Oklahoma Geological Survey
Charles J. Mankin, *Director*

Circular 103
ISSN 0078-4397

Marine Clastics in the Southern Midcontinent, 1997 Symposium

KENNETH S. JOHNSON, *Editor*

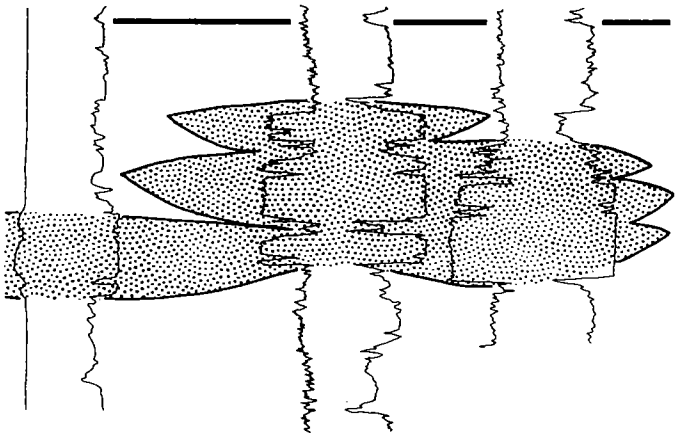

Proceedings of a symposium held March 25–26, 1997, in Norman, Oklahoma.

Co-sponsored by:

Oklahoma Geological Survey

and

National Petroleum Technology Office,
U.S. Department of Energy

The University of Oklahoma
Norman

2000

OKLAHOMA GEOLOGICAL SURVEY

CHARLES J. MANKIN, *Director*
KENNETH S. JOHNSON, *Associate Director*

SURVEY STAFF

JAMES H. ANDERSON, *Cartographic Draftsperson III*
RICHARD D. ANDREWS, *Geologist III*
LARRY T. AUSTIN, *Core and Sample Library Assistant*
BETTY D. BELLIS, *Word-Processing Operator II/Technical Typist*
MITZI G. BLACKMON, *Clerk-Typist I*
JERLENE A. BRIGHT, *Technical Project Specialist*
RAYMON L. BROWN, *Geophysicist III*
RUTH E. BROWN, *Assistant to the Director*
JOCK A. CAMPBELL, *Geologist IV*
BRIAN J. CARDOTT, *Geologist IV*
JAMES R. CHAPLIN, *Geologist IV*
JANISE L. COLEMAN, *Office Assistant IV*
CHRISTIE L. COOPER, *Editor*
TAMMIE K. CREEL, *Secretary II*
CHARLES R. DYER III, *Drilling Technician*
WALTER C. ESRY, *Manager, Core and Sample Library*
ROBERT O. FAY, *Geologist IV*
AMIE R. FRIEND, *Research Specialist I*
T. WAYNE FURR, *Manager of Cartography*
PATRONALIA M. HANLEY, *Chemist*
PRISCILLA A. JOHNSON, *Office Assistant IV*
MICHAEL A. KELLEY, *Computer Specialist*
JAMES W. KING, *Research Specialist I*
JAMES E. LAWSON, JR., *Chief Geophysicist*
KENNETH V. LUZA, *Geologist IV*
MICHAEL J. MERCER, *Manager, Log Library*
RICHARD G. MURRAY, *Copy Center Operator*
SUE M. PALMER, *Office Assistant II*
DAVID O. PENNINGTON, *Operations Assistant II*
CONNIE G. SMITH, *Promotion and Information Specialist*
PAUL E. SMITH, *Supervisor, Offset Press Copy Center*
THOMAS M. STANLEY, *Geologist II*
LLOYD N. START, *Assistant Drilling Technician*
JOYCE A. STIEHLER, *Chief Clerk*
MICHELLE J. SUMMERS, *Technical Project Coordinator*
NEIL H. SUNESON, *Geologist IV*
JANE L. WEBER, *Coordinator, Departmental Computer Systems*
STEPHEN J. WEBER, *Chief Chemist*

Cover Photo

Cross section illustrating lateral facies across Red Oak slope-channel deposit (from p. 134 of this volume).

This publication, printed by the Oklahoma Geological Survey, is issued by the Oklahoma Geological Survey as authorized by Title 70, Oklahoma Statutes, 1981, Sections 231–238. 1,050 copies have been prepared for distribution at a cost of $10,357 to the taxpayers of the State of Oklahoma. Copies have been deposited with the Publications Clearinghouse of the Oklahoma Department of Libraries.

PREFACE

The transfer of technical information will aid in the search for, and production of, our oil and gas resources. To facilitate this technology transfer, the Oklahoma Geological Survey (OGS) and the U.S. Department of Energy, National Petroleum Technology Office (DOE–NPTO), in Tulsa, cosponsored a symposium dealing with the search for, and production of, oil and gas resources from marine clastics in the southern Midcontinent. The symposium was held on March 25–26, 1997, in Norman, Oklahoma. This volume contains the proceedings of that symposium.

Research reported upon at the symposium focused on sandstones and other clastic rock units deposited in shallow- or deep-water marine environments. These clastics are major sources of oil and gas in the southern Midcontinent, and they have great potential for additional recovery using advanced technologies. The research reports on geology, depositional settings, diagenetic history, sequence stratigraphy, reservoir characterization, exploration, petroleum production, and enhanced oil recovery. In describing these marine clastics and their petroleum reservoirs, the researchers have increased our understanding of how the geologic history of an area can affect reservoir heterogeneity and our ability to efficiently recover the hydrocarbons they contain. We hope that the symposium and these proceedings will bring such research to the attention of the geoscience and energy-research community, and will help foster exchange of information and increased research interest by industry, university, and government workers.

Twenty talks and posters presented at the symposium are printed here as full papers or extended abstracts. An additional twelve talks and posters are presented as abstracts at the end of the volume. About 210 persons attended the symposium. Stratigraphic nomenclature and age determinations used by the various authors in this volume do not necessarily agree with those of the OGS.

This is the tenth symposium in as many years dealing with topics of major interest to geologists and others involved in petroleum-resource development in Oklahoma and adjacent states. These symposia are intended to foster the exchange of information that will improve our ability to find and recover our nation's oil and gas resources. Earlier symposia covered: Anadarko Basin (published as OGS Circular 90); Late Cambrian–Ordovician Geology of the Southern Midcontinent (OGS Circular 92); Source Rocks in the Southern Midcontinent (OGS Circular 93); Petroleum-Reservoir Geology in the Southern Midcontinent (OGS Circular 95); Structural Styles in the Southern Midcontinent (OGS Circular 97); Fluvial-Dominated Deltaic Reservoirs in the Southern Midcontinent (OGS Circular 98); Simpson and Viola Groups in the Southern Midcontinent (OGS Circular 99); Ames Structure in Northwest Oklahoma and Similar Features—Origin and Petroleum Production (OGS Circular 100); and Platform Carbonates in the Southern Midcontinent (OGS Circular 101).

Persons involved in the organization and planning of this symposium include: Kenneth Johnson and Charles Mankin of the OGS; and Tom Wesson and Chandra Nautiyal of DOE–NPTO. Other personnel who contributed include Michelle Summers and Tammie Creel, registration co-chairs; LeRoy Hemish, poster-session chair; Connie Smith, publicity chair; and Judy Schmidt, exhibits coordinator. Technical editing of this volume was done by Thomas W. Henry, Westminster, Colorado; layout and production was done by Sandra Rush, Denver, Colorado. Appreciation is expressed to each of them and to the many authors who worked toward a highly successful symposium.

KENNETH S. JOHNSON
General Chairman

CONTENTS

Petroleum Production from Marine Clastics in Oklahoma

Kenneth S. Johnson
Oklahoma Geological Survey
Norman, Oklahoma

Robert A. Northcutt
Independent Geologist
Oklahoma City, Oklahoma

G. Carlyle Hinshaw
Independent Geologist
Norman, Oklahoma

ABSTRACT.—Marine clastics include those clastic-rock units deposited in shallow- or deep-sea water. Their environments of deposition include delta front, barrier island, beach, offshore bar, continental shelf and slope, submarine fan, and transgressive sands. Most of Oklahoma's sedimentary rocks are of marine origin, and a significant part of those deposits consist of marine sandstones and conglomerates that are important sources of oil and gas in many parts of the state. Important marine-clastic reservoirs in Oklahoma are present in the Simpson (Wilcox and Bromide), Misener, Springer, Morrow, Cromwell, Atoka (Red Oak and Spiro), Red Fork, Cottage Grove, Layton, Tonkawa, Deese, Hoxbar, and others.

Production data for leases in Oklahoma were retrieved from the Geo Information Systems (GIS) data files by the geologic names of the producing intervals. The files contain 700 different geologic names for producing intervals, and about 300 of these are marine clastics. Some geologic names, such as Morrow and Red Fork, are used for units that are alluvial and/or deltaic in some parts of the state and marine in other areas. We identify these units as being among the marine clastics, and then separate out and eliminate those parts of the state where the alluvial/deltaic facies predominates.

We have prepared a series of eight maps to show the distribution of production from marine clastics by geologic age. The eight maps generated are for the following stratigraphic intervals: (1) Upper Cambrian and Ordovician; (2) Upper Devonian and Lower Mississippian (Woodford–Chattanooga); (3) Mississippian; (4) Upper Mississippian and Lower Pennsylvanian (Springer and Morrow); (5) Lower Pennsylvanian; (6) Middle Pennsylvanian; (7) Upper Pennsylvanian; and (8) Permian and Cretaceous. Cumulative production of oil and gas from 1979 through June 1996 for all of these stratigraphic intervals is 864 million barrels of oil and 12 trillion cubic feet of natural gas. Cumulative production for each of the eight intervals is shown separately.

INTRODUCTION

Oklahoma is one of the leading petroleum-producing states in the nation, and a significant part of the state's oil and gas has been produced from marine clastics. Marine clastics consist of sandstones, conglomerates, and shales deposited in shallow- or deep-sea water. The various environments of their deposition include delta front, barrier island, beach, offshore bar, continental shelf and slope, submarine fan, and transgressive sands. With petroleum exploration and production being of such great importance to the state, it is critical to understand the character and distribution of these prolific clastic reservoirs.

This paper provides an overview of the following: (1) the Paleozoic and Mesozoic geologic setting and marine clastics of Oklahoma, (2) the names and character of the principal marine-clastic reservoirs, and (3) the distribution of oil and gas production from the eight major groupings of marine clastics. The discussion that follows under Geologic Framework and the general geologic characterization of each of the eight groups of

Johnson, K. S.; Northcutt, R. A.; and Hinshaw, G. C., 2000, Petroleum production from marine clastics in Oklahoma, *in* Johnson, K. S. (ed.), Marine clastics in the southern Midcontinent, 1997 symposium: Oklahoma Geological Survey Circular 103, p. 1–17.

marine clastics is modified largely from earlier reports by Johnson and others (1988) and Johnson and Cardott (1992).

Production data for leases were retrieved from the Natural Resources Information System (NRIS) by Geo Information Systems (GIS), a research department of The University of Oklahoma, by the geologic names of the producing intervals. Oklahoma petroleum production is recorded by lease, *not by well*, by the Oklahoma Tax Commission. These data are public records and are marketed in several forms by commercial and governmental organizations. GIS provides the data six months in arrears, updated each six months. The data base begins in 1979, with oil, condensate, associated gas, and non-associated gas, recorded monthly. It is possible, through the mapping capabilities of SAS (an integrated system of software), to post a location map at almost any scale for one or several (or all) producing intervals by product or products. Also, individuals or companies can acquire the raw data and construct their own analyses.

GEOLOGIC FRAMEWORK

The geology of Oklahoma is complex, but it is remarkably well understood as a result of the extensive amount of drilling and seismic exploration in search of oil and gas. Great thicknesses of sedimentary rock are preserved in a series of major depositional and structural basins separated by orogenic uplifts that formed mainly during the Pennsylvanian (Figs. 1, 2). The major sedimentary basins contain as much as 20,000–40,000 ft of sediments, most of which are Paleozoic and marine, resting upon a basement complex of igneous rocks and some low-rank metasedimentary rocks (Denison and others, 1984; Johnson and others, 1988). Basement rocks beneath most of Oklahoma are Precambrian granites and comagmatic rhyolites; however, beneath the southern Oklahoma aulacogen, they are Early and Middle Cambrian granites, rhyolites, gabbros, and basalts. Basement rocks beneath the Ouachita province have not been penetrated by drilling and are unknown.

By early Paleozoic time, Oklahoma had three major tectonic/depositional provinces: the Oklahoma basin, the southern Oklahoma aulacogen, and the Ouachita trough (Fig. 3). The Oklahoma basin was a broad, shelf-like area that received a sequence of remarkably thick and extensive, shallow-marine carbonates interbedded with thinner marine shales and sandstones (Johnson and others, 1988). The southern Oklahoma aulacogen was the depocenter for the Oklahoma basin; it was a west-northwest–trending trough, where sediments generally are similar to those elsewhere in the basin, but they are two to three times thicker. The aulacogen embraced the Anadarko, Ardmore, and Marietta protobasins, along with the present-day Arbuckle anticline and Wichita Mountain uplift. The Ouachita trough was the site of deep-water sedimentation along a rift at the southern margin of the North American craton; later, these sediments were thrust northward as much as 50 mi to their present position in the Ouachita Mountain uplift.

Following Early Devonian sedimentation, the Oklahoma basin was uplifted epeirogenically, and large areas were exposed to erosion. Late Devonian inundation then caused the major pre-Woodford unconformity to extend over most parts of the state. The three major tectonic/depositional provinces persisted

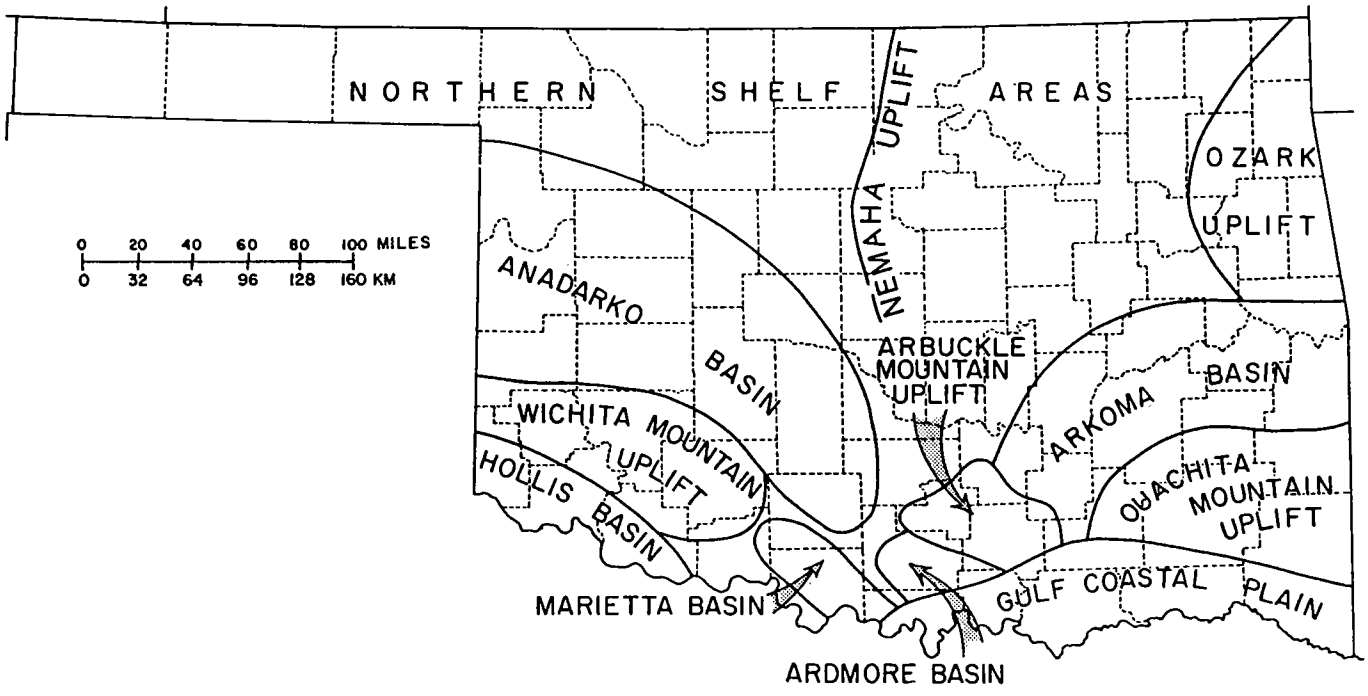

Figure 1. Map showing major geologic provinces of Oklahoma.

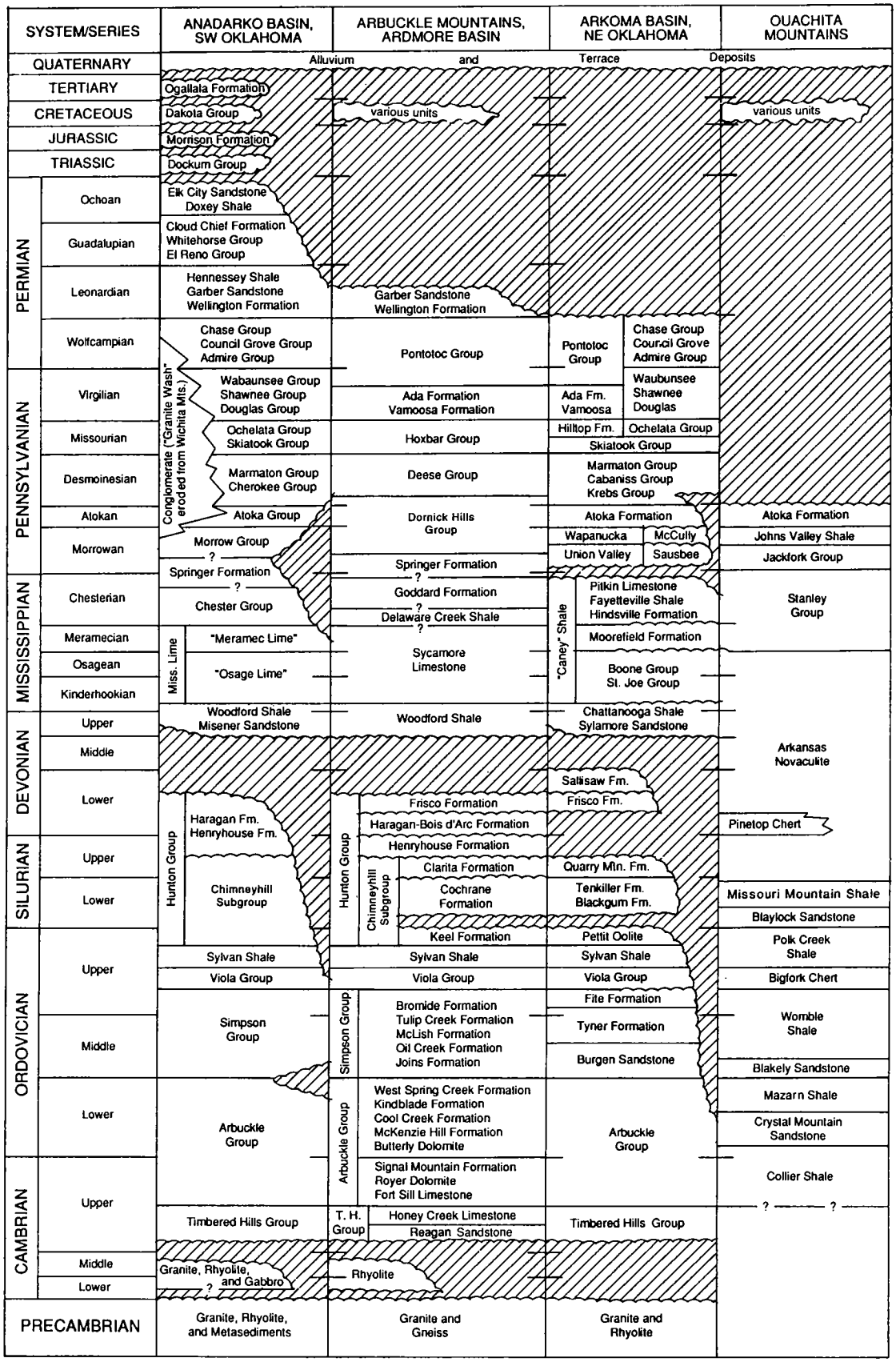

Figure 2. Generalized correlation of rock units in Oklahoma (modified from COSUNA charts by Hills and Kottlowski, 1983; Mankin, 1987) (reprinted, with modifications, from Johnson and Cardott, 1992). Height of boxes is not related to thickness of rock units.

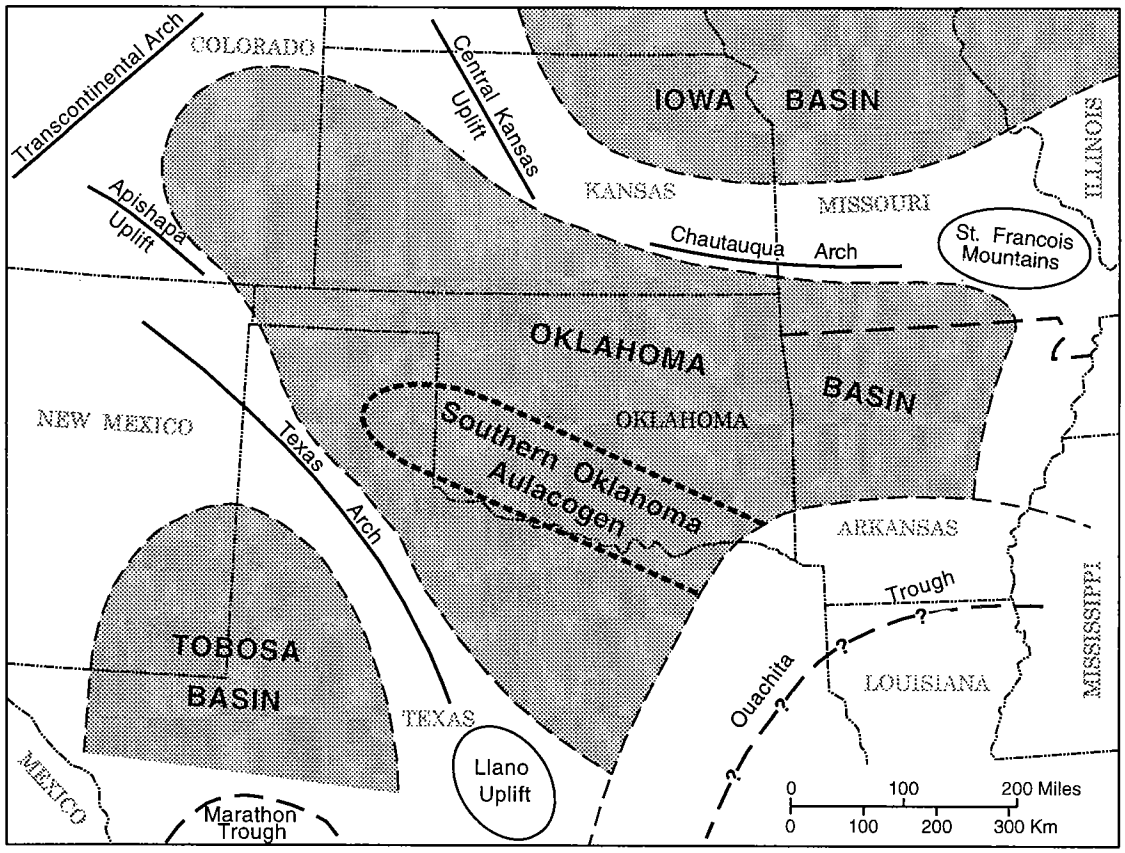

Figure 3. Map of southwestern United States, showing approximate boundary of the Oklahoma basin and other major features that existed in early and middle Paleozoic time (after Johnson and others, 1988).

until Pennsylvanian time, when the Oklahoma basin and the aulacogen were divided into a series of well-defined marine basins by sharply uplifted crustal blocks (Johnson and others, 1988; McBee, 1995). Northward thrusting and uplift during the Pennsylvanian destroyed the Ouachita trough. Pennsylvanian orogenic activity throughout the state was limited to folding, faulting, and uplift, and was not accompanied by igneous or high-grade metamorphic activity.

MARINE CLASTICS AND PETROLEUM PRODUCTION

For purposes of this report, it is practical to discuss the geology and petroleum production of marine clastics by subdividing the Paleozoic Era into eight stratigraphic intervals: (1) Upper Cambrian and Ordovician; (2) Upper Devonian and Lower Mississippian (Woodford–Chattanooga); (3) Mississippian; (4) Upper Mississippian and Lower Pennsylvanian (Springeran and Morrowan); (5) Lower Pennsylvanian; (6) Middle Pennsylvanian; (7) Upper Pennsylvanian; and (8) Permian and Cretaceous (Fig. 4).

Stratigraphic names used to identify individual producing units in the GIS files are the specific names used by various geologists, producers, or operators in reporting production data to the Oklahoma Tax Commission. Therefore, several names are typically given for the same unit, and a number of names present in the data base would not normally be published in the geologic literature. Also, different names commonly are used for stratigraphically equivalent producing units in northern Oklahoma and in southern Oklahoma. The equivalent names are shown in separate columns on the eight stratigraphic sequence tables (Tables 1–8). A heavy east-west line drawn across the state on the production maps (Figs. 6–13) shows the approximate boundary between the areas where these names are in common use.

Of the total 700 names in the GIS files that represent producing units, about 300 are names for marine clastics (Tables 1–8). Some geologic units, such as the Morrow and Red Fork, are marine deposits in some parts of the state and are nonmarine (alluvial and/or deltaic) in other areas; we list them here as being marine, but then show on the maps (Figs. 6–13) those areas where they are nonmarine by a cross-hatched pattern.

Cumulative-production figures presented for each of the eight sequences summarize data for production definitely assigned only to that sequence; they do not include commingled production, where reservoirs in two or more sequences were coproduced on the same lease. Therefore, cumulative production figures re-

GEOLOGIC AGE	MAJOR MARINE CLASTICS THAT YIELD PETROLEUM
Cretaceous	Trinity Group
Permian	Pontotoc Group
Upper Pennsylvanian	Virgilian Series Cisco Group Missourian Series Hoxbar Group
Middle Pennsylvanian	Marmaton Group Cherokee Group Deese Group
Lower Pennsylvanian	Atoka Group Upper Dornick Hills Group
Lower Pennsylvanian–Upper Mississippian	Morrow Group Lower Dornick Hills Group Jackfork Group Springer Group
Mississippian	Goddard Sycamore Mississippi Chat
Lower Mississippian and Upper Devonian	Woodford Misener
Ordovician	Viola Group Simpson Group
Upper Cambrian	Reagan

Figure 4. Stratigraphic intervals in the Paleozoic and Mesozoic of Oklahoma that contain petroleum-producing marine clastics. The eight intervals included in oil- and/or gas-production maps (Figs. 6–13) are bordered by bold lines.

ported here are minimal for the time period January 1, 1979, through June 30, 1996.

Upper Cambrian and Ordovician

Upper Cambrian and Ordovician strata form a vast blanket of marine rocks deposited throughout the Oklahoma basin (Fig. 5). These strata consist mainly of carbonates in the Arbuckle, Simpson, and Viola Groups and also include important clastics in the Reagan Sandstone and the several sands of the Simpson and Viola Groups.

Late Cambrian seas transgressed to the north and west, covering a basement-rock surface of modest to locally rugged relief. The time-transgressive basal Reagan Sandstone was deposited throughout most of the Oklahoma basin. It is a feldspathic and glauconitic sandstone deposited in an open, shallow-marine environment, and its thickness generally ranges from 100 to 400 ft.

Ordovician Simpson strata in the Oklahoma basin are cleanly washed, marine quartzose sandstones interbedded with shallow-marine limestones and greenish-gray shales. Simpson Group strata are thickest in the Anadarko and Ardmore basins, and aggregate more than 2,000 ft in the Ardmore basin (Schramm, 1964; Suhm, 1997). Individual high-purity silica sands (Joins, Oil Creek, McLish, Tulip Creek, Bromide, and Wilcox sands) generally are 50–400 ft thick. A recent comprehensive reference on the Simpson sands is a symposium on the Simpson and Viola Groups, edited by Johnson (1997).

The most commonly used names for petroleum-producing, marine-clastic intervals in the Upper Cambrian and Ordovician are listed in Table 1. The Reagan Sandstone, the oldest marine clastic rock in Oklahoma, produces oil in the complexly folded and faulted Eola-Robberson field in Garvin County—only one of the two known occurrences of Reagan oil or gas production in the state. Sands of the Simpson Group produce from structural traps and are among the most prolific oil and gas producing intervals in Oklahoma.

The Late Ordovician Viola Group is mainly a marine-limestone sequence, typically 200–600 ft thick in the Oklahoma basin. It contains a Simpson-like sand (commonly referred to as the Seminole sand or the "First Wilcox" sand), in much of central and north-central Oklahoma (Suhm, 1997). This Viola-age sand is typically 25–50 ft thick and locally reaches 70 ft thick.

Leases producing oil and gas from marine-clastic rocks of the Upper Cambrian and Ordovician sequence in Oklahoma are shown on Figure 6. The cumulative production from these reservoirs from January 1, 1979, through June 30, 1996, was 196,882,738 barrels (bbl) of oil and 295,592,480 thousand cubic feet (Mcf) of gas.

Upper Devonian and Lower Mississippian (Woodford–Chattanooga)

Following Middle Devonian epeirogenic uplift of most of Oklahoma, inundation of the region caused burial of the erosion surface under the organic-rich Woodford Shale, unquestionably the most prolific source rock for oil and gas in Oklahoma. The Woodford, which is equivalent to the Chattanooga Shale to the northeast, is dark gray to black fissile shale that also contains chert and siliceous shale. Where fractured, the brittle Woodford–Chattanooga Shale is a suitable reservoir rock. Anaerobic conditions on the Woodford seafloor inhibited almost all benthic organisms and favored the preservation of organic matter that settled to the bottom. The Woodford is present throughout most parts of the Oklahoma basin (Fig. 5); it ranges from 200–900 ft thick in the aulacogen to 50–100 ft thick in most of the shelf areas (Amsden, 1975, 1980; Johnson and others, 1988).

At the base of the Woodford in north-central Oklahoma is the Misener sand, which generally is 10–50 ft thick. The Misener consists of reworked, weathered clastic debris that was present on the pre-Woodford erosional surface.

Names of the Upper Devonian and Lower Mississippian reservoirs are listed in Table 2. The Woodford Shale and Arkansas Novaculite in southern Oklahoma produce from faulted and folded structures where the

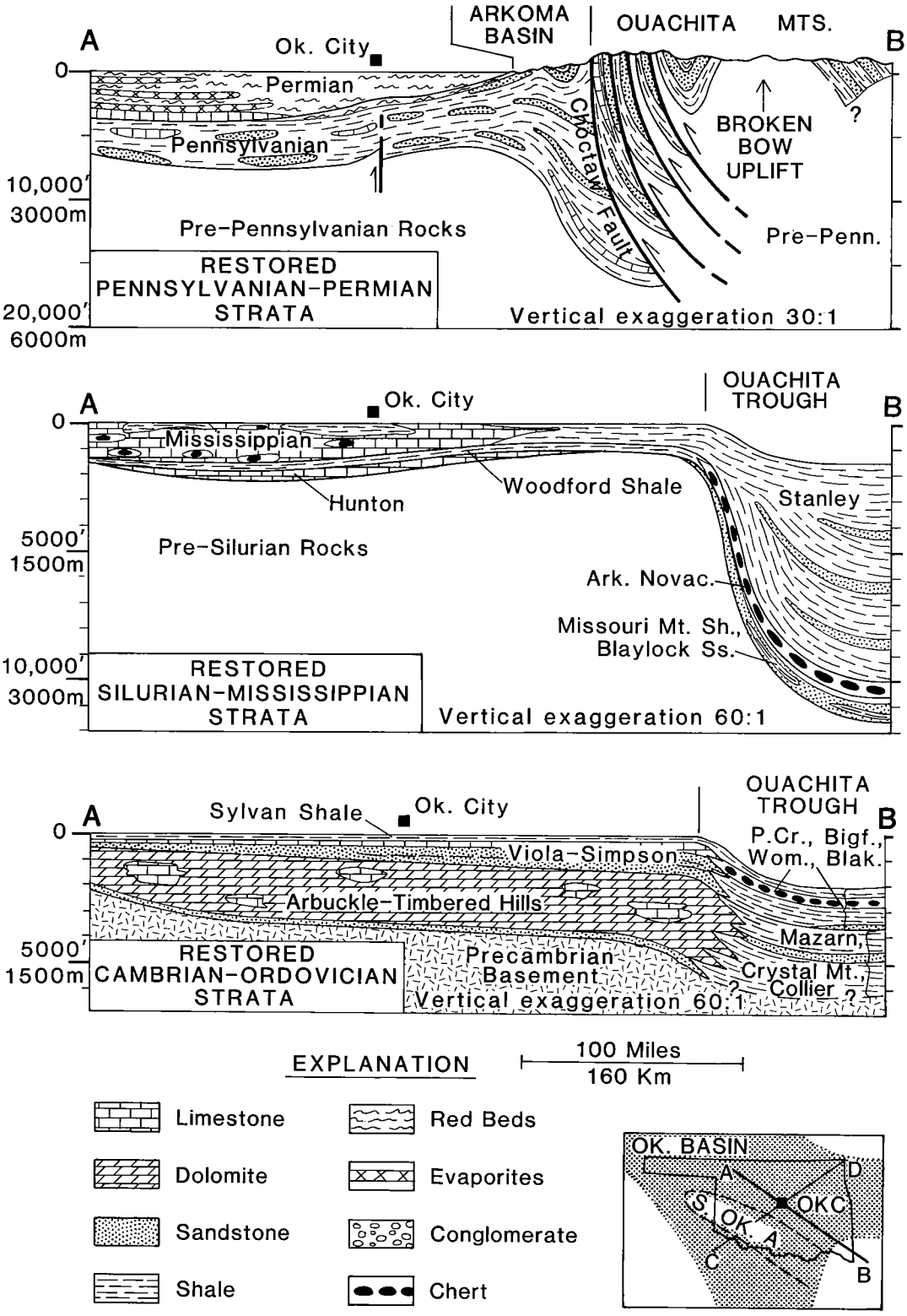

Figure 5 *(above and facing page)*. Schematic cross sections showing restored thickness of strata in Oklahoma at the end of early, middle, and late Paleozoic times (Johnson and Cardott, 1992). Top cross sections (Pennsylvanian–Permian) have less vertical exaggeration than other cross sections.

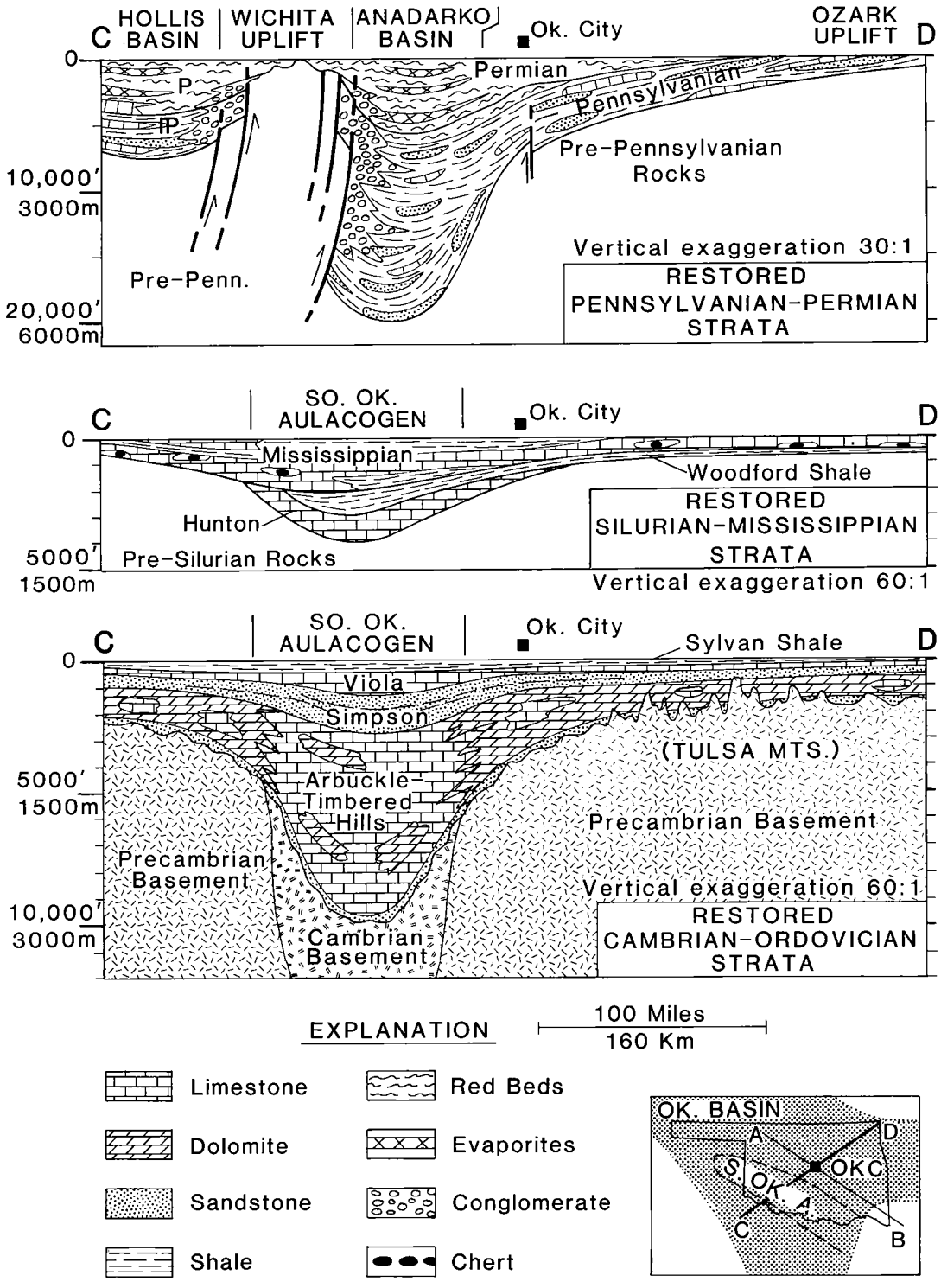

Figure 5 *(continued)*.

Table 1.—Names Used for Upper Cambrian and Ordovician Marine Clastics that Produce Petroleum in Oklahoma
(see Fig. 6)

Northern and east-central Oklahoma	Southern Oklahoma and deep Anadarko basin
ORDOVICIAN	
Viola Group	
Wilcox 1st	
Simpson Group	***Simpson Group***
Simpson	Bromide
Marshall	Bromide 1st
Wilcox	Bromide 2nd
Wilcox 2nd	Bromide 3rd
Tyner	Tulip Creek
	McLish
	McLish Basal
	Oil Creek
	Oil Creek Basal
CAMBRIAN	
	Reagan

Cumulative Production (1/1/79 through 6/30/96)
Oil: 196,882,738 bbl
Gas: 295,592,480 Mcf

siliceous facies has been heavily fractured. In north-central Oklahoma, the Misener sand is generally productive in stratigraphic traps along the depositional strike.

Leases producing oil and gas from Upper Devonian and Lower Mississippian reservoirs are shown on Figure 7. These reservoirs produced a cumulative 57,276,129 bbl of oil and 221,916,889 Mcf of gas from January 1, 1979, through June 30, 1996.

Mississippian

Mississippian strata are widespread over most of Oklahoma (Craig and others, 1979; Johnson and others, 1988). They consist of shallow-marine limestones and shales in most parts of the Oklahoma basin (Fig. 5), but thick, dark gray fissile shales (Caney and Goddard Shales), containing some thin marine sands, predominate in the eastern half of the aulacogen. Cherty limestone was deposited in the northern half of the state during the Osagean and Meramecian. The environment for deposition of most Mississippian strata was well-aerated, warm, shallow seas that supported abundant benthic life forms. Stratigraphic thicknesses generally range from 200 to 2,000 ft in the northern shelf areas, but the dark shale sequence in the aulacogen typically is 2,000–5,000 ft thick.

Mississippi "chat" consists of weathered and/or dense chert at the unconformable Mississippian–Pennsylvanian boundary in northern Oklahoma. The "chat" is a lag deposit that results from weathering and erosion of cherty limestone of the underlying Mississip-

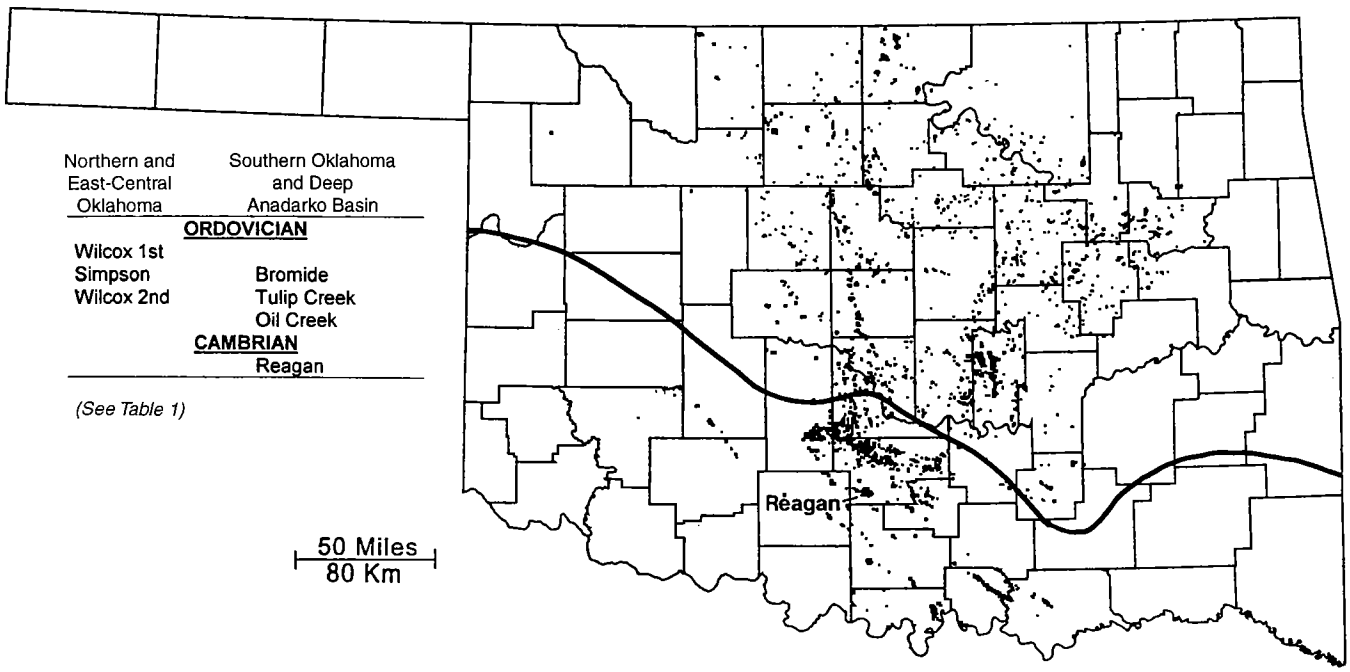

Figure 6. Oil and gas production from Upper Cambrian and Ordovician marine-clastic reservoirs in Oklahoma, 1979–1996. Heavy east-west line is approximate boundary for different nomenclature used in northern and southern Oklahoma. The only location of oil production from Reagan sand in Eola-Robberson field in southwestern Garvin County is annotated. Map generated by Geo Information Systems.

Table 2.—Names Used for Upper Devonian and Lower Mississippian Marine Clastics that Produce Petroleum in Oklahoma *(see Fig. 7)*

Northern and east-central Oklahoma	Southern Oklahoma and deep Anadarko basin
UPPER DEVONIAN AND LOWER MISSISSIPPIAN	
Woodford	Woodford
Misener	Arkansas Novaculite
Cumulative Production (1/1/79 through 6/30/96)	
Oil: 57,276,129 bbl	
Gas: 221,916,889 Mcf	

pian; easily weathered limestone is eroded, whereas weathering-resistant chert remains.

In southern Oklahoma, the Caney and Goddard are thick shale units that contain several marine sands. These strata represent deposition in slope to deep-water environments adjacent to and within the Ouachita trough.

Mississippian marine clastics in the Stanley, Goddard, and Sycamore of southern Oklahoma, and the Mississippi "chat" in northern Oklahoma (Table 3), are productive in both structural and stratigraphic traps. Reservoirs in the Mississippi "chat" tend to be in stratigraphic traps associated with structures or in truncated stratigraphic traps subsequently sealed by overlying Pennsylvanian beds. Reservoirs in the Stanley, Goddard, and Sycamore are generally in structural traps, where fracturing has enhanced the porosity and permeability of the sandstones.

The lease production map of Mississippian marine clastics (Fig. 8) shows the large area of Mississippi "chat" production in northern Oklahoma. Production from Goddard and Sycamore reservoirs in southern Oklahoma is located on structural trends in the Ardmore basin and in the Golden Trend of Garvin County. Stanley production is just now being developed in the Ouachita Mountains province of southeastern Oklahoma, and it is not yet posted on the map. Cumulative production from January 1, 1979, through June 30, 1996, for the Mississippian marine clastics is 109,477,118 bbl of oil and 389,304,661 Mcf of gas.

Upper Mississippian and Lower Pennsylvanian (Springeran and Morrowan)

The top of the Mississippian System is well marked by a pre-Pennsylvanian unconformity in most parts of the southern Midcontinent; however, the Mississippian–Pennsylvanian boundary occurs within the thick sequence of Springer and equivalent shales and sands where sedimentation was uninterrupted in the deep parts of the Anadarko and Ardmore basins. These Springer clastics (generally assigned a "Springeran" age) are commonly grouped with the overlying Morrowan strata, from which they are not easily distinguished. Here, we will group these units together on the map (Fig. 9), but we will discuss them as separate units.

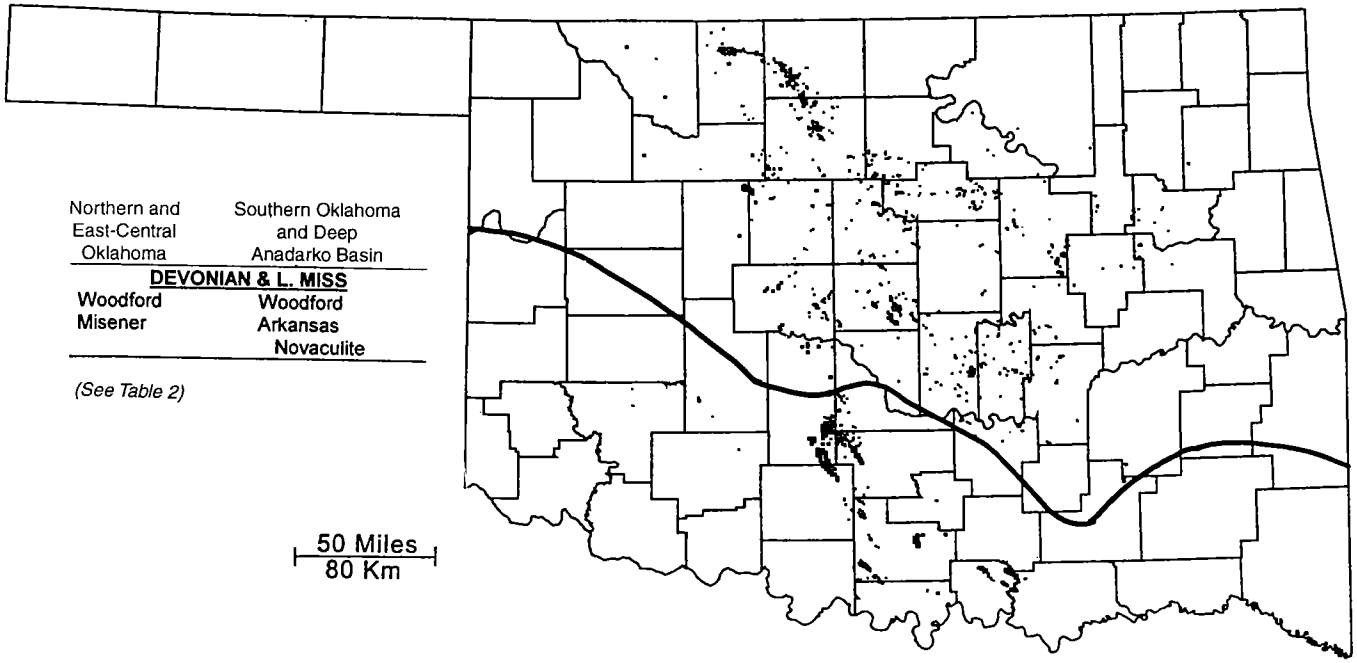

Figure 7. Oil and gas production from Devonian and Lower Mississippian (Woodford–Chattanooga) marine-clastic reservoirs in Oklahoma, 1979–1996. Heavy east-west line is approximate boundary for different nomenclature used in northern and southern Oklahoma. Map generated by Geo Information Systems.

Table 3.—Names Used for Mississippian Marine Clastics that Produce Petroleum in Oklahoma *(see Fig. 8)*

Northern and east-central Oklahoma	Southern Oklahoma and deep Anadarko basin
MISSISSIPPIAN	
Mississippi Chat	Stanley Goddard Sycamore

Cumulative Production (1/1/79 through 6/30/96)

Oil: 109,477,118 bbl

Gas: 389,304,661 Mcf

Deposition of the Springeran sandstones (Late Mississippian–Early Pennsylvanian) in the Anadarko-Ardmore basins marked a change from the dominantly carbonate and shale deposition of the Chester (Late Mississippian) to the clastic environments of the Early Pennsylvanian. Rapid subsidence of the Anadarko-Ardmore basins and the adjacent shelf areas in the Late Mississippian and Early Pennsylvanian caused transgression of the Springeran seas over the shelf areas of Chester carbonates and deposition of shallow-marine and shoreline sands of the Springer. Intervals of Springer sands in the Anadarko and Ardmore basins are as much as 250 ft thick in some areas, with discrete marine sand bars attaining a thickness of 50 ft or more for several miles (Brown and Northcutt, 1993).

Springer sands were first named after leases in the fields of southern Oklahoma where they produced oil and/or gas. Correlation of the individual sands was not attempted between fields, so some of the names of the Springer-producing intervals shown in Table 4 may, in fact, be equivalent.

Names of Morrowan producing intervals are also shown on Table 4. In southern Oklahoma, the Morrowan strata are named the lower Dornick Hills Group, and only the Primrose sand (the basal sand) is normally identified as a named member. In the Anadarko basin and shelf area of northern Oklahoma, individual Morrow Group sands have been named in some areas of western Oklahoma. Generally, throughout the basin and shelf area, the term "Morrow" has been applied to the various producing intervals without any attempt to name individual sands, because of the difficulty in correlation of the sands.

The production map for the Upper Mississippian and Lower Pennsylvanian (Springeran and Morrowan) sequence (Fig. 9) shows both Springer and Morrow (or lower Dornick Hills) production in southern Oklahoma and the deep Anadarko basin. Elsewhere, production is limited to only the Morrow in the Arkoma basin of eastern Oklahoma and in the shelf area of the Anadarko basin in western Oklahoma. The areas of upper Morrow deltaic deposits are shown by a cross-hatched pattern. Morrow sands in central and east-central Oklahoma generally produce from stratigraphic traps that occasionally are associated with structure, whereas the structural traps in the Arkoma basin along the frontal fault belt of the Ouachita Mountains provide the traps for gas production.

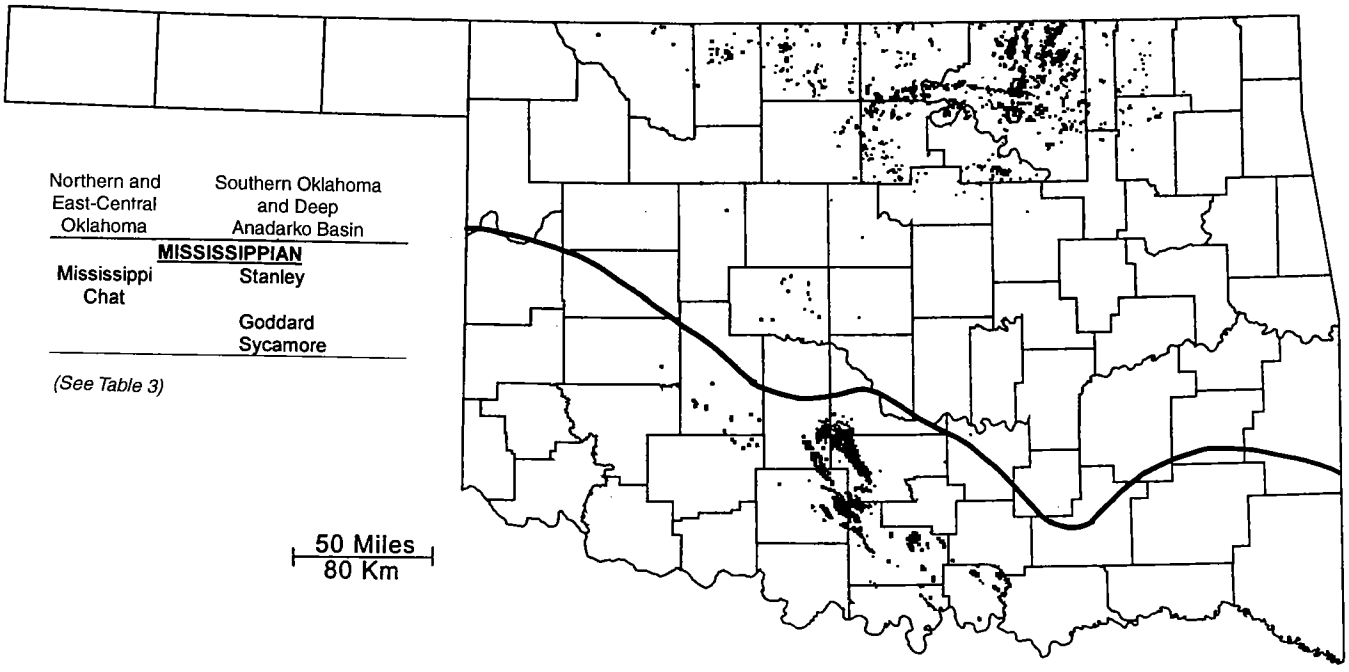

Figure 8. Oil and gas production from Mississippian marine-clastic reservoirs in Oklahoma, 1979–1996. Heavy east-west line is approximate boundary for different nomenclature used in northern and southern Oklahoma. Map generated by Geo Information Systems.

Table 4.—Names Used for Upper Mississippian and Lower Pennsylvanian (Springeran and Morrowan) Marine Clastics that Produce Petroleum in Oklahoma
(see Fig. 9)

Northern and east-central Oklahoma	Southern Oklahoma and deep Anadarko basin
LOWER PENNSYLVANIAN (MORROWAN)	
Morrow Group	***Lower Dornick Hills Group***
Morrow	Lower Dornick Hills
Mouser	Primrose
Purdy	
Purvis	***Jackfork Group***
Puryear	Jackfork
Hollis	
Pierce	
Bradstreet	
Lower Morrow	
Keyes	
Union Valley	
Cromwell	
Jefferson	
Mocane	

Northern and east-central Oklahoma	Southern Oklahoma and deep Anadarko basin
UPPER MISSISSIPPIAN–LOWER PENNSYLVANIAN (SPRINGERAN)	
	Springer Group
	Springer
	Woods
	Cunningham
	Markham
	Aldridge
	Humphreys
	Horton
	Hutson
	Britt
	Sims
	Goodwin
	Spiers
	Boatwright
	Anderson
	Stanley

Cumulative Production (1/1/79 through 6/30/96)

Oil: 316,371,420 bbl

Gas: 5,201,547,775 Mcf

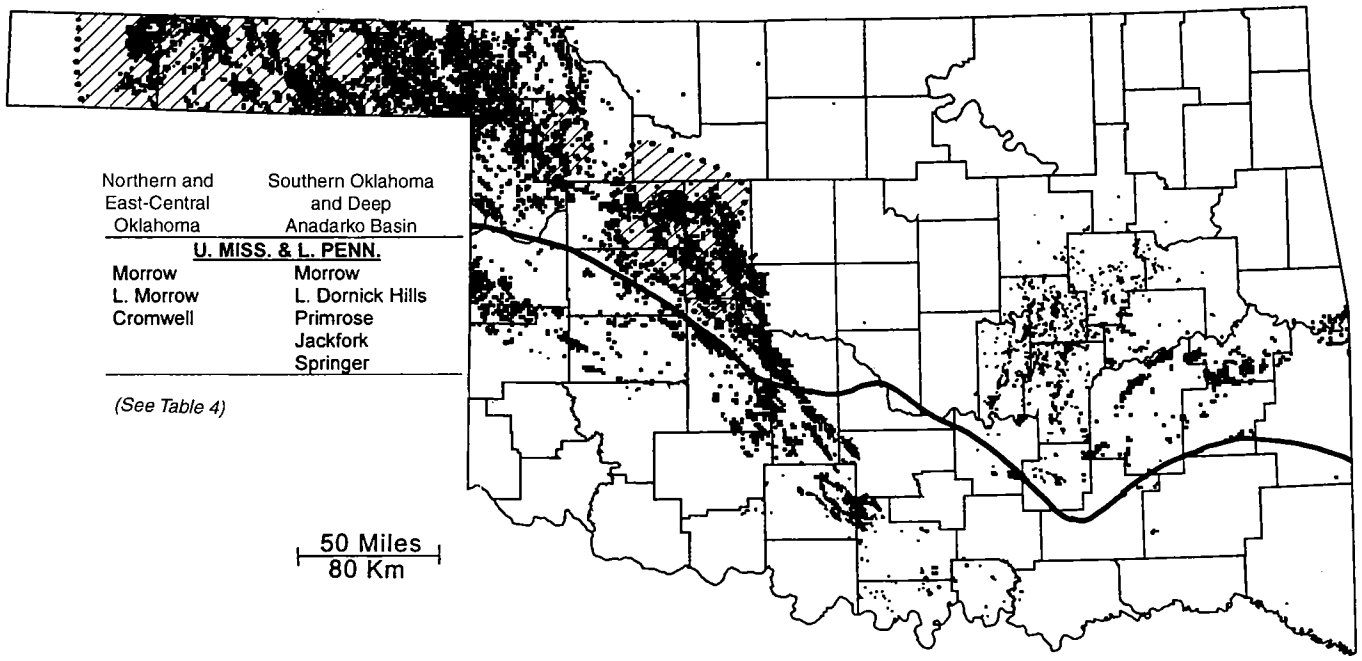

Figure 9. Oil and gas production from Upper Mississippian and Lower Pennsylvanian (Springeran and Morrowan) marine-clastic reservoirs in Oklahoma, 1979–1996. Heavy east-west line is approximate boundary for different nomenclature used in northern and southern Oklahoma. Cross-hatched area in northwestern Oklahoma denotes areas of Morrowan deltaic reservoirs. Map generated by Geo Information Systems.

Leases producing from Upper Mississippian and Lower Pennsylvanian (Springeran and Morrowan) reservoirs had a cumulative production of 316,371,420 bbl of oil and 5,201,547,775 Mcf of gas from January 1, 1979, through June 30, 1996.

Lower Pennsylvanian

Major changes took place in Oklahoma during Pennsylvanian time. Early and middle Paleozoic epeirogenic movements, accompanied by the deposition of relatively simple sequences of shelf carbonates (with some shales and sandstones) over vast regions of the Oklahoma basin, ended with a series of orogenic movements that subdivided the state into the tectonic provinces easily recognized today (Figs. 1, 5). First, an episode of Late Mississippian–Early Pennsylvanian epeirogenic uplift and erosion throughout most of the Oklahoma basin produced a widespread pre-Pennsylvanian unconformity, except where sedimentation was continuous along the axis of the aulacogen (the Springeran in the deep Anadarko and Ardmore basins). Then, a series of orogenic pulses in the aulacogen and the Ouachita trough through Early, Middle, and Late Pennsylvanian time caused, or contributed to, the following: (1) folding and thrusting of the Ouachita fold belt; (2) raising of the Wichita, Criner, Arbuckle, Nemaha, and Ozark uplifts; and (3) pronounced downwarping of the Anadarko, Ardmore, Marietta, Arkoma, and Hollis basins (Tomlinson and McBee, 1959; Ham and Wilson, 1967; Rascoe and Adler, 1983; Johnson and others, 1988; Sutherland, 1988; McBee, 1995).

Pennsylvanian strata in the state are sequences of marine and nonmarine shale, sandstone, conglomerate, and limestone that thicken markedly (to as much as 10,000–15,000 ft thick) into the rapidly subsiding basins (Fig. 5) (McKee and others, 1975; Johnson and others, 1988). The thick wedges of terrigenous clastic sediments were shed from nearby uplifts, mainly in the south; thinner carbonates were deposited in shallow-water shelf areas distal to the uplifts. Successively younger Pennsylvanian strata commonly overlap older units at the margins of the basins and across some of the uplifts.

Early Pennsylvanian sedimentation was largely restricted to the main sedimentary basins—the Anadarko, Ardmore, Arkoma, and Ouachita basins. Orogenic and epeirogenic uplift had raised most of the remainder of Oklahoma above sea level, thus providing a substantial source area for clastics deposited in shallow seas that occupied the basins. Lower Pennsylvanian strata in Oklahoma are almost entirely marine clastics of Morrowan and Atokan age. In most parts of the state, they are commonly referred to as the Morrow and Atoka Groups, respectively, although they are called the Dornick Hills Group in the south and southwest and the Jackfork Group in the Ouachita Mountains (Tables 4, 5). For purposes of this report, Morrowan strata and production are discussed mainly with the Springeran in the Upper Mississippian and Lower Pennsylvanian.

Names of producing reservoirs in the Lower Pennsylvanian (Atokan) are listed in Table 5. Most of the names in northern and east-central Oklahoma are used in the Arkoma basin and are named only in local areas. Gilcrease and Dutcher are names used in the western part of the Arkoma basin. Most of the producing reservoirs are just designated as "Atoka." Production is from both structural and stratigraphic traps; however, many are combination traps. The area of Lower Pennsylvanian (Atokan) production (Fig. 10) illustrates the concentration of production in the Arkoma basin. Some of the production shown in the Anadarko basin may be Middle Pennsylvanian but is incorrectly labeled as Atokan. In southern Oklahoma, the Atoka is called the Upper Dornick Hills.

Cumulative production from the Atokan reservoirs from January 1, 1979, through June 30, 1996, is 70,804,648 bbl of oil and 4,341,905,344 Mcf of gas. The large volume of natural-gas production is from the Arkoma basin.

Middle Pennsylvanian

The major mountain systems of southern Oklahoma and the surrounding highlands areas to the north and east of Oklahoma were uplifted and shedding clastic debris during most of the Middle Pennsylvanian (Desmoinesian). These strata were the first Pennsylvanian units to be deposited on the underlying eroded Mississippian surface across central and north-central Oklahoma. Throughout the Desmoinesian, this great amount of clastic debris was deposited in large deltas on the Cherokee platform and the Anadarko shelf in northeastern and northern Oklahoma. Shallow-water marine clastics were deposited in most of southern Oklahoma, whereas delta-front marine clastics were deposited in the southern part of the Anadarko basin.

The large number of names for producing sands in this sequence (Table 6) result, in part, from the many facies changes in Desmoinesian strata. Most of these sands have both marine and non-marine (deltaic) components. Several of these sands in northern and east-central Oklahoma are equivalent, and they can even be correlated to stratigraphic equivalents in southern Oklahoma and the deep Anadarko basin.

Reservoirs in these sands are primarily found in stratigraphic traps formed by updip pinchout of the sands. Some traps are combined with structural closure where the sands were deposited over post-depositional uplifts of small structures.

The lease production map for the Middle Pennsylvanian sequence (Fig. 11) illustrates the widespread petroleum production for these strata. The heavy east-west line across the state is the approximate boundary for the different nomenclature shown in Table 6. The cross-hatched areas indicate the large area of deltaic deposition for these producing units in northern Oklahoma.

For the period from January 1, 1979, through June 30, 1996, leases producing from Middle Pennsylvanian reservoirs, including deltaic reservoirs, had a cumulative production of 71,741,124 bbl of oil and 911,846,959 Mcf of gas. This production represents only the produc-

Table 5.—Names Used for Lower Pennsylvanian (Atokan) Marine Clastics that Produce Petroleum in Oklahoma
(see Fig. 10)

Northern and east-central Oklahoma	Southern Oklahoma and deep Anadarko basin
LOWER PENNSYLVANIAN (ATOKAN)	
Atoka Group	***Lower Dornick Hills Group***
Atoka	Upper Dornick Hills
Gilcrease	Carpenter
Dutcher	
Gose	
Alma	
Dirty Creek	
Morris	
Fanshawe	
Red Oak	
Panola	
Diamond	
Brazil	
Bullard	
Cecil	
Dunn	
Shay	
Atoka Lower	
Pope Chapel	
Spiro	
Atoka Basal	

Cumulative Production (1/1/79 through 6/30/96)
Oil: 70,804,648 bbl
Gas: 4,341,905,344 Mcf

tion from the mature stage of production from these reservoirs, since the greater amount of the production from these leases was prior to 1979.

Upper Pennsylvanian

Upper Pennsylvanian strata, which include the Missourian and Virgilian Series, were deposited in all parts of Oklahoma, except the eastern third of the state and the uplifted Ouachita, Arbuckle, and Wichita Mountain areas. Shallow seas inundated the western two-thirds of Oklahoma.

Upper Pennsylvanian strata are mostly marine shales, with numerous interbeds of sandstone and limestone. The marine sands were deposited in a variety of settings, including delta-front, shoreface, and offshore-bar environments. Also, thick conglomerates were deposited on the flanks of the still-rising Wichita and Arbuckle Mountain uplifts, and the term "granite wash" has been given to the predominantly arkosic conglomerates eroded from the Wichita uplift.

Names of marine clastics of the Upper Pennsylvanian that produce oil and/or gas are listed in Table 7. In northeast Oklahoma, many of these sands were deposited in both deltaic and marine environments. Throughout the rest of the state, sands of the Upper Pennsylvanian sequence were dominantly marine. Most of these sands were named locally and have stratigraphic equivalents with different names, especially in western Oklahoma.

Oil and gas production by lease for the Upper Pennsylvanian sequence is shown in Figure 12. The area of production from deltaic deposits in north-central Okla-

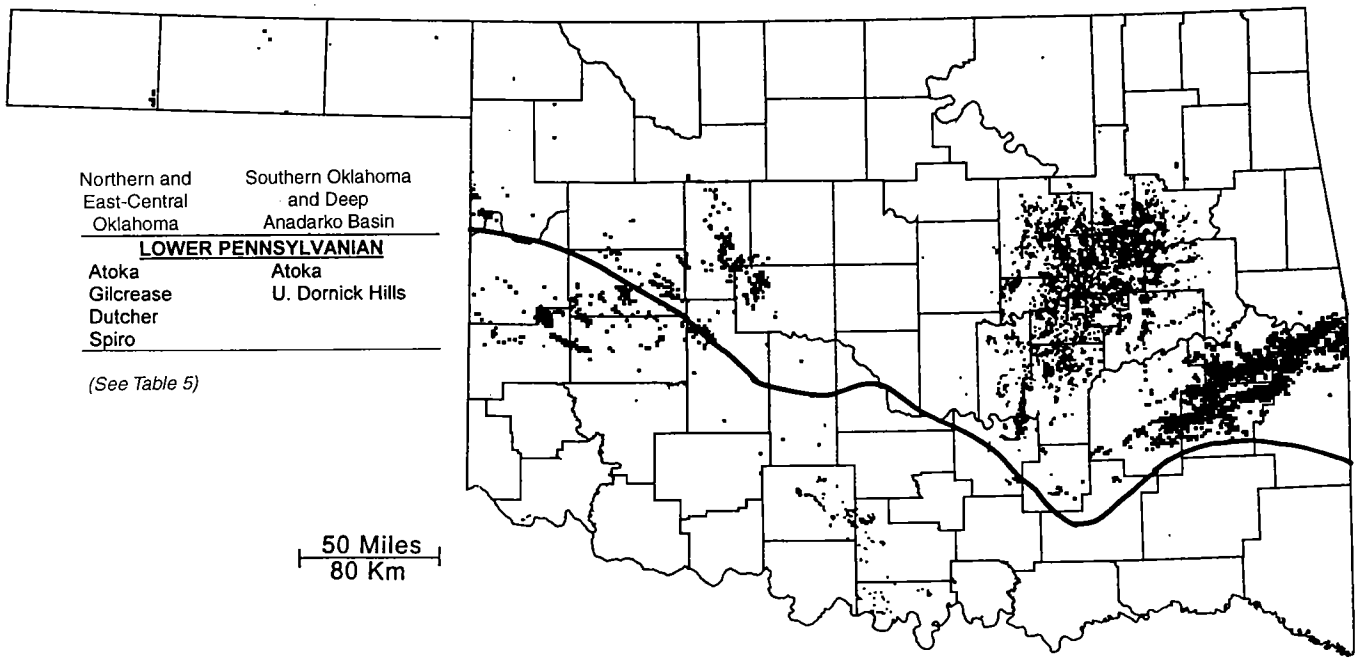

Figure 10. Oil and gas production from Lower Pennsylvanian (Atokan) marine-clastic reservoirs in Oklahoma, 1979–1996. Heavy east-west line is approximate boundary for different nomenclature used in northern and southern Oklahoma. Map generated by Geo Information Systems.

Table 6.—Names Used for Middle Pennsylvanian Marine Clastics that Produce Petroleum in Oklahoma
(see Fig. 11)

Northern and east-central Oklahoma	Southern Oklahoma and deep Anadarko basin
MIDDLE PENNSYLVANIAN	
Desmoinesian	
Marmaton Group	***Deese Group***
Boyd	Deese
Holdenville	Granite Wash Desmoinesian
Peru	Culberson
Wewoka	Deese 1st
Wetumka	Glover
Cherokee Group	***Cherokee Group***
Cherokee	Deese 2nd
Charleson	Rue
Calvin	Pharoah
Prue	Kistler
Lagonda	Gibson
Perryman	Deese 3rd
Senora	Fusulinid
Skinner	Arnold
Chelsea	Tatums
Olympic	Allen
Berry	Hart
Stuart	Deese 4th
Thurman	Pooler
Cherokee Middle	Tussy
Red Fork	Eason
Earlsboro	Osborne
Burbank	Carpenter
Bartlesville	Morris
Cherokee Lower	Hefner
Dutcher	Pickens
Boggy	Ashshalintubbie
McAlester	
Cameron	
Booch	
Tucker	
Brunner	
Taneha	
Tamaha	
Warner	
Burgess	
Hartshorne	

Cumulative Production (1/1/79 through 6/30/96)
Oil: 71,741,124 bbl
Gas: 911,846,959 Mcf

Table 7.—Names Used for Upper Pennsylvanian Marine Clastics that Produce Petroleum in Oklahoma
(see Fig. 12)

Northern and east-central Oklahoma	Southern Oklahoma and deep Anadarko basin
UPPER PENNSYLVANIAN	
Virgilian	
Wabaunsee Group	***Cisco Group***
Campbell	Cisco
Ragan	Granite Wash Pennsylvanian
Crews	Garner
Emporia	Ruel Blake
Vertz	Bateman
Garber	Coline
Vanoss	Griffin
	Rowe
Shawnee Group	Niles
Ada	Hervey
Hoover	
Carmichael	
Elgin	
Endicott	
Douglas Group	
Vamoosa	
Lovell	
Tonkawa	
Missourian	
Ochelata Group	***Hoxbar Group***
Perry	Granite Wash Missourian
Cottage Grove	Hoxbar
Mussellem	Briscoe
Hilltop	Yule-Funk
	Yule
Skiatook Group	Wade
Osage-Layton	Dyer
Pleasanton	Hedlund
Francis	Medrano
Layton	Marchand
Cleveland	Culp
Dillard	Culp-Melton
Jones	Melton
Wayside	Healdton

Cumulative Production (1/1/79 through 6/30/96)
Oil: 22,664,941 bbl
Gas: 323,089,221 Mcf

homa is shown by the cross-hatched pattern. In northwestern Oklahoma, the production is primarily from stratigraphic traps in the Hoover, Tonkawa, and Cottage Grove sands. In southern Oklahoma, the production is from stratigraphic traps in the Wade, Medrano, and Marchand sands, and from structural traps in other sands of the Cisco and Hoxbar Groups.

Cumulative production from all sands in the Upper Pennsylvanian sequence—marine and deltaic—for the period from January 1, 1979, through June 30, 1996, was 22,664,941 bbl of oil and 323,089,221 Mcf of gas.

Permian and Cretaceous

Permian strata are restricted to the western half of Oklahoma. Clastics were eroded from the Ouachitas (reduced to low mountains by this time) on the east, the ancestral Rocky Mountains on the west, and the Wichita uplift in southwestern Oklahoma. Lower Permian (Wolfcampian) carbonates and shales—both gray and red beds—are overlain by a major evaporite and red-bed sequence of Leonardian, Guadalupian, and Ochoan age. Evaporites (salt and gypsum /anhydrite)

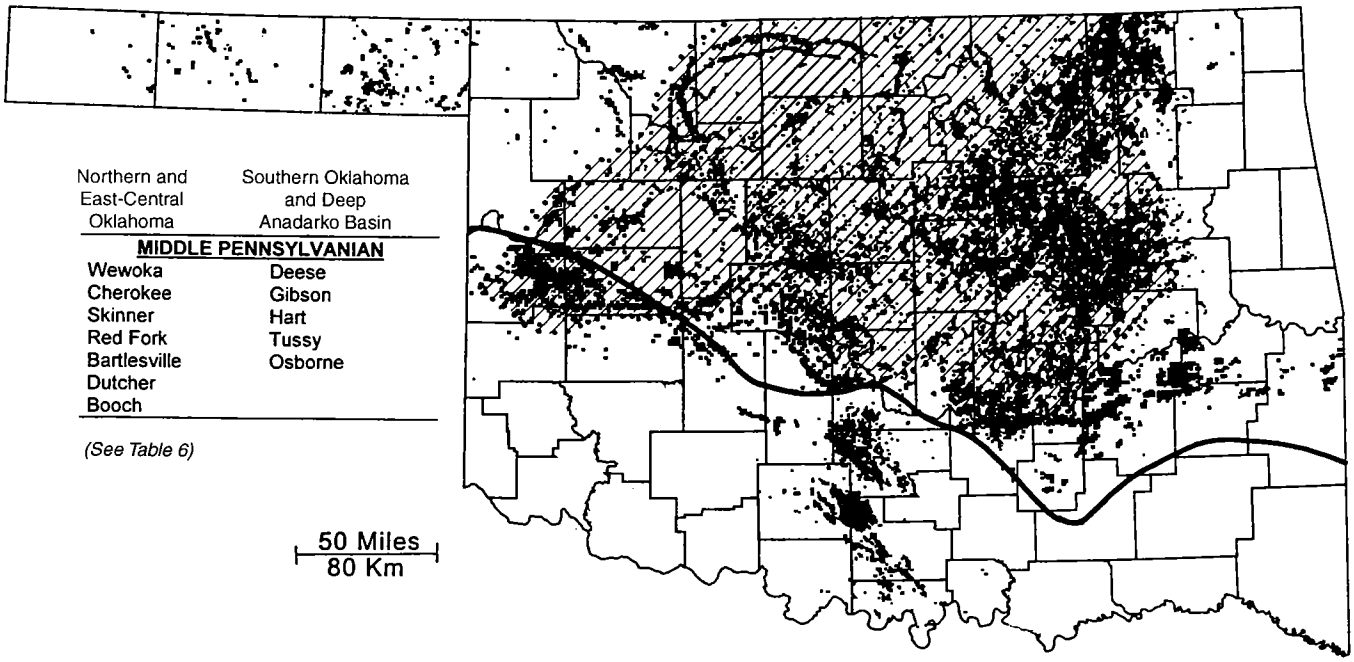

Figure 11. Oil and gas production from Middle Pennsylvanian (Desmoinesian) marine-clastic reservoirs in Oklahoma, 1979–1996. Heavy east-west line is approximate boundary for different nomenclature used in northern and southern Oklahoma. Crosshatched area denotes areas of Desmoinesian deltaic reservoirs. Map generated by Geo Information Systems.

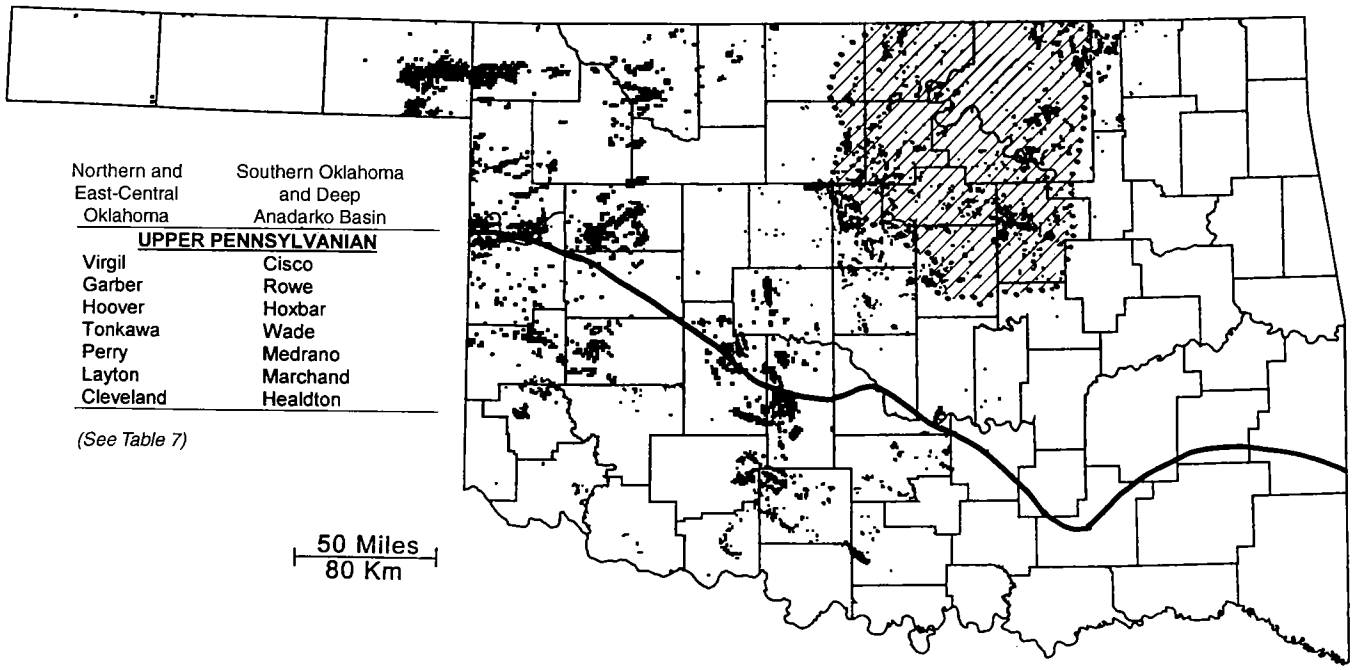

Figure 12. Oil and gas production from Upper Pennsylvanian marine-clastic reservoirs in Oklahoma, 1979–1996. Heavy east-west line is approximate boundary for different nomenclature used in northern and southern Oklahoma. Crosshatched area in east-central Oklahoma denotes area of Upper Pennsylvanian deltaic reservoirs. Map generated by Geo Information Systems.

thicken into the basins that continued to subside more than the adjacent uplifts and arches (Fig. 5). Permian marine sandstones (and "granite wash") were deposited mainly around the Wichita Mountain uplift and nearby parts of the Anadarko and Hollis basins; they also were deposited in shelf areas of north-central Oklahoma. Permian strata are as much as 7,000 ft thick in the Anadarko basin, 4,000 ft thick in the Hollis basin, and 1,000–3,000 ft thick in nearby shelf or platform areas (McKee and others, 1967; Johnson and others, 1988).

Table 8.—Names Used for Permian and Cretaceous Marine Clastics that Produce Petroleum in Oklahoma
(see Fig. 13)

Northern and east-central Oklahoma	Southern Oklahoma and deep Anadarko basin
CRETACEOUS	
	Trinity
	Paluxy
	Arbuckle sand
	Bilbo
PERMIAN	
	Granite Wash Permian
Leonardian	
Garber	
Wolfcampian	
	Pontotoc Group
Hoy	Pontotoc
Hotson	Nichols
Belveal	Ramsey
	Fortuna
	Noble-Olson

Cumulative Production (1/1/79 through 6/30/96)
Oil: 18,741,182 bbl
Gas: 332,352,616 Mcf

Lower and Upper Cretaceous shales, sandstones, and limestones are present in southeast, south-central, and westernmost Oklahoma. The Cretaceous seaway extended across most of southern and western Oklahoma during the last great marine inundation of the Western Interior of the United States. Cretaceous strata in southern Oklahoma are part of the Gulf Coastal Plain; they are a series of transgressive marine deposits that interfinger with alluvial and deltaic sediments to the north.

Names of marine clastics of the Permian and Cretaceous that produce oil and/or gas in Oklahoma are listed in Table 8. Oil and gas production by lease for the Permian and Cretaceous sequence is shown in Figure 13. Producing Permian marine clastics occur in both north-central and southern Oklahoma, whereas producing Cretaceous marine(?) clastics occur only in southern Oklahoma.

In northern and southern Oklahoma, Permian clastics produce on structural traps in fields where the source of the hydrocarbons is thought to be from vertical migration through fractures and faults from deeper and older reservoirs. Oil and gas production from Cretaceous strata occurs only in Marshall and McCurtain Counties of southeast Oklahoma (shown by the "K" on Fig. 13). The oil in these reservoirs is minor in quantity and is also considered to have leaked from deeper reservoirs below the Cretaceous.

During the period from January 1, 1979, through

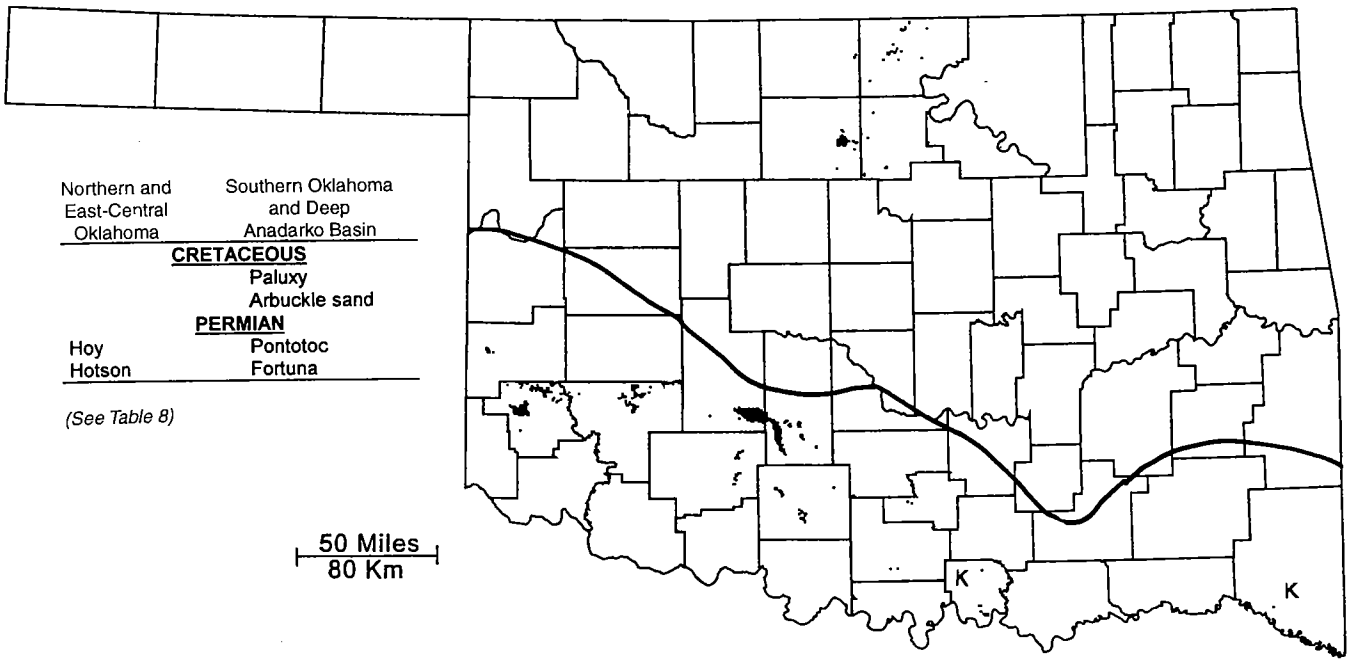

Figure 13. Oil and gas production from Permian and Cretaceous marine-clastic reservoirs in Oklahoma, 1979–1996. Heavy east-west line is approximate boundary for different nomenclature used in northern and southern Oklahoma. Two fields in southeastern Oklahoma with production from Cretaceous reservoirs annotated with letter "K." Map generated by Geo Information Systems.

June 30, 1996, oil and gas reservoirs in the Permian and Cretaceous sequence produced 18,741,182 bbl of oil and 332, 352,616 Mcf of gas. By far the greater amount of this production was from the Permian fields of southern Oklahoma.

SUMMARY

Oklahoma's marine clastics yield large amounts of oil and gas in most parts of the state. The geologic history of reservoir development and petroleum entrapment in these rocks encompasses many depositional, diagenetic, orogenic, and tectonic environments. Significant discoveries continue to be made throughout most of the Paleozoic sequence of marine clastics. As a result, Oklahoma remains a fertile field for explorationists, developers, and operators seeking optimization of producing properties. Cumulative production for all clastic units described in this report is 864 million bbl of oil and 12 trillion cf of gas from 1979 through June of 1996.

REFERENCES CITED

Amsden, T. W., 1975, Hunton Group (Late Ordovician, Silurian, and Early Devonian) in the Anadarko basin of Oklahoma: Oklahoma Geological Survey Bulletin 121, 214 p.

_____ 1980, Hunton Group (Late Ordovician, Silurian, and Early Devonian) in the Arkoma basin of Oklahoma: Oklahoma Geological Survey Bulletin 129, 136 p.

Brown, R. L.; and Northcutt, R. A., 1993, Springer marine sandstone—Anadarko basin, *in* Bebout, D. G.; White, W. A.; Hentz, T. F.; and Grasmick, M. K. (eds.), Atlas of major Midcontinent gas reservoirs: Texas Bureau of Economic Geology, p. 53–54.

Craig, L. C.; and others, 1979, Paleotectonic investigations of the Mississippian System in the United States: U.S. Geological Survey Professional Paper 1010, part I, p. 1–369; part II, 371–559; part III, 15 plates.

Denison, R. E.; Lidiak, E. G.; Bickford, M. E.; and Kisvarsanyi, E. B., 1984, Geology and geochronology of Precambrian rocks in the central interior region of the United States: U.S. Geological Survey Professional Paper 1241-C, 20 p.

Ham, W. E.; and Wilson, J. L., 1967, Paleozoic epeirogeny and orogeny in the central United States: American Journal of Science, v. 265, p. 332–407.

Hills, J. M.; and Kottlowski, F. E. (coordinators), 1983, Correlation of stratigraphic units in North America—Southwest/southwest Mid-Continent correlation chart: American Association of Petroleum Geologists, Tulsa, Oklahoma.

Johnson, K. S. (ed.), 1997, Simpson and Viola Groups in the southern Midcontinent, 1994 symposium: Oklahoma Geological Survey Circular 99, 275 p.

Johnson, K. S.; and Cardott, B. J., 1992, Geologic framework and hydrocarbon source rocks of Oklahoma, *in* Johnson, K. S.; and Cardott, B. J. (eds.), Source rocks in the southern Midcontinent, 1990 symposium: Oklahoma Geological Survey Circular 93, p. 21–37.

Johnson, K. S.; Amsden, T. W.; Denison, R. E.; Dutton, S. P.; Goldstein, A. G.; Rascoe, B., Jr.; Sutherland, P. K.; and Thompson, C. M., 1988, Southern Midcontinent region, *in* Sloss, L. L. (ed.), Sedimentary cover—North American craton; U.S.: Geological Society of America, The Geology of North America, v. D-2, p. 307–359. [Reprinted in 1989 as Oklahoma Geological Survey Special Publication 89-2, 53 p.]

Mankin, C. J. (coordinator), 1987, Correlation of stratigraphic units in North America—Texas-Oklahoma tectonic region correlation chart: American Association of Petroleum Geologists, Tulsa, Oklahoma.

McBee, William, Jr., 1995, Tectonic and stratigraphic synthesis of events in the region of the intersection of the Arbuckle and Ouachita structural systems, Oklahoma, *in* Johnson, K. S. (ed.), Structural styles in the southern Midcontinent, 1992 symposium: Oklahoma Geological Survey Circular 97, p. 45–81.

McKee, E. D.; and others, 1967, Paleotectonic maps of the Permian System: U.S. Geological Survey Miscellaneous Geologic Investigations Map I-450, scale 1:5,000,000.

_____ 1975, Paleotectonic investigations of the Pennsylvanian System in the United States: U.S. Geological Survey Professional Paper 853, part I, 349 p.; part II, 192 p.; part III, 17 plates.

Rascoe, B., Jr.; and Adler, F. J., 1983, Permo–Carboniferous hydrocarbon accumulations, Mid-Continent, U.S.A.; American Association of Petroleum Geologists Bulletin, v. 67, p. 979–1001.

Schramm, M. W., Jr., 1964, Paleogeologic and quantitative lithofacies analysis, Simpson Group, Oklahoma: American Association of Petroleum Geologists Bulletin, v. 48, p. 1164–1195.

Suhm, R. W., 1997, Simpson stratigraphy of the southern Midcontinent, *in* Johnson, K. S. (ed.), Simpson and Viola Groups in the southern Midcontinent, 1994 symposium: Oklahoma Geological Survey Circular 99, p. 3–38.

Sutherland, P. K., 1988, Late Mississippian and Pennsylvanian depositional history in the Arkoma basin area, Oklahoma and Arkansas: Geological Society of America Bulletin, v. 100, p. 1787–1802.

Tomlinson, C. W.; and McBee, W., Jr., 1959, Pennsylvanian sediments and orogenies of Ardmore district, Oklahoma, *in* Petroleum geology of southern Oklahoma: American Association of Petroleum Geologists, Tulsa, Oklahoma, v. 2, p. 3–52.

Sediment Transport around Islands, Ancient and Modern: Examples from the West Coast of Scotland and Southwestern Oklahoma

R. Nowell Donovan
Texas Christian University
Fort Worth, Texas

ABSTRACT.—The island of Iona, which lies off the western coast of Scotland, is built of Precambrian metamorphic rocks and is surrounded by an apron of bioclastic carbonate sands, with only about 20% siliciclastic grains. By contrast, quartz-feldspar sands with only about 4% shell debris mantle the adjacent granite shoreline of the nearby island of Mull. The two islands are separated by the Sound of Mull, a strip of water only ~0.5 mi (0.8 km) wide. Within the Sound, large—up to 400-yd (~400 m) long—transverse sand bars are kept more or less stationary by the balance of ebb and flood macrotides. The setting is a partial modern analog for the Late Cambrian southern Oklahoma archipelago in that it demonstrates partitioning of sediment—i.e., variable sediment contributions from different islands and the development of distinctive facies in localized settings.

INTRODUCTION

Rocky marine shorelines are rarely preserved in the geological record; even more rarely are they well exposed. In general, most major marine unconformities are planar surfaces. Rocky, island girt shorelines characterized by irregular relief generally involve rocks that are resistant to weathering, such as acidic igneous, high-grade metamorphic rocks, and (particularly in drier climates) limestones (e.g., George, 1970; Bucheit and Donovan, 1999, 2000). Preservation of this relief generally seems to involve rapid rates of subsidence (perhaps with contemporaneous fault activity), or rapid transgression, or some combination of the two. This paper describes a modern island setting—the island of Iona, off the western coast of Scotland—and draws some parallels to the Late Cambrian southern Oklahoma archipelago.

THE SOUTHERN OKLAHOMA ARCHIPELAGO

The major Late Cambrian (Franconian) transgression across the southern part of the Laurentian craton resulted in the inundation of a hilly landscape. Substantial remnants of this landscape are exposed in the St. Francis Mountains, the Arbuckles, and in the subsurface in northeastern Oklahoma (the "Tulsa Mountains"). However, the most informative outcrops are found in the Slick Hills of southwestern Oklahoma where precise contacts between sedimentary cover and basement (the Carlton Rhyolite Group) are well exposed (Donovan, 1986, 2000). In general six specific islands have been identified in the southern Oklahoma archipelago along a linear outcrop of approximately 15 mi (~39 km). Maximum relief on the unconformity is about 1,000 ft (~330 m). Detailed facies patterns have been tied to various settings between and around these islands; these patterns are superimposed on a general stratigraphic framework that records the following: (1) an upward passage from siliciclastic to carbonate sedimentation; (2) an upward decrease in the size or power of tidal currents; and (3) an upward decrease in the contribution of the local basement to the overlying sedimentary rocks.

These changes are reflected in the formal stratigraphic divisions of the Upper Cambrian into the basal, siliciclastic Reagan Formation and the overlying mixed carbonate/siliciclastic Honey Creek Formation, the two units comprising the Timbered Hills Group (McElmoyl and Donovan, 2000; Donovan, 2000).

Among the complexities of island-tied facies are: (1) the control of sand distribution by island geometries, resulting in the development of small tidally molded lenticular sandstones in high-energy shallow marine settings; (2) variability in paleocurrents; (3) the preservation of leeward and windward facies in both siliciclastic and carbonate sediments; and (4) a very small contribution of rhyolite fragments to carbonate facies, even at the more exposed island sites.

IONA

Iona is a small island, approximately 3.5 mi (5.6 km) long and 1.5 mi (2.4 km) broad. It is part of the Inner Hebrides, a chain of islands of varied geology that

Donovan, R. N., 2000, Sediment transport around islands, ancient and modern: examples from the west coast of Scotland and southwestern Oklahoma, *in* Johnson, K. S. (ed.), Marine clastics in the southern Midcontinent, 1997 symposium: Oklahoma Geological Survey Circular 103, p. 19–23.

extends along most of the west coast of Scotland. Iona is built of Precambrian rocks that form part of the foreland of the Caledonian orogenic belt. These rocks comprise an Archaean suite of complex gneisses (the Lewisian Group), which form most of the island, and upper Proterozoic siliciclastics (the Torridonian Group), which form a narrow strip along the east coast (Fig. 1). The island was heavily glaciated during the Pleistocene. Consequently, a thin veneer of till covers some low-lying areas. Glacial rebound has led to the erosion of three levels of raised beach, but sea level has been relatively stable for the past 7,000 years (Boulton and others, 1991).

Iona is separated from the adjacent large island of Mull by the 0.5 mi (0.8 km) wide Sound of Iona, a shallow marine channel that marks the trace of a major fault complex. The adjacent part of Mull is built of the Ross of Mull granite, a small funnel-shaped batholith that was probably intruded along the line of faulting. Iona faces the Atlantic Ocean and is subject to major weather systems arriving from the southwest. Much longshore-current transport is to the north, although this direction may be reversed during winter months when storms move south from the Arctic. The island is in a macrotidal zone. Tidal currents—both ebb and flood—are powerful in the constraining Sound.

BEACH SEDIMENTS ON IONA AND MULL

I assessed modern sediment patterns on either side of the Sound of Iona by collecting samples on several beaches, examining air photographs, and talking with local seamen. For the most part, Iona is a rock-girt island; only ~37.5% of the island's coastline is fronted by beaches. Most of these are pocket beaches, although more extensive sand strands occur around the north of the island and in the Bay at the Back of the Ocean. Rather more sand, >70%, mantles the opposing coastline of Mull.

Sediment on the beaches of Iona has three sources: (1) from glacial till, (2) from the local Precambrian rocks, and (3) from carbonate organisms.

Erosion of the glacial till has yielded large numbers of pebbles and boulders of diverse lithologies. Beaches made of these pebbles are most common on the south and west coasts of the island—e.g., at the Bay at the Back of the Ocean. Elsewhere, glacial erratics are common on both Iona and Mull. The local Precambrian rocks yield pebbles and quartz-feldspar-rock fragments; however, they make a surprisingly small contribution to the Iona beaches.

In fact most, about 80%, of the sand found on the beaches of Iona is of bioclastic origin; it records the shoreline activity of a remarkably extensive, temperate carbonate factory that extends along much of the exposed west coastline of the Western Highlands of Scotland (see, for example, Farrow and others, 1978; Farrow and others, 1979; Farrow, 1983). The most common constituents of the shoreline sands are angular fragments of a great variety of mollusks and barnacles, with lesser amounts of gastropods, echinoids, serpulids, and (sparsely) red algae. This sand is produced in such quantities that it forms substantial eolian dunes at the Bay at the Back of the Ocean and around the north end of the island. On many parts of the coastline, it seems likely that the relatively small contribution of sediment from the local Precambrian is due (at least in part) to the overwhelming abundance of this shell debris, which is of little abrasive significance and thus significantly retards erosion.

The composition of sand from Iona beaches stands in marked contrast to that found on beaches on the Ross of Mull (Fig. 2). There, most (~96%) of the grains are well-rounded siliciclastics, dominantly quartz but with substantial amounts of feldspar (both plagioclase and orthoclase) and rock fragments. The most likely source of these grains is from weathering of the Ross of Mull granite. The small percentage of carbonate fragments consists of well-rounded grains.

Clearly, the Sound of Iona effectively partitions the beach sands of the opposing islands. As noted, powerful tidal currents sweep the Sound. These currents have produced large transverse sand waves, up to 400 yd (~440 m) in length, that rise to within a few feet of the surface. They are composed partly of gravel made of fragments of the red alga *Lithothamnion*. Although individual storms may modify the shape of these sand waves (Pal Grant, 1996, personal communication), they are a persistent feature of the central part of the Sound, as is shown by a radiocarbon date of 3,893 ± 70 yr B.P. for a *Lithothamnion* grain collected from the surface of one of the sand waves (Farrow, 1983).

DISCUSSION

It is clear that there are limits to uniformitarian analogy in comparing modern Iona to Oklahoma in the Late Cambrian. The latitudinal position of the two areas differs; 500 million years ago, Oklahoma lay ~20° south of the equator on the southwestern side of the Laurentian craton (Donovan, 2000). Given constancy of meteorological patterns through time, the area probably would have been on the leeward side of the continent and subject to a seasonal climate with southeast trade winds. In contrast, Iona lies on the windward side of a continent in temperate stormy latitudes subject to strong westerly gales. Also, the fauna of the two areas can be compared only in the most general of terms.

In spite of these differences, some useful parallels can be drawn. For example, the stable sand bodies within the Sound of Iona can be translated by analogy into the lenticular cross-bedded sandstones that are a characteristic feature of the Reagan Formation. These sandstones are typically of small scale and display bimodal cross beds (Donovan, 1986, 2000). They are discrete and difficult to relate to overall facies trends within the Reagan and may well be records of sediment accumulation localized by tidal currents between islands of the southern Oklahoma archipelago. Subtle variations in the orientation of cross-beds between these sandstones may reflect local deviation of tidal currents such as occurs in the Sound of Iona.

Variations in the efficiency of longshore-transport

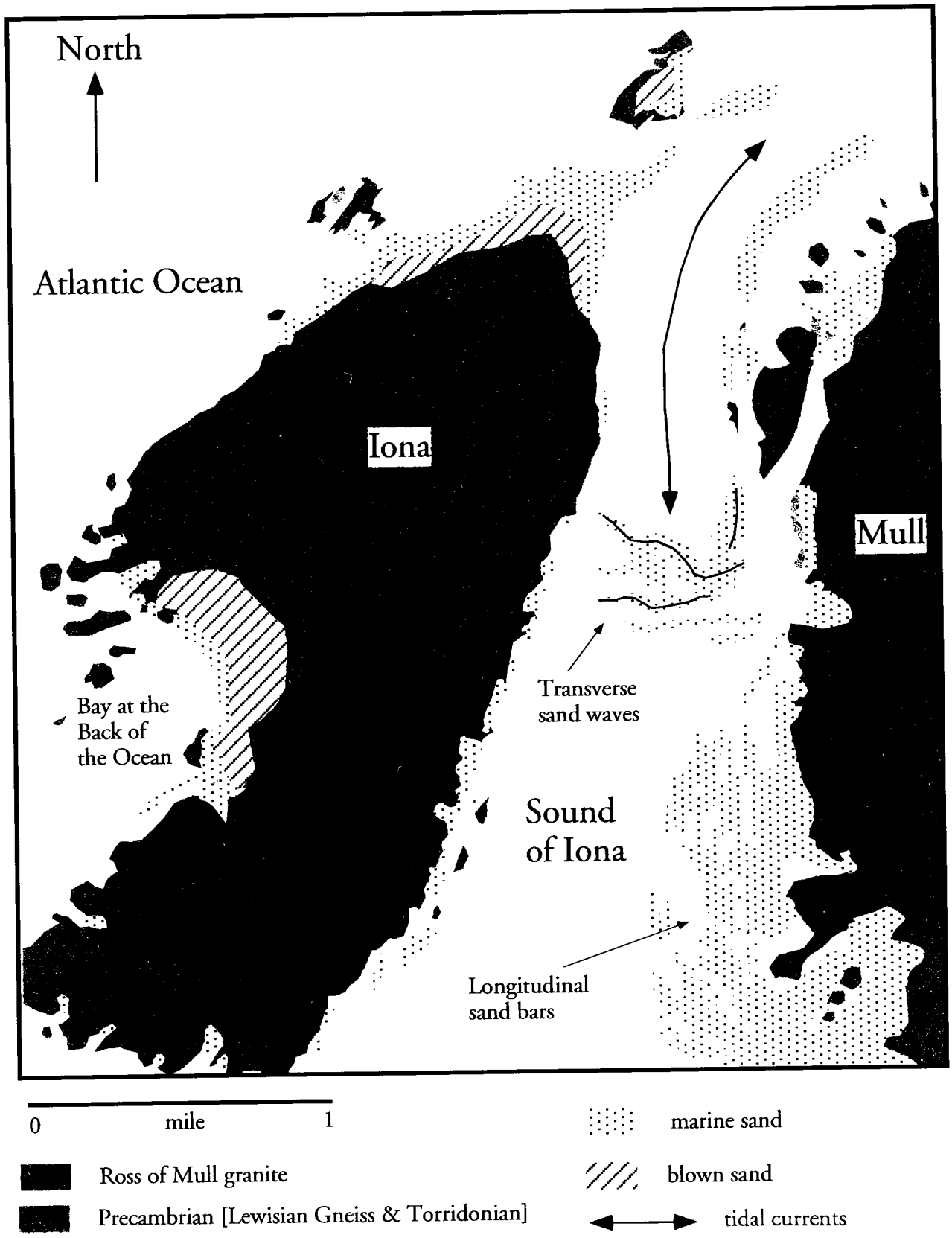

Figure 1. Map of the Iona area, Scotland, showing basic geology, principal beaches, tidal currents, and principal areas of mobile, shallow-marine sand.

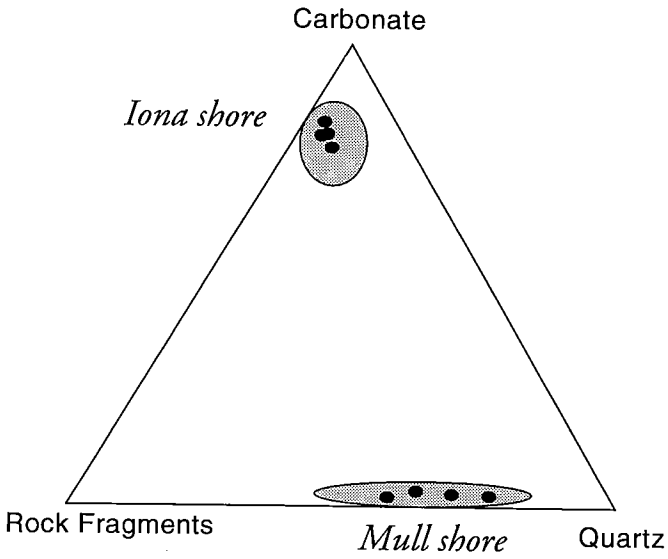

Figure 2. Triangular diagram contrasting the composition of shoreline sands from opposing coasts on the Sound of Iona.

mechanisms, apparent around the coastline of Iona, can be demonstrated in both general and specific detail in southern Oklahoma. For example, leeward and windward facies have been recognized at several island sites (Donovan and others, 1986; Donovan and others, 2000; Szabo and Donovan, 1999), and a detailed example of facies partitioning that extends through approximately 40 ft (~12 m) of the upper part of the Honey Creek Formation has been described by Bellamy and others (2000). In this example partitioning is detectable as (1) variations in the relative proportions and type of carbonate and siliciclastic grains; (2) variations in the petrography of the beds that overly the upper/lower Honey Creek hiatus; and (3) interruption of the meter-scale siliciclastic/carbonate cyclicity that is a persistent feature of the Honey Creek. The principal conclusion of that study was that islands in the archipelago "sheltered" leeward areas from influxes of siliciclastic grain populations that were blown off the Laurentian craton and subsequently reworked as marine shoreline sands. Variations in sea level superimposed cyclicity on this relationship.

Another feature of the Iona shoreline is the degree to which solid rock exposures are mantled by carbonate sands, thus undergo reduced erosion, and contribute little material to beach sediments. A similar mantling occurred at island sites in Oklahoma; a particularly good example of rock pedestals completely enveloped by carbonate sands is exposed in Blue Creek Canyon (Donovan and others, 1986). Where rhyolite pebbles are encountered in the Honey Creek Formation, they are generally angular or subangular. By contrast, rhyolite pebbles in the Reagan Formation generally are round to well rounded. To some extent, this difference in angularity probably reflects the cushioning of rhyolite pebbles by soft carbonate grains.

Carbonate sediments in both areas consist of mobile grains, varying in size from very fine sand to gravel, and mud content in both areas is low to nonexistent. In this respect, the Iona area is a typical temperate-water carbonate assemblage. The Honey Creek fauna was dominated by pelmatozoans, trilobites, and brachiopods and, as noted, was adapted to a high-amplitude tidal environment (Donovan, 2000). As a result, the dominant bed forms in both areas are varieties of crossbeds that record the migration of subaqueous sand dunes; and there is evidence in both areas of high energy in fauna (Farrow and others, 1979; Farrow, 1983; Donovan, 1986, 2000). This is a marked contrast to the mud-dominated facies that are characteristic of both modern tropical carbonate platforms and the Cambro–Ordovician platform on which the Arbuckle Group was deposited. The base of the Arbuckle Group records the initiation of an expansive microtidal platform and the conclusion of the tidally dominated conditions recorded by the Timbered Hills Group.

ACKNOWLEDGMENTS

Pal Grant of Iona provided valuable information on sediment movement in the Sound of Iona. The Kimbell family and Tommy Cavanagh are acknowledged for their continuing interest in the ongoing study of the geology of the Kimbell Ranch. The Moncrief Endowment supported this study.

REFERENCES CITED

Bellamy, J. B.; Denny, D. P.; Donovan, Matt; Donovan, R. N.; Pancake, Jim; and Sonnestine, Kevin, 2000, Sediment partitioning in the late Cambrian southern Oklahoma archipelago: Geological Society of America Abstracts with Programs, v. 32, no. 3, p. A-3.

Boulton, G. S.; Peacock, J. D.; and Sutherland, D. G., 1991, Quaternary, *in* Craig, G. Y. (ed.), Geology of Scotland (3rd edition): Geological Society of London, p. 503–543.

Bucheit, A. K.; and Donovan, R. N., 1999, Lower Jurassic borings and fissures: a rocky shoreline composed of Cambro–Ordovician limestone, Isle of Skye, Scotland: The Compass, Journal of Earth Sciences, Sigma Gamma Epsilon, v. 74, no. 2, p. 47–54.

_____ 2000, Initiation of a carbonate platform: a comparison between the Lower Jurassic Broadford Limestone, Isle of Skye, Scotland, and the Cambrian Honey Creek Limestone, Slick Hills, Oklahoma, *in* Johnson, K. S. (ed.), Platform carbonates in the southern Midcontinent, 1996 symposium: Oklahoma Geological Survey Circular 101, p. 57–64.

Donovan, R. N., 1986, The geology of the Slick Hills, *in* Donovan, R. N. (ed.), The Slick Hills of southwestern Oklahoma—fragments of an aulacogen?: Oklahoma Geological Survey Guidebook 24, p. 1–12.

_____ 2000, Initiation of the Arbuckle platform—view from the Slick Hills, Oklahoma, *in* Johnson, K. S. (ed.), Platform carbonates in the southern Midcontinent, 1996 symposium: Oklahoma Geological Survey Circular 101, p. 47–56.

Donovan, R. N.; and Bucheit, A. K., 2000, Marine facies and islands in the Reagan Sandstone (Upper Cambrian) in the Slick Hills, southwestern Oklahoma, *in* Johnson, K. S. (ed.), Marine clastics in the southern Midcontinent, 1997 symposium: Oklahoma Geological Survey Circular 103 [this volume], p. 25–37.

Donovan, R. N.; Beauchamp,, W.; Collins, K.; McConnell, D.; Rafalowski, M. B.; Ragland, D. A.; Sanderson, D. J.; and Tsegay, T., 1986, Geological highlights of the Blue Creek Canyon area, *in* Donovan, R. N. (ed.), The Slick Hills of southwestern Oklahoma—fragments of an aulacogen?: Oklahoma Geological Survey Guidebook 24, p. 84–91.

Donovan, R. N.; Ayan, Danielle; and Bucheit, A. K., 2000, Marine facies transitions in the Late Cambrian; the upper member of the Timbered Hills Group, Bally Mountain, Slick Hills, southwestern Oklahoma, *in* Johnson, K. S. (ed.), Marine clastics in the southern Midcontinent, 1997 symposium: Oklahoma Geological Survey Circular 103 [this volume], p. 39–50.

Farrow, G. E., 1983, Recent sediments and sedimentation in the Inner Hebrides, *in* Morton, J. M.; and Boyd, D. R. (eds.), The natural environment of the Inner Hebrides: Proceedings of the Royal Society of Edinburgh, v. 83B, p. 91–105.

Farrow, G.; Cucci, M.; and Scoffin, T., 1978, Calcareous sediments on the nearshore continental shelf of western Scotland: Proceedings of the Royal Society of Edinburgh, v. 76B, p. 55–76.

Farrow, G.; Scoffin, T.; Brown, B.; and Cucci, M., 1979, An underwater television survey of facies variation on the inner Scottish shelf between Colonsay, Islay, and Jura: Scottish Journal of Geology, v. 15, p. 13–29.

George, N. T., 1970, British regional geology: South Wales (3rd edition): Her Majesty's Stationery Office, London, 152 p.

McElmoyl, Courtney; and Donovan, R. N., 2000, Unconformity in the lower part of the Cambrian Honey Creek Limestone, Slick Hills, Oklahoma: candidate for a Grand Cycle boundary, *in* Johnson, K. S. (ed.), Platform carbonates in the southern Midcontinent, 1996 symposium: Oklahoma Geological Survey Circular 101, p. 65–78.

Szabo, S.; and Donovan, R. N., 1999, Iron-fixing stromatolites and pelmatozoans: ecological confrontation on a rocky Late Cambrian shoreline in southern Oklahoma: Geological Society of America Abstracts with Programs, v. 31, no. 1, p. A-35.

Marine Facies and Islands in the Reagan Formation (Upper Cambrian) in the Slick Hills, Southwestern Oklahoma

R. Nowell Donovan and Andrea K. Bucheit
Texas Christian University
Fort Worth, Texas

ABSTRACT.—A major transgression took place across the Laurentian (proto–North American) craton during the Late Cambrian. The record of this transgression in Oklahoma is preserved in the Timbered Hills Group (comprising the basal Reagan and overlying Honey Creek Formations) and the Arbuckle Group (specifically the lowermost Fort Sill Formation). The apparently straightforward model of Franconian transgression is complicated by occurrence of two major craton-wide regressions and an increasing tectonic response to the developing lower Paleozoic aulacogen. The first phase of this transgression, up to the earlier of the two major regressions—dated to the *Elvinia trilobite* zone of the Franconian—involves the Reagan Formation and the lowermost part of the Honey Creek Formation.

The transgressed land surface, formed by the Cambrian Carlton Rhyolite in the Slick Hills of southwestern Oklahoma, had a relief of several hundred feet. Initial deposits of alluvium filled in the low spots of the topography. As the transgression proceeded, topographic highs evolved into islands and siliciclastics were deposited as tidally influenced sand bars and heterolithics. The sand bars were molded by northwest to southeast currents; in general, current movement to the southeast—the ebb-tide direction—was dominant. The petrography of these sandstones is complex, involving quartz of cratonic origin, locally derived rhyolite clasts, and glauconite, ferruginous ooids, phosphate nodules, and shells, all of the latter of which formed in the depositional setting. Eventually, carbonate sandstones, derived from "production centers" associated with individual islands, mixed with siliciclastics, thus marking the base of the Honey Creek Formation. Both the siliciclastic and carbonate sequences are iron rich. This richness is manifest in several ways—as hematite cements, ferruginous ooids, glauconite, ankerite, pyrite, iron-rich illite, and ferroan-dolomite–calcite cements.

Individual islands in the southern Oklahoma archipelago partitioned tidal to estuarine siliciclastics and also supplied sheets of rhyolite-pebble conglomerate. This paper examines the Reagan Formation at two such islands.

INTRODUCTION

The purpose of this paper is to examine the Reagan Formation adjacent to two Late Cambrian islands in the Slick Hills of southwestern Oklahoma to determine effects of topography on sedimentation during a major marine transgression. The Slick Hills are located within Kiowa, Caddo, and Comanche Counties near the southwest corner of Oklahoma. They consist mainly of folded and fractured Cambrian–Ordovician limestones (with lesser amounts of siliciclastics) that rest unconformably atop the rhyolites of the Cambrian Carlton Group (Fig. 1). Since the Cambrian, the Laurentian craton has rotated approximately 70° counterclockwise from an equatorial position. "Oklahoma" lay about 15°–20° south of the equator during the Late Cambrian on the leeward side of the continent relative to major meteorologic systems. The two "island sites" analyzed in this study form part of the southern Oklahoma archipelago (Donovan, 1986, 2000b). One of these sites is located in the Bally Mountain range ("Bally Island"), the other lies near Ring Top Mountain in the eastern Slick Hills ("Ring Top Island") (Fig. 2).

The rocks of the Slick Hills were deposited in the southern Oklahoma aulacogen, the initial development of which, from the Precambrian to the Middle Cambrian, involved the extrusion and intrusion of a bimodal igneous suite of ultrabasic, basic, and acidic rocks. This igneous activity left the surface covered with a thick series of Cambrian rhyolites assigned to the Carlton Group (Ham and others, 1964). Tension faults facilitated the lava flows and helped to define the trend

Donovan, R. N.; and Bucheit, A. K., 2000, Marine facies and islands in the Reagan Formation (Upper Cambrian) in the Slick Hills, southwestern Oklahoma, *in* Johnson, K. S. (ed.), Marine clastics in the southern Midcontinent, 1997 symposium: Oklahoma Geological Survey Circular 103, p. 25–37.

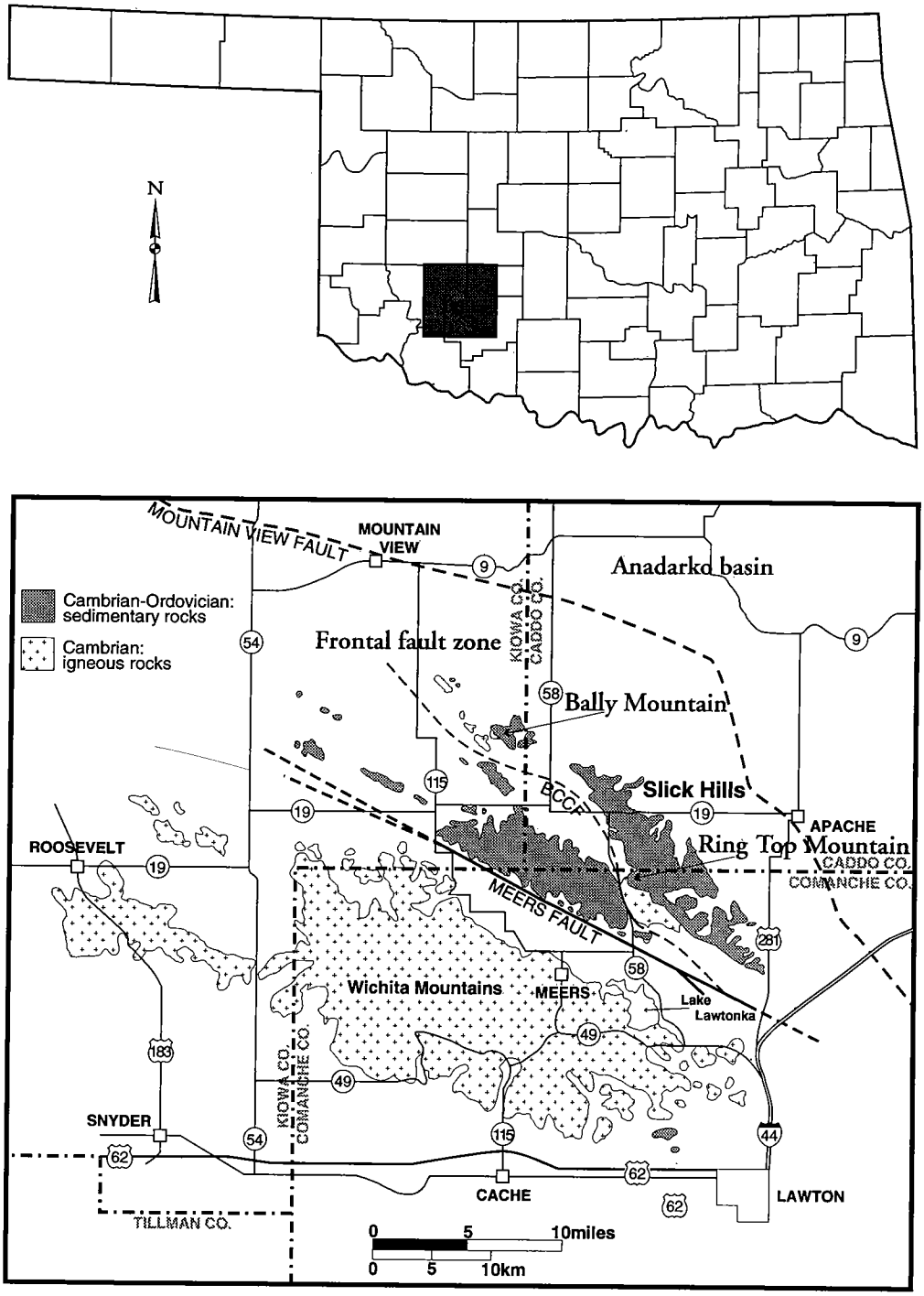

Figure 1. The location of Bally Mountain in the Slick Hills in southwestern Oklahoma.

of the aulacogen (N60°W); the basin extends laterally from southeastern Oklahoma into the Texas Panhandle. Following the igneous activity, a long period of crustal cooling, topographic contraction, and erosion ensued prior to a major Late Cambrian marine transgression across the entire continent.

A second stage of aulacogen definition during the early parts of the Paleozoic was marked by accelerating subsidence beneath siliciclastic and carbonate sequences deposited in this transgressive setting. These sequences are the Timbered Hills, Arbuckle, Simpson, and Viola Groups. The maximum rate of subsidence during this second stage coincided with deposition of the Signal Mountain Formation, the second oldest of the formations in the Arbuckle Group (Feinstein, 1981; Hosey and Donovan, 2000). Definition of the aulacogen during this stage is reflected in sediment isopachs that indicate thicknesses three to four times greater within the aulacogen than on the adjacent craton (Johnson and others, 1989).

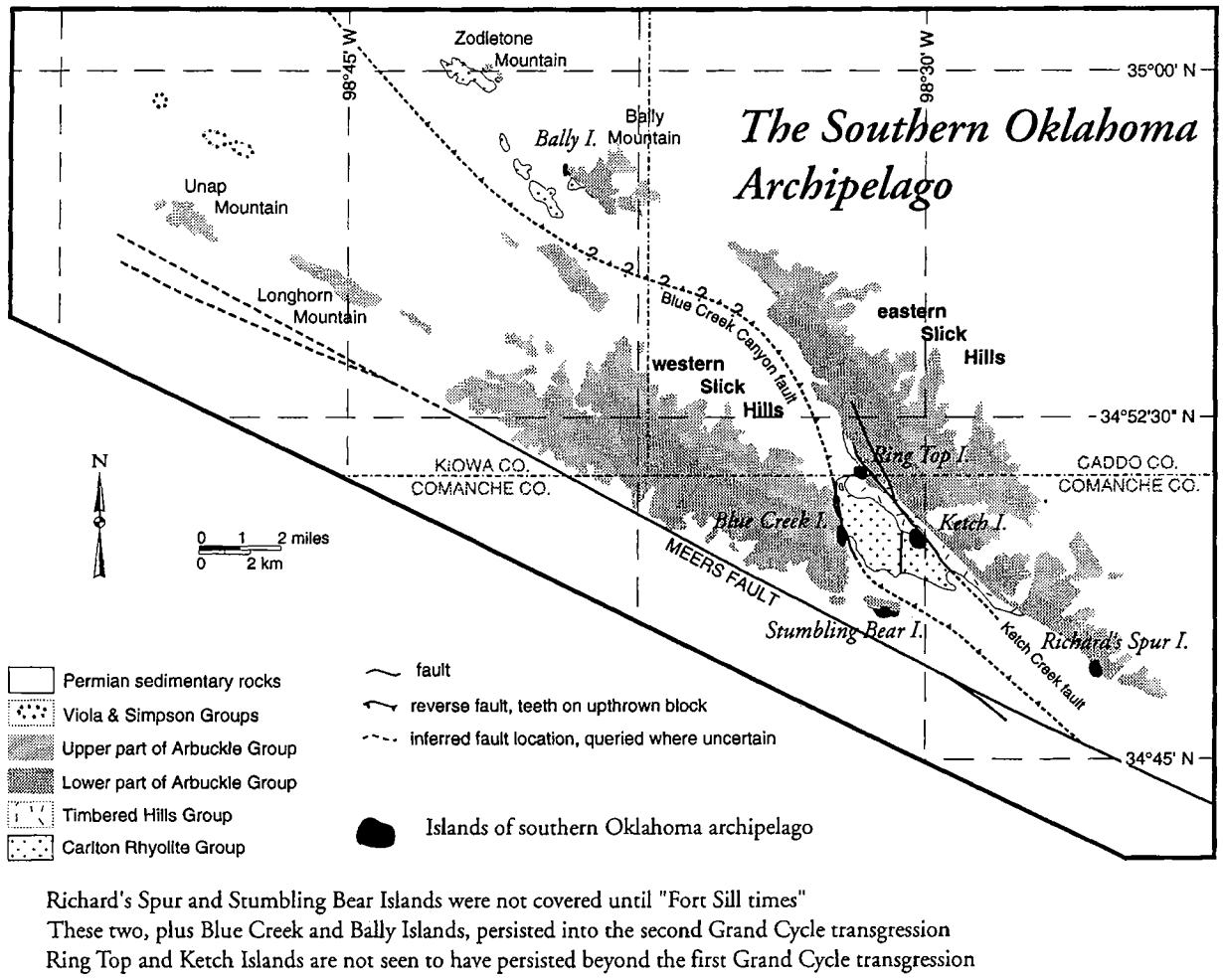

Richard's Spur and Stumbling Bear Islands were not covered until "Fort Sill times"
These two, plus Blue Creek and Bally Islands, persisted into the second Grand Cycle transgression
Ring Top and Ketch Islands are not seen to have persisted beyond the first Grand Cycle transgression

Figure 2. The islands of the southern Oklahoma archipelago; six islands are known thus far; facies distributions hint at the presence of others.

STRATIGRAPHIC SYNOPSIS

The oldest rock unit exposed in the Slick Hills is the Cambrian Carlton Group, which has a measured thickness at Bally Mountain (in the eastern Slick Hills) of about 3,600 ft (~1,100 m) (Ham and others, 1964). The Carlton Group forms a basement atop which the siliciclastics and carbonates of the lower Paleozoic rest with considerable unconformity. The Carlton Group is a thickly bedded sequence of rhyolitic lavas with lesser amounts of pyroclastic deposits.

Earlier studies of the age relationships between the Carlton Group and overlying Reagan Formation did not seem to allow time for substantial erosion or tectonism after the volcanism ended. In contrast, new dating by Gilbert and Hogan (1997) restricted the age of the basement to ca. 525–540 Ma and allows approximately 20 Ma of thermal subsidence and erosion prior to deposition of the overlying sediments. It is pertinent to note that Donovan (1995) suggested that significant pre-Reagan tectonism affected the Carlton Group, as shown by the existence of a series of north-south–trending fault and fracture patterns and a pre-Reagan dip to the rhyolite. At Bally Mountain, the rhyolite presently dips at 74° toward 050° (i.e., northeast), whereas the overlying rocks dip at approximately 50° to 060°. This suggests that the rhyolite had a pre-Reagan dip of about 22° to 260°. The pre-Reagan dip at Ring Top Mountain cannot be determined accurately because of widespread flow folds in the rhyolite.

During about 20 Ma of the Late Cambrian, the Carlton Group weathered and eroded into a series of hills with at least 1,000 ft (~300 m) of relief and gentle slopes of no more than 10° (Donovan, 1986; Donovan and Stephenson, 1991). Not surprisingly, the unconformity beneath the Cambrian sedimentary rocks is exceedingly irregular, and the stratigraphic architecture is complicated (Fig. 3).

The two lowest of the Carlton-covering formations, the Reagan and Honey Creek, are classified as the Timbered Hills Group. This series of rocks is generally marked by an upward increase in carbonate content coupled with a general decrease in grain size and amount of siliciclastic materials. The lowest part of the Reagan Formation consists of reddish-brown alluvial sandstones and conglomerates; this sequence grades into tidally influenced sand bars of purple and tan quartz sandstones interbedded with poorly exposed

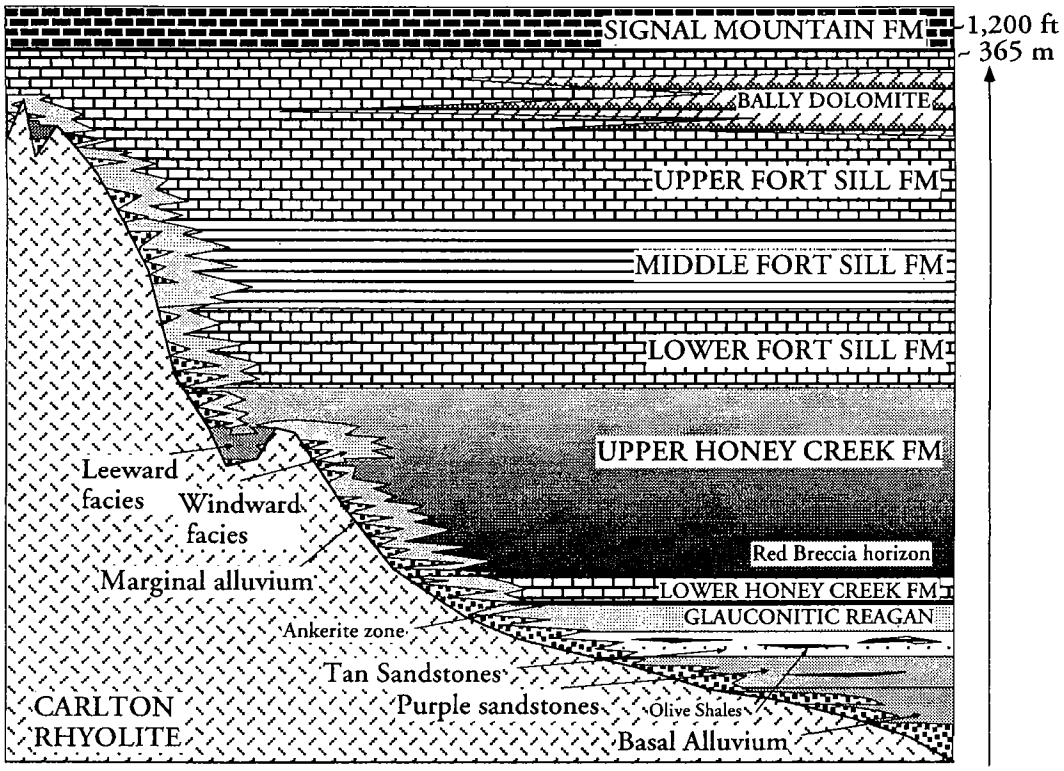

Figure 3. A synopsis of the stratigraphic relationships seen in the Cambrian rocks of the Slick Hills.

green shales. The topmost unit of the Reagan Formation is a tidally deposited, highly glauconitic sandstone. The base of the Honey Creek Formation is placed at the first occurrence of detrital carbonates (McElmoyl and Donovan, 2000). At and near this contact, much of the carbonate material has been altered to ankerite, which weathers to bright-orange limonite.

The Honey Creek Limestone is separated into "upper" and "lower" members by a pronounced disconformity. Beneath this disconformity, a bioclastic limestone the "red breccia" is locally present (McElmoyl and Donovan, 2000). These authors related the disconformity and breccia to a major, craton-wide regression that temporarily interrupted the continuity of the Franconian transgression (Chow and James, 1987). Meter-scale or less alternations between quartz sandstones and pelmatozoan-rich grainstones are common in both the upper and lower members of the Honey Creek Formation. The base of the Fort Sill Formation (lowest unit of the Arbuckle Group) is commonly taken as the change from grain-supported limestones to mudstones (Donovan and others, 2000).

SYNOPSIS OF THE SOUTHERN OKLAHOMA ARCHIPELAGO

The land surface in the Slick Hills was a hilly terrain with relief of at least 1,000 ft (~300 m) during Franconian time. Because of this topography, siliciclastics deposited in the early stages of transgression lapped onto the Carlton Group surfaces, and individual beds are laterally not persistent (Donovan, 1986). In addition, the sediments are diverse in composition and texture in part because they were partitioned by the rhyolite hills. The earliest sedimentary record consists of red beds formed by locally derived, braided-river sediments and alluvial talus. Alluvium continued to be shed off the rhyolite relief in decreasing amounts throughout the period of deposition of the Timbered Hills Group and even into the lowermost Arbuckle Group (Fort Sill Formation), when the last of the relief (Richard's Spur Island) was buried (Fig. 2). A tide-dominated, shallow, siliciclastic marine environment gradually lapped onto the topography as the transgression continued. Increasingly large amounts of quartz were incorporated into sediments; this quartz is thought to be contributed by the granites exposed on the craton to the north. The rocks contain an unusually large amount of iron. This probably was derived from the highly weathered rhyolite and is seen in the form of cements (ankerite, hematite, iron-rich illites), replacements (ankerite, pyrite, glauconite, and siderite), and intraformational grains (ferruginous ooids, glauconitic peloids) (Cloyd and others, 1986).

As the hills of the Carlton Group were increasingly isolated as islands, they ceased to be involved in continental-sedimentation dynamics and became relatively inert. The shallow, clear, and warm seas surrounding the newly formed islands supported sessile-pelmatozoan meadows and were further colonized by robust, thick-shelled trilobites and some orthid brachiopods. The widespread incursion of these organisms in skeletal grainstones demarcates the clearly diachronous base of the Honey Creek Limestone.

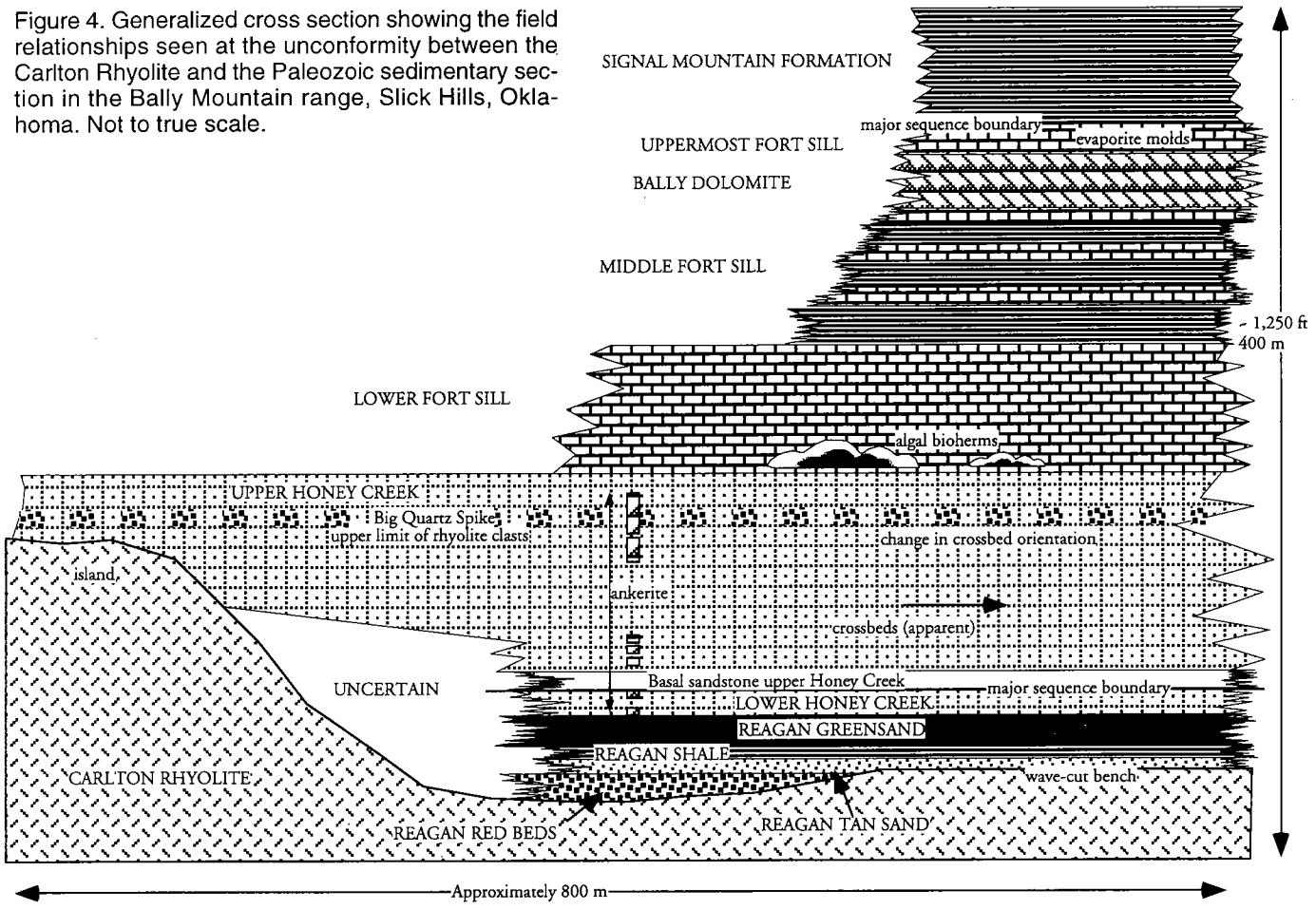

Figure 4. Generalized cross section showing the field relationships seen at the unconformity between the Carlton Rhyolite and the Paleozoic sedimentary section in the Bally Mountain range, Slick Hills, Oklahoma. Not to true scale.

BALLY AND RING TOP ISLANDS

The two northernmost islands in the southern Oklahoma archipelago are Bally Island and Ring Top Island (Fig. 2). The islands can only be observed as two-dimensional transects that are covered by veneers of Cambrian sedimentary layers and Permian conglomerates.

The Timbered Hills Group laps onto the rhyolite surface at Bally Island with considerable unconformity. The exposure at Bally Island is a 900-ft (~270-m) long transect oriented N27°W. Onlapping sediments strike N30°W on the average, and the plane of unconformity dips at ~50° to the east-northeast. The northwest end of the island and its overlying sediments are concealed by the Permian Post Oak Conglomerate; the southeast end displays excellent exposures other than a 210-ft (~65-m) length veiled by a grove of trees (Fig. 4). Farther to the southeast, the unconformity is also covered by Post Oak Conglomerate. Bally Island had a long existence, persisting well into the late Honey Creek time. The present exposure appears to be close to the true (three-dimensional) top of the island (Donovan and others, 2000).

The field relationships at Ring Top Island are more difficult to determine because of the imprint of Pennsylvanian folding; a major asymmetric anticline with a core of rhyolite plunges gently to the south-southeast and bisects an exposure of the unconformity that is ~650 ft (~200 m) in length. The Reagan Formation laps onto the northeast, south, and southwest sides of the island. Near the hinge of the anticline, small-scale folds and thrusts that are part of the Pennsylvanian folding deform the upper part of formation. To the north and west, the Permian Post Oak Conglomerate mask the field relationships. To the northeast of the fold hinge, sedimentary layers dip approximately 30° toward 080°; on the other limb of the fold, dips are much lower (5° to 225°–265°). Farther to the west-southwest, a block of Reagan Formation in unconformable contact with the rhyolite, displays a 60° dip to the southwest. This block is thought to have been displaced by a fault of uncertain orientation and throw. At the present level of exposure, the island projects into the topmost glauconite-rich member of the Reagan.

REAGAN FORMATION AT BALLY ISLAND

The lowermost part of the Reagan Formation at Bally Mountain consists of red beds. These are conglomerates, lithic sandstones, and shales, most of which appears to be generally poorly sorted rhyolitic debris deposited in an alluvial environment (Fig. 5). These deposits, which have a maximum thickness of 10 ft (~3 m), occupy a small valley cut into the underlying rhyolite surface. They are overlapped by a tan, pebbly, quartz-rich, well-sorted, coarse-grained sandstone

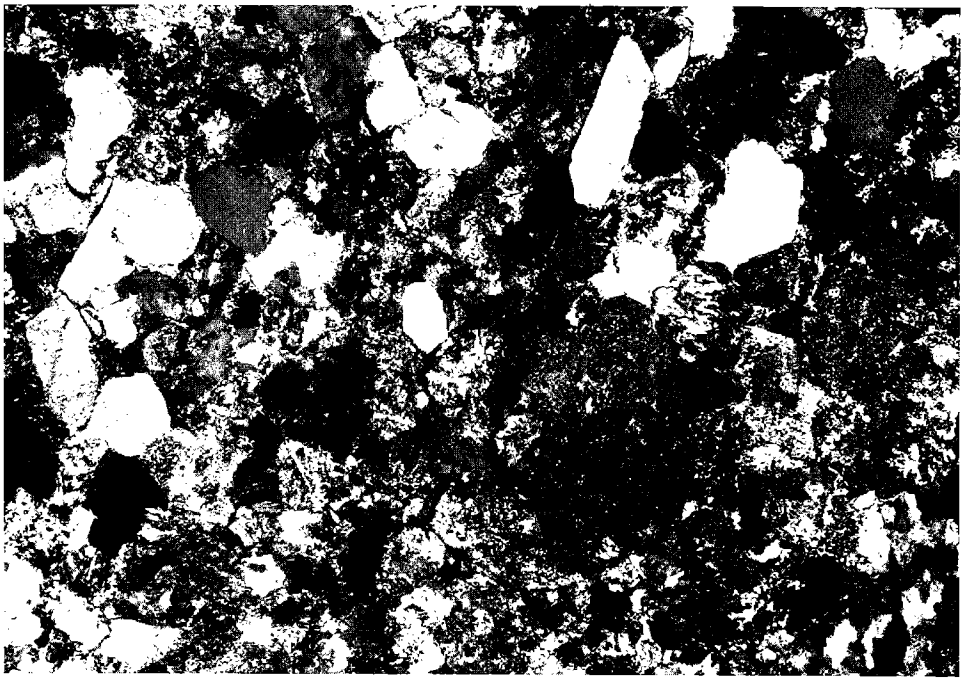

Figure 5. Photomicrograph (polarized light) of an example of the basal red beds seen at Bally Island. The rock is a poorly sorted, coarse-grained lithic sandstone in which ~70% of the grains are fragments of rhyolite of the Carlton Group, showing various degrees of devitrification. The remaining grains are quartz, derived either from phenocrysts in the rhyolite or from farther afield on the craton to the north. The principal cement is hematite; some illite is present. Field of view is ~3 mm across.

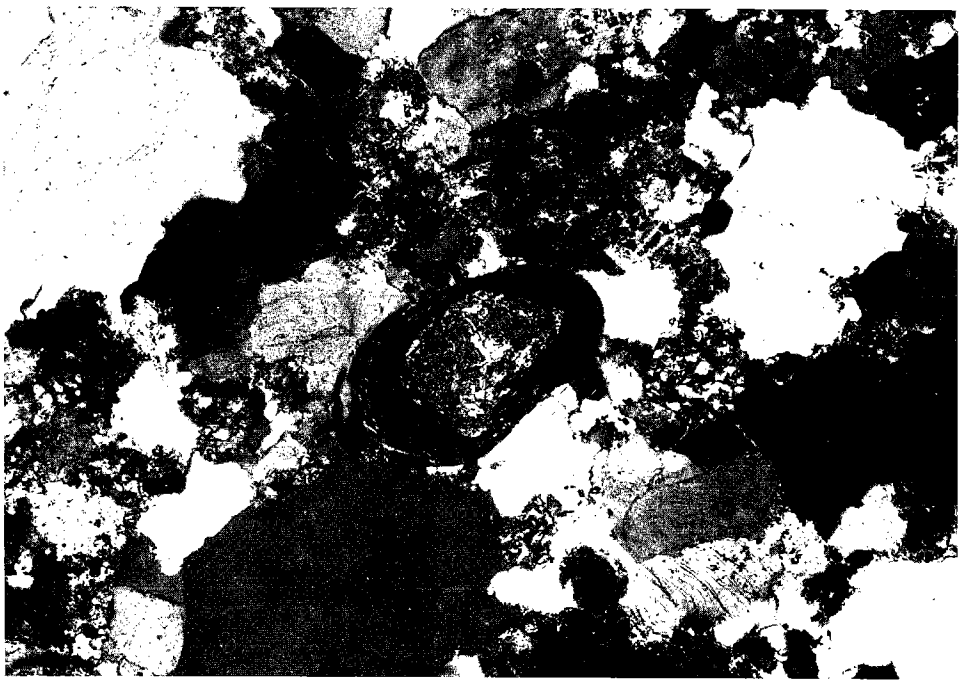

Figure 6. Photomicrograph (polarized light) of coarse-grained "shoreline"-facies sandstone at Bally. The most abundant grains are quartz and rhyolite, the latter being generally smaller in size and less common. A ferruginous ooid is present in the center of the picture. Some syntaxial quartz cement is present, but the rock was significantly compacted prior to lithification. This compaction was aided by devitrification of the rhyolite. Field of view ~3 mm across.

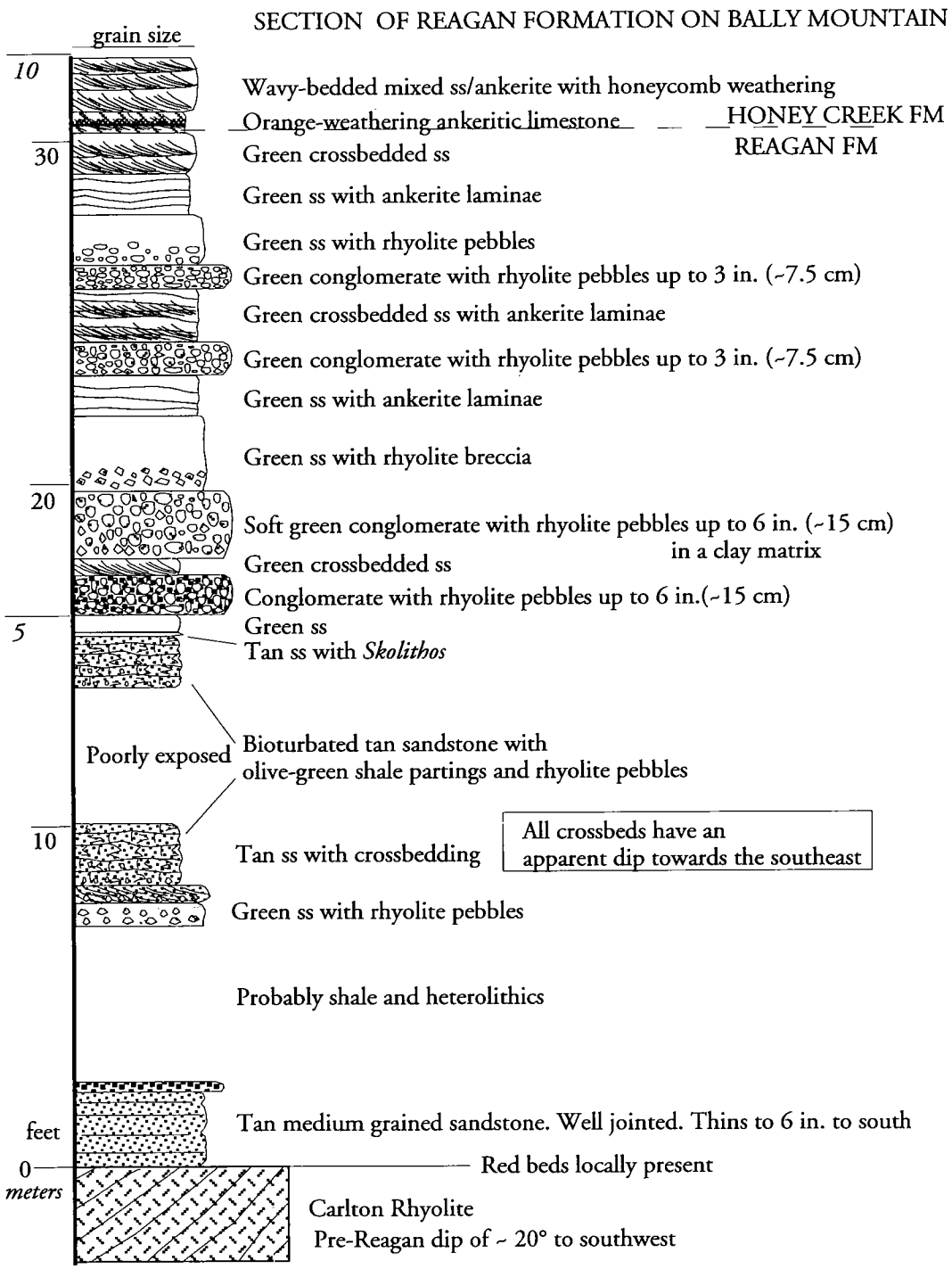

Figure 7. Measured section of the Reagan Formation at Bally Mountain; section located ~30 yds (27 m) northwest of small quarry.

that contains substantial amounts of rhyolite grains and as much as 15% ferruginous ooids (Fig. 6). This sandstone can be traced along the entire exposure at this level of the unconformity and varies from 0.5 to 3 ft (about 15–100 cm) in thickness. Parallel lamination is the principal sedimentary structure seen. The bed is interpreted as a shoreline sand and marks the commencement of the Franconian transgression at Bally Mountain (Fig. 7). Most of the quartz in the sandstone does not appear to have been come from the underlying rhyolite but has presumably been derived from a granitic terrane farther away on the craton. The ferruginous ooids now consist of concentric bands of tiny crystals of hematite and illite. They are an unlikely grains to have formed in a robust shoreline setting and may well have nucleated in quieter, offshore estuarine settings prior to their reworking into shoreline sands.

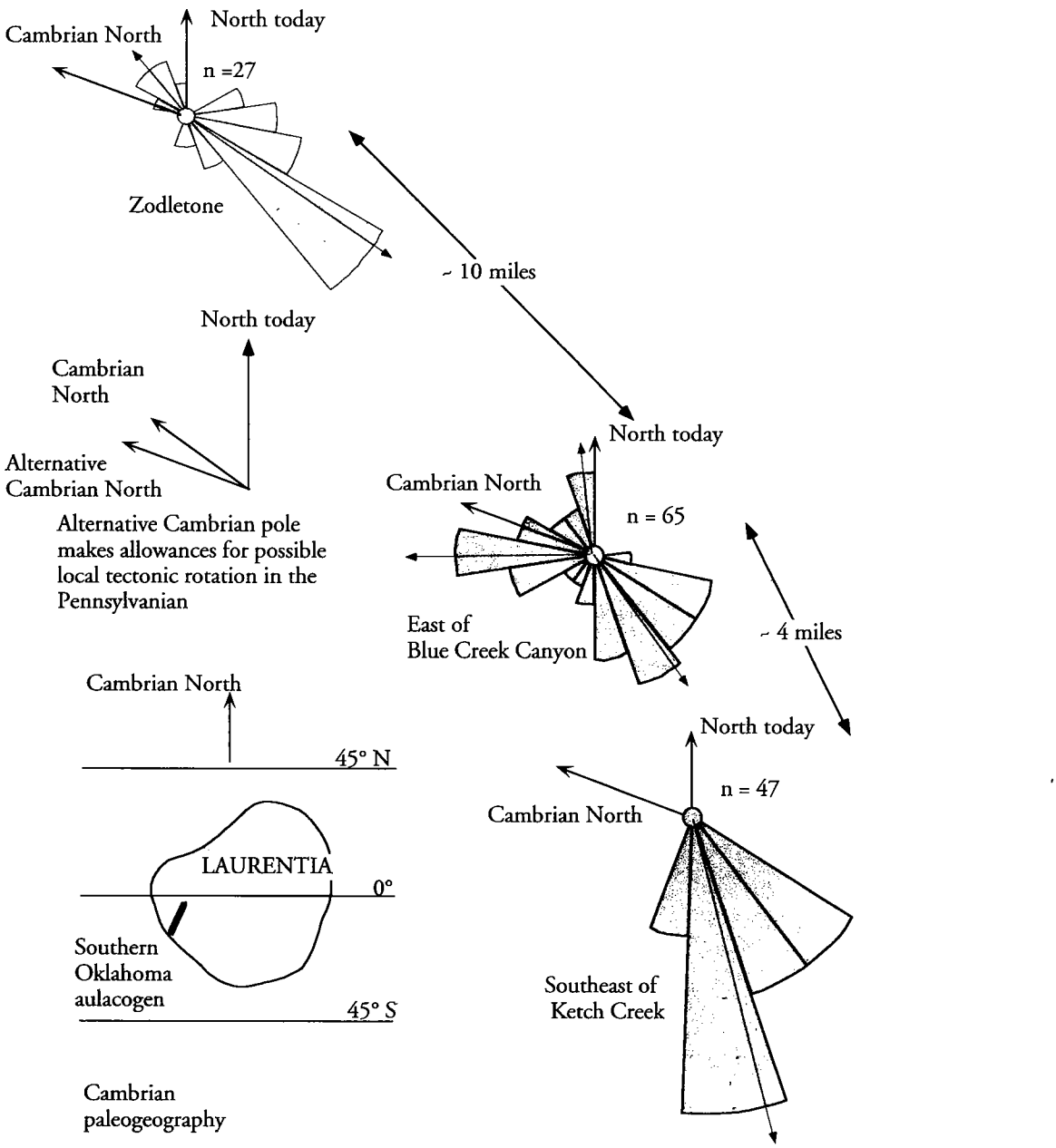

Figure 8. Cross-beddings orientations in the Reagan Formation, adjusted for plate-tectonic rotation.

The basal marine bed is overlain by about 10 ft (~3 m) of poorly exposed shales and thinly bedded sandstone-shale heterolithics. The shales are composed of olive-green illitic clay. In the middle of this shaly section is a lenticular tan, quartz-rich, medium- to coarse-grained sandstone that displays medium-scale cross-bedding. This sandstone does not persist for the length of the outcrop, being traceable for about 200 ft (~60 m). In its general characteristics, it is similar to other Reagan sandstones that have been interpreted as offshore, tidal sandbars (Donovan and others, 1986; Donovan and Ditzell, 1986). A common feature of these tan sandstones is that they display trace fossils of the *Skolithos* ichnofacies, indicating a degree of robust current flow. Horizontal bioturbation—i.e., crawling and mining traces—is a common feature of the thinner sandstones of the heterolithics, suggesting that they were deposited in quieter conditions.

All of the sandstones above the basal shoreline sand contain some glauconite in the form of medium- to fine-grained peloids that show various amounts of abrasion. Like other Reagan sections in the Slick Hills, the amount of glauconite present increases markedly up to the formational boundary and forms a very high percentage of noncarbonate grains in the overlying lower member of the Honey Creek Formation. This topmost green sandstone is representative of a conspicuous unit that varies from 15 to 20 ft (4.5–6 m) thick and that is found throughout the Slick Hills. Glauconite forms over half of the grains present in some of these beds. Other

grains include quartz, fragments of phosphatic brachiopods (*Lingula* sp.), rhyolite, and minor feldspar. There is a positive correlation between the abundance of glauconite peloids and phosphate fragments (i.e., broken shells), suggesting—but not proving—a genetic relationship. Bioturbation in the green sandstones is much less common than in the underlying tan sandstones and heterolithics and, where present, consists of crawling traces rather than vertical burrows.

Many of the green sandstones display cross-bedding. In some sections, cross-bedding sets up to 4 ft (~1.3 m) thick are present (Donovan, 1986). The general pattern of cross-bedding orientation in both tan and green sandstones in the Slick Hills is bipolar, with current flow alternating between the northwest and southeast (Fig. 8). The latter direction is the more prevalent. Given the orientation of the Slick Hills area to the Laurentian craton at this time, this stronger southeast flow direction is consistent with ebb-tide dominance.

The cross-beds at Bally are generally smaller than elsewhere in the Slick Hills, about 12 in. (~30 cm) and thus suggest generally calmer water. The exposures at Bally do not yield accurate cross-bedding vectors, but all the exposed two-dimensional profiles indicate transport to the southeast quadrant. A similar pattern is seen in the lower part of the upper member of the Honey Creek Formation (Donovan and others, 2000). One interpretation of this pattern is that tidal and other currents in the area were partially controlled by Bally Island, which, as exposed, lies to the northwest of this outcrop.

Conglomerates are more common in the Bally section than is usual for the green sandstones. Six pebble layers are present, and additional ones occur in both members of the Honey Creek Formation. Five of the pebble beds are conglomerates; one is a breccia. All the pebbles observed are rhyolite and the maximum pebble size is 6 in. (~15 cm). Bally Island is the likely source of these pebbles; they presumably represent shoreline beaches that were reworked into deeper and quieter offshore settings. Additionally, some of the most glauconitic strata at Bally display no visible internal structure and are poorly sorted deposits that may be storm related.

The rocks at Bally show a straightforward change in petrography that records the succession of transgressive environments. This change is matched by changes in the diagenetic imprint. The basal alluvium was cemented by hematite and silica, both of which were probably derived from the weathering and devitrification of the Carlton Group rhyolites. Syntaxial quartz cements are ubiquitous in the overlying tan shoreline and offshore-bar sandstones. This quartz was templated early, because minus cement porosities are high, around 30%. Lesser amounts of syntaxial quartz cements also are present in the green sandstones (Fig. 9). In the most glauconite-rich rocks, iron-rich illite forms a syndepositional matrix; many of these rocks show significant effects of compaction in which the glauconite peloids have been "fitted" against each other. Toward the top of the Reagan Formation, some patches of coarsely crystalline ankerite cement presumably record the presence of carbonate-rich waters in contact with the lower member of the overlying Honey Creek Formation.

Figure 9. Photomicrograph (polarized light) showing the contact between an upper medium-grained gray-green sandstone with a substantial content of quartz grains and a lower fine-grained sandstone in which most of the grains are glauconite peloids. The upper sandstone was lithified by syntaxial quartz cement, whereas the lower sandstone was lithified dominantly by compaction. Field of view ~3 mm across.

REAGAN FORMATION AT RING TOP ISLAND

The exposures at the Ring Top Island show that the island had a relief of at least 25 ft (~7.5 m) but apparently was buried before deposition of the lower member of the Honey Creek Formation (Figs. 10 and 11). Ring Top Island contributed little detritus to the sedimentary section. Only the basal breccia and sandy conglomerate contain more than 2% rhyolite. The physical characteristics of the island in the third dimension (i.e., the possibility of additional relief in the buried portion) are difficult to determine. The passage into the Honey Creek Formation is not exposed.

About 25 ft (~7.5 m) of gray and gray-green sandstones lap onto the rhyolite surface to the northeast of the island. Some of these sandstones are markedly

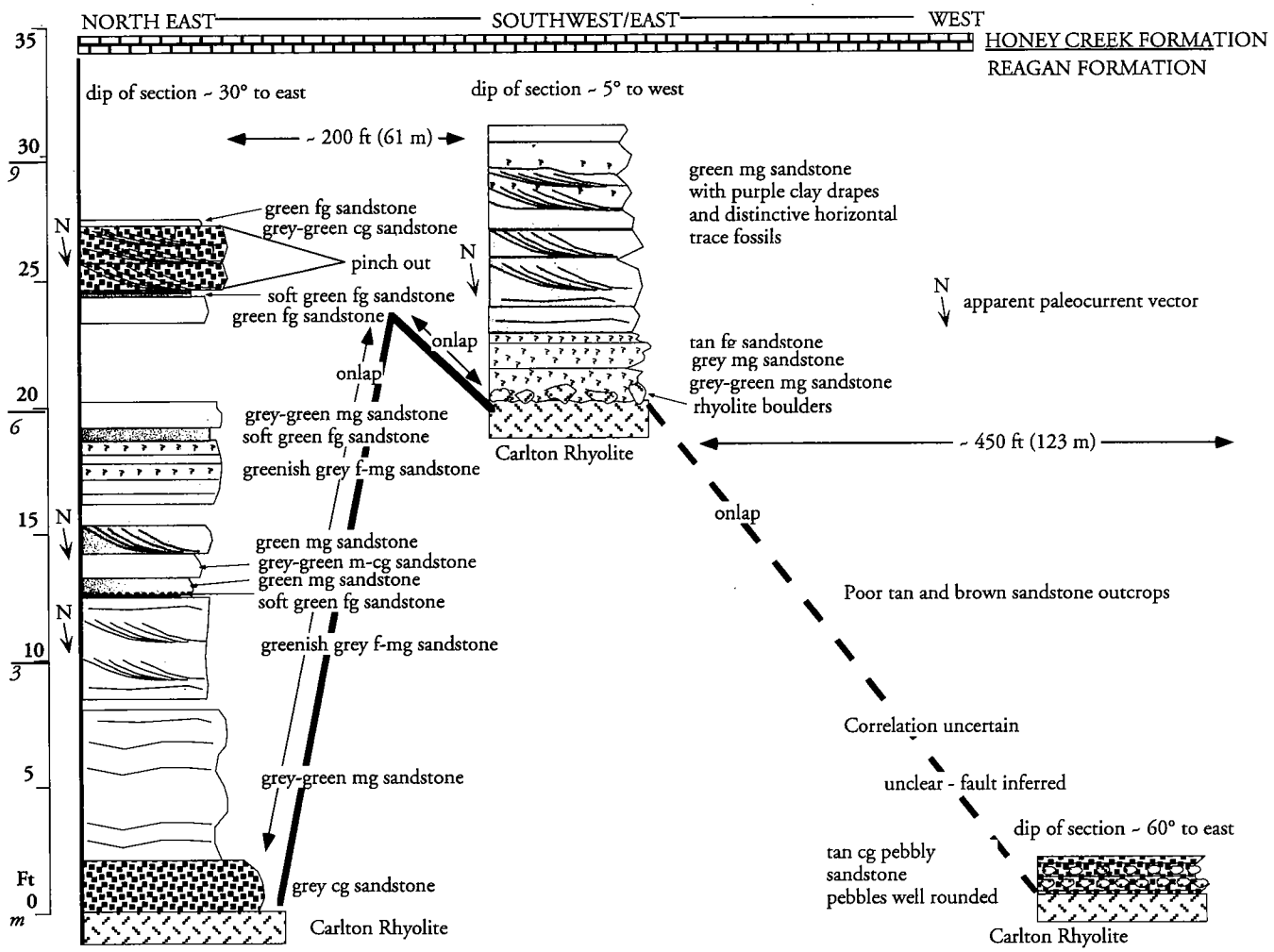

Figure 10. Logs of the Reagan Formation exposed around Ring Top Island. Abbreviations: fg—fine grained; mg—medium grained; cg—coarse grained.

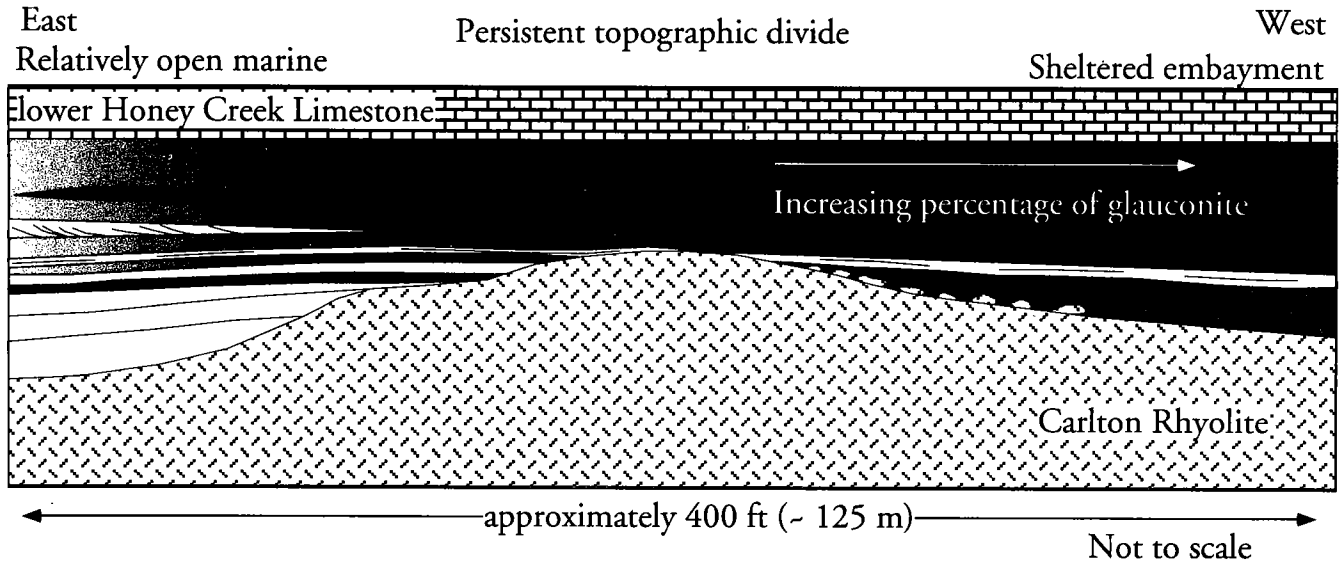

Figure 11. Cross section showing the facies relationships at Ring Top Island.

lenticular and appear to pinch out toward the crest of the island, suggesting that the island played a role in sediment partitioning. These sandstones range in grain size from fine to coarse; the finer lithologies contain more glauconite and less quartz (as noted, very little rhyolite is present). The petrology and diagenesis of these rocks resembles that seen at Bally. Sedimentary structures include some vertical burrows, parallel lamination, and medium-scale cross-bedding. The latter appears to have been deposited by currents moving to the south-southeast. The surface of unconformity is sharply defined although slightly faulted locally. The sandstones seem to have been banked against the island, which played a very limited role as a sediment provider.

Southwest of the crest of the island, the unconformity is marked by a basal breccia in which boulders of rhyolite as much as 31.5 in. (80 cm) long are embedded in intensely bioturbated tan and grayish-green, fine- to medium-grained sandstone that rests directly on the unconformity. This facies, which is unique in the Slick Hills, clearly records a major change in the environment from one side of the island to the other. A comparatively small amount of glauconite (<10%) is preserved in these lowest layers of rock; however, about 3 ft (~1 m) up into the section, an abrupt change in color to very dark green is due to a great increase in glauconite—as much as 50% of the rock in some cases. In addition, very high percentages of phosphatic brachiopods—up to 15%—are present. These intensely green rocks display medium- to large-scale cross-bedding, again indicating transport to the south-southeast. The impression gained from the section is of rapid inundation of the island by a sea-level rise that led to the development of anoxic conditions, because trace fossils are generally absent in the green sandstones. The only soft-bodied organisms that appear to have survived the flooding event are distinctive crawlers that produced long tracks that were ~0.5 in. (1.3 cm) wide. These traces are found on only two surfaces of purple mudstone that were probably clay drapes formed during periods of temporary sediment stability.

About 450 ft (~140 m) to the west of the island, an isolated exposure of the unconformity is overlain by about 2 ft (~60 cm) of tan, sandy conglomerate. The well-rounded pebbles in this conglomerate are all rhyolite clasts with maximum dimensions of 3 in. (~8 cm), although this bed also contains clasts of well-sorted quartz, subordinate rhyolite, and a trace of glauconite. The rock has been comprehensively cemented by syntaxial quartz. The sequence is interpreted as a shoreline deposit; its stratigraphic relationship to the main Ring Top outcrop is uncertain.

COMPARISON OF SETTINGS

The general transgressive-facies model (Fig. 12) for the Reagan Formation involves the inundation of a rhyolite coastline in a macrotidal setting in which ebb tides exerted a dominant control on sediment movement (Donovan, 1986). The sources of sediment (Fig. 13) were either the local basement (rhyolite), the distal craton (quartz and minor feldspar, probably transported from the interior of the craton by both rivers and the wind), and authigenic (glauconite peloids, phosphatic brachiopods, and ferruginous ooids). The upper green sandstones are interpreted to record a relatively rapid rate of sea-level rise that effectively drowned both the rhyolite topography and a lively shallow-water setting recorded by the tan sandstones. Both islands modified the general facies development.

Bally Island, the relief of which was greater than that of Ring Top Island, had a greater overall role as a sediment source to both the Reagan and Honey Creek Formations. This contention is supported by direct observation of the unconformity and by both the higher percentage and stratigraphically higher location of rhyolite fragments found at Bally. Early flanking sediments onlapping both Bally and Ring Top Islands varied notably in composition, but the lack of quality exposure on the north end of Bally Island makes a complete comparison impossible. Both islands appear to have partitioned facies development. At Bally, conglomerates are both coarser and more numerous, whereas, at Ring Top, an obvious and discrete development of individual shoreline facies exists on opposing sides of the island. In particular, the seemingly sheltered, southwest side of the island played host to numerous soft-bodied organisms, the trace fossils of which were not preserved in higher-energy areas on the northeast side of the island. Such partitioning is in accord with that found around modern archipelagos (Donovan, 2000b). Shoreline facies are found at both locations, but the basal red beds and shoreline sands rich in ferruginous ooids seen at Bally are not found at Ring Top.

ACKNOWLEDGMENTS

We would like to thank the Fort Worth Geological Society, Adkins Fund of Texas Christian University, Houston Geological Society, Mobil Foundation, and Moncrief family of Fort Worth for their generous financial support. Sincere appreciation is expressed to the Kimbell family for permitting us access to the site.

REFERENCES CITED

Chow, N.; and James, N. P., 1987, Cambrian Grand Cycles: a northern Appalachian perspective: Geological Society of America Bulletin, v. 98, p. 418–429.

Cloyd, Kelly; Donovan, R. N.; and Rafalowski, M. B., 1986, Ankerite at the contact between the Reagan Sandstone and the Honey Creek Limestone (Timbered Hills Group), *in* Donovan, R. N. (ed.), The Slick Hills of southwestern Oklahoma—fragments of an aulacogen?: Oklahoma Geological Survey Guidebook 24, p. 17–20.

Donovan, R. N., 1986, The geology of the Slick Hills, *in* Donovan, R. N. (ed.), The Slick Hills of southwestern Oklahoma–fragments of an aulacogen?: Oklahoma Geological Survey Guidebook 24, p. 1–12.

_____ 1995, The Slick Hills of Oklahoma and their regional tectonic setting, *in* Johnson, K. S. (ed.), Structural styles in the southern Midcontinent, 1992 symposium: Oklahoma Geological Circular 97, p. 178–186.

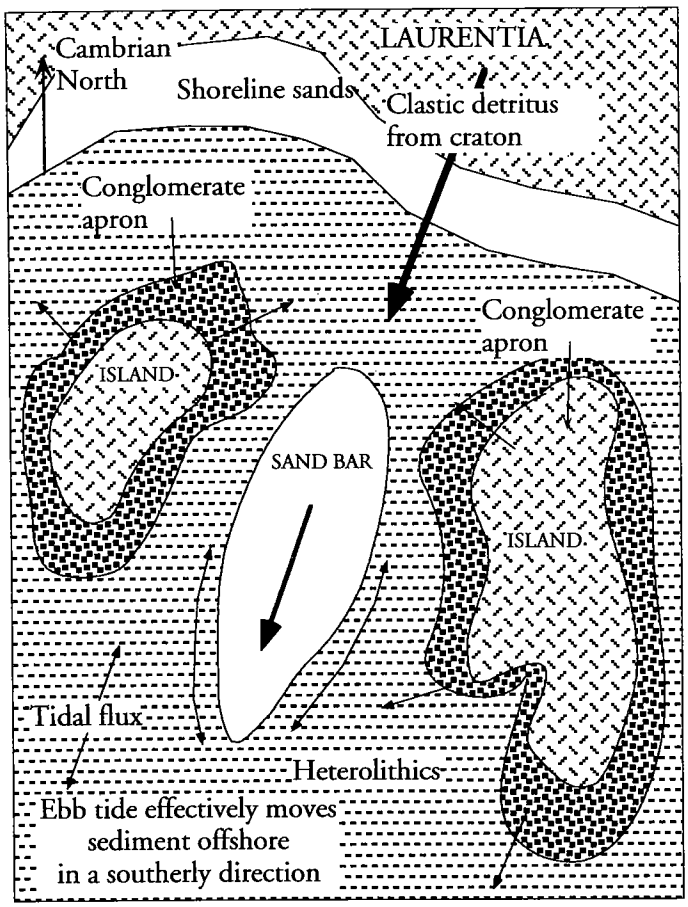

Figure 12. Depositional model illustrating major factors operating during the deposition of the Reagan Formation.

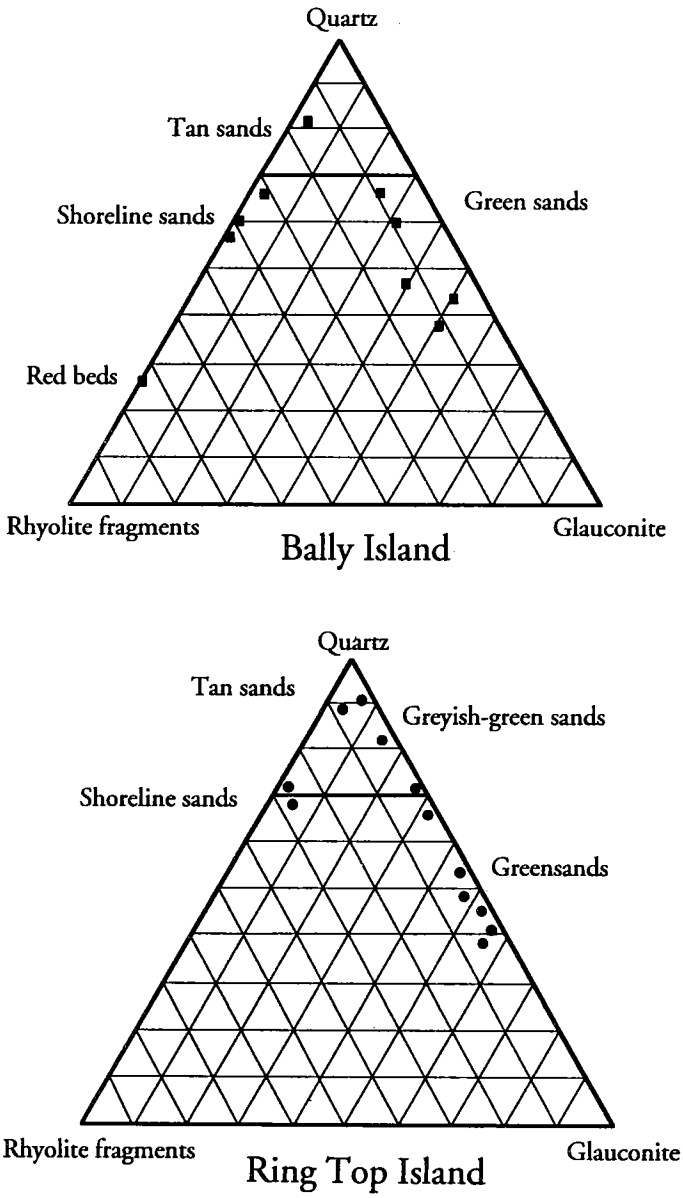

Figure 13. Contrast of the petrology of Reagan Formation sandstones seen at Bally and Ring Top Islands, respectively. Both show an upward decrease in rhyolite detritus and increase in glauconite peloids, but the details differ.

_____ 2000a, Initiation of the Arbuckle platform—view from the Slick Hills, Oklahoma, *in* Johnson, K. S. (ed.), Platform carbonates in the southern Midcontinent, 1996 symposium: Oklahoma Geological Survey Circular 101, p. 47–56.

_____ 2000b, Sediment transport around islands, ancient and modern: examples from the west coast of Scotland and southwestern Oklahoma, *in* Johnson, K. S. (ed.), Marine clastics in the southern Midcontinent, 1997 symposium: Oklahoma Geological Survey Circular 103 [this volume], p. 19–23.

Donovan, R. N.; and Ditzell, Curtis, 1986, Stop 3: Geologic highlights at Zodletone ("Stinking Mountain"), *in* Donovan, R. N. (ed.), The Slick Hills of southwestern Oklahoma—fragments of an aulacogen?: Oklahoma Geological Survey Guidebook 24, p. 96–99.

Donovan, R. N.; and Stephenson, M. D., 1991, A new island in the southern Oklahoma archipelago, *in* Johnson, K. S. (ed.), Late Cambrian–Ordovician geology of the southern Midcontinent, 1989 symposium: Oklahoma Geological Survey Circular 92, p. 118–121.

Donovan, R. N.; Ragland, D. A.; Cloyd, Kelly; Bridges, Steve; and Denison, R. E., 1986, Stop 2: Geological highlights of the Bally Mountain area, *in* Donovan, R. N. (ed.), The Slick Hills of southwestern Oklahoma—fragments of an aulacogen?: Oklahoma Geological Survey Guidebook 24, p. 92–95.

Donovan, R. N.; Ayan, Danielle; and Bucheit, A. K., 2000, Late Cambrian marine-facies transitions: upper member of the Timbered Hills Group, Bally Mountain, Slick Hills, southwestern Oklahoma, *in* Johnson, K. S. (ed.), Marine clastics in the southern Midcontinent, 1997 symposium: Oklahoma Geological Survey Circular 103 [this volume], p. 39–50.

Feinstein, S., 1981, Subsidence and thermal history of southern Oklahoma aulacogen: implications for petroleum exploration: American Association of Petroleum Geologists Bulletin, v. 65, p. 2521–2533.

Gilbert, M. C.; and Hogan, J. P., 1997, What's new in Oklahoma's old basement [abstract]: American Association of Petroleum Geologists Bulletin, v. 81, p. 1351.

Ham, W. E.; Denison, R. E.; and Merritt, C. A., 1964, Basement rocks and structural evolution of southern Oklahoma: Oklahoma Geological Survey Bulletin 95, 302 p.

Hosey, R. M.; and Donovan, R. N., 2000, Boundary between the Fort Sill and Signal Mountain Formations in the Lower Arbuckle Group, Slick Hills: candidate for a Grand Cycle boundary, *in* Johnson, K. S. (ed.), Platform carbonates in the southern Midcontinent, 1996 symposium: Oklahoma Geological Survey Circular 101, p. 79–88.

Johnson, K. S.; Amsden, T. W.; Denison, R. E.; Dutton, S. P.; Goldstein, A. G.; Rascoe, Bailey, Jr.; Sutherland, P. K.; and D. M. Thompson, 1989, Geology of the southern Midcontinent: Oklahoma Geological Survey Special Publication 89-2, 53 p.

McElmoyl, Courtney; and Donovan, R. N., 2000, Unconformity in the lower part of the Cambrian Honey Creek Limestone, Slick Hills, Oklahoma: candidate for a Grand Cycle boundary, *in* Johnson, K. S. (ed.), Platform carbonates in the southern Midcontinent, 1996 symposium: Oklahoma Geological Survey Circular 101, p. 65–78.

Late Cambrian Marine-Facies Transitions: Upper Member of the Timbered Hills Group, Bally Mountain, Slick Hills, Southwestern Oklahoma

R. Nowell Donovan, Danielle Ayan, and Andrea K. Bucheit
Texas Christian University
Fort Worth, Texas

ABSTRACT.—A major transgression took place across the Laurentian (proto–North American) craton during the Late Cambrian. By the Early Ordovician, the continent had been inundated to form one of the greatest carbonate platforms in the earth's history. The units that record the commencement of this transgression in Oklahoma are the Timbered Hills Group (consisting of the basal Reagan and overlying Honey Creek Formations) and the Arbuckle Group (specifically the lowermost Fort Sill Formation). The initial character of this transgression is well displayed in the Slick Hills of southwestern Oklahoma, specifically in a section in the Bally Mountain range. In the Slick Hills, the transgressed land surface, formed by the Cambrian Carlton Rhyolite, had a relief of several hundred feet. In other words, hills/islands of igneous rocks jut through the Timbered Hills and lower Arbuckle Group sedimentary rocks, forming a highly irregular unconformity. This irregularity has led development of an "archipelago model" to explain some of the complex field relationships seen in the Slick Hills. Evolution of the topography was independent of the tectonic evolution of the southern Oklahoma aulacogen and was in fact a characteristic of the Laurentian craton as a whole—i.e., wherever basement rocks of whatever age resisted erosion, topographic highs developed (e.g., the subsurface Tulsa Mountains of northeastern Oklahoma). The biggest of the paleohills evolved into islands as the Franconian transgression continued.

Within this geomorphic framework a complex sequence of interrelated environments controlled sedimentation patterns. Initial deposits of alluvium filled in the low spots of the topography. Subsequently marine siliciclastics were deposited as shoreline sandstones, tidally influenced sand bars, and heterolithics. Eventually, carbonate sandstones, derived from "production centers" associated with individual islands, mixed with siliciclastics, thus serving to initiate the carbonate system that would come to dominate Oklahoma during the deposition of the Arbuckle Group. It is possible to recognize in detail windward and leeward facies of carbonate adjacent to individual islands. Similarly, individual islands partitioned tidal and estuarine siliciclastics. Both the siliciclastic and carbonate sequences are iron-rich. This richness is manifest in several ways—as hematite cements, ferruginous ooids, glauconite, ankerite, pyrite, and ferroan calcite cements.

The apparently straightforward model of Franconian transgression is complicated by occurrence of two major regressions and an increasing tectonic response to the developing early Paleozoic aulacogen.

This paper describes the transition from marine siliciclastics to carbonate platform by evaluating the upper part of the Honey Creek Formation at Bally Mountain. The impact of the transgression controlled environments of deposition, sediment petrography, and early diagenesis.

INTRODUCTION

A record of Franconian (Late Cambrian) transgression across the Laurentian craton is preserved in the Slick Hills of southwestern Oklahoma (Fig. 1). A general lithostratigraphic trend upward, from basal siliciclastic detritus to mud-dominated carbonates, can be recognized throughout the area. This trend records a gradual change from alluvial environments to tide-dominated siliciclastic shoreline and shallow-marine

Donovan, R. N.; Ayan, Danielle; and Bucheit, A. K., 2000, Late Cambrian marine-facies transitions: upper member of the Timbered Hills Group, Bally Mountain, Slick Hills, southwestern Oklahoma, *in* Johnson, K. S. (ed.), Marine clastics in the southern Midcontinent, 1997 symposium: Oklahoma Geological Survey Circular 103, p. 39–50.

settings into which increasing amounts of carbonate detritus found their way. Ultimately the area became part of the immense Late Cambrian–Early Ordovician microtidal carbonate platform that circled the Laurentian craton. This craton was astride the equator during the Late Cambrian; southern Oklahoma was ca. 20° south of the equator and has rotated ca. 70° anticlockwise since then (McElmoyl and Donovan, 2000).

Although this general pattern can be recognized throughout the area, facies analysis is greatly complicated by the nature of the land surface that was transgressed—a range of hills built of the middle to Late Cambrian Carlton Rhyolite. During the course of the transgression, the topography evolved from a range of hills, with summits rising to at least 1,000 ft (ca. 300 m), to an archipelago that was not inundated until the carbonate platform was well developed. The archipelago environment dictated that sharp facies changes occurred within the enveloping sediments, particularly during early phases of the transgression (Donovan, 1986).

Two major and several minor regressions punctuated the developing transgression, creating further complexity to the history of the area. These major regressions are marked by clear evidence of withdrawal of marine waters and contemporary erosion. The archipelago persisted through the earlier but not the later of these two regressions (Donovan, 2000).

Another feature of special interest is the abundance of iron that is associated with the drowned land surface. This iron is manifest in both valency states, as hematite cements, ferruginous ooids, a variety of forms of glauconite, iron-fixing bacterial stromatolites, ferroan-calcite and ankerite cements, and the widespread replacement of calcite by ankerite.

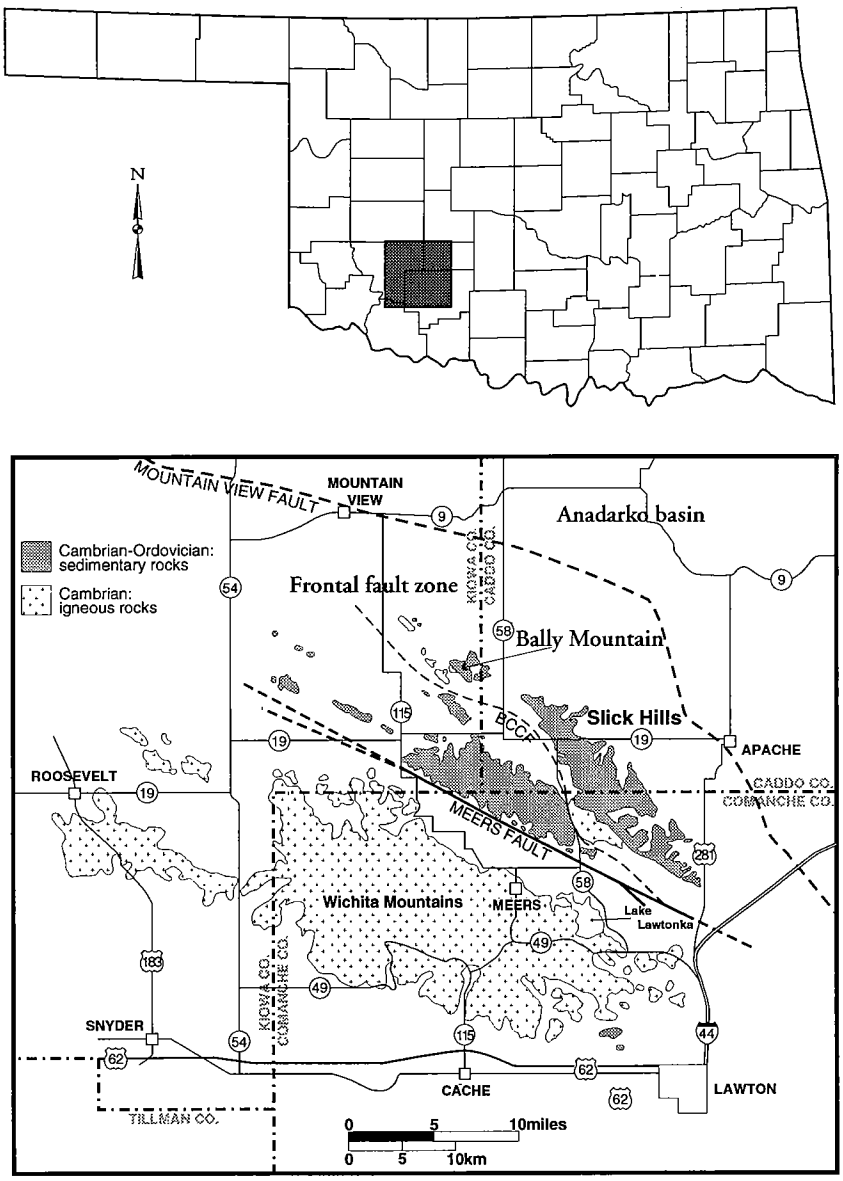

Figure 1. The location of Bally Mountain in the Slick Hills in southwestern Oklahoma.

STRATIGRAPHIC SYNOPSIS

The formal stratigraphic breakdown of the sequence recognizes the broad lithostratigraphic pattern outlined in the previous section. The basal siliciclastics are assigned to the Reagan Formation and the mixed carbonate and siliciclastics to the Honey Creek Formation. These two formations constitute the Timbered Hills Group. The overlying platform carbonates are assigned to the Arbuckle Group. In this paper, we are concerned only with the Fort Sill Formation, which is lowermost division of the Arbuckle Group (Fig. 2).

McElmoyl and Donovan (2000) discussed the convoluted evolution of the stratigraphic terminology. In this paper we follow their placement of boundaries, using the following two criteria.

(1) The base of the Honey Creek Formation is taken as the first incursion of detrital carbonates (pelmatazoan-rich grainstones), and (2) the base of the Arbuckle Group is taken as the lowest occurrence of stratigraphically persistent lime mudstones. This usage honors established lithostratigraphic practice. Both boundaries are easy to determine in the field and can be traced throughout the area without difficulty.

McElmoyl and Donovan (2000) divided the Honey Creek into "Lower" and "Upper" members. They erected this informal subdivision in order to recognize a stratigraphic break that can be traced throughout the Slick Hills. In places, this break is a slight angular unconformity; in other areas, it is a disconformity. Locally a "Red Breccia" is sandwiched between the two

members. They correlated the break with a craton-wide regression, previously recognized as a "Grand Cycle" boundary by Chow and James (1987). McElmoyl and Donovan (2000) suggested that the complexities of the stratigraphic relationships—e.g., the restricted occurrence of the red breccia and localized angular relationships—reflect the geographic complexities of the archipelago.

We present in this paper a detailed description of the upper member of the Honey Creek Formation as exposed at Bally Mountain in the northwest part of the eastern Slick Hills. Our purpose is to interpret the changes that took place as a siliciclastic-dominated setting was replaced by a carbonate platform dominated by mud-producing carbonate processes.

BALLY MOUNTAIN EXPOSURE

The sequence at Bally Mountain dips to the northeast at 40–60°, is well exposed, and displays many of the relationships discussed in the previous section (Donovan and others, 1986). Of particular interest is the presence of one of the rhyolite islands of the southern Oklahoma archipelago on the northwestern edge of the exposure. This island persisted throughout deposition of the Reagan Formation and at least the lowermost two thirds of the Honey Creek Formation, including most of the upper member (Fig. 2). The apparent "height" of the island in the exposure may be close to its real height because clasts of rhyolite are not found much above the present level of exposure of the unconformity surface.

Reagan Formation and Lower Part of the Honey Greek Formation

This part of the section lies below the stratigraphic break recognized by McElmoyl and Donovan (2000) and is described in detail elsewhere (Donovan and Bucheit, 2000). A synopsis is offered here. The lowermost part of the sequence consists of alluvial red beds that occupy a small valley cut into the underlying rhyolite surface. These beds are overlapped by a tan, well-sorted, coarse-grained, pebbly, quartz-rich, sandstone that can be traced along the entire exposure at this level of the unconformity and is interpreted as marine shoreline sand, marking the commencement of the Franconian transgression at Bally Mountain. Shales and heterolithics overlying this sandstone are overlain by glauconitic and quartz-rich sandstones that form the uppermost part of the Reagan Formation. These rocks record continuing transgression and faunal colonization. Most of the glauconite is peloidal and appears to be derived from either trace fossils and/or the abundant phosphatic brachiopod *Lingula*.

The base of the Honey Creek Formation is defined as the first incursion of detrital carbonate, as noted previously. The base is marked by broken and abraded pelmatozoans with subordinate fragments of thick-shelled trilobites and brachiopods. This detritus was worked into the existing mix of quartz, glauconite, rhyolite, and phosphatic grains. Diagenetic carbonate takes two forms: (1) as calcite cement, principally syntaxial overgrowths around the pelmatozoans, and (2) as ankerite which replaces calcite. The latter is concentrated near the basal contact with the Reagan Formation and beneath the contact with the upper member of the Honey Creek Formation. Ankerite zones throughout the Honey Creek are conspicuous because the mineral has weathered to limonite, and the resulting rocks have a bright orange veneer (Cloyd and others, 1986).

A feature of both the Reagan Formation and the lower member of the Honey Creek Formation at Bally is the occurrence of conglomerates throughout the section, regardless of general lithology. These conglomerates form beds as much as 3 ft (ca. 1 m) thick and consist of rhyolite pebbles as much as 6 in. (ca. 15 cm) in diameter. Similar conglomerates are found throughout the Slick Hills at this level; their prevalence at Bally probably records erosion of the adjacent rhyolite hill/island terrain. Unfortunately, the contact of the beds with the island is not exposed at this low level in the section, and thus this relationship cannot be confirmed (Fig. 2).

Upper Member of the Honey Creek Formation

This member lies above a widespread stratigraphic break (McElmoyl and Donovan, 2000). Contact with the underlying beds is sharp. We have not seen unambiguous evidence of erosion, and no basal conglomerate occurs. The "red breccia," described above, is not present at Bally. The upper member is 146 ft (ca. 45 m) thick (Fig. 3A–E).

The basal bed of the upper member is a tan, fine-grained, well-sorted, quartz-rich sandstone, characterized by parallel lamination and small-scale trough crossbeds. This sandstone forms a conspicuous ledge that can be traced throughout the Slick Hills.

Strata above the basal sandstone consist of thin sandstone layers that are intermixed and dominated either by quartz or carbonate grains. These two types of sandstones have differentially weathered to a distinctive wavy "honeycomb" texture (Bucheit and Donovan, 2000).

The percentage of carbonate gradually increases upward through the section until ca. 93 ft (ca. 28 m) above the base of the member, at which point a substantial and persistent tan, quartz-rich sandstone, ca. 4 ft (ca. 1.3 m) thick, interrupts the prevailing trend. This sandstone, which is characterized by parallel lamination and bimodal small-scale trough crossbeds, contains abundant rhyolite pebbles. Above this level, the proportions of carbonate to quartz are approximately equal, until about 140 ft (ca. 43 m) above the base, where the proportion of carbonate increases to ca. 85%.

The contact between the Honey Creek and Fort Sill is placed at 146 ft (ca. 45 m) above the base of the upper member of the Honey Creek Formation, where a distinctive purple hardground heralds the domination of lime mud in the sequence. Although this hardground is only about 1 in. (ca. 2.5 cm) thick, it can be traced across the width of outcrop at Bally. The hardground

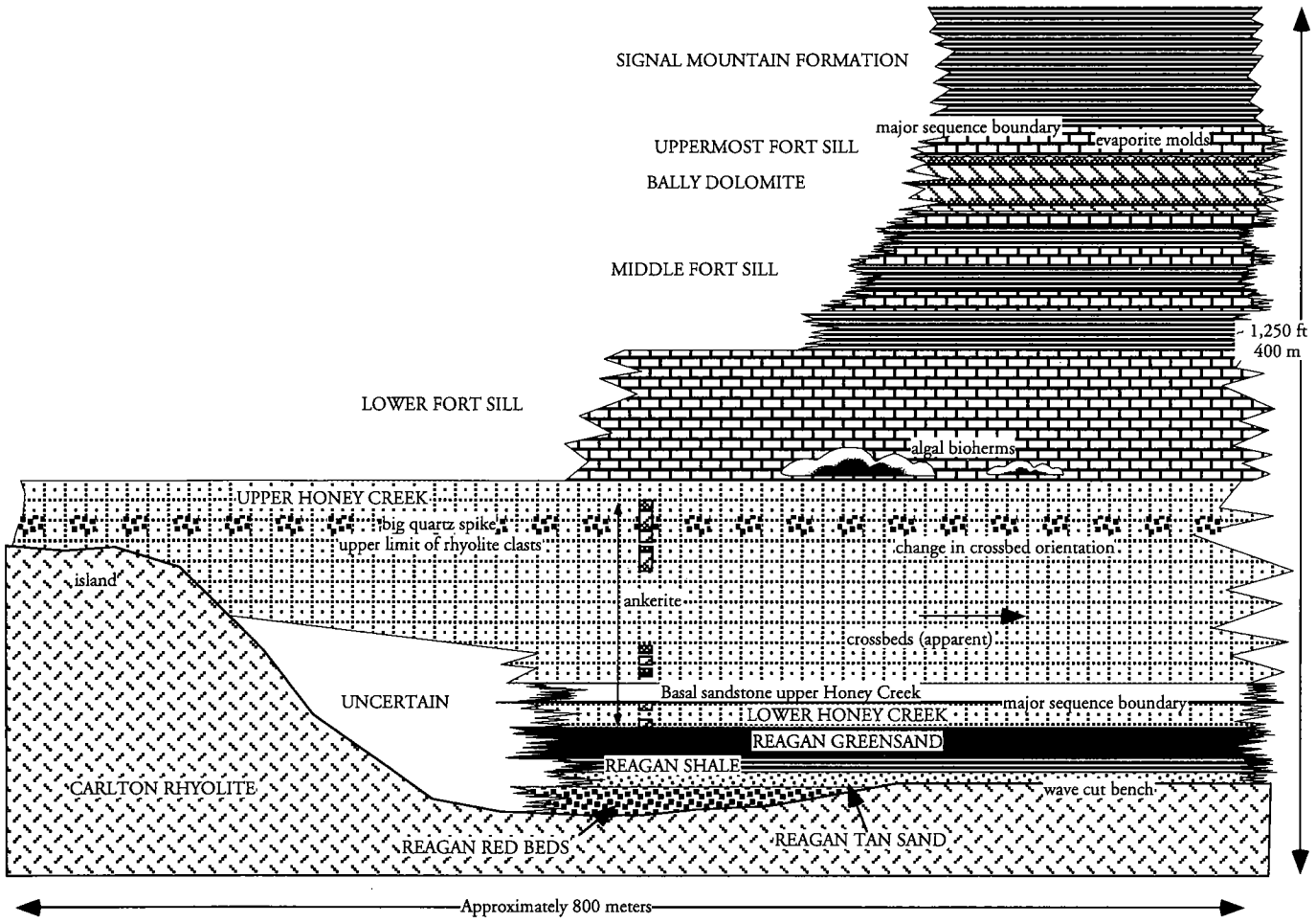

Figure 2. Cross section showing the field relationships at the unconformity between the Carlton Rhyolite and the Paleozoic sedimentary section in the Bally Mountain Range, Slick Hills, Oklahoma. Figure not to true scale.

surface is associated with disseminated hematite, glauconite, and phosphate, and it has formed a growth platform for pelmatozoans and the alga *Renalcis* (Fig. 4). Overlying strata in the Fort Sill Formation display a variety of mud-supported bioclastic textures, more hardgrounds, some stromatolites and a distinctive mud-mound buildup at 20 ft (ca. 6 m) above the base of the formation. Although the presence of lime mud brings a distinctive regular order to the outcrop, many petrographic features of the Honey Creek Formation persist into the Fort Sill, including detrital quartz, glauconite, and *Lingula* valves.

Four additional petrographic features in the section require comment.

1. Rhyolite pebbles, most of which are angular, are found up to the level of the distinctive sandstone at ca. 93 ft (ca. 28 m). This level is a few feet above the presently exposed "top" of the adjacent rhyolite island, suggesting that this "top" may be close to the "real" summit of the island. Twelve pebbly levels are present, but only in the highest (93-ft, ca. 28-m) level are the pebbles obviously associated with thicker siliciclastic accumulations. An inference is that, with the exception of this uppermost occurrence, the input of rhyolite clasts was independent of both the input of carbonate and siliciclastic grain populations.
2. From 114 to 127 ft (ca. 35–39 m) above the base of the member, the variety and grain size of the siliciclastics increase markedly. Granules and very coarse grains of quartz, feldspar, and granophyre, up to 5 mm in diameter, are scattered throughout the section, and a bimodal grain population of siliciclastics is present. This occurrence, the "Big Quartz Spike," has been interpreted as a record of tectonic activity that rejuvenated geomorphic relief in the area and led to exposure and erosion of the Wichita granites (Jusczuk and others, 1999).
3. Widespread and (in some cases) complete replacement of calcite by ankerite has taken place at several horizons, notably: (1) from 15 to 30 ft (ca. 4.5–9 m); (2) above and below the "93 ft sandstone," from 90 to 104 ft (ca. 27–32 m); and (3) associated with the "Big Quartz Spike," from 105 to 125 ft (32–38 m). The ankerite completely obliterated preexisting carbonate textures (Fig. 5). Ankerite

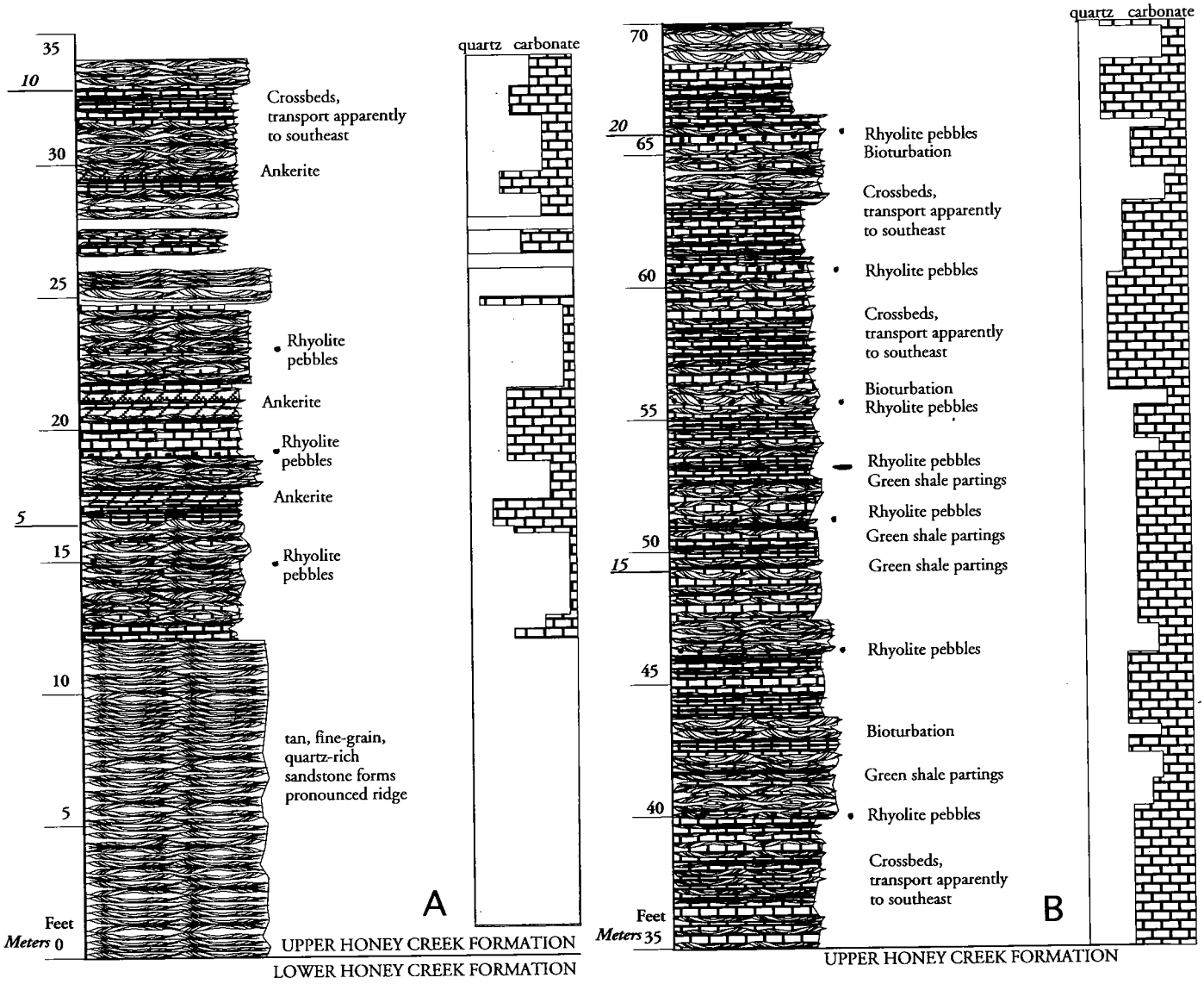

Figure 3 *(above and following pages).* Detailed log (A–E) of the upper member of the Honey Creek Formation and the lowest part of the Fort Sill Formation at Bally Mountain. See Figure 3E for explanation of symbols.

is also present as late cement in variable amounts throughout the section. Both varieties of ankerite are coarse grained and xenotopic and show extinction partitioning within individual crystals. This partitioning may reflect the deep-burial history of the sequence—approximately 12,000 ft (ca. 3,650 m) for almost 200 million years. In general, the abundance of ankerite must reflect the widespread availability of iron in the diagenetic environment. The timing of and mechanism of formation of the mineral, however, are uncertain. Given the general transgressive setting, precipitation from modified seawater seems likely. In most cases ankerite zones are loosely tied to horizons of change—e.g., at (2) and (3) above—and at the base and top of the lower member of the Honey Creek Formation, as noted in a previous section. It can be argued that these "horizons of change" may coincide in one way or another with periods of flushing of the continental land surface.

4. In marked contrast to the Reagan Formation, very little detrital clay occurs in the section—just a few thin layers of green illitic shale.

Sedimentary Structures

The upper member of the Honey Creek is characterized by the distinctive "wavy"-bedded weathering profile (Bucheit and Donovan, 2000) that has resulted from diagenetic modification of a mixed siliciclastic-carbonate sandstone texture. The siliciclastic sandstones are composed of fine- to medium-grained quartz (about 70–80%), fine-grained glauconite peloids, most of which show signs of abrasion (about 5–15%), and

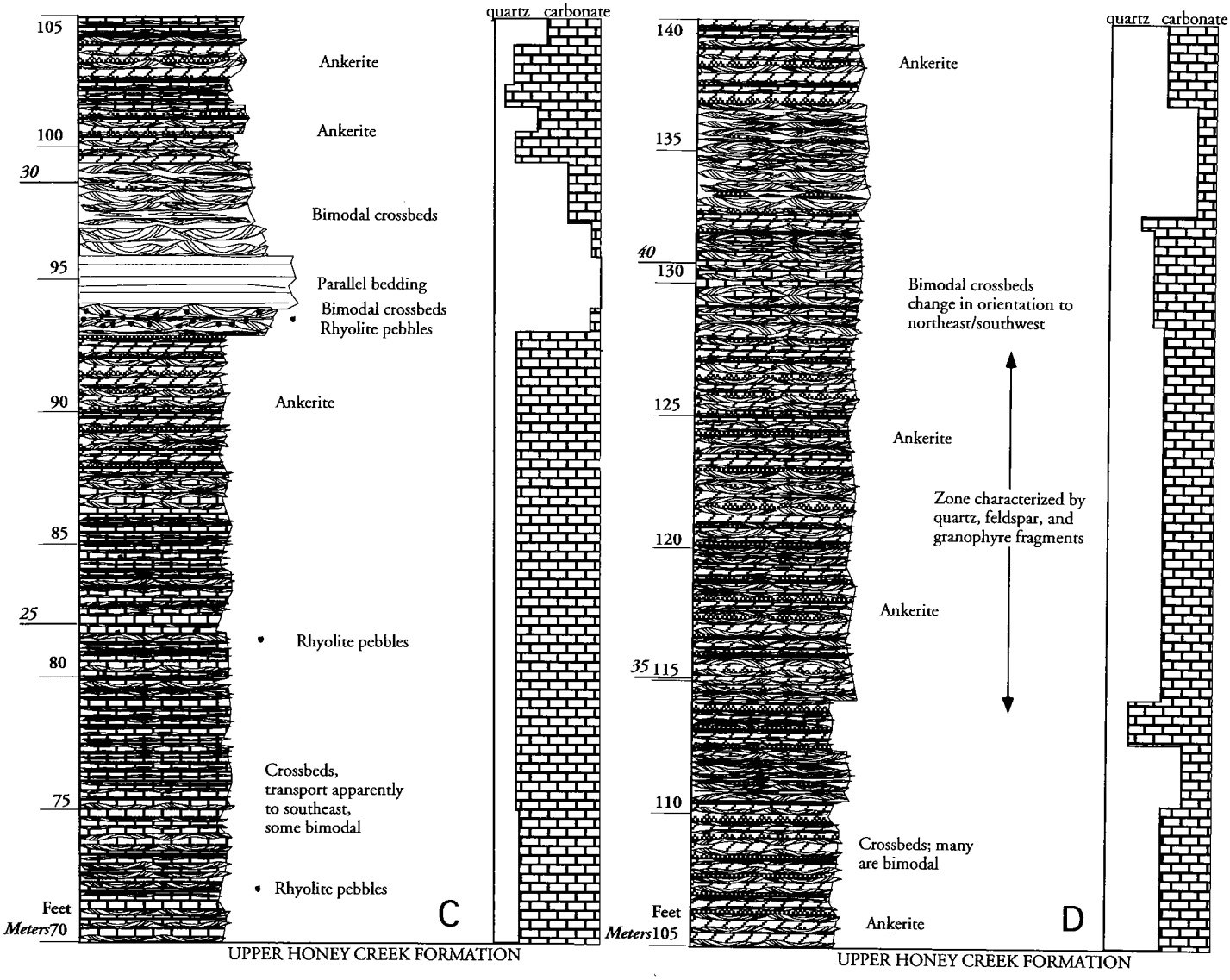

Figure 3 *(continued).*

subordinate fresh feldspar (microcline, orthoclase, and plagioclase) and phosphatic brachiopod fragments (Fig. 6). The carbonate sandstones are dominated by coarse-grained (up to 5 mm) pelmatozoan clasts but contain subordinate trilobite and brachiopod fragments (both calcareous and phosphatic) and glauconite peloids (Fig. 7). Although some mixing of the two grain populations has taken place, discrete layering of the two lithologies can be observed at the millimeter scale.

Each sandstone type is typified by parallel lamination and small-scale (up to 3 in., ca. 7.5 cm) trough crossbedding, some of which display herringbone patterns (Fig. 8). Some of the coarser pelmatozoan accumulations, however, display no clear evidence of primary internal structure. To some extent, the primary bedding fabric has been disturbed by horizontal burrowing and, more comprehensively, by differential compaction. This differential compaction is due to rapid cementation of the pelmatozoan grains by syntaxial calcite. Consequently, they were lithified before the quartz sands were and functioned as rigid plates during compaction of the sequence. The templating of calcite by pelmatozoans in some of these rocks was so effective that the minus cement porosity of the rock exceeds 50%. One result of this early cementation is that single-set carbonate ripple marks may resemble lenticular nodules; this resemblance is further enhanced by differential pressure solution of the carbonate at the contact with the enveloping siliciclastics.

Depositional Environment

Analysis of the unusual bipolar character of the sequences suggests that the depositional environment was a shallow-marine setting in which there was insufficient energy to comprehensively mix the available sediment. The coarse-grained fragments of pelmatozoans appear to have responded as a discrete grain population, hydraulically partitioned from the finer silici-

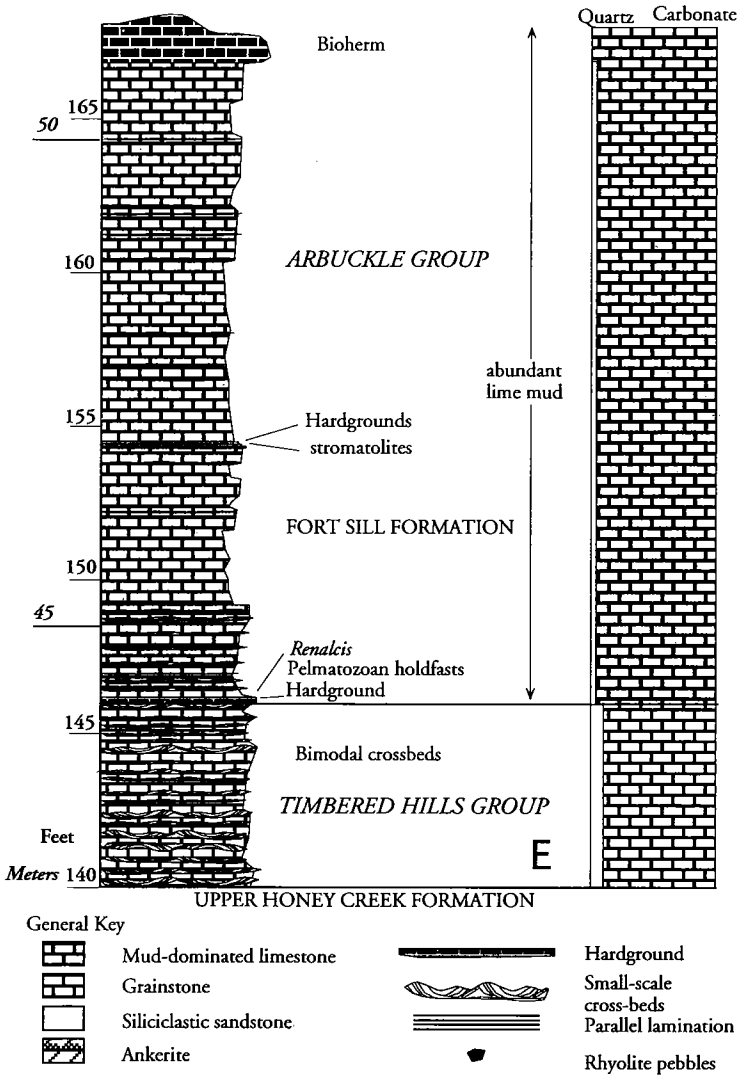

Figure 3 *(continued).*

clastics. In this context, it is pertinent that some of the pelmatozoan fragments were too coarse to be involved in small-scale ripple-mark generation and may well have accumulated as small lags, the initial lenticular shape of which was essentially a mold of the underlying rippled surface. The rocks display a tidal imprint, as evidenced both by the herringbone bimodal nature of some of the crossbeds and by their internal detail, in the form of cross-lamination spacing that is compatible with the influence of neap and spring tides (Nio and Yang, 1989). However, none of the tidal sandbars with large-scale crossbeds exist that are commonly seen in the Reagan Formation (Donovan, 1986). Nor is there much evidence of storm-controlled deposition.

The evidence suggests that the "Honey Creek" environment was an open shelf to which the supply of siliciclastics was gradually cut off. Tidal and meteorologic energy initially was sufficient to prevent stabilization of the bottom, particularly as the siliciclastics were slow to lithify (see subsequent discussion). In essence, the beginning of "Fort Sill"—i.e., "Arbuckle-style"—deposition marks the moment when the sea bed stabilized sufficiently to allow both (1) colonization of the sea bed by organisms (particularly algae) that produced large amounts of lime mud, and (2) the widespread development of hardgrounds. These events followed as a consequence of the continuing Late Cambrian transgression and the increasing inundation of the Laurentian craton.

Although evidence of burrowing is present, bioturbation was not intense enough to destroy most primary stratification. It seems likely that the detrital sands (of either type) either yielded limited nourishment and/or were too unstable for continued occupation by the available Cambrian infauna.

Sources of Sediment

The general asymmetry recognized in the upper member of the Honey Creek Formation throughout the Slick Hills is the decrease in the amount of siliciclastics upward through the sequence. Making allowances for the exceptions noted in the preceding section, this siliciclastic grain population is generally fine grained and well sorted. This is in notable contrast to the underlying Reagan Formation and lower member of the Honey Creek Formation, where grain size is considerably coarser.

The petrography of the grain population (dominantly quartz with subordinate feldspar and trace rhyolite) is not compatible with a local source (i.e., the Carlton Rhyolite). We suggest that the grains were transported into the area by trade winds blowing off the Laurentian continent. This argument is supported by the location of the Slick Hills area a few degrees south of the Late Cambrian equator on the lee side of the continent with respect to wind-circulation patterns. We further suggest that the siliciclastics accumulated as eolian dunes on an exposed land surface during the preceding (post-lower–pre-upper Honey Creek) regression and were then reworked as marine sediments when the overall transgression recommenced (Fig. 9). Likely wind patterns suggest that longshore transport was significant. It is pertinent that grain size does not show an upward decrease through the section, suggesting that winds continued to deliver siliciclastics to the area even though the grains had farther to travel and were increasingly "diluted" by carbonates.

Most of the carbonates in the section are fragments of pelmatozoans, which were sessile organisms that require a stable substrate. Such substrates are not preserved in this sedimentary section but are preserved around the islands of the southern Oklahoma archipelago where they take the form of rhyolite rock surfaces and various localized hardgrounds developed in island-tied facies (Donovan and Rafalowski, 1984; Szabo and Donovan, 1999). Donovan (1986) suggested that the islands and similar rock-girded coastlines were surrounded by "meadows" of pelmatozoans, and that

Figure 4. Photomicrograph (ordinary light) showing the irregular hardground proposed as the local base of the Arbuckle Group at Bally Mountain. The most conspicuous feature is a pelmatozoan holdfast that is anchored on a protrusion of the hardground. The hardground surface is erosional; an eroded fragment of *Renalcis* is visible to the left of the pelmatozoan (below the hardground surface), and another specimen of the same alga coats the upper surface of the holdfast. To the left of the holdfast, sediment above the hardground consists of a poorly sorted mix of pelmatozoan fragments, fine-grained quartz and lime mud. Field of view is ca. 12 mm across.

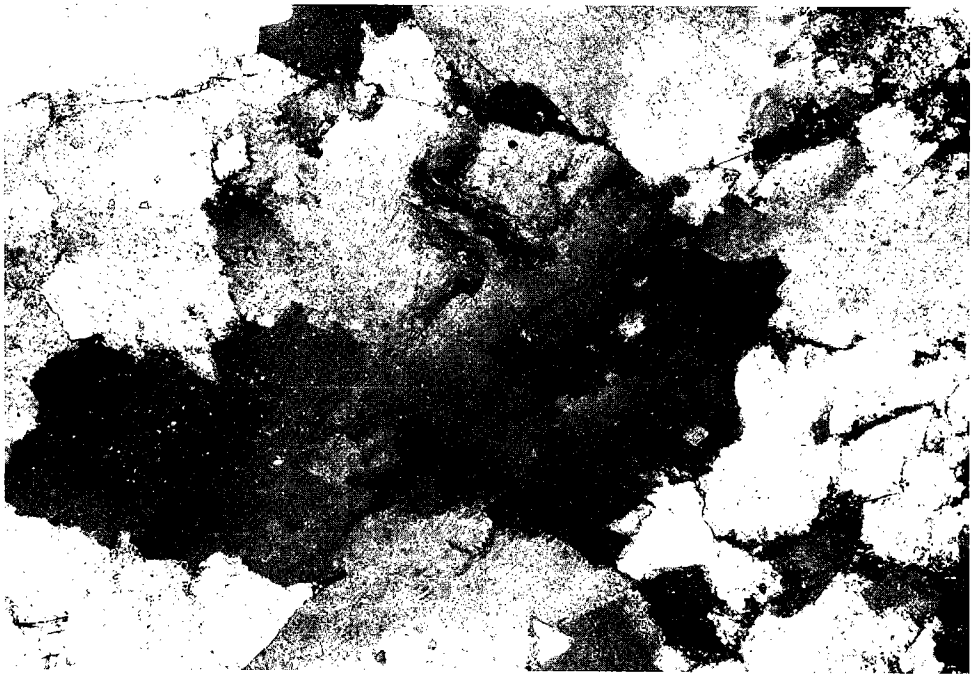

Figure 5. Photomicrograph (polarized light) of coarse-grained ankerite replacement of calcite from the "Big Quartz Spike" section, showing mostly anhedral boundaries and slightly strained extinction, with some discrete strain partitioning in individual crystals. Field of view ca. 3 mm across.

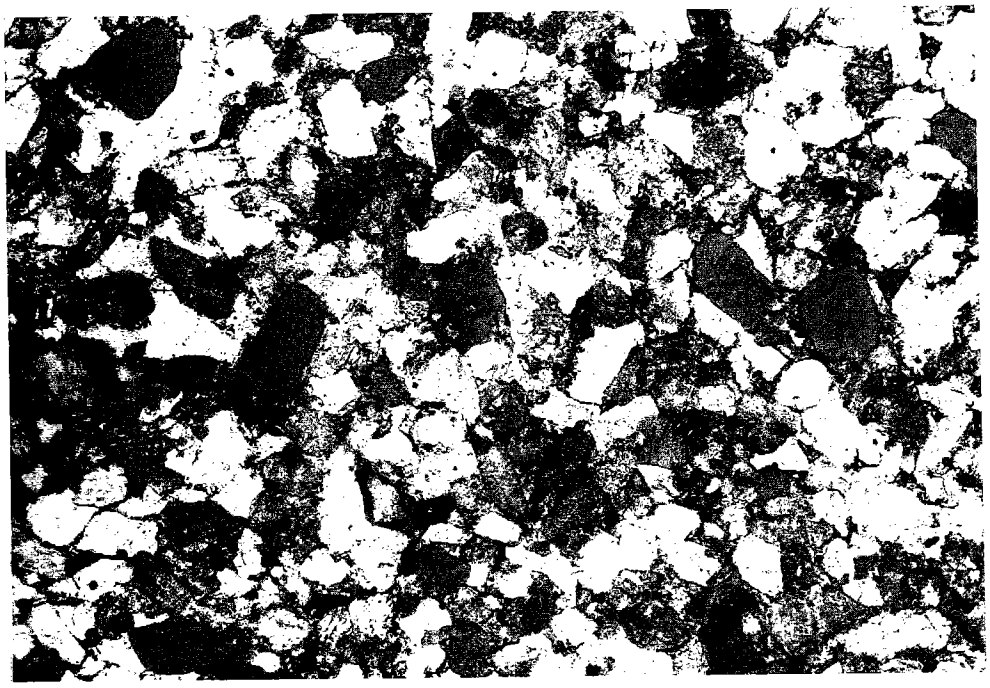

Figure 6. Photomicrograph (ordinary light) showing a characteristic fine- to medium-grained siliciclastic sandstone containing mostly angular quartz (white) and glauconite (medium grey). The sandstone was well compacted before cementation by ferroan calcite—seen as dark grey crystals—that forms no more than 5% of the rock. Field of view ca. 3 mm across.

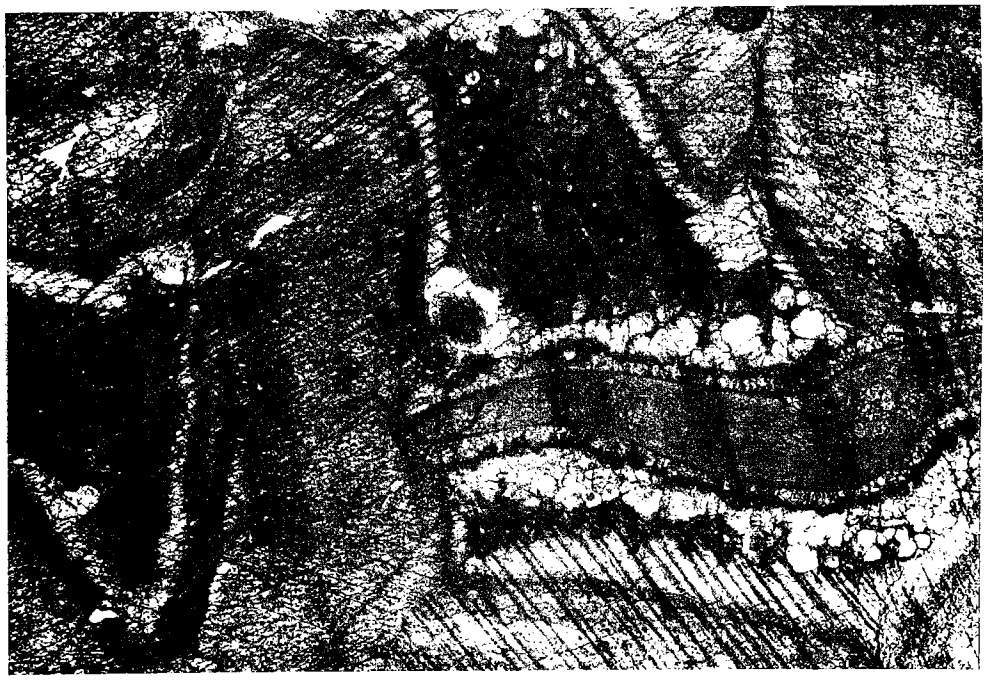

Figure 7. Photomicrograph (ordinary light) showing a characteristic pelmatozoan grainstone. A sinuous fragment of a trilobite is coated by an isopachous fringe of small calcite crystals; the rest of the rock consists of syntaxial overgrowths of calcite on pelmatozoan fragments (difficult to see). This cement shows a compositional zoning (due to the incorporation of ferrous iron into the lattice) that has been highlighted by staining. The youngest cements are the most iron rich (dark grey in the picture). The sandstone was cemented very quickly after deposition—there was no significant compaction prior to cementation. The minus cement porosity in this view is ca. 55%. Field of view ca. 3 mm across.

Figure 8. Outcrop photograph of the upper member of the Honey Creek Formation at the 110-ft (ca. 36-m) level showing characteristic small-scale crossbedding of pelmatozoan-rich grainstones (light) and siliciclastics (darker and in relief).

these meadows were the principal source of carbonate grains for both members of the Honey Creek Formation. Other carbonate organisms—principally trilobites and brachiopods—presumably lived in these meadows, and their detritus was similarly distributed by waves and tides.

Glauconite peloids are found throughout the section but are less commonly encountered in the basal sandstone. Their origin is uncertain, but their occurrence shows a positive correlation with that of phosphatic brachiopod fragments. Alternatively, they may be the fecal products of trace-fossil organisms.

Sequence of Events at Bally

Within the overall record of transgression outlined herein, certain specific features of the section require some comment. The thick basal sandstone is by far the thickest siliciclastic unit in the section and presumably represents the "purest" reworked product of the dune system that had accumulated during the preceding regression. This interpretation is supported by the lower-than-usual content of glauconite peloids in the deposit—i.e., this sandstone was less "diluted" by authigenic marine bioclasts.

The thick siliciclastic sandstone at ca. 93 ft (ca. 28 m) above the base of the member may be a regressive unit with characteristics similar to the basal sandstone. An alternative explanation is that it records a change in the local geography associated with the burial of the Bally rhyolite island. As noted, the highest occurrence of rhyolite pebbles in the section is seen in this sandstone. Further support for this suggestion is provided by a change in the orientation of crossbeds at this point. Although the quality of the exposure is not compatible with precise crossbed-orientation measurements, the apparent movement of sediment below the "93-ft level" was consistently to the southeast (using today's geographic directions) away from the island. This direction also is seaward from the Laurentian craton, suggesting that the island (for as long as it existed) impeded sediment movement off of the continent. Upward from the "93-ft level," crossbeds generally are more variable in their orientation and herringbone crossbeds are much more common, suggesting that tidal flow was no longer impeded or controlled by the local topography. The "Big Quartz Spike" (Jusczuk and others, 1999) has been discussed previously; it is worth noting that it is located within the upper part of the section and clearly indicates that sediment transport paths were geographically diverse at this time.

Diagenetic Imprint

Some aspects of the diagenesis of the sequence have been discussed previously. In essence, the story is one of the timing and nature of carbonate cementation. Although some syntaxial quartz cement is present in the basal sandstone, it is quantitatively minor. The earliest carbonate cement was nonferroan calcite, most of which nucleated on pelmatozoan fragments as syntaxial overgrowths. In addition, small, isopachous, nonferroan-calcite crystals coated trilobite and brachiopod fragments. Subsequent calcite tends to be increasingly ferroan. Some of these syntaxial overgrowths show two or three alternating zones of ferroan and nonferroan calcite. The final cementation was by ankerite, and comprehensive replacement of all the carbonate by ankerite took place within the grainstones in some parts of the section. By contrast, cementation of the siliciclastics involved sparry ferroan calcite; this sparite appears to have precipitated relatively late in the perigenesis in that it postdated significant compaction.

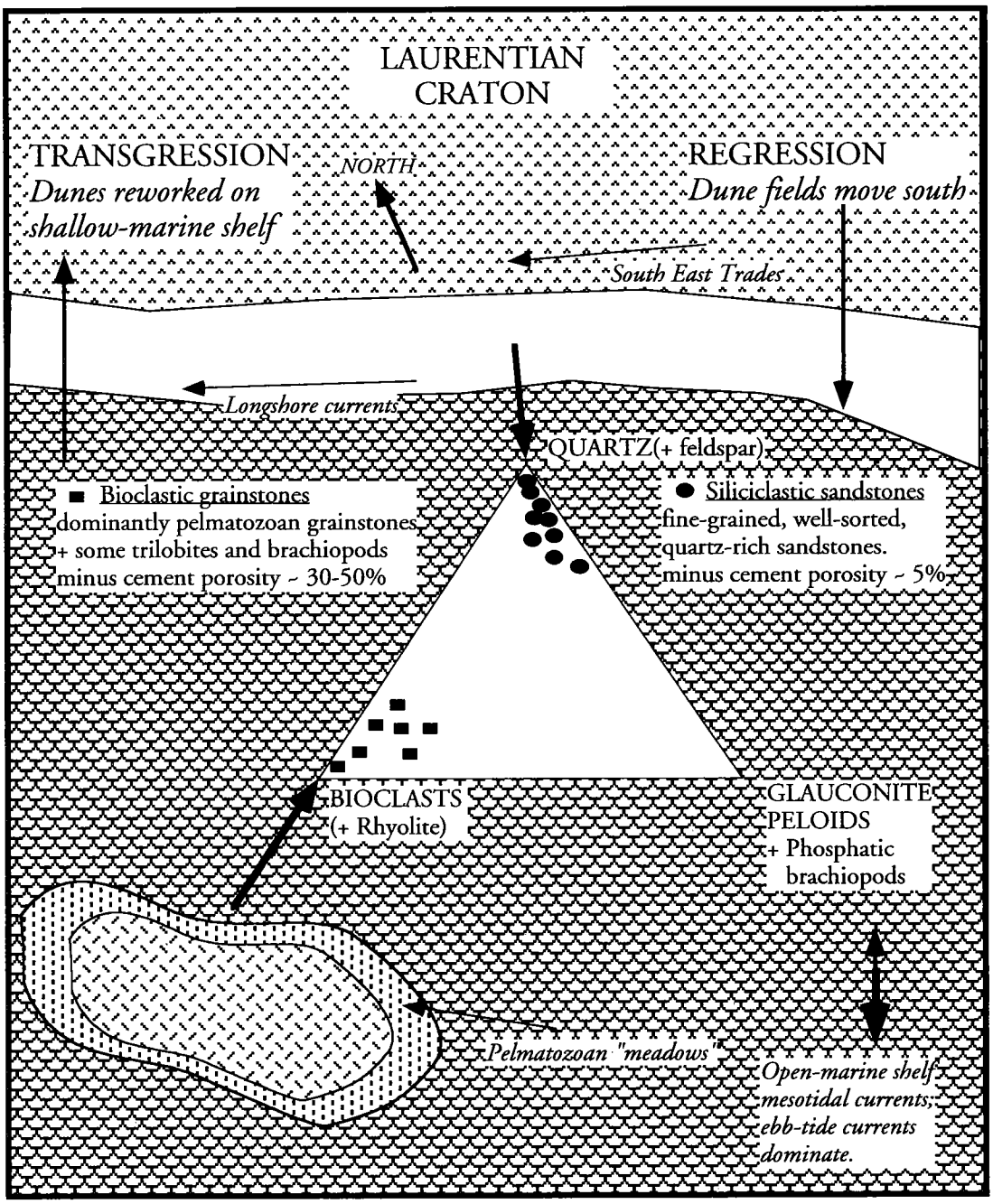

Figure 9. Depositional model illustrating major factors operating during the deposition of the upper member of the Honey Creek Formation.

In summary, early diagenesis records burial beneath a transgressive sea in which carbonate saturation was partitioned and templated by pelmatozoan fragments. Because iron was abundant on the continental land surface, the iron content of cements and replacement minerals was high. The ankerite essentially occupies a diagenetic niche that would normally be occupied by dolomite. It seems likely that most cementation was from modified marine waters of increasingly reducing character. The principal later diagenetic imprint involved pressure solution of carbonates during Paleozoic burial when the section was buried to a depth of ca. 12,000 ft (ca. 3,650 m) for almost 200 million years.

ACKNOWLEDGMENTS

We would like to thank the Fort Worth Geological Society, Adkins Fund of Texas Christian University, Houston Geological Society, Mobil Foundation, and the Moncrief family of Fort Worth for their generous financial support. Sincere appreciation is expressed to the Kindblade family, Earl Davis, and Ricky Clerk for permitting us access to the site.

REFERENCES CITED

Bucheit, A. K.; and Donovan, R. N., 2000, Initiation of a carbonate platform: a comparison between the Lower Jurassic Broadford Limestone, Isle of Skye, Scotland, and the Cambrian Honey Creek Limestone, Slick Hills, Oklahoma, *in* Johnson, K. S. (ed.), Platform carbonates in the southern Midcontinent, 1996 symposium: Oklahoma Geological Survey Circular 101, p. 57– 64.

Chow, N.; and James, N. P., 1987, Cambrian Grand Cycles: a northern Appalachian perspective: Geological Society of America Bulletin, v. 98, p. 418–429.

Cloyd, Kelly; Donovan, R. N.; and Rafalowski, M. B., 1986, Ankerite at the contact between the Reagan Sandstone and the Honey Creek Limestone (Timbered Hills Group), *in* Donovan, R. N. (ed.), The Slick Hills of southwestern Oklahoma—fragments of an aulacogen?: Oklahoma Geological Survey Guidebook 24, p. 17–20.

Donovan, R. N., 1986, The geology of the Slick Hills, *in* Donovan, R. N. (ed.), The Slick Hills of southwestern Oklahoma—fragments of an aulacogen?: Oklahoma Geological Survey Guidebook 24, p. 1–12.

_____ 2000, Initiation of the Arbuckle platform—view from the Slick Hills, Oklahoma, *in* Johnson, K. S. (ed.), Platform carbonates in the southern Midcontinent, 1996 symposium: Oklahoma Geological Survey Circular 101, p. 47–56.

Donovan, R. N.; and Bucheit, A. K., 2000, Marine facies and islands in the Reagan Sandstone (Upper Cambrian) in the Slick Hills, southwestern Oklahoma, *in* Johnson, K. S. (ed.), Marine clastics in the southern Midcontinent, 1997 symposium: Oklahoma Geological Survey Circular 103 [this volume], p. 25–37.

Donovan, R. N.; and Rafalowski, M. B., 1984, The anatomy of an Early Cambrian shell bank in the Honey Creek Formation, southwestern Oklahoma [abstract]: Geological Society of America Abstracts with Programs, v. 16, no. 2, p. 82.

Donovan, R. N.; Ragland, D. A.; Cloyd, Kelly; Bridges, Steve; and Denison, R. E., 1986, Stop 2: Geological highlights of the Bally Mountain area, *in* Donovan, R. N. (ed.), The Slick Hills of southwestern Oklahoma—fragments of an aulacogen?: Oklahoma Geological Survey Guidebook 24, p. 92–95.

Jusczuk, S. J.; Trice, David; Walters, M. C.; and Donovan, R. N., 1999, On granophyre fragmants and variations in siliciclastic grain size—a possible late Cambrian tectonic spike in the Slick Hills of southwestern Oklahoma. The Compass, Journal of Earth Sciences, Sigma Gamma Epsilon, v. 74, no. 4, p. 125–132.

McElmoyl, Courtney; and Donovan, R. N., 2000, Unconformity in the lower part of the Cambrian Honey Creek Limestone, Slick Hills, Oklahoma: candidate for a Grand Cycle boundary, *in* Johnson, K. S. (ed.), Platform carbonates in the southern Midcontinent, 1996 symposium: Oklahoma Geological Survey Circular 101, p. 65–78.

Nio, S. D.; and Yang, C. S., 1989, Recognition of tidally influenced facies and environments: Short Course Note Series #1, International Geoservices BV, Leiderdorp, The Netherlands, 230 p.

McLish Formation—Influence of "Ames Crater" on Reservoir Lithofacies and Petrophysical Characteristics?

Michael D. Kuykendall
Solid Rock Resources, Inc.
Tulsa, Oklahoma

The McLish Formation of Oklahoma is the middle formation of the Simpson Group (Whiterockian Series, Chazyian Stage), which consists of the Bromide, Tulip Creek, McLish, Oil Creek, and Joins Formations, in ascending order. The McLish Formation consists of both widespread transgressive and locally regressive, shallow-marine sequences deposited following the initial transgression of the Tippecanoe Sequence.

Detailed reservoir characterization of the Ames impact structure ("Ames crater") in Major County, Oklahoma, synthesis of petrographic descriptions of the McLish and other Simpson Group units from the literature, and integration of recent biostratigraphic and lithostatigraphic information from the buried impact crater, led to the development of the following working hypothesis. Exposure, weathering, and reworking of the lithofacies of the Ames crater provided a local point-source of the apparently anomalous detrital grains, fragments, and finer constituents noted in the McLish sandstones. This interpretation may help explain lithologic and mineralogic differences and apparent provenance discrepancies, as well as petrophysical anomalies, in portions of the McLish, as compared with other formations of the Simpson Group, in areas of central Oklahoma and the Anadarko basin. Several lines of evidence supporting a McLish-age episode of crater filling and exposure include: (1) conodont age constraints (middle Simpson Group; McLish–lower Bromide Formations) of the crater-filling shales (Repetski, 1997); (2) biostratigraphic recognition of a major regional unconformity in southern Oklahoma between the Oil Creek and McLish Formations interpreted to be the Sauk-Tippecanoe Sequence boundary (Derby and others, 1991); and (3) regional lithostratigraphic correlations revealing the onlapping and/or unconformable relationship of the middle lower Simpson with Arbuckle Group rocks on the northern shelf of the Anadarko basin.

The reservoir lithofacies of the Ames crater primarily include: (1) ejecta/fallout dolomite micro- and megabreccias of the Arbuckle Group; (2) devitrified, pseudopyroclastic, impact-melt rocks containing shocked quartz; (3) and centrally rebounded and ejected granodiorite (micro- and mega-breccias) derived from basement rocks of the Central Oklahoma Granite Group. Lithologic and mineralogic variations in the sandstone (McLish) directly overlying the crater-filling shales (originally believed to be Oil Creek) and in the McLish in other parts of Oklahoma contrast to other compositionally mature quartzarenites of the Simpson Group. These contrasting features include: (1) relatively high percentages (up to 15%) of equant to subangular feldspar (plagioclase and orthoclase) grains (granodiorite-derived?); (2) higher than normal concentrations of iron minerals (pyrite and limonite); (3) a relative increase in amounts of illitic and chloritic clay (detrital and authigenic) and "heavy minerals"; (4) angular to tabular and rounded black "shale"? particles (which may actually be mafic-rock [diabase] fragments, also observed in granodiorite breccia rocks from the Ames crater, suggesting either the presence of a local diabase dike within the rebounded and ejected basement rocks, or possibly even fragments of an achondritic meteorite, the impact of which created the Ames structure); (5) aggregates of dolomite crystals (detrital dolomite?); (6) interbedded reddish-maroon shales among otherwise green to greenish-gray shales; and (7) sand-size grains/spheres of partially to completely devitrified (silicified) glass (microtektites?) in the vicinity of the Ames impact structure.

Integration of the combined lithostratigraphic and biostratigraphic information supports the working hypothesis that the Ames structure was formed by meteor impact in Sauk (pre-Tippecanoe) Sequence rocks, presumably in truncated, southward-dipping (basinward), dolomites of the upper Arbuckle Group (West Spring Creek Formation) that were subaerially exposed in a regional shelfal position (possibly as late as Joins–Oil Creek time). Deposition of thin Oil Creek marine muds and silts may have occurred subregionally around the exposed and relatively high-relief impact crater, making subsurface differentiation between marine shales of the Oil Creek (Sauk Sequence) and McLish (Tippecanoe Sequence) shales very difficult without biostratigraphic control. The exposed, eroded, and karstified crater subsequently was inundated and filled with organic-rich, McLish-age, marine muds and silts (primary source rocks) during the initial marine transgression of the Tippecanoe Sequence. Then, this structure was completely (?)

Kuykendall, M. D., 2000, McLish Formation—influence of "Ames crater" on reservoir lithofacies and petrophysical characteristics?, *in* Johnson, K. S. (ed.), Marine clastics in the southern Midcontinent, 1997 symposium: Oklahoma Geological Survey Circular 103, p. 51–52.

buried by a sandy shallow-marine shoreface complex, which is quite thin (<10 ft) along the crater rim, but thickens to nearly 100 ft in the area over the crater floor.

An awareness and understanding of potential impact-influenced McLish lithofacies should provide an alternative explanation of provenance for the subtle mineralogic differences observed between the McLish and other Simpson sandstones, lead to refinement of regional Lower and Middle Ordovician stratigraphy, and provide a better understanding of petrophysical anomalies associated with many McLish reservoirs, which in turn should create new strategies for hydrocarbon exploration.

Lithology and Cyclicity in Middle Ordovician McKee Sandstone Member (Tulip Creek Formation, Simpson Group) in the Tobosa Basin, Southeast New Mexico and West Texas

Michael J. Bosco and Jim Mazzullo
Texas A&M University
College Station, Texas

ABSTRACT.—The lower Paleozoic rocks deposited on the inner craton of North America are characterized by thick sections of carbonate rocks separated by thin units of sandstones and shales. The origins of these sandstones are poorly understood, but it is generally agreed upon that they were deposited in a nearshore environment during a relative highstand in a shallow epicontinental sea. One of these sandstones, the McKee Sandstone Member (Tulip Creek Formation, Simpson Group), attains a maximum thickness of approximately 230 ft in the Tobosa basin and appears to be abnormally thick to have been deposited during a single sea-level–highstand event. We conclude that the McKee was deposited as a result of several smaller progradational highstands and transgressions as opposed to a single, higher-order highstand. Changes in quartz sand grain size and percentage of clay and carbonate composition accompanied by sharp breaks and repetition in facies delineate this cyclicity.

The McKee Sandstone consists largely of sandstones, muddy sandstones, and sandy mudstones. The sandstones are generally subquartzose to quartzose (50–100%), moderately well sorted and very fine to fine grained. Very fine to medium-sand–sized detrital collophane is occasionally common (<16%), as are fossils, but feldspars in the McKee are sparse (<2%), making the McKee sandstones overall quartzarenites. Medium sand to cobble-gravel–sized, rounded to well-rounded, mudstone lithoclasts are locally abundant and commonly deformed.

Four facies can be distinguished in the McKee Sandstone Member based on sediment lithology and sedimentary structures. Cyclic breaks in lithology occur above tidal-flat or tidal-channel facies (facies 3 and 4, respectively) at the maximum flooding surface. Above the maximum flooding surface lies the most-basinward facies, either the inner-shelf facies (facies 1), or, more commonly the wave-dominated beach facies (facies 2). In general, a sequence in the McKee Sandstone Member consists of the most-basinward facies overlain by progressively landward facies. A composite sea-level curve showing this cyclicity can be extrapolated from this information.

INTRODUCTION

The lower Paleozoic rocks deposited on the inner craton of North America are characterized by thick sections of carbonate rocks separated by thin units of quartzose sandstones and shales that were deposited during a relative sea-level highstand (Wilson, 1975). The origins of these sandstones are poorly understood, but it is generally agreed upon that they were deposited in a nearshore environment in a shallow epicontinental sea. One of these quartzose sandstones, the McKee Sandstone Member (Middle Ordovician), was first recognized as the basal member of the Tulip Creek Formation in the carbonate-dominated Simpson Group of west Texas by the West Texas Geological Society in 1941 (Cole and others, 1942). Until the present day, this is the only published material specifically on the McKee Sandstone.

Two other quartzose sandstones are recognized in the basal parts of other formations of the Simpson Group: the Connell Sandstone Member of the Joins Formation (Schweers, 1949), and the Waddell Sandstone Member of the McLish Formation (Cole and others, 1942). No further specific research has been published on the Connell or the Waddell Sandstone Members.

The McKee Sandstone Member is the basal subdivision of the Tulip Creek Formation of the Simpson Group and rests directly on the McLish Formation. The McKee consists of quartzose sandstones with a complex

Bosco, M. J.; and Mazzullo, Jim, 2000, Lithology and cyclicity in Middle Ordovician McKee Sandstone Member (Tulip Creek Formation, Simpson Group) in the Tobosa basin, southeast New Mexico and west Texas, *in* Johnson, K. S. (ed.), Marine clastics in the southern Midcontinent, 1997 symposium: Oklahoma Geological Survey Circular 103, p. 53–64.

mineralogy of matrix and cements, separated by and intermixed with sandy mudstones and carbonates. The McKee has a maximum thickness of approximately 230 ft and appears abnormally thick to have been deposited during a single sea-level highstand event on the cratonic interior in an area of little relief.

The purpose of this study is to correlate sea-level fluctuations with the lithology of the McKee Sandstone in the Tobosa basin of southeast New Mexico and west Texas (Fig. 1). Materials examined include conventional cores (Fig. 2) for determination of bedding characteristics, core samples for petrological and grain-size analysis, as well as other information. In addition, this study will attempt to characterize the petrology and environment of deposition of the McKee Member.

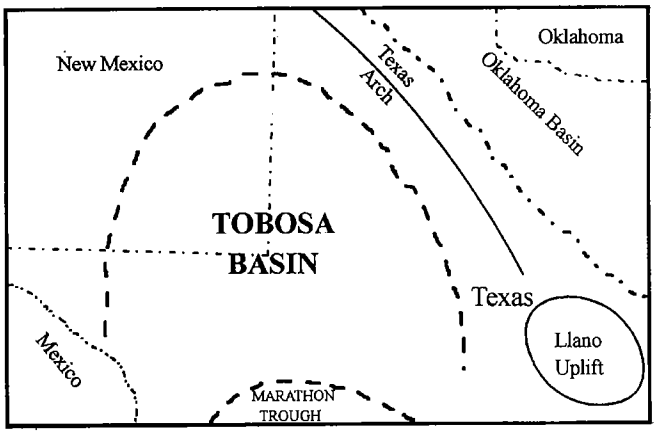

Figure 1. Map of the southwestern United States showing the approximate location of the Tobosa basin and other major features present in the early to middle Paleozoic (modified from Johnson and others, 1988).

CHARACTERISTICS OF THE MCKEE SANDSTONE MEMBER

Lithology

The McKee Sandstone Member consists principally of sandstones, muddy sandstones, and sandy mudstones. The sandstones are generally subquartzose to quartzose (50–100%), moderately well sorted, and very fine to fine grained, and the detrital grains are subangular to rounded when quartz overgrowths are not present. Some well-rounded, medium-grained quartz sand is also present. Very fine to medium sand-sized detrital collophane is occasionally common (<16%), as are fossils, but feldspars in the McKee are sparse (<2%), making the McKee sandstones overall quartz arenites. Medium-grained sand to cobble-gravel–sized, rounded to well-rounded, mudstone lithoclasts are locally abundant and commonly deformed.

The detrital clays in the McKee have a mixed mineralogical composition. Illite tends to be the predominant detrital and authigenic species, but glauconite, berthierine, odinite, kaolinite, smectite, and chlorite clays along with hematite and micrite may also be present.

The authigenic cements in the McKee Sandstone Member are carbonates, clays, and quartz. Pore-filling carbonate cements occur in the forms of crystalline calcite, dolomite, ankerite, and siderite. They can also occur as recrystallized micrite and recrystallized fossils. Authigenic clays occur as grain-lining cements.

Finally, the McKee exhibits a wide range of colors and a variable, but generally high, degree of bioturbation. Green sandstones tend to be dominated by glauconite and illite clay, and the lighter-green sandstones, which have less clay, are the most friable. Brown and yellow sandstones tend to have more authigenic quartz cement and are generally clay free. Gray sandstones have abundant carbonate cement and micritic mud, whereas red sandstones have more hematitic clay. Bioturbation tends to mix and mottle these colors in a wide range of proportions.

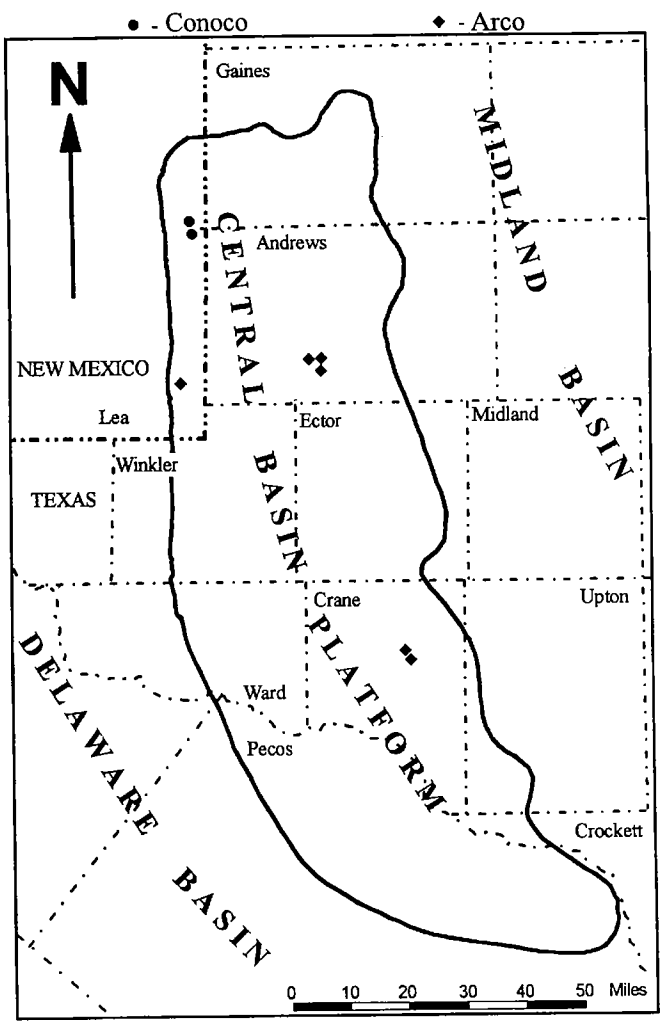

Figure 2. Political map of study area showing core locations and commonly used Permian basin physiographic features.

Facies

Four facies (designated simply facies 1–4) can be distinguished in the McKee Sandstone Member based on sediment lithology and sedimentary structures.

Facies 1

Facies 1 is composed of very thin to thick-bedded, bioturbated, planar-parallel and wavy, nonparallel laminated (Fig. 3), grayish-green to yellow, nonfossiliferous, very fine to fine-grained, muddy quartzose sandstones. It is distinguished from other facies by its (1) abundant detrital clay content, (2) considerably lesser and smaller (generally sand-sized) lithoclasts, (3) sparse fossils, and (4) absence of carbonates, cross-laminae, flasers, mudcracks, and interbedding of mudstone and sandstone (Figs. 4 and 5). The mean detrital grain sizes of the sandstones range from 103 to 169 μm, and their standard deviations from 33 to 115 μm. When plotted on a maximum-entropy histogram (Full and others, 1984), the grain-size data show either relatively even distributions of sizes or negative skewing (Fig. 6A,B). Facies thickness ranges from 3 to 18 ft.

The planar and wavy laminae of facies 1 are commonly 0.1–2.0 cm thick when present, but are commonly convoluted and disrupted by burrows. The laminae are bioturbated to varying degrees. The laminae may be visible despite burrowing, or may be mottled, burrowed, or obliterated and "massive."

The detrital composition of facies 1 is primarily dominated by quartz (62–80% of detrital composition) and detrital clay (20–38% of detrital composition) with lesser amounts of collophane (<9% of detrital composition) and lithoclasts (<10% of detrital composition) (Fig. 7). Where lithoclasts are small enough to be identifiable in thin section, they consist of rounded, medium-grained to coarse-grained, gray to black mudstone, and appear to contain a high concentration of collophane (Fig. 7A,B).

The authigenic-cement content of facies 1 is the least of all four facies (Fig. 8). Quartz cement and carbonates (Fig. 8E,F) are sparse (<1% of total composition), and authigenic clays (Fig. 8A,B) occur only occasionally (<2% of total composition). It is difficult to distinguish pre-Simpson from post-Simpson authigenic quartz overgrowths due to the presence of rounded-quartz overgrowths (Fig. 9). Porosities are consequently the highest for this facies (1–25% of total composition), and rocks of facies 1 are generally the most friable of all four facies.

Facies 2

Facies 2 consists of very thin to medium-bedded, bioturbated, planar-, wavy-, and cross-laminated, yellowish-brown and yellowish-gray, very fine to fine-grained, quartzose sandstones. It is distinguished from other facies by the following: (1) abundance of carbonates, (2) the common lithoclasts and detrital clay, (3) the occasional presence of fossils, (4) the rare occurrence of flasers, and (5) the absence of mudcracks and interbedded mudstone and sandstone. The mean detrital grain sizes of the sandstones range from 113 to 309 μm, and their standard deviations range from 39 to 144 μm. Facies 2 is generally coarser and more poorly sorted then facies 1 and 4 and similar in grain size and sorting to facies 3. When plotted on a maximum-entropy histogram, the grain-size data generally show either bimodal distribution of sizes or positive skewing (Fig. 6C,D). Facies thickness ranges from 0.5 to 20 ft.

Facies 2 is the most bioturbated facies of the McKee Sandstone Member and is generally mottled to burrowed. When the laminae are visible, they are planar, wavy, and from 0.1 to 3.0 cm thick. Once again, the laminae are bioturbated to varying degrees. In some beds, they are visible despite burrowing; in others, they are mottled, in others, they are burrowed; and in others, they are obliterated and the beds are massive.

The detrital composition of facies 2 is primarily dominated by quartz (79–100% of detrital composition), with lesser amounts of detrital clay (<15% of detrital composition), lithoclasts (<15% of detrital composition), and collophane (<12% of detrital composition). The lithoclasts consist of rounded, medium-grained sand to cobble-sized, gray to black mudstone.

The authigenic composition of facies 2 is dominated by carbonates (<39% of total composition), with lesser amounts of authigenic clay (<12% of total composition) and quartz (<9 % of total composition) (Fig. 10). Porosities are the second highest in this facies (0–21%).

Facies 3

Facies 3 consists of very thin to medium-bedded, bioturbated, planar-, wavy-, and flaser-laminated, fossiliferous, green, gray, red, and black, very fine to medium-grained, muddy quartzose sandstones and sandy mudstones with occasional cross-bedding, mudcracks, and dark-gray, rounded, medium-grained sand to cobble-gravel–sized mudstone lithoclasts. It is distinguished from other facies by its abundant detrital clay, lithoclasts, carbonates, fossils, flasers, and interbedded mudstone and sandstone, and common mudcracks. The mean detrital grain size of the sandstones range from 102 to 319 μm, and their standard deviations from 30 to 154 μm. When plotted on a maximum-entropy histogram, the grain-size data generally show either bimodal distribution of sizes or positively skewing (Fig. 6E,F). Facies thickness ranges from 0.4 to 13 ft.

The planar, wavy, and cross-laminae of facies 3 are commonly 0.1–3.0 cm thick when present, but are commonly convoluted and disrupted by burrows. The laminae are bioturbated to varying degrees. They are visible despite burrowing in some beds, or mottled, burrowed, or obliterated with "massive" beds) in others. Mudcracks, when visible, are filled with clean, very well rounded, medium-grained, quartzose sand. The thin nature of bedding of very different lithologies combined with burrows greater in length then individual beds in this facies makes composition unreliable as being indicative of this facies.

The detrital composition of facies 3 is primarily dominated by quartz (21–93% of detrital composition), detrital clay (<74% of detrital composition), lithoclasts (<40% detrital composition), and lesser amounts of collophane (<16% of detrital composition). This facies has the largest amount of lithoclasts seen during core description and in thin section (Fig. 7A,B). In addition,

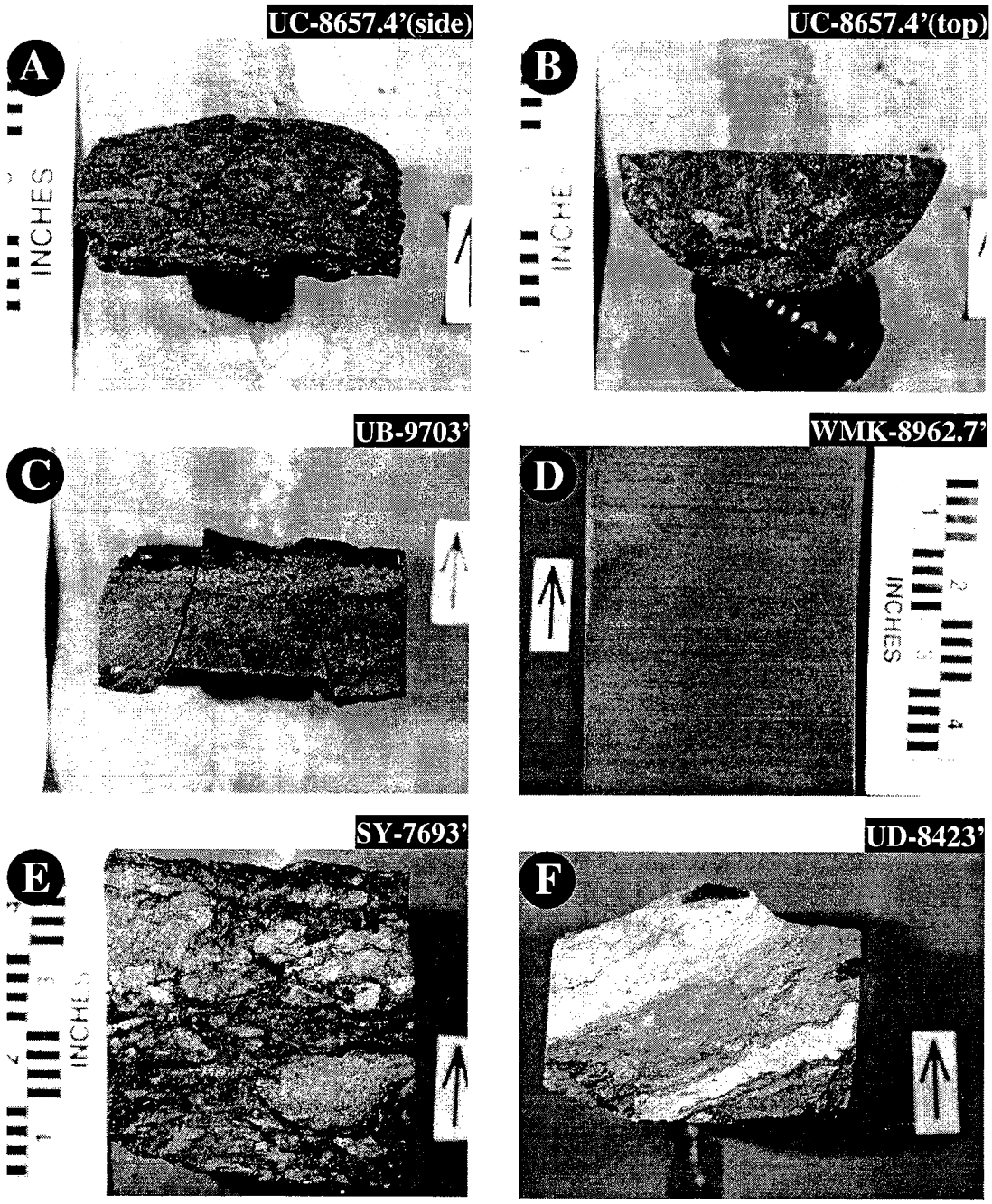

Figure 3 *(above and facing page).* Core photos showing examples of types of bedding, sedimentary structures, and varying degrees of bioturbation in the McKee Sandstone Member: (A) mudcracks (side view), (B) mudcracks (top view), (C) sand stringer, (D) parallel planar laminae, (E) non-parallel wavy laminae, (F) parallel wavy laminae, (G) flaser laminae, (H) cross-laminae, (I) mottled bedding, (J) mottled bedding, (K) burrowed bedding, (L) massive bedding.

this facies tends to contain the highest concentration of collophane pellets per sample.

The authigenic-cement content of facies 3 is dominated by carbonates (<50% of total composition), and authigenic clay (<13% of total composition), with lesser amounts of quartz (<2% of total composition). In general, the lower the detrital clay content, the higher the carbonate content. Porosities are the lowest for this facies (0–9%). Low porosities may be due to its mud and carbonate content, and it is commonly friable.

Facies 4

Facies 4 consists of very thin to thin bedded, bioturbated, planar-parallel, wavy-, and cross-laminated, yellowish-brown, very fine quartzose sandstones and occasional interlaminated green to brown mudstones.

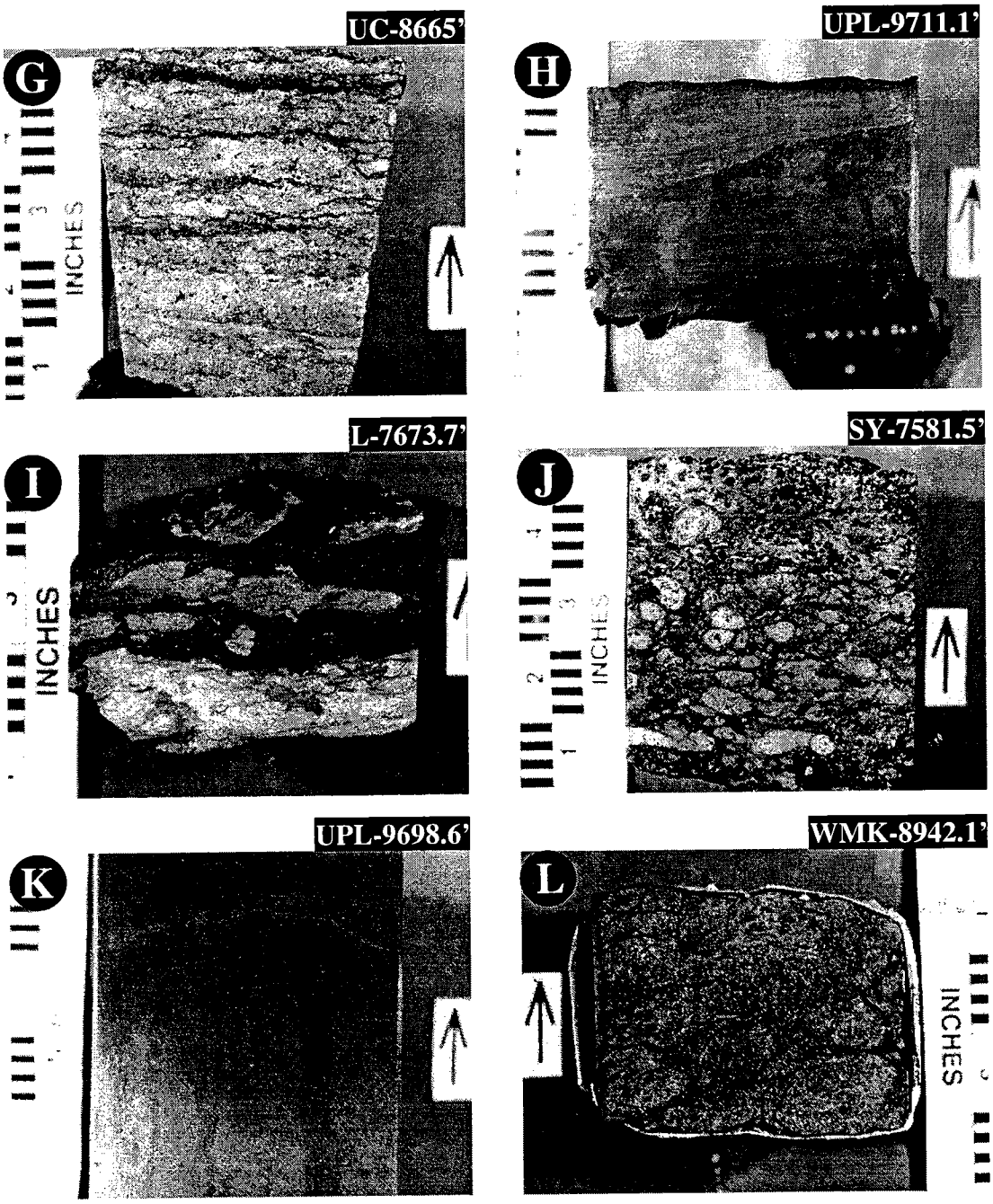

Figure 3 *(continued).*

It is distinguished from other facies by its (1) common fossils; (2) occasional detrital clay, carbonates, and interbedded mudstone and sandstone; (3) sparse occurrence of lithoclasts; and (4) absence of flasers and mudcracks. The mean detrital grain sizes of the sandstones range from 89 to 114 μm, and their standard deviations range from 18 to 60 μm. Of all the facies, this is the cleanest, finest, and best sorted. When plotted on a maximum-entropy histogram, the grain-size data show negative skewing (Fig. 6G). Facies thickness ranges from 1 to 4.5 ft.

The planar-, wavy-, and cross-laminae of facies 4 are commonly 0.1–1.0 cm thick when present and are commonly convoluted and broken by burrows. The laminae are bioturbated to varying degrees. In some beds, they may be visible despite burrowing, mottled and burrowed, or obliterated, and the beds are massive.

The detrital composition of facies 4 is primarily dominated by quartz (89–98% of detrital composition), and lesser amounts of detrital clay (2–8% of detrital composition) and collophane (<7% of detrital composition).

Facies	Primary Structures: wavy parallel	wavy non-parallel	planar parallel	cross-lamination	flasers	Secondary Structures: mud cracks	bioturbation	Grain Size (μm): # of samples	range of mean	range of std. dev.
One (inner shelf)		●	●				■	18	103-169	33-115
Two (beach/barrier)	☒	☒	☒	☒	○		■	53	113-309	39-144
Three (tidal flat)	☒	☒	☒	●	■	☒	■	48	102-319	30-154
Four (tidal channel)	☒	☒	☒	☒			■	10	89-114	18-60

Facies	Detrital Composition: quartz	rock fragments	clay	collophane	fossils	Authigenic Composition: quartz	clay	carbonate	porosity
One (inner shelf)	■	●	■	●	○	○	○	○	■
Two (beach/barrier)	■	☒	☒	☒	●	●	☒	■	☒
Three (tidal flat)	■	■	■	☒	■	○	☒	■	●
Four (tidal channel)	■	○	●	●	☒	☒	☒	●	●

■ abundant (>25%) ● occasional (2–10%)
☒ common (10–25%) ○ sparse (<2%)

Figure 4. Characteristics of the four facies of the McKee Sandstone Member.

The authigenic composition of facies 4 is dominated by quartz (<12% of total composition) and authigenic clays (<13% of total composition) and lesser amounts of carbonates (<10% of total composition) (Fig. 11). Microprobe EDS analysis of an authigenic clay crystal from this facies revealed it to be illite (Fig. 11B). Porosities are low to moderate for this facies (2–10%) due to the high authigenic clay content.

INTERPRETATION

Depositional Environment

The McKee Sandstone Member is a cyclic transgressional and highstand progradational, inner-shelf, beach, and tidal-flat complex that was deposited in an overall restricted shallow-marine–shelf environment. Cyclic breaks in lithology occur above tidal flat or tidal channel facies (facies 3 and 4, respectively) at the maximum flooding surface (Fig. 12). Above the maximum flooding surface lies the most basinward facies either the inner-shelf facies (facies 1) or, more commonly, the wave-dominated beach facies (facies 2). A composite sea-level curve showing this cyclicity can be extrapolated from this information.

Facies 1 is likely to have been deposited in an inner-shelf environment as is evident from its moderate mud content, low carbonate content, and finer grain size

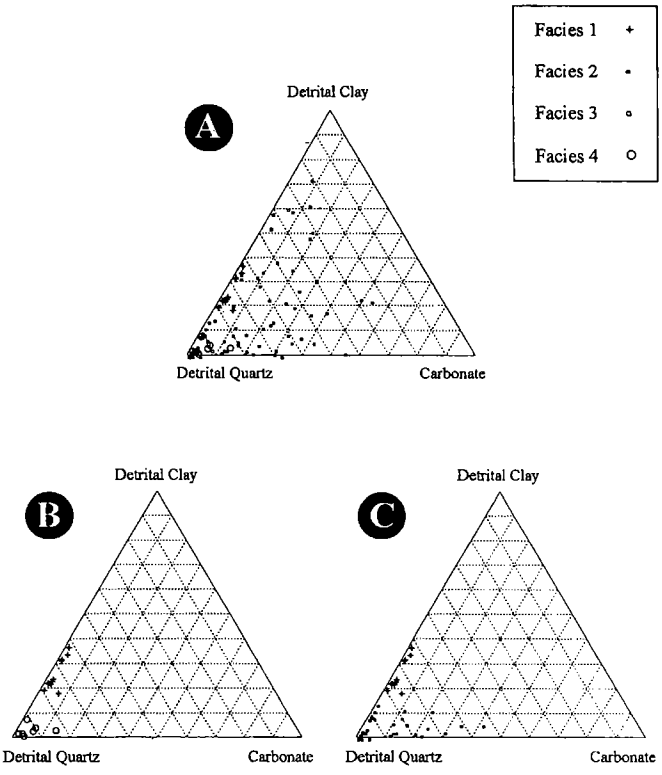

Figure 5. Ternary diagrams displaying the compositions of the McKee Sandstone Member: (A) all four facies plotted, (B) only facies 1 and 4 plotted, (C) only facies 1 and 2 plotted.

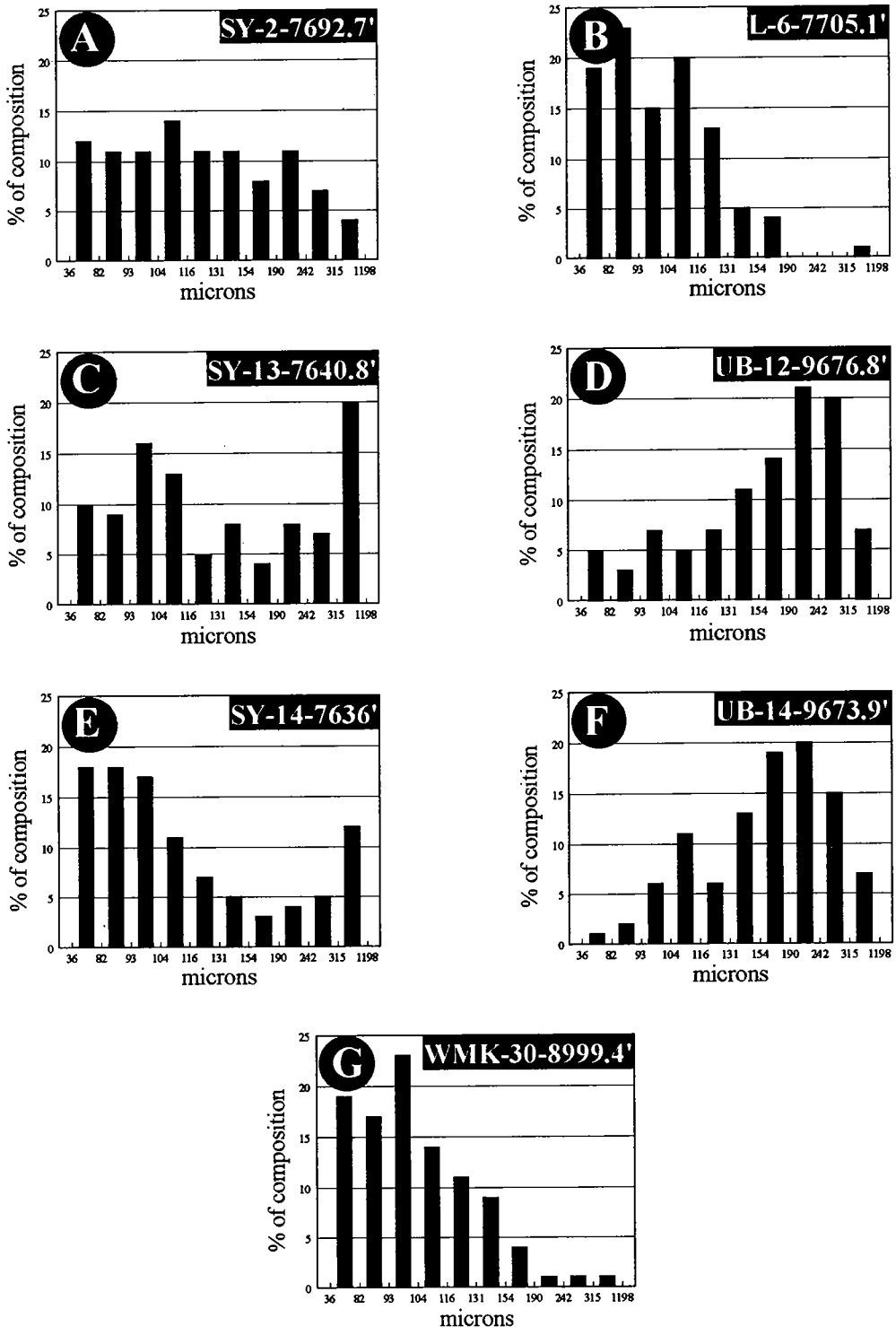

Figure 6. Typical maximum-entropy histograms for (A and B) facies 1, (C and D) facies 2, (E and F) facies 3, and (G) facies 4.

relative to other facies. The occasional occurrences of mudstone lithoclasts are likely to have been the result of storm deposits (Stride and others, 1982). The common occurrence of green and presumably glauconitic clay is restricted to a marine continental-shelf environment (Porrenga, 1967). Glauconite is primarily formed in marine areas with low sedimentation rates and in the presence of some organic activity. Modern-day conditions analogous to this exist in the Celtic Sea on the continental shelf of southwest England (George and Murray, 1977). However, the sediments in the Celtic Sea are considerably more fossil- and carbonate-rich.

Facies 2 is likely to have been deposited in a wave-dominated beach or nearshore environment, as is evi-

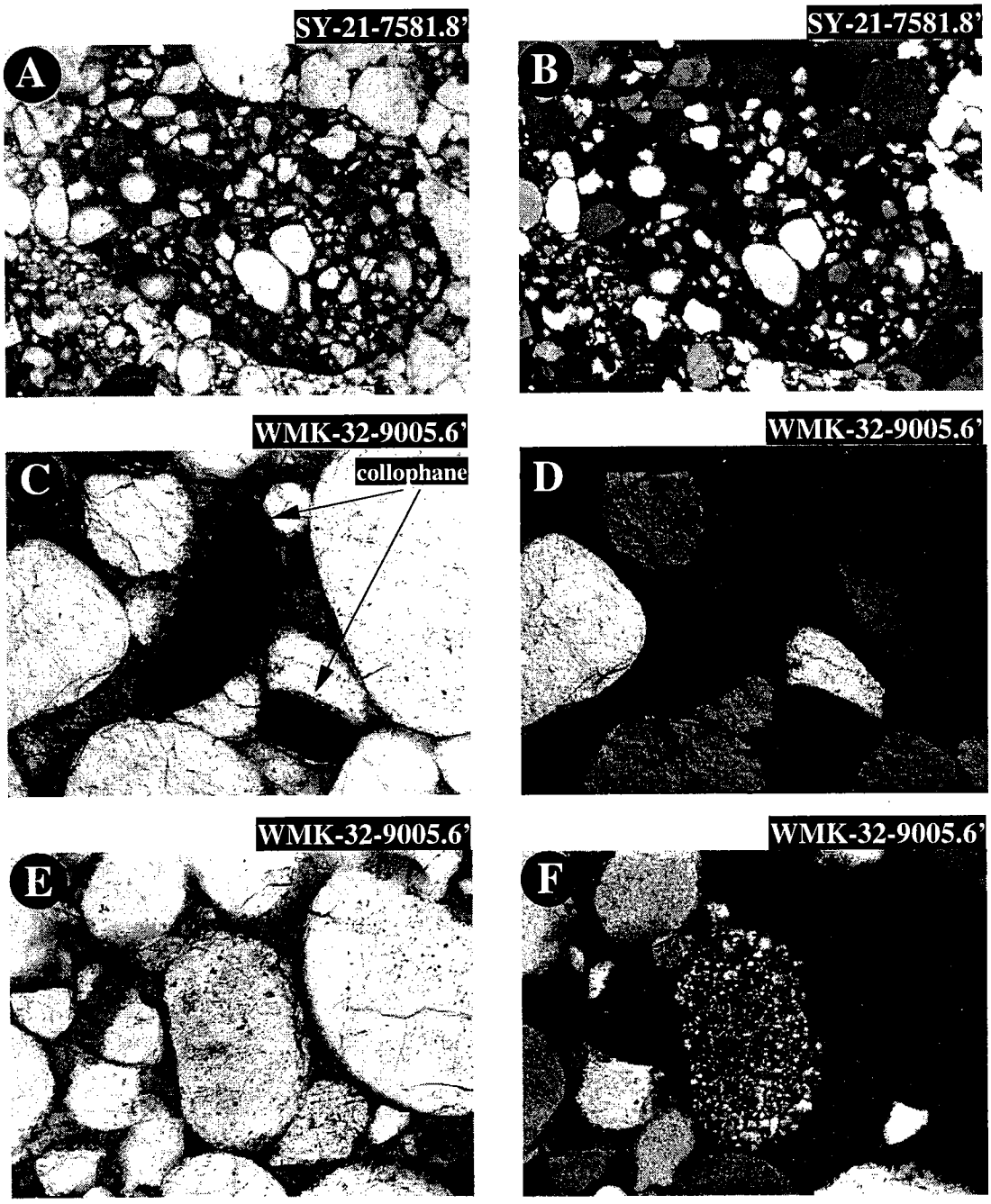

Figure 7. Thin-section photos showing examples of detrital components present in the McKee Sandstone Member: (A) mudstone lithoclast in plane light and (B) under crossed nicols, (C) collophane grains in plane light and (D) under crossed nicols, (E) monocrystalline quartz grains with sparse polycrystalline-quartz grain in center in plane light and (F) under crossed nicols.

dent from the low mud content, high carbonate content, and cross-laminae. Modern-day conditions such as this exist in Sapelo Island, Georgia (Howard, 1969). The presence of mudstone lithoclasts and the sparse occurrence of flasers suggest a tidal influence, and hence a mesotidal coastal environment (Klein, 1977).

Facies 3 was deposited in a tidal-flat environment, as is evident from mudcracks, interbedded mudstones and sandstones, flasers, and high fossil content. Modern-day conditions analogous to this exist in the tidal flat of Mont Saint-Michel Bay, France (Larsonner, 1975). Collophane, which is also common *in situ* as well as in mudstone lithoclasts in this facies, has been suggested to indicate high organic productivity relative to sedimentation rate in a shallow marine environment (Cook, 1976). Mudstone lithoclasts in other facies appear to contain a high amount of collophane (Fig. 7A,B). Therefore, it is reasonable to assume that their origin is from facies 3.

Facies 4 is likely to have been deposited in a tidal

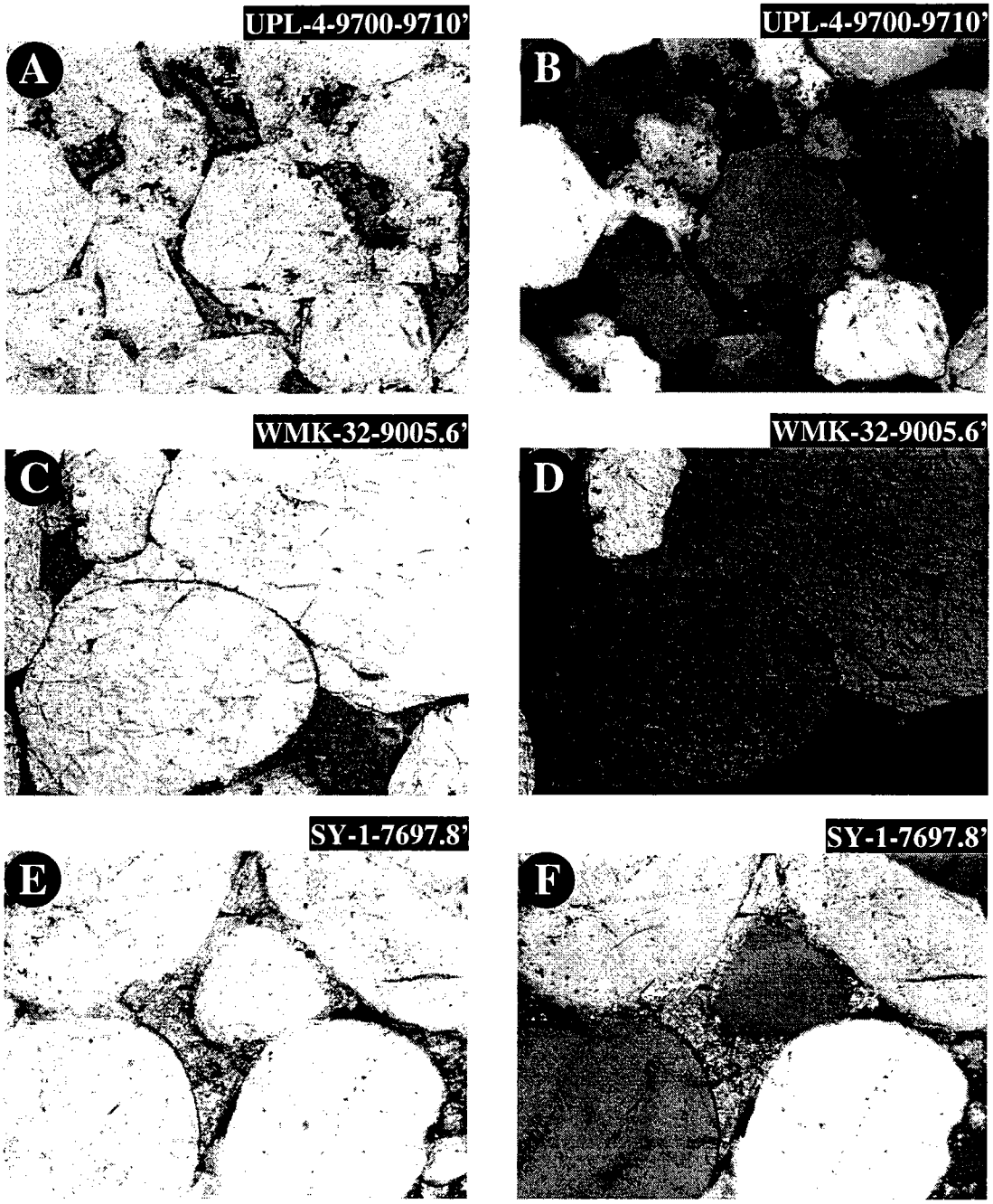

Figure 8. Thin-section photos showing examples of authigenic components present in the McKee Sandstone Member: (A) authigenic clay lining pores and quartz overgrowths in plane light and (B) under crossed nicols, (C) quartz overgrowths in plane light and (D) under crossed nicols, (E) pore filling carbonate in plane light and (F) under crossed nicols.

channel environment as is evident from the very fine sand size and high degree of sorting, high fossil content, bed thickness, and lack of detrital mud, as well as its intimate association with facies 3. Lateral accretion of point bars in tidal channels is likely to have been the mechanism for creation of a sand of this nature (Weimer and others, 1982). The lack of mudstone lithoclasts in this facies, may be attributed to their disintegration through abrasion due to high transport velocities in this tidal-channel environment. Also, this would explain the lack of mud and high degree of sorting in the facies.

Stratigraphic Sequence

The vertical succession of facies in a section of the Conoco Warren McKee #27 core (Fig. 13) represents an ideal stratigraphic sequence observed in the study of the McKee Sandstone Member. An ideal sequence consists of facies 1, bounded below by facies 3 or 4, overlain by facies 2, and then followed by either facies 3 or 4.

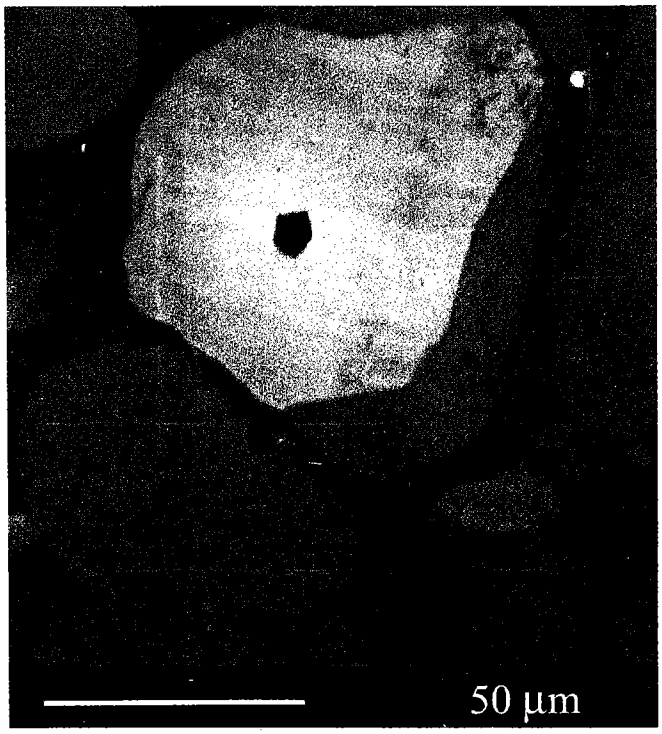

Figure 9. Image of quartz grain under cathodoluminescence showing rounded quartz overgrowths along with zircon inclusion.

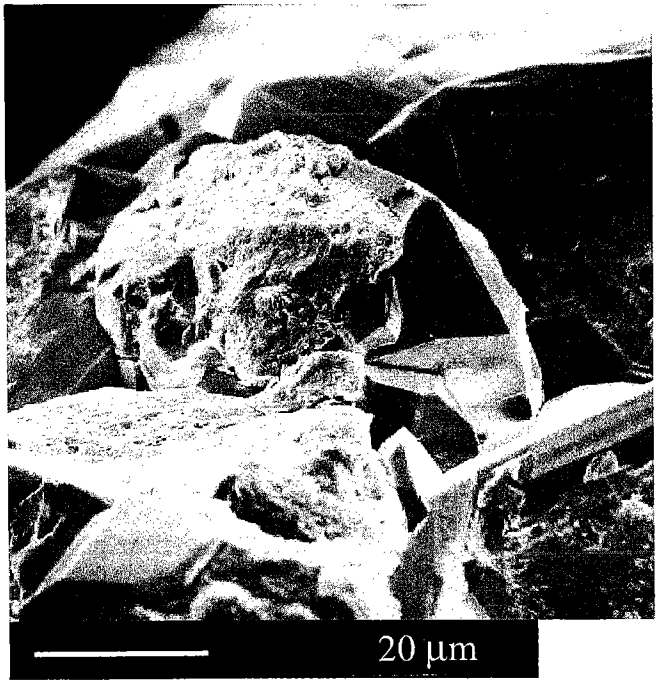

Figure 10. SEM image of quartz overgrowth from the Warren McKee #27 core at a depth of 8,955.3 ft (sample WMK-12).

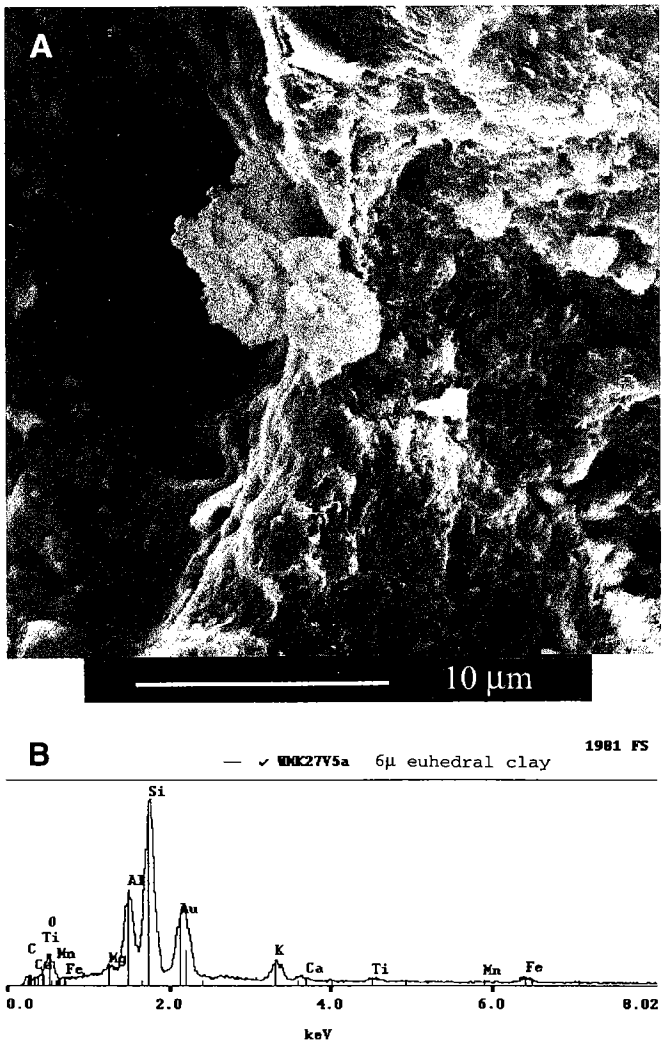

Figure 11. (A) Image of authigenic clay grain in facies 4 from sample WMK-5 along with (B) EDS spectra of the grain.

Facies 1 is part of the transgressive systems tract. Facies 2 may also be part of the transgressive systems tract, when it is bounded below by facies 1. However, where facies 1 is not present, facies 2 solely represents the transgressive systems tract. Facies 3 and 4 represent the highstand systems tract. In general, a sequence in the McKee Sandstone Member consists of the most basinward facies overlain by progressively landward facies.

CONCLUSIONS

The lower Paleozoic rocks deposited on the inner craton of North America are characterized by thick sections of carbonate rocks separated by thin units of sandstones and shales that were deposited during a relative highstand (Wilson, 1975) in a shallow epicontinental sea. One of these sandstones, the McKee Sandstone Member in the Tobosa basin, is a result of cyclic sea-level changes, during a relative highstand on the North American craton. Changes in quartz-sand grain

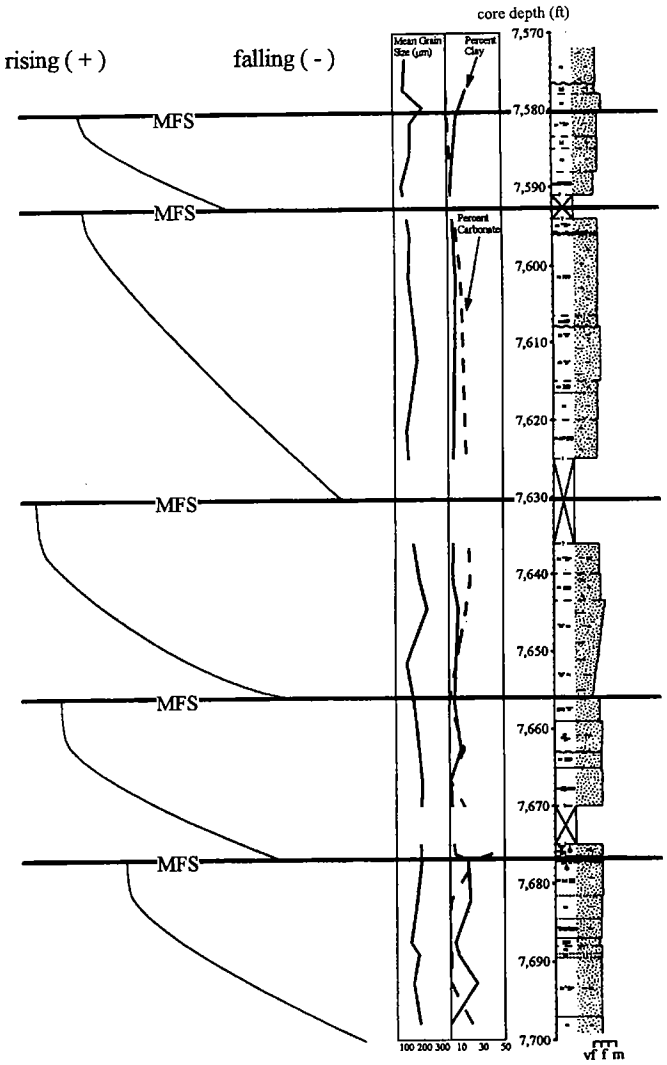

Figure 12. Maximum flooding surfaces (MFS) and sea-level curve extrapolated from the Arco State Y-4 core.

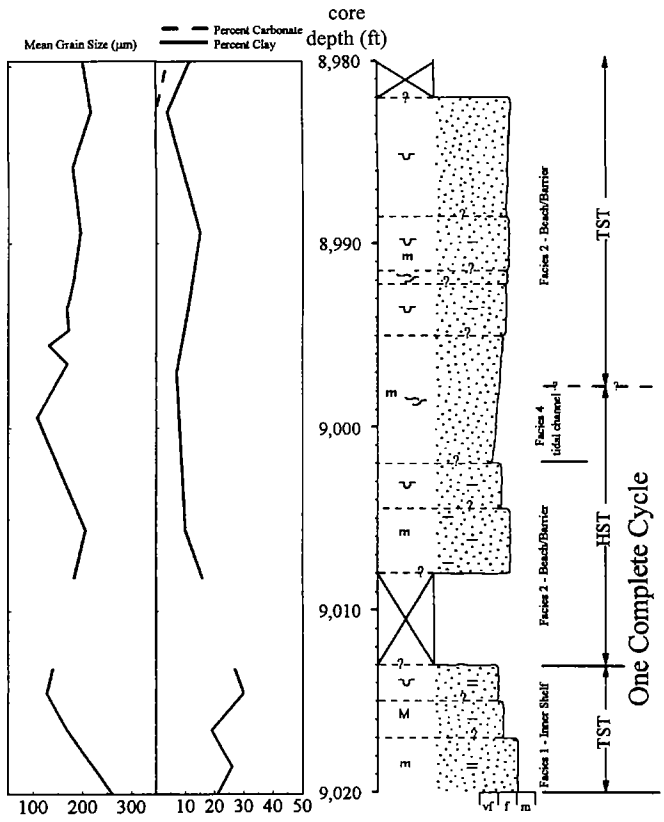

Figure 13. Ideal stratigraphic sequence in the McKee Sandstone Member from the Conoco Warren McKee #27 core showing a single cycle of transgressive systems tract (TST) innershelf facies (facies 1) overlain by highstand systems tract (HST) beach/barrier and tidal-channel facies (facies 2 and 4, respectively).

size and percentage of clay and carbonate composition accompanied by sharp breaks and repetition in facies delineate this cyclicity. Therefore, the McKee was deposited as a result of several smaller progradational highstands and transgressions as opposed to a single, higher-order highstand event.

REFERENCES CITED

Cole, C. T.; Cordry, C. D.; and Hemphill, H. A., 1942, McKee and Waddell Sands, Simpson Group, west Texas: American Association of Petroleum Geologists Bulletin, v. 26, p. 279–282.

Cook, P. J., 1976, Sedimentary phosphate deposits, *in* Wolf, K. H. (ed.), Handbook of strata-bound and stratiform ore deposits: Elsevier, Amsterdam, p. 505–535.

Full, W. E.; Ehrlich, R.; and Kennedy, S. K., 1984, Optimal configuration and information content of sets of frequency distributions: Journal of Sedimentary Petrology, v. 54, p. 117–126.

George, M.; and Murray, J., 1977, Glauconite in Celtic Sea sediments: Proceedings Ussher Society, v. 4, p. 94–101.

Howard, J. D., 1969, Radiographic examination of variations in barrier island facies; Sapelo Island, Georgia: Gulf Coast Association of Geological Societies Transactions, v. 14, p. 217–232.

Johnson, K. S.; Amsden, T. W.; Denison, R. E.; Dutton, S. P.; Goldstein, A. G.; Rascoe, B., Jr.; Sutherland, P. K.; and Thompson, D. M., 1988, Southern Midcontinent region, *in* Sloss, L. L. (ed.), Sedimentary cover—North America craton; U.S.: Geological Society of America, The Geology of North America, v. D-2, p. 307–359. [Reprinted in 1989 as Oklahoma Geological Survey Special Publication 89-2, 53p.]

Klein, G. deV. (ed.), 1977, Clastic tidal facies: Continuing Education Publication, Champaign, Illinois, 149 p.

Larsonneur, C., 1975, Tidal deposits, Mont Saint-Michel Bay, France, *in* Ginsburg, R. N. (ed.), Tidal deposits: Springer-Verlag, Heidelberg, p. 24.

Porrenga, D. H., 1967, Glauconite and chamosite as depth indicators in the marine environment, *in* Hallam, A. (ed.), Depth indicators in marine sedimentary rocks: Marine Geology, Special Issue no. 5/6, p. 495–502.

Schweers, R. H., 1949, Connell Sandstone, Oil Creek Formation, Simpson Group, west Texas: American Association of Petroleum Geologists Bulletin, v. 33, p. 2029–2036.

Stride, A. H.; Belderson, R. H.; Kenyon, N. H.; and Johnson, M. A., 1982, Offshore tidal deposits: sand sheet and

sand bank facies, *in* Stride, A. H. (ed.), Offshore tidal sands: processes and deposits: Chapman and Hall, London, p. 95–125.

Weimer, R. J.; Howard, J. D.; and Lindsay, D. R.,1982, Tidal flats and associated tidal channels, *in* Scholle, P. A.; and Spearing, D. (eds.), Sandstone depositional environments: American Association of Petroleum Geologists Memoir 31, p. 191–245.

Wilson, J. L., 1975, Carbonate facies in geologic history: Springer-Verlag, New York, 471 p.

Sedimentology and Sequence Stratigraphy of Jackfork Group, U.S. Highway 259, Le Flore County, Oklahoma[1]

Roderick W. Tillman
Consulting Sedimentologist and Stratigrapher
Tulsa, Oklahoma

ABSTRACT.—The Morrowan Jackfork Group, where it crops out in the Ouachitas, has long been regarded as a deep-water, primarily turbidite deposit. Recent work in southeastern Oklahoma indicates that at least two or more periods of significant shallowing occurred during the deposition of the Jackfork. I have revisited and redescribed outcrops along U.S. Highway 259, originally described by Lewis Cline and Frank Moretti in 1956, and have interpreted these outcrops to include shelf, slope, and deltaic deposits. These relatively shallow-water deposits occur in the Markham Mill and Prairie Mountain Formations of the Jackfork Group.

Several significant sequence-stratigraphic surfaces occur in the Jackfork Group. Relatively abrupt shallowing is evident at what are interpreted to be sequence boundaries at the base of the Prairie Mountain Formation and at the base of the shelf and deltaic deposits that form the lower part of the Markham Mill Formation. Significant flooding surfaces are observed between the slope and overlying shelf deposits in the upper Prairie Mountain Formation and either in the upper part of the Markham Mill Formation or at the base of the Wesley Formation. A third flooding surface may occur at or near the base of the Game Refuge Formation.

Slope, shelf, and deltaic deposits in the Jackfork Group are characterized by features distinctly different from those of the turbidites in the Wildhorse Mountain Formation, which forms much of the Jackfork along U.S. 259.

The slope deposits are characterized by the presence of locally abundant, rounded and transported, primarily sandstone blocks supported in a fine-grained matrix of mudstone and shale. The clasts range in diameter from several centimeters to several meters and occur at numerous positions within the upper-middle part of the Jackfork. Shelf deposits in the Prairie Mountain Formation are characterized by thin, generally undeformed, subhorizontally laminated 1- to 3-ft–thick sandstones interbedded with shales. The upper surfaces of some of the thinner shelf sandstones have burrows, including *Zoophycos*.

Deltaic deposits are primarily thinly bedded, current-rippled, and subhorizontally laminated, lenticular splay sandstones interbedded with shales. In the deltaic deposits, local channeling and thicker sandstone beds occur, as does localized soft-sediment deformation.

INTRODUCTION

The outcrops along U.S. 259, south of Big Cedar, Oklahoma, were the subject of extensive work by Lewis Cline and his University of Wisconsin students in the mid-1950s. One of the key measured sections that grew out of their work was published by Cline and Moretti in 1956. Their section extends from below the base of the Jackfork Group (Jackfork Group of this paper) to what they defined as the Atoka Formation at the top. Their "Atoka top" was included by Briggs (1973) in the Game Refuge Formation (Game Refuge Formation of this paper) of the Jackfork Group. This paper focuses on the Jackfork Group outcrops along U.S. 259, one of the best-exposed and most complete Jackfork sections in eastern Oklahoma.

At the time Cline and Moretti measured the section in this area, U.S. 259 had just been finished, and there were numerous well-exposed outcrops along the right-

[1]This paper is reprinted with slight modifications from Tillman, R. W., 1994, Sedimentology and sequence stratigraphy of Jackfork Group, U.S. Highway 259, Le Flore County, Oklahoma, *in* Suneson, N. H.; and Hemish, L. A. (eds.), Geology and resources of the eastern Ouachita Mountains frontal belt and southern Arkoma basin, Oklahoma: Oklahoma Geological Survey Guidebook 29, p. 203–223.

Tillman, R. W., 2000, Sedimentology and sequence stratigraphy of Jackfork Group, U.S. Highway 259, Le Flore County, Oklahoma, *in* Johnson, K. S. (ed.), Marine clastics in the southern Midcontinent, 1997 symposium: Oklahoma Geological Survey Circular 103, p. 65–85.

Table 1.—U.S. Highway 259 Measured Section (Units 1–63)*

	Thickness (feet)
Atoka Formation—*Note: What is designated here as Atoka is actually Game Refuge Formation, the uppermost formation in the Jackfork Group according to Briggs (1973, p. 29).*	
63. Poorly exposed sandy shale with rectangular blocks of hard quartzitic sandstone. Sandstone float containing a sandstone cast fauna was found in this interval. The fauna may be Honess' "Morrow fauna." *(Crinoids.)*	
62. Poorly exposed blue-gray shale	90
61. Shale and thin-bedded sandstone. Shale predominates near the base but at the top the well-bedded, thin, white sandstone may comprise 40% of the rock	245
60. Sandstone and sandy shale; hard, white, quartzitic sandstone comprises 60% of the interval	165
JACKFORK GROUP	
Wesley Formation	
59. Shale; weathers light blue-gray; contains at least one 5-inch bed of black green-gray weathering chert	150
Markham Mill Formation	
58. Sandstone; soft, green-gray, a small amount of interbedded lignitic sandy shale near top	38
57. Shale; sandy; exposed at sharp curve in road	27
***Prairie Mountain Formation**—Top of formation occurs near the base of Unit 56. Top of formation marked by sequence boundary.*	
56. Sandstone; some very hard white massive rock but toward the top becomes green and friable	148
55. Light blue-gray sandy shale with rounded boulder-like masses of brown-gray quartzitic sandstone *(boulder shale)*	105
54. Poorly exposed, massive, yellow-weathering sandstone	90
53. Shale and sandstone	195
52. Massive to medium bedded, fine-grained, firm white sandstone; weathers yellow; thickness of interval hard to calculate *(includes flooding surface)*	230
51. Poorly exposed light blue-gray sandy shale with some intercalated hard, thinly bedded, quartzitic sandstone. *(Measured Section 6A-93 starts about 450 feet above the base of this unit.)*	650
50. Light gray yellow-weathering sandstone and sandy shale in about equal proportions	278
49. Shale; soft, slightly sandy at base; weathers light gray	52
48. Massive yellow sandstone	20
47. Covered; some poorly exposed yellow-weathering sandstone	50
46. Poorly exposed sandy blue-gray shale and soft sandstone; exposed in the saddle where the new highway intersects the old road to Big Cedar. *(Now at this location there is only a short north-south road linking Kiamichi Mountain crestal road and U.S. Highway 259.)*	327
Wildhorse Mountain Formation, *Upper Part*	
45. Sandstone; soft, *friable* medium-grained, *(200 μm)*, light gray, weathers yellow. *(Sharp lower contact with 1-foot erosional relief. This unit probably belongs in Prairie Mountain Formation.)*	40
Sequence Boundary	
44. Shale with subordinate sandstone; dark blue-gray laminated shale with interlaminated gray siltstone and sandstone with evenly bedded white quartzitic sandstone; sandstone comprising 35% of upper portion of interval, relatively unimportant in lower portion	120
43. Sandstone and shale; 80% of interval comprised of fine-grained, hard, well bedded, quartzitic sandstone in beds up to 1½ feet thick; dark gray sandy shale intercalated, becoming important toward the base	55
42. Shale and sandstone; soft white sandstone at base grading upward into blue-gray laminated silty shale. *("Ouachita National Forest" sign near base of unit.)*	35
41. Covered; poor exposures indicate sandy shale	310
40. Sandstone; soft, yellow-weathering; thickness hard to calculate because road parallels strike	50
39. Sandstone; hard, white to light gray, well bedded in even beds two feet thick	75
38. Lower one-half of interval covered; upper one-half appears to be badly weathered gray sandy shale with interbedded fine-grained quartzitic sandstone	155
Big Stick Monument (at roadside, 5.4 miles south of Big Cedar)	
37. Sandstone; hard, white to pink, fine-grained, quartzitic sandstone; forms crest of ridge where highway cuts through	170
36. Shale and sandstone; dark blue-gray sandy shale and hard to firm gray sandstone; sandstone-shale ratio 60:40	135
35. Sandstone and shale; sandstone comprises 65–70% of interval; remainder composed of dark blue-black shale with alternating laminae of gray siltstone and some sandstone beds up to a foot in thickness	117
34. Shale; black with interlaminated gray siltstone (35%); one bed of hard, quartzitic sandstone	9.5
33. Sandstone; predominantly hard, medium blue-gray, subquartzitic sandstone in beds averaging from 2 to 6 feet; rarely, a well bedded silty shale intervenes *(includes thickening-upward sandstone)*; includes a fault with small displacement down to west	265
32. Shale and sandstone; dark blue-gray shale with interlaminated 1 to 2 inch beds of hard quartzitic gray sandstone occurring in 30% of interval; total sandstone content estimated at 45% of interval	52
31. Predominantly dark gray laminated shale interbedded with thin 1 to 2 inch beds of gray sandstone; occasional 2 to 5 foot beds of soft, dirty, poorly sorted, yellow-weathering sandstone; grades into zone 32 above where the sandstone merely becomes more quartzitic and better jointed; about 60% shale and 40% sandstone	105

Table 1 *(continued)*.—U.S. Highway 259 Measured Section (Units 1–63)

	Thickness (feet)
PRAIRIE HOLLOW MAROON SHALE MEMBER	
30. Shale and sandstone; mostly *pinkish to* gray shale and green-gray, silty, massive sandstone that weathers yellow; some brownish-red shale and silty shale at intervals	130
Wildhorse Mountain Formation, Lower Part	
29. Sandstone; massive below becoming bedded above and containing a small amount of shale at top; hard and quartzitic below, becoming poorly sorted and brown-gray above	30
28. Shale; dark blue-gray laminated shale with some silty and sandy beds included	39
27. Sandstone; fine-grained, blue-gray, hard, quartzitic, weathers brown; well defined beds about 2 feet thick	50
26. Shale; dark blue-gray to black, blocky clay-shale; some rounded hard quartzitic masses near the top that may be concretionary *"glupes" and "globs," a nontectonic, sedimentary, slurried unit. Above deformed unit is a generally thinning-upward unit overlain by shale.*	52
25. Sandstone; gray, weathers brown-gray	73
24. Dark laminated shale and interlaminated hard, white, quartzitic sandstone in about equal amounts	135
23. Sandstone; soft, white, weathers yellowish; beds up to 2 and 3 feet thick	45
22. Shale and sandstone; dark blue-gray laminated shale interbedded with white, well bedded, quartzitic sandstone occurring as thin laminae in the shale; sand-shale ratio 4:6	173
21. Sandstone; soft, dirty, massive, weathers yellowish	40
20. Shale; blue-gray with beds of dirty gray sandstone	22
19. Covered	20
18. Interval 65% sandstone, 35% sandy shale; silty, poorly sorted, yellow-weathering sandstone; blue gray shale with interlaminated light gray siltstone or fine-grained sandstone; center of cut faulted; displacement unknown but not great	115
17. Predominantly laminated blue-gray shale with laminae of ash-gray siltstone; one 8-foot bed of yellow-weathering friable sandstone one-third the distance above the base	60
16. Covered; estimated	50
15. Sandstone; soft, friable, gray, weathers yellowish, in beds averaging about a foot in thickness: 95% sandstone in lower part of interval decreasing to 80% above	40
14. Shale; dark gray, well-bedded shale with some light gray, hard, quartzitic sandstone in beds up to 6 inches; soft, friable, yellow sandstone begins to be prominent toward top	100
13. Sandstone and sandy shale; firm to friable yellow-weathering gray sandstone and separating sandy gray shales (30%)	80
12. Covered	125
11. Sandstone with perhaps 30% purple-gray to brown-gray, sandy, lignitic shale and some laminated dark blue-gray shale; firm to friable, fine to medium-grained, ash-gray, yellow-weathering sandstone in beds averaging 1½ feet thick; many beds have ripple-marked upper surfaces	140
10. Shale and sandstone; predominantly dark blue-gray, laminated shale with thin even-bedded sandstone layers; at top of zone about 5 feet of white, hard, ripple-marked sandstone	25
9. Alternating sandstone and shale in subequal proportions (ratio 6:4); sandstone is light gray, medium to fine-grained, poorly sorted, in well developed beds averaging less than 2½ feet and with some poorly developed ripple marks; dark gray to brown shale, the brown layers being sandy, lignitic, and containing many plant remains	135
8. Covered	35
7. About 50% of interval medium-gray, poorly sorted sandstone in beds up to 1½ feet, the units averaging 20 feet; separated by subequal amounts of dark blue-gray sandy shale; shale laminated with 1 to 3 inch beds of brown-gray lignitic sandstone	95
6. Shale and sandstone; blue-gray shales with thin laminae of silty, poorly sorted, fine-grained sandstone with intercalated medium-grained, brown-weathering sandstone; sandstone-shale ratio 6:4	37
STANLEY SHALE GROUP	
Chickasaw Creek Siliceous Shale Formation	
5. Shale; soft, dark gray to black when fresh, weathers light blue-gray; a few 1 to 4 inch beds of white siltstone and brown-gray poorly sorted sandstone *(Briggs moved unit 5 into Jackfork Group, 1973, p. 39; location is NE¼NE¼ sec. 26, R. 25 E., T. 1 N.; 2.35 miles south of Big Cedar, intersection of Highways 254 and 63.)*	205
4. Siliceous shale, black laminated siliceous shale containing several thin beds of blue-black chert mottled with white almond-shaped siliceous areas	15
3. Shale; poorly exposed, dark gray to black, laminated, weathers light blue-gray; includes some siliceous shale and some minor amounts of fine-grained ash-gray siltstone and sandstone	55
2. Siliceous shale; dark gray to black laminated siliceous shale with thin 1 to 3 inch hard, ash-gray siltstones comprising about 20% of the interval; dark blue–black chert in 1 to 3 inch bands, speckled with white siliceous areas	15
1. Dark blue gray to black laminated shale predominating (60–65%); fine-grained ash-gray sandstone in even beds up to 3 feet in thickness second in importance; sandy shale, 5%	55

*Originally measured by Cline and Moretti, 1956; modified, refined, and interpreted by R. W. Tillman in 1993 and 1994. Italicized parts are changes and additions made to section by Tillman.

of-way. Since their work was completed, many of the outcrops have deteriorated, and a few new ones have been excavated. During the course of my work, I visited most of the currently well-exposed outcrops along the highway and, for the most part, was able to consistently locate myself on Cline and Moretti's measured section. Suggested revisions and additions to their section on a unit by unit basis are included in the slightly revised version of their measured section (Table 1). A more detailed description of part of their measured section is the subject of this paper and should be referred to often while reading this paper (see Fig. 5).

APPROACHES TO DEFINITION OF JACKFORK STRATIGRAPHY

The area of this study is in the interval between the Windingstair fault and the Octavia fault in southeastern Oklahoma, near the Arkansas state line. A number of workers have mapped and interpreted the stratigraphy of parts of this and adjoining thrust-fault blocks (Fig. 1). Garrett Briggs has done the most detailed work to date in the area of the Cline and Moretti section on U.S. 259.

The stratigraphy of the Jackfork Group in southeastern Oklahoma has been in flux almost from the first day a geologist began to study the unit. The name "Jackfork Formation" was first used by Taff (1902) to designate the thick sequence of sandstones and shales that he encountered on Jackfork Mountain in Atoka County, Oklahoma.

Harlton (1938) elevated the Jackfork Formation to the Jackfork Group and subdivided it into four formations on the basis of laterally persistent shales present in the Round Prairie syncline east of the town of Atoka. The Jackfork Group was further redefined 35 years later by Briggs (1973) to include the following formations, from bottom to top: Chickasaw Creek, Wildhorse Mountain, Prairie Mountain, Markham Mill, Wesley, and Game Refuge (Fig. 2). Briggs did not recognize all six formations in his mapping of the area in Le Flore County, Oklahoma (Fig. 3). He grouped the Prairie Mountain, Markham Mill, and Wesley into one mappable unit. I believe that subdivision of these three formations is possible for purposes of mapping and to better understand the sequence stratigraphy of the Jackfork. I follow Cline and Moretti's (1956) units and Briggs's (1973) reassignment of ages in the following discussion of the geology of the study area. The reader is referred to Briggs (1973) for a detailed discussion of the stratigraphy and regional aspects of the formations in the Jackfork Group in southern Le Flore County (Fig. 1).

A generalized north-south cross section through the Mississippian and Pennsylvanian strata (including the Jackfork Group) in the area of Cline and Moretti's (1956) measured section shows the relation between the stratigraphic units and the thrust faulting (Fig. 4). In an effort to define the environments of deposition and sequence stratigraphy of the Jackfork Group, I measured a 1,260-ft section through most of the upper part of the Jackfork (Fig. 5). For individual units, lithology, mean grain size, sorting, sedimentary structures, and inferred sedimentary environments are indi-

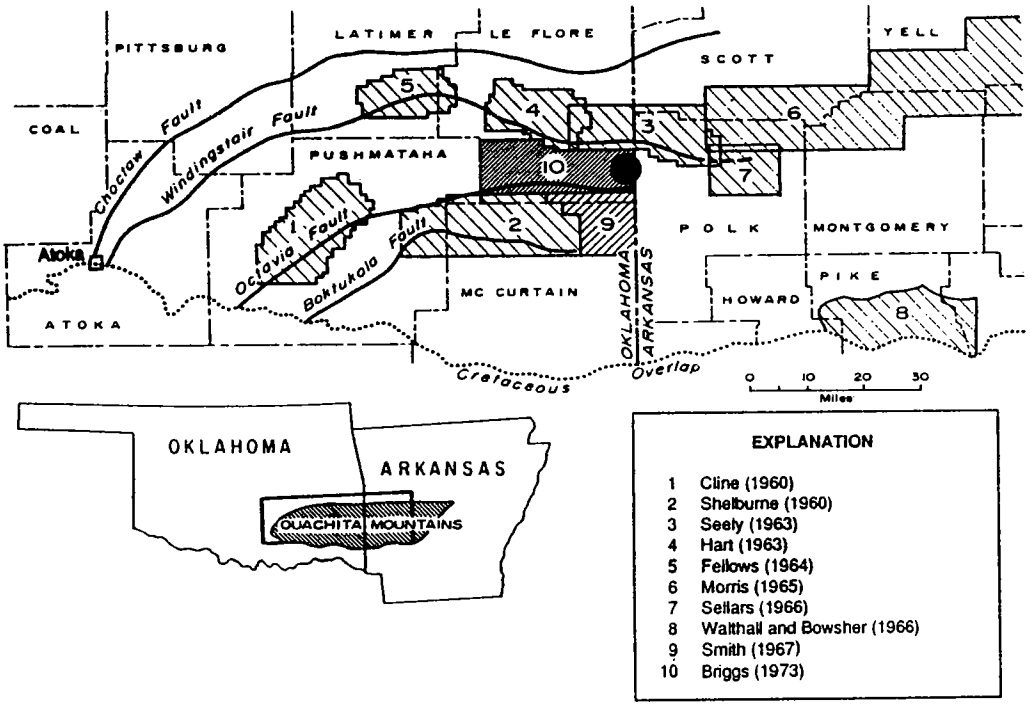

Figure 1. Location map for Ouachita Mountains in southeastern Oklahoma and western Arkansas. Black circle is location of U.S. Highway 259 measured section. (Modified from Briggs and Smith, 1973.)

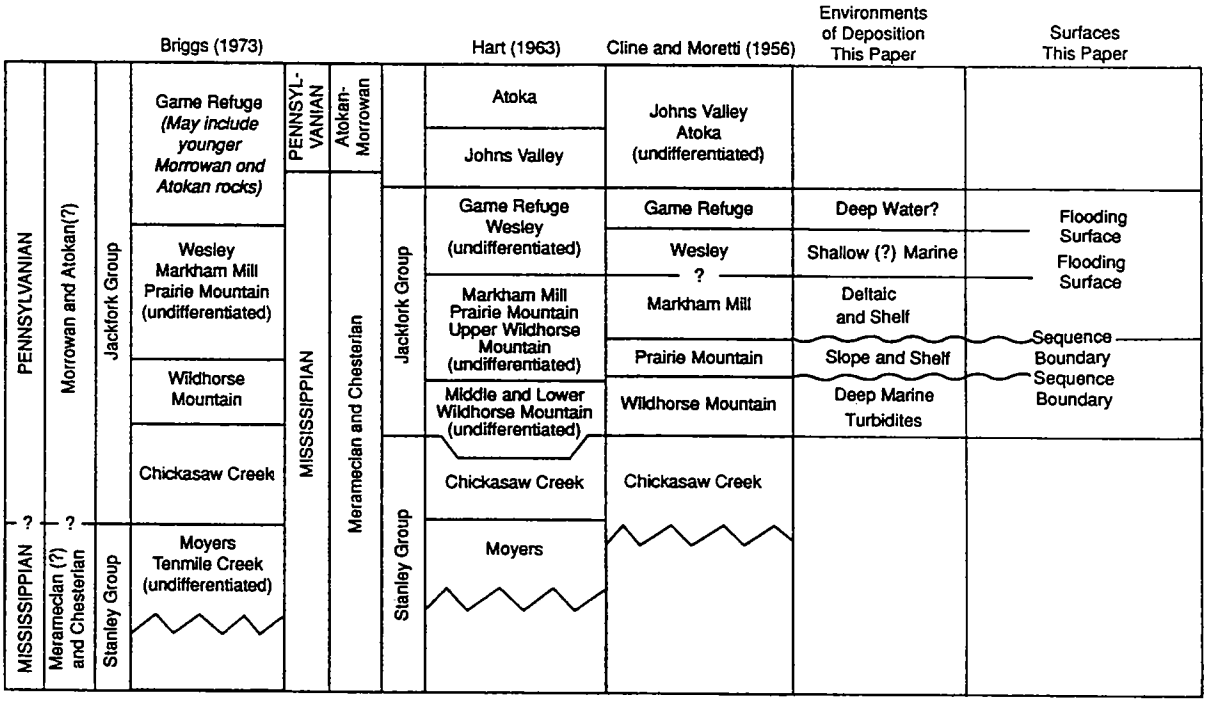

Figure 2. Stratigraphic reference sections of previous workers in southeastern Oklahoma. Cline and Moretti's (1956) units are used in this paper. Sequence stratigraphic surfaces are indicated. (Modified from Briggs, 1973.)

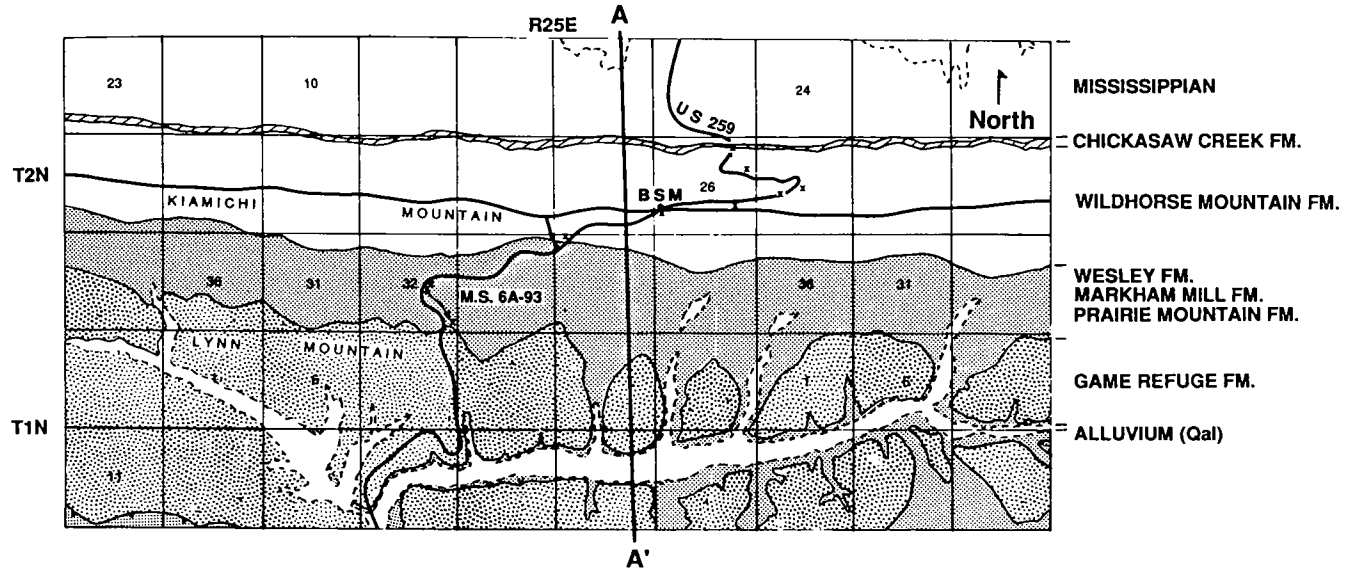

Figure 3. Geologic map of part of Lynn Mountain syncline in study area. Locations of measured section 6A-93 in Section 32 and stratigraphic cross section A–A' are indicated. Base of Chickasaw Creek Formation is 2.4 mi south of Big Cedar. BSM = Big Stick Monument; x = diagnostic Jackfork Group outcrops along U.S. 259. (Modified from Briggs and Smith, 1973.)

cated. Variation in mean grain size is commonly one of the keys to recognizing unit boundaries. Table 2 is a unit by unit comparison of units described in Figure 5 with the units described by Cline and Moretti.

WILDHORSE MOUNTAIN FORMATION

The Wildhorse Mountain Formation, which probably forms 70% of the Jackfork Group along U.S. 259, is like most other Jackfork turbidites described in the literature (Morris, 1974, 1975). However, the upper part of the Jackfork Group (Prairie Mountain Formation and higher) is poorly documented and significantly underinterpreted in the literature.

Thick Wildhorse Mountain Formation turbidites crop out east and southwest of Big Stick Monument (Fig. 3). Most of the turbidite sandstones are thick and

well cemented; they were deposited in deep water. Near and southwest of Three Sticks Monument along U.S. 259, the upper part of the Wildhorse Mountain Formation becomes slightly shalier, and distinct packages of turbidite sandstones occur between shales. Several of the sandstones contain accumulations of coalified plant fragments and carbonaceous debris. These accumulations of shallow-water, carbonaceous detritus occur in the turbidite sandstones in several forms including: (1) carbonaceous fragments disseminated throughout the quartz sandstones, (2) as accumulations on bedding or lamination surfaces, and (3) as the dominant fraction in "slurried beds" (Fig. 6).

Erosion on an outcrop scale at the base of the turbidite packages is generally minimal. In the outcrops along U.S. 259, erosion within the packages at the base of individual beds is generally also minor and has a relief of less than 1 ft (Fig. 7). Rarely, erosion at the base of some packets of beds has resulted in a relief of up to 1.5 ft. Characteristics of Jackfork turbidites are summarized in Table 3.

Table 2.—Comparison of Units and Thicknesses in Jackfork Group

Formations	Units		Thicknesses	
	This paper	Cline and Moretti (1956)	This paper	Cline and Moretti (1956)
Wesley	30–32	59	71 ft (part)	150 ft
Markham Mill[a]	29	58	35 ft	38 ft
	28	56 (part), 57	156 ft	175 ft (part)
	19–27[b]	56 (part)	58 ft	148 ft (part)
Prairie Mountain				
	18	55 and 56 (part)	105 ft	105 ft and 148 ft (part)
	9–17	53, 54	400 ft	285 ft
	4–8[b]	52	240 ft	230 ft
	1–3	51	200 ft (part)	650 ft

[a]Base of Markham Mill Formation as designated at this location is a sequence boundary.
[b]Flooding surfaces occur above Unit 8 (this paper) and above Unit 27 (this paper).

PRAIRIE MOUNTAIN FORMATION

I interpret the top of the Wildhorse Mountain Formation to be at the base of Unit 45 of Cline and Moretti (1956). Cline and Moretti picked the base of the Prairie Mountain Formation just above Unit 45, rather than at the base of the unit. I interpret the contact at the base of Unit 45 to be a sequence boundary that represents significant shallowing.

The basal sandstone of the formation (not included in Tillman measured section) is friable and generally massive appearing; it forms 2- to 3-ft–thick lenses that thin and thicken over the length of the outcrop (Fig. 8). Horizontal bedding or lamination is absent. The sandstone may include large troughs and white to pink shale drapes on some 3- to 6-ft–wide depressions. The total volume of shale in outcrop is <2%. Laterally, shales are truncated (by troughs?). Erosional relief at the contact of the units is as much as 1.5 ft. Only a trace of burrowing is observed. Grain size ranges from 125 to 250 μm; mean grain size 175–200 μm. Sorting is moderate to poor. There is a strong grain-size contrast between the basal beds of this unit and the underlying, thinly bedded turbidites (mean grain size 100–125 μm). In hand sample, Cline and Moretti's (1956) Unit 45 appears to be relatively porous and permeable. This sandstone (channel?) probably was deposited entirely by traction currents. Pauli (1994) described similar channels in roughly the same stratigraphic interval.

Greenish-pink clayey shale occurs just above the porous sandstone. The clayey shale is typical of that observed in the Prairie Mountain and some parts of the Atoka Formations in other areas in Le Flore County and is interpreted to have been deposited by processes other than turbid flow. This type of clayey shale may have been deposited in relatively shallow water and is quite different from the mudstones interbedded with or associated with the turbidites of the underlying Wildhorse Mountain Formation.

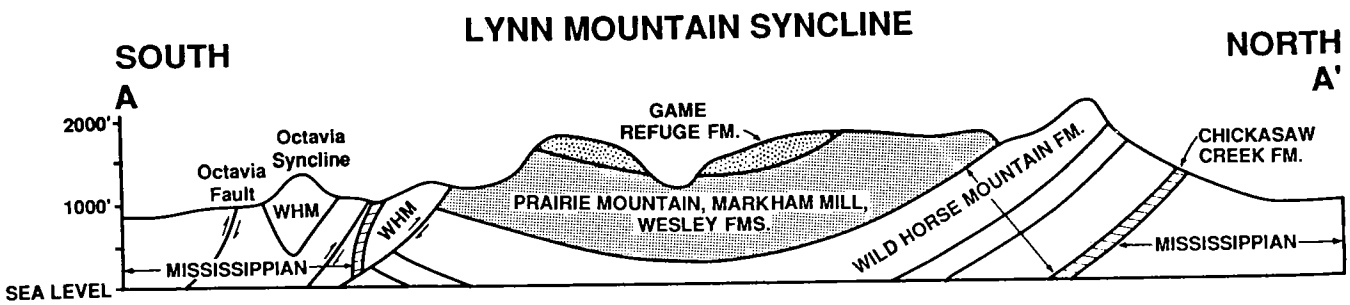

Figure 4. Stratigraphic cross section A–A'. WHM is Wildhorse Mountain Formation. Location is ~1.7 mi east of measured section 6A-93 along U.S. Highway 259. (Modified from Briggs and Smith, 1973.)

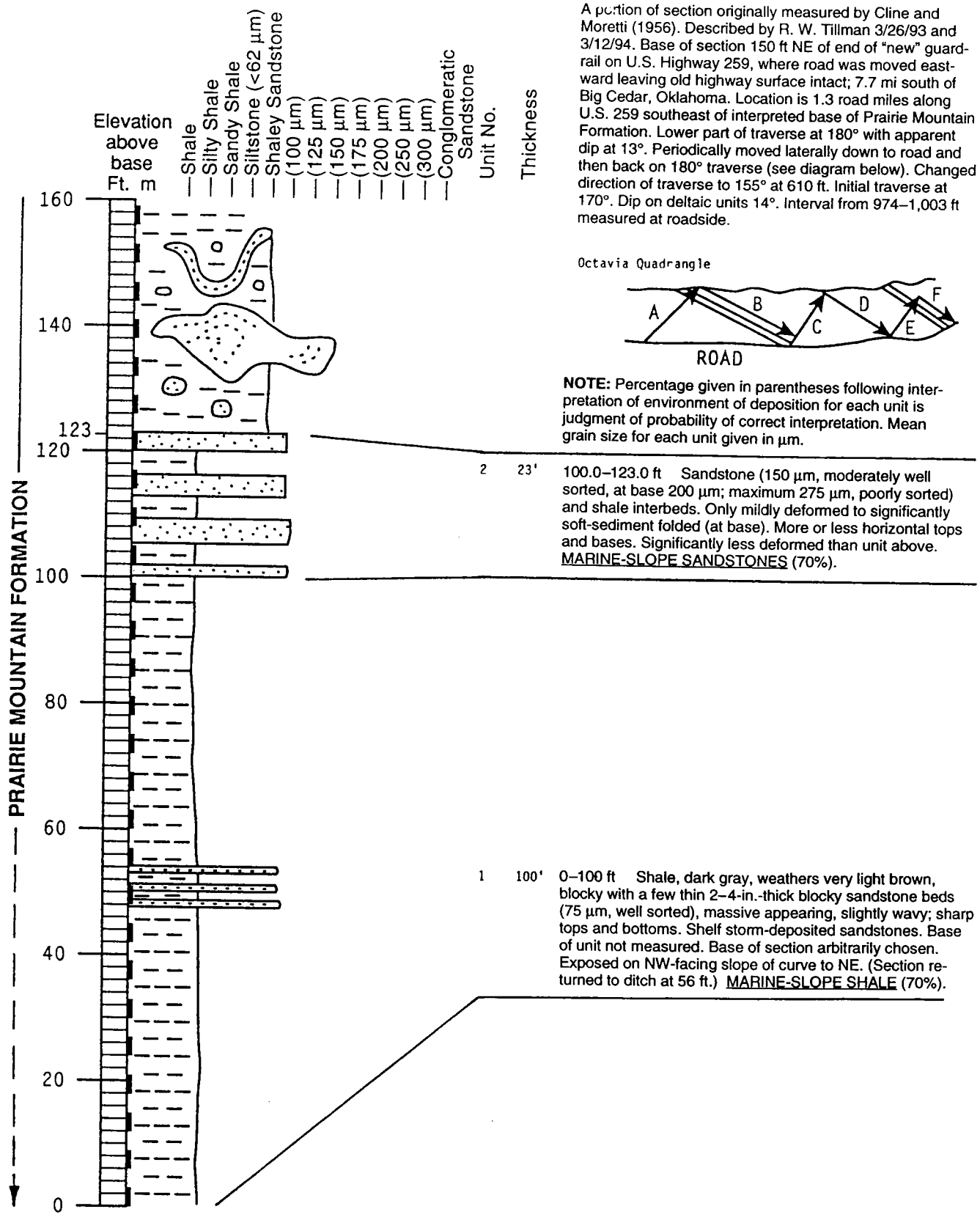

Figure 5 *(pages 71–77)*. Jackfork Group, Measured Section 6A-93, along U.S. Highway 259, NW¼SE¼ to SE¼SE¼ sec. 32, T. 2 N., R. 25 E., Le Flore County, Oklahoma.

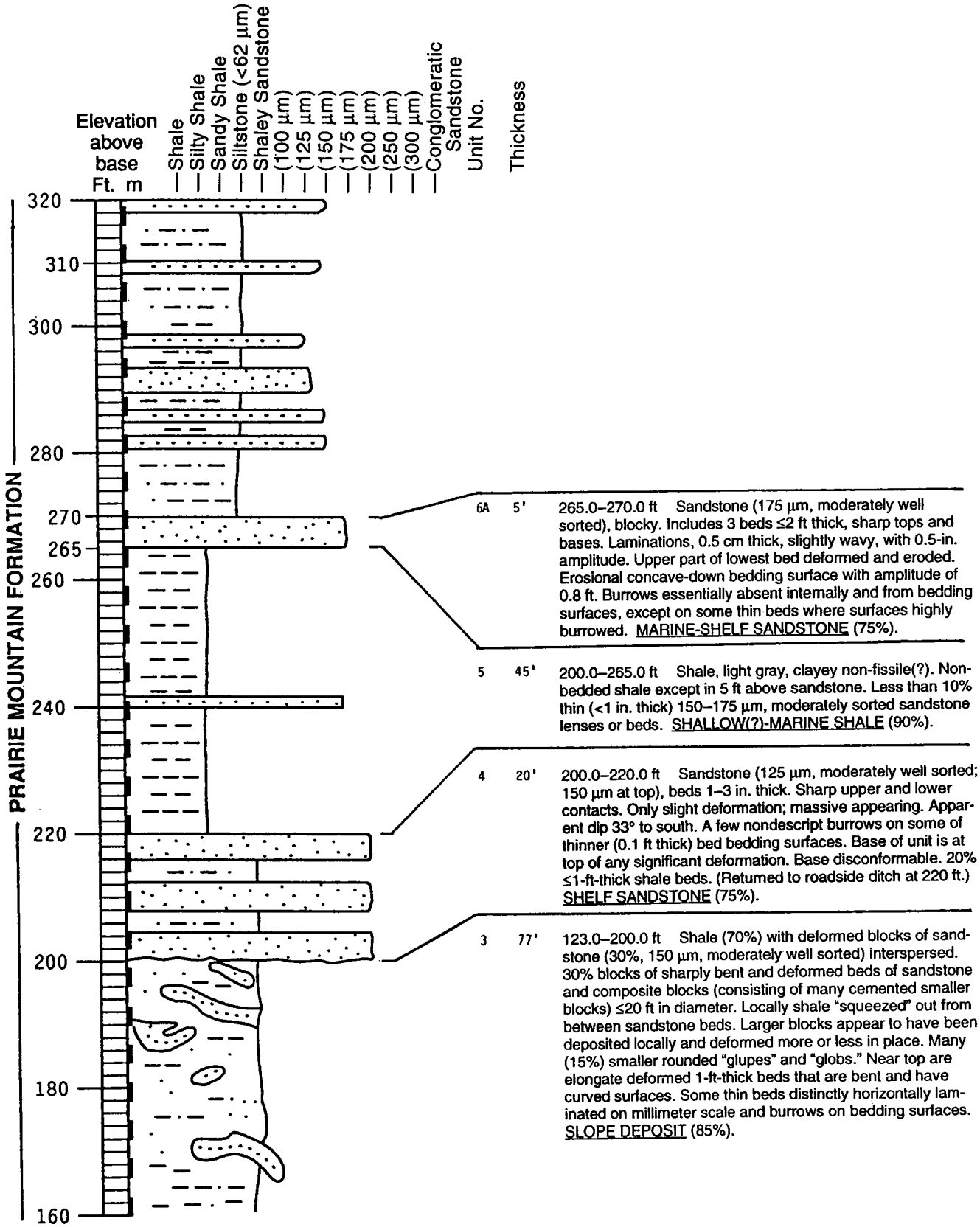

Figure 5. *(continued)*

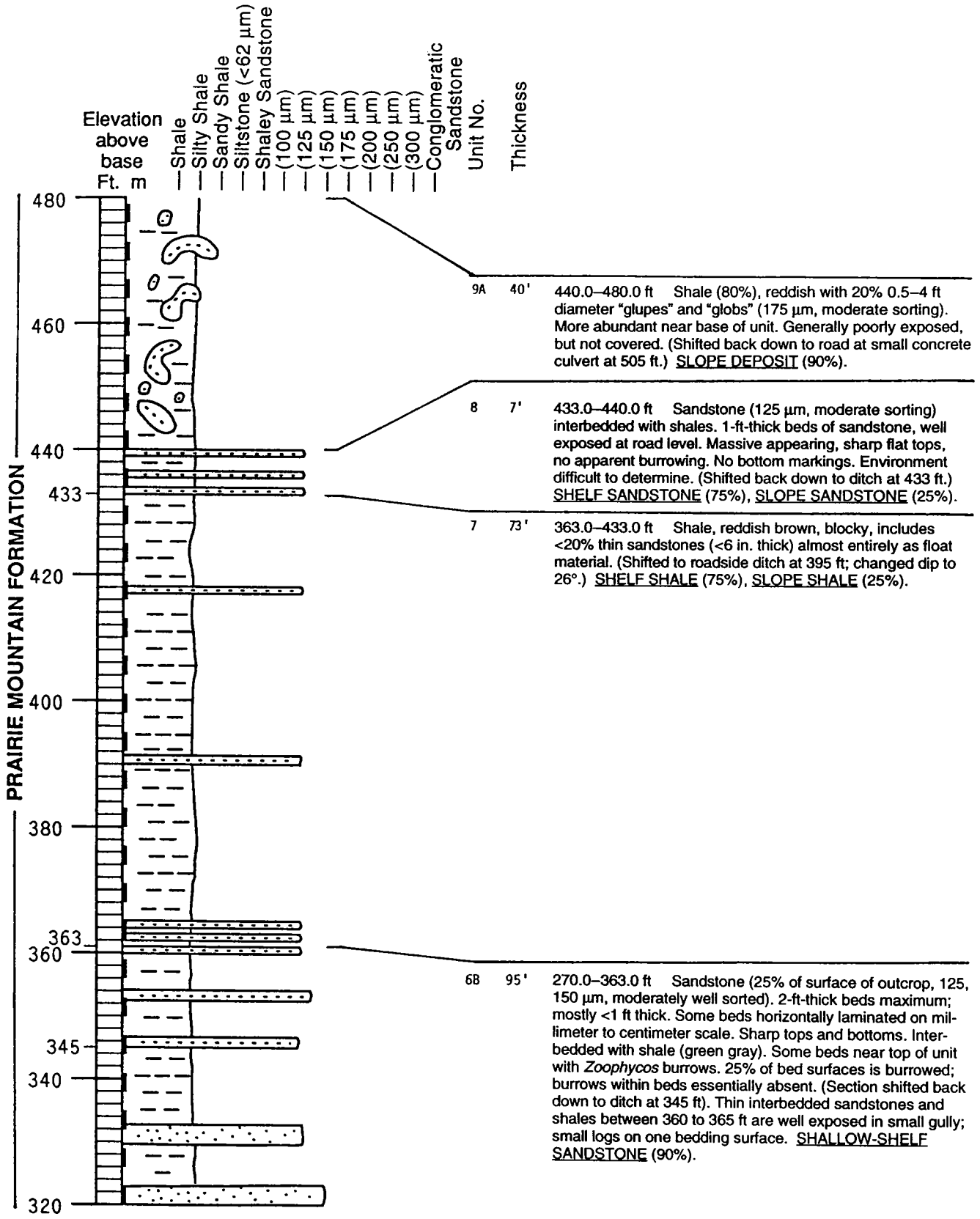

Figure 5. *(continued)*

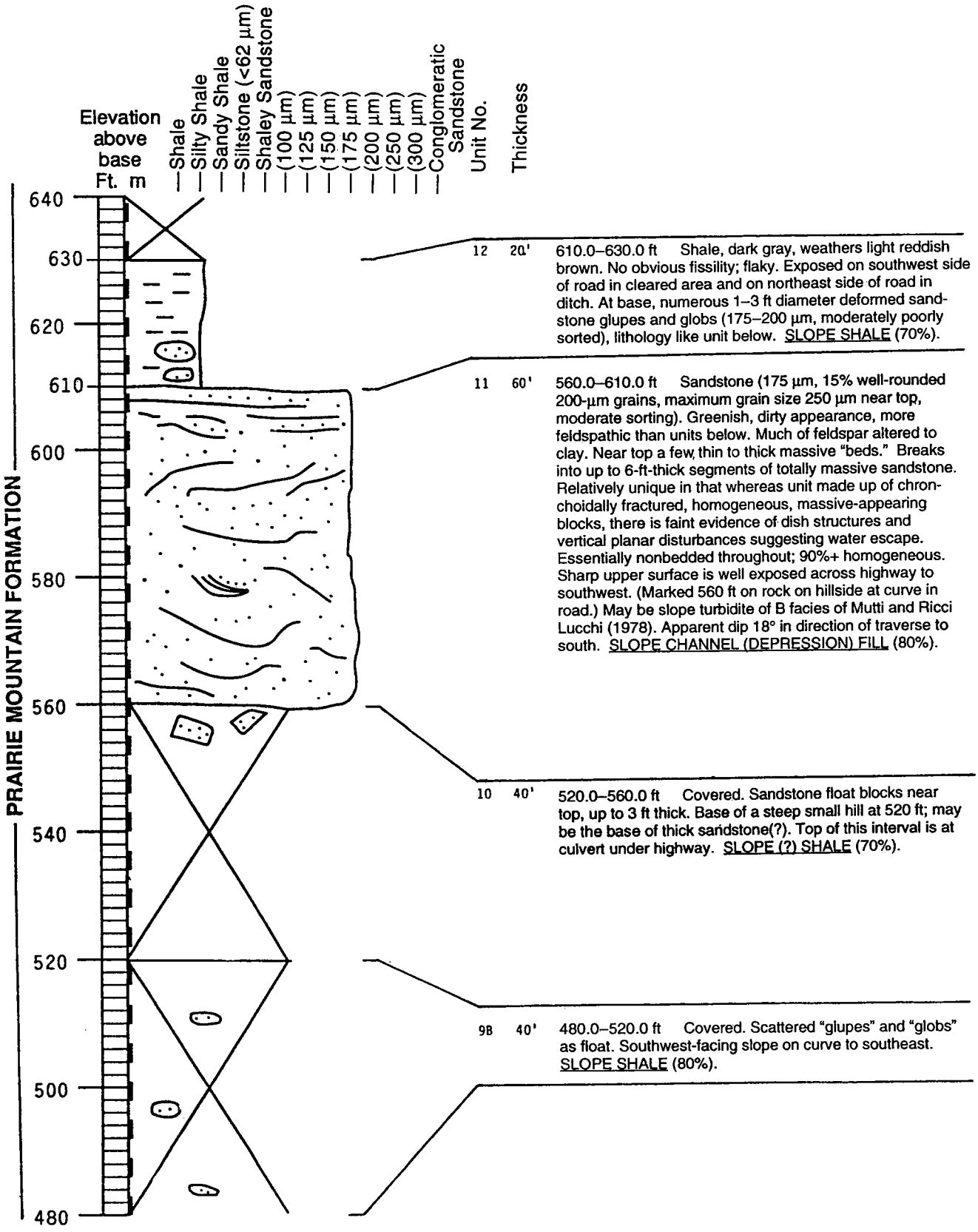

Figure 5. *(continued)*

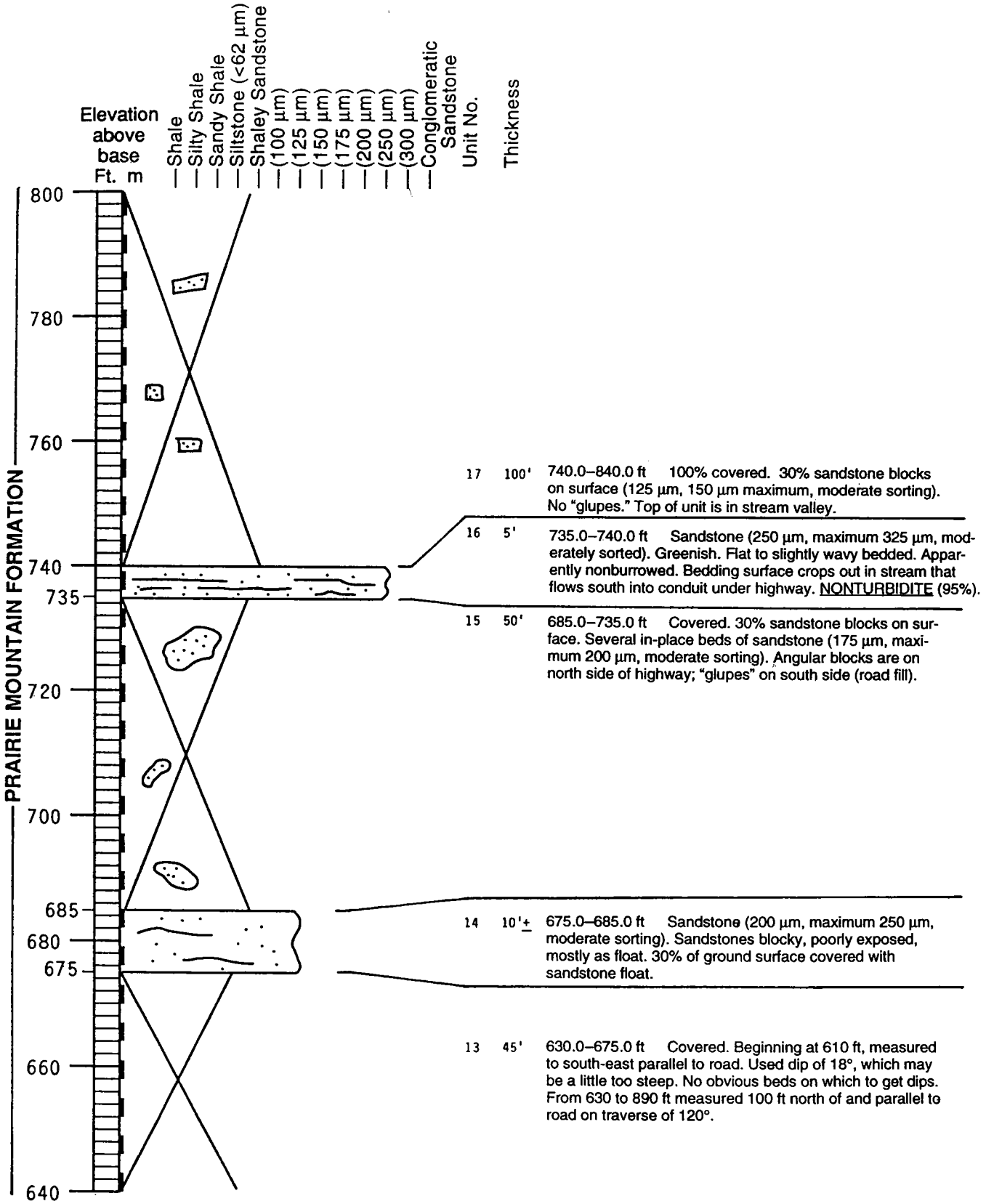

Figure 5. *(continued)*

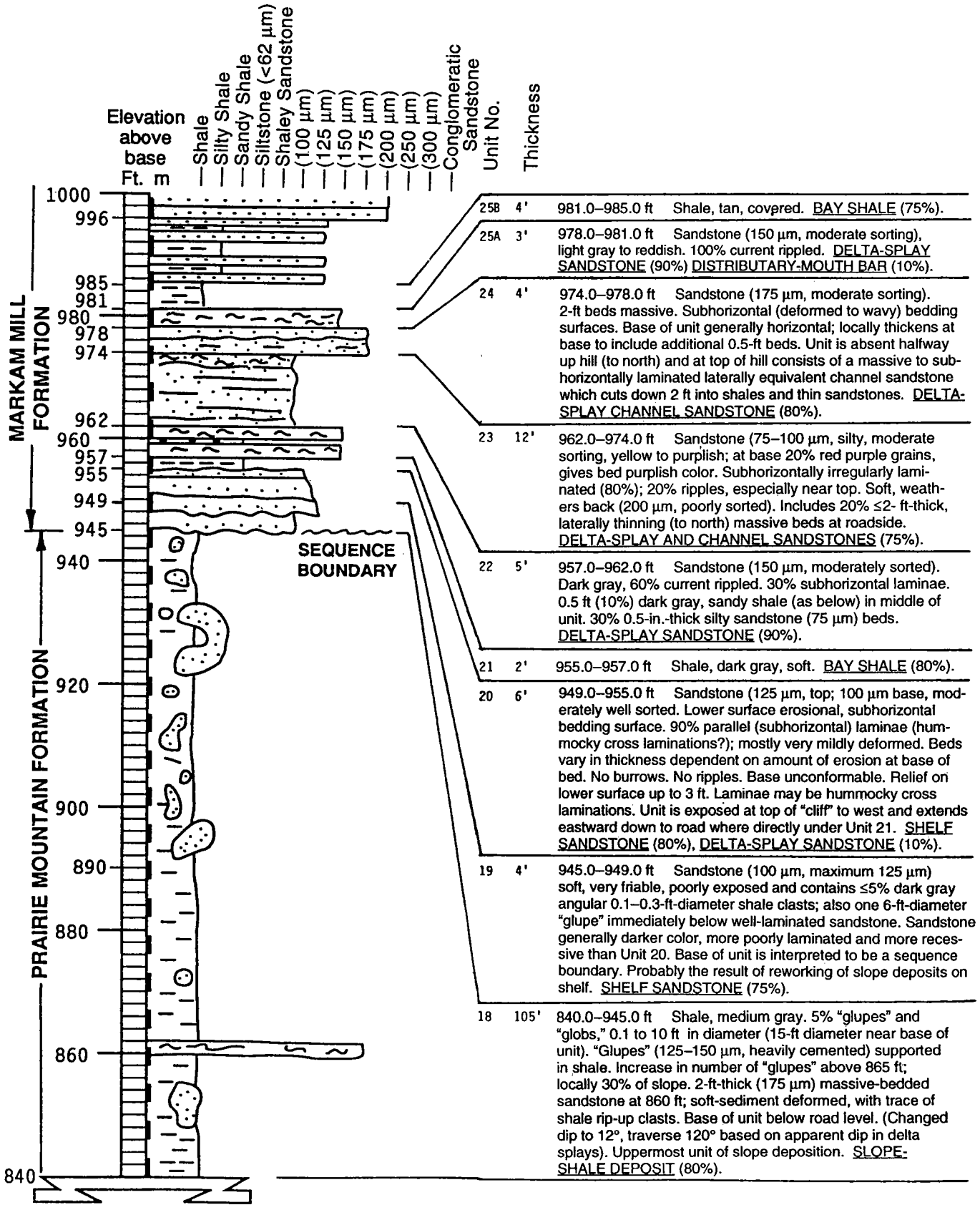

Figure 5. *(continued)*

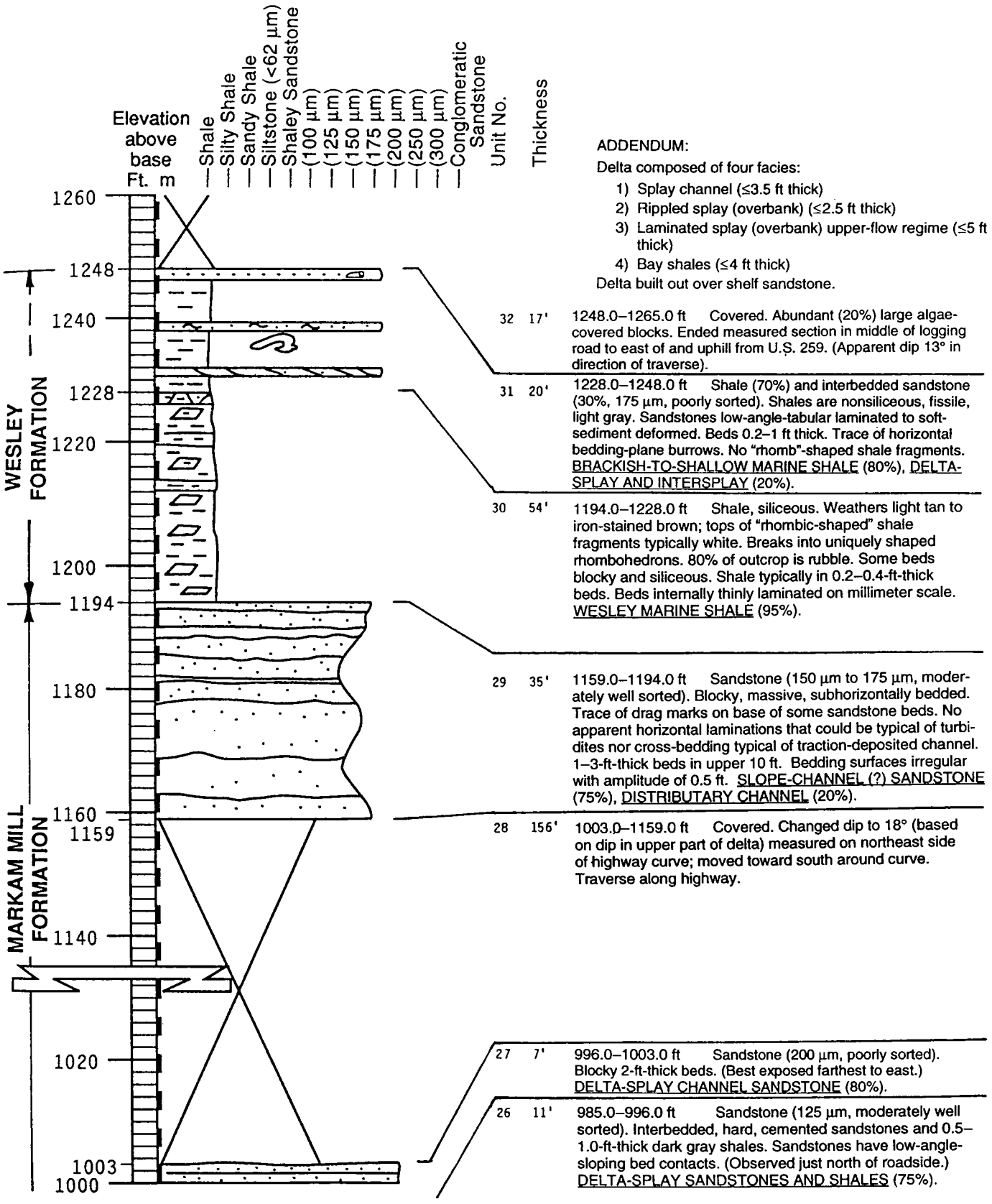

Figure 5. *(continued)*

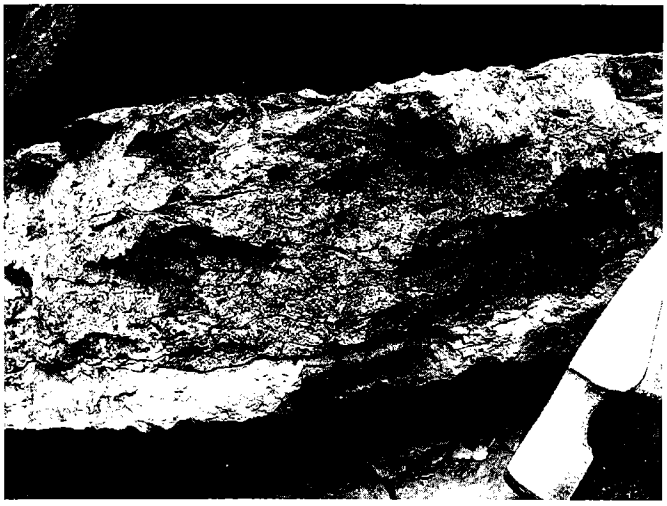

Figure 6. Wildhorse Mountain Formation of Jackfork Group. Slurried "turbidite" (blue-bed) containing abundant plant and wood fragments. Plant fragments are jumbled and have no preferred orientation. Thin turbidite sandstones are interbedded with thin shales (hammer head for scale). Bed is just below strata shown in Figure 7.

Figure 7. Turbidites in Wildhorse Mountain Formation of Jackfork Group. Note abrupt horizontal upper and lower bed contacts typical of turbidites. Beds are 0.5–3 ft thick and are located along U.S. Highway 259, 1.3 mi northeast of measured section 6A-93.

Table 3.—Suite of Turbidite Features Observed in Wildhorse Mountain Formation of Jackfork Group

Horizontal bedding
Sharp tops and bases of beds
Bouma sequences
Partial Bouma sequences
Asymmetrical current ripples (as opposed to symmetrical wave ripples)
Absence of traction features larger than ripples
Horizontal laminations
Normal grading
Inverse grading
Bottom marks Flutes (directional) Grooves (bidirectional)
Deep-water trace fossils
Water-escape features Dish structures Pipes
Rip-up clasts concentrated at top of beds
Local interbedding of shale and sandstone on fine scale Levee deposits Overbank deposits

Boulder beds occur at several locations along U.S. 259. The lowest "boulder bed" is Unit 3 (123–200 ft, Fig. 5). The boulders in these beds are rounded blocks of sandstones that, for the most part, are not in contact with one another; rather, individual boulders are separated by a silty- and muddy-shale matrix. Units such as these are commonly associated with slope deposits (Table 4). These beds (Units 3, 9, and 18; Fig. 5) were not singled out in Cline and Moretti's (1956) measured section but were noted by Briggs (1973) and Black

Figure 8. Base of Prairie Mountain Formation. Possible shallow-water, yellowish white, friable, 50-ft-thick channel sandstone. Sandstone is in sharp contact (below photo) with Wildhorse Mountain sandstone turbidites. Outcrop is stratigraphically above and a short distance west of rocks shown in Figure 7 (location: NW¼NW¼NW¼ sec. 34, T. 2 N., R. 25 E).

Table 4.—Characteristics of Slope Deposits

Primarily fine grained (shale, mudstone, and silt)

Thin mudstones (1–5 cm) may show grading

Variable size clasts may be common
- (a) Deposited primarily by gravity
- (b) Most had intrabasinal source
- (c) May contain a relatively narrow range of rock types, mostly sandstones
- (d) Commonly rounded and/or includes "bottom marks" on all sides ("glupe") or on one side ("glob")
- (e) Very variable in size; 1 cm to several meters diameter
- (f) Commonly matrix-supported

May include slope-channel sandstone filling

May form very thick accumulations
- (a) Where relative sea level rises
- (b) Where down-to-basin faulting occurs
- (c) Seaward of delta

May contain both "shallow-water" and "deep-water" burrows, including *Zoophycos*

Figure 9. Wood fragments on bedding surface of shelf sandstone at top of Unit 6B at 364 ft in measured section 6A-93 (Fig. 5). Fragments are oriented parallel to bedding.

(1969). They occur in several units in the upper part of the Prairie Mountain Formation.

Measured section 6A-93 (Fig. 5) extends from the middle of the Prairie Mountain Formation to near the top of the Wesley Formation, Cline and Moretti's Unit 59. The newly measured section, which is the subject of this paper, does not include units below Cline and Moretti's Unit 51. The section will be described generally from the base upward.

Figure 10. Tracks and trails on thin-bed bedding surface in shelf sandstone. Fine grazing pattern visible below and to the left of end of pen. Unit 4 in measured section 6A-93 (Fig. 5). (Pen for scale.)

Figure 11. Trails of pellets on bedding surface of shelf sandstone. Unit 4 in measured section 6A-93 (Fig. 5). (Pen for scale.)

Shelf Sandstones and Shales

A thick shale interval from 200 to 440 ft in the upper part of Prairie Mountain Formation contains <25% sandstone and is interpreted to consist of shelf deposits. A shelf interpretation is supported by the presence of thinly bedded, horizontally laminated sandstones with burrows of moderately shallow-water type (including *Zoophycos*). Wood fragments occur on some bedding surfaces (Fig. 9). Burrows and trails are generally limited to bedding surfaces (Figs. 10 and 11). The tops and bases of some of the sandstones are gradational; others are sharp. Slightly wavy laminations also occur. Interbedded shales are pastel colors (light gray, pink, and light green). Neither fissility nor bedding is observed in

the shales except where sandy lenses occur, and there bedding is horizontal. Deformation and transported clasts typical of the slope deposits are absent, as are packages of sharp-based and sharp-topped turbidite sandstones. The absence of typical slope and turbidite characteristics adds further to a shelf interpretation for this interval.

The characteristics of shelf sandstones are listed in Table 5. Many of the characteristics listed under "Nearshore and Shoreface Attached Shelf-Ridge" are observed in those Prairie Mountain Formation strata interpreted as shelf deposits. The characteristics of offshore-shelf sandstones are also listed in Table 5 to contrast with the characteristics observed in the Jackfork.

Table 5.—Characteristics of Shelf Sandstones

Nearshore and Shoreface Attached Shelf Ridge

1. Primarily wave deposited
   (a) HCS (hummocky cross-stratification), lower shoreface and offshore transition
   (b) SCS (swaley cross-stratification), middle shoreface
   (c) Subhorizontally to horizontally laminated
   (d) "Smeared-out troughs"; formed by combined flow
   (e) Commonly fine-grained; moderately well sorted
2. May contain some tidal and storm deposits
3. Suite of trace fossils will be those from nearshore zone

Offshore Shelf Ridge (Not present in Jackfork)

1. Primarily storm-current deposits
2. Marine sand body surrounded by shale; sides, bottom, and top
3. Coarsens upward, facies by facies, from silt to medium-grained sand
4. Facies may climb stratigraphically in oblique fashion
5. Glauconitic (trace to 30% locally)
6. Predominently angle of repose or combined flow cross-lamination; upper portion. Current rippled; lower and lateral parts of ridge
7. Sand body asymmetrical
   (a) In form
   (b) In distribution and types of lithofacies
   (c) In occurrence of siderite and clay rip-up clasts
8. Relatively uniform flow directions (oriented subparallel to regional bottom contours)
9. Absence of shoreline-type burrows such as *Asterosoma*
10. Absence of littoral-zone foraminifera suite
11. Absence of evidence of subaerial exposure
12. May contain wave-generated deposits near top of shallowing-up sequence

Slope Deposits

Overlying the lowest shelf deposit is one of at least three thick "boulder shale" intervals (Unit 9, 440–520 ft). There, as in the "boulder beds" below (Fig. 12; Unit 3 and Unit 9, Fig. 5), the clasts occur as "raisins in a pudding" rather than being clast-supported. These boulders are sedimentary and as much as 8 ft in diameter (Fig. 13). The exact composition of the boulders was not documented by me; however, Briggs (1973) noted the following:

> In Unit 55 [of Cline and Moretti, 1956] the "boulders are not concentrated at any particular horizon but are randomly distributed throughout the shale. Most of the boulders are composed of sandstone but the sandstone boulders vary considerably in size, color, matrix content and induration. Ironstone concretions and a few small chert cobbles were also observed. No limestone boulders were found.

As with the "boulder beds" in Unit 3 (Fig. 5), these deposits suggest at least significant local relief, possibly on a slope. The slope may have been the margin of a continent or the result of faulting.

MARKHAM MILL FORMATION

The top of the "boulder shale" (945 ft) is interpreted to be a sequence boundary separating moderately deep-water slope deposits below from the overlying shallow-marine shelf and deltaic sandstones above (Figs. 14 and 15).

Shelf Deposits

The interval from 945 to 955 ft is interpreted as a shelf sandstone deposit and includes two distinct units (19 and 20). These units lie between what are interpreted as slope deposits below and deltaic deposits above. A sequence boundary probably exists at the base of these shelf deposits, and parasequence boundaries occur within (at the unit boundary, Fig. 5) and at the top of the deposits. The lower shelf unit (Unit 19) is interpreted as a reworked sandstone that may have resulted from reworking of underlying slope sandstones. Because of the reworking, the lower contact of this unit appears to be slightly transitional. The lower shelf sandstones (Unit 19) are darker colored, more poorly laminated, and less well cemented than the overlying shelf sandstones (Unit 20).

Unit 20 (949–955 ft) is a very distinct and resistant sandstone that is well exposed in outcrop (Figs. 14 and 15). The internal laminations are 90% subhorizontal with a suggestion of hummocky cross-stratification (HCS). The unit, as a whole, is mildly soft-sediment deformed. Beds vary in thickness depending on the amount of erosion at the base of individual beds and at the base of the unit (3 ft). The absence of ripples in this unit probably eliminates any possibility that this is a distributary-mouth–bar sandstone.

Deltaic Deposits

The sandstones in the interval above the proposed sequence boundary (near the base of Cline and Moret-

Figure 12. Aerial photograph showing "boulder bed" near base of measured section 6A-93, Unit 3 (Fig. 5). "Boulders" are rounded, transported fragments of sandstone beds that may have "bottom marks" on all sides, informally designated as "glupes," or only on one side, "globs." May represent a slope deposit.

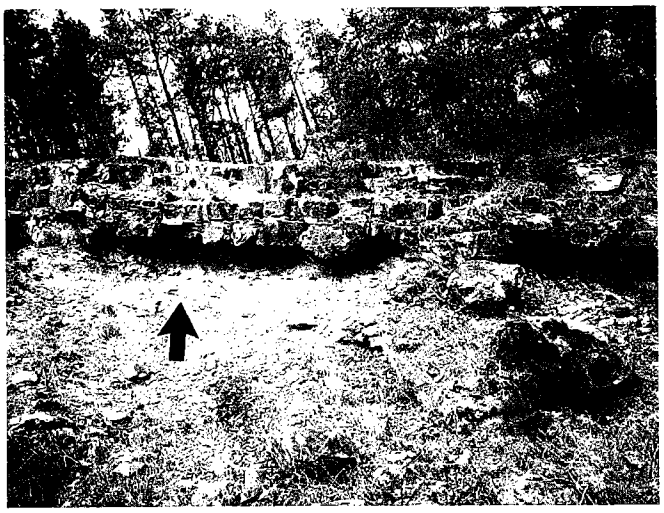

Figure 14. Sequence boundary (arrow) between slope deposits (below) and shelf sandstone (above). Contact is between Units 18 and 19 at 945 ft in measured section 6A-93 (Fig. 5). "Glupes" near right side of photo are in slope deposit at the very top of Unit 18. Unit 19 (above arrow) is a sandstone (reworked on shelf?) that is more friable and more recessive than resistant sandstone above (Unit 20). Markham Mill Formation of Jackfork Group.

Figure 13. Large, transported, rounded clasts "floating" in shale matrix. Maximum diameter of "glupes" and "globs" in this unit is 10 ft. Location of photograph is near top of Unit 18 in measured section 6A-93.

Figure 15. Planar to hummocky laminae in sandstone (Unit 20 of measured section 6A-93, Fig. 5) just above sequence boundary. Upward curving of laminae may be hummocky cross-stratification (HCS), which is indicative of wave or combined-flow deposition. Environment probably inner-shelf deposition, possibly delta fringe.

ti's [1956] Unit 56, Table 1) are interpreted to include a variety of shallow-marine, brackish, and possibly continental deposits including deltaic sandstones (Figs. 16–19). The interval from 949 to 996 ft (Units 22–27; 47 ft thick, Fig. 5) is interpreted to be deltaic, and the deposits are characterized primarily by thick sets of thinly bedded current ripples varying from 20% (Unit 23) to 100% (Unit 25A) ripples. Subhorizontal lamination is also prominent in some units, varying from 30% (Unit 22) to 80% (Unit 23). The mean grain size varies from 100 to 150 μm in the rippled and laminated beds.

Massive to laminated channeled sandstones that are as much as 4-ft thick, but thin laterally to 0 ft, are also observed (Unit 24, Fig. 5; Figs. 20 and 21). Massive to laminated beds 2-ft thick and interbedded with thinner-bedded sandstones form as much as 20% of Unit 23 and the entirety of Unit 27 (Fig. 5). Lateral

Figure 16. Interbedded, thin, rippled delta-splay sandstones and "lagoonal" shales and mudstones. Photograph taken 50 ft north of U.S. Highway 259 and location of measured section 6A-93 (Fig. 5). Equivalent to Units 23 and 24.

Figure 17. Relatively thick sets of rippled, very fine grained (100 μm) sandstone interbedded with irregular, subhorizontally bedded and laminated sandstone beds. Delta-splay sandstone, Unit 23 in measured section 6A-93 (Fig. 5).

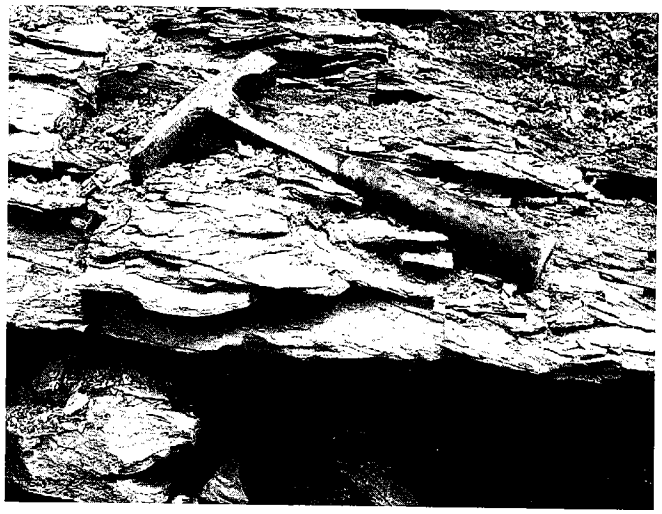

Figure 18. Ripples typical of very fine grained (100–125 μm) sandstones in delta splays. Markham Mill Formation of Jackfork Group. Unit 23 in measured section 6A-93 (Fig. 5).

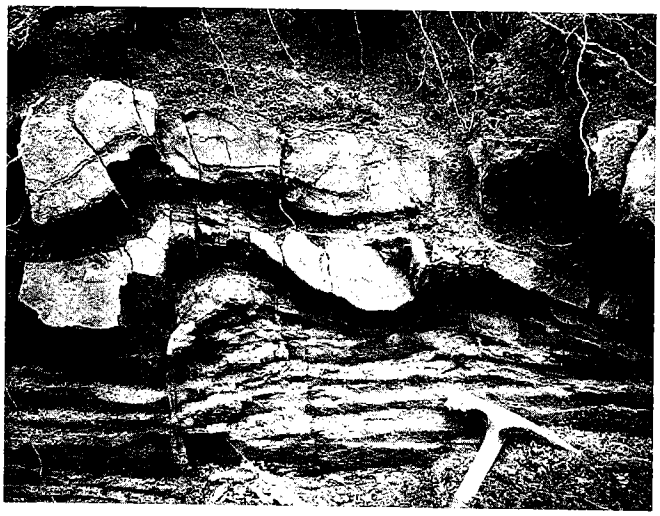

Figure 19. Soft-sediment-deformed, thin-bedded sandstones in delta splay (Unit 24 in measured section 6A-93, Fig. 5). Located 3 ft above small channel in Figure 20. (Hammer for scale.)

variation of bedding types over short distances (<10 ft) is common. No burrowing was observed. All the deposits in the deltaic interval were emplaced by traction and are interpreted to represent delta splays and delta-splay channels. A relatively thick distributary channel, near the measured section, is postulated as a source for the splay sandstones. A summary of the features observed in the deltaic deposits of the Jackfork Group is given in Table 6. The shelf and deltaic deposits (Units 19–26 and the shelf deposits in the interval from 200 to 440 ft; Fig. 5) were deposited in a much shallower environment than has been previously interpreted for the

Figure 20. Lens-shaped delta-splay channel sandstone equivalent to Unit 24 in measured section 6A-93 (Fig. 5). Sharp lower base. Eroded into thinly bedded mudstones and sandstones. Thins toward both edges of photo. Width of channel is ~15 ft. (Hammer on left for scale.)

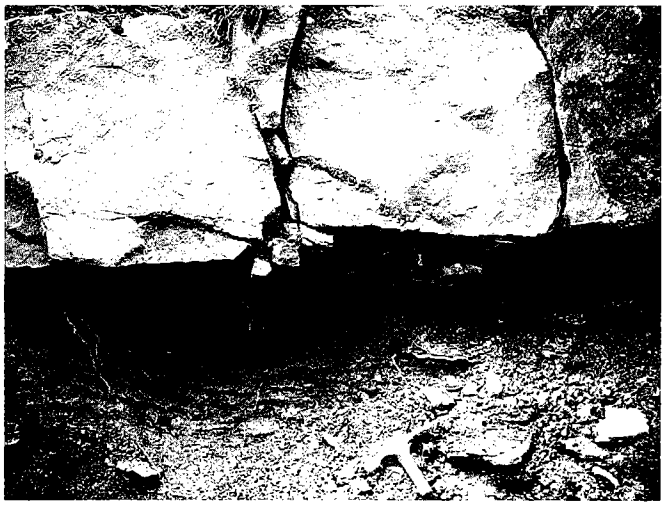

Figure 21. Close-up of Unit 24 in Figure 20. Note sharp base of channel sandstone. Internally massive to faintly horizontally laminated. (Hammer for scale.)

Table 6.—Characteristics of Deltaic Deposits (Markham Mill Formation)

1. All deposits show evidence of traction current deposition
2. Interbedded sandstones and shales
3. Sandstones are current rippled (most common) and horizontally laminated (high-flow regime)
4. Distributary and fluvial channels must be present locally(?) but not in measured section outcrop
5. Splay and overbank sandstones and lagoonal shales predominate
   (a) Locally silty
   (b) Locally lenticular
   (c) Interbedded on variety of scales
   (d) Shales are pastel in color and generally lack fissility
6. Sandstones commonly have sharper bases than tops
7. Burrowing sparce to absent
8. Locally carbonaceous; more carbonaceous than most of deeper-water facies
9. Base of delta only a few feet above sequence boundary that separates shelf sandstones from underlying slope deposits
10. Absence of shoreface, slope, and turbidite features

Jackfork Group. The fluvial channel (Table 7) or distributary channel, which must be the source of the delta splays, is probably not present in the U.S. 259 outcrop unless the sandstone in the interval from 1,159 to 1,194 ft (Fig. 5) is a distributary channel. Sedimentary features are sparse in this unit (29), and a precise interpretation of environment of deposition cannot be made.

Slope and/or Deltaic Channel Sandstones

Approximately 56 ft are covered above the top of the well-exposed deltaic deposits. A thick sandstone in the interval from 1,159 to 1,194 ft (Unit 29, Fig. 5) is superficially like Unit 11, which is a 60-ft-thick sandstone. Both sandstones are generally massive appearing and subhorizontally bedded. Bedding surfaces are slightly irregular with an amplitude of 0.5 ft. Angle-of-repose traction cross-lamination is absent. Both units (11 and 29) have mean grain sizes slightly coarser (175 μm) than most of the deposits interpreted as deltaic and shelf. Unit 11 contains grains as large as 250 μm and appears to be less quartzose than most other units.

Some beds in Unit 11 are 6 ft thick and break into conchoidally fractured, homogeneous blocks having faint dish structures and vertical planar disturbances that probably were avenues for water escape from the sand soon after deposition. Unit 11 is interpreted to be a slope channel-fill deposit and may be a "B" facies turbidite deposit (terminology of Mutti and Ricci Lucchi, 1978). Although these two units appear to be similar, the mechanism of deposition of Unit 29 is less interpretable; however, it may also be a slope channel-fill sandstone.

WESLEY FORMATION

The Wesley Formation is the highest stratigraphic unit redescribed and interpreted along U.S. 259 (Fig. 5). This cherty black shale has a very distinctive appearance—it breaks into numerous, small, well-cemented rhombohedrons that typically have "chalky"-white bedding surfaces (Fig. 22). The cherty shale is interbedded with very thin friable sandstones (Fig. 23). The Wesley Formation (Units 30 and 31, Fig. 5) is interpreted to be marine.

Table 7.—Characteristics of Fluvial Sandstones

Scoured base of channel
Beds show cut and fill (1–3 ft minimum)
Laterally variable
Cross-laminated (a) Troughs (b) Planar-tabular (braided)
Traction deposits (absence of turbidity deposition features)
Current ripples
Planar-horizontal (upper flow regime) laminations
Locally fining upward (point bar) (a) Decrease in mean grain size upward (b) Increase in amount of clay upward
May have lateral accretion beds
May be poorly sorted
May contain wood and carbonaceous fragments
Interbedded shales are light colored
Clay rip-up clasts may be common locally
Interbedded relatively thin sandstones and shales (a) Interbedded overbank sandstones (b) Rippled splay sandstones

Figure 22. Wesley Formation of Jackfork Group. Distinct rhombohedron shapes and white bedding surfaces typical of cherty, thin-bedded marine mudstones that make up most of this unit. Black pen for scale near base. Unit 30 in measured section 6A-93 (Fig. 5).

Figure 23. Wesley Formation. Typical black, blocky, siliceous mudstone interbedded with shale. (Hammer for scale.) Unit 30, near top of measured section 6A-93 (Fig. 5).

The Game Refuge Formation was not included in the newly measured section, but was observed in the course of measuring and describing several unpublished sections.

SEQUENCE STRATIGRAPHY

Several important sequence-stratigraphic surfaces occur in the series of outcrops along U.S. 259. The base of the Prairie Mountain Formation, which is well below the newly measured section, is interpreted to be a sequence boundary (Fig. 2). Near the top of the Prairie Mountain, the water in which sands were deposited shallowed. Just above the "boulder shale" at the top of the Prairie Mountain Formation, a sequence boundary apparently separates "slope" deposits below from shallow-marine, shelf and deltaic deposits of the Markham Mill Formation above. At least one flooding surface may occur near the top of the Markham Mill Formation or at the base of the Wesley Formation. A flooding surface probably also occurs at or near the base of the Game Refuge Formation. Several parasequence boundaries may be present in the Prairie Mountain Formation and the upper part of the Markham Mill Formation.

CONCLUSIONS

Relatively thick sections of the Jackfork Group are interpreted as significantly shallower water deposits than many previous workers have indicated. A 240 ft thick interval (Units 2–8, Fig. 5) and a 10 ft thick interval (Unit 20, Fig. 5) interpreted as shelf deposits and a 46 ft thick deltaic sequence (Units 22–27, Fig. 5) are the shallowest water deposits observed. The shelf deposits are characterized by thin, predominantly subhorizontally laminated sandstones; some have burrowed upper surfaces, and a few have internal burrowing. These sandstones are interbedded on a variety of scales with shale and mudstone.

Deltaic units are characterized throughout by traction deposition in the form of thick rippled beds; thin, laterally discontinuous channels; local soft-sediment deformation; and several "massive-appearing," relatively thicker, more resistant sandstones.

Several thick intervals, which may have been deposited on slopes (either fault-related or on the edge of a continent), are present. These slope deposits are marked by numerous small to large deformed blocks of sandstone in a mudstone or shale matrix.

Sequence boundaries are interpreted at the base and the top of the Prairie Mountain Formation. A significant flooding surface occurs at or near the top of the Markham Mill Formation. Additional flooding surfaces and parasequence boundaries may be interpreted between several units of the measured section. These shallower-water deposits may be part of a separate thrust-fault block that was translated more than 100 miles in a northerly direction.

ACKNOWLEDGMENTS

David Pauli aided in the reconnaissance of the area, and James Hopper aided in measuring section 6A-93 (Fig. 5). Field work done at the request of Weyerhaeuser in 1992 stimulated my interest in doing a detailed interpretation of the section. Neil Suneson's careful editing significantly improved the paper. Brenda Howell and Teresa Gamsky drafted the figures. Robert and Margaret Draughon typed the manuscript.

REFERENCES CITED

Black, B. A., 1969, Origin of isolated sandstone masses in shales of Late Paleozoic flysch, Ouachita Mountains, southeastern Oklahoma: University of Wisconsin unpublished Ph.D. dissertation, 191 p.

Briggs, Garrett, 1973, Geology of the eastern part of the Lynn Mountain syncline, Le Flore County, Oklahoma: Oklahoma Geological Survey Circular 75, 34 p.

Briggs, Garrett; and Smith, D. L., 1973, Geologic map and sections of eastern part of Lynn Mountain syncline and adjacent areas, *in* Briggs, Garrett, Geology of the eastern part of the Lynn Mountain syncline, Le Flore County, Oklahoma: Oklahoma Geological Survey Circular 75, pl 1.

Cline, L. M., 1960, Stratigraphy of the late Paleozoic rocks of the Ouachita Mountains, Oklahoma: Oklahoma Geological Survey Bulletin 85, 113 p.

Cline, L. M.; and Moretti, F. J., 1956, Two measured sections of Jackfork Group in southeastem Oklahoma [description and correlation of two complete stratigraphic sections of the Jackfork Sandstone in Kiamichi Mountains, central Ouachita Mountains, Oklahoma]: Oklahoma Geological Survey Circular 41, 20 p.

Fellows, L. D., 1964, Geology of the western part of Winding Stair Range, Latimer and Le Flore Counties, Oklahoma: Oklahoma Geological Survey Circular 65, 102 p.

Harlton, B. H., 1938, Stratigraphy of the Bendian of the Oklahoma salient of the Ouachita Mountains: American Association of Petroleum Geologists Bulletin, v. 22, p. 852–914.

Hart, O. D., 1963, Geology of the eastern part of Winding Stair Range, Le Flore County, Oklahoma: Oklahoma Geological Survey Bulletin 103, 87 p.

Morris, R. C., 1965, A geologic investigation of the Jackfork Group of Arkansas: University of Wisconsin unpublished Ph.D. dissertation, 179 p.

_____ 1974, Sedimentology and tectonic history of the Ouachita Mountains, *in* Dickinson, W. (ed.), Tectonics and sedimentation: Society of Economic Paleontologists and Mineralogists Special Publication 22, p. 120–142.

_____ 1975, Stratigraphy and structure of part of the frontal Ouachita Mountains, Arkansas: American Association of Petroleum Geologists Bulletin, v. 59, p. 747–765.

Mutti, E.; and Ricci Lucchi, F., 1978, Turbidites of the northern Apennines: introduction to facies analysis: International Geology Review [translated by T. H. Nilsen], v. 20, no. 2, p. 125–166. [Reprinted as American Geological Institute Reprint Series 3, Falls Church, Virginia, 66 p.]

Pauli, David, 1994, Friable submarine channel sandstones in the Jackfork Group, Lynn Mountain syncline, Pushmataha and Le Flore Counties, Oklahoma, *in* Suneson, N. H.; and Hemish, L. A. (eds.), Geology and resources of the eastern Ouachita Mountains frontal belt and southeastern Arkoma basin, Oklahoma: Oklahoma Geological Survey Guidebook 29, p. 179–202.

Seely, D. R., 1963, Structure and stratigraphy of the Rich Mountain area, Oklahoma and Arkansas: Oklahoma Geological Survey Bulletin 101, 173 p.

Sellars, R. T., Jr., 1966, Geology of the Mena–Board Camp quadrangles, Polk County, Arkansas: Tulane Studies in Geology, v. 4, p. 141–172.

Shelburne, O. B., Jr., 1960, Geology of the Boktukola syncline, southeastern Oklahoma: Oklahoma Geological Survey Bulletin 88, 84 p.

Smith, D. L., 1967, Geology of northeast McCurtain and southeast Le Flore Counties, Oklahoma: University of Wisconsin unpublished M.S. thesis, 46 p.

Taff, J. A., 1902, Description of the Atoka quadrangle [Indian Territory]: U.S. Geological Survey Geologic Atlas Folio 74, 6 p.

Walthall, B.; and Bowsher, A. L., 1966, Geology of part of southern Ouachitas, Arkansas, *in* Flysch facies and structure of the Ouachita Mountains: Kansas Geological Society Guidebook, 29th Field Conference, p. 125–139.

Turbidite Elements of the Jackfork Group in Arkansas

Roger M. Slatt[1]
Colorado School of Mines
Golden, Colorado

Paul Weimer
University of Colorado
Boulder, Colorado

Charles G. Stone
Arkansas Geological Commission
Little Rock, Arkansas

Hisham Al-Siyabi, and Eugene T. Williams
Colorado School of Mines
Golden, Colorado

ABSTRACT.—Five basic elements are common to turbidite depositional systems— channels and their fill, overbank deposits, lobes, channel-lobe–transition features, and major erosional features. All five of these elements are interpreted to be present at different outcrops of the Lower Pennsylvanian upper Jackfork Group[2] in southwest-central Arkansas. An understanding of turbidite elements in the Jackfork Group in southwest-central Arkansas is important because: (1) this area is a common training ground for petroleum-industry geoscientists and engineers working on deep-water clastic deposits worldwide; (2) there is an active Jackfork gas play in the frontal Ouachita overthrust belt of eastern Oklahoma, with production probably from similar turbidite elements; and (3) controversy currently exists over interpretation of the depositional system of the Jackfork Group, which has much broader implications to exploration and development of turbidite reservoirs.

Each of the five elements in the Jackfork Group exhibits characteristic sedimentologic and stratigraphic features that allow identification in vertical section and recognition of such important features as bed connectivity and perhaps potential reservoir quality. Some Jackfork outcrops are suitable for determining lateral aspects such as bed continuity and correlatability, whereas other outcrops are less suitable. A preliminary sequence-stratigraphic framework is also developed. Comparison of the Jackfork outcrops with more generalized, published characteristics of these elements provides additional insight into lateral and vertical attributes, as determined from well logs, cores, and seismic reflection profiles. The Arkansas Jackfork strata can be used as analogs for potentially gas-productive Jackfork strata in eastern Oklahoma.

INTRODUCTION

The classic publications of Mutti and Normark (1987, 1991) defined five basic elements common to both modern and ancient turbidite systems: channels and their fill, overbank deposits, lobes, channel-lobe transition deposits and their morphologic features, and major erosional features (excluding channels)—especially scours and shelf-edge slump scars. More recent publications focusing on descriptive or formative classifications all contain the same elements, although the names may differ (Posamentier and Erskine, 1991; Chapin and others, 1994; Mahaffie, 1994; Reading and Richards, 1994; Yielding and Apps, 1994). Some of the many factors that control deep-sea sedimentation are eustatic sea-level variations, local tectonic setting, basin size and configuration, type of sediment within the system, and frequency and volume of gravity flows (Baruffini and others, 1994). These factors give rise to

[1]Present address: University of Oklahoma, Norman, Oklahoma.

[2]Identified by various investigators as "Jackfork Sandstone, "Jackfork Formation," and "Jackfork Group" in Arkansas.

Slatt, R. M.; Weimer, Paul; Stone, C. G.; Al-Siyabi, Hisham; and Williams, E. T., 2000, Turbidite elements of the Jackfork Group in Arkansas, *in* Johnson, K. S. (ed.), Marine clastics in the southern Midcontinent, 1997 symposium: Oklahoma Geological Survey Circular 103, p. 87–103.

a variety of sizes, geometries, facies, and stacking patterns of deposits. Thus, lateral and vertical attributes that may be important to exploration and development may vary significantly, making it difficult to generalize from one system to another.

Each of these five elements is present within the Lower Pennsylvanian Jackfork Group in the Ouachita Mountains of southwest-central Arkansas. This area is especially significant for three reasons.

First, the area has for many years been a training ground for the petroleum industry, where geoscientists and engineers can examine superb Jackfork outcrops as an analog to fine-grained, turbidite reservoirs in the Gulf of Mexico and elsewhere (Slatt and others, 1997a). Many ideas and observations have emerged from such interchanges on the outcrop.

Second, the Jackfork Group in eastern Oklahoma has been the prime target of recent gas exploration (Pauli, 1994; Montgomery, 1996; Petzet, 1996). Although some prior interpretations of the regional depositional system of the Jackfork Group predicted that only basinal, sand-poor turbidite facies would be present in eastern Oklahoma (summarized in Jordan and others, 1993, and in Roberts, 1994), an outgrowth of the exploration activity has been the indication that sandier facies, including some possibly of shallower water origin, are present (Pauli, 1994; Tillman, 1994, 2000; Montgomery, 1996). Petzet (1996) stated: "Jackfork depositional models will remain speculative, at least until stratigraphic and sedimentological analysis of Jackfork outcrops in eastern Oklahoma and western Arkansas can be carried out and integrated with well data from the current play." We concur with Petzet's statement and add that the excellent outcrop exposures in southwest-central Arkansas, which have been studied in detail and examined by numerous petroleum geologists, geophysicists, and engineers through the years, can provide additional insights into the nature of the productive depositional system(s) in Oklahoma. Based upon published information on the Jackfork in Oklahoma, the same depositional elements described below in southwest-central Arkansas should all be present in the productive area.

Third, controversy has recently emerged over a publication by Shanmugam and Moiola (1995), who interpreted these deposits predominantly as debrites rather than high- and low-density turbidites. Although such controversy can be beneficial in forcing geoscientists to critically review geologic concepts and ideas, the broader implications of this publication to exploration for and development of turbidites has drawn strong critical review from the geoscientific community in publication (Bouma and others, 1997; Coleman, 1997; D'Agostino and Jordan, 1997; Lowe, 1997; Slatt and others, 1997) and at the 1997 American Association of Petroleum Geologists Annual Convention (SEPM, 1997a,b).

With these three reasons in mind, this paper presents examples of each of the turbidite elements that we have observed and studied in southwest-central Arkansas. Although the term "turbidite" was used by Mutti and Normark (1987) to describe their five elements, it should be remembered that processes in addition to true turbidity-current transport and deposition are common in deep-sea environments (Winn and Armentrout, 1995).

TURBIDITE ELEMENTS

Channels and Their Fill

According to Mutti and Normark (1987) a channel is the expression of negative relief that represents a long-term pathway for sediment transport. On modern submarine fans, the two main types of channels are large, leveed valleys—the primary sediment-feeder systems—and smaller, unleveed, distributary channels. Topographic relief and features in modern channels and ancient channel-fills can be erosional, depositional, or mixed origin. Erosional channel-fills are characterized by relatively coarse-grained, scour-based, lenticular conglomerates, debrites, graded beds, and horizontal to cross-stratified alternations of coarse sandstone and granule-to-pebble conglomerate. Depositional channel-fill units consist of thick, scoured, amalgamated, graded, axial sandstones and pebbly sandstones that become finer-grained and thinner-bedded toward the channel margins and into overbank settings. Either type of channel-fill generally passes upward into mudstones or thin-bedded, finer-grained sandstones, occasionally exhibiting lateral-accretion surfaces during the waning stages of channel filling.

Such features in the Jackfork are displayed in at least two areas in the vicinity of DeGray Lake, Arkansas, and in one area near North Little Rock, Arkansas (Haley and others, 1976). At all three areas, outcrop gamma-ray logs (Slatt and others, 1992, 1995) have been obtained adjacent to measured sections for comparison with subsurface gamma-ray logs.

The first area in which channel-fill facies are well exposed is at an active quarry immediately north of Hollywood, Arkansas. Hollywood Quarry is a 600 by 375 by 150 ft excavation that exposes more than 130 ft of strata near the top of the upper Jackfork. Four units have been identified and mapped in the quarry (Jordan and others, 1993; Slatt and others, 1994b, 1997; see Fig. 1). From the base to the top, these (using lowercase letters) are designated on Figure 1 as follows: unit "a"—a shale unit, containing abundant sandstone, pebbly sandstone, and shale clasts; unit "b"—90 ft of mainly massive, medium-grained quartzose, amalgamated sandstone beds with some conglomerates and pebbly sandstones; unit "c"—10 ft of black shale with thin, very fine grained sandstone to siltstone beds; and unit "d"—30 ft of medium-grained turbidite and slurried sandstones interbedded with mudstones. The basal part of unit "b" has an erosional contact with underlying unit "a." Unit "b" consists of a series of offset-stacked, lenticular sandstones separated by thin shales where it has been exposed by quarrying operations (Fig. 2) and contains pebbly sandstone. Sandstone and shale beds within units "c" and "d" are continuous across the length of the quarry (Slatt and others, 1997). It is likely that the strata exposed at Hollywood Quarry

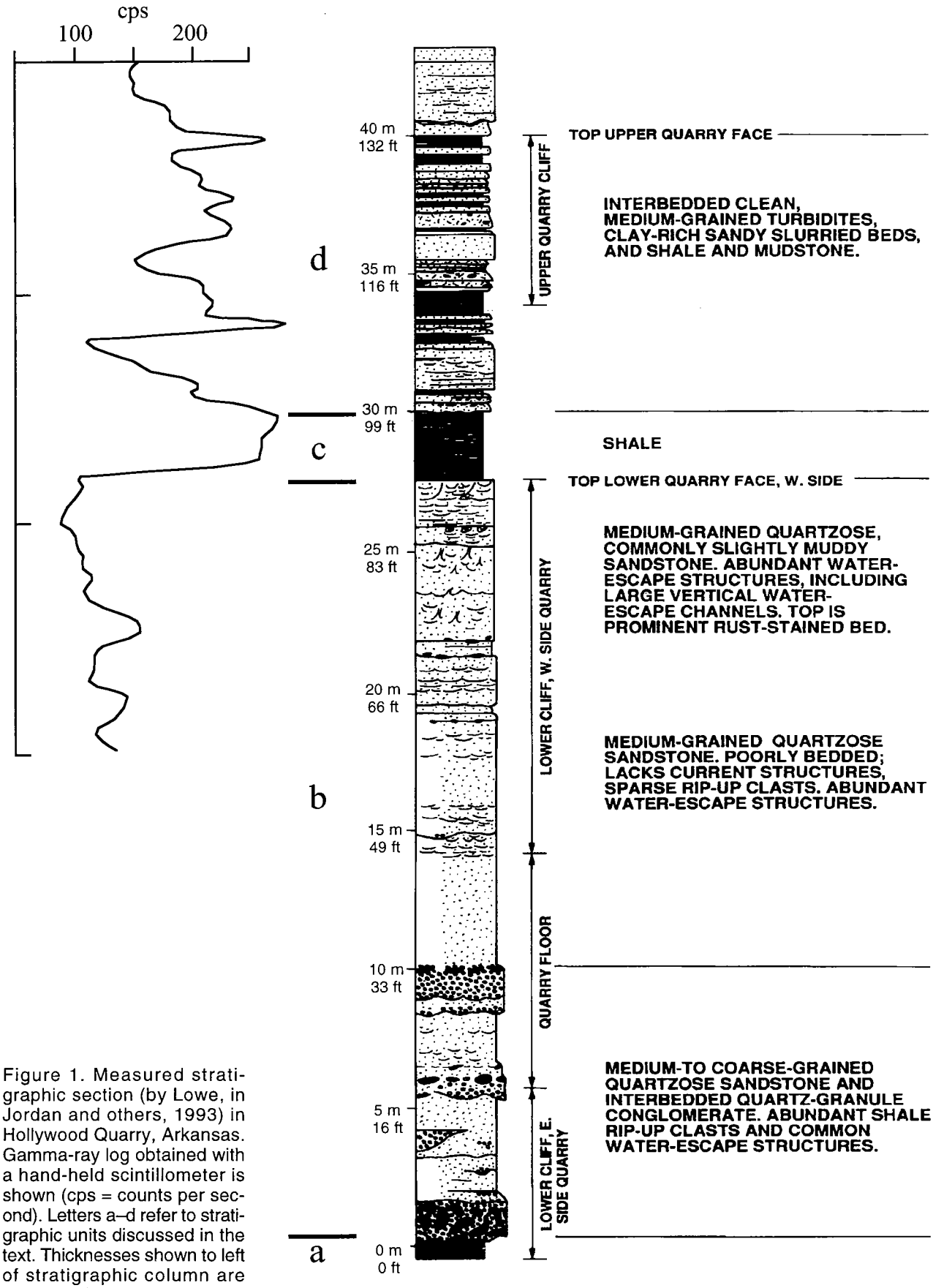

Figure 1. Measured stratigraphic section (by Lowe, in Jordan and others, 1993) in Hollywood Quarry, Arkansas. Gamma-ray log obtained with a hand-held scintillometer is shown (cps = counts per second). Letters a–d refer to stratigraphic units discussed in the text. Thicknesses shown to left of stratigraphic column are accumulative.

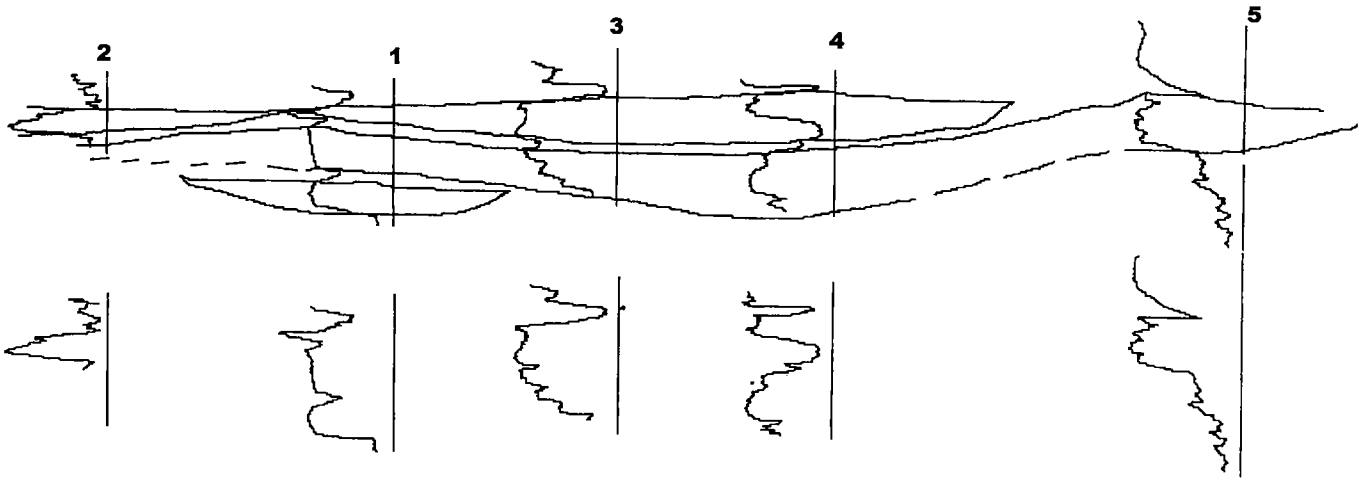

Figure 2. Sketch of pseudo-outcrop gamma-ray logs and the offset-stacked nature of channel-fill of the lower, massive sandstone interval along the east wall of Hollywood Quarry (after Jordan and others, 1993). Distance between log 2 and 5 is approximately 150 ft.

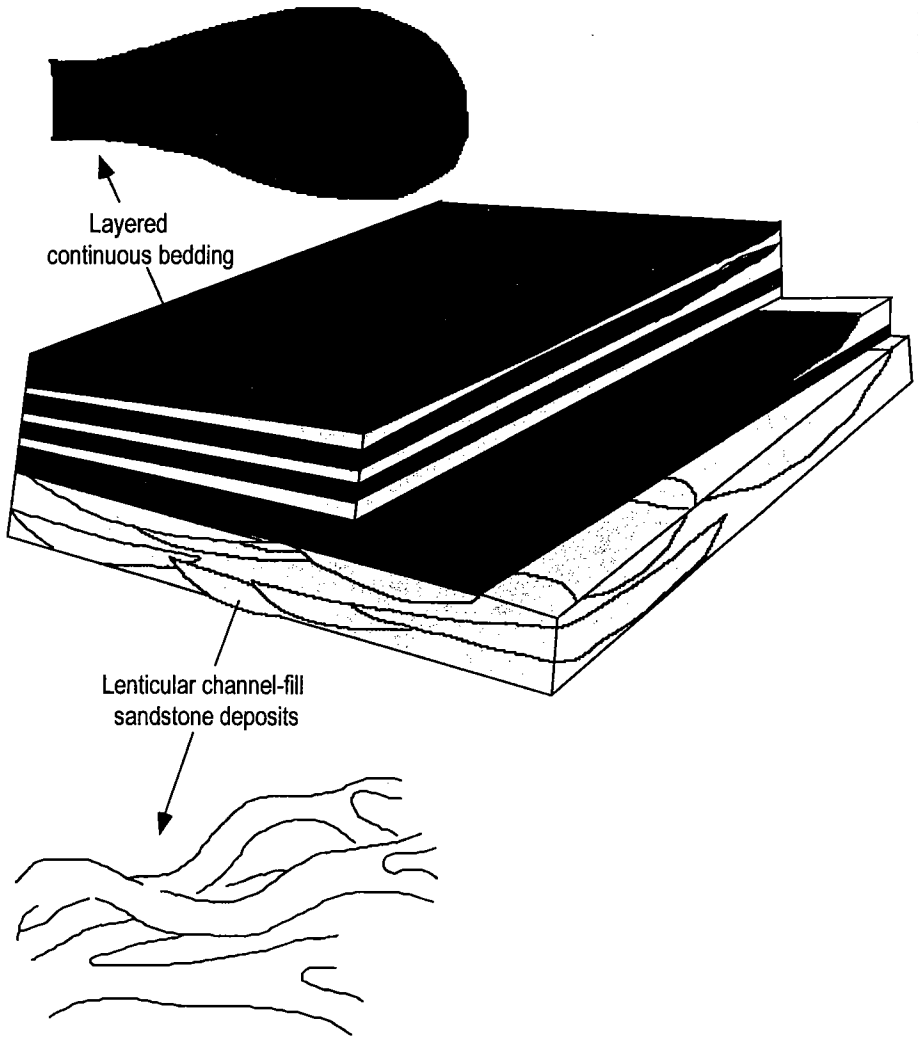

Figure 3. Channel-fill depositional model for Hollywood Quarry.

represent an upward-fining and upward-thinning, channel-fill (and perhaps overbank) succession (Fig. 3), although the quarry is too small to determine lateral relationships. This section has many similarities to the uppermost channel sequences at the DeGray Lake Spillway, but it is stratigraphically about 1,200 ft higher and located near the top of the Jackfork. The Hollywood Quarry section is probably the stratigraphic equivalent of the Murray Quarry section described by Jordan and others (1993).

The second area of well-exposed channel-fill deposits is at Pinnacle Mountain State Park (Fig. 4) southwest of Little Rock. In that area, an east-west–trending linear chain of steep, discontinuous hills consisting of thick, moderately to steeply dipping sandstones and shales of the lower Jackfork extends for about 6 mi. At the abandoned Fulk Mountain Quarry near the Visitors Center, three lithologic units have been gamma-ray logged but not measured (Jordan and others, 1993; Fig. 5). From the base upward, these are designated: unit "a"—50–60 ft of stratified, lenticular sandstone; unit "b"— a sequence >100 ft thick of chaotic, disarticulated and contorted blocks (some of which contain fossiliferous, platform-derived masses [Gordon and Stone, 1977]) and beds of sandstone encased in unstratified, contorted mudstone; and unit "c"—a sequence >100 ft thick of resistant, evenly bedded,

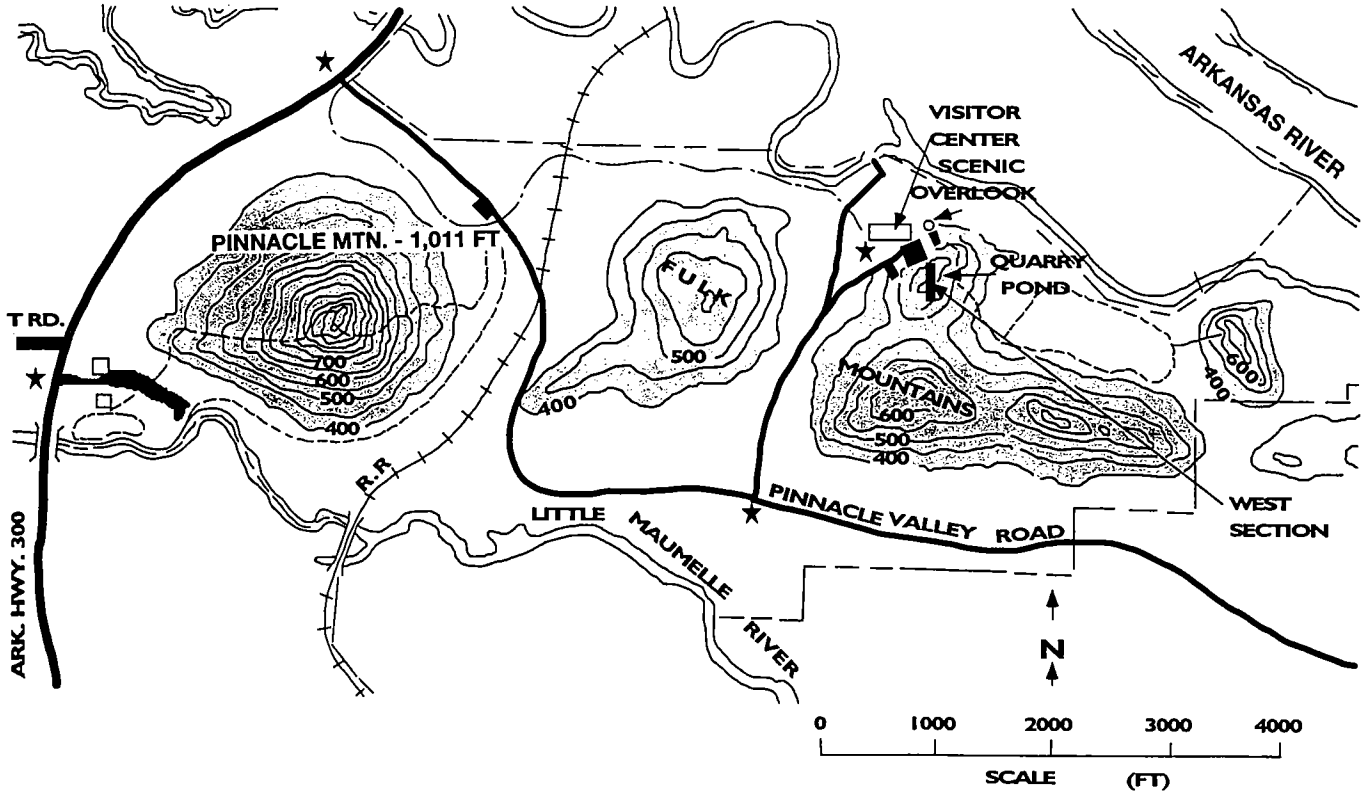

Figure 4. Geographic features in proximity of Pinnacle Mountain State Park, Arkansas; location of Visitors Center, where gamma-ray log was obtained with a hand-held scintillometer ("West Section") (Fig. 5) is shown. Elevation contours in feet.

laminated, clean, quartzose, fine- to medium-grained sandstones that exhibit some channeling. We interpret these unusual thick sandstone deposits (unit "c") as large, discontinuous pods of very high energy turbidite sandstones that were transported through a linear channel on a relatively steep, unstable muddy slope and deposited within slope depressions, perhaps formed as lows between topographically high slump blocks. Where complete sections of sandstone units can be mapped, they appear to form upward-fining and upward-thinning, channel-fill units (Jordan and others, 1993). Modern turbidite sands have been found in a similar setting on the upper Nova Scotia continental slope (Hill, 1984). Other origins proposed for these deposits include: (1) resistant sandstone beds mixed with mudstones in a tectonic mélange (Maumelle) zone at the toe of an accretionary wedge (Viele and Thomas, 1989; Davis, 1994), and (2) partially to completely lithified sandstone slabs and shale masses that have slid, in part from the shelf edge, down a depositional paleoslope (Jordan and others, 1993).

The third area is in the classic DeGray Lake Spillway, which exposes a 1,000 ft thick stratigraphic section mostly near the top of the middle Jackfork (Fig. 6). The section consists of thin- to thick-bedded, low- to high-density turbidite sandstones, thick pebbly sandstones to sandy conglomerates, thick debris-flow shales, and laminated shales and siltstones (DeVries, 1991; Jordan and others, 1993; Chester, 1994; Slatt and others, 1994a). A gamma-ray log of this outcrop interval is shown in Figure 6 alongside a measured stratigraphic section. Figure 7 shows correlations of the spillway section to DeGray Lake Dam, Lakeshore, and Intake measured sections (Fig. 8). The sandstones and conglomerates occur in intervals separated by debris flows and laminated shales.

The upper 230 ft of the DeGray Lake Spillway section is interpreted as a channel/proximal-lobe complex. From the base upward, this 230 ft consists of the following: unit "a"—a 20 ft thick debrite consisting of contorted shale with abundant sandstone and mudstone clasts, including a large, folded slab of sandstone near its top; unit "b"—130 ft of thick-bedded, massive-appearing to amalgamated sandstones separated by thin mudstones; unit "c"—40 ft of shale; and unit "d"—40 ft of clean, quartz-cemented, medium- to coarse-grained sandstones, pebbly sandstones, and sandy conglomerates that grade at the top to fine- to medium-grained sandstones with sparse granules (Jordan and others, 1993; Fig. 6). Pebbly sandstones and conglomerates within unit "d" exhibit erosional bases and normal or reverse grading, and scour surfaces are common. Unit "d" has been mapped for a distance of 13 mi in the general down-current direction (Coleman and others, 1994). It is interpreted as an axial, coarse-grained, channel-fill deposit. Unit "b" has been correlated laterally for at least a mile distance where it grades to pebbly sandstone and sandy conglomerate beds (Fig. 7); it

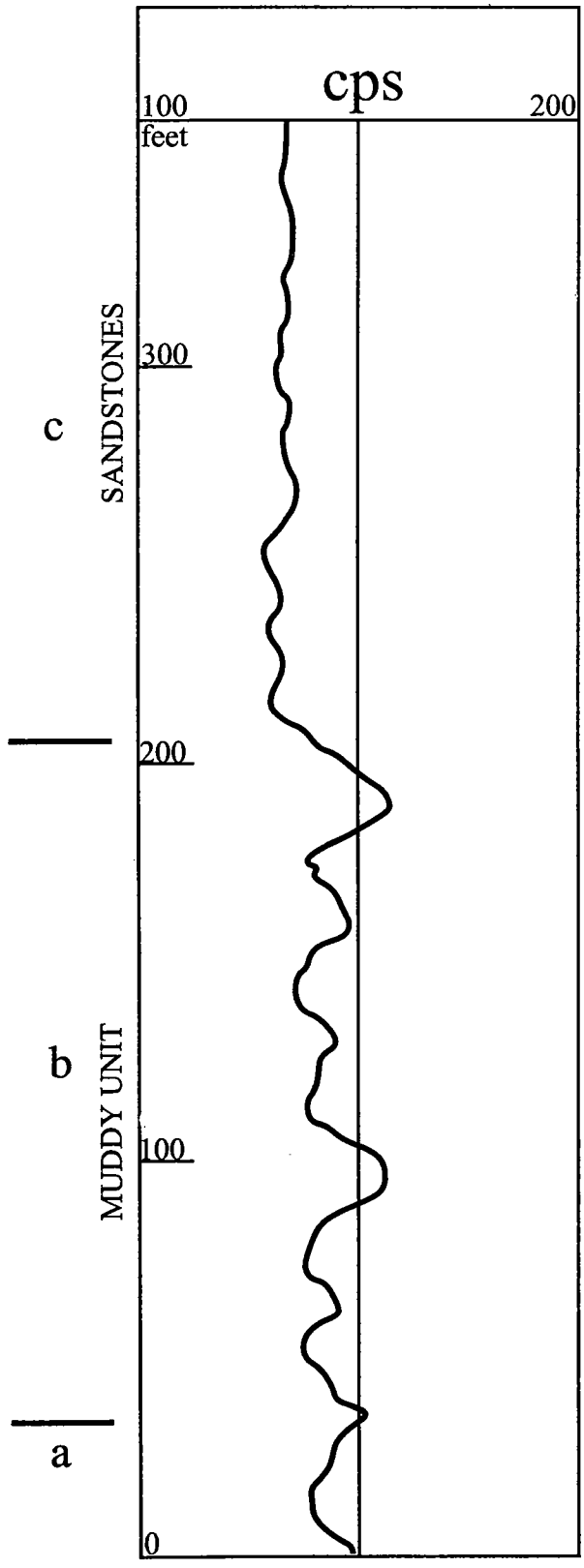

Figure 5. Outcrop gamma-ray log obtained with a hand-held scintillometer along the west wall of the stratigraphic section at the Visitors Center (see Fig. 4). Units "a," "b," and "c" shown on left. (cps = counts per second).

may be a proximal-lobe or channel deposit. Shaley units "a" and "c" represent periods of fine-grained sedimentation, punctuated by sporadic debris flows.

Lobes

According to Mutti and Normark (1987), the term "lobe" has different connotations for modern and ancient fans. Lobes defined for modern fans are based mainly on morphological character, whereas lobe interpretations in ancient fans are based primarily on their stratigraphic character. Differences between the two are a result of the different modes of analysis—seismic reflection, echo-sounding, and side-scan sonar for modern fans (and not deep-penetration cores) versus outcrop, seismic, log, and core observations (mainly vertical) for ancient fans. On modern fans, such features can be tens to hundreds of square miles in extent. Ancient lobes are characterized by the lack of channelized deposits, their tabular and laterally extensive nature (as much as hundreds of square miles), and vertical-stacking pattern. Individual sandstone beds are generally parallel sided, although scoured bases can occur and can be of variable thickness and grain size depending upon the nature of the source material and individual turbidite-flow characteristics. Individual lobe packages are considered to generally display an upward-thickening and upward-coarsening vertical sequence. However, because of compensation-style deposition, upward-thinning and upward-fining lobe sequences can occur (Slatt and others, 1994a). Sandstone-rich intervals may alternate stratigraphically with mudstone-rich, interlobe deposits. Lobes may either be attached to channel-fill facies or be detached, basin-floor features; and they may either onlap onto adjacent slope facies or be convex-upward bodies that wedge down-current into thinner-bedded and finer-grained lobe-fringe deposits.

We interpret the lower 770 ft at the DeGray Lake Spillway section as predominantly lobe deposits, because many of the criteria mentioned above can be observed. Mutti (1992) also interpreted this interval as lobes. One such example is a cleaning- and thickening-upward, sandstone-mudstone succession at 540–640 ft within unit "g" (Fig. 6). Individual beds have been described and measured within this succession and correlated across both walls of the spillway (Jordan and others, 1993; Slatt and others, 1997a). The succession thickens upward and exhibits individual beds that thicken and thin laterally in alternate directions across the Spillway (Slatt and others, 1997a). Some beds pinch out within the outcrop area, but Jordan and others (1993) made calculations and determined that individual beds may extend for hundreds to thousands of feet before pinching out. This and adjacent successions have been correlated with outcrops and subsurface core borings obtained about a mile away, at the site of the DeGray Lake Dam and Intake (Fig. 7). At a larger scale, this succession also has been correlated with reasonable certainty with a 140 ft thick succession in a subsurface well 6 mi to the south (Shell Oil Co., No. 1

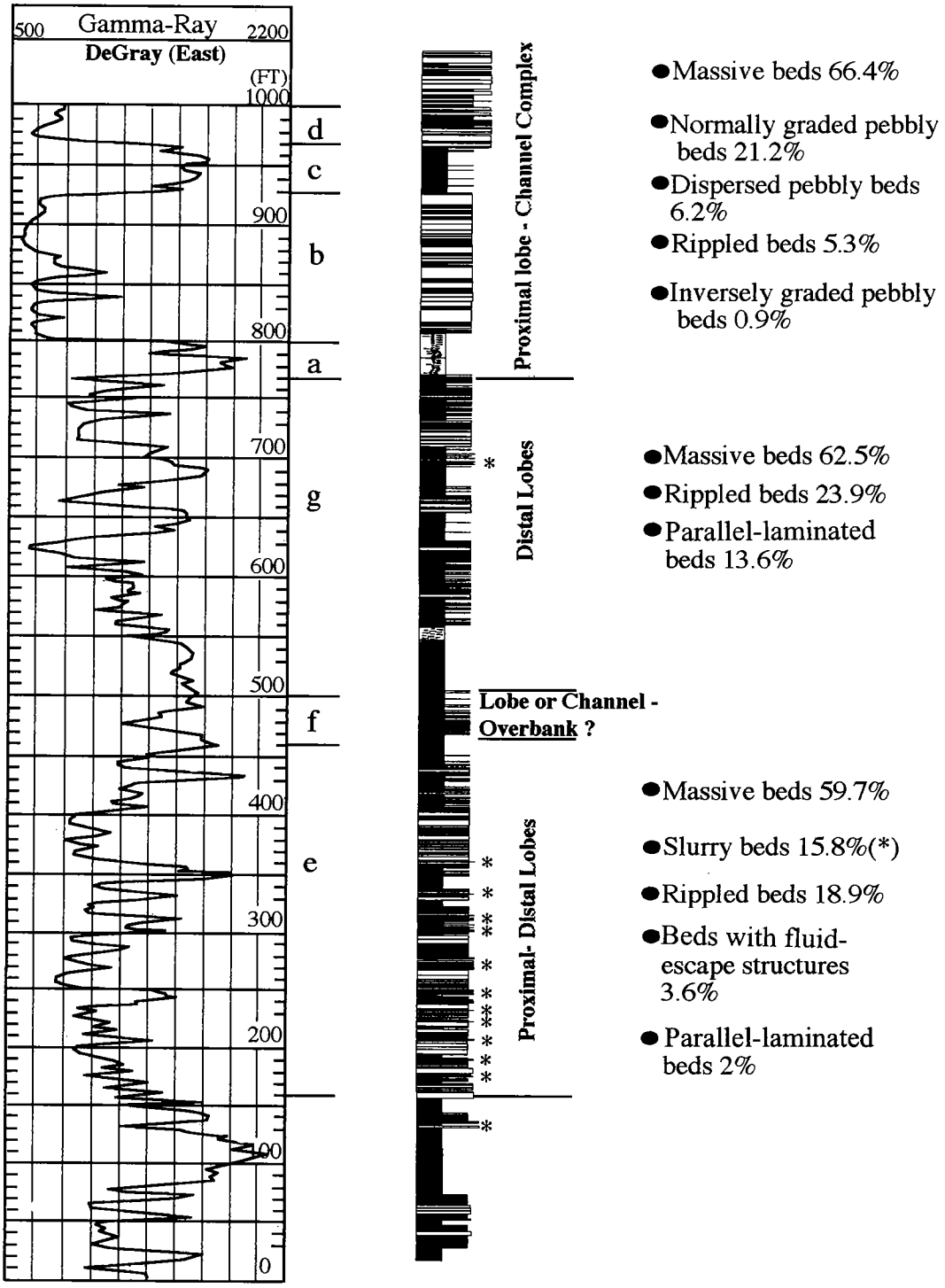

Figure 6. Outcrop gamma-ray log of the 1,000-ft stratigraphic section at DeGray Lake Spillway. Measured section by Al-Siyabi is shown at the right, along with proportions of bedding types (asterisks show the location of slurry beds). Letters a–f refer to stratigraphic units (intervals) discussed in the text. Gamma-ray output is in counts per second (cps).

Rex Timber; Jordan and others, 1993; Coleman and others, 1994). The different thicknesses between the Spillway and Rex Timber well suggest a lobate or wedge-shaped character (based upon only the two data points) to the succession.

Muddy sandstone "slurry beds" (Jordan and others, 1993) occur sporadically within the lower half of unit "e" (Fig. 6). Such beds are not present in other intervals at DeGray Lake Spillway, although they do occur within interval "d" at Hollywood Quarry (Fig. 1). A few

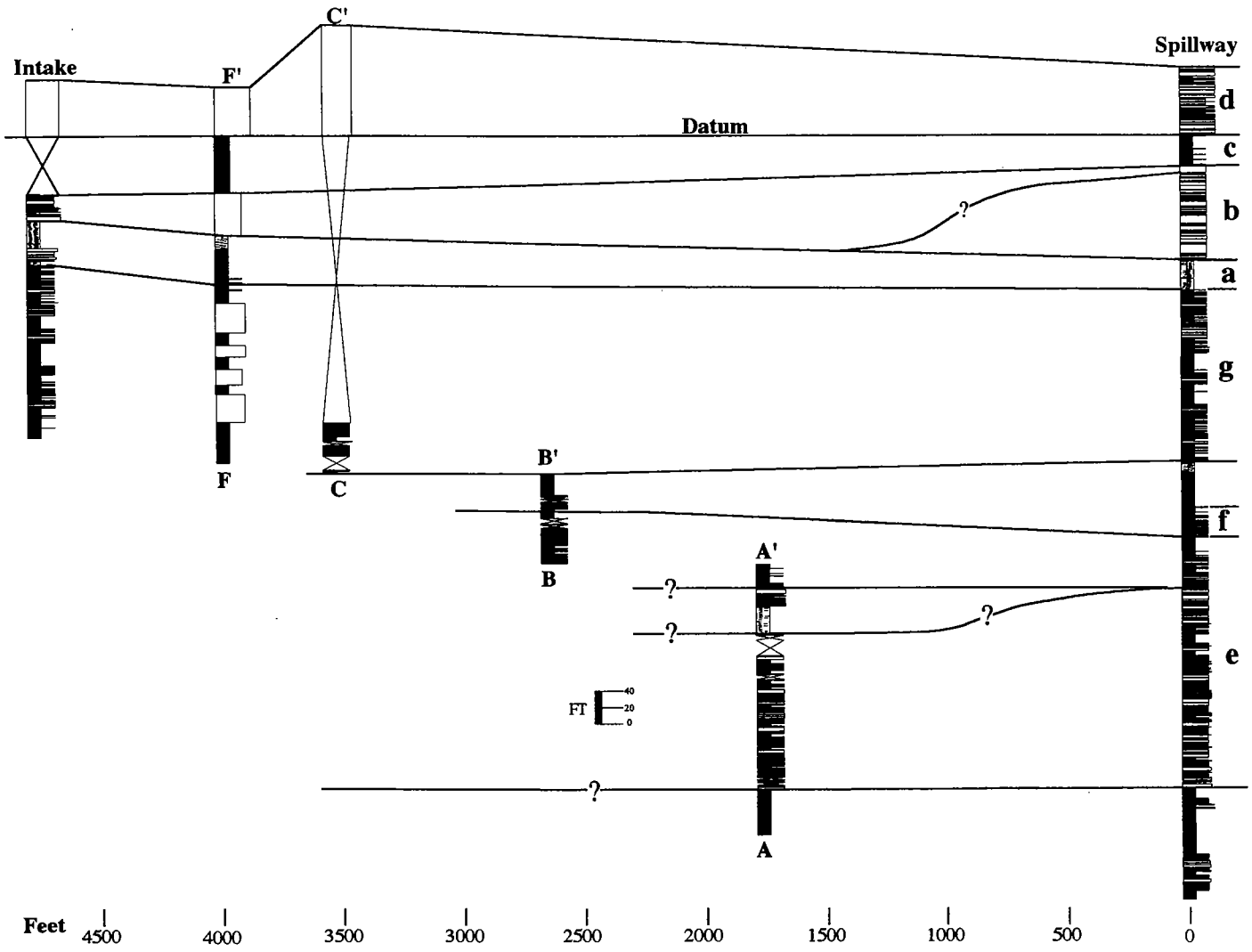

Figure 7. Stratigraphic sections measured and correlated by Al-Siyabi (see Fig. 8 for locations of sections). Spillway section is shown in Figure 6. Horizontal scale (in ft) is distance between measured outcrop sections.

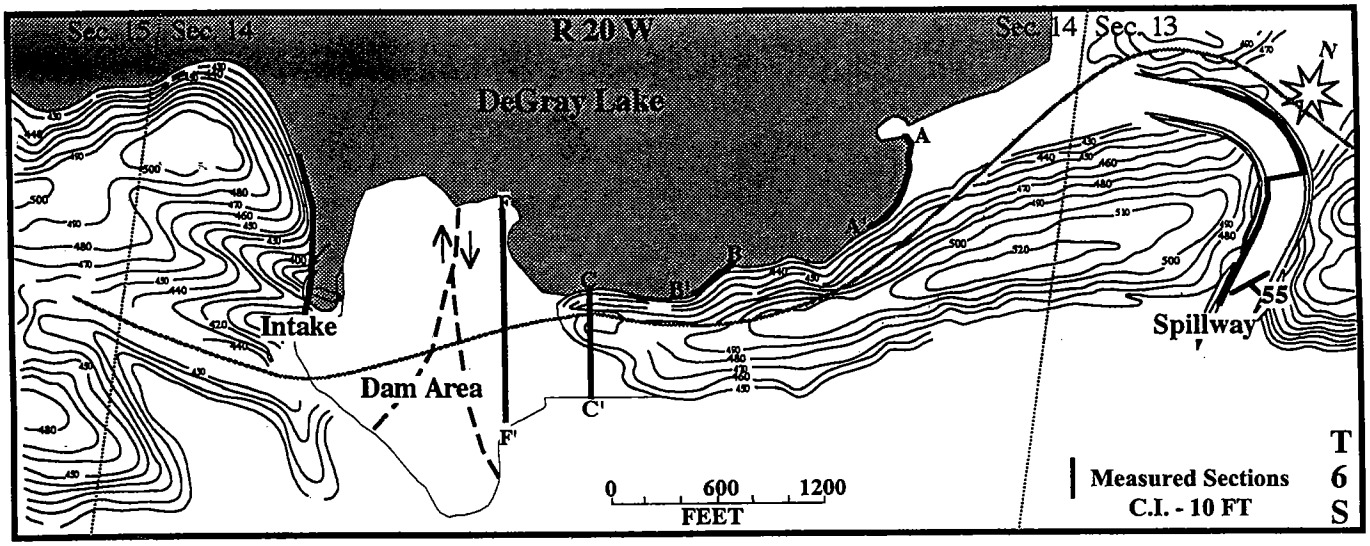

Figure 8. Location of measured stratigraphic sections shown in Figure 7. Contours depict ground surface topography.

slurried beds grading laterally (presumably down the depositional dip) into more massive turbidite beds can be observed. We interpret these slurried beds as having been deposited on a slightly higher-gradient slope than that upon which nonslurried beds of unit "g" were deposited. Therefore, sets of strata containing the slurried beds represent the somewhat more proximal lobe deposits than sets of strata that do not contain these beds.

Overbank Deposits

Overbank deposits can form more than 50% of a fan area on some large deep-sea systems, according to Mutti and Normark (1987). Such deposits dominate in levee-valley or channel-levee systems, reaching widths exceeding 47 mi. On modern levee surfaces, sediment waves can develop that can have wavelengths up to 1.3 mi and wave heights up to 130 ft. However, such features are only likely to be preserved in ancient deposits as cross-bed sets. Like those of modern levees, ancient levee or overbank deposits consist of alternating beds of mudstone and current-laminated, fine-grained sandstone. Associated deposits include relatively thin slumps, debris flows, channel sandstones, and crevasse-splay deposits. Beds can be laterally continuous or discontinuous depending upon the extent of local slumping or scouring. Overbank deposits form wedge-shaped bodies that can either thin or thicken stratigraphically upward.

Bouma and others (1993) interpreted unit "f" (Fig. 6) at DeGray Lake Spillway as a channel-levee–overbank deposit produced by a migrating channel. The walls of the Spillway consists of generally thin-bedded Bouma Tb and Tc, low-density turbidites interbedded with mudstones (Chester, 1994). The following criteria were used by DeVries (1991) and Bouma and others (1993) in their interpretation. (1) Paleocurrent indicators for part of the interval show a westerly direction in the lower part of the exposure—the general, basin-wide paleocurrent trend is westerly (Morris, 1977)—but shifts progressively toward the south upsection. (2) A high degree of correlation (up to 80%) of individual beds exists over the 250-ft lateral distance between both walls of the Spillway. (3) Individual sandstone-mudstone intervals within the section are wedge-shaped. Up to 35% thinning of these beds occurs over this lateral distance. (4) Thinning occurs in alternate directions (east-to-west or west-to-east) within different intervals, indicating compensation-style bedding (Mutti and Sonnino, 1981). (5) The entire interval thins and fines upward. (6) And, finally, the basal sandstone within unit "f" is interpreted as a massive, thick-bedded channel deposit (Fig. 6). However, Bouma and others (1993) pointed out that, of all these criteria, the only one that may be uniquely diagnostic of a channel-levee–overbank deposit is the progressive shift in paleocurrent direction up the stratigraphic section.

Channel-Lobe Transition Zone

The channel-lobe transition zone within any turbidite system, according to Mutti and Normark (1987), is the region that separates well-defined channels or channel-fill facies from well-defined lobes or lobe facies. As such, this zone can exhibit some of the characteristics of both the channels and lobes. Characteristic features of this zone are related to changes that occur when a turbidity current undergoes a hydraulic jump or rapid change from high-velocity flow within a high-gradient, channelized area to a lower-velocity flow within a flatter, unchannelized area. This transition is marked by increased turbulence and flow enlargement, resulting in increased erosion on the fan surface and sediment bypass to down-current positions. This transition can occur in a number of settings—e.g., from a feeder canyon to a fan, from a fan channel to a lobe or levee, or from a high- to low-gradient slope induced by a fault or a salt dome. According to Mutti and Normark (1987), it is this process that can lead to detachment of depositional lobes from their feeder channels. Features considered to be diagnostic of channel-lobe transition zones in ancient deposits include the coarsest-grained sediments within the system, amalgamated beds, scoured surfaces, shallow cut-and-fill features, outsized mudstone rip-up clasts, localized disrupted and chaotic units formed by impact, mud-draped scours, and cross-stratified, tractive-transport deposits.

This type of deposit is well exposed at quarries near Murfreesboro (Souter Quarry) and Arkadelphia, Arkansas (Murray Quarry; Jordan and others, 1993). More than 200 ft of Jackfork are superbly exposed at the Souter Quarry along steeply dipping bedding planes (Fig. 9). This section may be equivalent stratigraphically to the top of the DeGray Lake Spillway section, discussed above. About 20 ft of these strata consist of pebbly sandstone to sandy conglomerate beds. The upper surfaces of some of these bedding planes are literally covered by outsized, platy-shale clasts or their molds. The tops of some bedding planes are very irregular, giving an almost worty appearance, and exhibit complex fluid-flow features. Other beds contain an abundance of molds of wood fragments. The most spectacular feature is a series of large erosional scours on the upper surface of a few sandstone beds. These scours are spoon-shaped with mutually parallel long axes. Where this surface is overlain by another sandstone, the scours are seen to be amalgamated, sand-on-sand, flute molds. The same features have been noted at Murray Quarry, although they are not as well exposed.

Scours and Large-Scale Erosional Features

Mutti and Normark (1987) define scours as isolated, roughly equidimensional cut-and-fill features where erosion and subsequent depositional fill are most commonly produced by the same flow. Such features do not constitute "channels" because they are not long-term, sediment-transport conduits. On modern fans, such scours range up to hundreds of yards wide. Although Mutti and Normark (1987) did not specifically include large-scale erosional features in their classification, they were described in earlier work (Mutti, 1985), and they are included in this category here. Mutti and Normark (1987) claimed that filled scours have not

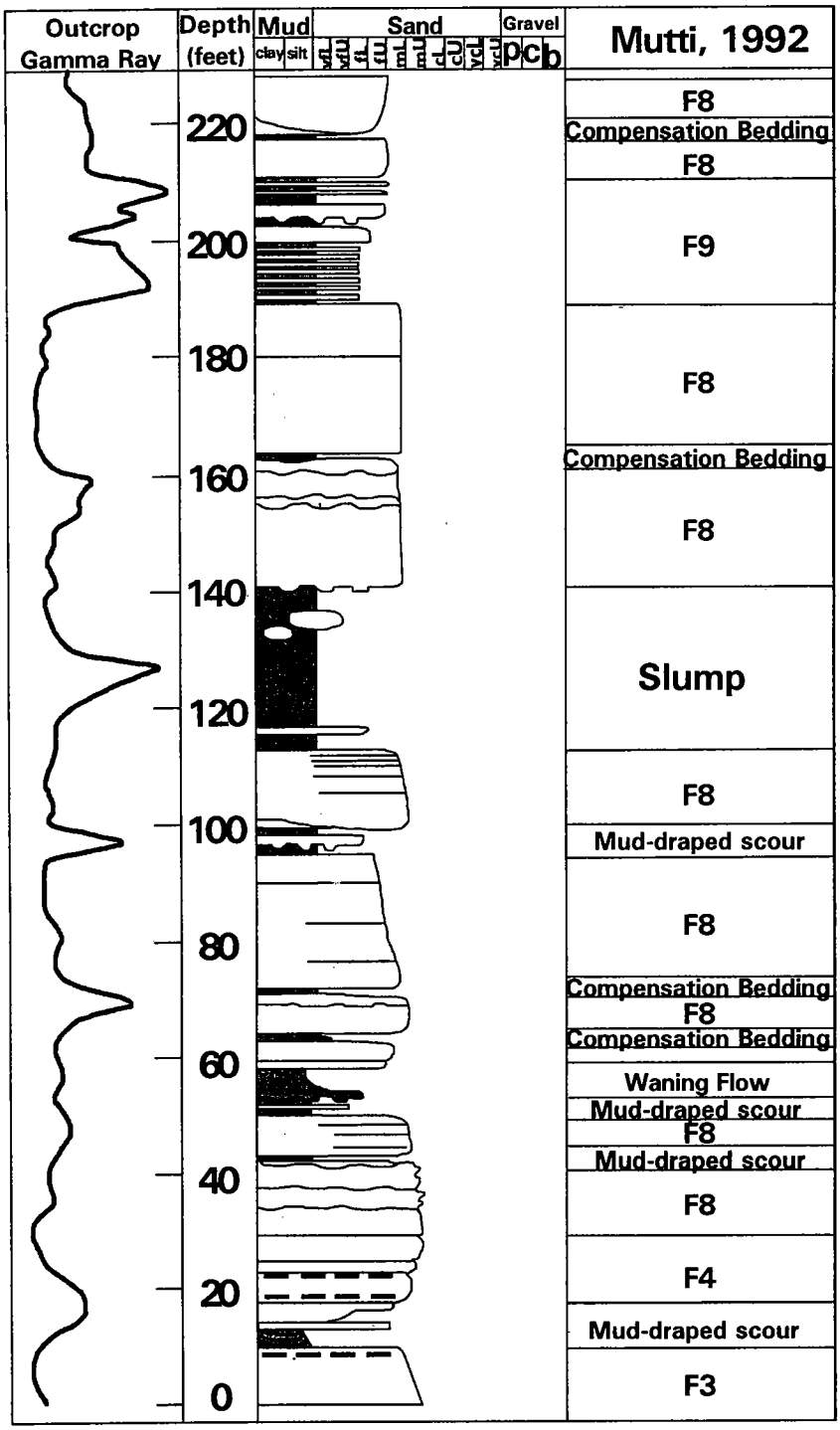

Figure 9. Measured stratigraphic section and outcrop gamma-ray log obtained with a hand-held scintillometer at Murfreesboro (Souter Quarry), Arkansas. Mutti's (1992) turbidite-classification scheme is shown (F3 = clast-supported conglomerates with erosional bases; F4 = gravelly high-density turbidity current deposits; F8 = sandy, high density turbidity-current deposits; F9 = low-density turbidity-current deposits).

been observed on modern fan environments. Hackbarth and Shew (1994) recently described a Pleistocene channel-levee fill within a large slump scar in the Gulf of Mexico.

Small- to large-scale scours, slump scars, and other erosional features are well exposed at the abandoned Big Rock Quarry, a spectacular Jackfork outcrop near North Little Rock, Arkansas. This quarry, visited by many geoscientists and engineers through the years, exposes a 300 ft thick by 2,750 ft wide highwall section of complexly interstratified, almost flat-lying sandstones and mudstones (Fig. 10). In very general terms, the quarry can be divided into three major parts (Jordan and others, 1993): (1) unit "a"—a basal mudstone, which represents the top of the lower Jackfork (shown as light-gray unit below arrow on Fig. 10A); (2) unit "b"—an unconformably overlying 150-ft complex of thick, lenticular sandstones and interbedded shales and mudstones of the basal part of the upper Jackfork; and (3) unit "c"—a capping unit of thinner-bedded sandstones and shales (also shown with a light-gray pattern on Fig. 10A).

It is generally not possible to study details of the rocks in outcrop because of the sheer quarry walls; however, examination of a vertical section of the same strata a few miles away and a core obtained behind the quarry wall by Shell Oil Co. (Link and Stone, 1986) reveals the middle unit "b" consists of massive, dark-gray, fine- to very fine grained, quartzose sandstones interbedded with laminated shales and (more commonly) with muddy debrites comprised of contorted and occasionally stretched mudstones (Jordan and others, 1993; Slatt and others, 1994a). The debrites line the bottoms of depressions, which are capped by sandstones, indicating that the depressions were first produced by slumping or scouring, followed by lining of the depressions with mudstone, then filled by turbidite sands. Other beds exhibit erosional truncation. Consequently, beds within unit "b" are discontinuous at all scales (Cook and others, 1994), such that virtually no beds represented on three outcrop gamma-ray logs across the quarry are correlative (Fig. 10B–D). The upper unit "c" consists of thin sandstones and unusual shale-clast, slurry breccias that exhibit inclined, accretionary bedding (Jordan and others, 1993; Slatt and others, 1994a), suggesting that this unit was deposited as levees and small channels during the waning stages of deposition. The overall thickness of the sandy units exposed at Big Rock Quarry decreases in northwesterly and southeasterly directions, which—assuming a southwesterly sediment

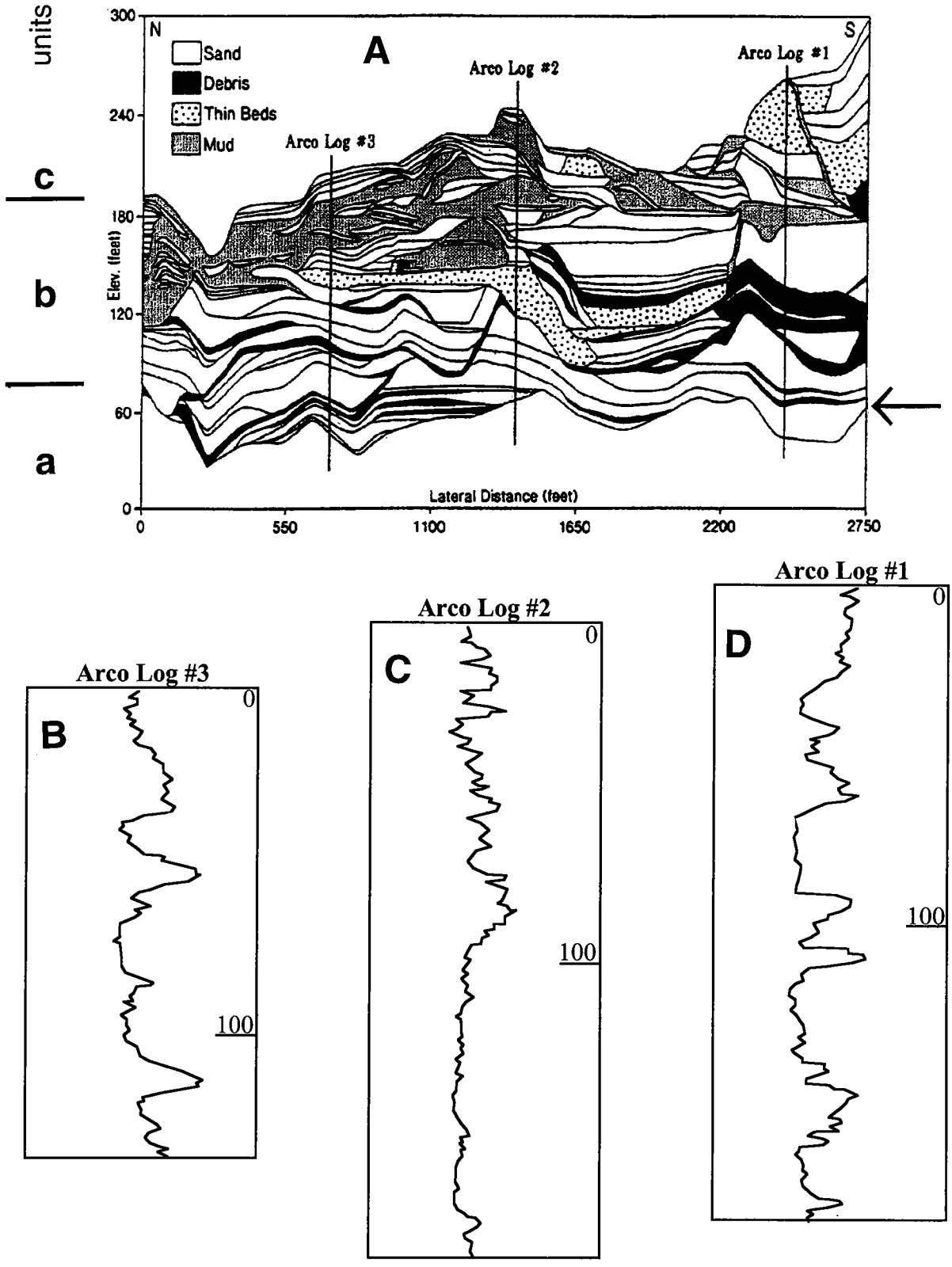

Figure 10. (A) Schematic diagram modified slightly from Cook and others (1994) showing the generalities of stratal discontinuity in highwall of Big Rock Quarry, Arkansas. Lower-case letters ("a," "b," and "c") refer to units (stratigraphic intervals) discussed in the text. Arrow (on right side of figure) points to erosional base of unit "b." Unit "a" and unit "c" are shown by light-gray pattern. Location of three outcrop gamma-ray logs, obtained with an Arco Research and Technical Services Co. logging truck (Slatt and others, 1992), are shown by vertical lines. (B–D) The three outcrop gamma-ray logs, the locations of which are shown in Figure 10A.

transport direction (Thomson and LeBlanc, 1975; Roberts, 1994)—suggests that the basal portion of the upper Jackfork sandstone in this area is broadly lenticular in its strike dimension over several miles.

Cook and others (1994) have interpreted this section at Big Rock Quarry as a nested submarine-fan–channel complex, in contrast to Jordan and others (1993), who interpreted the quarry section as a slope canyon fill, formed by recurrent slope failures. We favor this latter interpretation because sandstone unit "a" sits in angular discordance with underlying contorted mudstone, because similar mudstone also overlies the sandstone, and because the basal portion of the upper Jackfork in this area is broadly lenticular over several miles. Figure 3 of Mutti (1985) provided a schematic illustration of our interpretation of the Big Rock Quarry section.

PRELIMINARY SEQUENCE-STRATIGRAPHIC FRAMEWORK

Establishing a sequence stratigraphic framework for bathyal turbidite systems exposed in outcrops is challenging because few outcrops exist where key stratal surfaces can be traced unequivocally from shelf to base-of-slope, and stratal-stacking patterns can be seen at a scale similar to that on seismic profiles. Unfortunately, well-exposed, regionally continuous outcrops of the Jackfork Group are absent in southwest-central Arkansas because of the heavy vegetation and extensive structural overprint. Our attempts to use the aerial photostratigraphic interpretation technique of Sgavetti (1991) have not been fruitful. We have instead constructed a preliminary sequence-stratigraphic framework for the DeGray Spillway section, based on key observations at both regional and outcrop scale. This work follows that of Baquero and others (1994).

Regional Observations

The Jackfork Group was deposited during Morrowan (Early Pennsylvanian) time, while active thrusting associated with the collision of North and South America was occurring to the south. The foreland basin subsided isostatically, and the receiving basin was continuously changing shape during deposition. By the Early Permian, continued thrusting had telescoped the basin and deformed these turbidite systems. The Morrowan was also a time of well-documented glacial eustasy, which clearly affected deposition of sediments in the cratonic basin north and northwest of the Ouachita basin (e.g., Bowen and others, 1993). Presumably, these eustatic cycles affected the timing of deposition and amount of sediment that was delivered to the deeper Ouachita basin. Deposition of the Jackfork clearly was affected by both tectonic and eustatic factors, although their relative importance in controlling deposition is unknown.

Local Observations at DeGray Lake Spillway

Interpretation of the thicker shale packages is critical to regional interpretation. The shale packages can be interpreted as (1) condensed sections—i.e., the basinal equivalents of the Prograding Complex, Transgressive Systems Tract and Highstand Systems Tract (allocyclic control on deposition); or (2) deposited during major channel/lobe switches (autocyclic controls). One key technique used in industry to evaluate the relative significance of the shale packages is the relative abundance of various planktic biota (i.e., calcareous nannoplankton). Unfortunately, these outcrops are largely devoid of any fossils.

Another technique that is used to evaluate the regional significance of shales is the relative amount of radioactivity. Several authors have observed that shale intervals with higher radioactivity ("hot shales") commonly correspond to increased content of organic matter and longer periods of deposition (e.g., Loutit and others, 1988; Slatt and others, 1992, 1995). These "hot" shales commonly are basinal equivalents of one or several sequences in the deep basin (distal basinal equivalents to the Prograding Complex, Transgressive Systems Tract, and Highstand Systems Tract). On seismic profiles these can appear as one or two reflections that exhibit good regional distribution. One dark, laminated shale interval at 110 ft (Fig. 6) in the DeGray Lake Spillway section clearly has higher gamma-ray response than others. Thus, there is at least one potential condensed section in the outcrop. The regional extent of this shale is not known. Several stratigraphically higher shales exhibit high gamma-ray responses (e.g., at 240 ft, 350 ft, 420 ft, 460 ft, 650 ft, 690 ft, 780 ft, and 950 ft on Fig. 6).

Petrography of Jackfork sandstones can be used to establish the timing of significant events. In a tectonically active basin, discrete tectonic pulses can be recorded by the compositional change in sediments supplied to the basin. Numerous early petrographic studies on Jackfork strata (summarized in Jordan and others, 1993) suggested sediment sourcing from the northeast, in the vicinity of the Illinois basin and Appalachia, as well as from a southern ("Llanoria") landmass. A more recent, comprehensive petrographic study by Thomson and others (1994) supported a mature Illinois basin source to the northeast, a less mature Llanoria source from the south, and an easterly source from the Ouachita-Appalacian orogen. A recent study of rare-earth element isotopes suggested a dominantly Appalachian provenance (Gleason and others, 1994). In the DeGray Lake Spillway section, sandstones are lithic arenites in the basal 800 ft (Jordan and others, 1993). However, a major petrographic change from lithic arenites occurs to clean chert-quartz arenites in the upper 200 ft of section (Fig. 6). This change is interpreted to reflect changes in the source area from the northeast to the south. Such influxes of sediment from distinctly different source areas are interpreted to reflect discrete, regionally significant depositional events—be they tectonic and/or eustatic in origin.

Possible Interpretation of Sequence-Stratigraphic Framework

Two end-member depositional-sequence scenarios and one intermediate scenario are presented below

for the DeGray Lake Spillway succession in order to illustrate the uncertainty in developing a sequence-stratigraphic framework from vertical succession alone. These scenarios are: (1) high-frequency eustatic control on deposition; (2) low-frequency, no eustatic control (one sequence); and (3) an intermediate model between 1 and 2. In our opinion, not enough data are available to unequivically identify a preferred interpretation.

High-Frequency Eustatic Control

According to the model of high-frequency eustatic control of deposition, each major sandstone package is interpreted to reflect deposition within one eustatic cycle. Using criteria of Mutti and others (1994), eight depositional sequences are interpreted to exist at the DeGray Lake Spillway section, each about 100–150 ft thick (Fig. 6). Each shale package would reflect the deep-water equivalents to the Prograding Complex, Transgressive Systems Tract, and Highstand Systems Tract.

Low-Frequency, No Eustatic Control

The model of low frequency, no eustatic control (one sequence) requires that all of the sedimentary cycles present must reflect ongoing autocyclic processes within a single depositional sequence. Major sandstone packages reflect deposition within lobe and channel-complexes (Fig. 6), and their subsequent switching and abandonment are reflected in the shale packages that overlie the sandstones. According to this interpretation, the only possible sequence boundary overlies the hot shale at 140 ft on Figure 6.

Intermediate Interpretation

With this scenario, some of the major sandstone packages are interpreted to reflect deposition associated with a drop in relative sea level and a sequence boundary at the base of each package. Three or four depositional sequences are interpreted to be present at the DeGray Lake Spillway section. The most likely position of sequence boundaries are at 140 ft, 550 ft, 800 ft, and 960 ft on Figure 6 (or possibly at the bases of underlying shales of units "a" and "c" in the latter two cases). The hot shale at 110 ft is the best condensed section. With this intermediate interpretation, the sandstone packages may also reflect a combination of depositional sequences within higher- and lower-frequency cycles. Such a scenario is easy to envision for glacio-eustatic times; similar interpretations have been described for other basins (Mitchum and others, 1993; Brown and others, 1996).

APPLICATIONS TO INTERPRETING SUBSURFACE DATA OF TURBIDITE ELEMENTS

From extensive study of outcrops from many parts of the world, Chapin and others (1994) and Mahaffie (1994) classified turbidite reservoir types into thin-bed levees, channels, and sheets. These classes are equivalent to Mutti and Normark's (1987) overbank, channel, and lobe depositional elements, respectively. Chapin and others (1994) outlined a set of characteristics for these three types that are broadly applicable to turbidites. These include well-log and core characteristics and attributes of lateral continuity, correlation, and connectivity. Measured outcrop sections and gamma-ray document most of the Jackfork elements discussed above. Also, in some instances, Jackfork outcrop and quarry exposures are of sufficient size to evaluate lateral attributes. Because this is not always the case, it is important to summarize those aspects described by Mahaffie (1994) and Chapin and others (1994) that can be used to predict Jackfork attributes in the subsurface or where outcrops are not exposed.

Rock and Log Characteristics and Correlations

More commonly than not, channel-fill elements will exhibit sharp bases on logs and core, and the overall channel-fill sequence will exhibit a blocky or upward-thinning and upward-fining character. Massive to graded, thick-bedded, amalgamated Bouma Ta sandstones will be the predominant lithology. If gravel was present in the source area, then conglomerates and pebbly sandstones may occur. Entire channel-fill sequences may be difficult to correlate laterally, because of their lenticular nature; however, this is a matter of scale of features on log or core to be correlated. Internally, channel-fill sequences will exhibit considerable discontinuity because of slumping, scouring, resedimentation, and cut-and-fill. Thus, internal continuity of sequences will be low, and connectivity may vary from high to low. Such features will not be observable on wire-line logs but will be visible in core and on borehole image logs (Slatt and others, 1994a). Features of erosional canyon-fills should be similar to those of channel-fills.

Chapin and others (1994) divided sheets or lobe elements into two types—layered and amalgamated. Amalgamated-sheet sandstones may exhibit a blocky well-log pattern similar to that of channels, but lateral continuity and correlation will be better. Layered sheets, by definition, consist of interbedded sandstones and mudstones, both of which can be expected to be laterally continuous and correlatable for relatively long distances. Well-log response of individual beds within a layered sheet interval may or may not be resolvable on logs depending upon the thickness of the beds and the resolution of the tool. The entire layered-sheet interval may exhibit a blocky, upward-coarsening or upward-fining log response (Slatt and others, 1994a). Amalgamated and layered sheets should be distinguishable in core and on borehole image logs. Connectivity of amalgamated-sheet sandstones will be high, whereas that of layered-sheet sandstones will be low. Because of the higher flow energy associated with amalgamated sheets, sandstone beds are more apt to be Bouma Ta beds, whereas layered-sheet sandstones might be Ta, Tb, and/or Tc beds.

Because of their thin-bedded nature, overbank or levee elements will exhibit a subdued, "ratty" log response and will appear thin bedded in core. Sandstones are characteristically Bouma Tb and Tc (includ-

ing climbing-ripple beds), and mudstones may be silty or clayey. Borehole image logs will also exhibit the same thin-bedded character as in cores (Slatt and others, 1994a), but details of sedimentary textures and structures may not be resolvable (Spang and others, 1997). Individual beds may be laterally continuous for long distances, but correlation will be difficult (if not impossible) on well logs and in core. In such situations, bed continuity will be high, but bed connectivity will be low because of sandstone-mudstone interbedding. In proximal levee positions, individual beds may be scoured and cut-out and, thus, not laterally continuous (Browne and Slatt, 1997). Connectivity may be high in such cases. Scour features will be subtle in cores and borehole image logs.

Seismic Stratigraphic Expression of Turbidite Elements

Our own studies (mainly Weimer) have provided a basis for suggesting some seismic-stratigraphic–recognition criteria for turbidite depositional elements. The seismic stratigraphic expression of turbidite elements is expected to be variable because resolution depends upon frequency content of the seismic data, depth of the features to be imaged, thickness of the elements, and acquisition and processing parameters. Three-dimensional seismic and seismic-coherence technology have dramatically improved industry's ability to image these elements (Brown and others, 1996; Lopez and others, 1996; Weimer and Davis, 1996). Discussed below are the salient seismic characteristics of turbidite elements in a mud-dominated system such as the Jackfork Group.

In modern fans, levees (overbank deposits) adjacent to channels have a "gull-wing" shape—topographically elevated levees that are wedge-shaped in cross section and that thin away from the channel. However, in buried turbidite systems, leveed channels are generally thin and lack the gull-wing shape, probably because of compaction. Instead, the reflection character of levees is hummocky to slightly mounded to subparallel. Amplitude is generally low to moderate in these settings, and continuity is generally good. Channel-fill reflections are generally parallel to slightly mounded and hummocky. Amplitude is variable—from low to high—and continuity is poor. Buried leveed channels are best imaged using horizon slices from 3-D seismic data.

Lobes (sheet sands) by themselves are probably not resolvable on 2-D seismic or on 3-D horizon slices. If sufficiently thick (amalgamated), they can be resolved on multifold seismic data, where they will consist of parallel to subparallel, generally high-amplitude seismic reflections with good continuity. Three-dimensional horizon slices indicate high-amplitude reflections can be traced over a few to hundreds of square miles.

The features of the channel-lobe transition zone cannot be resolved on 2-D seismic data. If there is sufficient relief on the erosional features associated with these deposits, 3-D seismic horizon slices might be able to image them.

Large-scale erosional features are probably the easiest to identify on multifold seismic data because of the truncation of individual seismic reflections. Seismic stratigraphic expression of the fill of these features is highly variable, consisting of subparallel to chaotic to mounded reflections with variable amplitude and continuity.

Some Considerations for Reservoir Simulation and Production

Gas and oil production can occur out of any of the turbidite elements described above. However, hydrocarbon volumes and production characteristics might differ among elements. For example, channel- and canyon-fill sandstones of the type described above probably will exhibit good vertical connectivity, but they will be elongate in character and contain internal discontinuities at a variety of scales so that hydrocarbon migration will follow a tortuous path. Lobe (and overbank) deposits contain thin sandstones that are more apt to be laterally continuous away from the well bore, but their vertical connectivity is typically poor. Lobe and overbank deposits commonly cover larger areas than channel deposits, but net-to-gross is lower in the former.

Jackfork wells in eastern Oklahoma are being produced from fractured, tight-gas sandstones that are hydraulically fractured (Montgomery, 1996; Petzet, 1996). If so, then reservoir simulation probably is not applicable. However, there is a potential for more porous stratigraphic accumulations of gas (Pauli, 1994). If such accumulations are discovered, simulation might become important, in which case, the design of numerical simulation models will be dependent on the nature of the interpreted depositional architecture. Different approaches toward numerical modeling are necessary for the two types of deposits. The first type is where the interval is layered and has good lateral continuity but poor vertical connectivity (e.g., lobes and overbank deposits). The second type of deposit is where the interval is massive and unlayered and has good vertical continuity but perhaps limited lateral extent (e.g., channels and canyon-fill). Other factors that will affect simulation model design include the degree of natural fracturing, the probability of sand-on-sand contacts due to fault juxtaposition (as is the case at Hollywood Quarry), and the dip angles of beds.

CONCLUDING REMARKS

A variety of turbidite elements are contained within Jackfork Group strata in southwest-central Arkansas. These elements are also thought to occur in potentially gas-productive Jackfork strata in eastern Oklahoma. The elements are well exposed in outcrop and thus offer the opportunity to observe the vertical and occasionally lateral attributes of turbidite elements. Such observations can improve interpretation of the depositional framework and reservoir attributes of Jackfork strata in the subsurface, where well logs, seismic records, and occasionally production information constitute the main database. Thus, observation and study

of these outcrops can lead to improved exploration for and development of Jackfork turbidite reservoirs.

ACKNOWLEDGMENTS

We would like to thank our colleagues who have worked on various aspects of the Jackfork Group with us over the years, especially J. K. Arbenz, Jim Coleman, Anthony D'Agostino, Robert Gillespie, Boyd Haley, Douglas Jordan, Don Lowe, Mark Scheihing, Alan Thomson, and B. H. Walthall. Graduate students in Slatt and Weimer's "Petroleum Geology of Turbidite Depositional Systems" course at Colorado School of Mines/University of Colorado completed some of the work reported here. Financial support for this work by Amoco, Arco, Chevron, Exxon, Marathon, Mobil, Phillips, Schlumberger, Shell, Texaco, Union Pacific, and Vastar is gratefully acknowledged.

REFERENCES CITED

Baquero, E. J.; Peterson, J.; Weimer, P.; and Slatt, R. M., 1994, Preliminary sequence stratigraphic framework, Pennsylvanian Jackfork Group turbidites, DeGray Lake area, Arkansas [abstract]: Geological Society of America Abstracts with Programs, v. 26, p. 2.

Baruffini, L.; Cavalli, C.; and Papani, L., 1994, Detailed stratal correlation and stacking patterns of the Gremiasco and Lower Castagnola turbidite systems, Tertiary Piedmont basin, northwestern Italy, *in* Weimer, P.; Bouma, A. H.; and Perkins, B. F. (eds.), Submarine fans and turbidite systems: Gulf Coast Section Society of Economic Paleontologists and Mineralogists 15th Annual Research Conference Proceedings, p. 9–21.

Bouma, A.H.; DeVries, M.B.; and Cook, T. W., 1993, Correlation efficiency as a tool to better determine depositional subenvironments in submarine fans: Transactions of the Gulf Coast Association Geological Societies, v. 43, p. 31–40.

Bouma, A. H.; DeVries, M. B.; and Stone, C. G., 1997, Reinterpretation of depositional processes in a classic flysch sequence (Pennsylvanian Jackfork Group), Ouachita Mountains, Arkansas and Oklahoma: discussion: American Association of Petroleum Geologists Bulletin, v. 81, p. 470–472.

Bowen, D. W.; Weimer, P.; and Scott, A. J., 1993, The relative success of siliciclastic sequence stratigraphy in exploration: examples from valley fill and turbidite systems reservoirs, *in* Weimer, P.; and Posamentier, H. W. (eds.), Siliciclastic sequence stratigraphy: American Association of Petroleum Geologists Memoir 58, p. 11–38.

Brown, L. F.; Benson, J. M.; Brink, G. J.; Doherty, S.; Jollands, A.; Jungslager, E. N. A.; Keenan, J. H. G.; Muntingh, A.; and Van Wyck, J. S., 1996, Sequence stratigraphy in offshore South African divergent basins: American Association of Petroleum Geologists Studies in Geology 41, 184 p.

Browne, G. H.; and Slatt, R. M., 1997, Thin-bedded slope fan (channel-levee) deposits from New Zealand: an outcrop analog for reservoirs in the Gulf of Mexico [abstract]: Gulf Coast Association Geological Societies, New Orleans, v. 47, p. 75–86.

Chapin, M. A.; Davies, P.; Gibson, J. L.; and Pettingill, H. S., 1994, Reservoir architecture of turbidite sheet sandstones in laterally extensive outcrops, Ross Formation, western Ireland, *in* Weimer, P.; Bouma, A. H.; and Perkins, B. F. (eds.), Submarine fans and turbidite systems: Gulf Coast Society of Economic Paleontologists and Mineralogists 15th Annual Research Conference Proceedings, p. 53–68.

Chester, T. L., 1994, Analysis of vertical cyclicity patterns in two sediment gravity flow sequences: Stanford University unpublished M.S. thesis, 169 p.

Coleman, J. L., Jr., 1997, Reinterpretation of depositional processes in a classic flysch sequence (Pennsylvanian Jackfork Group), Ouachita Mountains, Arkansas and Oklahoma: discussion: American Association of Petroleum Geologists Bulletin, v. 81, p. 466–469.

Coleman, J. L., Jr.; Swearingen, G. V.; and Breckon, C. E., 1994, The Jackfork Formation of Arkansas—a test for the Walker-Mutti-Vail models for deep-sea fan deposition: Arkansas Geological Commission Guidebook 94-2, 56 p.

Cook, T. W.; Bouma, A. H.; Chapin, M. A.; and Zhu, H., 1994, Facies architecture and reservoir characterization of a submarine fan cannel complex, Jackfork Formation, Arkansas, *in* Weimer, P.; Bouma, A. H.; and Perkins, B. F. (eds.), Submarine fans and turbidite systems: Gulf Coast Section Society of Economic Paleontologists and Mineralogists 15th Annual Research Conference Proceedings, p. 69–81.

D'Agostino, A. E.; and Jordan, D. W., 1997, Reinterpretation of depositional processes in a classic flysch sequence (Pennsylvanian Jackfork Group), Ouachita Mountains, Arkansas and Oklahoma: discussion: American Association of Petroleum Geologists Bulletin, v. 81, p. 473–475.

Davis, M. H., 1994, Maumelle chaotic zone, *in* Stone, C. G.; Haley, B. R.; and Davis, M. H., Guidebook to Paleozoic rocks in the eastern Ouachita Mountains, Arkansas: Arkansas Geological Commission Guidebook 94-1, p. 1–8.

DeVries, M. B., 1991, Correlation trends in thinner-bedded turbidites, Chatsworth Formation, Simi Hills, California and Jackfork Group, DeGray Lake, Arkansas: Louisiana State University unpublished M.S. thesis, 88 p.

Gleason, J. D.; Patchett, P. J.; Dickinson, W. R.; and Ruiz, J., 1994, Nd isotopes link Ouachita turbidites to Appalachian sources: Geology, v. 22, p. 347–350.

Gordon, M., Jr.; and Stone, C. G., 1977, Correlation of the Carboniferous rocks of the Ouachita trough with those of the adjacent foreland, *in* Stone, C. G. (ed.), Symposium on the geology of the Ouachita Mountains, v. 1: Arkansas Geological Commission, Little Rock, p. 70–91.

Hackbarth, C. J.; and Shew, R. D., 1994, Morphology and stratigraphy of a mid-Pleistocene turbidite leveed channel from seismic, core, and log data, northeastern Gulf of Mexico, *in* Weimer, P.; Bouma, A. H.; and Perkins, B. F., Submarine fans and turbidite systems: Gulf Coast Section Society of Economic Paleontologists and Mineralogists 15th Annual Research Conference Proceedings, p. 127–133.

Haley, B. R.; Glick, E. E.; Bush, W. V.; Clardy, B. F.; Stone, C. G.; Woodward, M. B.; and Zachry, D. L., 1976, Geologic map of Arkansas: Arkansas Geological Commission and U.S. Geological Survey, scale 1:250,000.

Hill, P. R., 1984, Sedimentary facies of the Nova Scotia upper and middle continental slope, offshore eastern Canada: Sedimentology, v. 31, p. 293–309.

Jordan, D. W.; Lowe, D. R.; Slatt, R. M.; Stone, C. G.; D'Agostino, A.; Scheihing, M. H.; and Gillespie, R. H., 1993, Scales of geological heterogeneity of Pennsylvanian Jackfork Group, Ouachita Mountains, Arkansas: applications to field development and exploration for deep-water sandstones: Arkansas Geological Commission Guidebook 93-1, 141 p.

Link, M. H.; and Stone, C. G., 1986, Jackfork Sandstone at the abandoned Big Rock Quarry, North Little Rock, Arkansas, *in* Stone, C. G.; and Haley, B. R., Sedimentary and igneous rocks of the Ouachita Mountains of Arkansas: Arkansas Geological Commission Guidebook 86-3, p. 1–8.

Lopez, J. A.; Haskell, N. L.; Nissen, S. E.; and Bahorich, M. S., 1996, 3-D seismic coherency and the imaging of sedimentological features, *in* Pacht, J. A.; Sheriff, R. E.; and Perkins, R. F. (eds.), Stratigraphic analysis utilizing advanced geophysical, wireline and borehole technology for petroleum exploration and production: Gulf Coast Section Society of Economic Paleontologists and Mineralogists 17th Annual Research Conference, Houston, p. 191–197.

Loutit, T. S.; Hardenbol, J.; Vail, P. R.; and Baum, G. R., 1988, Condensed sections: the key to age dating and correlation of continental margin sequences: Society of Economic Paleontologists and Mineralogists Special Publication 42, p. 183–215.

Lowe, D. R., 1997, Reinterpretation of depositional processes in a classic flysch sequence (Pennsylvanian Jackfork Group), Ouachita Mountains, Arkansas and Oklahoma: discussion: American Association of Petroleum Geologists Bulletin, v. 81, p. 460–465.

Mahaffie, M. J., 1994, Reservoir classification for turbidite intervals at the Mars discovery, Mississippi Canyon 807, Gulf of Mexico, *in* Weimer, P.; Bouma, A. H.; and Perkins, B. F., Submarine fans and turbidite systems: Gulf Coast Section Society of Economic Paleontologists and Mineralogists 15th Annual Research Conference Proceedings, p. 233–244.

Mitchum, R. M., Jr.; Sangree, J. B.; Vail, P. R.; and Wornardt, W. W., 1993, Recognizing sequences and systems tracts from well logs, seismic data, and biostratigraphy: examples from the late Cenozoic of the Gulf of Mexico, *in* Weimer, P.; and Posamentier, H. W. (eds.), Siliciclastic sequence stratigraphy: recent developments and applications: American Association of Petroleum Geologists Memoir 58, p. 163–197.

Montgomery, S., 1996, Jackfork Group: Ouachita Mountains: Petroleum Frontiers, v. 13, no. 1, 59 p.

Morris, R. C.; 1977, Flysch facies of the Ouachita trough—with examples from the spillway at DeGray Dam, Arkansas, *in* Sloan, C. G. (ed.), Symposium on the Geology of the Ouachita Mountains: Arkansas Geological Commission, Little Rock, p. 158–169.

Mutti, E., 1985, Turbidite systems and their relations to depositional sequences, *in* Zuffa, G. G. (ed.), Provenance of arenites: Reidel, Holland, p. 65–93.

_____ 1992, Turbidite sandstones: Agip and Istituto di Geologia, Universita di Parma [Italy], 275 p.

Mutti, E.; and Normark, W. R., 1987, Comparing examples of modern and ancient turbidite systems: problems and concepts, *in* Leggett, J. K.; and Zuffa, G. G. (eds.), Marine clastic sedimentology: Graham and Trotman, London, p. 1–38.

_____ 1991, An integrated approach to the study of turbidite systems, *in* Weimer, P.; and Link, M. H. (eds.), Seismic facies and sedimentary processes of submarine fans and turbidite systems: Springer-Verlag, New York, p. 75–106.

Mutti, E.; and Sonnino, M., 1981, Compensation cycles: a diagnostic feature of turbidite sandstone lobes: International Asscciation of Sedimentologists, 2nd European Regional Meeting, Bologna, Italy, p. 120–123.

Mutti, E.; Davoli, G.; Mora, S.; and Papani, L., 1994, Internal stacking patterns of ancient turbidite systems from collisional basins, *in* Weimer, P.; Bouma, A. H.; and Perkins, B. F. (eds.), Submarine fans and turbidite systems: Gulf Coast Section Society of Economic Paleontologists and Mineralogists 15th Annual Research Conference Proceedings, p. 257–268.

Pauli, D., 1994, Friable submarine channel sandstones in the Jackfork Group, Lynn Mountain syncline, Pushmataha and Le Flore Counties, Oklahoma, *in* Suneson, N. H.; and Hemish, L. A. (eds.), Geology and resources of the eastern Ouachita Mountains frontal belt and southeastern Arkoma basin, Oklahoma: Oklahoma Geological Survey Guidebook 29, p. 179–202.

Petzet, G. A.,1996, Jackfork play grows, but economics tough: Oil and Gas Journal, v. 94, no. 28, p. 60–61.

Posamentier, H. W.; and Erskine, R. D., 1991, Seismic expression and recognition criteria of ancient submarine fans, *in* Weimer, P.; and Link, M. H. (eds.), Seismic facies and sedimentary processes of submarine fans and turbidite systems, Springer-Verlag, New York, p. 197–222.

Reading, H. G.; and Richards, M., 1994, Turbidite systems in deep-water basin margins classified by grain size and feeder system: American Association of Petroleum Geologists Bulletin, v. 78, p. 792–822.

Roberts, M. T., 1994, Geologic relations along a regional cross section from Spavinaw to Broken Bow, eastern Oklahoma, *in* Suneson, N. H.; and Hemish, L. A. (eds.), Geology and resources of the eastern Ouachita Mountains frontal belt and southeastern Arkoma basin, Oklahoma: Oklahoma Geological Survey Guidebook 29, p. 137–160.

Roberts, M. T.; and Compani, B., 1996, Miocene example of a meandering submarine channel-levee system from 3-D seismic reflection data, Gulf of Mexico basin, *in* Pacht, J. A.; Sheriff, R. E.; and Perkins, B. F. (eds.), Stratigraphic analysis utilizing advanced geophysical, wireline, and borehole technology from petroleum exploration and production: Gulf Coast Section Society of Economic Paleontologists and Mineralogists 17th Annual Research Conference Proceedings, p. 241–254.

SEPM (Society of Economic Paleontologists and Mineralogists, Society for Sedimentary Geology), 1997a, Processes of deep-water clastic sedimentation and their reservoir implications: what can we predict?: Society for Sedimentary Geology Debate, American Association of Petroleum Geologists Convention, Dallas, 23 p.

SEPM (Society of Economic Paleontologists and Mineralogists, Society for Sedimentary Geology), 1997b, Fine-grained submarine fan architecture and turbidite nomenclature, Jackfork Group, Arkansas: Society for Sedimentary Geology Field Trip #14, American Association of Petroleum Geologists Convention, Dallas.

Sgavetti, M., 1991 Photostratigraphy of ancient turbidite systems, *in* Weimer, P.; and Link, M. H. (eds.), Seismic facies and sedimentary processes of submarine fans and

turbidite systems: Frontiers in Sedimentary Geology, Springer-Verlag, New York, p. 107–126.

Shanmugam, G.; and Moiola, R. J., 1995, Reinterpretation of depositional processes in a classic flysch sequence (Pennsylvanian Jackfork Group), Ouachita Mountains, Arkansas and Oklahoma: American Association of Petroleum Geologists Bulletin, v. 79, p. 672–695.

Slatt, R. M.; Jordan, D. W.; D'Agostino, A. E.; and Gillespie, R. H., 1992, Outcrop gamma-ray logging to improve understanding of subsurface well log correlations, *in* Hurst, A.; Griffiths, C. M.; and Worthington, P. F. (eds.), Geological applications of wireline logs II: The Geological Society (England) Special Publication 65, p. 3–19.

Slatt, R. M.; Jordan, D. W.; and Davis, R. J., 1994a, Interpreting formation microscanner log images of Gulf of Mexico Pliocene turbidites by comparison with Pennsylvanian turbidite outcrops, Arkansas, *in* Weimer, P.; Bouma, A. H.; and Perkins, B. F. (eds.), Submarine fans and turbidite systems: Gulf Coast Section Society of Economic Paleontologists and Mineralogists 15th Annual Research Conference Proceedings, p. 335–348.

Slatt, R. M.; Jordan, D. W.; Stone, C. G.; and Wilson, M. S., 1994b, Stratigraphic and structural compartmentalization observed within a "model turbidite reservoir," Pennsylvanian upper Jackfork Formation, Hollywood Quarry, Arkansas, *in* Weimer, P.; Bouma, A. H.; and Perkins, B. F. (eds.), Submarine fans and turbidite systems: Gulf Coast Section Society of Economic Paleontologists and Mineralogists 15th Annual Research Conference Proceedings, p. 349–356.

Slatt, R. M.; Borer, J. M.; Horn, B. W.; Al-Siyabi, H. A.; and Pietraszek, S. W., 1995, Outcrop gamma-ray logging applied to subsurface petroleum geology: The Mountain Geologist, v. 32, p. 81–94.

Slatt, R. M.; Weimer, P.; and Stone, C. G., 1997a, Reinterpretation of depositional processes in a classic flysch sequence (Pennsylvanian Jackfork Group), Ouachita Mountains, Arkansas and Oklahoma: discussion: American Association of Petroleum Geologists Bulletin, v. 81, p. 449–459.

Slatt, R. M.; Weimer, P.; Al-Siyabi, H. A.; and Williams, E. T., 1997b, Outcrop analogs of turbidite petroleum reservoirs for assessing volumetric, development drilling, and simulation scenarios [abstract]: American Association of Petroleum Geologists Annual Meeting, Dallas.

Spang, R. J.; Slatt, R. M.; Browne, G. H.; Hurley, N. F.; Williams, E. T.; Davis, R. J.; Kear, R.; and Foulk, L. S., 1997, Formation microscanner image logs for evaluating stratigraphic features and key surfaces in thin-bedded turbdite sequences: Gulf Coast Association of Geological Societies, New Orleans, v. 47, p. 643–646.

Thomson, A.; and LeBlanc, R. J., 1975, Carboniferous deep-sea fan facies of Arkansas and Oklahoma: Geological Society of America Abstracts with Programs, v. 7, p. 1298–1299.

Thomson, A.; Danielson, S. E.; Hankinson, P. K.; and Kitchings, K. D., 1994 , Provenance of the Jackfork Sandstone, Ouachita Mountains, Arkansas and eastern Oklahoma [abstract]: Geological Society of America Abstracts with Programs, v. 26, no. 1, p. 28.

Tillman, R. W., 1994, Sedimentology and sequence stratigraphy of Jackfork Group, U.S. Highway 259, Le Flore County, Oklahoma, *in* Suneson, N. H.; and Hemish, L. A. (eds.), Geology and resources of the eastern Ouachita Mountains frontal belt and southeastern Arkoma basin, Oklahoma: Oklahoma Geological Survey Guidebook 29, p. 203–223. [Note: This article is reprinted with minor modifications as Tillman (2000) in this volume on p. 65–85.]

Viele, G. W.; and Thomas, W. A., 1989, Tectonic synthesis of the Ouachita orogenic belt, *in* Hatcher, R. D.; Thomas, W. A.; and Viele, G. W. (eds.), The Appalachian-Ouachita orogen in the United States: Geological Society of America, Boulder, Colorado, Decade of North American Geology, v. F-2, p. 695–728.

Weimer, P.; and Davis, T. L., 1996, Applications of 3-D seismic data to exploration and production: American Association of Petroleum Geologists Studies in Geology No. 42, and Society of Exploration Geophysicists Development Series No. 5, 270 p.

Winn, R. D., Jr.; and Armentrout, J. M. (eds.), 1995, Turbidites and associated deep-water facies: Society of Economic Paleontologists and Mineralogists Core Workshop No. 20, Houston, Texas, 176 p.

Yielding, C. A.; and Apps, G. M., 1994, Spatial and temporal variations in the facies associations of depositional sequences on the slope: examples from the Miocene-Pleistocene of the Gulf of Mexico, *in* Weimer, P.; Bouma, A. H.; and Perkins, B. F. (eds.), Submarine fans and turbidite systems: Gulf Coast Section Society of Economic Paleontologists and Mineralogists 15th Annual Research Conference Proceedings, p. 425–437.

Effects of Depth on Reservoir Characteristics and Production on Morrow and Springer Gas-Well Completions in the Anadarko Basin, Western Oklahoma

Paul W. Smith, Walter J. Hendrickson, and Ronald J. Woods
Petroleum Information/Dwights LLC
Oklahoma City, Oklahoma

ABSTRACT.—A recently published report by the Gas Research Institute (GRI) entitled "Gas Well Recovery versus Depth in the Anadarko Basin of Western Oklahoma" (Smith, 1996) suggested that the observed increase in gas-well recovery with increased depth is influenced more by increased reservoir volume than by increased pressure. The GRI conclusions are based upon the physical volumes at depth required to contain the produced gas. The study did not include an investigation into the physical reservoir parameters (i.e., thickness or porosity). Trends in well recovery (and required reservoir volumes) versus depth resulting from the GRI study will be presented.

Independent of the GRI study, detailed reservoir-characteristic studies for numerous fields producing from the Morrow and the Springer have been conducted. Approximately 375 wells producing from Morrow sandstones and 300 wells producing from Springer sandstones were evaluated. The distribution of wells represents a wide spectrum of depth ranges. The results of the reservoir characterization studies will be presented to include trends in reservoir thickness, reservoir porosity, water saturation, and well spacing. These factors can be used to determine the reservoir volume and demonstrate trends in physical reservoir volume with depth. Using original bottomhole pressure and temperatures, an expansion coefficient can be derived for each completion. This method can be used to make estimates of original gas in place for each completion. The original gas in place for each well was calculated using the perforated thickness and perforated porosity; the same was done using saturated thickness and saturated porosity. An interesting set of plots and data resulted that can be used to expedite exploration strategies, exploitation strategies, and/or acquisition strategies. Guidelines for estimating the productivity of the specific reservoirs resulting from the reservoir characterization studies were generated and are presented.

INTRODUCTION

A recently published report by the Gas Research Institute (GRI) (Smith, 1996) suggests that the observed increase in gas-well recovery with increased depth must be influenced by increased reservoir volume because observed increases in gas recovery are greater than could be accomplished by increased pressure. The GRI conclusions are based upon the physical volumes at depth required to contain the produced gas. The study did not include an investigation into the physical reservoir parameters (i.e., thickness or porosity). Subsequent to the GRI study, the reservoir characteristics of about 675 Morrow and Springer completions were evaluated to determine trends in reservoir quality.

DEPTH VERSUS THICKNESS AND POROSITY

The logs of 300 wells producing from Springer sandstones and 375 wells producing from Morrow sandstones were evaluated representing a wide spectrum of depth ranges. The investigation included an evaluation of gross reservoir thickness, saturated thickness, perforated thickness, and the porosity information for each reservoir definition. Discussions within this report will be limited to perforated and saturated intervals of wells having a single-zone completion. This step was necessary to relate known production to reservoir parameters.

Figure 1A shows the trend in perforated thickness with depth for Morrow sandstone completions. Figure 1B shows the average porosity for the same Morrow wells. At depths above 12,000 ft, porosity degrades with increased depth. Below 12,000 ft, porosity does not show a continued degradation with depth. In fact, at depths of 15,000–17,500 ft, the porosity improved over the 12,000–15,000-ft interval to a quality slightly superior to that observed at 11,000 ft. The deep porosity is likely to be secondary porosity, which tends to have

Smith, P. W.; Hendrickson, W. J.; and Woods, R. J., 2000, Effects of depth on reservoir characteristics and production on Morrow and Springer gas-well completions in the Anadarko basin, western Oklahoma, *in* Johnson, K. S. (ed.), Marine clastics in the southern Midcontinent, 1997 symposium: Oklahoma Geological Survey Circular 103, p. 105–118.

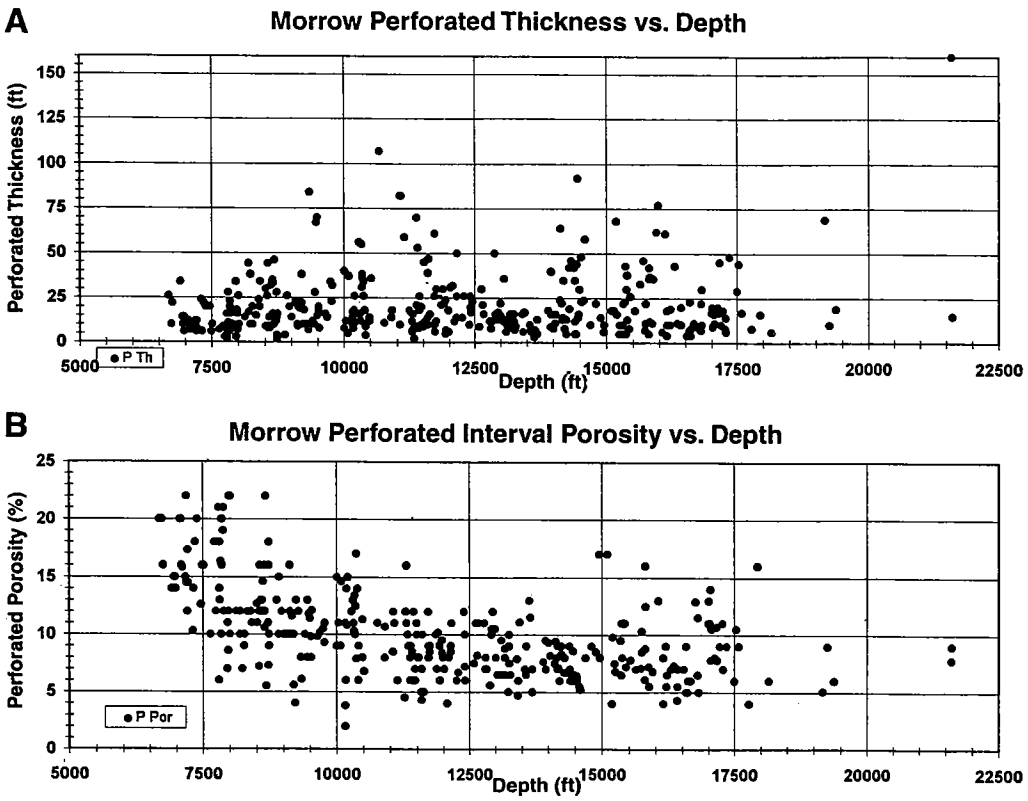

Figure 1. Trends in Morrow sandstones for 357 completed gas wells in the Anadarko basin. (A) Perforated thickness (in ft) versus depth (in ft). (B) Perforated interval porosity (in percentage of bulk volume) versus depth (in ft).

better connectivity; thus, improved permeability should be expected.

Figure 2A depicts the trend in perforated thickness with depth for completions in the Springer sandstones. At depths below 14,000 ft, an increase in perforated thickness is observed for Springer completions. In contrast, the trend is fairly flat for perforated thickness in Morrow completions (see Fig. 1A). Figure 2B shows the average porosity for the same Springer wells. A slight increase in porosity is present at depths between 15,000 ft and 17,500 ft, a trend that is interestingly similar to the trend in Morrow sandstones (Fig. 1B).

The saturated interval commonly differs significantly from the perforated thickness. There does not appear to be any standard rule to aid in determining what percentage of the saturated interval should be perforated. As shown in Figures 3A and 4A (the ratio of perforated to saturated thickness versus depth for the Morrow and Springer sandstones, respectively), as little as 5% of the hydrocarbon-saturated interval may be perforated in a specific well. These discrepancies are not related to porosity as might first be surmised. Most of the saturated porosities are within 80% of the perforated porosity, and in several cases the saturated porosity is better then the perforated porosity (see Figs. 3B and 4B). This situation may suggest the presence of by-passed gas.

We examined reservoir heterogeneities in our evaluations. Typically, Morrow and Springer sandstones are highly compartmentalized both vertically and horizontally. The degree of vertical reservoir heterogeneity typically increases with thickness.

WELL SPACING, RESERVOIR DRAINAGE, AND PRESSURE

Figures 5A and 6A (Morrow and Springer, respectively) show the relationships between well spacing and the radius of drainage for the saturated interval with depth. It would appear that Morrow wells typically drain less than 160 acres regardless of spacing. Springer wells demonstrate a similar habit, although more scatter is observed. The radius of drainage was calculated by determining the area required to contain the produced hydrocarbons considering the log-determined thickness, porosity, reported initial reservoir pressure, bottomhole temperature, and a 75% recovery. Some of the large radii of drainage could result from increased reservoir thickness and porosity outside the investigation range of a well log. In other cases, large drainage radii could result from capturing gas likely contained in undrilled offset acreage. The trend in recovery does not appear to demonstrate the need for larger spacing units with increased depth. At depths below 15,000 ft, most wells drain less than 320 acres, and a majority drain less than 160 acres. This characteristic may be caused by reservoir compartmentalization, a strong characteristic of these reservoirs. The

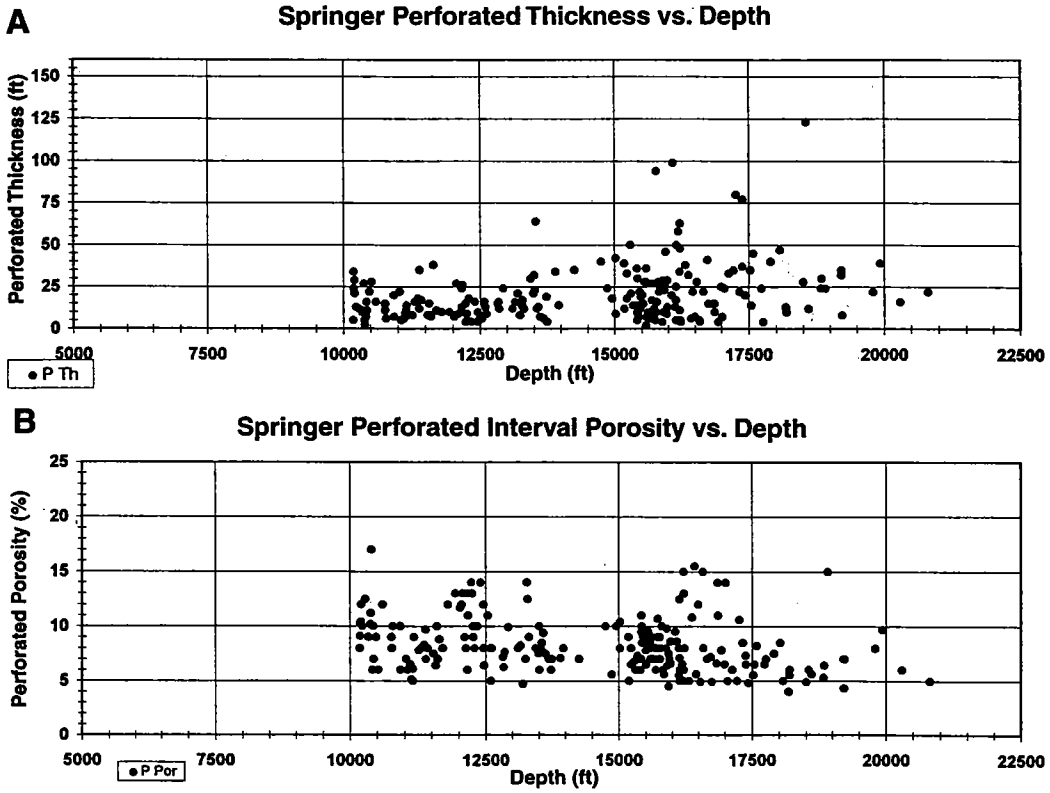

Figure 2. Trends in Springer sandstones for 300 completed gas wells in Anadarko basin. (A) Perforated thickness (in ft) versus depth (in ft). (B) Perforated interval porosity (in percentage of bulk volume) versus depth (in ft).

trend suggests that reservoir depth does not have much impact on the radius of drainage (Fig. 7) and is in keeping with the entire sample population. The pattern observed in Figure 7B (pressure drawdown versus radius of drainage) is nearly identical to the pattern shown in Figure 7A (ultimate recovery versus radius of drainage). As the amount of gas produced per pound of pressure depletion increases, the "reservoir size" (the volume from which it is being produced) necessarily increases. This observation is in keeping with the so-called perfect gas law.

Trends in reservoir pressure as a function of depth are shown in Figure 5B (Morrow) and 6B (Springer). Morrow sandstones appear to enter an overpressured regime at 13,000 ft. Springer sandstones were found overpressured at all depth intervals. A significant increase in pressure is observed in Springer completions below 15,000 ft. Increased pressure yields more gas per volume of reservoir. Thus, a 13,500-ft Morrow completion is apt to recover more gas than a Morrow reservoir of similar size at 12,500 ft.

GAS IN PLACE AND ULTIMATE RECOVERY

As suggested in the GRI study (Smith, 1996), reservoir volume in the Morrow and Springer sandstones must increase with depth. Both Morrow and Springer completions confirm that saturated gas in place increases with depth (Figs. 8A and 9A, Morrow and Springer, respectively). Although not shown, perforated gas in place increases with depth. This increase in reservoir volume with depth can be attributed to several factors evaluated during these studies. The average reservoir thickness improves with depth. Reservoir porosity does not show continued degradation with depth, and does show improvements with depth. Observed water saturations improve with depth for both Morrow and Springer completions. Thus, the physical ("tank") size of the reservoir increases with depth. Increased pressure amplifies the increases in gas reserves with depth.

The summarized data (Table 1) show single-zone-completion–well counts, average perforated thickness, average perforated porosity, and ultimate recoveries segregated by depth. Figure 10A–D presents histograms derived from data presented in Table 1 and provides a basis for comparisons of the Morrow and Springer trends.

This study highlights a practice of perforating a portion of the saturated interval. This practice probably leads to a significant decrease in ultimate production. A disparity of varying size between perforated gas in place and gas recovery exists throughout the depth spectrum for Morrow and Springer completions. Some wells have produced 30–40 billion cubic feet (BCF) of gas more than the calculated volumetrics would indicate is within reach of the perforated volume (see Figs. 8B and 9B, for the Morrow and Springer sandstones,

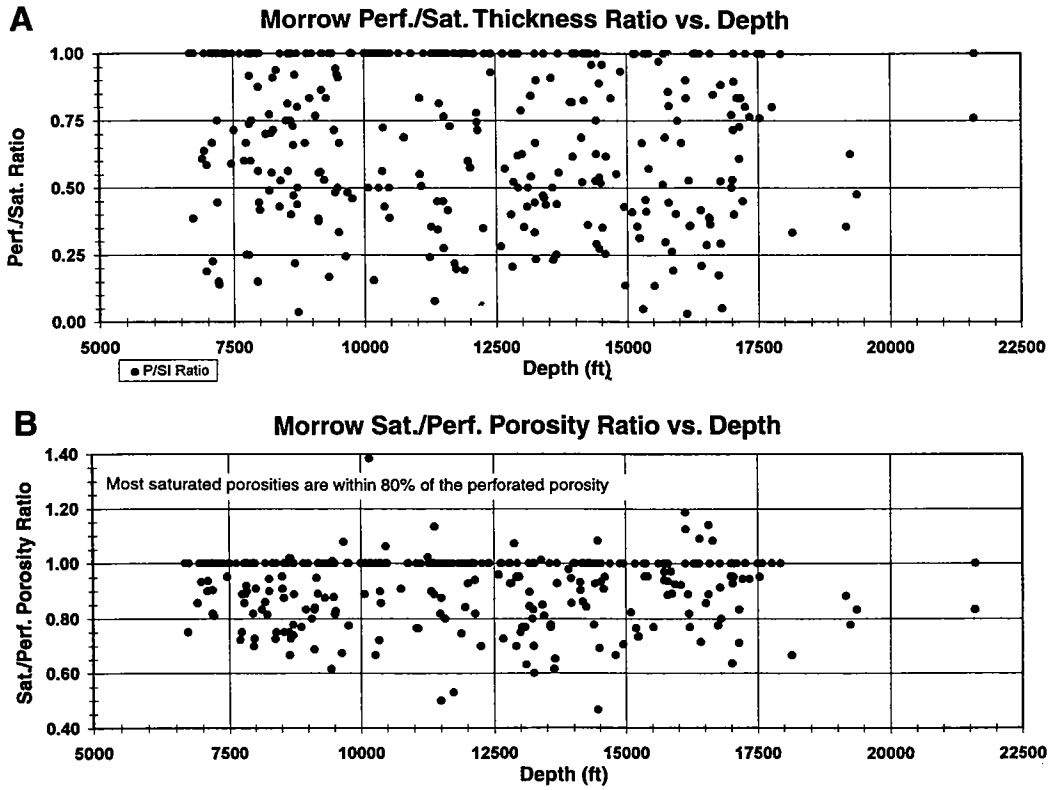

Figure 3. Trends in Morrow sandstones for 357 completed gas wells in Anadarko basin. (A) Ratio of perforated to saturated thickness versus depth (in ft). (B) Ratio of saturated to perforated porosity versus depth (in ft).

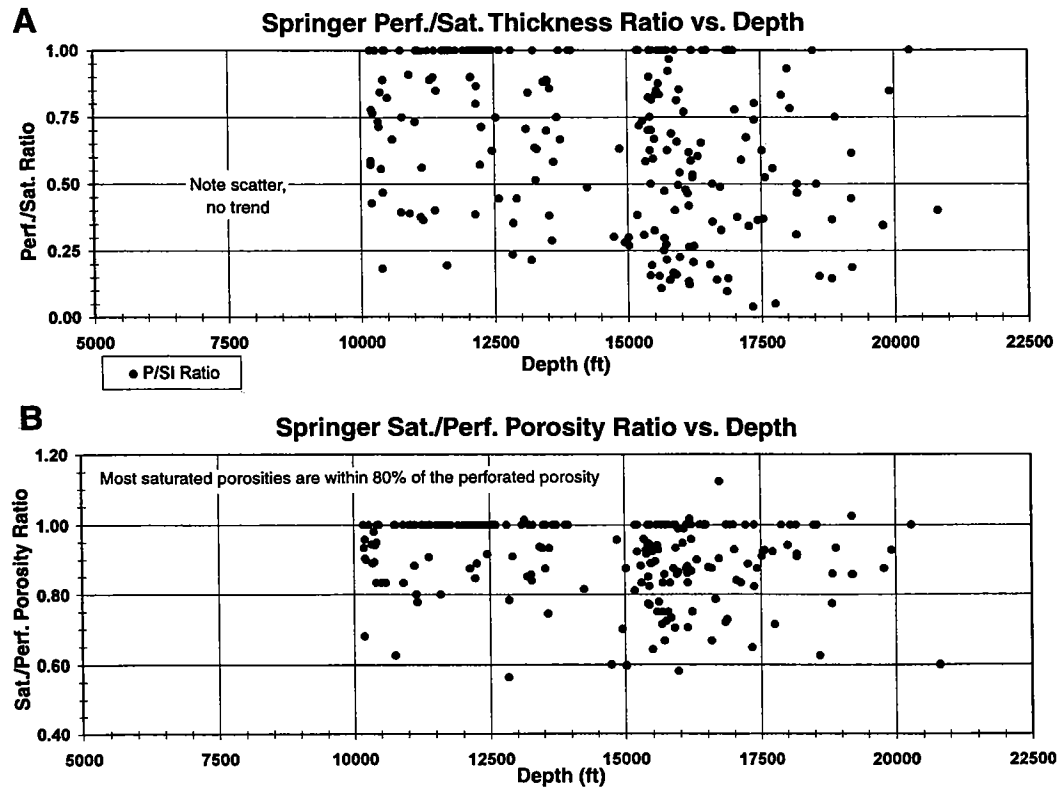

Figure 4. Trends in Springer sandstones for 300 completed gas wells in Anadarko basin. (A) Ratio of perforated to saturated thickness versus depth (in ft). (B) Ratio of saturated to perforated porosity ratio versus depth (in ft).

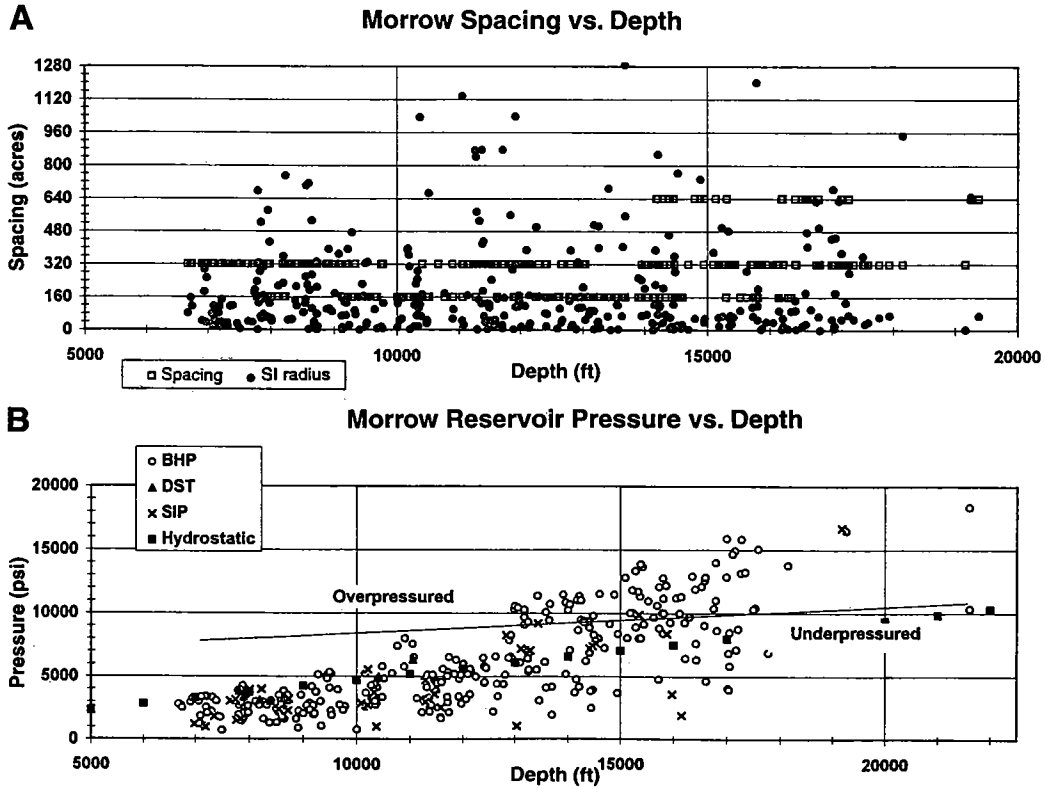

Figure 5. Trends in Morrow sandstones for 357 completed gas wells in the Anadarko basin. (A) Well spacing (in acres, shown by open squares) or saturated-interval radius (SI rad, in acres, shown by filled circles) versus depth (in ft). (B) Pressure (in pounds per square inch, psi) versus depth (in ft). Pressure measurements from bottomhole (BHP, shown by open circles), drill-stem tests (DST, shown by filled triangles), saturated-interval pressure (SIP, shown by x's), or hydrostatic pressure (shown by filled squares). Solid line represents boundary between underpressured and overpressured measurements.

respectively). In many of the "over-produced" cases, the stimulation treatment may have succeeded relative to the interval perforated. However, it is difficult to separate a successful stimulation from an increased drainage radius or improved reservoir characteristics outside the "view" of the well logs. It can be determined if it is likely that a specific well produced more gas than the volumetric approach would suggest by subtracting the saturated gas in place from the ultimate recovery. This exercise reveals that many wells must be draining outside acreage. Further investigation certainly is warranted on these wells.

This method of evaluation also helps screen out wells that do not warrant further investigation. Many wells produce about what they should—within a reasonable margin of error. There is a large population of wells that do not produce much of the perforated gas in place. Consequently, examples where the stimulation failed to access all the perforated reservoir volume are also present. Figures 8B and 9B show wells that have under produced by 20–30 BCF of gas. Wells that fail to drain the perforated volume certainly fail to drain the saturated volume. These imbalances lead to several important questions. For many of these wells, were the stimulation techniques used in the 1970s and 1980s optimum? How much of that gas is recoverable by current techniques? Investigation indicates that some of the "under-produced" wells were drained by adjacent "over-produced" wells; but many were not. Further geologic and engineering investigation is warranted to determine how much gas may have been overlooked.

CAUSE AND EFFECT

Reserve estimates were calculated for the perforated intervals and saturated intervals of each well. Observed water saturation, initial pressure, reservoir temperature, spacing derived from drill patterns, interval thickness, interval porosity, and a recovery factor of 75% was used to calculate gas in place. A comparison of the volume of saturated gas in place versus the volume of perforated gas in place is shown in Figure 11A (Morrow). In Example #1 for the Morrow, the well has a perforated volume of 1 BCF of gas and a saturated volume of 9 BCF. This disparity resulted because only 6 ft of a 40-ft-thick sandstone with an average porosity of 12% was perforated through each interval. This specific example has two 5-ft-shale streaks that separate the reservoir into three distinct lobes. An example of an over-producing Morrow well is provided in Figure 11B as Example #2. This example well has produced 27.5

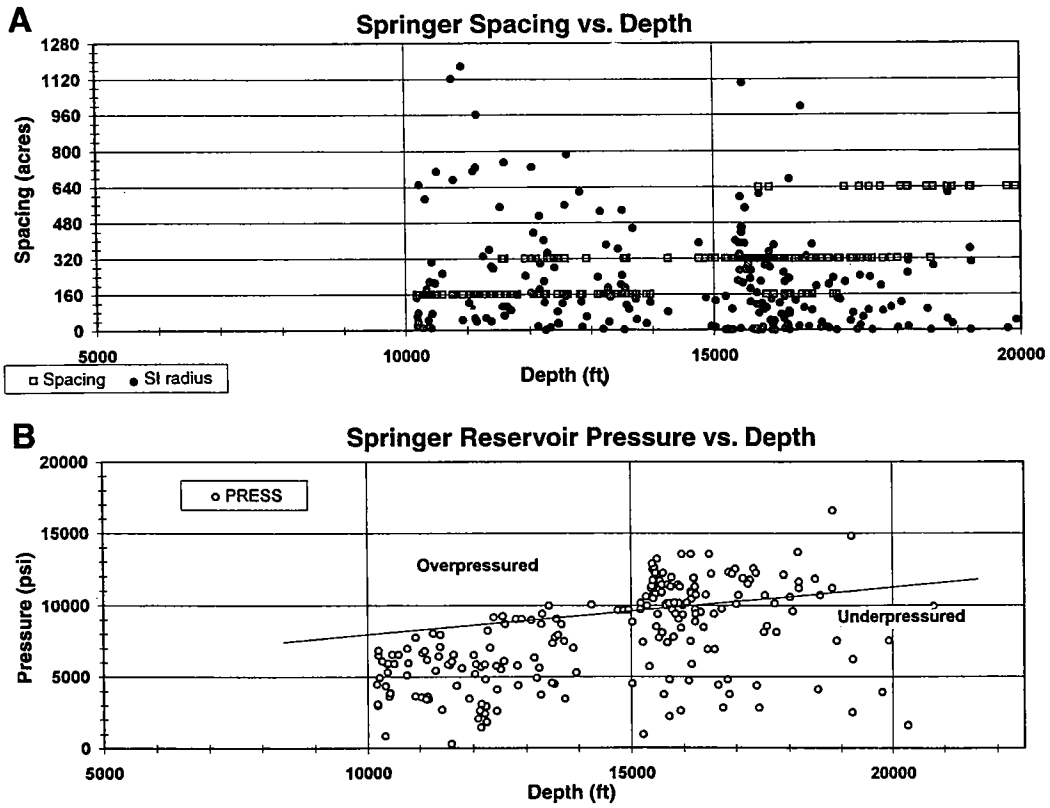

Figure 6. Trends in Springer sandstones for 300 completed gas wells in the Anadarko basin. (A) Well spacing (in acres, shown by open squares) or saturated-interval radius (SI rad, in acres, shown by filled circles), versus depth (in ft). (B) Pressure (in pounds per square inch, psi) versus depth (in ft). Solid line represents boundary between underpressured and overpressured measurements.

BCF of gas, about 17.5 BCF gas more than the perforated volume suggests that it should produce, and it has produced more than 8 BCF more gas than calculated for the saturated volume. This specific well is likely draining the acreage in the north offset direction. The offsetting section to the north is held by production from a Red Fork well and no Morrow test has offset the prolific 27 BCF well. The prolific well is not anomalous to the field in which it lies; the reservoir characteristics in this well are only average for the field. Is it too late for the competitor to drill an offset and recover a few BCF gas?

Reserve estimates were also calculated for the Springer completions. Springer Example #1 (see Fig. 12A) shows a well with less than 2 BCF reserves in the perforated interval and about 15 BCF reserves in the saturated interval. Figure 12B (volume of ultimate recovery versus volume of perforated gas in place) demonstrates that the well has failed to capture about 1.3 BCF of the perforated gas in place. Only 15 ft of a 155-ft saturated interval was perforated in this example. The reservoir has a high degree of vertical heterogeneity and is highly compartmentalized vertically. It appears the stimulation failed to communicate the perforations with most of the saturated reservoir. It appears that the early 1980s vintage completion failed to adequately drain the reservoir. Further investigation is warranted.

Figure 13 (volume of ultimate recovery versus volumetric balance for the Morrow sequence) and Figure 14 (the same plot for the Springer) demonstrate that anomalous wells can be identified quickly by detailed reservoir analysis. Most of the wells that cluster about the origin on these figures do not represent significant opportunities. Upon detailed geologic and engineering investigation, many anomalies of the over-production can be explained by offset under-production. One well drained the other. However, this type of data can be plotted quickly on a map as well, and volumetric balances for wells, fields, and trends can be established. Figure 14 shows two anomalous wells. Could the 13 BCF well benefit from a work-over and how did the offset(s) to the 18 BCF well perform? Were they offset? Why not? These anomalies may lead to further development opportunities.

GAS PRODUCED BY DRAWDOWN VERSUS ULTIMATE RECOVERY

The amount of gas produced per pound of pressure drawdown creates very interesting figures. As one would expect, better wells produce more gas per pound

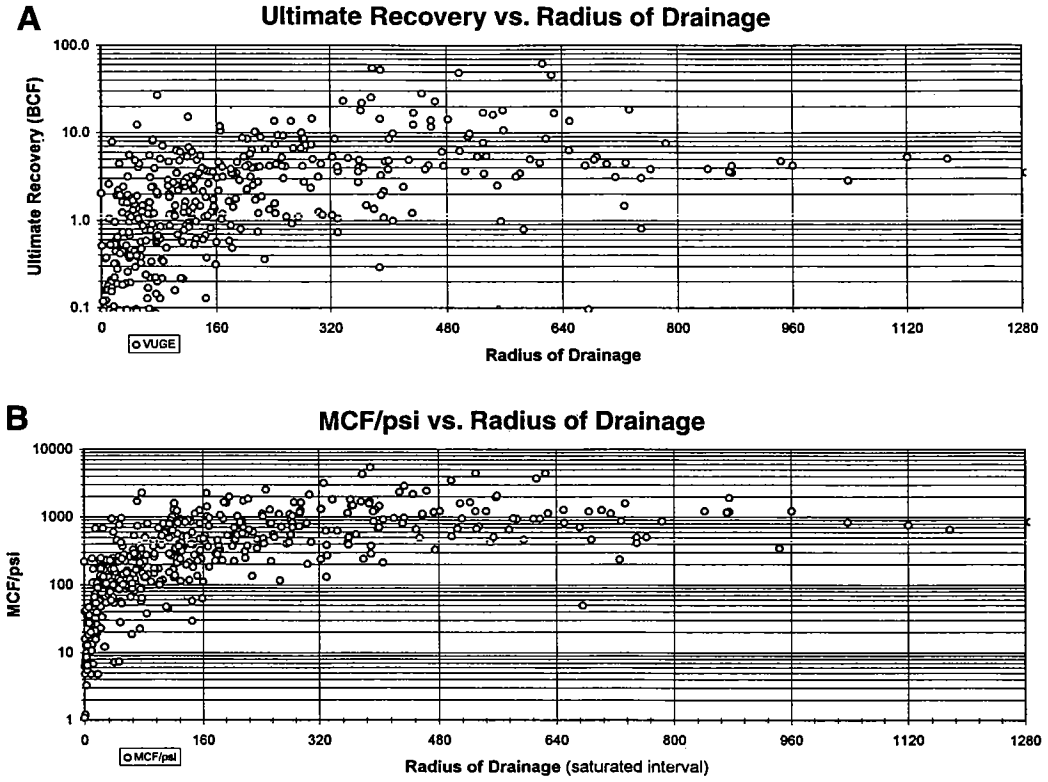

Figure 7. Trends in Springer and Morrow sandstones for 657 completed gas wells in the Anadarko basin. (A) Ultimate recovery (in billion cubic feet, BCF) versus radius of drainage (in ft). (B) Pressure drawdown (in thousand cubic feet, MCF, per pound per square inch, psi) versus radius of drainage of saturated interval (in ft).

of pressure drawdown than do poor wells. This expectation can be demonstrated in Figures 15 and 16 (Morrow and Springer, respectively). The figures are nearly identical in slope and trend. From these data, we might conclude that big wells drain large reservoirs ("tanks") and small wells drain small "tanks." This explanation would be in keeping with the *perfect gas law*:

Volume Factor = pressure × (volume/temperature)

Although intuitively correct, this explanation for the trends is not confirmed by the data. No definitive trend exists that demonstrates that increased recovery per pound of pressure drawdown (thousand cubic feet per pound per square inch, MCF/psi) is related to one of the volumetric parameters derived from the reservoir evaluations. Figure 17A–D shows the scattered distribution of porosity, thickness, and saturated porosity-feet in comparison to Morrow and Springer drawdown versus ultimate recovery. We found that a slight relationship could be established between observed water saturation and pressure drawdown. These results appear to defy the perfect gas law. Thicker reservoirs and more porous reservoirs *should* produce more gas per pound of pressure drawdown than the thinner and less porous reservoirs. A 100-ft^3 "tank" will produce twice the gas per pound of pressure drawdown that a 79.4-ft^3 "tank" would. This relationship must hold true for gas reservoirs.

The perfect gas law does apply to geologic "tanks." The reservoir may not deliver the gas to the borehole at rates acceptable to the individual operator, which may result in premature abandonment of the well. Reservoir permeability may be poor or have been damaged during the drilling and completion of the well. Furthermore, reservoir characteristics are likely to change away from the borehole, which may alter the size of the "tank." The reservoir conditions may improve or degrade away from the borehole; consequently, reservoir calculations were made for each well with the assumption that the characteristics observed in the well represent the average conditions for the drained area. At this point, geologists and engineers should integrate these results with other existing data (i.e., maps) to determine if the production behavior of an individual well is within expectations. In many cases, we find that poor performance in one well can be attributed to great performance in an offset well. We have investigated several anomalous wells and found that the anomalous well had been ignored by industry.

As shown by looking "vertically" at Figure 17D, wells may have delivered from 100 to 2,000 MCF per pound

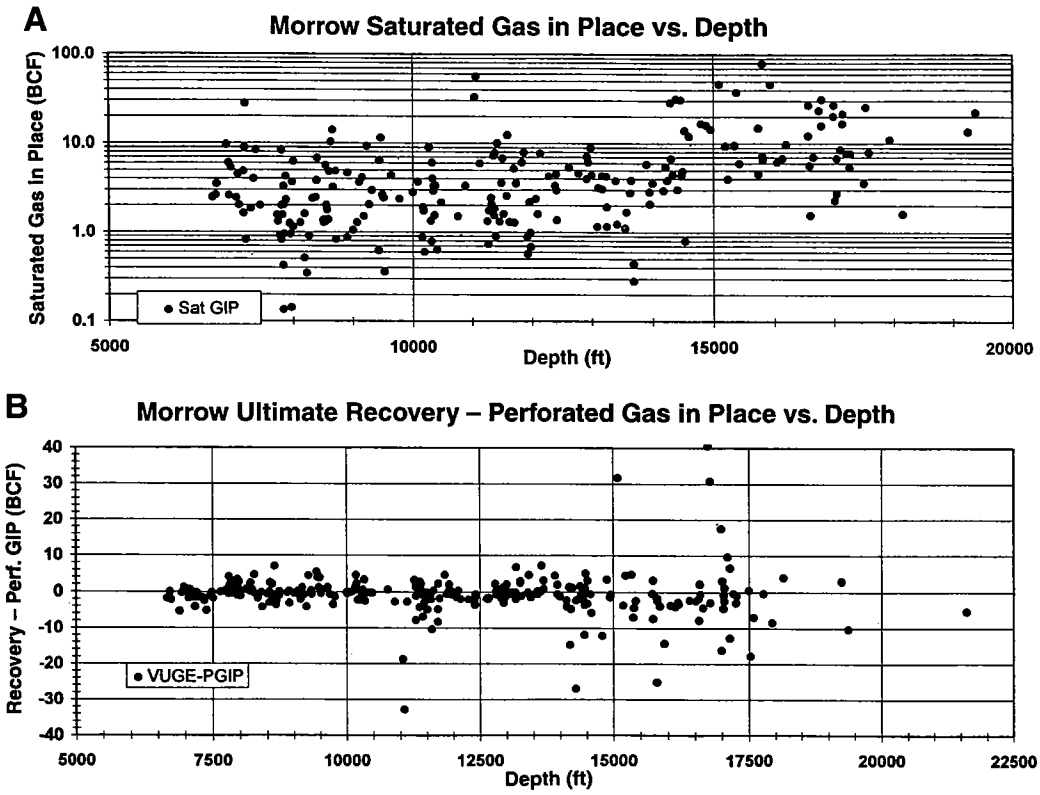

Figure 8. Trends in Morrow sandstones for 357 completed gas wells in the Anadarko basin. (A) Volume of saturated gas in place (Sat, in billion cubic feet, BCF) versus depth (in ft). (B) Volume of ultimate recovery of perforated gas in place (PGIP, in BCF) versus depth (in ft).

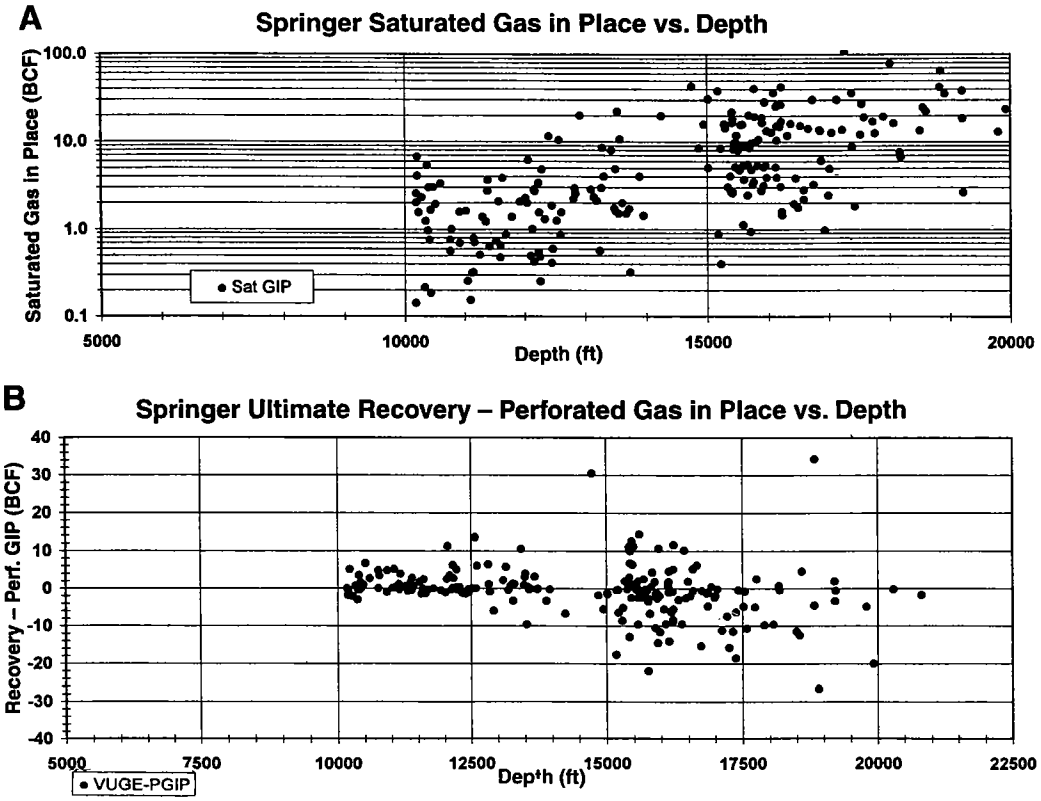

Figure 9. Trends in Springer sandstones for 300 completed gas wells in the Anadarko basin. (A) Volume of saturated gas in place (Sat, in billion cubic feet, BCF) versus depth (in ft). (B) Volume of ultimate recovery of perforated gas in place (PGIP, in BCF) versus depth (in ft).

Table 1.—Numbers of Single-Zone Completion Wells in Morrow and Springer Sandstones in the Anadarko Basin with Average Perforated Thickness, Average Perforated Porosity, and Ultimate Recoveries Segregated by Depth

Depth cell (ft)	Single-zone-completion count			Average perforated thickness (ft)			Average perforated porosity (%)			Ultimate recovery (BCF)		
	Morrow	Springer	Grand total	Morrow	Springer	Average	Morrow	Springer	Average	Morrow	Springer	Average
7,000	24	0	24	14		14	16.1		16.1	1.120		1.120
8,000	35	0	35	16		16	13.7		13.7	1.990		1.990
9,000	35	0	35	21		21	12.0		12.0	2.493		2.493
10,000	29	16	45	23	16	20	11.3	10.0	10.9	1.923	1.649	1.826
11.000	23	17	40	25	14	20	9.1	8.1	8.6	2.119	2.694	2.363
12,000	27	26	53	22	12	17	8.0	10.1	9.0	1.802	3.055	2.417
13,000	26	26	42	14	15	14	8.6	8.3	8.4	2.521	5.062	3.489
14,000	29	11	40	22	23	22	7.7	7.5	7.6	3.245	2.586	3.063
15,000	15	18	33	21	20	21	9.3	8.2	8.7	7.642	10.255	9.067
16,000	13	27	40	20	31	28	9.0	8.2	8.5	3.047	5.858	4.944
17,000	23	12	35	14	34	21	9.2	8.1	8.9	8.999	6.650	8.194
18,000	6	6	12	20	98	59	8.6	6.3	7.4	2.447	4.701	3.574
19,000	2	6	8	15	26	23	7.5	7.4	7.5	8.017	14.714	13.040
20,000	0	2	2		31	31		8.9	8.9		0.868	0.868
21,000	0	1	1		22	22		5.0	5.0		0.075	0.075
22,000	1	0	1	15		15	9.0		9.0	1.039		1.039
Grand total	288	158	446	19	24	21	10.5	8.5	9.8	3.089	5.075	3.793

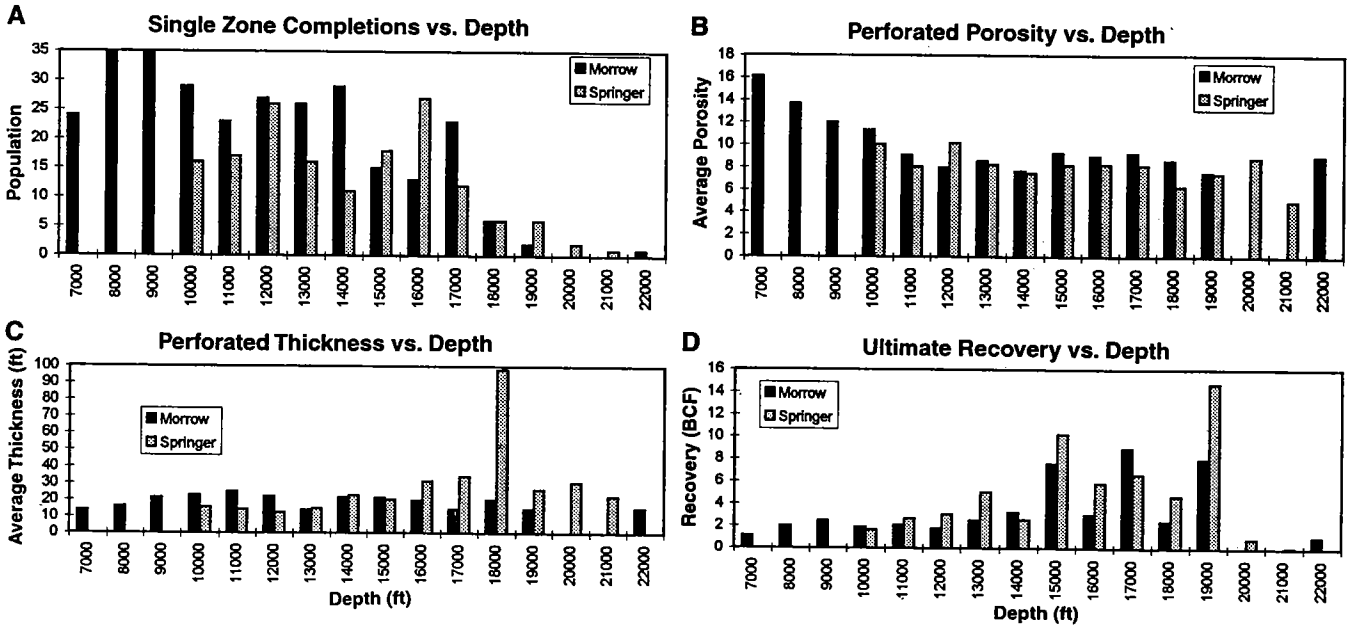

Figure 10. Trends in Morrow and Springer sandstones for 446 single-zone-completion gas wells in the Anadarko basin. Morrow data shown by dark-gray bars; Springer by light-gray bars. Data from Table 1. (A) Histogram of number of single-zone-completion wells (population) versus depth (in ft). (B) Average perforated porosity (in %) versus depth (in ft). (C) Average perforated thickness (in ft) versus depth (in ft). (D) Volume of ultimate recovery (in billion cubic feet, BCF) versus depth (in ft).

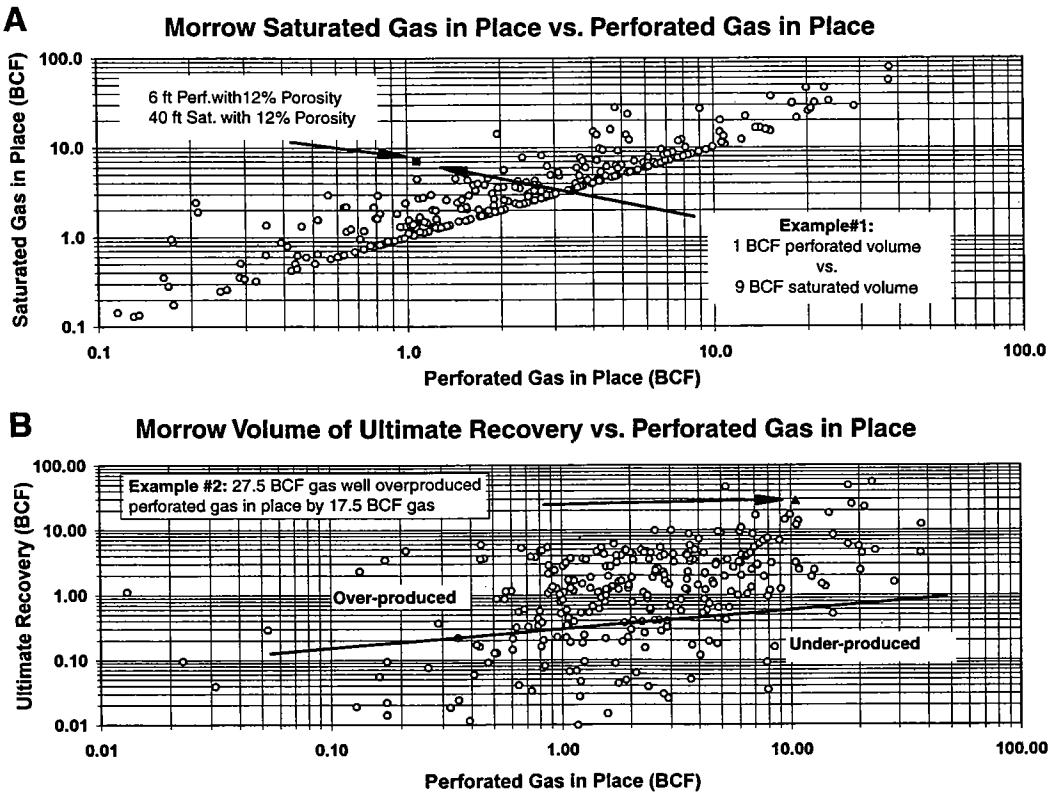

Figure 11. For Morrow sandstones in the Anadarko basin, logarithmic plots of ultimate perforated gas in place (in billion cubic feet, BCF) versus (A) volume of saturated gas in place (in billion cubic feet, BCF), and (B) volume of ultimate recovery (in BCF); boundary between under-produced wells and over-produced wells is shown by solid line. Example #1 (solid square) and Example #2 (solid triangle) are discussed in text.

of pressure drawdown to produce 1 BCF of gas. This suggests a 20-fold range in the reservoir size "tank-volume." This observation can be explained by either (1) a limited reservoir having delivered all the gas possible, or (2) a large reservoir having delivered only a limited amount of gas to the borehole. By reviewing the same data "horizontally," wells producing 100 MCF/psi drawdown may have produced between 0.15 and 1.5 BCF of gas—a 10-fold range. We can envision explanations for the spectrum between end scenarios. These data can be mapped to examine their relationships to each other and to obtain insights to their spatial relationships.

CONCLUSIONS

This study confirms the observation proposed by Smith (1996) that reservoir degradation is not continuous with depth. It can be shown that, at deep depths, some Morrow and Springer reservoir characteristics improve with depth. Trends in reservoir characteristics with depth show that the rapid degradation in porosity ceases below 12,000 ft, and, in many wells, the trend actually reverses. Increases in reservoir thickness also are observed with depth. Trends showing increased reservoir volume with depth are provided for Morrow and Springer reservoirs. Although not presented, calculated water saturation tends to improve with depth as well.

This study demonstrates that a strong relationship exists between ultimate recovery and the amount of gas produced per pound of pressure drawdown. According to the *perfect gas law*, the amount of gas produced per pound of pressure drawdown is controlled by "tank volume" (reservoir size). The study indicates that little (if any) observable relationship exists between log characteristics and volume of gas produced per pound of pressure depleted. This observation suggests that reservoir heterogeneity and/or drilling and completion practice play very significant roles in productivity. The observation also implies that many opportunities exist for future development within known productive areas.

Examples were provided that demonstrate that wells having anomalous reservoir characteristics relative to production could identify these opportunities. Reservoir characterization studies on a large scale provide a screening method by which only those wells can be identified that are deemed to be worthy of focused attention for possible opportunities. A large reservoir-

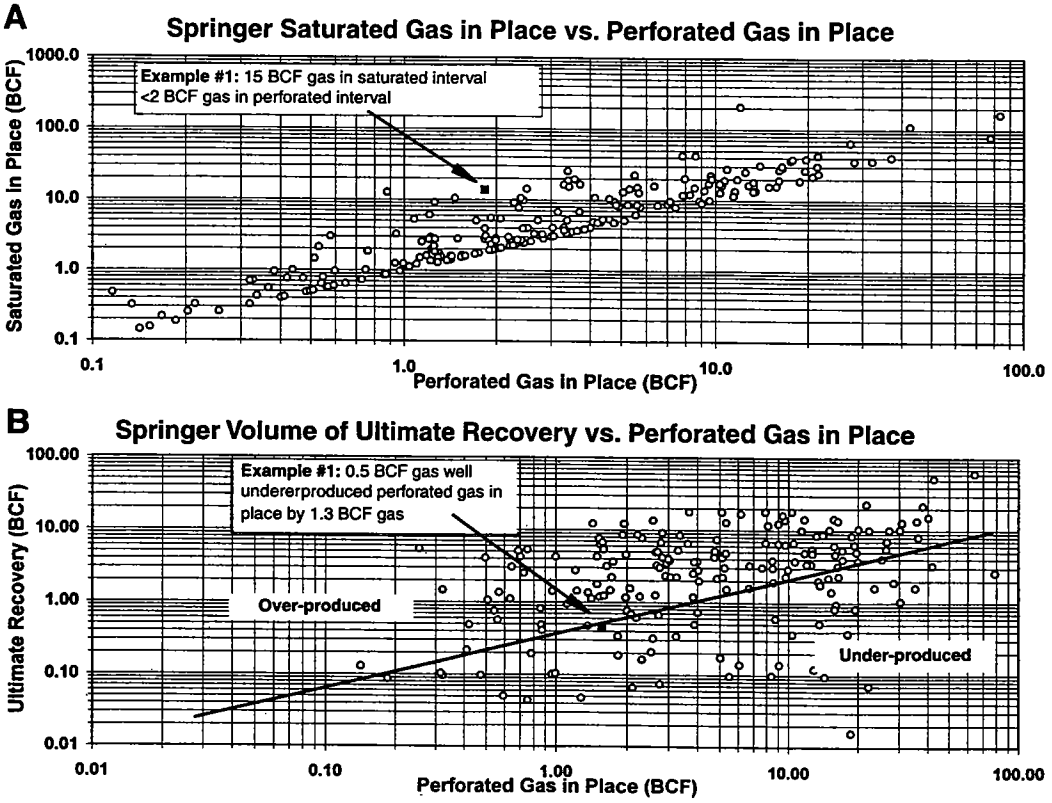

Figure 12. For Springer sandstones in the Anadarko basin, logarithmic plots of volume of saturated gas in place (in billion cubic feet, BCF) versus (A) volume of saturated gas in place (in BCF), and (B) volume of ultimate recovery (in BCF); boundary between under-produced wells and over-produced wells is shown by solid line. Example #1 (solid squares) is discussed in the text.

characteristics database can be used for many types of screening mechanisms, such as prospect "reality checking." Reservoir studies can aid management in developing exploration and exploitation strategies. For example, drilling for a Morrow sandstone target below 13,000 ft should have a higher priority than a 12,000 ft target if the target sizes are fairly equivalent. The 13,000-ft Morrow prospect has the potential of gaining 3,000–4,000 lbs of additional reservoir pressure, which may lead to increased recovery of 50% per well.

RECOMMENDATIONS

Wells are graded by production. Some wells are great (very profitable), most are average and many are neither. Other than production, what separates the great wells from the average wells? And why are the dog wells so poor? Reservoir-characterization studies can identify wells having anomalous reservoir characteristics relative to their production. Wells that have only average production may be underachievers relative to their reservoir characteristics.

Unfortunately, there are more wells than available manpower to identify all the opportunities. Reservoir studies on a basin level allow geologists and engineers to determine if the wells for which they are responsible are producing normally, above average, or at substandard level relative to wells with similar characteristics. Trends that are hidden at the well or field level may become obvious at the basin level. If some wells in a field are producing above average amounts of oil and gas, then, strategically, those wells producing substandard amounts of oil and gas should be considered potential opportunities. The question can be posed, "What has been done to wells with above average production to cause them to perform so well, and can the same strategies be applied to substandard wells to increase their production?" Geologists and engineers can use the results of reservoir-characterization studies in conjunction with existing maps and interpretations to identify areas of overlooked potential.

Reservoir permeability certainly affects the producibility of a reservoir. However, available permeability data is scant. Permeability is the only reservoir factor that can be altered during the drilling and completion phase. Low permeability can be caused by the introduction of fluids reactive with reservoir constituents (especially swelling clay minerals) during the drilling and/or completion phase of a well. This observation

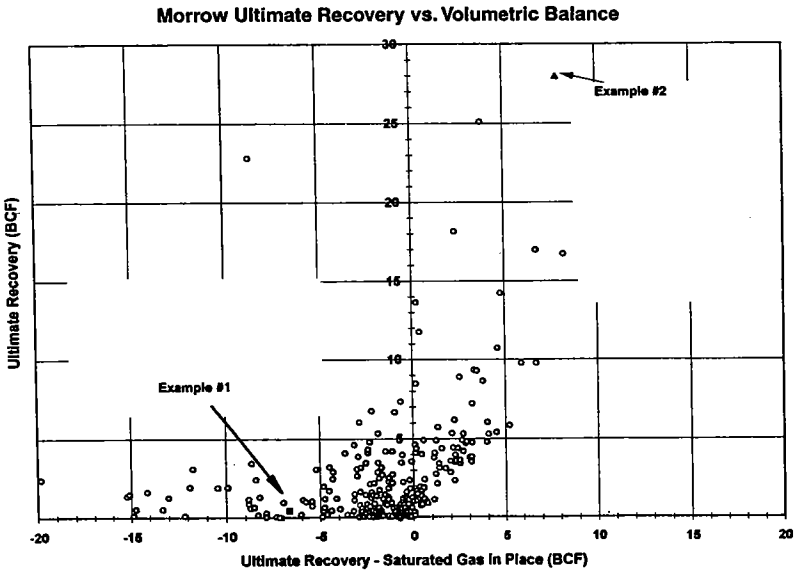

Figure 13. Volume of ultimate recovery (in billion cubic feet, BCF) versus volumetric balance (in BCF) for Morrow sandstone wells in the Anadarko basin. Example #1: Saturated interval is underproduced by 7 BCF gas; however, perforated interval is underproduced by 0.5 BCF gas. Perforated only 6 ft in a 40-ft-thick saturated interval. Example #2: Perforated interval is overproduced by 17.5 BCF gas and saturated interval is overproduced by about 8 BCF gas. North offset section is operated by competitor who has not drilled to the Morrow. This well has reservoir characteristics that are average for the field.

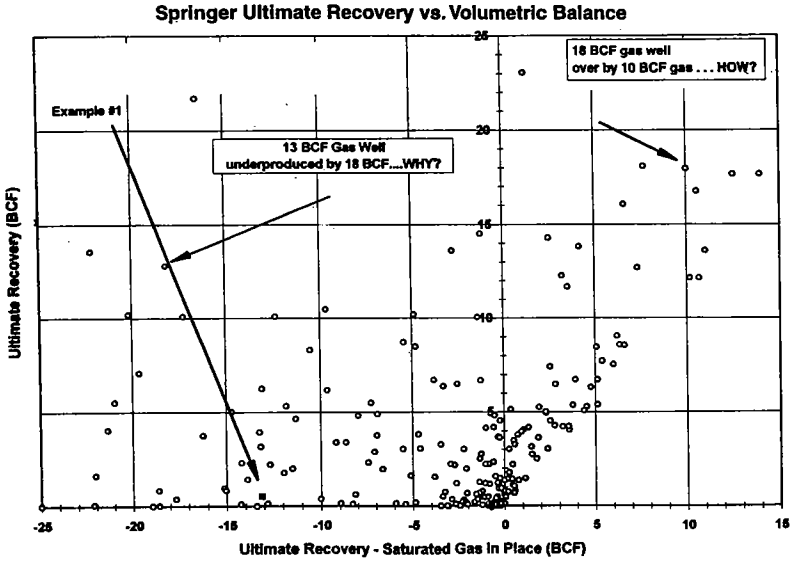

Figure 14. Volume of ultimate recovery (in billion cubic feet, BCF) versus volumetric balance (in BCF) for Springer sandstone wells in the Anadarko basin. Example #1: Saturated interval is underproduced by 13 BCF gas. Fifteen feet of a 155-ft saturated interval was perforated.

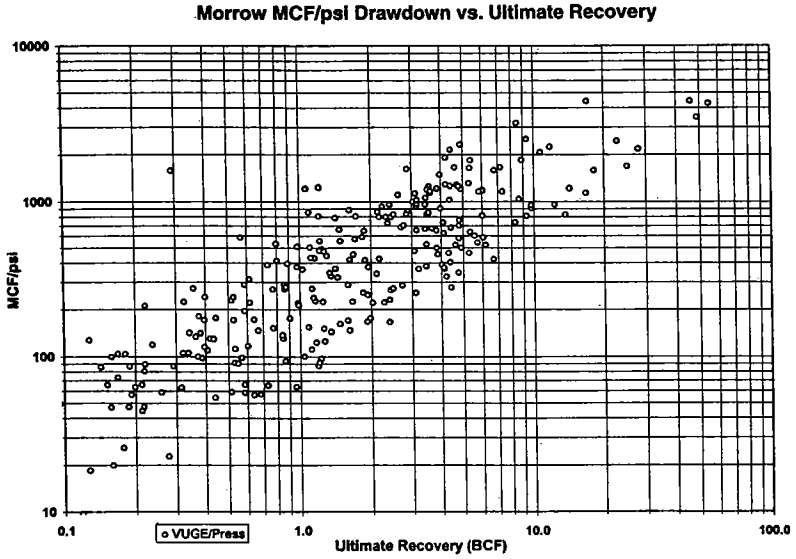

Figure 15. Log/log plot of amount of gas produced per pound of pressure drawdown (in thousand cubic feet per pound per square inch of pressure, MCF/psi) versus volume of ultimate recovery (in billion cubic feet, BCF) for Morrow sandstones in the Anadarko basin.

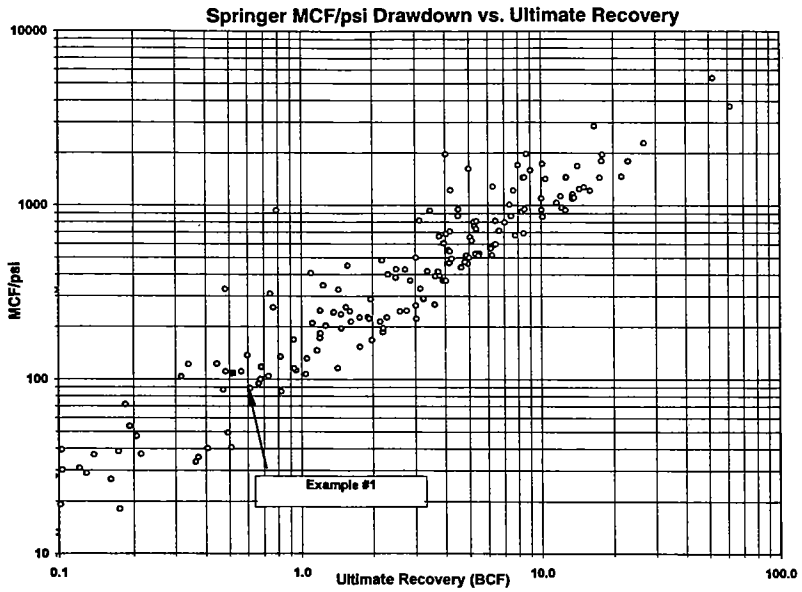

Figure 16. Log/log plot of amount of gas produced per pound of pressure drawdown (in thousand cubic feet per pound per square inch of pressure, MCF/psi) versus volume of ultimate recovery (billion cubic feet, BCF) of gas for Springer sandstones in the Anadarko basin. Example is discussed in text.

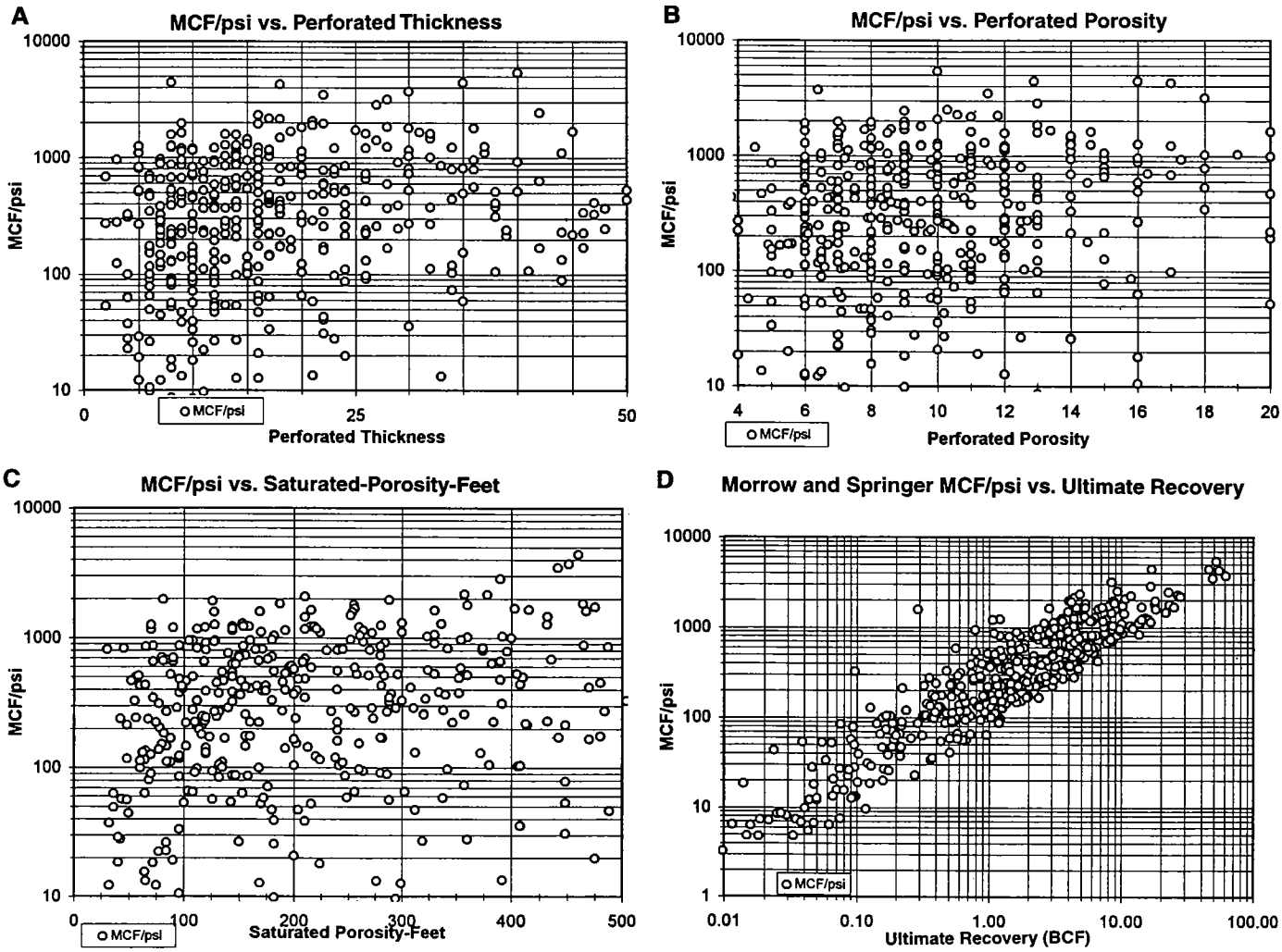

Figure 17. Logarithmic plots for Morrow and Springer sandstones in the Anadarko basin of (A) pressure drawdown (in thousand cubic feet per pound per square inch, MCF/psi) versus perforated thickness (in ft); (B) pressure drawdown (in MCF/psi) versus perforated porosity (in %); (C) pressure drawdown (in MCF/psi) versus saturated porosity (in ft); and (D) log/log plot of pressure drawdown (in MCF/psi) versus volume of ultimate recovery (in BCF).

poses the question, "What effects do various drilling and completion techniques have upon production rates and ultimate recovery?" With advancements in geological understanding, techniques used in the 1970s and 1980s may not have had optimum response compared with a well drilled and completed with the technology that is available today.

In many companies, the expertise jumps from one project to another or from one region to another without time being taken to make in-depth evaluations. During 1995, more than 90% of the additions to reserves came from existing fields. Less than 10% were due to wildcat discoveries. Reservoir-characterization studies can provide a powerful advantage.

REFERENCE CITED

Smith, P. W., 1996, Anadarko basin statistical studies: gas well recovery versus depth in the Anadarko basin of western Oklahoma: Gas Research Institute, Chicago, Contract No. C5095-890-3448, GRI Final Report GRI-96/0196, 65 p.

Heterogeneity of Morrow Sandstone Reservoirs Measured by Production Characteristics

Thaddeus S. Dyman, James W. Schmoker, and John C. Quinn
U.S. Geological Survey
Denver, Colorado

ABSTRACT.—Production parameters from oil and gas wells, including peak monthly production, peak consecutive-12–month production, and cumulative production, are tested as tools to quantify and understand the heterogeneity of marine clastic reservoirs in fields where current monthly production is ≤10% of peak monthly production. Variation coefficients, defined as $VC = (F_5 - F_{95})/F_{50}$, where F_5, F_{95}, and F_{50} are the 5th, 95th, and 50th (median) fractiles of a probability distribution, are calculated for peak and cumulative production and examined for internal consistency, type of production parameter, conventional vs. unconventional accumulations, and reservoir depth. These production parameters measure the net result of complex geologic, engineering, and economic processes. Our fundamental hypothesis is that well-production data provide information about subsurface heterogeneity in older fields that would be impossible to obtain using geologic techniques with smaller measurement scales such as petrographic, core, and well-log analysis.

Well-production data for this study were compiled for 69 oil and gas fields in the Pennsylvanian Morrow Sandstone of the Anadarko basin, Oklahoma. Of these, 47 fields represent production from marine clastic facies. The Morrow data were supplemented by data from the Arbuckle (Cambrian–Ordovician), Simpson (Ordovician), Atoka (Pennsylvanian), and Hunton (Devonian) Groups of the Anadarko basin, one large gas field in Upper Cretaceous reservoirs of north-central Montana (Bowdoin Dome), and three areas of the continuous-type (unconventional) oil accumulation in the Bakken Formation (Devonian–Mississippian) in the Williston basin, North Dakota and Montana.

Our analysis shows that: (1) variation coefficients derived from the cumulative-production records of older wells are larger than those for the peak yearly production or peak monthly production, implying that heterogeneity associated with reservoir volume accessed by wells is greater than heterogeneity associated with the flow rates controlled by the plumbing system of a well. (2) Of the fields studied, Morrow gas reservoirs of the Anadarko basin are less heterogeneous than Morrow oil reservoirs. Bakken, fracture-controlled, shale reservoirs of the Williston basin are most homogeneous in terms of production characteristics and are thus the most predictable. (3) Depth exerts little control on heterogeneity for the fields in this study (depth range of 8,000 ft). (4) The heterogeneity of cumulative well production between fields is equal to or less than that within fields. Results such as these indicate that quantitative measures of production rates and production volumes of wells, expressed as dimensionless variation coefficients, are potentially valuable tools for documenting reservoir heterogeneity in older fields for field redevelopment and risk analysis.

INTRODUCTION

For this study, we test the use of the well-production parameters of peak monthly production, peak consecutive-12–month production, and cumulative production in older wells as tools to quantify and understand the heterogeneity of oil and gas reservoirs. We define measures of variability (variation coefficients) in peak production and cumulative production and examine calculated variation coefficients with respect to internal consistency, type of production parameter, conventional vs. unconventional accumulations, and reservoir depth. We also evaluate the use of well-production parameters for planning of long-range field development. The bulk of the test data represent Morrowan-age clastic reservoirs of the Anadarko basin. Well-production data from

Dyman, T. S.; Schmoker, J. W.; and Quinn, J. C., 2000, Heterogeneity of Morrow Sandstone reservoirs measured by production characteristics, *in* Johnson, K. S. (ed.), Marine clastics in the southern Midcontinent, 1997 symposium: Oklahoma Geological Survey Circular 103, p. 119–127.

other formations of the Anadarko basin, Williston basin, and north-central Montana are also included in the data set to include a broader population of reservoirs to compare with the Morrow.

BACKGROUND

Production parameters in oil and gas reservoirs vary significantly from well to well for a variety of geologic and engineering reasons. The fundamental hypothesis of this study is that well-production variability carries information about the heterogeneity of reservoirs that would be difficult or impossible to obtain using traditional geologic techniques such as petrographic study, core and well-log analysis, and outcrop observations. The flow of oil or gas to a wellbore is visualized as integrating all aspects of geology that are relevant to reservoir performance over an area of tens to hundreds of acres.

In addition to *in situ* geologic factors, completion and production practices might also influence well-production characteristics. An aspect of this preliminary study is to examine the extent to which systematic characteristics reflecting reservoir heterogeneity are masked by variability in engineering practices.

Measures of Well Production

Peak monthly production is defined as the volume of oil or gas produced in the most productive calendar month in the history of a well. In identifying the peak month, production volumes should be adjusted to account for the fact that a calendar month can consist of 28, 29, 30, or 31 days. Variations in peak monthly production reflect variations in the rates at which hydrocarbons can flow to the wellbore (well deliverability). Because of the short measurement period, the peak monthly production is not commonly affected by factors relating to depletion of hydrocarbons in a reservoir. However, the short measurement period also means that variations in peak monthly production in some cases might reflect human-induced engineering factors rather than *in situ* natural reservoir factors.

Peak consecutive-12–month production (for convenience, referred to in the remainder of this paper as peak yearly production), is defined as the volume of oil or gas produced in the most productive 12-month period (as differentiated from the most productive calendar year) in the history of a well. Peak yearly production is in some ways a compromise indicator of well deliverability. The longer measurement period (compared to peak monthly production) increases the probability that variations in peak yearly production are indicative of geologic factors rather than engineering factors. However, over a one-year period, reservoir depletion could start to play a role, so that peak yearly production might be a mixed measure of reservoir volume as well as production rate.

Cumulative production is the total volume of oil or gas recovered throughout the producing history of a well. Because most wells exhibit exponential or hyperbolic production decline as a function of time, cumulative production from older wells (that is, wells in which the curve of production vs. time has flattened) asymptotically begins to approximate ultimate recovery. Although cumulative production from older wells is not an ideal measure of ultimate recovery (cumulative production being too low unless the well is abandoned), it has the advantage of precision—cumulative production is a direct measurement, whereas ultimate recovery is an estimate based on projections into the future. In older wells, variations in cumulative production reflect variations in the reservoir volume accessed by the wellbore. Older wells are defined for this study as wells for which current monthly production is less than 10% of initial monthly production.

Lognormal Distributions

Many geologic processes result in physical properties whose values form a lognormal distribution. A lognormal distribution is one in which the logarithms of the observations in question follow a normal distribution. Therefore, most of the observed values of a lognormal data set are relatively small, and a few are very large. Lognormal distributions in geology include such diverse properties as the grain sizes of sediments, magnitudes of earthquakes, gold-assay values from mineral deposits, frequencies of floods, and sizes of oil and gas fields (Koch and Link, 1970; Davis, 1986).

The production parameters of peak monthly production, peak yearly production, and cumulative production measure the net result of multiplicative geologic processes and thus might be expected to approximate a lognormal distribution. For this reason, production data in this study are plotted on graph paper having axes arranged (as shown in Fig. 1) such that a lognormal distribution plots as a straight line.

In actual practice, plots of peak monthly production, peak yearly production, and cumulative production will not form exact lognormal distributions. A true lognormal distribution has no cutoff at the high end, but offers an increasingly small chance for an increasingly large value. However, peak monthly production, peak yearly production, and cumulative production all have finite upper limits that are dictated by hydrocarbons in place, drainage area, permeability, and other factors; and the upper end of the probability distribution is therefore truncated. The lower end of the distribution might also be truncated, by economic considerations, in that some poor wells might not be completed and produced to become part of the data set.

Quantitative Measures of Production Variability

The slopes of the probability distributions for peak monthly production, peak yearly production, or cumulative production (Fig. 1) are direct indicators of the variability of the data set. Steeper slopes equate to greater production heterogeneity. A horizontal line on Figure 1 would represent an oil or gas field with perfectly uniform production characteristics.

A parameter that is proportional to the slopes of the four probability distributions of Figure 1 would provide a quantitative numerical representation of production

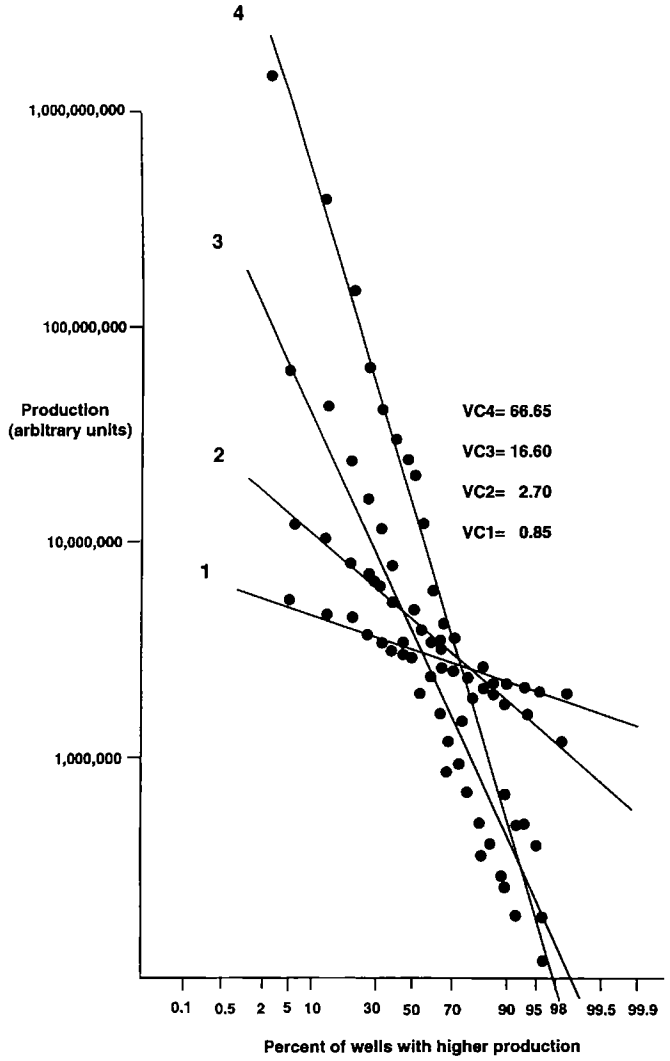

Figure 1. Probability distributions based on hypothetical data for production from wells of an oil or gas field (peak monthly production, peak 12-month production, or cumulative production). Each point represents a well; four different fields are depicted. This figure illustrates a type of plot in which: (1) lognormal distributions plot as straight lines; and (2) steeper slopes of lines correspond to a greater range of production and thus greater production variability. The variation coefficient VC = $(F_5 - F_{95})/F_{50}$ provides a dimensionless numerical value for the variability of each data set, and increases as slope increases.

heterogeneity. Such a parameter, referred to here as a variation coefficient, can be calculated using a measure of the dispersion (range) of the data set divided by a measure of central tendency such as the mean or the median (Stell and Brown, 1992; Schmoker, 1996; Dyman and others, 1996). For this study, a dimensionless variation coefficient (VC) is calculated as:

$$VC = (F_5 - F_{95})/F_{50},$$

where F_5, F_{95}, and F_{50} are the 5th, 95th, and 50th (median) fractiles of the probability distribution for peak monthly production, peak yearly production, or cumulative production. These fractiles are picked directly from plots such as illustrated by Figure 1.

Note in Figure 1 that increasing VC corresponds to increasing slope of the probability distribution, and thus to increasing well-production variability. Because VC is a dimensionless variable, with the range of values normalized by the median of the values, it is independent of the magnitude of production. In other words, VC does not depend on whether overall production of a group of wells is "good" or "poor."

Other variation coefficients could be defined whereby the range of production values is represented by perhaps the 10th and 90th fractiles, the maximum and minimum measurements, or the standard deviation, or if the central tendency is represented by the mean rather than the median. Test calculations indicate that all these approaches result in similar rankings of variability.

DATA

Well-production data developed for this study represent 69 primarily gas fields in the Morrow Sandstone (Pennsylvanian) of the Anadarko basin, Oklahoma, one gas field each in the Arbuckle Group (Cambrian–Ordovician), Simpson Group (Ordovician), Atoka Group (Pennsylvanian), and Hunton Group (Devonian) of the Anadarko basin and one gas field in undifferentiated Upper Cretaceous (Phillips, Greenhorn, and Bowdoin) reservoirs of north-central Montana (Table 1; Fig. 2). The Anadarko basin gas accumulations are conventional fields. The Bowdoin field is a localized "sweet-spot" in an accumulation of shallow, regionally extensive, unconventional, biogenic gas of the type termed continuous by Schmoker (1995). These data are supplemented by previously developed data (Schmoker, 1996)

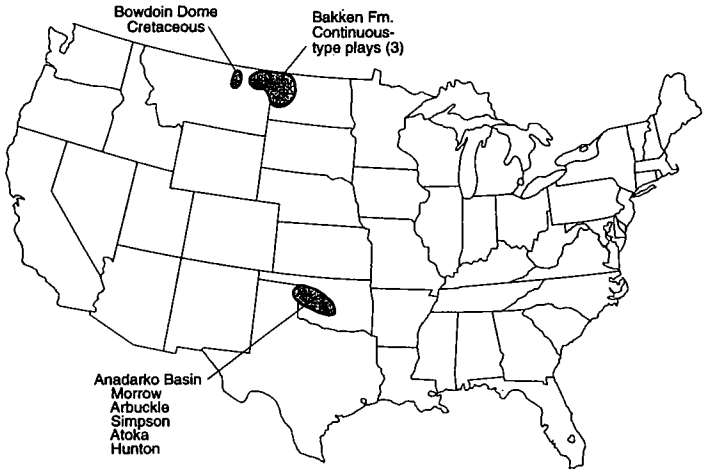

Figure 2. Map of the conterminous United States showing the locations of fields from which wells were derived for this study.

TABLE 1. — Data Generated in Study of Reservoir Heterogeneity as Measured by Production Characteristics of Vertical Wells by Region or Basin

Field	Depth (ft)	Env.	No.	Gas VC_{cp}	Gas VC_{pyp}	Gas VC_{pmp}	Oil VC_{cp}	Peak well
MORROW GROUP GAS FIELDS (ANADARKO BASIN)								
Adams Ranch	5,700	m	23	24.92	—	—	—	6,586,443
Angell	5,608	m	29	3.28	2.92	2.23	46.75	2,229,561
Anthon	13,028	m	16	9.99	5.92	6.92	46.62	6,515,234
Arkalon	5,700	m	27	9.11	3.68	4.96	10.39	7,331,340
Arapahoe	—	m	12	19.95	7.93	7.53	—	6,943,859
Arnett Southeast	11,409	m	19	72.41	26.90	18.36	57.74	14,773,401
Balko South	7,642	m	44	13.15	16.03	16.70	11.74	5,172,653
Boiling Springs North	7,050	m	57	7.22	5.64	5.08	13.00	5,345,138
Borchers North	5,607	fd	19	3.45	—	—	3.05	9,429,664
Camrick	—	fd	197	6.43	3.96	2.62	23.41	19,792,874
Camrick Gas Area	6,871	fd	48	7.22	4.40	2.96	91.11	2,567,568
Carthage	5,059	fd	55	9.12	4.34	3.39	9.54	26,026,988
Carthage Northeast	—	fd		—	—	—	5.88	—
Cestos Southeast	9,432	m	15	7.08	7.22	5.23	5.36	4,158,977
Clark Creek East	5,685	e	14	16.22	—	—	27.20	6,012,261
Como Southwest	—	—	12	4.79	8.37	9.83	—	229,434
Crane Southeast	11,010	m	14	7.08	—	—	9.67	5,161,790
Custer City East	12,490	m	14	5.48	2.68	7.81	13.82	3,054,591
Eagle City South	9,750	m	14	11.22	3.59	4.46	4.71	3,816,420
Elm Grove	12,063	m	12	33.01	35.60	15.61	27.36	10,004,990
Evalyn-Condit	5,636	m	34	6.45	14.81	10.21	20.88	7,016,788
Fay East	10,578	m	58	9.96	4.79	3.10	15.42	13,460,837
Gage	8,716	m	140	9.95	5.60	4.21	20.35	9,971,786
Gentzler	5,992	m	21	17.73	14.82	8.88	8.35	4,240,002
Gooch	5,926	m	11	2.44	—	—	34.67	7,757,186
Grand West	—	m	14	7.22	8.31	5.34	—	3,630,084
Guymon-Hugoton	6,217	fd	168	4.34	4.96	4.21	3.22	17,569,159
Guymon South	6,583	fd	79	3.82	4.00	4.26	2.87	11,759,974
Harmon East	10,254	m	52	14.45	9.47	7.59	7.17	9,949,396
Harper Ranch	5,437	e	31	26.36	9.90	4.82	8.20	9,245,994
Higgins South	11,897	m	29	11.21	7.57	5.39	43.64	9,651,127
Hooker Southwest	—	m	60	4.56	8.05	8.97	9.09	15,791,981
Ivanhoe	8,250	m	63	12.99	9.49	4.91	9.09	9,189,029
Keys Gas Area	4,437	fd	25	8.41	4.67	2.19	21.36	3,204,188
Kinsler	5,175	fd	39	13.77	4.19	3.99	501.15	13,866,396
Liberal Southeast	6,202	m	19	9.97	—	—	16.87	12,302,149
Logan South	8,300	m	66	7.50	4.79	4.64	16.56	4,652,107
Lovedale	6,113	e	49	11.46	7.32	3.66	15.16	5,287,262
Lovedale Northwest	5,728	e	62	7.74	4.20	4.78	23.79	5,447,140
Mayfield Northeast	—	m	10	13.60	7.15	12.97	—	8,094,077
Milder	8,886	m	41	10.21	13.57	7.99	17.50	11,067,421
Mocane-Laverne	7,000	m	1,462	6.27	4.65	4.04	10.72	17,139,891
Mohler Northeast	5,690	m	14	6.09	—	—	13.57	3,277,300
Mouser	6,244	fd	47	4.87	3.97	3.14	9.99	21,348,342

(continued on next page)

TABLE 1. — *(Continued)*

Field	Depth (ft)	Env.	No.	Gas VC_{cp}	Gas VC_{pyp}	Gas VC_{pmp}	Oil VC_{cp}	Peak well
Nobscott Northwest	10,283	m	23	6.02	4.34	4.05	12.34	6,284,542
Oakwood North	9,420	m	64	6.45	4.33	3.38	7.72	8,472,153
Okeen Northwest	7,886	m	16	4.86	5.25	5.61	58.74	4,259,750
Peek Northeast	11,514	m	18	8.20	4.79	5.07	6.45	2,511,460
Postle	6,119	fd	31	12.87	—	—	4.05	11,275,268
Putnam	10,326	m	167	18.18	5.72	4.00	8.50	23,465,695
Richfield	4,744	fd	30	8.67	4.69	7.56	16.62	12,503,325
Sampsel Northeast	4,591	fd	48	10.42	5.65	4.06	67.50	8,297,998
Sharon West	9,144	fd	43	16.54	5.85	4.32	25.09	14,960,625
Shuck	5,628	fd	15	6.90	9.30	5.47	13.38	3,007,304
Singley	5,803	m	11	4.64	—	—	25.10	2,287,632
Snake Creek	5,452	e	13	7.52	4.18	4.56	—	4,833,944
Squaw Creek	—	m	11	3.08	2.65	11.50	—	—
Sparks	5,254	m	26	3.79	—	—	5.27	11,149,646
Stevens	5,560	m	16	6.86	—	—	48.80	3,622,547
Taloga	4,428	m	19	32.96	—	—	12.29	4,830,872
Tangier	9,035	m	110	15.84	6.42	4.88	27.51	15,576,109
Tyrone	6,384	m	26	2.03	22.98	14.16	10.01	5,510,136
Walkemeyer	6,145	m	13	5.45	—	—	10.08	6,039,016
Watonga-Chickasha Trend	9,953	m	794	12.28	7.47	5.59	17.76	34,932,228
Wilburton	4,808	fd	17	11.46	—	—	3.68	13,143,092
Woodward North	7,729	m	32	9.77	7.60	6.53	19.28	4,057,792
Woodward Northeast	—	m	16	30.39	22.20	7.32	15.60	5,885,149
Woodward South	8,658	m	19	12.94	12.69	6.55	31.61	6,867,064
Woodward Southeast	7,999	m	14	10.67	—	—	50.10	15,885,406
NON–MORROW GROUP FIELDS (ANADARKO BASIN)								
Mayfield West (Arbuckle)	16,500	m	8	3.56	3.34	1.94	—	25,134,000
Mayfield West (Hunton)	18,200	m	20	4.27	4.19	1.85	—	27,193,000
Carpenter (Atoka)	15,000	f	30	8.46	5.42	5.16	—	22,000,000
Verden (Springer)	18,000	m	37	7.41	3.78	3.08	—	6,981,000
CRETACEOUS (NORTH-CENTRAL MONTANA)								
Bowdoin dome	1,700	m	29	7.00	2.84	3.23	—	777,438
BAKKEN SHALE (WILLISTON BASIN)								
Antelope (Sanish Pool)	10,500	m	39	—	—	—	3.63	1,119,000
Fairway Area Play	10,500	m	75	—	—	—	4.35	515,000
Intermediate Play	10,500	m	67	—	—	—	2.40	299,000

NOTES: Columns give field or area name (Field), average field depth, ft (Depth), depositional environment of reservoir (Env.), number of wells used to calculate variation coefficients (No.), dimensionless variation coefficient calculated for cumulative production (VC_{cp}), peak yearly production (VC_{pyp}), and peak monthly production (VC_{pmp}) of wells, and the highest cumulative well production in each field or area, thousand cubic feet of gas (Peak well). Only VC_{cp} identified for oil fields. See text for description of variation coefficient. fd, fluvial-deltaic; m, marine; e, estuarine. Dashed lines indicate missing data. Production data for wells taken from Petroleum Information Corporation National Production System on CD-ROM.

for three areas (treated here as fields) of the Mississippian–Devonian Bakken Formation continuous (unconventional) oil accumulation in the Williston basin of North Dakota and Montana (Table 1).

Production data for the wells of these 77 fields were obtained from the Petroleum Information Corporation (PI) National Production System (NPS) (ver. August, 1995) on CD-ROM. The NPS data contain identification, location, completion, and monthly production information by well for many basins in the United States.

Variation coefficients for gas production for each field were calculated for peak monthly production, peak yearly production, and cumulative production (from older wells in which cumulative production was approaching ultimate production) of wells and are listed in Table 1. Variation coefficients for cumulative production of oil are also listed in Table 1.

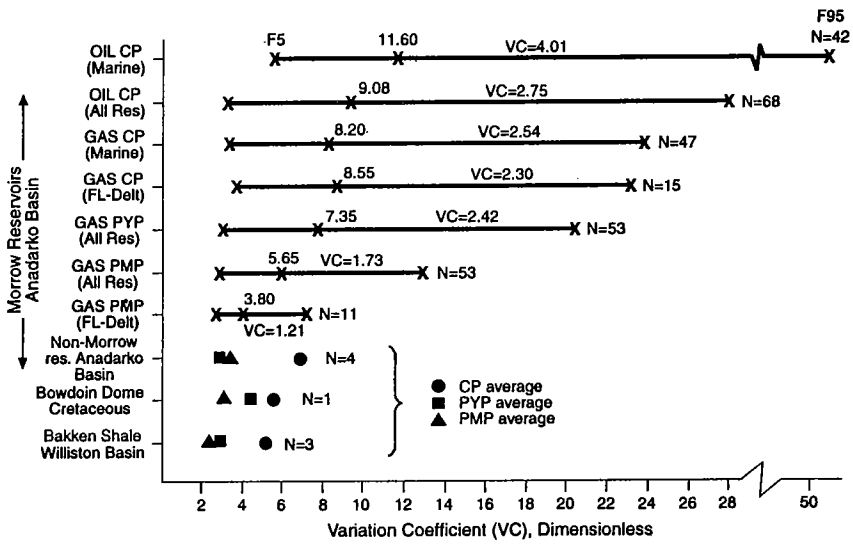

Figure 3. Range and average variation coefficients for cumulative production, peak twelve-month production, and peak monthly production for the fields in this study. For Morrow reservoirs, the two outer X's represent the 5th and 95th percentiles of wells in each data set, and the middle X represents the 50th percentile of wells. For non-Morrow gas fields of the Anadarko basin, Cretaceous fields in Bowdoin dome of north-central Montana, and Bakken fields of the Williston basin, only mean or actual values were plotted because of the limited data points. Data taken from Table 1.

ANALYSIS

The variation coefficients listed in Table 1 change significantly from field to field but are generally consistent within a field. For 44 of the 58 gas fields for which comparisons can be made, VC derived from cumulative production is larger than VC calculated from peak yearly production or peak monthly production. Assuming that cumulative production of older wells is proportional to ultimate production, this relation suggests that heterogeneity associated with the reservoir volume accessed by a well is greater than heterogeneity associated with the plumbing system controlling flow rates to a well. An alternative interpretation is that engineering practices within a field, pipeline capacity, contract constraints, seasonal demand, and other market factors are acting as filters that reduce the variability of flow rates.

Data in Table 1 illustrate that variation coefficients vary widely from field to field. Among the 68 Morrow-reservoir gas fields, for example, VC_{cum} (the cumulative variation coeffecient) for gas ranges from 2.03 to 72.41. Perhaps a sorting of these fields according to some causal geologic variable (e.g., depositional environment of reservoir) would reduce VCs within the subgroups formed, but for the class of Morrow reservoirs as a whole, the degree of well-production heterogeneity varies significantly between fields.

Figure 3 offers a smoothed presentation of the VC data of Table 1 for all reservoirs, thereby making general relations more apparent. For each of the 10 reservoir groupings shown: (1) heterogeneity of cumulative production is significantly greater than the heterogeneity of peak monthly or peak yearly production, and (2) heterogeneity of peak monthly production and peak yearly production are approximately equal for the non-Morrow reservoirs but slightly higher for Morrow reservoirs.

A consistent hierarchy is maintained among the 10 groupings of Figure 3. Regardless of whether cumulative production, peak yearly production, or peak monthly production is considered, Morrow reservoirs of the Anadarko basin are most heterogeneous; and non-Morrow reservoirs of the Anadarko basin, the reservoirs of the Bakken Formation of the Williston basin, and the Bowdoin reservoir of north-central Montana are the least heterogeneous.

The Bakken Formation and the Cretaceous reservoirs of Bowdoin field have extremely low matrix permeability, ranging from less than 0.1 millidarcies (md) to 6 md or more. Production is controlled by fracture systems, whereas Morrow sandstone reservoirs commonly have conventional matrix permeability. The relatively low variation coefficients for the Bakken fields (Fig. 3) suggest that the fracture systems for this reservoir, which might be extremely heterogeneous on the scale of inches, are, in fact, quite homogeneous on the scale of the drainage area of wells. This circumstance was noted also by Stell and Brown (1992), who examined the Bakken Formation along with two fractured chalk reservoirs. Effects such as depositional environment, burial diagenesis, and position of wells within a trap make production from conventional Morrow fields more heterogeneous than that from fractured Bakken shales (Fig. 3).

Figure 3 also illustrates that, for cumulative produc-

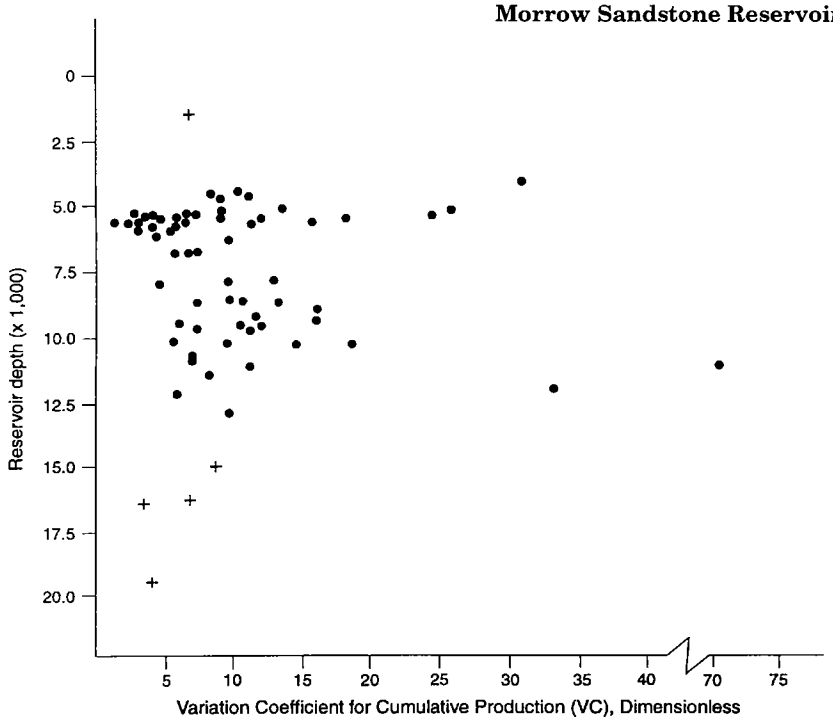

Figure 4. Plot of variation coefficients of cumulative production for 23 fields used in this study vs, depth in feet (Table 1). Dots represent Morrow fields, and plus signs represent non-Morrow fields for which depth data are available.

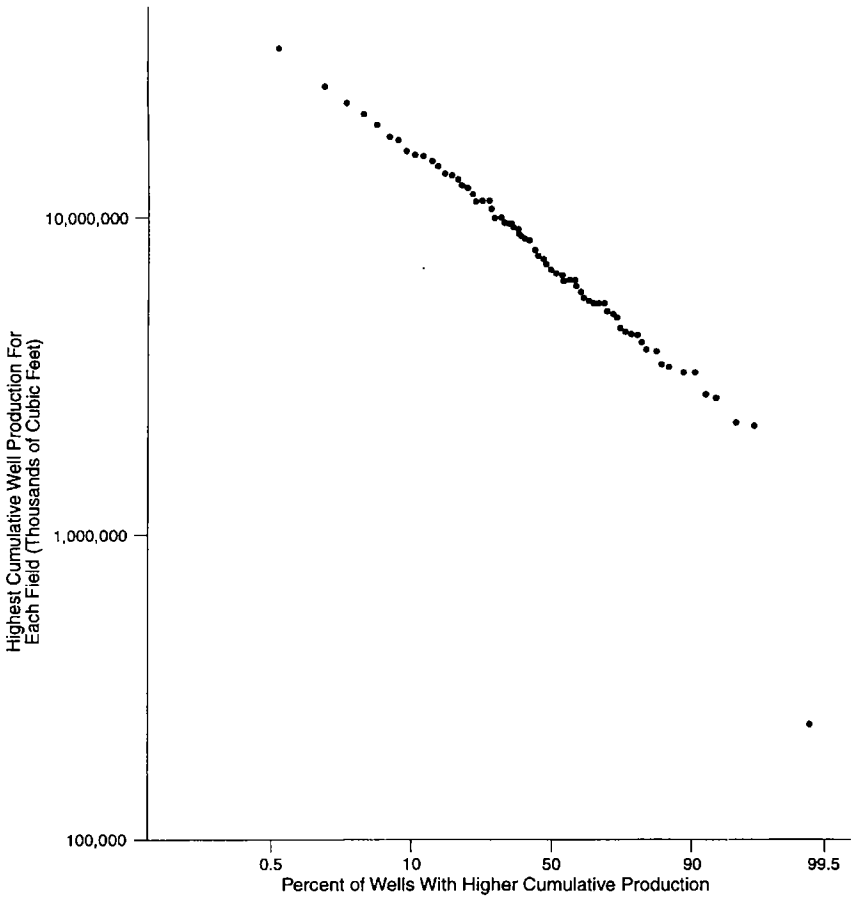

Figure 5. Probability distribution for highest cumulative well production in each of the 67 Morrow gas fields of this study. Data are from "Peak well" column of Table 1. Variation coefficient (VC) of this data set is 2.49.

tion, Morrow oil production is more heterogeneous than Morrow gas production for reservoirs that produce both gas and oil. The greater oil-production heterogeneity may be related to the nature of the fluid characteristics of oil vs. gas (e.g., oil is more viscous and less mobile than gas). For Morrow gas reservoirs, limited variation exists based on differences in depositional environments. The variation coefficient for Morrow marine gas reservoirs is 2.54, whereas the variation coefficient for fluvial-deltaic gas reservoirs is 2.30.

The Morrow fields in this study extend over a depth range of more than 8,000 ft (Table 1). The depth range is much greater when non-Morrow fields are included. As an example of an effort to relate reservoir heterogeneity to a causal variable, variation coefficients of cumulative production for gas are plotted against depth in Figure 4. If the Morrow Elm Grove and Arnett Southeast fields are discounted as outliers (VC_{cum} = 33.01 and 72.41), shallow reservoirs (less than 10,000 ft) are only slightly more variable (mean VC_{cum} = 10.06) than deeper reservoirs (greater than 10,000 ft, mean VC_{cum} = 9.90) based on the 60 Morrow reservoirs in this study for which depth data are available. When the deep non-Morrow fields are added to the average, the deeper reservoirs (greater than 10,000 ft) have a slightly lower mean VC_{cum} (8.79). Figure 4 illustrates that depth exerts limited control on reservoir heterogeneity, at least for the gas fields in this study.

The preceding discussion is focused on the production variability of wells within a field (intra-field), but the concept of the variation coefficient can also be applied to production variability between fields (inter-field), as illustrated by Figure 5. This figure is a probability distribution for the highest cumulative well production in each Morrow gas field of a 67-field group (non-Morrow fields are excluded). The VC of this data set is 2.49. Comparison to Figure 3 shows that, for the fields of this study, the heterogeneity of cumulative well production *between* fields (VC = 2.49) is slightly less than the average heterogeneity of cumulative well production *within* fields (VC = 2.75; Fig. 3).

Figure 6 is a plot of field size (represented here by the number of wells in

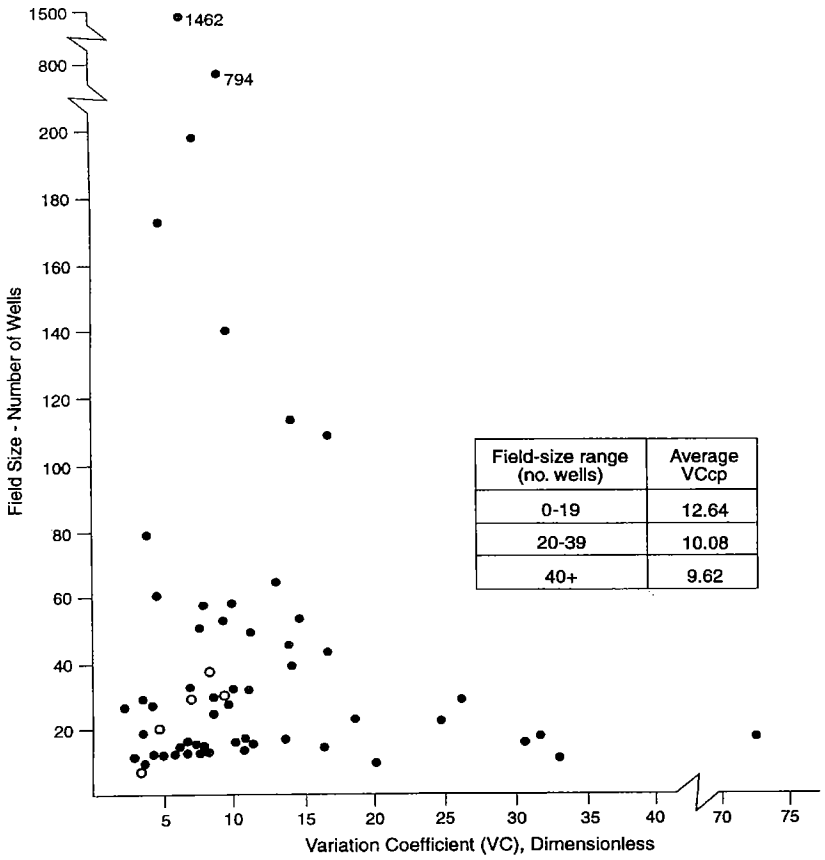

Figure 6. Plot of field size (measured as the number of wells in a field) vs. variation coefficient (VC) for gas fields in this study. Dots represent Morrow fields, and open circles represent non-Morrow fields. Data taken from Table 1.

each field) vs. VC for cumulative production (VC_{cp}) for gas fields. Figure 6 was prepared in order to determine whether small fields in this study are more heterogeneous with respect to production than large fields. A general trend of decreasing heterogeneity with increasing field size can be identified on Figure 6. When VCs are averaged within arbitrary field-size classes (e.g., 0–19, 20–39, and 40 or more wells in each field as shown in Figure 6 using VC_{cp} data from Table 1), a slight decrease in average VC is recognized with increasing field size from 12.64 (0–19 well range) to 9.62 (40 or more wells in field). We cannot yet determine whether this trend occurs for fields in general or why it occurs based on the information available for the fields in this study. An hypothesis for simple domal traps attributes this trend to the "edge effect" along the margins of fields. The ratio of interior wells with good production to wells on the edge of the field with poor production is greater for larger fields than for smaller ones.

APPLICATIONS TO LONG-RANGE FIELD DEVELOPMENT

Reserve growth refers to the typical increases in estimated sizes of fields that occur as oil and gas accumulations are developed and produced. Highly compartmentalized reservoirs tend to have significant reserve growth through time, as formerly isolated rock volumes are accessed by infill drilling. The economic significance of such reserve growth can be enormous. Among conventional fields grouped according to basic geologic similarities, the degree of reservoir compartmentalization might correlate with the degree of heterogeneity as indicated by the variation coefficients discussed here. If so, a ranking of VCs for fields of a group might be interpreted as a ranking of potential for future reserve growth. This hypothesis could be tested by: (1) calculating variation coefficients for conventional fields as of a given time in the past (let us say, 1975, as an example), and (2) comparing these variation coefficients to the actual reserve growth of the fields between 1975 and the present.

Production characteristics of unconventional accumulations such as coalbed gas, oil or gas in shales, and basin-centered gas commonly vary significantly from well to well. Economic advantage accrues to an operator who can develop a predictive model for identifying the better well locations in an unconventional accumulation. However, the benefits of such risk reduction decrease as the level of reservoir heterogeneity decreases. To illustrate this point, consider the end-member case of a very homogeneous unconventional reservoir. In this uniform reservoir, random drilling would yield about the same results as drilling from detailed geologic knowledge obtained at considerable expense. Studies aimed at reducing risk in the development of unconventional accumulations might be best directed towards the most heterogeneous reservoirs. The variation coefficients discussed in this report provide a quantitative screening parameter for identifying the most heterogeneous unconventional reservoirs.

SUMMARY

This study shows that quantitative measures of the variability of production rates and production volumes of wells, expressed as dimensionless variation coefficients, are potentially valuable tools for documenting heterogeneity in conventional and continuous-type reservoirs. Analysis of well-production data in 69 Morrow gas fields indicates that trends in variation coefficients exist that are indicative of *in situ* geologic factors. Masking effects relating to engineering-induced production variability are less likely to affect variation coefficients derived from longer-term measures of well production.

Results of this preliminary study offer sufficient

encouragement to continue examination of production heterogeneities of gas reservoirs. A larger data set needs to be developed, in part because the relative effects upon production heterogeneity of geologic factors vs. engineering factors are not easily separated in the present small data set. A larger data set is also needed for statistical credibility in searching for: (1) correlations between well-production variation coefficients and reservoir lithology, size, depth, depositional environment, diagenetic history, structural style, trap type, age, etc.; (2) methods to differentiate conventional and continuous (unconventional) accumulations using well-production variation coefficients; and (3) analog models based on production heterogeneity that empirically establish classes of reservoirs useful for analysis of exploration risk, exploitation methods, and field growth (reserve appreciation).

A thorough analysis of production heterogeneities in wells and reservoirs may shed light on some important questions including the following. (1) What is the range of variation in production parameters for different reservoirs? (2) Can reservoirs be compared and categorized using measures of production? (3) Can conventional and unconventional continuous-type reservoirs be differentiated using measures of production variability? (4) Can production-variability models be defined which empirically capture effects of lithology, trap type, fracture development, and other geologic factors? (6) Can measures of production variability be used to rank the potential for future reserve growth and as a screening parameter for prioritization of research aimed at risk reduction in the development of unconventional accumulations?

REFERENCES CITED

Brown, R. L.; Parham, K. D.; and Campbell, J. A., 1993, Morrow sandstones—Anadarko basin and Hugoton embayment, Kansas and Oklahoma, *in* Bebout, D. G., White, W. A.; Hentz, T. F.; and Grasmick, M. K. (eds.), Atlas of major Midcontinent gas reservoirs: Gas Research Institute, 85 p. (oversized).

Davis, J. C., 1986, Statistics and data analysis in geology (2nd edition): John Wiley and Sons, New York, 550 p.

Dyman, T. S.; Schmoker, J. W.; and Quinn, J. C., 1996, Reservoir heterogeneity as measured by production characteristics of wells—preliminary observations: U.S. Geological Survey Open-File Report 96-059, 14 p.

Koch, G. S.; and Link, R. F., 1970, Statistical analysis of geological data: John Wiley and Sons, New York, 374 p.

Schmoker, J. W., 1995, Method for assessing continuous-type (unconventional) hydrocarbon accumulations, *in* Gautier, D. L.; Dolton, G. L.; Takahashi, K. L.; and Varnes, K. L. (eds.), 1995 national assessment of United States oil and gas resources—results, methodology, and supporting data: U.S. Geological Survey Digital Data Series DDS-30 [CD-ROM].

_____ 1996, A resource evaluation of the Bakken Formation (Upper Devonian and Lower Mississippian) continuous oil accumulation, Williston basin, North Dakota and Montana: The Mountain Geologist, v. 33, no. 1, p. 1–10.

Stell, J. R.; and Brown, C. A., 1992, Comparison of production from horizontal and vertical wells in the Austin Chalk, Niobrara, and Bakken plays, *in* Schmoker, J. W.; Coalson, E. B.; and Brown, C. A.(eds.), Geological studies relevant to horizontal drilling—examples from western North America: Rocky Mountain Association of Geologists, Denver, p. 67–87.

Depositional Systems and Diagenesis of Slope and Basin Facies, Atoka Formation, Arkoma Basin

T. A. (Mac) McGilvery
Phillips Petroleum Company
Bartlesville, Oklahoma

David. W. Houseknecht
U.S. Geological Survey
Reston, Virginia

ABSTRACT.—Strata of the lower and middle Atoka Formation in the Arkoma basin accumulated in a rapidly evolving foredeep during convergent tectonism associated with Ouachita orogenesis. Marine slope and deep-basin facies reflect tectonic influence on subsidence rates, facies distributions, and sediment-distribution patterns. Sandstones deposited in three distinct settings may be considered as potential objectives for natural-gas exploration activity. Slope channel sandstones were deposited within channel-levee complexes localized above syndepositional normal faults. Marginal submarine fan sandstones were deposited within discrete submarine fans at the base of the slope at points where slope channels debouched onto the basin floor. Sandstones deposited within a regionally extensive, longitudinal-apron complex on the deep floor of the basin represent a variety of turbidite facies that display both westward proximal-to-distal characteristics on a gross scale and randomly interspersed facies on a local scale.

The abundance and distribution of detrital clay minerals exerted significant influences on diagenesis and reservoir quality of Atoka sandstones. Sandstones within slope-channel and marginal submarine-fan deposits tend to be grain-supported and contain variable amounts of dispersed clay emplaced during dewatering. Those that lack dispersed clay have little reservoir potential because porosity was occluded by compaction and quartz cementation. Those with dispersed clay have fair to excellent reservoir potential because porosity was preserved by clay inhibiting quartz cementation and was subsequently enhanced by dissolution of silicate grains. Sandstones within the longitudinal apron complex tend to be matrix-supported. They have little reservoir potential because of low original porosity, destruction of porosity by compaction during shallow burial, and meager enhancement of porosity by grain dissolution during deeper burial.

INTRODUCTION

The Arkoma is one of a series of foreland basins that formed along the North American side of the Ouachita mountain belt during Carboniferous orogenesis. Atokan strata of the basin record a remarkably rapid transition from sedimentation on a marine shelf of a passive continental margin to sedimentation in a foreland basin formed in response to convergent tectonism. Basal Atokan strata were deposited along a tidally swept coastline on a tectonically stable shelf that had prevailed since the Late Cambrian. The remainder of Atokan strata were deposited during the breakdown of that shelf by normal faults, apparently induced by obduction of the Ouachita accretionary prism onto the southern margin of North American continental crust. The resulting wedge of sediment represents progressive filling of the basin by submarine fan, marine slope, and deltaic facies that record the dynamic evolution of tectonic style, sediment-distribution patterns, and sediment composition as the orogenic belt pushed northward onto the continent. By the end of the Atokan, flexural subsidence and deposition of coal-bearing molasse characterized the final phase of foreland-basin development.

This paper summarizes the main depositional facies observed in the lower through middle portion of the Atoka Formation, an interval of strata deposited on the

McGilvery, T. A.; and Houseknecht, D. W., 2000, Depositional systems and diagenesis of slope and basin facies, Atoka Formation, Arkoma basin, *in* Johnson, K. S. (ed.), Marine clastics in the southern Midcontinent, 1997 symposium: Oklahoma Geological Survey Circular 103, p. 129–140.

slope and basin floor of a rapidly and dynamically evolving foreland basin. These strata episodically have been the focus of natural gas exploration activity for several decades, and this emphasis likely will increase in the future as exploration concepts and technologies improve and as industry seeks additional exploration targets in this prolific basin.

GEOLOGIC SETTING

The Ouachita Mountains, extending from central Arkansas into southeastern Oklahoma, represent the largest exposure of an orogenic belt that lies mostly buried beneath Mesozoic and Cenozoic strata of the Gulf coastal plain. The foreland region along the entire length of the Ouachita orogenic belt generally shared a common history of rifted-margin sedimentation during the early through middle Paleozoic followed by foreland basin development induced by convergent tectonism during the late Paleozoic (Flawn and others, 1961; Graham and others, 1975; Thomas, 1985; Meckel and others, 1992). During the final phases of Ouachita orogenesis, the foreland region was segmented into individual structural basins, one of which is the Arkoma.

The Arkoma basin is an arcuate synclinorium that extends from east-central Arkansas to southeastern Oklahoma (Fig. 1). It lies immediately north of the Ouachita orogenic belt, to which it is genetically intimately related. Although the southern margin of the basin is historically defined as the northern edge of the Ouachita frontal thrust belt, Atokan strata exposed in the frontal thrust belt were deposited in continuity with Arkoma basin strata and older Arkoma basin strata extend southward for an unknown distance beneath the thrust belt.

Stratigraphy

Stratigraphy of the Arkoma basin reflects the opening and subsequent closing of a Paleozoic ocean basin. Pre-Atokan strata are composed of mostly shelf carbonates, with subordinate sandstones and shales that accumulated on a passive continental margin following opening of the ocean basin. These strata display gradual thickening to the south. Sediment-accumulation rates were low (average ~7 m/m.y.), sand was derived from the North American craton, and sediment dispersal was mostly southward.

Strata of the Atoka Formation (lower–Middle Pennsylvanian) are mostly shales and sandstones deposited during convergent tectonism that caused breakdown of the precursor shelf and development of the foreland basin. Atoka strata thicken dramatically southward, with abrupt increases in thickness across basement-rooted normal faults that were active during sedimentation (Fig. 2). Sediment accumulation rates were high (average ~1,100 m/m.y.), and sediment entering the basin from both the north and east (see subsequent section) was transported longitudinally westward within the basin.

Post-Atokan strata are shales, sandstones, and coal beds deposited during final phases of foreland-basin sedimentation. These strata thicken to the south but do not display abrupt thickening across normal faults, indicating that syndepositional normal faulting had ceased. Sediment accumulation rates were moderate (average ~250 m/m.y.); sand was mostly derived from the evolving Ouachita orogenic belt to the east and south; and sand dispersal was mostly westward.

Structure

The structural style of the basin reflects rheology and geometry of the stratigraphic units described above, as well as their age relative to major compressional events associated with Ouachita orogenesis. Pre-Atokan shelf strata and the Precambrian granitic basement are mostly deformed by Atokan-aged normal faults. Most of these normal faults dip southward and display displacements of a few hundred meters to more

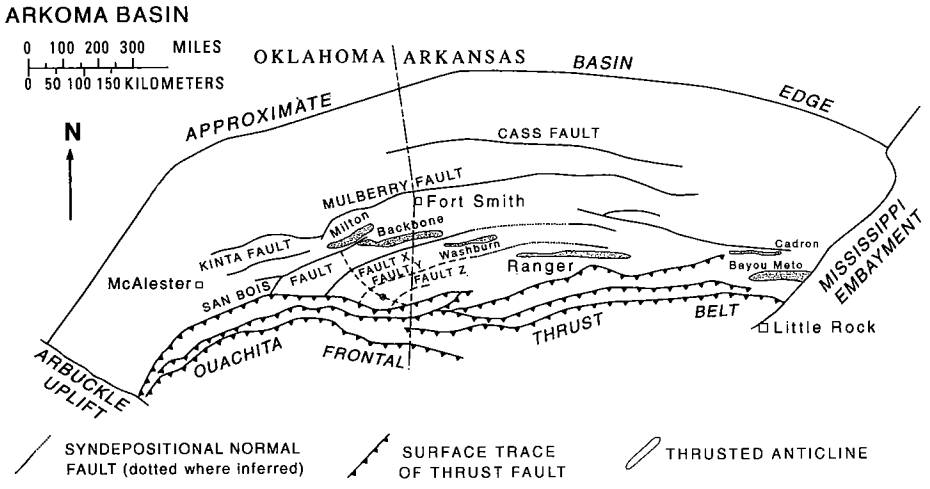

Figure 1. Map of Arkoma basin showing locations of known syndepositional normal faults, main thrust faults in Ouachita frontal zone, anticlines within basin that have Atoka Formation exposures, and stratigraphic cross section (Fig. 2).

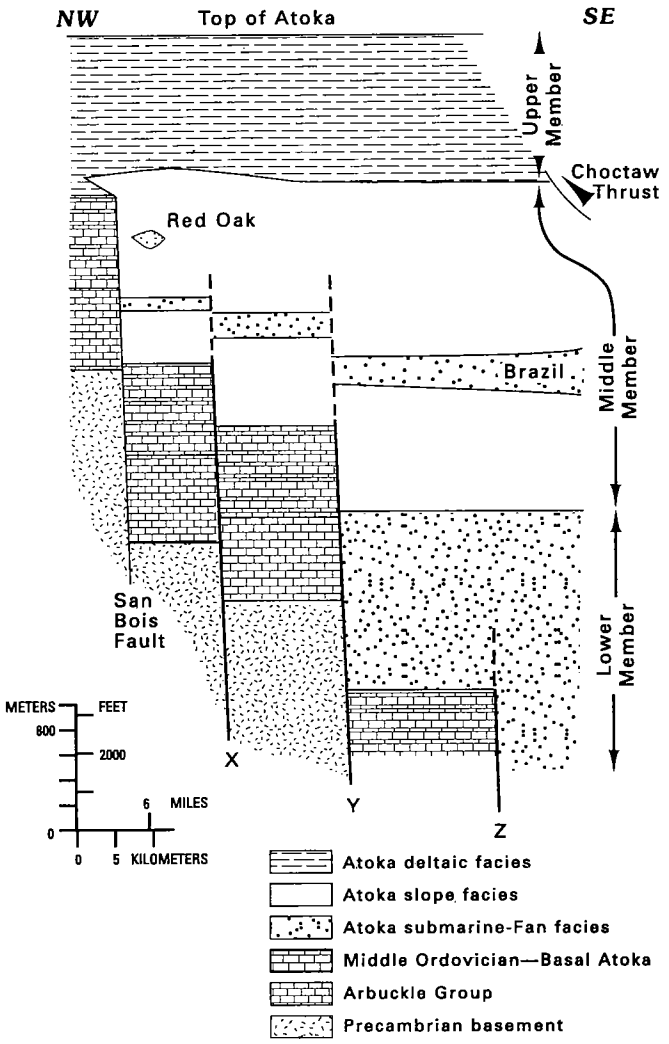

Figure 2. Generalized stratigraphic cross section illustrating stratigraphy and facies distribution relative to syndepositional normal faults. Cross section is based on subsurface data, including wire-line logs and reflection seismic data. Location of cross section shown in Figure 1. Modified from Houseknecht and Ross (1992).

than 4 km, thereby producing the step-like stratigraphic geometry of the Atoka Formation illustrated in Figure 2. All of these Atokan aged normal faults are thought to have formed within a compressional tectonic setting as a result of lithospheric bending into a subduction zone coupled with vertical loading during obduction of the Ouachita orogenic pile onto the edge of North American continental crust (Houseknecht, 1986; Bradley and Kidd, 1991). Some of these normal faults were reactivated as reverse faults during later phases of Ouachita compressional deformation.

The structural style is different above the wedge of shelf strata. In the Arkoma basin proper, Atokan and younger strata are deformed into broad synclines and narrow anticlines whose axes are generally parallel to the Ouachitas. Listric thrust faults underlie much of the folded section and ramp to the surface along the crests of many anticlines. Southward, in the Ouachita frontal thrust belt (Fig. 1), thrust faults increase in number and displacement. Rocks involved in this thrust faulting are mostly Atokan strata that were deposited in deeper portions of the foreland basin and locally include the uppermost strata deposited on the precursor shelf.

ATOKA FORMATION PALEOGEOGRAPHY

The paleogeography of the Arkoma basin evolved rapidly during the Pennsylvanian as the result of tectonic events related to Ouachita orogenesis. Interpretations of the tectonic and paleogeographic history have been presented by several workers (Graham and others, 1975, 1976; Houseknecht and Kacena, 1983; Thomas, 1985; Houseknecht, 1987; Johnson and others, 1988; Meckel and others, 1992; Roberts, 1994). This section summarizes the regional setting during deposition of the lower and middle portions of the Atoka Formation.

Paleotectonic and paleogeographic reconstructions of the Arkoma basin and surrounding region suggest that the basin received sediment from several major dispersal systems during Atokan sedimentation. Detritus entered the basin from the north (Fig. 3), with specific sources of sediment probably including older platform strata exposed around the Ozark and Nemaha uplifts, as well as sedimentary and crystalline rocks of the distant Canadian shield (Hayes, 1963). Sand reaching the Arkoma basin from these mature and/or distant sources was predominately composed of spherical and well-rounded quartz grains like those deposited in the underlying Spiro Sandstone (Houseknecht and McGilvery, 1990; Houseknecht and others, 1993). Within the context of the entire Atoka Formation, this was the volumetrically least important of the three sediment sources, although sand of this provenance may form conspicuously large proportions of the Atoka Formation along the northern rim of the basin (Fig. 3).

Sediment also was funneled southward through the Illinois basin into the eastern Arkoma basin (Fig. 3), and sand associated with that dispersal system also was composed predominately of quartz grains, although small volumes of feldspar and pelitic lithic fragments likely were included during the late Atokan (Potter and Glass, 1958; Houseknecht and others, 1993). The ultimate provenance of this sediment may have included cratonic rocks of the Canadian shield and orogenic rocks of the central and northern Appalachians (Houseknecht and others, 1993). Within the context of the entire Atoka Formation, this sediment source was likely of intermediate volumetric importance, although it may have contributed significantly to depositional systems in the northern half of the Arkoma basin (Fig. 3).

A third dispersal system flowed into the eastern Arkoma basin from the Black Warrior basin in Alabama and Mississippi. It derived sediment from the Ouachita orogenic belt, which already had been uplifted and exposed to erosion along the southwestern margin of the Black Warrior basin (Mack and others,

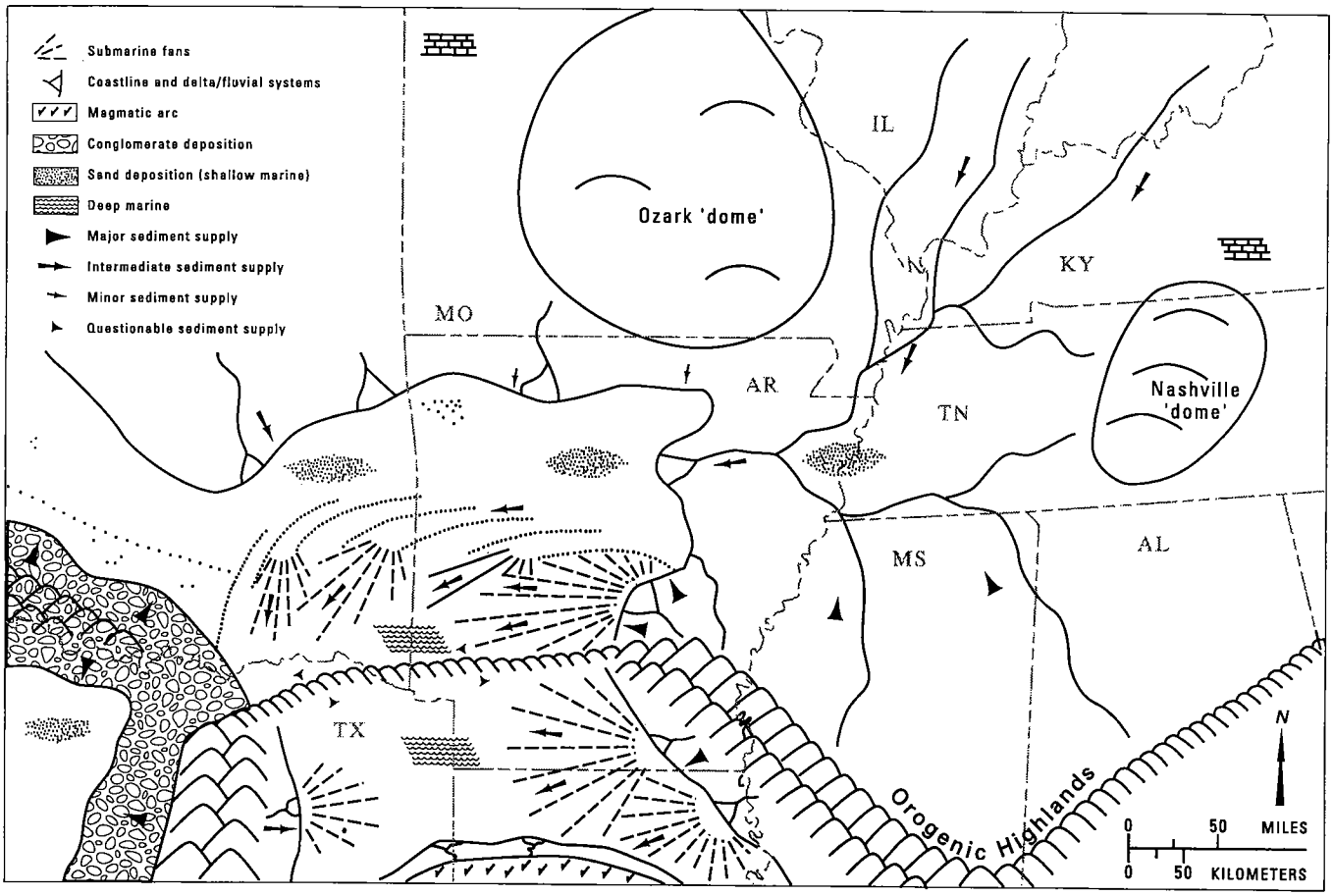

Figure 3. Early–middle Atokan paleogeography of southern Midcontinent. Modified from Houseknecht (1987).

1983), and from the southern Appalachians along the southeastern margin of the Black Warrior basin. Sand derived from the orogenic provenance contains a significant volume of lithic fragments and some feldspar, indicating derivation from metamorphic and volcanic source rocks (Mack and others, 1983; Houseknecht and others, 1993). This sediment source likely was a significant contributor to the Atoka Formation as a whole and probably fed sediment to both the nonmarine through shallow-marine systems in the north and the deep-marine systems in the south.

As suggested by Figure 3, it is likely that sediment from the Illinois basin and Black Warrior basin may have mixed within the sediment-dispersal system in the easternmost Arkoma basin. However, it is significant to note that sediment entering the nonmarine through shallow-marine depositional systems in the easternmost Arkoma basin would have been transported a significant distance and may have spent a significant residence time, probably in fluviatile systems, before reaching sites of deposition in Arkansas and Oklahoma.

The western end of the emerging Ouachita orogenic belt can be considered a fourth sediment-dispersal system during deposition of the Atoka Formation. In contrast to the dispersal system of the Black Warrior basin discussed above, it appears likely that sediment entering the deep marine depositional systems in the easternmost Arkoma–Ouachita basin would have been transported more directly from the emerging Ouachita orogenic highlands with little or no residence time in fluviatile systems (Fig. 3). Evidence in support of this inference includes the immature-textural and -compositional nature of Atoka Formation sandstones in the Ouachitas.

Consideration of basin geometry suggests that the greatest sediment volume would have entered the eastern end of the Arkoma basin (in the area of the Mississippi embayment) and would have been dispersed to other parts of the basin by westward longitudinal transport (Fig. 3). This broad interpretation is supported by paleocurrent data collected by many workers throughout the Arkoma basin and Ouachita frontal thrust belt. The paleogeographic evolution of the middle Atoka succession within this context was characterized by compound, tectonically controlled sediment-dispersal systems.

ATOKA DEEP-WATER DEPOSITIONAL SYSTEMS

There have been significant advances in the understanding and classification of slope/basin-depositional systems in recent years. Improved resolution of seismic

data and side-scan sonar imaging of Pliocene to Holocene systems, such as that of the continental margin of southeast Africa and the Mississippi, Amazon, Rhone, Ebro, and Navy systems, provide detailed analogues for the interpretation of ancient systems (Dingle and Robson, 1985; Droz and Bellaiche, 1985; Normark and Piper, 1985; Damuth and others, 1988; Alonso and others, 1990; Twitchell and others, 1991). Models for deep-water depositional systems have been expanded from the early submarine-fan models of Normark (1978) and Walker (1978) to include the influence of sediment-supply geometry and sediment calibre on system architecture (Heller and Dickinson, 1985; Surlyk, 1987; Nelson and others, 1991; Reading and Richards, 1994; Galloway and Hobday, 1996). Sediment-supply geometry can be defined as point-sourced/canyon-fed, arc-linear/delta-fed, or linear/shelf-fed dispersal (Galloway and Hobday, 1996). Depositional systems influenced by supply geometry include point-sourced submarine fans, delta-fed aprons, and slope-fed aprons (Galloway and Hobday, 1996). Sediment calibre (texture and grain size), classified as mud-rich, mud/sand-rich, sand-rich, and gravel-rich, is a primary control on system morphology in the absence of significant depositional topography. Mud-rich fan systems, such as the Rhone and Mississippi, are generally elongate, exhibit relatively low relief, and range in size from tens of square miles to hundreds of square miles (Droz and Bellaiche, 1985; Twitchell and others, 1991). Sand-rich fan systems, such as the Navy, tend to be radial in geometry, exhibit relatively high relief, and average tens of square miles in size. The primary internal depositional components are effectively controlled by sediment calibre. Channel/levee systems characterize mud-rich sediment dispersal in much the same way as in fluvial systems, whereas low-relief channels lacking well-developed levees and mounded lobe complexes characterize sand-rich dispersal systems.

The middle Atoka succession records clastic deposition in multiple, coeval deep-water systems. The sediment-supply calibre was dominantly mud-rich to sand/mud-rich and feeder system geometry ranged from point-sourced to line-sourced dispersal. The resultant depositional systems included slope-channel/levee complexes, marginal submarine fan systems, and longitudinal-apron complexes (Fig. 4). The evolution and

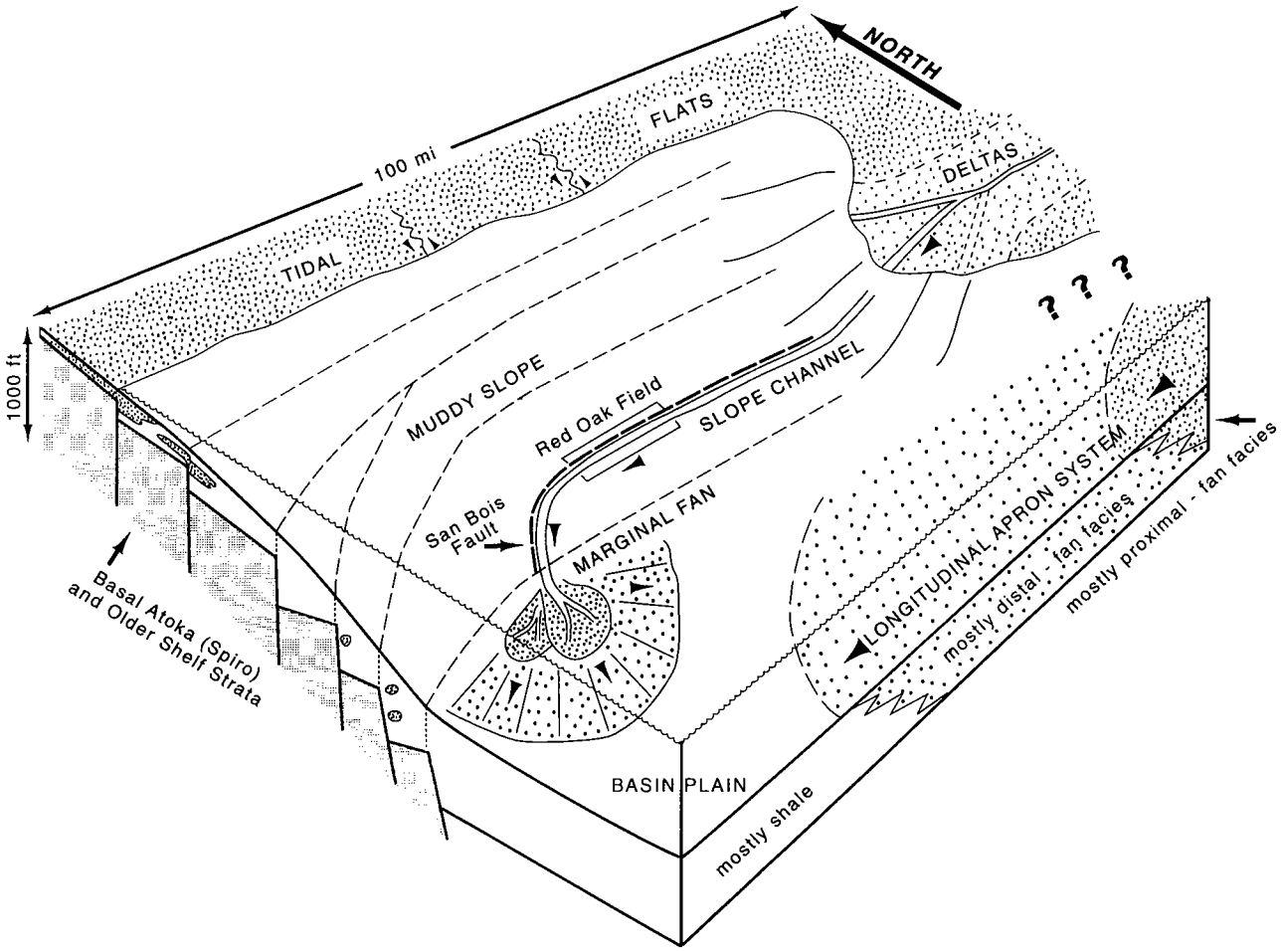

Figure 4. Reconstruction of depositional system in which Atoka facies were deposited. Dash-dot lines represent sea-floor traces of syndepositional normal faults illustrated in Figure 2. The Red Oak sandstone was deposited in the slope-channel complex depicted near the center of the figure. Shaftless arrowheads indicate direction of sediment transport. Vertical and lateral scales approximate. Figure modified from Houseknecht (1986) and Houseknecht and McGilvery (1990).

paleogeographic distribution of these systems were controlled by syndepositional tectonics.

Slope-Channel Systems

In that part of the Arkoma basin where the section thickens significantly across syndepositional faults, the Atoka Formation is composed of dark gray mudstone and numerous localized sandstones. A substantial mud-rich sediment supply combined with flexural down-bending of the northern margin of the basin resulted in the development of a muddy slope depositional setting, which lacked a bathymetrically distinct shelf-slope-rise geometry (Fig. 4). Linear sand bodies and numerous semi-cohesive slump complexes punctuated this slope. Sediment was delivered to the slope through linear to arc-linear feeder systems developed in front of tide-dominated shore-zone and deltaic systems. Despite significant syndepositional displacement along many normal faults, numerous widespread key beds display continuity across the faults, and there is no evidence of erosional truncation of strata upthrown to the faults (Houseknecht, 1986). These relationships imply that the rate of mud deposition kept pace with the rate of subsidence and that the sea floor above the faults displayed little or no relief.

Sand-rich facies within this setting were concentrated in elongate multistoried, channel-levee complexes (Fig. 5), which were focused along the downthrown margins of syndepositional normal faults. Most of the sand bodies that occur in this setting are lenticular (0.5–3 mi wide; 30–150 ft thick) and elongate (several miles to tens of miles long). The movement on some normal faults apparently resulted in a slight depression on the sea floor, which was sufficient to localize sediment gravity flows that entered the slope environment. The flows were erosive into unconsolidated slope muds, thereby channelizing the slope along the sea floor trace of syndepositional faults (Fig. 4). The Red Oak sandstone, the most prolific gas reservoir in the basin, has been interpreted as a slope channel complex (Houseknecht, 1986; Houseknecht and McGilvery, 1990; Houseknecht and Ross, 1992). Gravity-driven depositional processes, inferred from core and outcrop sedimentology, included turbidity flow, fluidized flow, and cohesive flow. In core, the base of each sandstone bed is erosive, either into shale or a somewhat older sandstone bed. The sandstone is uniform in grain size (very fine to fine sand) and sorting (moderately well to well sorted) and displays a limited range of sedimentary structures, with most cores appearing massive (lacking obvious sedimentary structures). Other common structures include diffuse flat laminations and a diverse spectrum of dewatering structures, including dish structures, convolute laminations, diffuse vertical laminations, swirled laminations, and dewatering pipes (Red Oak sandstone core photographs are included in Houseknecht and McGilvery, 1990, and in Houseknecht and Ross, 1992). Silty sandstone displaying parallel laminations occurs along the lateral margins of the channel-fill complexes. These complexes include massive, amalgamated sand bodies and locally

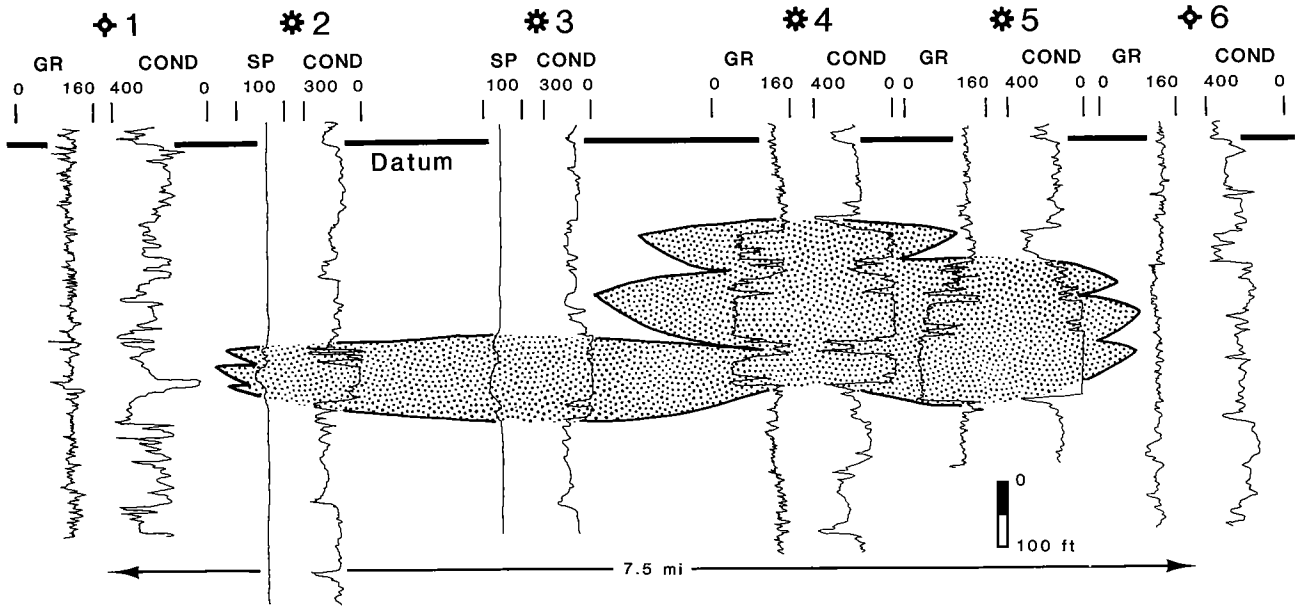

Figure 5. Cross section illustrating lateral facies across Red Oak slope-channel deposit. Cross sectional width of composite channel deposits is exaggerated because line of section is oblique to trend of sandstone body. Key to wells: (1), Slawson #1-2 Ivanhoe (sec. 2, T. 6 N., R. 21 E.); (2), Midwest #1 Gallagher (sec. 13, T. 6 N., R. 21 E.); (3), Midwest #1 Rider (sec. 17, T. 6 N., R. 22 E.); (4), Pan Am #1 Parks Unit-B (sec. 27, T. 6 N., R. 22 E.); (5), Leben Drilling #1-26 Major Realty (sec. 26, T. 6 N., R. 22 E.); (6), Snee & Eberly #1 Askew (sec. 35, T. 6 N., R. 22 E.). Log responses and scales: GR, gamma ray, scale in API Gamma Ray Units; SP, spontaneous potential, scale in millivolts; COND, conductivity, scale in millimhos/m. From Houseknecht and McGilvery (1990).

derived slump complexes consisting of remobilized heterolithic levee facies (Fig. 6).

Atoka sandstones like the Red Oak have long been attributed to deposition in "deep water" because of the predominance of sedimentary structures indicative of sediment gravity-flow mechanisms. As a result, many previous workers have inferred that the syndepositional normal faults acted as fundamental bathymetric features within the depositional basin, with shelfal conditions prevailing upthrown and "deep-water" conditions prevailing downthrown to a major fault (e.g., Vedros and Visher, 1978). This inference does not seem compatible with the continuity of correlative beds across many syndepositional faults and needs to be reevaluated in light of recent work demonstrating that the only requisite for accumulation and preservation of facies deposited by sediment gravity flow mechanisms is water depths below storm wave base (e.g., Walker, 1992). Within a tidally dominated basin like the Arkoma, it is feasible for such deposits to have accumulated in water depths that would not normally be considered "deep." In support of this interpretation, in the area of the Red Oak gas field, inferred esturine and tidal-flat facies occur in the Fanshawe sandstone just 700 ft above Red Oak slope channel facies (Mankowski, 1991). Assuming that neither uplift of the basin nor a significant drop in sea level occurred after deposition of the slope-channel facies and before deposition of the tidal-flat facies, 700 ft is a reasonable estimate for the depth of water in which the Red Oak slope channel sand was deposited.

Marginal Submarine-Fan Complexes

Marginal submarine-fan complexes were developed in the toe-of-slope position (Fig. 4). These are comparable to the limited lobe complexes described by Reading and Richards (1994) in mud-rich systems. The distinction of these marginal fans is that they are point-sourced, at the distal ends of the slope channels, rather than from an associated submarine canyon. Production from marginal submarine-fan facies has been established in the Panola field. Producing components are approximately 3 × 6 mi in size and exhibit lobate external geometries. Log motifs within the field are serrate with crude upward-thickening trends, consistent with fan-lobe complexes (Galloway and Hobday, 1996).

In outcrops along the frontal thrust belt, these facies can be distinguished from those associated with the longitudinal apron complexes (described below) in three ways. (1) The marginal fans are composed of cleaner, grain-supported sandstones (see later discussion). Petrographic analysis reveals that the framework grain composition of sandstones in the two facies is similar, but samples of the apron system contain significantly more matrix and are more poorly sorted than samples of the marginal fan system. (2) Deposits associated with the apron system display paleocurrent indicators that are predominantly west-directed, whereas marginal-fan facies display south to southwestward indicators (Fig. 7). (3) The marginal-fan deposits display internal facies architecture that suggests progradation from north to south. For example, channelized proximal lobe facies (Fig. 7) grade both westward and eastward along the strike of the frontal thrust belt into more distal lobe facies characterized by beds deposited by unconfined sediment gravity flows. The dimensions of such lateral facies sequences are typically 9–15 mi, suggesting the original size of the marginal fans, although recent field development in this facies (e.g., Panola) suggests that economic reservoirs are restricted to the central, more channelized, sand-rich portions of the fan deposits. Abundant evidence for interfingering of marginal and longitudinal apron facies (Fig. 7)

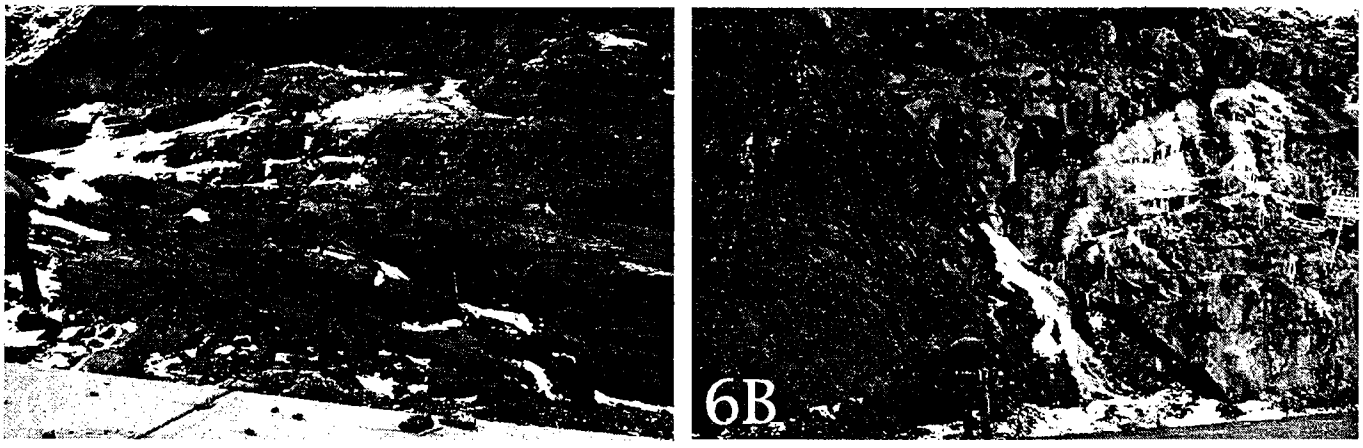

Figure 6. Slope and slope-channel facies in the Atoka Formation exposed at Blue Mountain Dam, Yell County, Arkansas. (A) Laminated and burrowed mudstones, siltstones, and very fine grained sandstones typical of Atoka slope facies. Bedding discordance is inferred to represent a rotational slump within slope facies. Person at left for scale. (B) Slope channel sandstone (right) in erosive contact with slump-contorted deposit of laminated mudstones, siltstones, and very fine grained sandstones (left). The slump-contorted unit may represent slope deposits or slope-channel levee deposits. Person for scale. This exposure is an analogue for productive slope-channel sandstones such as the Red Oak sandstone in Oklahoma.

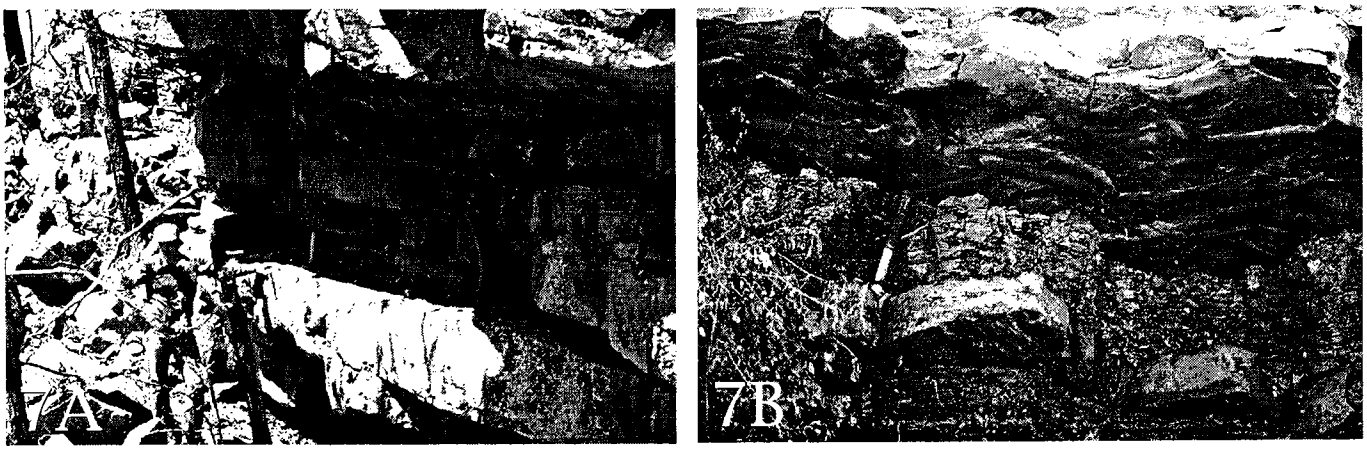

Figure 7. Marginal submarine-fan facies in the Atoka Formation exposed on Blue Mountain, south of Wilburton, Latimer County, Oklahoma. (A) Amalgamated channel deposits near the center of a marginal submarine-fan lobe. Each bed represents a single depositional event, rests erosionally on underlying bed, and internally displays abundant dewatering structures similar to those observed in cores of slope channel facies of the Red Oak sandstone. Person at left for scale. (B) Two thin turbidites and interbedded shale. The lower turbidite (just below hammer head) is interpreted as part of the lateral fringe of the marginal submarine fan the channelized facies of which are shown in A. This bed displays a grain-supported fabric and south-directed sole marks; it is inferred that the sand was transported through a slope channel from the north and deposited on a marginal fan such as the one shown in Figure 4. The sandstone bed above the hammer handle is interpreted to be part of the longitudinal apron system. It displays a matrix-supported fabric, poorer sorting than the underlying bed, and west-directed sole marks.

suggests that the two systems evolved simultaneously but were fed by different sediment-dispersal systems.

Longitudinal-Apron Complexes

The foredeep portion of the Arkoma basin was the site of an evolving longitudinal apron complex. This succession has been described previously as an "axial fan system" (Houseknecht, 1986, 1987; Houseknecht and McGilvery, 1990), which implies a single canyon-fed, point-source for sediment dispersal (Galloway and Hobday, 1996). The authors now define this as an "apron complex" in acknowledgment of multiple dispersal systems supplying sediment to this basinal setting (Fig. 3). The primary sediment input was from the eastern and southeastern margin of the basin, with a predominantly longitudinal dispersal vector driven by sediment influx and progressive closure of the basin. This is supported by paleocurrent measurements and a regional westward-thinning and -fining trend, which reflects a geographically proximal to distal transition within the apron (Fig. 8). However, the proximal-to-distal transition is not meant to imply an inner lobe to outer lobe transect within a single submarine fan. In addition to the lack of a single point-source, bedding architecture is not systematically organized such as that typical of submarine fans (Walker, 1978). In outcrop, large-scale slump and debris-flow deposits are randomly interspersed with thin to thick sandstones deposited as turbidity, grain flow, or fluidized flow units. Locally organized successions 10–50 ft in thickness reflect individual channel or lobe depositional events. Stratigraphic successions greater than 1,000 ft in thickness observed on wire-line logs and in outcrop are dominated by event stratification, which is consistent with multiple, coeval sediment-dispersal systems (Heller and Dickinson, 1985; Galloway and Hobday, 1996). The scale of these complexes (tens to hundreds of square miles) is consistent with mud- to mud/sand-rich systems (Reading and Richards, 1994).

SANDSTONE DIAGENESIS AND RESERVOIR QUALITY

The sediment-dispersal and -depositional systems described in preceding sections exerted significant influences on petrology and reservoir quality of sandstones within the lower and middle Atoka Formation. These linkages between depositional processes and reservoir quality have been documented by Houseknecht and Ross (1992), and this section summarizes the important relationships that may be useful for anticipating reservoir quality.

Clay minerals are the key to understanding reservoir quality in Atoka sandstones deposited in slope and deep-water environments. Although Houseknecht and Ross (1992) recognized five modes of clay mineral occurrence in Atoka sandstones, two modes comprising detrital clay emplaced during or immediately following deposition were recognized as most influential on diagenesis and reservoir quality. (1) "Depositional matrix" in the Atoka Formation comprises a heterogeneous mixture of illitic clays, chlorite, and silt-sized quartz and feldspar grains that results in a matrix-supported fabric. It is mostly detrital in origin and probably was emplaced as part of the depositional medium in sandy debris flows. (2) "Dispersed clay minerals" are mixtures of illitic clays and chlorite that form grain coatings, bridges between grains, and consolidation laminations (concentrations of clay minerals, or-

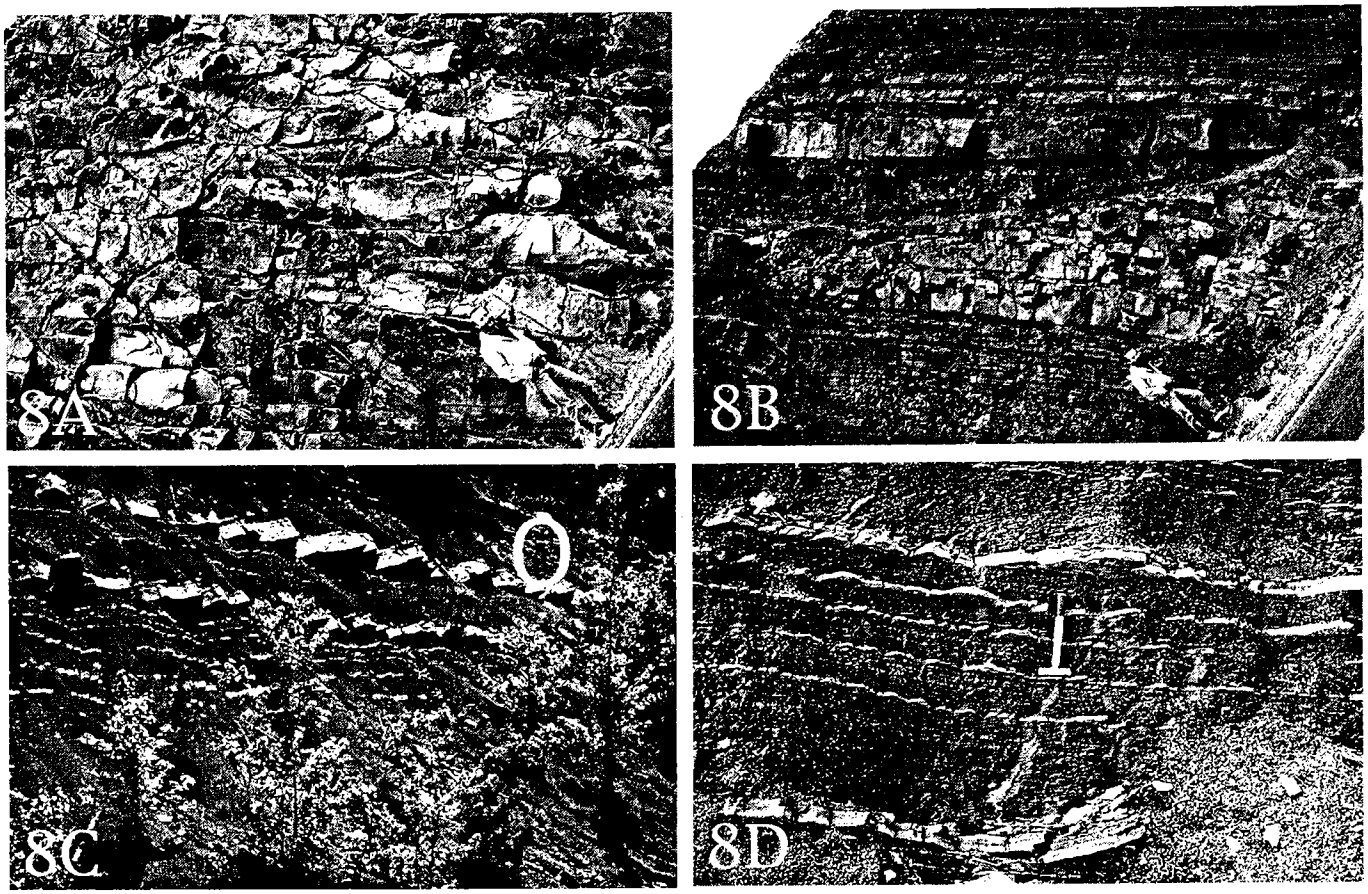

Figure 8. Proximal (A and B) and distal (C and D) facies of the Atoka longitudinal apron system. (A) Thick, amalgamated channel deposits exposed along Bayo Meto anticline, Pulaski County, Arkansas. Each depositional unit is 1–2 m thick and rests erosionally on underlying unit. Camera was rotated so that bedding is parallel to photo frame. (B) Thin-bedded submarine-fan lobe deposits above and below channelized facies, including a mud-filled channel. Same outcrop as A. (C) Mud-dominated distal deposits of the Atoka longitudinal-apron system, near axis of Spring Mountain syncline, McCurtain County, Oklahoma. Sandstone beds all display partial Bouma sequences but collectively do not define systematic lobe-aggradation patterns. Person in upper right for scale. (D) Mud-dominated, distal deposits of the Atoka longitudinal-apron system on Blue Mountain south of Wilburton, Latimer County, Oklahoma.

ganic particles, and other grains resulting from dewatering during sediment consolidation). They are most abundant in samples that display secondary sedimentary structures, and are inferred to represent detrital clays emplaced during turbidite dewatering.

The evolution of reservoir quality in Atoka sandstones was influenced primarily by the abundance and distribution of clay minerals, which are summarized schematically in Figure 9. The presence or absence of depositional matrix fundamentally influenced the subsequent diagenesis and reservoir quality of Atoka sandstones. Sandstones that contain abundant depositional matrix (Fig. 9, right branch) display matrix-supported fabrics and relatively poor sorting. Initial porosity was probably low (25–30%), and primary porosity and permeability likely were reduced substantially by mechanical compaction during shallow burial (Fig. 9). This reduction of porosity and permeability apparently inhibited diagenetic reactions during deeper burial because these sandstones display evidence of a rather subdued diagenetic history relative to those discussed below. Matrix-supported sandstones have poor reservoir potential because original porosity was relatively low, porosity was reduced by compaction during shallow burial, and subsequent diagenesis did not effectively enhance porosity (Fig. 9).

Sandstones that contain little or no depositional matrix display grain-supported fabrics and relatively good sorting. In these sandstones, diagenesis and evolution of reservoir quality were influenced by the abundance and distribution of dispersed clay minerals emplaced by dewatering. Sandstones that lack dispersed clay (Fig. 9, left branch) display evidence of a simple diagenetic history in which most original porosity (35–40%) was occluded by compaction and quartz cementation, resulting in less than 5% porosity. Although these sandstones were subjected to additional diagenesis during deeper burial, they generally contain insufficient porosity to be economic reservoirs.

Grain-supported sandstones that contain dispersed

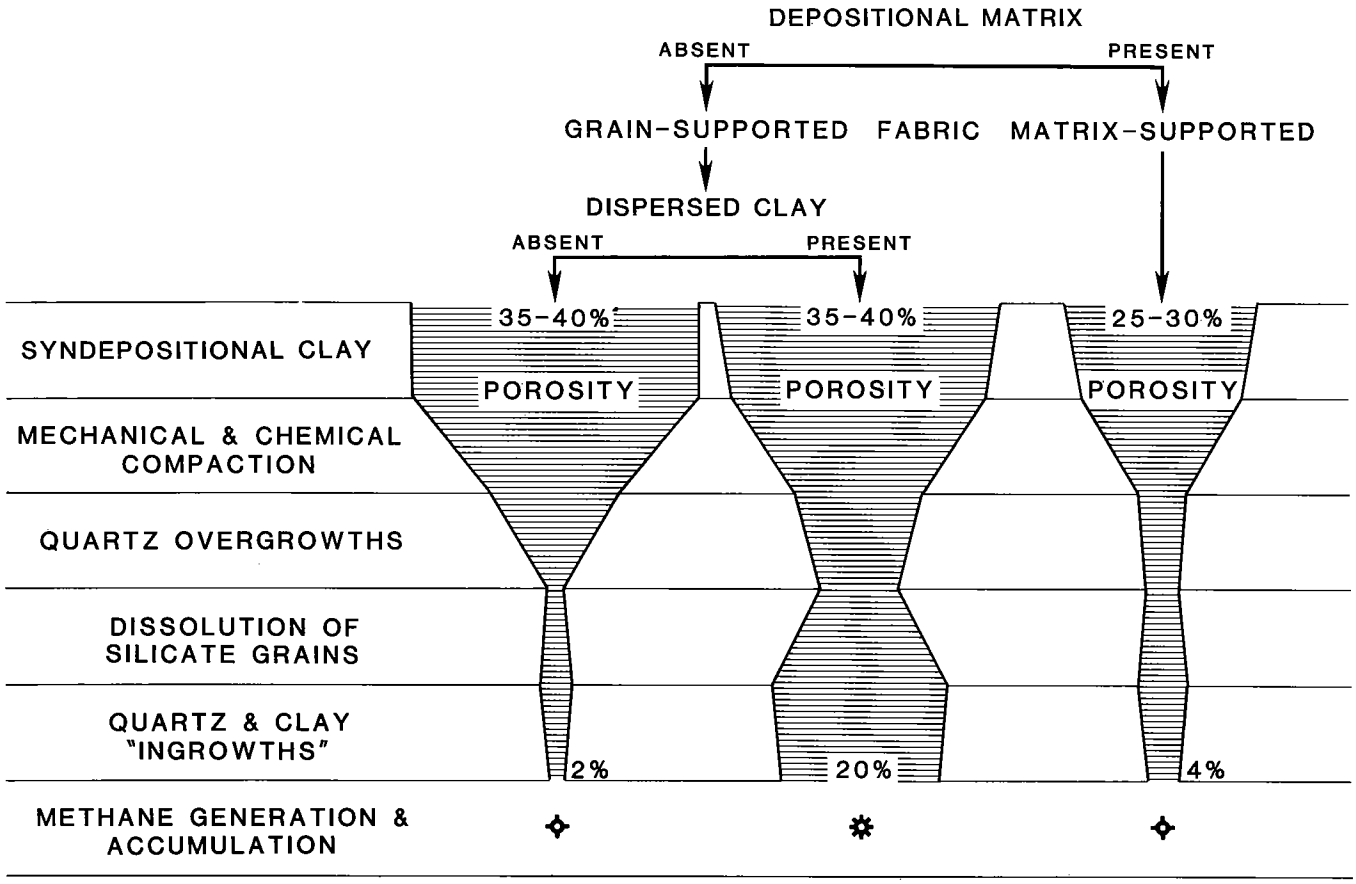

Figure 9. Summary of paragenesis of Atoka Formation slope and deep-water sandstones. Paragenesis of three end members of clay content are illustrated—samples with grain-supported fabrics that contain little or no dispersed clay (left branch); samples with grain-supported fabrics that contain dispersed clay (middle branch); and samples with matrix-supported fabrics that contain abundant depositional clay (right branch). Diagenetic events are listed at left in general sequence of occurrence (although there was some overlap in timing), and width of striped areas depicts average porosity. Following one branch downward depicts evolution of sandstone porosity through time as burial depth increased. From Houseknecht and Ross (1992).

clay (Fig. 9, middle branch) display evidence of a more complex diagenetic history. Although original porosity (35–40%) was reduced by compaction during shallow burial, subsequent quartz cementation was inhibited by abundant clay coatings on detrital quartz grains. Therefore, these sandstones retained good porosity, which was enhanced during deeper burial by widespread dissolution of silicate grains (feldspars and lithic fragments). Even though some porosity reduction occurred subsequently as the result of quartz and clay precipitation ("ingrowths" into pores resulting from silicate grain dissolution), these sandstones generally retain good porosity and represent the best reservoir quality among all Atoka slope and submarine-fan facies.

CONCLUSIONS

The Atoka Formation in the Arkoma basin accumulated in a dynamically evolving foredeep developed in response to convergent tectonism (Ouachita orogenesis). Detrital sediment delivered to the basin from multiple dispersal systems mostly entered the eastern end of the basin and was transported longitudinally westward.

The northern half of the basin was characterized by a delta-fed marine slope system that included slope channels localized above syndepositional normal faults. These slope channels, in turn, fed sediment to marginal submarine fans that accumulated at the base of the slope. The southern half of the basin was characterized by a longitudinal-apron complex, comprising debris-flow, turbidite, and basin-plain deposits. The deep-water deposits display a westward proximal-to-distal facies transition on a gross scale. However, proximal and distal facies interspersed on a local scale probably reflect the multiple dispersal systems that fed sediment to the apron complex.

Sediment dispersal patterns and depositional processes primarily influenced the abundance and distribution of clay minerals in Atoka sandstones. Sands deposited in the northern half of the basin, both in slope-channel and marginal submarine-fan systems, were part of a long-distance, long-residence time sediment-dispersal system that favored the introduction into slope and basin environments of turbidity currents

(as opposed to debris flows; Middleton and Hampton, 1976). The result is a predominance of sandstones that display grain-supported fabrics. Within these sandstones, the abundance and distribution of detrital clays were controlled by the amount and intensity of dewatering. Reservoir potential in these sandstones varies from poor to excellent, depending on the amount and distribution of dispersed clays emplaced by dewatering and on subsequent diagenesis.

Sands deposited in the southern half of the basin (deep Arkoma–Ouachita basin) were mostly part of a short-distance, short residence-time sediment-dispersal system that favored the introduction into slope and basin environments of debris flows composed of a more heterogeneous mixture of sand and clay. The result is a predominance of sandstones that display matrix-supported fabrics. Reservoir potential in these sandstones is generally poor.

REFERENCES CITED

Alonso, B.; Gardner, M. E.; and Maldanado, A., 1990, Sedimentary evolution of the Pliocene and Pleistocene Ebro margin, northeastern Spain: Marine Geology, v. 95, p. 313–331.

Bradley, D. C.; and Kidd, W. S. F., 1991, Flexural extension of the upper continental crust in collisional foredeeps: Geological Society of America Bulletin, v. 103, p. 1416–1438.

Damuth, J. E.; Flood, R. D.; Kowsmann, R. O.; Belderson, R. H.; and Gorini, M. A., 1988, Anatomy and growth pattern of Amazon deep-sea fan as revealed by long-range side-scan sonar (GLORIA) and high resolution seismic studies: American Association of Petroleum Geologists Bulletin, v. 72, p. 885–911.

Dingle, R. V.; and Robson, S., 1985, Slumps, canyons, and related features on the continental margin off East London, southeast Africa (southwest Indian Ocean): Marine Geology, v. 67, p. 37–54.

Droz, L.; and Bellaiche, G., 1985, Rhone deep-sea fan: morphostructure and growth pattern: American Association of Petroleum Geologists Bulletin, v. 69, p. 460–479.

Flawn, P. T.; Goldstein, A., Jr.; King, P. B.; and Weaver, C. E., 1961, The Ouachita System: University of Texas, Austin, Bureau of Economic Geology Publication 6120, 401 p.

Galloway, W. E.; and Hobday, D. K., 1996, Terrigenous clastic depositional systems [2nd edition]: Springer–Verlag, New York, 489 p.

Graham, S. A.; Dickinson, W. R.; and Ingersoll, R. V., 1975, Himalayan-Bengal model for flysch dispersal in the Appalachian-Ouachita system: Geological Society of America Bulletin, v. 86, p. 273–286.

Graham, S. A.; Ingersoll, R. V.; and Dickinson, W. R., 1976, Common provenance for lithic grains in Carboniferous sandstones from the Ouachita Mountains and Black Warrior basin: Journal of Sedimentary Petrology, v. 46, p. 620–632.

Hayes, M. O., 1963, Petrology of Krebs Subgroup (Pennsylvanian, Desmoinesian) of western Missouri: American Association of Petroleum Geologists Bulletin, v. 47, p. 1537–1551.

Heller, P. L.; and Dickinson, W. R., 1985, Submarine ramp facies model for delta-fed, sand-rich turbidite systems: American Association of Petroleum Geologists Bulletin, v. 69, p. 960–976.

Houseknecht, D. W., 1986, Evolution from passive margin to foreland basin: the Atoka Formation of the Arkoma basin, south-central U.S.A., *in* Allen, P. A.; and Homewood, P. (eds.) Foreland basins: International Association of Sedimentologists Special Publication 8, p. 327–345.

_____ 1987, The Atoka Formation of the Arkoma basin: Tectonics, sedimentology, thermal maturity, sandstone petrology: Tulsa Geological Society, Short Course Notes, 72 p.

Houseknecht, D. W.; and Kacena, J. A., 1983, Tectonic and sedimentary evolution of the Arkoma foreland basin, *in* Houseknecht, D.W. (ed.), Tectonic-sedimentary evolution of the Arkoma basin: Society of Economic Paleontologists and Mineralogists Midcontinent Section, v. 1, p. 3–33.

Houseknecht, D. W.; and McGilvery, T. A., 1990, Red Oak field, *in* Beaumont, E. A.; and Foster, N. H. (eds.), Structural traps II; traps associated with tectonic faulting; treatise of petroleum geology atlas of oil and gas fields: American Association of Petroleum Geologists, Tulsa, p. 201–225.

Houseknecht, D. W.; and Ross, L. M., 1992, Clay minerals in Atokan deep water sandstone facies, Arkoma basin: origins and influence on diagenesis and reservoir quality, *in* Houseknecht, D. W.; and Pittman E. D. (eds.), Origin, diagenesis, and petrophysics of clay minerals in sandstones: Society of Economic Paleontologists and Mineralogists Special Publication 47, p. 227–240.

Houseknecht, D.; Wood, G.; Jaques R.; and Gresham A., 1993, Influence of Ozark uplift on Pennsylvanian sediment dispersal patterns: Geological Society of America, Abstracts with Programs, v. 25, no. 3, p. 26–27.

Johnson, K. S.; Amsden, T. W.; Denison, R. E.; Dutton, S. P.; Goldstein, A. G.; Rascoe, B., Jr.; Sutherland, P. K.; and Thompson, D. M., 1988, Southern Midcontinent region, *in* Sloss, L. L. (ed.), Sedimentary cover—North American craton: Geological Society of America, Boulder, Colorado, The Geology of North America, v. D-2, p. 307–359.

Mack, G. H.; Thomas, W. A.; and Horsey, C. A., 1983, Composition of Carboniferous sandstones and tectonic framework of southern Appalachian-Ouachita orogen: Journal of Sedimentary Petrology, v. 53, p. 931–946.

Mankowski, M., 1991, Depositional and diagenetic controls of reservoir quality, Fanshawe sandstone, Red Oak gas field, Oklahoma: University of Missouri, Columbia, unpublished M.S. thesis, 95 p.

Meckel, L. D.; Smith, D. G.; and Wells, L. A., 1992, Ouachita foredeep basins; regional paleogeography and habitat of hydrocarbons, *in* MacQueen, R. W.; and Leckie, D. A. (eds.), Foreland basins and fold belts: American Association of Petroleum Geologists Memoir 55, p. 427–444.

Middleton, G.; and Hampton, M., 1976, Subaqueous sediment transport and deposition by sediment gravity flows, *in* Stanley D.; and Swift, D. (eds.), Marine sediment transport and environmental management: Wiley, New York, p. 197–218.

Nelson, C. H.; Maldonado, A.; Barber, J. H., Jr.; and Alonso, B., 1991, Modern sand-rich and mud-rich siliciclastic aprons: alternative base-of-slope turbidite systems to

submarine fans, *in* Weimer, P.; and Link, M. H. (eds.), Seismic facies and sedimentary processes of submarine fans and turbidite systems: Springer-Verlag, New York, p. 171–190.

Normark, W. R., 1978, Fan valleys, channels and depositional lobes on modern submarine fans: characters for recognition of sandy turbidite environments: American Association of Petroleum Geologists Bulletin, v. 62, p. 912–931.

Normark, W. R.; and Piper, D. J. W., 1985, Navy fan, Pacific Ocean, *in* Bouma, A. H.; Normark, W. R.; and Barnes, N. E. (eds.), Submarine fans and related turbidite systems: Springer-Verlag, New York, p. 87–94.

Potter, P. E.; and Glass, H. D., 1958, Petrology and sedimentation of the Pennsylvanian sediments in southern Illinois—a vertical profile: Illinois Geological Survey R.I. 204, 60 p.

Reading, H. G.; and Richards, M., 1994, Turbidite systems in deep-water basin margins classified by grain size and feeder system: American Association of Petroleum Geologists Bulletin, v. 78, p. 792–822.

Roberts, M. T., 1994, Geologic relations along a regional cross section from Spavinaw to Broken Bow, eastern Oklahoma, *in* Suneson, N. H.; and Hemish, L.A. (eds.), Geology and resources of the eastern Ouachita Mountains frontal belt and southeastern Arkoma basin, Oklahoma: Oklahoma Geological Survey Guidebook 29, p. 137–159.

Surlyk, F., 1987, Slope and deep shelf gully sandstones, Upper Jurassic, East Greenland: American Association of Petroleum Geologists Bulletin, v. 71, 464–475.

Thomas, W. A., 1985, The Appalachian–Ouachita connection: Paleozoic orogenic belt at the southern margin of North America: Annual Review Earth Planetary Science, v. 13, p. 175–199.

Twitchell, D. C.; Kenyon, D. C.; Parson, L. M.; and McGregor, B. A., 1991, Depositional patterns of the Mississippi Fan surface: evidence from GLORIA II and high-resolution seismic profiles, *in* Weimer, P.; and Link, M. H. (eds.), Seismic facies and sedimentary processes of submarine fans and turbidite systems: Springer-Verlag, New York, p. 349–363.

Vedros, S. G.; and Visher, G. S., 1978, The Red Oak sandstone: a hydrocarbon-producing submarine fan deposit, *in* Stanley, D.; and Kelling, G. (eds.), Sedimentation in submarine canyons, fans, and trenches: Dowden, Hutchinson, and Ross, Stroudsburg, Pennsylvania, p. 292–308.

Walker, R. G., 1978, Deep water sandstone facies and ancient submarine fans: models for exploration for stratigraphic traps: American Association of Petroleum Geologists Bulletin, v. 62, p. 932–966.

_____ 1992, Turbidites and submarine fans, *in* Walker, R. G.; and James, N. P. (eds.), Facies models; response to sea level change: Geological Association of Canada, p. 239–263.

Influence of Initial Calcite Grains and Diagenesis on Porosity Development in Spiro Sandstone of South Haleyville, South Hartshorne, and South Panola Fields, Pittsburg and Latimer Counties, Oklahoma

James M. Forgotson, Jr., and Huaibo Liu
University of Oklahoma
Norman, Oklahoma

Harvey Blatt
Hebrew University of Jerusalem
Jerusalem, Israel

Neil H. Suneson
Oklahoma Geological Survey
Norman, Oklahoma

W. Philip Schreiner
Texaco
Denver, Colorado

ABSTRACT.—The Spiro sandstone, and the underlying Foster unit are composed of sandstone, limestone, shale, and chert in the South Haleyville, South Hartshorne, and South Panola gas fields, southeastern Oklahoma. Based on the relative amounts of depositional carbonate grains, the gas-producing reservoir sandstones can be divided into three main sublithofacies that strongly controlled the diagenesis and porosity evolution: (1) carbonate-grain–poor sandstone, (2) carbonate-grain–bearing sandstone, and (3) carbonate-grain–rich sandstone.

Petrology, geochemistry, and fluid-inclusion thermometry indicate that the Spiro and Foster sandstones have undergone five stages of diagenetic alteration: (1) early compaction and quartz cementation, (2) calcite cementation, (3) calcite dissolution, (4) ferroan-dolomite and ankerite precipitation, and (5) pyrobitumen emplacement and later quartz cementation. Three diagenetic events (compaction, cementation, and dissolution) significantly influenced reservoir quality. In response to these diagenetic events, the carbonate-grain–poor sandstone has undergone chlorite and quartz cementation that variably reduced the amount of initial interparticle porosity. Calcite cementation and dissolution have created significant secondary porosity in the carbonate-grain-bearing sandstone. The carbonate-grain–rich sandstones have been tightly compacted and calcite cemented and did not develop significant solution porosity.

Six kinds of cements—chlorite, quartz, calcite, ferroan-dolomite, ankerite, and bitumen—are recognized within the reservoir rocks. The homogenization and melt temperatures (homogenized at 71°C to 140°C and first melted at –32°C to –22°C and finally melted at –9°C to –5°C) of the two-phase fluid inclusions within the calcite cement indicate that it formed in a NaCl-H_2O system with 10–20 wt% of NaCl equivalence at 5,000–6,000 ft (1,500–1,800 m) depth of burial. The ferroan dolomite and ankerite cements precipitated in a NaCl-$MgCl_2$-H_2O system with a 20–30% concentration of NaCl equivalence and at a depth of 8,200–9,800 ft (2,500–3,000 m). The later overgrowth quartz was formed at a depth of 12,500 ft (3,800 m) or deeper.

Forgotson, J. M., Jr.; Liu, Huaibo; Blatt, Harvey; Suneson, N. H.; and Schreiner, W. P., 2000, Influence of initial calcite grains and diagenesis on porosity development in Spiro sandstone of South Haleyville, South Hartshorne, and South Panola fields, Pittsburg and Latimer Counties, Oklahoma, *in* Johnson, K. S. (ed.), Marine clastics in the southern Midcontinent, 1997 symposium: Oklahoma Geological Survey Circular 103, p. 141–155.

INTRODUCTION

The Spiro and Foster sandstones are well-known gas reservoirs in the Arkoma basin and along the thrust-faulted trend at the basin's southern margin. Many papers on the stratigraphy and sedimentation of these sandstones have been published (Grayson, 1980; Frost, 1983; Hinde, 1990; Suneson and Campbell, 1990), but only a few authors discussed diagenesis and the evolution of porosity. Pittman and Lumsden (1968) and Lumsden and others (1971) described the cementation and noted that chlorite coatings retarded pressure solution and quartz overgrowth. Pittman (1972) illustrated pressure solution and quartz overgrowth from some Spiro sandstone samples using scanning electron microscopy. Houseknecht and McGilvery (1991) gave a summary description of the Red Oak gas field to the east of this study area, and Gross and others (1995) described the gas reservoirs.

Gas-production rates and cumulative volumes indicate that the Spiro and Foster sandstones have good but highly variable reservoir quality that is closely related to their lithological characteristics in the fields studied. The purpose of this paper is to present the results of sedimentological, petrological, and geochemical studies of sedimentary facies and diagenesis to determine the factors controlling porosity of the Spiro and Foster reservoirs within the study area.

Location and Geological Background

The study area includes the South Haleyville gas field, the western part of the South Hartshorne gas field located in T. 3 N.–T. 4 N., R. 16 E.–R. 17 E., Pittsburg County, and the South Panola gas field, located in T. 5 N., R. 19 E., Latimer County, Oklahoma (Fig. 1). In the Ouachita frontal belt, the lower part of the Pennsylvanian section includes, from bottom to top, the Wapanucka, Atoka, and Hartshorne Formations (Grayson, 1980; Frost, 1983; Houseknecht, 1986). The Foster and Spiro were considered to be the upper part of the Wapanucka Formation by Hendricks and others (1947), Grayson (1980), and Frost (1983). Based on subsurface studies, the Spiro was assigned to the bottom of the Atoka Formation by Lumsden and others (1971), Houseknecht and MacGilvery (1991), and Gross and others (1995). Gross and others (1995) further divided the interval between the top of the Wapanucka limestone and lower Atoka shale into a sub-Spiro shale member and a Spiro sandstone member. In the South Haleyville and South Hartshorne fields, the Spiro sandstone consists of about equal amounts of sandstone and limestone. The sandstone and shale sequence that occurs between the Spiro and the Wapanucka is equivalent to the Foster in the South Panola gas field.

Data Collection and Analyses

Conventional cores from the Garrett B-1 and Jennings 24-1A wells, sidewall cores from the Dromgold 35-1 well, and cuttings from three other wells were used in this study (Fig. 1). In addition to these subsurface materials, samples were collected from five Spiro outcrops, and four other outcrops were examined along the western part of the Ouachita frontal belt. Thin sections were made from the cores, drill cuttings, and outcrop samples. All of the thin sections were examined using a polarizing microscope and cathodoluminoscope. All of the thin sections of the sandstones and some of the thin sections of limestones from the cores and sidewall plugs were point-counted to determine their textures, compositions, and porosities.

Selected thin sections were polished for microprobe analyses using a Cameca SX50 electron microprobe. Ten thick sections with calcite and dolomite cements from cores of the Garrett B-1 well were prepared for fluid inclusion analyses using a Lan Kam TH600 heating and cooling stage.

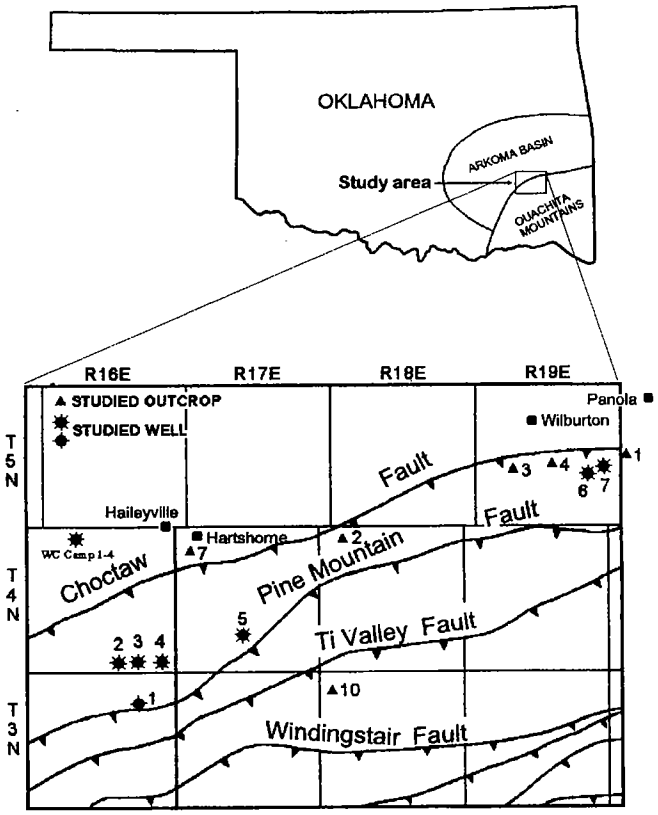

Figure 1. Index map showing study area and location of wells and outcrops.

LITHOFACIES AND DEPOSITIONAL ENVIRONMENTS

The Spiro interval contains sandstone, limestone, shale, and chert in the region of the South Haleyville, South Hartshorne (Figs. 2 and 3), and South Panola (Fig. 4) fields and displays a similar lithofacies assemblage throughout the western part of the frontal belt of the Ouachita Mountains. The Foster is composed of sandstone and shale in the South Panola field. Five lithofacies have been recognized within the Spiro and Foster rock units: (1) sandstone, (2) grain-/packstone, (3) mottled wacke-/packstone, (4) chert, and (5) shale.

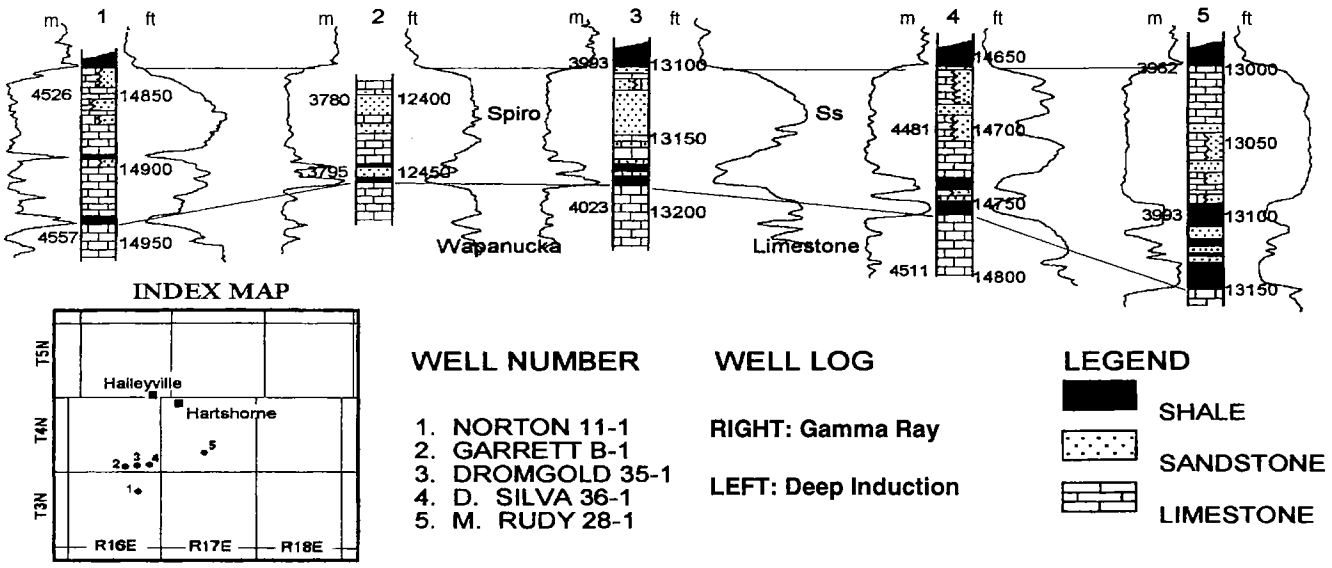

LITHOLOGIC COLUMNS FROM WELLS IN SOUTH HALEYVILLE AND SOUTH HARTSHORNE FIELDS

Figure 2. Wells studied in the South Haleyville and South Hartshorne fields. The Spiro sandstone interval in these wells is composed of interbedded sandstone and limestone. The bottom boundary of the Spiro is a layer of shale. The shale, sandstone, and limestone interval above the Wapanucka limestone is equivalent to the Foster sandstones in the South Panola field. Lithologic columns were interpreted from drill cuttings, cores, and sidewall cores.

Sandstone

The sandstones were divided into three sub-lithofacies, based upon the strong influence of the depositional components on the diagenesis and porosity evolution. These sub-lithofacies are: (1) carbonate-grain–rich sandstone, containing 15% or more fossil fragments and other calcite grains; (2) carbonate-grain–bearing sandstone, containing 5–15% calcite grains, mostly fossil fragments; and (3) carbonate-grain–poor sandstone, containing less than 5% carbonate grains. Fossil fragments including crinoids, bryozoans, brachiopods, ostracodes, and foraminifers are common in the Spiro sandstones but sparse in the Foster sandstones. The sandstones of the Spiro interval in the South Haleyville field are dominated by sub-lithofacies 2; in the South Panola field, they are dominated by sub-lithofacies 1 (Figs. 3 and 4). The Foster sandstones in the South Panola field and equivalent sandstones in the South Haleyville and South Hartshorne fields are poor in carbonate-grains, sub-lithofacies 3.

The Spiro and Foster sandstones examined on outcrops are very fine to medium grained and moderately to very well sorted. Quartz is the dominant detrital component (generally >95%) with minor to trace amounts of chert, feldspar, zircon, tourmaline, rutile, and leucoxene. Marine-fossil fragments, including crinoids, bryozoans, brachiopods, ostracodes, and foraminifers, range from 1% to 20%. Large- to medium-scale cross-bedding (including trough cross-bedding and low-angle, planar cross-bedding) are prominent. The sandstones observed in several Spiro sandstone outcrops are interpreted as parts of a barrier-island system. The cross-bedded sandstones that contain a mixture of quartz sands and carbonate grains are interpreted to be the foreshore–offshore bars that are characterized by low-angle, planar cross-bedding and/or multi-directional cross-bedding.

The Spiro sandstone in the wells studied is predominantly very fine to fine-grained. Wave-ripple and bioturbation structures are present and medium-scale, trough cross-bedding occurs sparsely. In the Garrett B-1 well, this sandstone facies, which is the major reservoir, is interbedded with limestone (Fig. 3). In the Jennings 24-1A well, this sandstone facies, which is rich in bioclasts, is interbedded with limestone and shale (Fig. 4). The interbedded marine limestone and high content of marine fossils indicate that the sandstone is a marine deposit. Wave ripples and bioturbation indicate a shallow-marine environment. It is interpreted to be a shallow-marine sand sheet deposited in a wide shoreface zone.

The Foster sandstones display upward-fining, tabular cross-bedding and contain mud clasts. In the Jennings 23-1A well, 10 upward-fining sandstone sequences occur within the cored interval from 13,853.9 to 13,872 ft (4,223 to 4,228 m), where the cores ended (Fig. 4). The thicknesses of the individual sandstone beds range from 0.5 to 3 ft (~0.2 to 0.9 m). Each contains medium-grained quartz sandstone in the lower part that grades upward into medium- to fine-grained quartz sandstone. The mostly porous sandstones in the

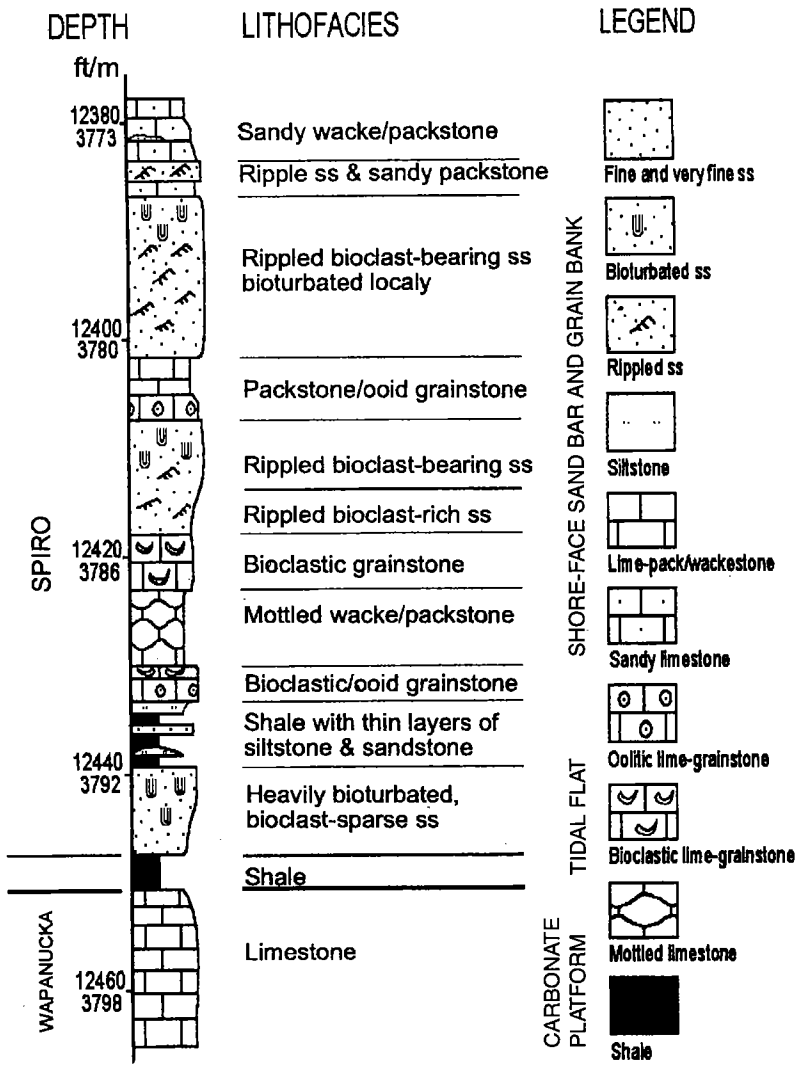

Figure 3. Core-log profile and interpretation of depositional environments of the Spiro and upper part of the Wapanucka limestone, Garrett B-1 well.

lower parts of each bed are cross-bedded with well-rounded, moderately sorted grains. The upper parts of the sandstone beds are typically nonporous, structureless with well-sorted, tightly compacted grains. Black mud-pebbles are common, especially in the upper parts. The typical Foster facies in the Arkoma basin is considered to be local stream deposits (Lumsden and others, 1971). The upward-fining sequence, bidirectional, tabular-bedding, and dark-shale fragments indicate that the Foster sandstone facies in the south Panola field was deposited in a shallow nearshore to subaqueous environment with lateral erosion and sedimentation. It could be a tidal-dominated channel deposit.

In the Garrett B-2 well, the sandstone equivalent to the Foster is interbedded with shale and exhibits abundant vertical bioturbation, indicating a tide-related environment. This sandstone and shale may have been deposited in a sand/mud tidal flat.

Grain/Packstone and Sandy Grain/Packstone

The grains of this limestone facies include bioclasts (crinoids, bryozoans, brachiopods, ostracodes, foraminifers, and spicules) and ooids, generally accompanied by significant amounts of detrital quartz. The types of the limestone and grains indicate a medium- to high-energy environment. This facies was interpreted to be a shallow-marine, grainstone bank/shoal deposit.

Chert

Chert commonly occurs at the top of the Spiro and is characterized by abundant siliceous spicules. The siliceous spicules and associated bioclasts, such as crinoids, bryozoans, and foraminifers, suggest a slightly deeper shelf environment.

Shale

Shale occurs in the middle and lower parts of the Spiro and Foster sandstone intervals. This facies is black to dark gray and contains marine fossils and thin lenticular layers of gray sandstone and siltstone. This facies is interpreted as shallow-shelf or mud-flat deposits.

SANDSTONE DIAGENESIS

The Spiro and Foster sandstones have undergone complex diagenetic modifications during burial. Three diagenetic events—(1) compaction and pressure solution, (2) cementation, and (3) dissolution—have significantly influenced the reservoir quality within the study area. In response to these diagenetic effects, the carbonate-grain–poor sandstone—especially the Foster and its equivalent sandstones—have been altered dominantly by compaction and chlorite and quartz cementation. The carbonate-grain–bearing sandstones have been strongly modified by calcite cementation and dissolution; and the carbonate-grain–rich sandstones and sandy limestones have been tightly compacted and cemented with calcite.

Other type of diagenesis including replacement of carbonate grains by quartz, ankerite, and feldspar are less important.

Compaction and Pressure Solution

The maximum thickness of sediments above the Spiro was about 25,000 ft (7,600 m) along the southern margin of the Arkoma basin. Current burial depths of the Spiro range from 12,000 to 15,000 ft (3,700 to 4,600 m). Compaction caused by the overburden sediments resulted in both grain rearrangement and pressure solution, both of which reduced primary porosity mainly in grainstone, sandy grainstone and partial-bioclast–

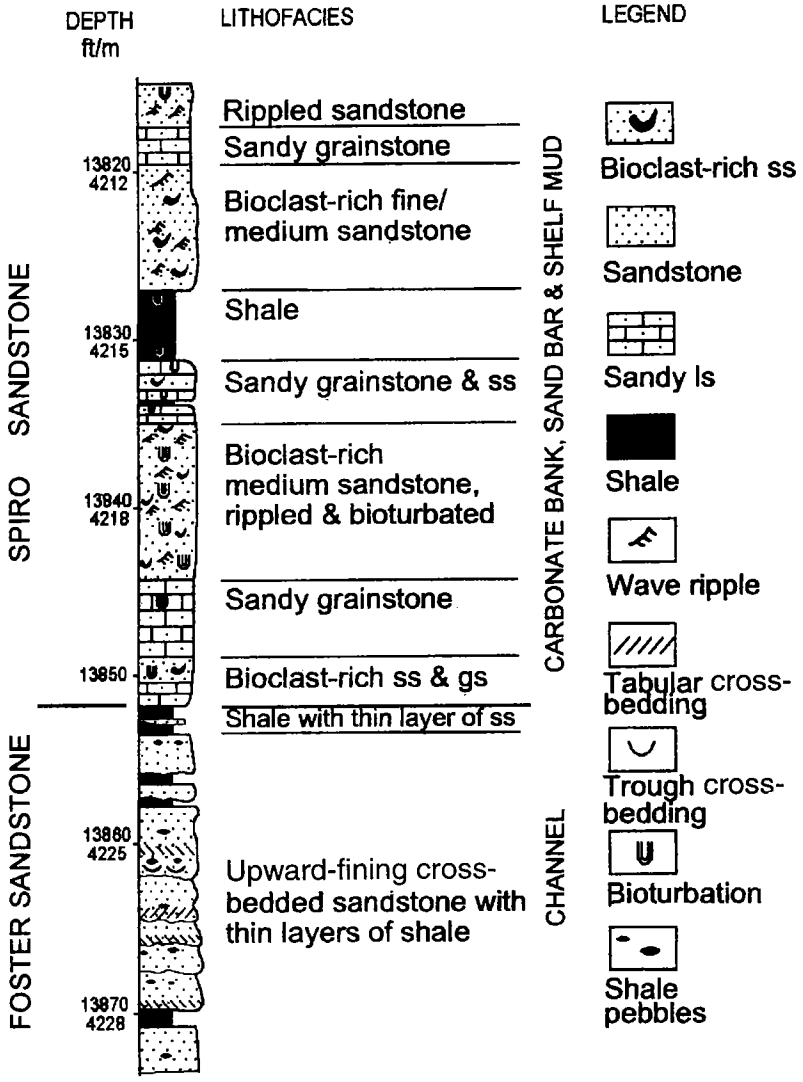

Figure 4. Core-log profile and interpretation of depositional environment of the Spiro and Foster sandstones, Jennings 23-1A well (shown as well no. 6 on Fig. 1).

rich sandstone. In these rocks, the grains are tightly connected. The quartz particles were forced into relatively soft and soluble carbonate grains (Fig. 5A). The primary intergranular porosity in some sandy-grainstone samples was reduced almost to zero by this process. The pressure solution caused by overburden has produced styolites and microstyolites between grains. These processes added $CaCO_3$ to the pore water for calcite cementation. However, in most sandstones, the minus-cement porosity ranging from 30% to 38% (Fig. 6) indicates that early calcite cementation deterred further compaction.

In the carbonate-grain–poor sandstone, pressure solution resulted in sutured contacts of the quartz grains and provided SiO_2 for quartz cementation (Lumsden and others, 1971; Pittman, 1972). The minus-cement porosity in these sandstones ranges from 20% to 38%. If the primary porosity was 40–45%, the compaction and pressure solution have reduced porosity by 5–20%. A much stronger pressure solution effect is recognized in the tightly quartz-cemented sandstone in which the minus-cement ranges from 20% to 30%.

Cementation

Six kinds of cements are significant in both quantity and their effect on the reservoir in the wells studied. They are chlorite, quartz, calcite, ferroan-dolomite, ankerite, and pyrobitumen cements. Petrological evidence indicates the following cementation sequence: chlorite → overgrowth quartz (phase 1) → calcite (phase 1) → ferroan dolomite → ankerite → pyrobitumen → overgrowth quartz (phase 2) → calcite (phase 2).

The first diagenetic event affecting the Spiro was the formation of chlorite, and the second diagenetic event was the syntaxial quartz overgrowth (Houseknecht and McGilvery, 1991). The quartz overgrowth in the South Haleyville field could nucleate on quartz grains with a chlorite coat, which shows that the chlorite coating was not as thick and complete as in the Spiro sandstone of the South Panola and Red Oak fields, where it effectively prevented quartz overgrowth. The third diagenetic event was calcite cementation. Point-count data from porous, partially calcite-cemented sandstone show that the content of quartz cement is much lower in the calcite-cemented part than in the porous part (Table 1, 12,392A,B; and 12,395A,B), which indicates calcite cement prior to the late quartz overgrowth. The pyrobitumen cement is clearly later than phase I overgrowth quartz but is earlier than the last calcite cement and at least a part of the phase II quartz cement.

Quartz Cements

Authigenic quartz cements including overgrowth quartz cement and pore-filling chert are common in the Spiro sandstones and are much more developed in the Foster sandstones. Based on the point counts from the thin sections of cores taken in the Garrett B-1 and Dromgold wells, the amounts of quartz cement in the Spiro sandstones range from 1.7 to 21.0 vol% (Table 1). The overgrowth quartz ranges from 8% to 25% in the Foster sandstones. Two phases of overgrowth quartz were recognized by cathodoluminescence analysis: (1) luminescence color following the parent quartz—dull red and dull blue, and (2) dull black luminescence. The phase 1 quartz cement directly precipitated on the host grain and preceded calcite cement (Fig. 5B); the phase 2 quartz cement occupies the center of the intergranular pore space. Solidified pyrobitumen may occur between phase 1 and phase 2 authigenic quartz,

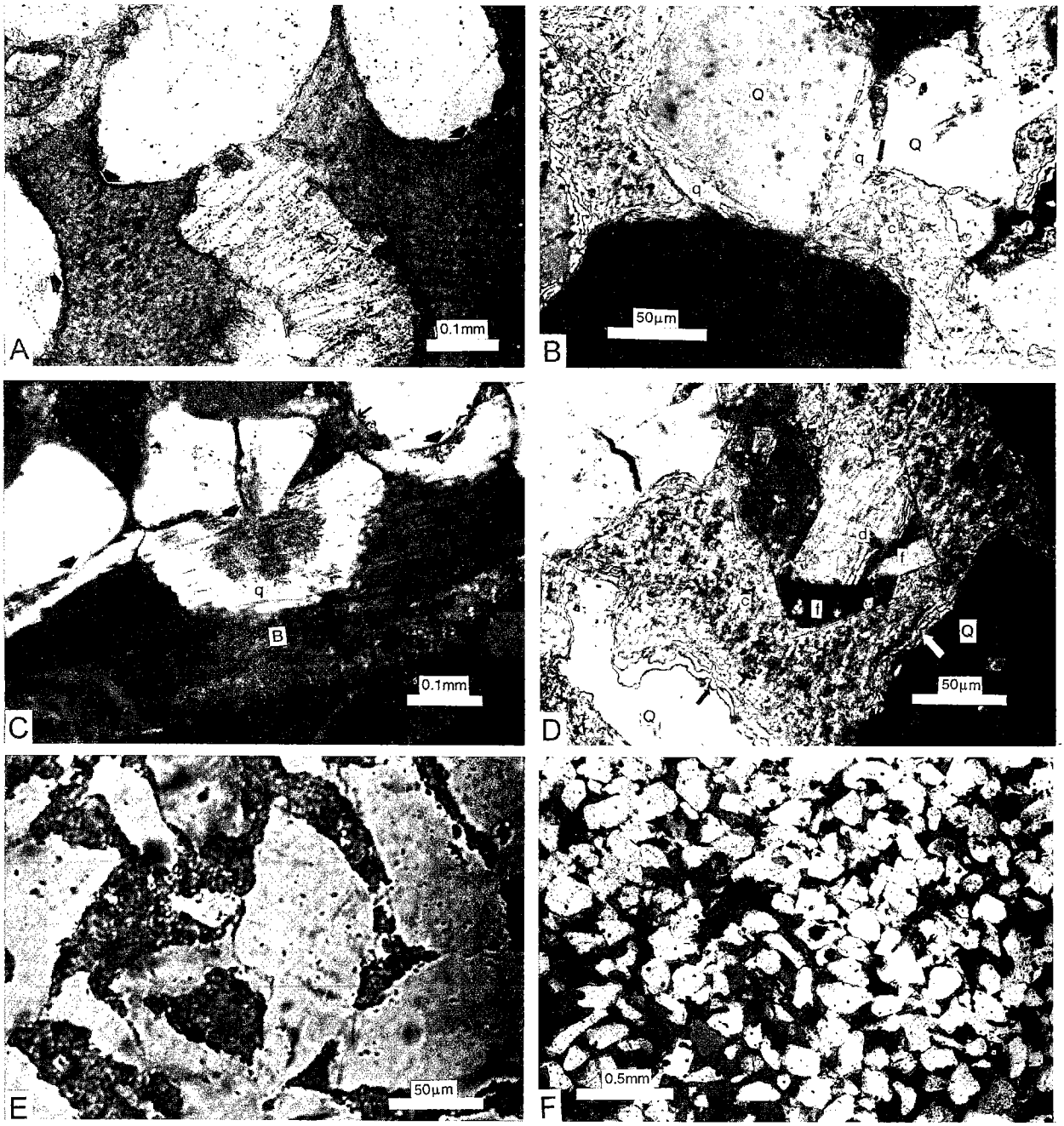

Figure 5. Photographs of thin sections showing diagenetic fabrics: ***A***—Tight contact between grains due to compaction, resulting in loss of primary intergranular porosity. Note the detrital quartz squeezed into crinoid grain (arrows). Sample from core of Garrett B-1 well, depth 12,405 ft (3,781 m), plane light, scale bar 0.1 mm. ***B***—Petrological relationship between overgrowth quartz (q) and calcite cement (c): calcite cement filled the interparticle pores and slightly replaced both quartz grains (Q) and their overgrowths. Note also the hackly shaped boundary between calcite cement and quartz (both Q and q, arrow). Sample from core of Garrett B-1 well, depth 12,391 ft (3,776.8 m), crossed-polarized light, scale bar 50 µm. ***C***—Brachiopod shell (B) replaced by overgrowth quartz beginning at the pressure-solution contacts (thick arrows). Note that overgrowth quartz did not replace calcite cement (thin arrow), indicating that calcite cementation was later than quartz overgrowth and replacement. Sample from core of Garrett B-1 well, depth 12,382 ft (3,774 m), crossed-polarized light, scale bar 0.1 mm. ***D***—Relationship between calcite cement (c), authigenic feldspar (f), and ferroan dolomite (d). Note the platy euhedral feldspar that replaced calcite cement. The rhombohedral ferroan dolomite is associated closely with feldspar. Note also the hackly boundary between calcite cement and detrital quartz (arrows). Sample from core of Garrett B-1 well, depth 12,391 ft (3,776.8 m), crossed-polarized light, scale bar 50 µm. ***E***—Polished thin section shows the shapes of the porosity margin. The intergranular porosities (darker) display a typically hackly shape at the boundaries of the detrital and the overgrowth quartz. These shapes record the marginal replacement of quartz particles and phase 1 quartz cement by now-absent calcite cement. Sample from the core of Garrett B-1 well, depth 12,413 ft (3,783.5 m), plane light, scale bar 50 µm. ***F***—Sharp contact between porosity dissolved part (upper and right) and cemented part (lower left) within a fine-grained quartzarenite. Sample from core of Garrett B-1 well, depth 12,391 ft (3,776.8 m), plane light, scale bar 0.5 mm.

TABLE 1.—Point-Count Data, Spiro Sandstone

Sample	Detritus (%) Q	CG	OD	Cements (%) OQ	Cal	DA	OC	Porosity (%)
Garrett B-1 well:								
12382	54.5	31.7	0.7	3.0	17.9	1.1	–	0.9
12385	40.3	28.3	0.3	6.2	16.9	4.4	–	3.2
12391	53.6	3.4	0.9	21.0	2.7	7.2	–	9.3
12392A	55.6	11.5	0.3	2.2	28.1	0.5	–	1.5
12392B	56.8	5.8	0.2	14.7	1.1	2.8	–	17.4
12393	57.1	8.0	0.2	12.5	0.8	5.3	–	14.2
12395A	53.2	10.1	–	2.8	29.1	2.4	–	2.4
12395B	60.7	5.6	–	13.6	1.6	4.8	–	12.9
12399	61.8	4.5	–	7.5	6.0	4.0	–	15.3
12401	57.1	11.0	0.1	1.7	20.2	0.5	–	8.8
12405	37.3	58.0	–	0.5	3.3	0.4	–	0.1
12411	53.5	7.5	0.1	7.8	9.6	8.5	1.9c	12.3
12413	55.2	12.0	1.5	4.7	5.9	3.5	0.8c	9.4
12414	38.9	21.5	1.1	0.5	25.0	2.9	–	0.0
12422	32.0	55.3	–	0.1	11.2	0.3	–	0.0
12433	57.1	19.9	–	3.4	12.2	4.6	2.8p,c	0.0
12439	66.5	1.4	–	5.4	0.2	6.0	20.6p,c	0.0
Dromgold 35-1 well:								
13116	32.3	33.3	0.3	0.1	31.1	0.1	0.1b	2.6*
13120	52.2	12.2	0.3	3.6	25.7	0.3	2.4p	3.3*
13122	57.1	3.4	–	16.8	5.8	6.6	0.8c,p	9.4
13124	37.0	36.1	–	3.2	21.0	0.8	1.9p,c	2.1*
13128	32.6	30.1	0.4	1.3	25.3	3.9	0.4p	4.6*
13130	35.1	23.6	–	3.3	26.9	6.2	4.6c	0.2*
13132	64.1	5.0	0.2	7.9	15.8	1.5	0.3p	5.3*
13136	63.7	2.4	0.2	7.6	0.7	5.1	5.8h,c	14.4*
13140	29.1	42.7	–	2.6	20.5	2.9	2.9a	2.2*
13144	57.2	7.7	1.6	2.9	18.2	2.2	3.8c,p	7.3*
13148	44.4	19.4	0.7	5.1	21.4	6.1	1.5c,p	1.4*
13156	42.7	19.4	0.6	4.8	25.9	0.6	2.6c,l	3.5*
13164	31.6	49.3	–	0.8	4.1	–	13.1c,p	1.1*
13168	35.8	23.7	0.3	2.8	29.8	3.3	2.0c,p	2.4*
Outcrop sample:								
S1-1	55.7	–	0.8	34.9	–	–	0.4c	15.2
S1-4	62.3	–	–	22.7	–	–	–	15.0
S2-1	68.7	–	0.4	14.0	–	–	2.0c	14.9
S3-1	57.7	–	–	8.5	–	–	13.3c	20.4
S5-1	65.2	0.2	–	13.3	0.1	–	7.7h	13.6
S5-7	74.1	–	–	12.2	–	–	9.2ch	4.5
S5-10	68.7	1.4	–	9.0	–	–	11.8h,c	9.1
S7-3	56.1	–	3.0	7.7	–	–	9.1ch,p	24.0
S7-4	58.7	–	2.7	15.3	–	–	10.8c	12.5
S7-S	64.8	1.3	–	8.6	–	–	9.1c	16.3

NOTES: Q, quartz detritus; CG, bioclasts and other carbonate grains; OD, other detritus including heavy minerals, chert and lithic detritus; AQ, authigenic quartz; Cal, calcite; DA, ferroan dolomite and ankerite; OC, other cements including clay (c), chlorite (ch), hematite (h), pyrobitumen (p), and lime-mud (l). Porosity data from core analysis.

indicating that the quartz cementation began prior to and continued after pyrobitumen emplacement. Syntaxial overgrowth of the secondary quartz appears to have penetrated very thin chlorite films. At the pressure solution contacts between quartz grains and bioclasts, the secondary overgrowth quartz selectively replaced carbonate bioclasts, especially brachiopods and bryozoans, rather then calcite cement (Fig. 5C). Quartz cementation decreased with increased calcite cement (Fig. 7), and overgrowth quartz tends to be absent in fully calcite-cemented areas. The quartz cement contains almost no fluid inclusions. Only one two-phase inclusion was found; the homogenization temperature was 140°C (Table 2).

Calcite Cements

Calcite cement, ranging from 1.1 to 29.1 vol% (Table 1), occurs in the subsurface Spiro sandstones mainly as coarse crystals occupying intergranular pores and to a lesser degree as poikilitic cement. Samples from Spiro outcrops show that nearly all the calcite cement as well as the bioclasts have been leached out during subaerial exposure. Protrusions of the calcite into quartz grains are very common in thin section and give the impression that the replacement of quartz by calcite was extensive (Fig. 5B,D). This appearance may be caused largely by calcite overlaps, and the replacement may be slight. (McBride, 1987). However, the protrusion boundaries between quartz grains and calcite cements have provided evidence for recognizing the secondary porosity after dissolution of calcite cement (see Dissolution section below).

The two-phase fluid inclusions within the calcite cements homogenized at 71°C to 123°C (Table 2). Several inclusions were big enough for measuring melting temperatures. After freezing, their first melting was at –22°C to –24°C, and final melting was at –5°C to –6°C. According to Crawford's data chart (1981) and the experiments of Davis and others (1990), these calcite cements probably formed in a NaCl-H_2O system with 10–20 wt% of NaCl equivalence at 5,000–6,000 ft (1,500–1,800 m) burial depth.

Ferroan-Dolomite Cement

Poikilitic ferroan dolomite cement spots, 0.3–1 mm across, constitute a maximum of 8.5 vol% of the whole rock (Table 1). Microprobe analysis shows

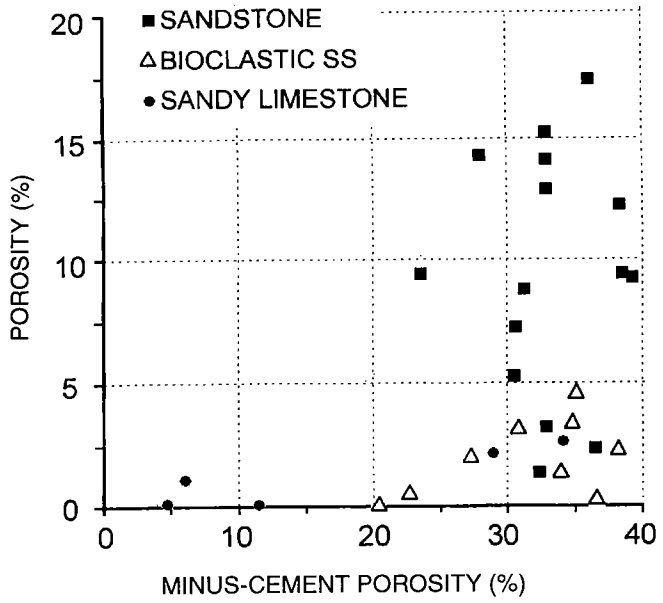

Figure 6. Plot of minus-cement porosity versus percent porosity shows that most of the sandstones have 30–38% of minus-cement porosity, indicating compaction only had a small influence on the reduction of initial porosity. The wide variation in present porosity is from dissolution of primary calcite cement. Sandy limestones and some bioclastic sandstones were highly compacted. Data from point counting of thin sections of Garrett B-1 and Dromgold 35-1 (no. 7 on Fig. 1) wells.

Table 2.—Analyses of Fluid Inclusions within the Cements from the Spiro Sandstones of Garrett B-1 Well

Number	Host mineral	Melt First (°C)	Melt Final (°C)	Homogenization (°C)
12385-A	Calcite	–24	–6	123
12385-B	Calcite	–22	–6	71
12385-C	Calcite	–24	–5	91
12385-D	Calcite			121
12385-E	Calcite			114
12389-A	Quartz*			140
12389-B	Ankerite	–32	–9	124
12389-B	Ankerite			129
12389-C	Calcite			101
12389-D	Calcite			76
12389-D	Calcite			81
12395	Calcite			96
12400-A	Calcite	–26?	–7	108
12400-B	Calcite			105
12400-C	Calcite			74
12400-D	Calcite			121
12406-A	Calcite			74
12406-B	Fe-dolomite	–27	–8	126
12406-B	Fe-dolomite			112
12406-B	Fe-dolomite			116
12410-A	Fe-dolomite			134
12410-A	Fe-dolomite			116
12411-A	Fe-dolomite	–28	–8	108
12411-B	Fe-dolomite			109
12411-C	Fe-dolomite			124

*Phase-2 quartz cement.

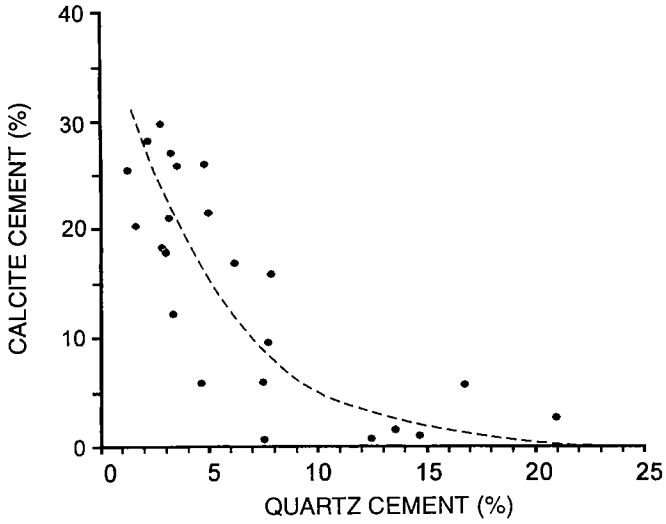

Figure 7. Plot of percent overgrowth quartz versus percent calcite cement shows a decrease in quartz cement with increased calcite cement. Overgrowth quartz is <8% of the bulk rock volume and generally <5% where higher percentages of calcite cement are present. This suggests that the phase 1 quartz cement may be no more than 5–8%. Point-counting data from the thin sections of Garrett B-1 and Dromgold 35-1 wells.

that the poikilitic ferroan dolomite contains 15–18% $FeCO_3$ (Table 3). Petrological relationships indicate that ferroan-dolomite cement postdated phase 1 calcite cement (Fig. 5D).

The homogenization temperatures of two-phase fluid inclusions in the poikilitic ferroan dolomite range from 108°C to 124°C; the first- and final-melting temperatures are –27°C to –28°C and –8°C, respectively (Table 2). The measured temperatures indicate a deeper burial and higher salinity for the precipitation of the ferroan dolomite than for precipitation of the calcite cement. The first melting temperatures suggest a $NaCl$-$MgCl_2$-H_2O parent-solution system with 20–30% concentration of NaCl equivalence and a depth from 8,200 to 9,800 ft (2,500–3,000 m) during precipitation of the ferroan dolomite.

Ankerite

Ankerite occurs in minor amounts, 0.3–3.3 vol%, as disseminated crystals. Individual, 0.1–0.5 mm in diameter, disseminated ankerite crystals are generally larger than the quartz detritus. They are interpreted to have formed by precipitation in larger interstitial pores after dissolution of calcite cement. The ankerite cement contains 23% $FeCO_3$ (Table 3). Two fluid inclusions

Table 3.—Result of Microprobe Analysis: Carbonate Cements, Garrett B-1Well

Number	Sample*	Contents (%)			
		$FeCO_3$	$MgCO_3$	$CaCO_3$	$SrCO_3$
12413-1	DAC	23.4	23.0	54.0	0.05
12413-2	DAC	23.5	22.1	54.1	0.031
12411-1	PAC	14.8	24.6	59.4	0.098
12411-2	PAC	17.9	24.4	57.5	0.085
12411-3	PAC	18.1	23.1	58.5	0.098
12411-4	CC	0.07	1.2	97.3	0.19

*DAC, disseminated ankerite cement; PAC, poikilitic ankerite cement; CC, calcite cement.

Table 4.—Result of Microprobe Analysis (%): Chlorite, Garrett B-1 Well*

Number	SO_2	Al_2O_3	MgO	CaO	FeO	K_2O
12439	30.5	21.8	5.5	0.1	22.3	1.5

*Average of 30 analyses.

found in the ankerite had homogenization temperature of 124°C and 129°C, a first-melting temperature of –32°C and a final-melting temperature of –9°C (Table 2). These data indicate a slightly higher salinity of parent solution and a much higher temperature of formation than that of the ferroan dolomite.

Pyrobitumen

Pyrobitumen is solidified asphalt cement that occurs in cutting chips from several wells. The most abundant pyrobitumen, however, is in the fine- to very fine grained sandstones above and below the Spiro producing interval in the WC Camp 1-4 well (Fig. 1), where the pyrobitumen occurs as a solid-phase cement filling intergranular pore space. This pyrobitumen produced by loss of volatiles also occurs as fragment-shaped relics within the intergranular pores. The lithological relationship indicates that the pyrobitumen cementation preceded phase 2 quartz overgrowth.

Chlorite

Chlorite occurs in the Spiro sandstones as crystalline plates oriented normal to the detritus surface. In the South Haleyville and South Hartshorne fields, it is volumetrically unimportant, generally <1 vol%, and occurs as a very thin film, generally <5 μm thick on the detrital quartz grains. Microprobe analysis shows a small amount of K_2O (Table 4) that may indicate a minor amount of illite. This cement type increases toward the east, and coats from 5–15 μm thick occur on the quartz grains.

This cement type is more abundant in the coarser lower parts than in the finer upper parts of the Foster sandstone sequences. Chlorite also sparsely occurs as intergranular-filling cement in some very fine grained Foster sandstones.

Other Cements and Authigenic Minerals

Clay and hematite lining or filling pores resulting from dissolution of carbonate components are abundant and quite visible in outcrop samples but are very sparse in subsurface Spiro samples (Table 1). Pyrite spots (≤1 mm across) are rarely associated with the pyrobitumen cement. A matrix composed of a mixture of clay, leucoxene, quartz, and apatite occurs occasionally in the sandstone core from the Garrett B-1 well. Authigenic feldspar occurs as small euhedral crystals that have replaced calcite (Fig. 5D).

Dissolution

Dissolution of carbonate bioclasts and calcite cement has provided the main porosity system in both the outcrop and subsurface Spiro sandstones. Crinoid bioclasts, the most soluble detritus, have been dissolved completely on the outcrop and have been dissolved to a great extent in subsurface samples. The other fossils (bryozoans, brachiopods, ostracodes, and foraminifers) are also completely dissolved in outcrop samples but appear more stable than crinoids in the subsurface. Petrologically, the extent of dissolution of the bioclasts is related to the total calcite content (Fig. 8). The point-count data from subsurface samples show that the dissolution within the Spiro sandstones was largely an uneven process controlled probably by both the lithological characteristics and the movement of the corrosive solution. Based on the wells studied, the dissolution intensity in the Spiro interval of the South Haleyville and South Hartshorne fields is greater than that in the South Panola field. In the South Haleyville field, the dissolution intensity in the Garrett B-1 well is greater than in the Dromgold 35-1 well. Petrologically, the extent of dissolution of the calcite cement and bioclasts is related to the total amount of initial calcite (carbonate grains plus calcite cement). The dissolution was most pervasive in the sandstones with <15% carbonate grains or with 15–30% initial calcite (Figs. 9 and 10). Residual calcite cement in these reservoir sandstones ranges from 2% to 10%. Dissolution was minor in the limestones and the carbonate-grain–rich sandstones.

Similar dissolution observed in the Red Oak field has been interpreted by Houseknecht (1987) to have been promoted by organic acids and carbon dioxide generated by thermal maturation of organic matter. The differential movement of these corrosive solutions resulted in the differential dissolution of calcite cement and bioclasts between gas fields, wells, and intervals within each well.

RESERVOIR POROSITY

Two types of porosity were recognized in the Foster sandstones. Partial preservation of the primary inter-

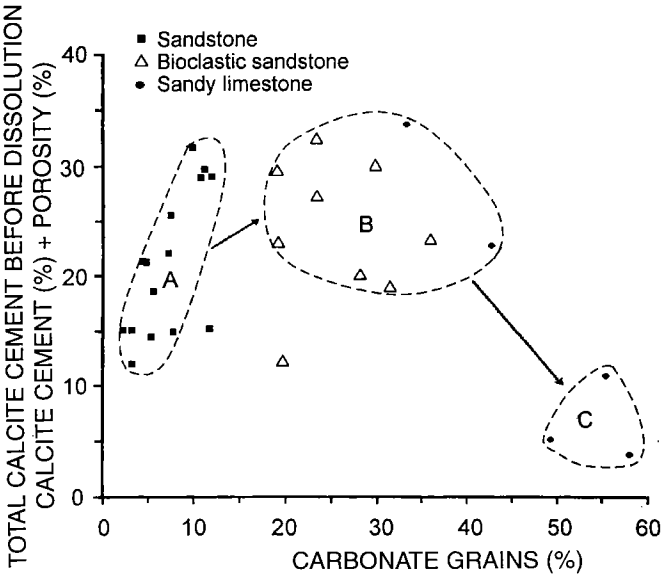

Figure 8. Plot of carbonate grains versus amount of calcite cement plus porosity (equals total calcite cement before dissolution). Most of the data fall into three groups: (1) group A shows that if the amount of carbonate grains is <15%, the calcite cement plus porosity increases with an increase in carbonate grains; (2) group B indicates that if the carbonate grains range from 20% to 40%, the calcite cement stops increasing; and (3) group C, sandy limestone containing 45–60% of carbonate grains, has very low values of calcite cement plus porosity. The decrease of calcite cement from group B to C suggests a decrease of the intergranular porosity due to greater compaction and pressure solution in the sandy grainstones.

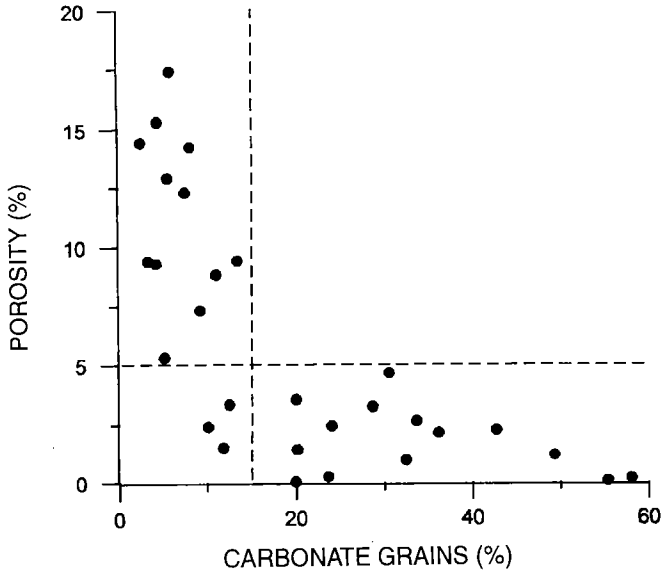

Figure 9. Plot of carbonate grains versus porosity shows: (1) varied development of porosity in the sandstones with <15% carbonate grains; and (2) porosity poorly developed in the rocks with ≥20% carbonate grains, indicating increased compaction and calcite cementation may have obstructed formation of the secondary porosity.

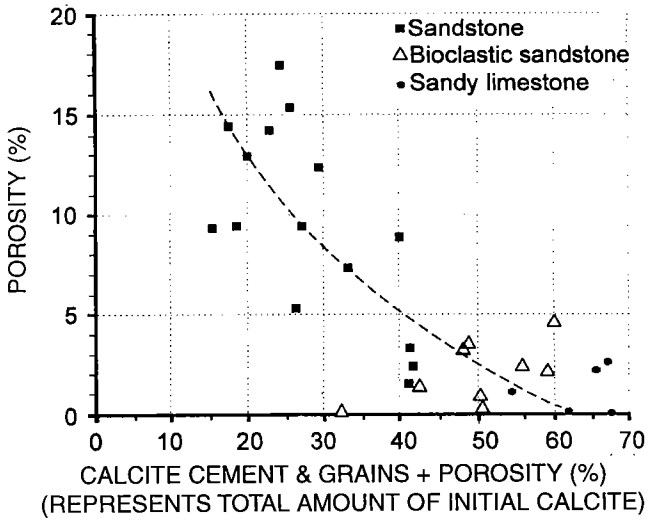

Figure 10. Plot of percent porosity against percent of porosity + calcite grains + calcite cement. The parameter porosity% + calcite grains% + calcite cement% represents initial abundance of total calcite prior to dissolution of calcite cement. The figure shows: (1) porosity decreases with increasing initial total calcite; and (2) the sandstones with 15–30% initial calcite have the highest porosity. Point-count data from thin sections of Garrett B-1 (dots) and Dromgold 35-1 (circles) wells.

granular porosity is the main porosity type within the Foster facies and is interpreted to be the result of retarded pressure solution and quartz overgrowth because of chlorite coating on the quartz grains (Lumsden and others, 1971). The other results from the dissolution of bioclasts to produce moldic pores larger than those of the quartz grains.

Porosity in the Spiro sandstones includes primary and secondary types. The primary intraparticle porosity, mostly occurring in apertures of bryozoans and foraminifers and pores in echinoderm plates, has minor importance in the Spiro reservoir. Thin sections from the Garrett B-1 and Dromgold 35-1 wells show that the reservoir pore space is dominated by secondary intergranular porosity formed by dissolution of calcite cement and grains. The solution origin of this porosity can be distinguished from primary porosity using polished, thinner thin sections. The boundaries of the intergranular porosities in this kind of thin section display a typical hackly shape that records the marginal replacement of quartz detritus by now-absent calcite cement (Fig. 5E). Generally, a sharp contact that records the action boundary of the corrosive liquid occurs between the areas of dissolution and the areas that are still cemented (Fig. 5F). The quantitative relationship between porosity and rock texture supplies important information about the origin of porosity in Spiro sandstones. Figures 6, 11, and 12 give information on the dissolution. Figure 6 is a plot of minus-cement porosity versus porosity. If the reservoir porosity were mainly primary, the compaction of interstitial pores would continue to decrease the porosity to the lowest value, esti-

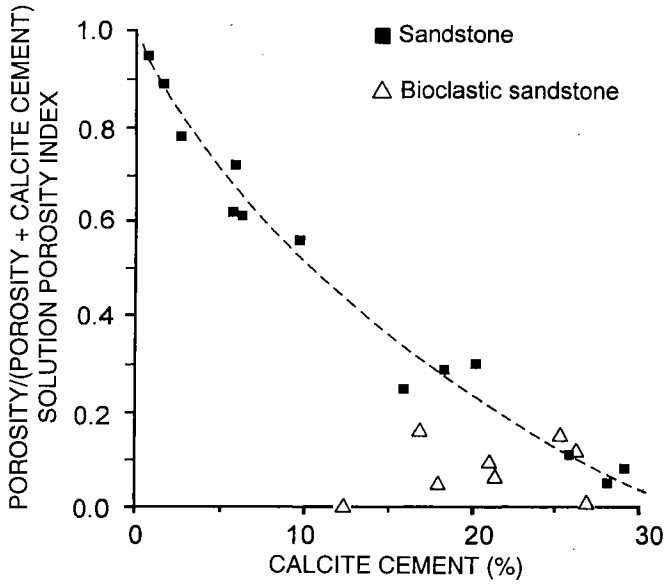

Figure 11. Plot of calcite cement versus porosity/(porosity + calcite cement). The ordinate porosity/(porosity + calcite cement) represents the abundance of secondary porosity (secondary porosity index) resulting from dissolution of original calcite cement. The plot shows a negative correlation between secondary porosity and calcite cement in normal sandstones.

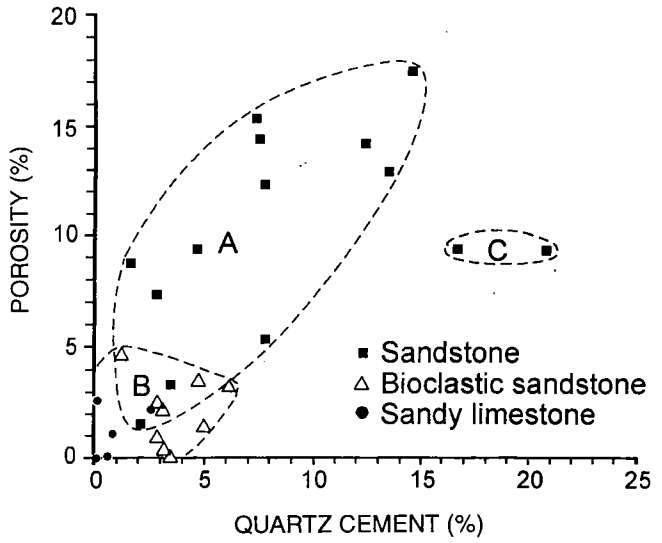

Figure 12. Plot of percent of quartz cement versus porosity. The data points fall into three groups: (1) group I, sandstones showing a positive-correlation between porosity and quartz cement (porosity increases with increasing quartz cement); (2) group II, carbonate-grain–rich sandstone and sandy limestone, showing no correlation between the low values of quartz cement and low porosity; and (3) group III showing a decrease in porosity where the quartz cement exceeds 15%. The positive correlation between porosity and quartz cement in group I indicates: (1) phase 2 quartz cement formed after calcite dissolution, and (2) dissolution origin of the reservoir porosity. Note the sandstones with lower porosity have <8% of quartz cement, meaning phase 1 overgrowth quartz is <8% (~5%).

mated to be 21% by Mou and Brenner (1982). However, many of the Spiro sandstones, especially the porous sandstones, have 30–40% of minus-cement porosity, which suggests that an earlier pore-filling cementation contributed to rock strength and inhibitedcompactional effects. Figure 12 is a plot of quartz cement versus porosity. These data show a tendency of porosity to increase with increasing quartz cement if the amount of quartz cement is less than 15%. This is because the major quartz cementation occurred after calcite cement dissolution. Thus, the greater the dissolution the greater was the secondary porosity and the more developed was the quartz cementation (see also caption of Fig. 12). The porosity of the Spiro reservoir sandstones in the Garrett B-1, Dromgold 35-1, and Jennings 23-1A wells ranges from 8% to 20%. The dissolution is also supported by degrees of porosity development (solution porosity index) being highly negatively correlated with the percent of carbonate cement (Fig. 11).

The moldic porosity after bioclasts, especially crinoids, may form 10% to 15% of the total pores in reservoir rocks but may form the major type of pores in the carbonate-grain–rich, low-porosity sandstones.

The data from core analysis combined with point-counting information show a porosity-distribution pattern formed by large-scale, uneven dissolution of calcite cement. The Spiro sandstone in the Garrett B-1 well consists of interbedded alternating porosity beds, 8–15 ft (2.5–5 m) thick, and tight streaks, 6–20 ft (2–6 m) thick (Fig. 3). The most porous interval from 12,387.7 to 12,401.8 ft (3776.7 to 3781.0 m) in this well consists of porous, 10–80 cm thick, and calcite-cemented, 3–25-cm-thick layers (Fig. 13). These layers in the cores are irregular in shape and varied in size. The Spiro sandstones in the Dromgold 35-1 well have less porosity and more initial total calcite than those in the Garrett B-1 well. These observations suggest significant vertical and lateral heterogeneity within the Spiro in the South Haleyville and South Hartshorne fields.

BURIAL HISTORY AND POROSITY EVOLUTION: A DISCUSSION

Following the termination of Spiro and Foster sedimentation on the stable shelf (Houseknecht, 1986), the study area was buried maximally by no less than 15,000–25,000 ft (4,600–7,600 m) of sedimentary rocks, mainly shale. Important aspects of the burial history of the Spiro sandstones are connate formation water, overburden, hydrocarbon maturity, and an anomalous geothermal gradient. Diagenetic alteration and porosity evolution that reflect the effects of these variables are summarized into the following six stages. Figure 14 summarizes the diagenetic processes, and Figure 15 shows porosity evolution within the three sandstone sublithofacies.

Stage of Early Compaction and Quartz Cementation

This stage includes the period from the beginning of burial until calcite cementation. Based on the mea-

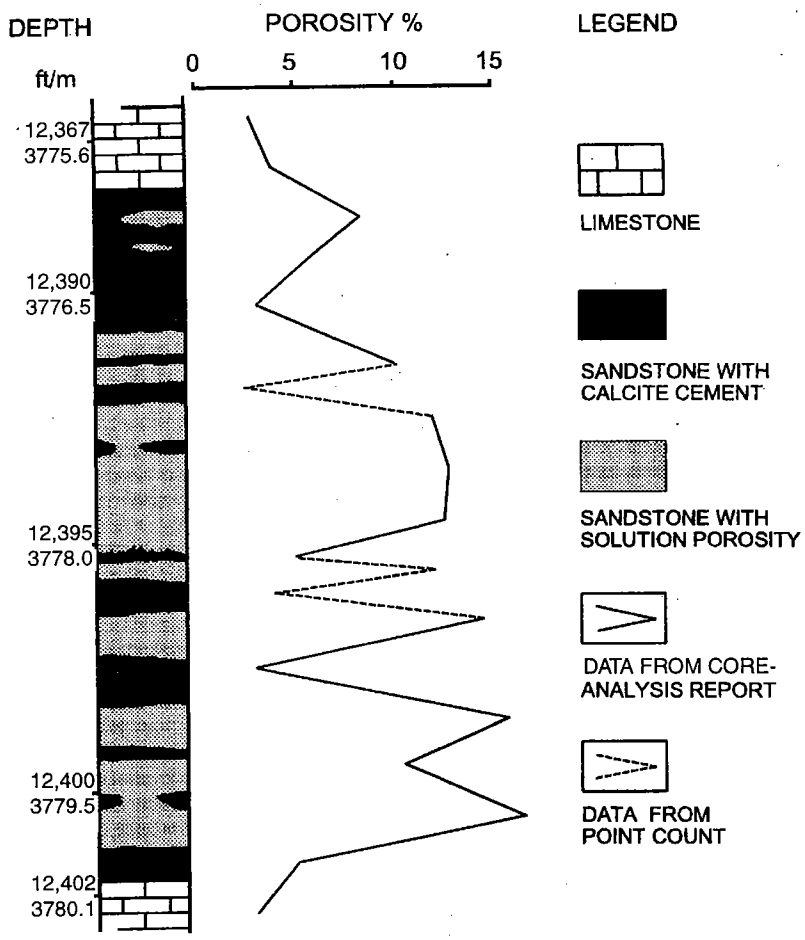

Figure 13. Profile shows the major porosity intervals in the Spiro sandstones of Garrett B-1 well. The sandstones consist of calcite-cemented sandstone and sandstone with secondary porosity, which results in a strong reservoir heterogeneity.

sured homogenization temperatures of fluid inclusions within calcite cement (see below), the maximum temperature during this stage of diagenesis may be lower than 70°C. The interstitial solution was connate seawater. Diagenetic events of this stage were predominantly compaction and the first phase of quartz cementation.

The well-rounded and well-sorted Spiro sandstones probably had primary porosities of 40–45% when deposited. The present minus-cement porosity of the sandstones in the Garrett B-1 well ranges from 20% to 40%, which indicates that primary porosity has been reduced by 10–50% of the original value because of reorientation and pressure solution during compaction. Most of the reservoir sandstone has minus-cement porosity of 30–40 (Fig. 6), not far below the estimated depositional value, indicating that pre-cement compaction did not greatly reduce the sandstone's reservoir porosity.

The chlorite cementation might have started before substantial compaction. It may mainly have occurred in the sandstones associated with shale beds. The clay from the shale may have contributed to the forming of chlorite.

Cementation by overgrowth quartz reduced the primary porosity to a varied extent. The relationship between overgrowth quartz and porosity shows that the quartz cement prior to the calcite cement is <8% and commonly <5% of the whole rock volume. In porous sandstones, however, the total quartz cements range from 3% to 20%, and, if it is <15 vol%, tends to increase with increasing porosity (Fig. 12). This suggests that overgrowth quartz increases with increasing secondary porosity because most of the quartz cement in the porous sandstones precipitated after the dissolution of the early calcite cement. After early compaction and the first phase of quartz cementation, the porosity in the Spiro sandstones had decreased from 40–45% to about 35%.

Stage of Calcite Cementation

Diagenesis was dominated by compaction and pressure solution before and during calcite cementation of the quartz sandstones in the limestones and carbonate-grain–rich sandstones of the Spiro interval. Point-count data show that 50–80% of the interstitial porosity of the limestones and carbonate-grain–rich sandstones was destroyed by compaction and pressure solution. The interbedded limestones and carbonate-grain–rich sandstones acted as calcium and carbonate exporters. During the stage of calcite cementation, pressure solution of limestones provided $CaCO_3$ to the interstitial water of the adjacent porous sandstones; cementation occurred at temperatures probably ranging from 70°C to 80°C. Measured homogenization temperatures of the inclusions in the calcite cement

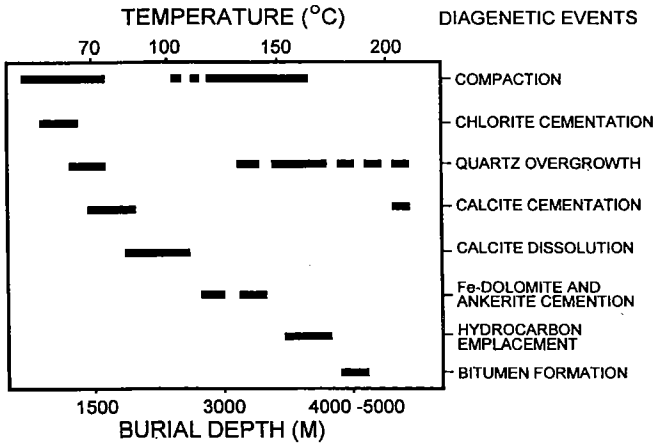

Figure 14. Sequence of burial digenesis and diagenetic products in the Spiro sandstones of South Haleyville and South Hartshorne fields.

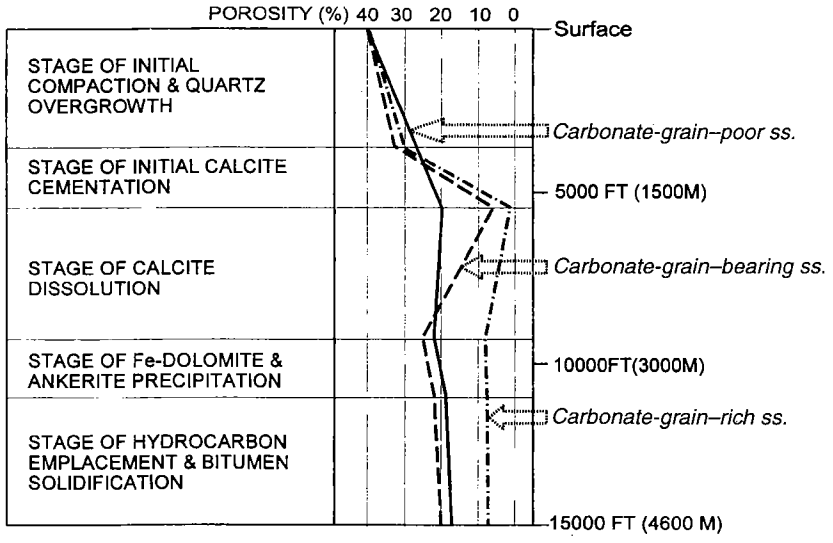

Figure 15. Diagenetic stages and porosity evolution; the porosity curves show the maximum porosities of three main sandstone sublithofacies in every stage.

range from 71°C to 123°C. The low values may be more reliable because fluid inclusion stretching increases homogenization temperatures. The wide range of homogenization temperatures reflects a population of fluid inclusions that was trapped at relatively shallow depth and consequently underwent varying amounts of stretching during further burial. Using a normal geothermal gradient (30°C per 1,000 m), the depth of burial during calcite cementation would be 5,000–6,000 ft (1,500–1,800 m). The solution water with 10–20 wt% salinity was saturated with $CaCO_3$ derived from adjacent limestone or carbonate-grain–rich sandstone. Intergranular calcite cement then precipitated and partially replaced early quartz. The intergranular porosity was largely filled by blocky or poikilitic calcite. In the sandstones of the Garrett B-1 and Dromgold 35-1 wells, calcite cement occupies up to 31 vol% of the rock. Thus, after calcite cementation (at least in some sandstone beds), only a few percent of interparticle porosity was left.

In the Foster sandstones, because of lack of calcite cementation following the phase of chlorite cementation, compaction and widespread quartz overgrowth continued and reduced porosity to 5–25% .

Stage of Calcite Dissolution

According to MacGowan and Surdam (1990), the organic-acid–anion concentration is increased in sandstone/shale systems within the temperature range of ~80°C to ~120°C—the intermediate burial zone of Surdam and others (1989). As burial progressed, the Spiro and Foster sandstones entered this zone where the organic-acid anions dominated, and calcite cement and bioclasts became unstable and soluble. The incomplete and uneven dissolution of calcite suggests a diagenetic system in which the effects of bicarbonate, carbonate, carboxylic acid, and CO_2 varied both spatially and temporally. Secondary intergranular porosity and moldic porosity that resulted from dissolution of calcite cement and calcite grains ranged from 10% to 30%. After calcite dissolution, further compaction and pressure solution may have reduced secondary porosity by 2%.

Stage of Ferroan-Dolomite and Ankerite Precipitation

At temperatures above 100°C, the rock system was subjected to increasingly elevated partial pressure of CO_2 because of decarboxylation of carboxylic acids, but the pH was still dominated by the monofunctional organic-acid anion (Surdam and others, 1989). The destabilization of Fe-bearing organometallic complexes provided Fe into the diagenetic system (Surdam and others, 1989). The breakdown of smectite to illite in mixed-layer clays may also provide iron and magnesium. During this stage of diagenesis, the ferroan dolomite and ankerite became a stable phase and precipitated as poikilitic and disseminated crystals as the temperature increased. These ferrous carbonates also replaced bioclasts, calcite cement, and other detritus. The varied percentage of $FeCO_3$ (14.8–18.1 wt%, Table 3) in the ferroan dolomite contained in the Spiro may reflect the difference in depth during its formation. The ankerite that contains $FeCO_3$ and $MgCO_3$, totaling about 23 wt% (Table 3) formed later and at a greater depth. Boles (1978) noted that shallow ankerite has an appreciable excess of calcium. The homogenization temperatures of the inclusions in the ferroan dolomite and ankerite show that the ferroan dolomite probably formed at temperatures of 100°C to 120°C, and the ankerite formed at temperatures of 120°C to 130°C, corresponding respectively to depths from 9,200 to 10,500 ft (2,800 to 3,200 m) and from 10,500 to 11,500 ft (3,200 to 3,500 m). The first-melt temperatures (–32°C for ankerite and –27°C for ferroan dolomite, Table 2) of the inclusions in the ferroan carbonates suggest a NaCl-$MgCl_2$-H_2O parent solution. The final-melt temperatures (–9°C and –8°C, Table 2) of the fluid inclusions indicate that the salinity of the host solution was 20–30 wt% NaCl equivalent. Point-count data show that 1% to 8% of the bulk rock volume is occupied by ferroan dolomite and ankerite cements.

Stage of Pyrobitumen Emplacement

Hydrocarbon migration into the porous sandstones followed calcite dissolution. At least a portion of the hydrocarbon was liquid. With increasing depth of burial and temperature, the Spiro and Foster were subjected to an increase in temperature, which has been determined by measuring vitrinite reflectance from the Red Oak field to the Wilburton field (Hathon and Houseknecht, 1987). Some of the vitrinite reflectance values (R_o = 1.49 – 2.25) measured for samples taken

from the wells close to the South Hartshorne field indicate that the highest temperature to which the Spiro was subjected in the study area may have reached 180°C to 300°C. The hydrocarbon maturation reached at least the dry-gas stage. The liquid hydrocarbons were degraded thermally to solid asphalt and gas. The porosity of the reservoirs initially occupied by oil may have been totally or partially obliterated by the pyrobitumen. In the studied gas fields, the pyrobitumen commonly occurs as degradation relicts that partially occupy a few percent of the interparticle porosity.

Later Stage of Quartz Cementation

A second phase of quartz cementation occurred after the formation of the secondary porosity by calcite dissolution and a partial infilling by hydrocarbons. This phase came later than the ankerite. Therefore, the temperature during this stage of diagenesis must have been higher than 130°C. The homogenization temperature (140°C, Table 2) of the fluid inclusions within the quartz cement supports this contention. This later quartz cementation lasted until temperatures higher than 200°C were reached, because this later quartz cement clearly postdated the relict pyrobitumen. After this later quartz-cementation stage, the diagenetic process most devastating to porosity ended, and the porosity of the reservoir sandstones ranged from 8% to 20%.

CONCLUSIONS

1. The Spiro and Foster sandstones in the frontal Ouachita Mountains can be divided into three major sandstone sublithofacies—carbonate-grain–poor, carbonate-grain–bearing, and carbonate-grain–rich sandstones—that were deposited in nearshore marine environments. The Spiro is mainly composed of carbonate-grain–bearing and carbonate-grain–rich sandstones with about equal amounts of limestones. The sandstone in the Foster is dominantly carbonate-grain poor.

2. The sandstones underwent a continuous burial diagenesis that was controlled by connate water, overburden, hydrocarbon maturation, increased burial temperature, and original composition. Compaction, cementation, and dissolution are the main diagenetic processes that influenced the reservoir porosity.

3. The three different sandstone sublithofacies displayed different diagenetic results in response to the burial diagenesis. The carbonate-grain–poor sandstones underwent compaction, pressure solution, and chlorite and quartz cementation. The residual primary porosity after these diagenetic events provided the potential reservoir porosity in the South Panola field. The carbonate-grain–bearing sandstones have been altered mainly by compaction, calcite cementation, and calcite dissolution. Secondary-dissolution porosity after calcite cement formed the major reservoir porosity in the South Haleyville and South Hartshorne fields. The carbonate-grain–rich sandstones that were tightly compacted and locally calcite cemented have poorly developed intraparticle porosity and dissolution porosity.

4. Secondary porosity formed by the dissolution of calcite cement and bioclasts is the result of decreased pH that accompanied maturation of organic matter to petroleum.

ACKNOWLEDGMENTS

We thank Texaco Oil and Gas Company for supporting this study and the School of Geology and Geophysics of the University of Oklahoma for providing research facilities.

REFERENCES CITED

Boles, J. R., 1978, Active ankerite cementation in the subsurface Eocene of southwest Texas: Contributions to Mineralogy and Petrology, v. 68, p. 13–22.

Crawford, M. L., 1981, Phase equilibria in aqueous fluid inclusions: Mineralogical Association of Canada Short Course Handbook 6, p. 75–100.

Davis, D. W.; Lowenstein, T. K.; and Spencer, R. J., 1990, Melting behavior of fluid inclusions in laboratory-grown halite crystals in the systems NaCl-, NaCl-KCl-H_2O, NaCl-$MgCl_2$-H_2O, and NaCl-$CaCl_2$-H_2O: Geochimica et Cosmochimica Acta, v. 52, p. 1019–1025.

Frost, R. W., 1983, The subsurface stratigraphy of the Wapanucka Formation in the Arkoma basin of Oklahoma: Baylor University unpublished M.S. thesis, Waco, Texas, 118 p.

Grayson, R. C., Jr., 1980, The stratigraphy of the Wapanucka Formation (Lower Pennsylvanian) along the frontal margin of the Ouachita Mountains, Oklahoma: University of Oklahoma unpublished Ph.D. dissertation, Norman, 318 p.

Gross, J. G.; and others, 1995, Reservoir description and exploration potential of the Choctaw trend, Arkoma basin, Oklahoma and Arkansas: American Association of Petroleum Geologists Bulletin, v. 79, p. 159–185.

Hathon, L. A.; and Houseknecht, D. W., 1987, Hydrocarbon in an overmature basin, 1. Thermal maturity of Atoka and Hartshorne Formation, Arkoma basin [abstract]: American Association of Petroleum Geologists Bulletin, v. 71, p. 993–994.

Hendricks, T. A.; Gardner, L. S.; Knechtel, M. M.; and Averitt, P., 1947, Geology of the western part of the Ouachita Mountains of Oklahoma: U.S. Geological Survey Oil and Gas Investigation Preliminary Map 66, sheet 1 of 3.

Hinde, L. K., 1990, Stratigraphic facies relationships and structural trends of the Spiro Formation, frontal Ouachita Mountains, southeastern Oklahoma [abstract]: American Association of Petroleum Geologists Bulletin, v. 75, p. 200.

Houseknecht, D. W., 1986, Evolution from passive margin to foreland basin: the Atoka Formation of the Arkom a basin, south-central USA: International Association of Sedimentologists Special Publication 8, p. 327–345.

_____ 1987, The Atoka Formation of the Arkoma basin: Tectonics, sedimentology, thermal maturity, sandstone petrology: Tulsa Geological Society Short Course Notes, 72 p.

Houseknecht, D. W.; and McGilvery, T. A., 1991, Red Oak field, *in* Beaumont, E. A.; and Foster, N. H. (compilers), Structural traps II—Traps associated with tectonic faulting: American Association of Petroleum Geologists

Treatise of Petroleum Geology, Atlas of Oil and Gas Fields, A-107, p. 201–225.

Lumsden, D. N.; Pittman, E. D.; and Buchanan, R. S., 1971, Sedimentation and petrology of Spiro and Foster sands (Pennsylvanian), McAlester basin, Oklahoma: American Association of Petroleum Geologists Bulletin, v. 55, p. 254–266.

MacGowan, D. B.; and Serdam, R. C., 1990, Importance of organic reaction to modeling water-rock interactions during progressive clastic diagenesis, *in* Melchoir, D.; and others (eds.), Chemical modeling of aqueous system II: American Chemical Society Symposium Series 416, p. 494–507.

McBride, E. F., 1987, Diagenesis of the Maxon sandstone (Early Cretaceous), Marathon region, Texas: a diagenetic quartzarenite: Journal of Sedimentary Petrology, v. 57, p. 98–107.

Mou, D. C.; and Brenner, R. L., 1982, Control of reservoir properties of Tensleep Sandstone by depositional and diagenetic facies: Lost Soldier Field, Wyoming: Journal of Sedimentary Petrology, v. 52, p. 367–381.

Pittman, E. D., 1972, Diagenesis of quartz in sandstones as revealed by scanning electron microscopy: Journal of Sedimentary Petrology, v. 42, p. 507–519.

Pittman, E. D.; and Lumsden, D. N., 1968, Relationship between chlorite coatings on quartz grains and porosity, Spiro Sand, Oklahoma: Journal of Sedimentary Petrology, v. 38, p. 668–670.

Surdam, R. C.; and others, 1989, Porosity evolution in sandstone/shale system, *in* Hutcheon, I. E. (ed.), Short course in burial diagenesis: Mineralogical Association of Canada, Montreal, p. 61–134.

Suneson, N. H.; and Campbell, J. A., 1990, Oil and gas exploration in the western Ouachita region, Oklahoma: The Oil and Gas Journal, v. 88, p. 85–87.

Chamosite: A Key Mineral for Interpretation of the Depositional Environment of the Spiro Sandstone

Zuhair Al-Shaieb and Phebe Deyhim
Oklahoma State University
Stillwater, Oklahoma

ABSTRACT.—Chamosite, or iron-rich chlorite, is well documented in sedimentary ironstones and generally agreed to have formed in a particular shallow-marine environment with specific geochemical and sedimentological controls. However, chamosite is not restricted to ironstones. For example, chamosite is a common constituent in several productive Pennsylvanian formations, such as the Spiro sandstone in the Arkoma basin and Springer sandstone in the Anadarko basin.

Chamosite forms penecontemporaneously with deposition or early in diagenesis in several distinct morphologies, including coated grains consisting of concentric laminae around detrital nuclei, granules/nodules, thick pore coatings, and pseudomorphous replacement of bioclastic debris. Under plane-polarized light, chamosite varies in color from light green to light brown. X-ray diffraction analysis shows that the variety with 14 Å basal-spacing is very common; however, a 7 Å chlorite (berthierine) is also present in lesser quantity.

The presence of chamosite in sandstone is highly significant in determining both depositional environment and postdepositional diagenetic history, including reservoir preservation. In the Pennsylvanian sandstones studied, chamosite-rich facies exhibit highly distinctive diagenetic patterns compared with other facies with less clay. Preservation of primary porosity is the common denominator in all chamositic sandstones, whereas quartz overgrowths and/or other types of cements tend to occlude the pore space in the cleaner facies. Thus, differentiation of these Pennsylvanian sandstones into reservoir-quality and tightly cemented types is directly related to the presence of chamosite.

INTRODUCTION

The occurrence of chamosite ooids, peloids, granules, and cements in sedimentary ironstones has been well documented and explained to a fair degree. The notion that these unique sedimentary deposits formed in a somewhat specialized marine environment has been substantiated repeatedly, and the supposed geochemical and sedimentological characteristics of that environment have been reasonably defined. Recently, chamositic ooids, granules, and clay coatings have been observed in some productive Lower Pennsylvanian sandstones of the Arkoma basin in Oklahoma and Arkansas (Fig. 1). It is unlikely that these clastic sequences represent incipient ironstone sedimentation, although they may indicate deposition under similar conditions. The object of this paper is not to critique or propose models for the formation of sedimentary ironstones but rather to apply the viable concepts developed by previous workers to the problem of chamosite occurrence in clastic sequences. For a more comprehensive synopsis of the ironstone problem, the reader is referred to Kimberley (1979, 1980) and Van Houten and Purucker (1984). It is hoped that the following discussion will (1) describe the depositional environment of these sandstones by analogy rather than strict adherence to sedimentary ironstone depositional models, and (2) assess the role of chamosite- and non-chamosite–bearing lithofacies as potential hydrocarbon reservoirs.

GEOCHEMISTRY

The clay mineral chamosite is an iron-rich, 14 Å, trioctahedral member of the chlorite group that resembles and may be genetically related to berthierine, a 7 Å, iron-aluminum, trioctahedral serpentine (Tucker, 1981; Brindley, 1982). Although some workers (Iijima and Matsumoto, 1982; Bhattacharyya, 1983) have contended that the term berthierine should be used for all chamositic minerals, other workers (Bailey, 1980; Van Houten and Purucker, 1984; Curtis and

Al-Shaieb, Zuhair; and Deyhim, Phebe, 2000, Chamosite: a key mineral for interpretation of the depositional environment of the Spiro sandstone, *in* Johnson, K. S. (ed.), Marine clastics in the southern Midcontinent, 1997 symposium: Oklahoma Geological Survey Circular 103, p. 157–170.

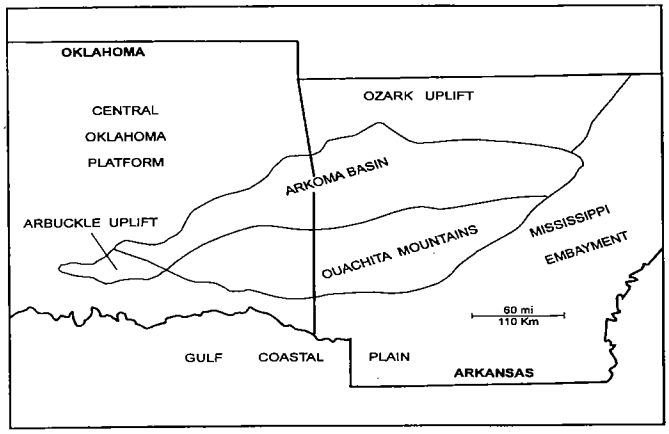

Figure 1. Geologic provinces of eastern Oklahoma and western Arkansas. (After Camp and Ratliff, 1991.)

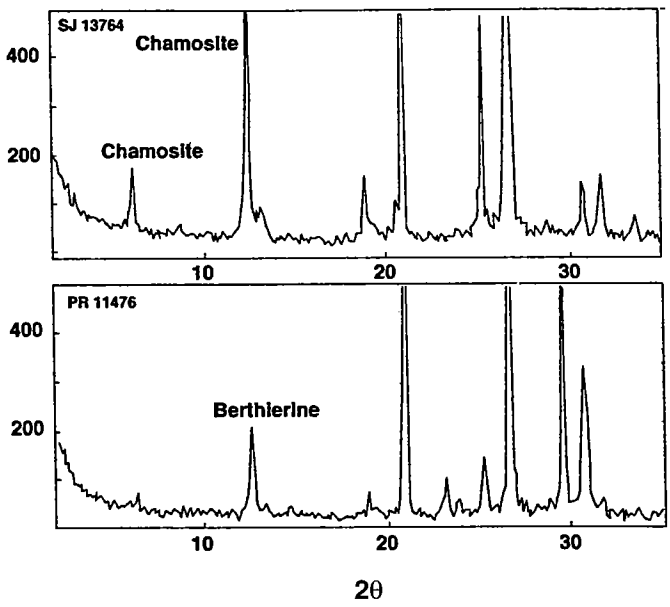

Figure 2. X-ray diffraction patterns of chamosite and berthierine.

others, 1985; Maynard, 1986) have maintained that the name chamosite should be delegated to iron-rich chlorites with a discernable 14 Å basal spacing and that bertherine should likewise be used to identify 1:1-type, layered silicates having only 7 Å basal spacing (Fig. 2).

Uncertainty surrounds the formation of chamosite. Chamositic clays are ferrous silicates and, as such, are theoretically stable only under reducing conditions. It therefore has been hypothesized that chamosite forms either in locally reducing, anoxic-marine settings or as the result of diagenetic alteration of a precursor that was stable under normal oxic-marine conditions. Chamosite is commonly found in rocks of normal shallow-marine facies. These deposits are characteristic of settings that are typified by normal pH and positive values of Eh (oxidation potential) in the water column (Curtis and Spears, 1968). Thus, it is unlikely that chamosite would have formed as a primary stable precipitate in these settings. Currently, the consensus is that chamositic ooids, peloids, and clay films formed as a product of the early anoxic alteration of a gelatinous precursor cf $Fe(OH)_3$, $Al(OH)_3$, and $SiO_2 \cdot nH_2O$ that was presumably stable in normal oxic-marine settings (Tucker, 1991). Velde and others (1974) and Odin and Matter (1981) further specify that 7 Å berthierine probably formed first and diagenetically alters to 14 Å chamosite with time. Other workers (e.g., Bhattacharyya, 1983) suggest that chamositic clays and ooids are the possible alteration products of detrital kaolinite. Questions as to the mode of formation and the mechanism of iron supply and enrichment are yet unresolved. It is likely that intense weathering of continental landmasses supplied the iron via fluvial systems. A comprehensive list of the various iron-enrichment models can be found in Kimberley (1979, 1980).

FORMATION OF CHAMOSITIC CLAYS

Chamositic clay commonly occurs in sedimentary ironstones as ooids, peloids or granules, pore-filling and grain-coating clays, films, and replacements after fossil fragments (Van Houten and Purucker, 1984). All of these morphologies are manifest in the sandstones of this study. Chamositic ooids in thin section exhibit concentric laminae of tangentially arranged clay particles (Rohrlich, 1974). Van Houten and Purucker (1984) propose that coatings of a quasi-chamositic Fe-Al-Si gel were mechanically layered onto the surface of the proto-ooid as the grains were lying on a soft, muddy substrate and being jostled by currents above. Many of these ooids—termed spastoliths—are commonly stretched and flattened parallel to bedding, suggesting that they were malleable at the time of deposition (Tucker, 1981). Diagenetic alteration of these gelatinous ooids to more ordered and stable 14 Å chamosite would presumably occur in the low Eh regimes that exist some distance below the sediment-water interface (Tucker, 1981). Similar methods of formation are invoked for the formation of peloids and clay films. Peloids may be either of fecal origin or consist of clay floccules (Van Houten and Purucker, 1984). Clay films may form from early coating of detrital grains by the chamositic gel or by clay infiltration following burial. Replacement of skeletal debris, notably echinoids, was probably accomplished by the coating and filling of shell pores by the clay-gel and later replacement of calcite or aragonite by chamosite.

In summary, chamosite formed through the alteration of a malleable gelatinous precursor, and chamosite clay films may have formed locally as a primary precipitate in water-filled pore spaces beneath the sediment/water interface, where negative Eh values are commonly encountered.

GEOLOGIC SETTING OF THE ARKOMA BASIN

The Arkoma basin is an east-west–trending, arcuate foreland basin that lies adjacent to the northern front of the Ouachita fold belt in Arkansas and Oklahoma

(Fig. 1). The basin has an asymmetrical trough-shaped profile that deepens from its northern limits along the Ozark dome and the central Oklahoma platform toward its thrusted southern margin along the frontal zone of the Ouachita fold belt.

The Arkoma basin is genetically related to the Ouachita fold belt, and the history of sedimentation within the basin reflects the changes in the tectonic character of the Ouachita region throughout most of the Paleozoic. Upper Cambrian to Lower Pennsylvanian carbonates, sandstones, and shales were deposited on a shelf along a passive- and rifted-continental margin (Houseknecht, 1987). Deep-marine shales, bedded chert, and submarine-fan deposits of Mississippian to Late Pennsylvanian age constitute a flysch assemblage that was deposited in a rapidly subsiding basin concomitant to the southward subduction of the North American trailing edge. This subduction may have been affected by the northern migration of an island arc or continental mass toward the Ouachita region (Morris, 1974; Briggs, 1974; Graham and others, 1976; Houseknecht and Kacena, 1983). Consumption of the remnant ocean basin culminated in the late Atokan with the thrusting of the northward-advancing subduction complex onto the trailing southern edge of North America. Subsequent east-west–trending, down-to-the-south, normal faulting occurred, cutting the entire Paleozoic section as well as the basement rock. These faults greatly affected sediment dispersal within the basin. Typical molasse facies of late Atokan and Desmoinesian age represent the foreland stage of basin development, during which the Arkoma basin achieved essentially its present-day architecture.

ATOKAN STRATIGRAPHY

The Atoka Formation (Fig. 3) typically contains seven major sandstone sequences, which, in ascending order, are the Spiro (or Cecil Spiro), the Paul Barton, the Dunn, the Jenkins, the Sells, the Vernon, and the Casey sandstones. Houseknecht (1987) suggested that the sandstones of the Atoka Formation represent a transitional stage of deposition between the earlier passive-margin and later foreland-type deposits. The basal Atokan Spiro sandstone probably represents the last stage of deposition upon the stable Atlantic-type passive margin. The Atoka Formation unconformably overlies the Wapanucka Limestone (Morrowan) and the sandstones of the Bloyd Formation (Morrowan) and is overlain throughout the axial part of the basin by the Hartshorne Formation and the McAlester Formation, both of Desmoinesian age (Zachary and Sutherland, 1984) (Fig. 3).

DEPOSITIONAL MODEL OF THE CHAMOSITE-BEARING SPIRO SANDSTONES

Reliable determination of depositional environments requires a detailed knowledge of the geological setting in which a rock unit formed. Ideally, petrographic analyses should be coupled with detailed subsurface mapping and correlation of individual sandstone bodies

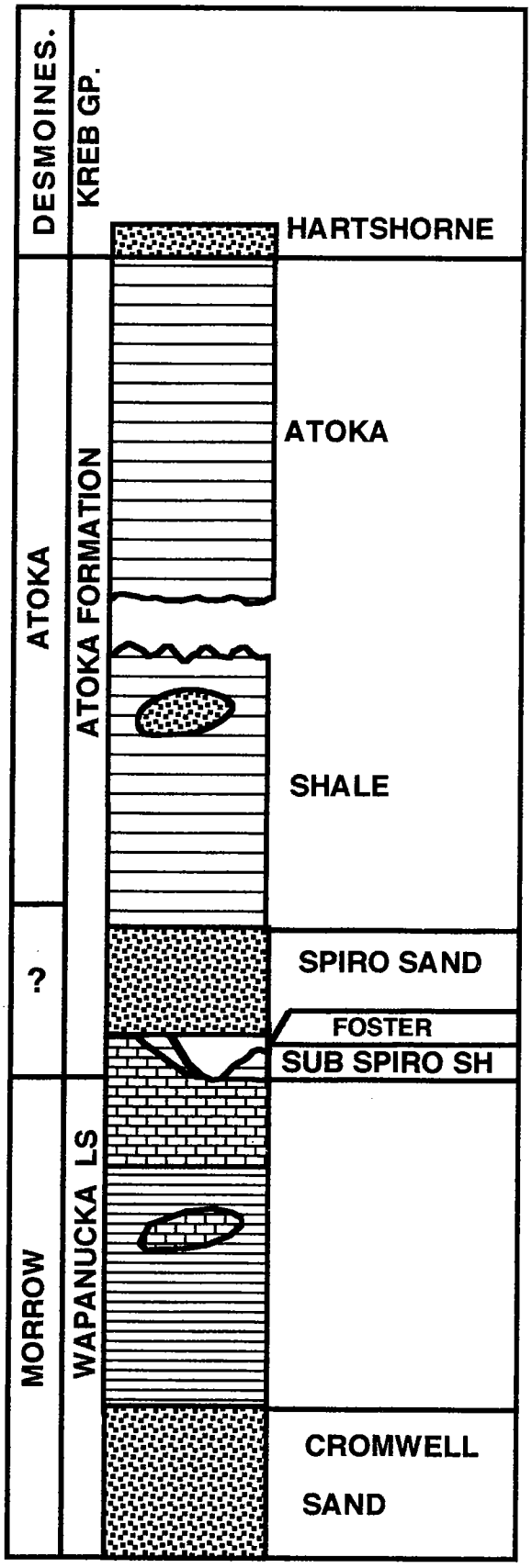

Figure 3. Generalized stratigraphic column of the Arkoma basin, showing stratigraphic position of Spiro sandstone.

to determine the regional development of sediment trends. This type of analysis requires a vast store of data and is quite beyond the scope of this study. However, the data obtained from the cores analyzed can prove invaluable in establishing a depositional model and commonly can be used to construct a vertical succession of facies changes within the area immediately adjacent to the wellbore from which the core was obtained.

Fossil fragments, glauconite, chamosite, and collophane were detected in varying amounts in the four cores of Spiro sandstone from the Wilburton field of southeastern Oklahoma (Fig. 4). These detrital and diagenetic constituents are considered indicative of deposition under marine conditions. Moreover, Porrenga (1966) suggests that chamosite forms in tropical waters at depths ranging from 30 to 500 ft, and that glauconite forms typically in deeper (100–2,400 ft) and relatively cooler water (Heckel, 1972).

Chamosite pellets were observed in two of the Spiro sandstone cores and the Sells sandstone core, whereas glauconite was found in one Spiro core. Thus, the above-described constituents suggest very strongly that the Spiro sandstones were deposited under shallow-marine conditions. Facies analysis of the Spiro sandstone in the available cores is based on the assemblage of sedimentary structures and the occurrence of the aforementioned detrital and diagenetic constituents. The sandstones of the Spiro in the study area were deposited in what is termed the Wilburton embayment. The major facies observed are incised valley-fill channel sands, tidal channels with associated tidal mud, silt, and sand-flat deposits, and marine bars on tidal-ridge complexes.

During the late Morrowan, a marine regression exposed the upper Arkoma shelf, resulting in the incision of valleys into the sub-Spiro shale and locally into the underlying Wapanucka Limestone. The sediments were transported across the shelf by these valleys. In the early Atokan, a northward marine transgression resulted in the backstepping and infilling of the valleys. In this environment, chamositic facies were dominant in the more restricted nearshore environment of the embayment, whereas glauconite facies occurred in the more-agitated offshore facies (Fig. 5).

PETROLOGY, PETROGRAPHY, AND DIAGENESIS OF THE SPIRO SANDSTONE

Four cores were examined in the vicinity of Wilburton field, Latimer County, Oklahoma (Fig. 4). Each core was slabbed and logged using specifically designed

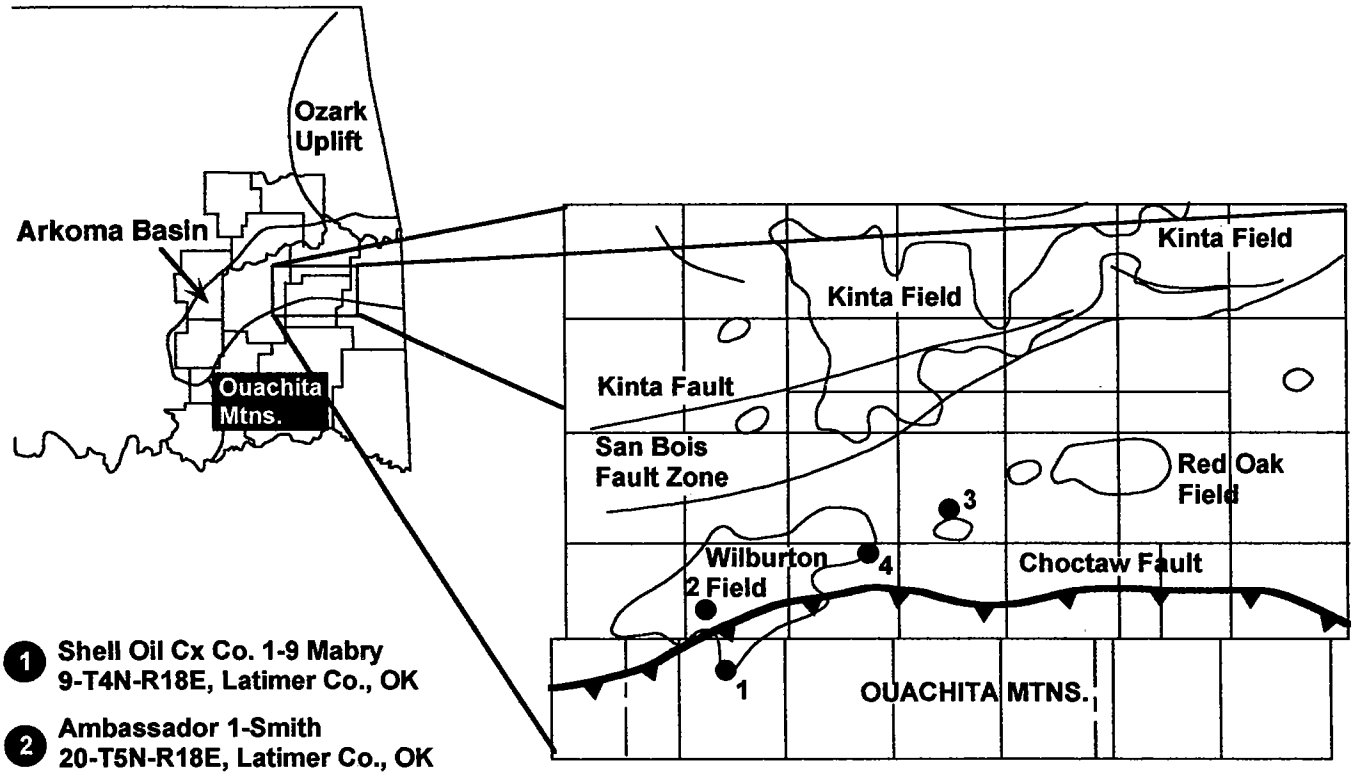

Figure 4. Index map of study area showing core locations.

petrolog to show stratigraphic intervals, depth, lithology, sedimentary structure, color, grain size, sorting, porosity, constituents, and location of samples selected for thin section and other analyses. The Spiro is very fine to medium-grained sandstone that is moderately to well sorted. Quartz is the major constituent, although feldspar, rock fragments, and skeletal fragments are present in subordinate amounts. Quartzarenite, sublitharenite, and calcarenaceous sand were the major sandstone lithologies observed. Chamosite and glauconite are present, and collophane is a minor constituent.

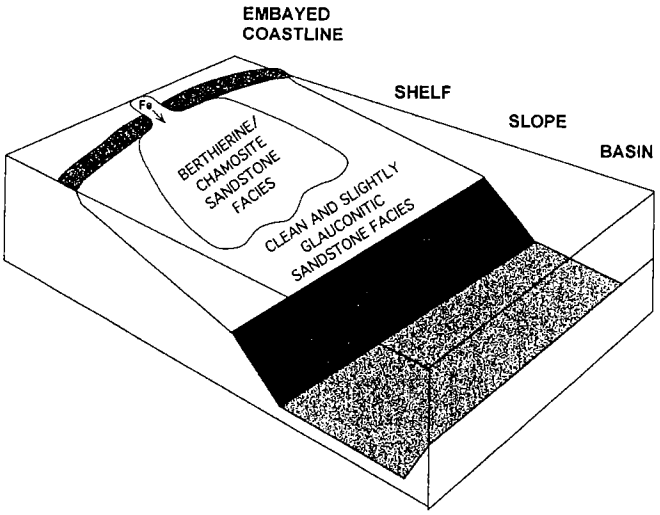

Figure 5. Schematic block diagram of an embayment showing the distribution of iron-bearing minerals, especially the chamositic and glauconite facies.

Major Primary Grain Constituents

The most abundant grain type in the Spiro sandstone is quartz. Most of the quartz grains are single crystals with uniform extinction. Vacuoles and inclusions are present in minor amounts. Most of the polycrystalline quartz observed represents either a metamorphic or sedimentary source. Very fine to fine-grained sand is the dominant grain size of most sandstones, although other grain sizes (i.e., medium) are present. Plagioclase and K-feldspar are present in minor amounts. Plagioclase grains are easily identified by their albite twinning (Fig. 6). Untwinned orthoclase is identified by its cloudy appearance due to alteration. Perthite and microcline are less common than orthoclase in the Spiro sandstone. Rock fragments are not very common in the Spiro. Metamorphic and sedimentary fragments are the dominant type.

Other Primary Grain Constituents

A variety of bioclastic materials occur within the Spiro sandstone (Fig. 6). Their percentages range from trace to amounts typical of calcarenaceous sandstone. Fossil types include echinoderm plates and columnals, brachiopod shells and spines, and bryozoan fragments. Trilobites, ostracodes, gastropods, fusulinids, and coral

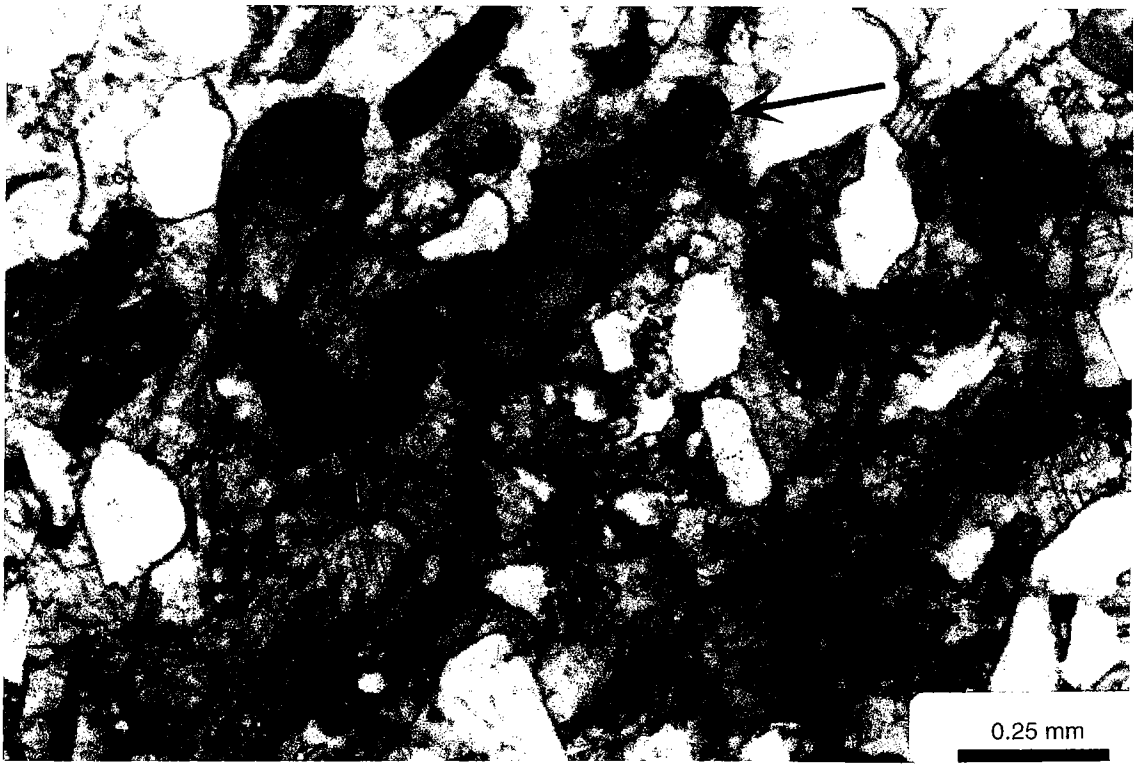

Figure 6. Typical calcarenaceous sandstone with fossil fragments. Note the infilling of chamosite (arrow). (Plane-polarized light.)

fragments occur in lesser quantities. These bioclasts range in size from medium pebbles to medium-grained sand.

Collophane grains are not common and are characterized by a reddish-brown color in plane-polarized light; they are isotropic under crossed nicols. Collophane grains are present as phosphatic brachiopods and other skeletal fragments. Muscovite, biotite, zircon, illite, rutile, and other minerals are present in minor amounts. Detrital clays are also present as components of true matrix and/or pseudomatrix. The latter was formed by ductile deformation of soft fragments, such as chamosite, glauconite, and shales.

Diagenetic Constituents

Sandstones that are not cemented in early diagenesis generally show signs of compaction and grain deformation. Elongated muscovite crystals are bent or may be fractured by harder grains. Chamosite and glauconite were deformed during compaction and flowed between quartz grains forming pseudomatrix. Styolitic surfaces are very common and are generally associated with higher clayey matrix and organic matter. Pyrite commonly occurs along styolites. Partial dissolution of quartz and other grains along styolites is evidence of pressure solution. The compaction features of the Spiro sandstones account for the partial reduction of their primary porosity.

Chemical diagenesis has significantly further modified the Spiro sandstone. These rocks have undergone several cementation and dissolution episodes. Although these modifications are common diagenetic features exhibited in the Spiro sandstones, drastic local variations may be related to the original sediments composition and textures.

Silica Cements

Silica cements in the form of syntaxial quartz overgrowths are very common in the Spiro sandstone (Fig. 7). The overgrowth is separated from the detrital grain by a "clayey rim" that consists mainly of an early diagenetic product such as chlorite and, to a lesser extent, illite. Lumsden and others (1971) indicated that early chlorite coating on quartz grains inhibited the formation of quartz overgrowth and retarded the pressure-solution features. Where several quartz grains occur together in clusters, the contacts between adjacent overgrowths are sinuous and irregularly compromise boundaries, produced by mutual interference during crystal growth. In few cases are the boundaries between detrital grains and overgrowth cement indistinct. Advanced stages of overgrowth occur where sandstones are clean and contain small amounts of clay and relatively high amounts of quartz. Chalcedony is a minor cement but occurs in several episodes and, in some instances, replaces the grain.

Carbonate Cements

Calcite cement is present in several forms. It varies from being patchy or spotty to being widespread. The

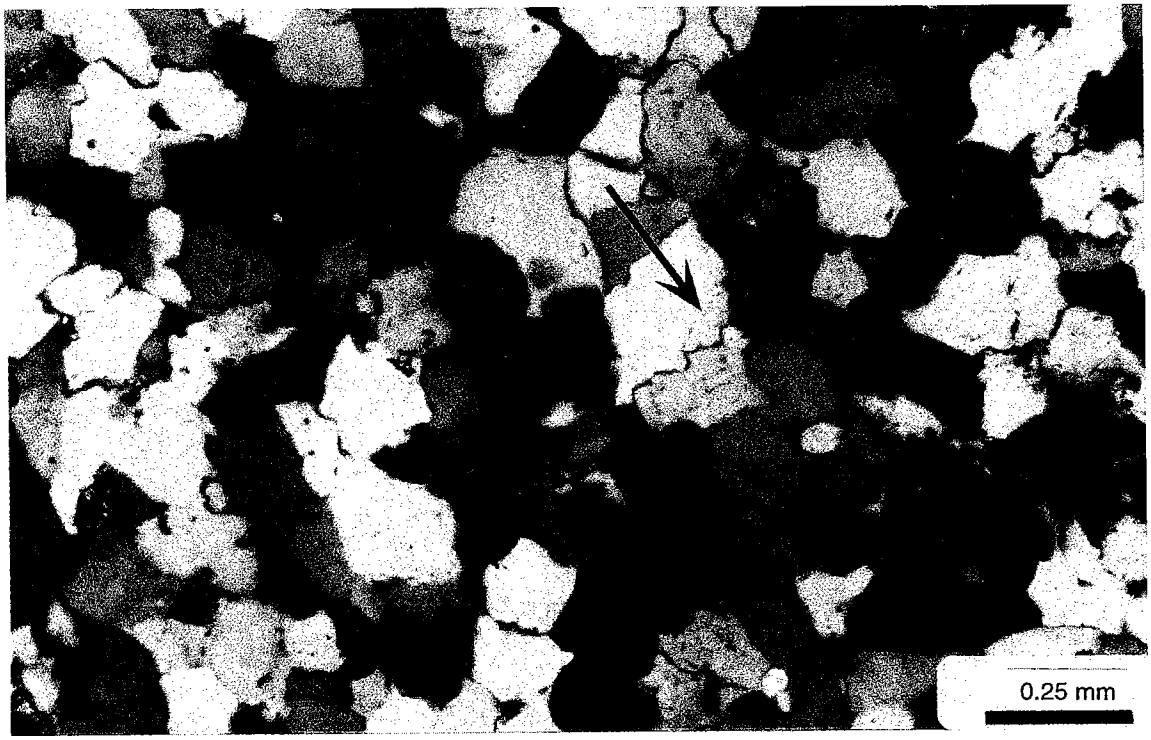

Figure 7. Syntaxial quartz overgrowth separated from detrital grains by clay rim (arrow); pressure-solution along stylolite to the left. (Plane-polarized light.)

latter condition is exhibited by quartz grains floating in calcite cement to form poikilotopic texture (Fig. 8).

Two types of dolomite were observed. Early small hypidiotopic rhombs replace authigenic clays, lining pores and coating detrital grains. The late-stage dolomite consists of large idiotopic rhombs that are infilled voids (Fig. 9). Some of the dolomite is ferroan (ankerite).

Siderite is a minor constituent and occurs as subhedral to euhedral crystals (Fig. 10), genetically associated with chamosite pellets.

Chamosite Pellets

Chamosite is an iron silicate with a structure similar to that of chlorite. Chamosite has a green color and a low birefringence. It typically occurs as ooids; however,

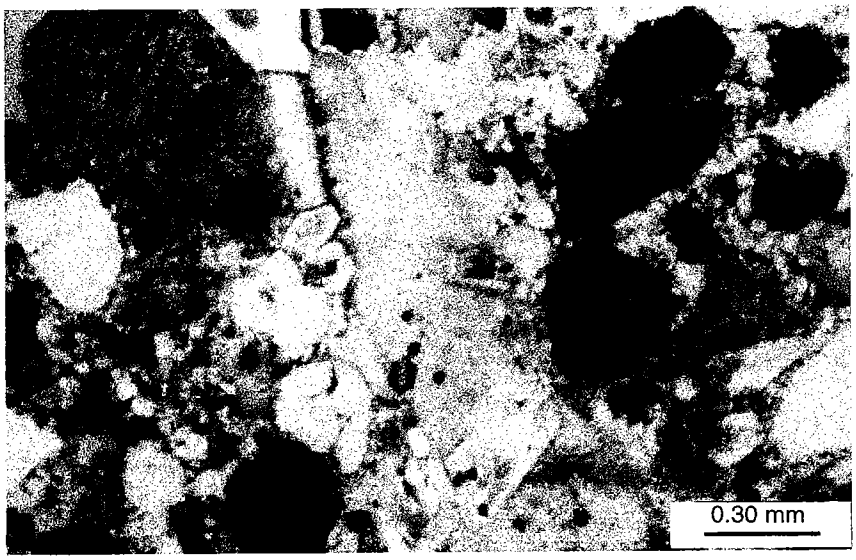

Figure 8. Poikilotopic calcite cement displacing and replacing quartz grains. (Crossed nichols).

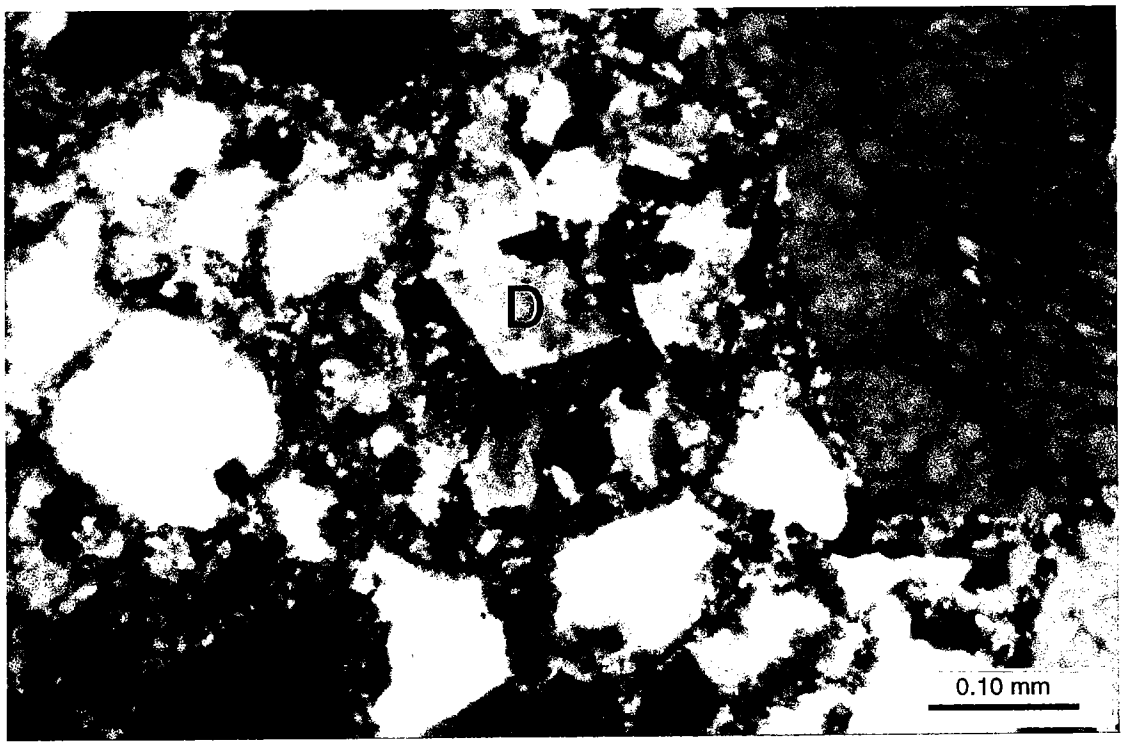

Figure 9. Late-stage pore-filling euhedral dolomite (D). (Crossed nichols.)

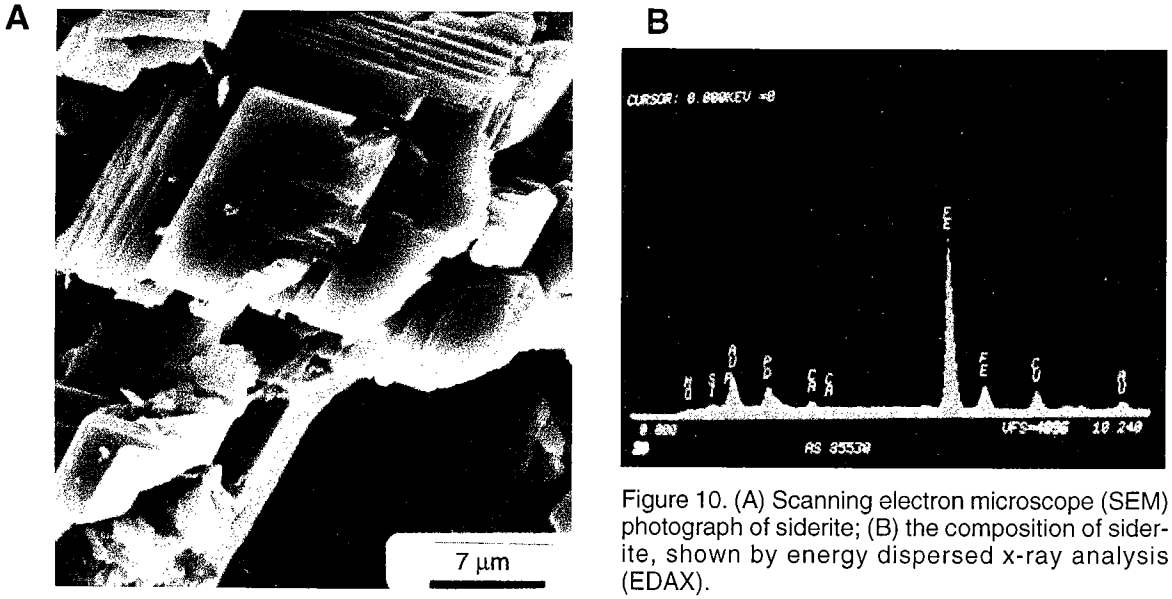

Figure 10. (A) Scanning electron microscope (SEM) photograph of siderite; (B) the composition of siderite, shown by energy dispersed x-ray analysis (EDAX).

it also forms flakes and pellets and is finely disseminated in mudrocks. It has been suggested that chamosite is precipitated as a mixed gel of $Fe(OH)_3$, $Al(OH)_3$, and $SiO_2 \cdot H_2O$, which is stable under positive Eh (Tucker, 1981). It is thought that chamosite gel is carried by rivers, stabilized by colloidal organic substances, and absorbed on clay minerals. These colloids carry positive charges, and, on entering the sea, they become flocculated and precipitation soon follows. Conversion of this gel to chamosite would take place after burial within the reducing environment beneath the sediment-water interface.

Chamosite occurs as pellets in the Spiro sandstone (Figs. 11 and 12). They are typically green; however, partially altered chamosite changes in color to yellow and golden brown with darker limonitic zones. The pellets will be almost opaque when they are totally replaced by limonite. Siderite occurs as brown stains—that may or may not exhibit well-crystalline habits—within or near the outer margin of the pellets. Siderite is identified by its high birefringence. Chamosite pellets were originally soft and are commonly deformed or flattened (Fig. 12A). When severe deformation occurred, a pseudomatrix would form.

Glauconite

Glauconite occurs as rounded pellets, which are aggregates of small crystals and are easily identifiable by their bright green color (Fig. 13). Glauconite has a moderate birefringence. Some green glauconite may be altered partially or completely to brown glauconite. The brown color results from oxidation of the ferrous iron in glauconite.

Clay Minerals

Chamosite, or iron chlorite, is the most abundant diagenetic clay mineral present. Two stages of chlorite were observed in the Spiro sandstone. An early stage occurs as pellets and as a coating on quartz grains, as discussed earlier. The morphology of this stage ranges from poor near the grain boundaries to moderately crystalline in an outwardly direction. The late stage of chamosite is typically authigenic and is characterized by well-developed crystal morphology (Fig. 14). Authigenic illite is the most abundant clay in rocks with very low chamosite content.

Pyrite

Pyrite occurs as cement or along styolites associated with higher organic content.

Organic Matter

Organic matter was observed in the majority of the thin sections examined. Their content ranges from trace to >9%. Organic matter occurs in seams, along styolites, and as pyrobitumen in pore spaces (Fig. 11). The brown to black color is a function of thermal maturation and the type of organic matter.

Porosity

Both primary and secondary porosity types were observed in the Spiro sandstone. Volumetrically, secondary porosity is as significant as primary porosity. It is important to recognize that primary porosity has provided avenues for pore-fluid migration, which has resulted in partial or complete dissolution of metastable constituents to generate secondary porosity. During the course of this investigation, some differences between estimated thin-section porosity and measured core-lab porosity were observed. Perhaps the only way to examine this relationship is to cut a thin section of the same plug used to measure porosity.

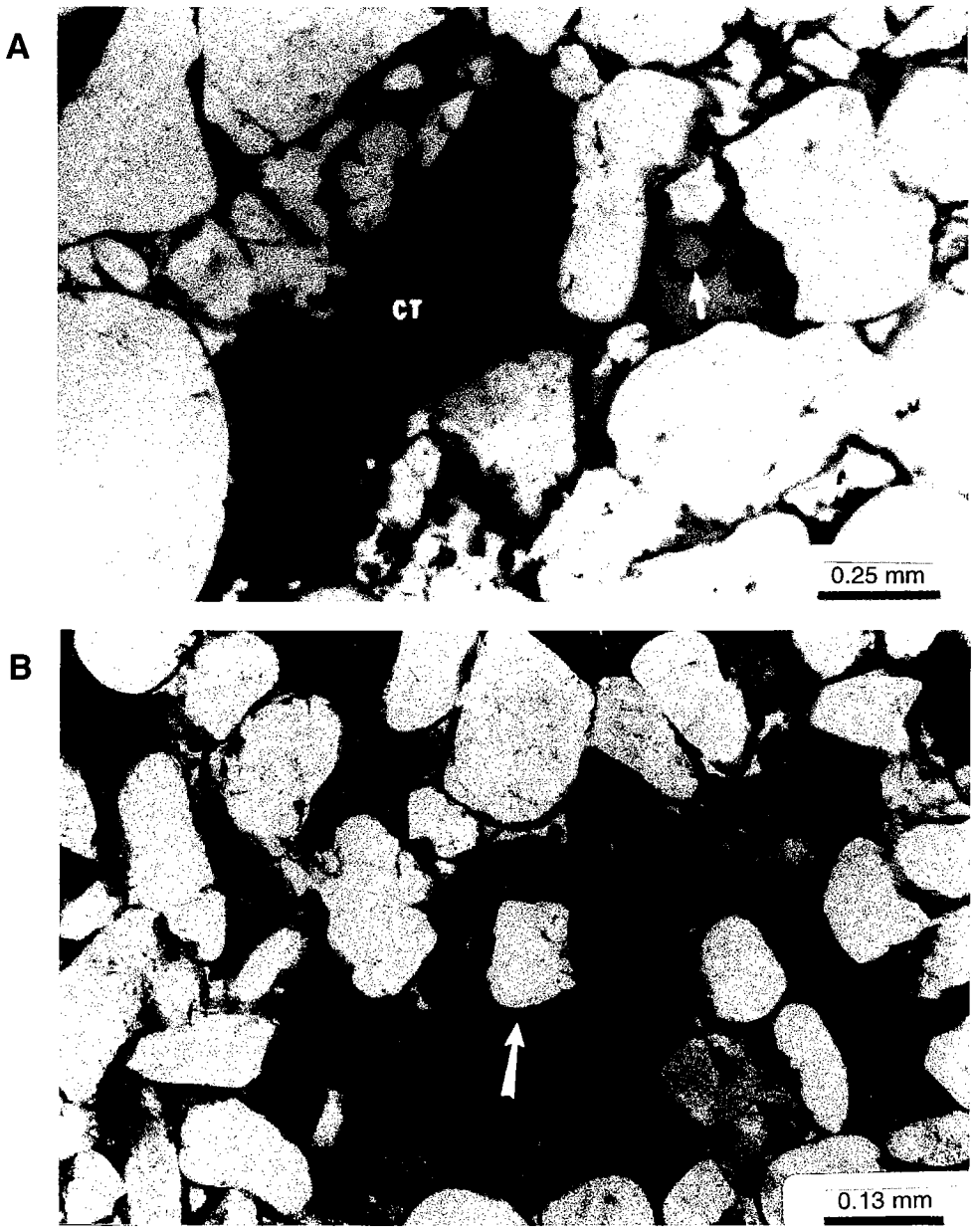

Figure 11. (A) Green chamosite pellet (CT); pyrobitumen in spore space (arrow). (B) Chamosite ooid (arrow). (Plane-polarized light.)

Primary Porosity

Intergranular porosity is considered the most common primary porosity. However, this type was modified by compaction, cementation, and dissolution. Complete preservation of the original primary porosity is rare (Fig. 15). In very clean sandstone, destruction of primary porosity by quartz overgrowths is very common. Primary porosity was preserved where the quartz grains were lined with thick coats of early-stage chamosite. It is very evident that both syntaxial quartz overgrowth and pressure solution roles in the destruction of primary porosity were minimal. Illite coats may have played a similar role. Figure 16 shows the positive correlation between core-lab porosity and the total chamosite content.

Secondary Porosity

Secondary porosity is a very significant type observed in the Spiro sandstone. It can be attributed to the partial and/or complete dissolution of metastable siliceous constituents. The development of secondary porosity may depend largely on the composition and texture of the sandstones. Partial dissolution, oversized and elongated pore spaces, and enlarged intergranular porosity are the major configuration of the secondary

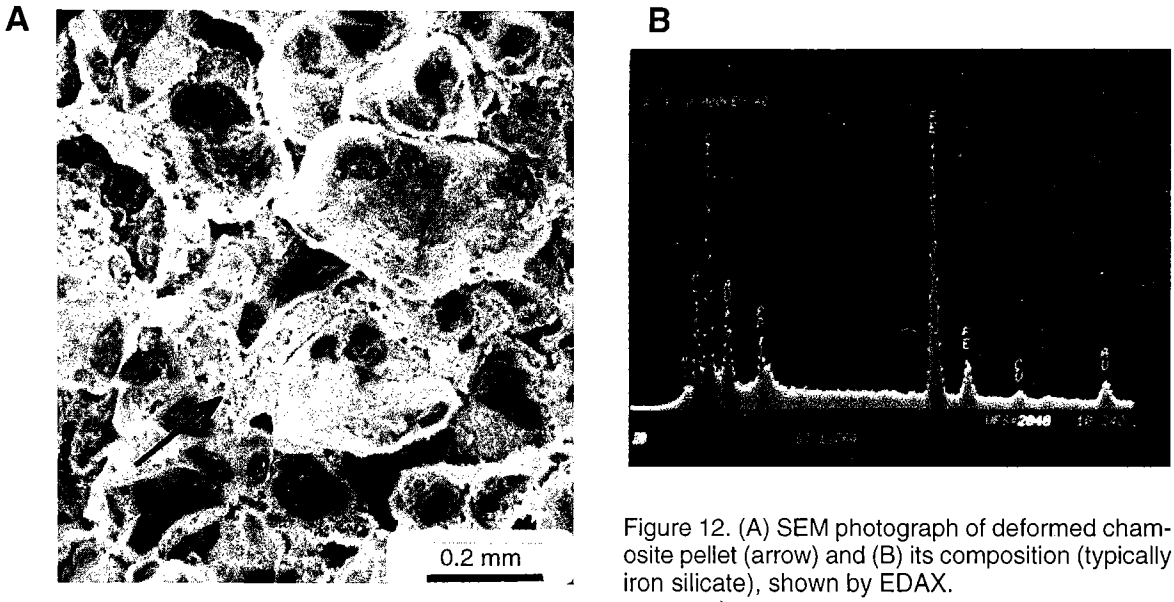

Figure 12. (A) SEM photograph of deformed chamosite pellet (arrow) and (B) its composition (typically iron silicate), shown by EDAX.

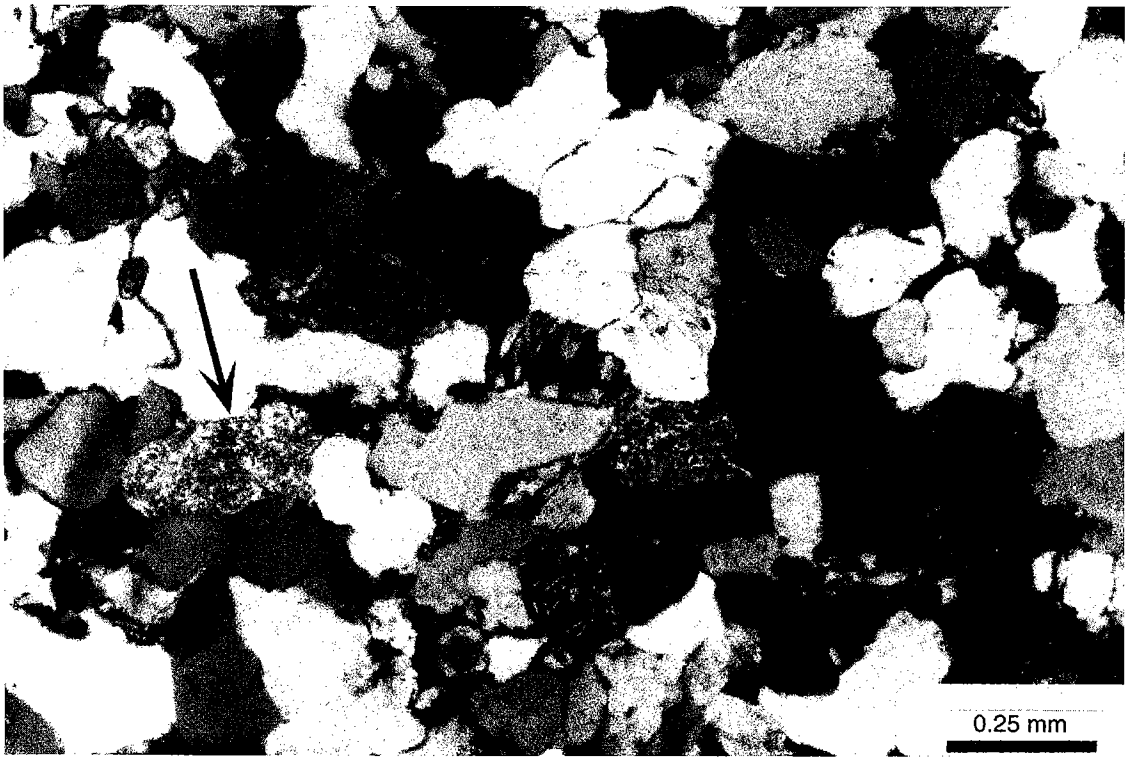

Figure 13. Green glauconite pellet (arrow) rimmed by high-birefringent illite. (Crossed nichols.)

pores. It is important to recognize that early-stage chamosite pellets played a significant role in the process of secondary-porosity development. Although partial dissolution of chamosite pellets was observed, formation of oversized pores is somewhat complex and may be due to the dissolution of multiple chamosite pellets and chamosite matrix. Elongated pore spaces may be formed as the result of dissolution of deformed chamosite pellets (Fig. 17) or dissolution of material (i.e., organic material, pyrite, and clay) along styolites. Moldic porosity was present in intervals where skeletal fragments were abundant. Dissolution of calcite cement is considered a very minor feature. Microporosity was developed when available pore space was loosely filled with late-stage chamosite and/or illite and kaolinite.

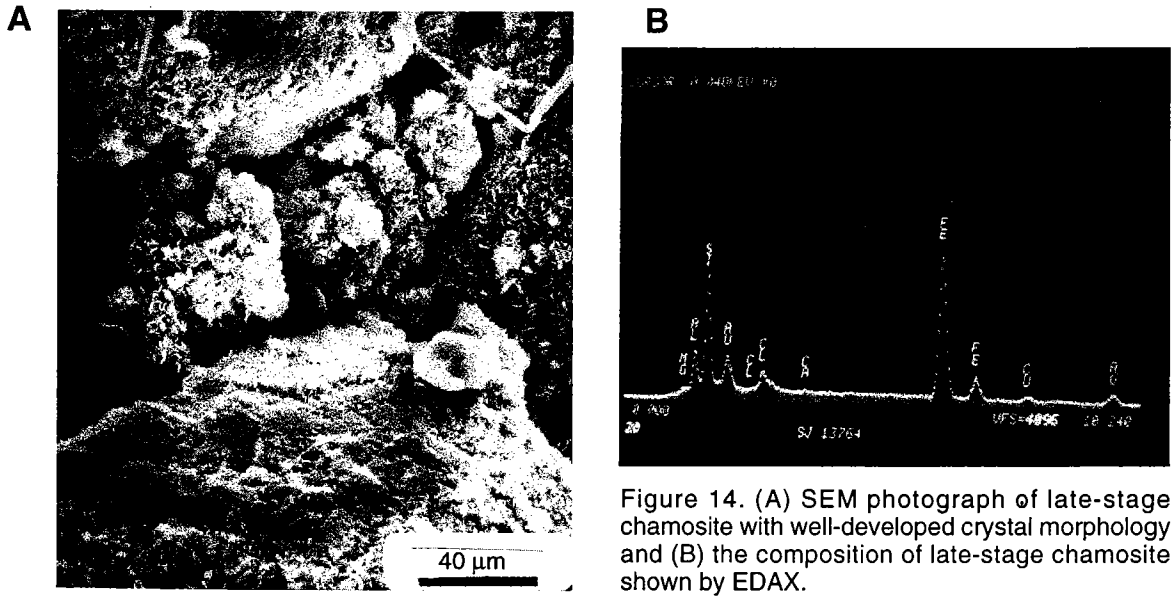

Figure 14. (A) SEM photograph of late-stage chamosite with well-developed crystal morphology and (B) the composition of late-stage chamosite shown by EDAX.

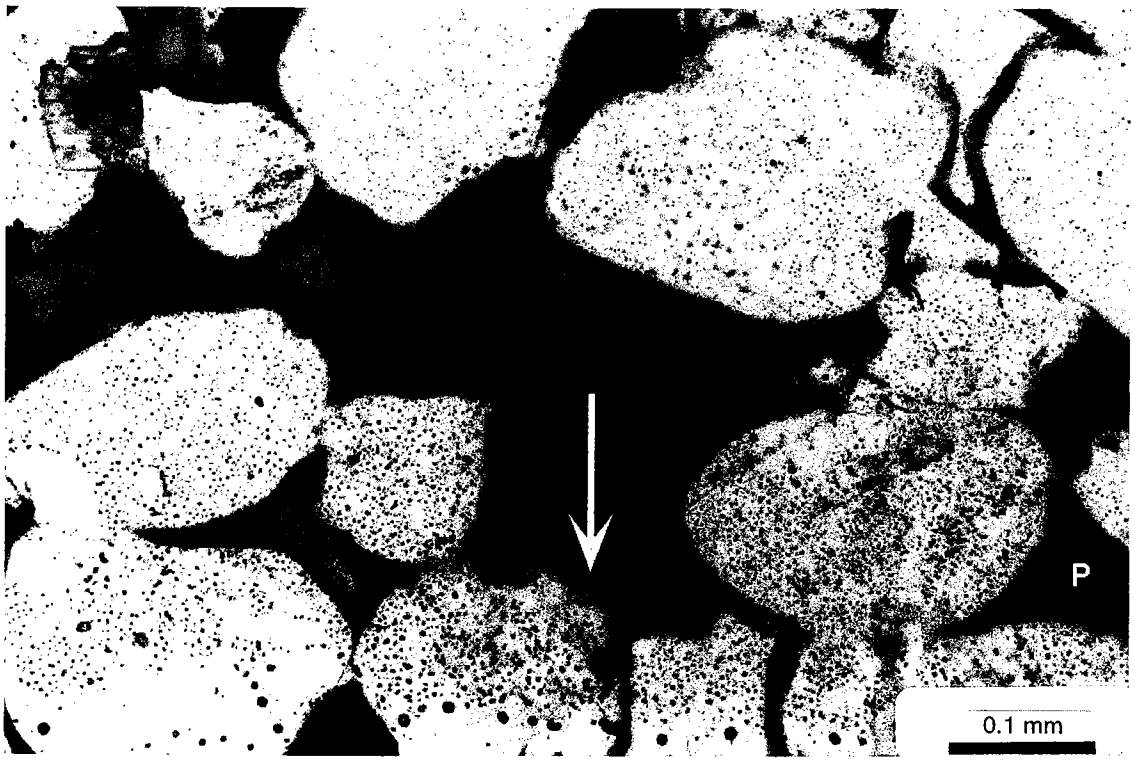

Figure 15. Preserved primary pore space (P) with thick coat of chamosite (arrow).

Diagenetic History

Diagenesis of the Spiro sandstones was initiated shortly after deposition just below the sediment-seawater interface. Soft, diagenetic chamosite pellets were in part flattened and deformed and infiltrated pore spaces. Quartz grains in chamosite rich zones were coated with thick coats of chamosite. In a relatively chamosite-poor environment, quartz grains remained relatively clean. In this early stage, siderite was observed to be associated with chamosite. Subhedral dolomite/siderite rhombs appear to nucleate and perhaps replace early diagenetic chamosite coating quartz grains. With increasing depth of burial,

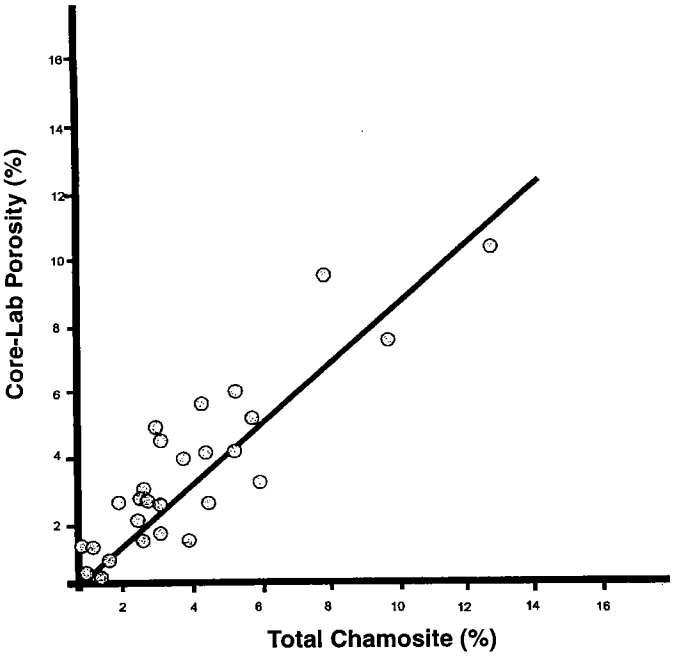

Figure 16. Plot of core-lab porosity (%) versus total chamosite content (%). Note strong linear correlation.

compaction processes—such as ductile deformation of soft constituents and rearrangement of original grains—were early processes, which reduced part of the primary porosity.

Quartz overgrowth represents a significant diagenetic stage with drastic effects on primary porosity. Syntaxial quartz overgrowths are very common in clean Spiro sandstone with "clay rims" that separate overgrowths from detrital quartz grains. Where the dust rims are not present, the overgrowths are not readily distinguishable. Advanced stages of overgrowths generally occluded pore space completely. On the other hand, quartz grains with thick coats of chamosite or illite will inhibit the nucleation process, and overgrowth will be minimal. In addition, the thick coats of clay will also retard pressure solution related to fluid circulation. It is also observed that when early dolomite and/or siderite replaces clays, overgrowth nucleation takes place, and silica is able to infill voids with dolomite and/or siderite rimming detrital grains. Calcite cement followed the quartz-overgrowth stage. Poikilotopic and mosaic calcite were common in clean, quartz-dominated sandstone. Syntaxial calcite overgrowth was observed around skeletal grains, such as crinoid bioclasts and bryozoans. Calcite cement was minor in chamosite-rich facies. By the end of this stage, porosity was completely obliterated in clean-sandstone facies by either quartz overgrowths or carbonate cements. However, significant portions of primary porosity were still preserved in the relatively clay-rich (chamosite and illite) sandstones. It is also important to note that diagenetic fluids up to this point may be described as "Constructive Type Fluids." On the other hand, hydrogen-ion–rich fluids may have been generated during thermal maturation of organic matter with increasing depth of burial. The hydrogen ions may be supplied by organic and/or carbonic acids (Carothers and Kharaka, 1978; Surdam and others, 1984; Al-Shaieb and Walker, 1987). These fluids could be described as "Destructive Type Fluids." The only available avenues for migration of these fluids were areas with preserved primary porosity. Hence, these fluids

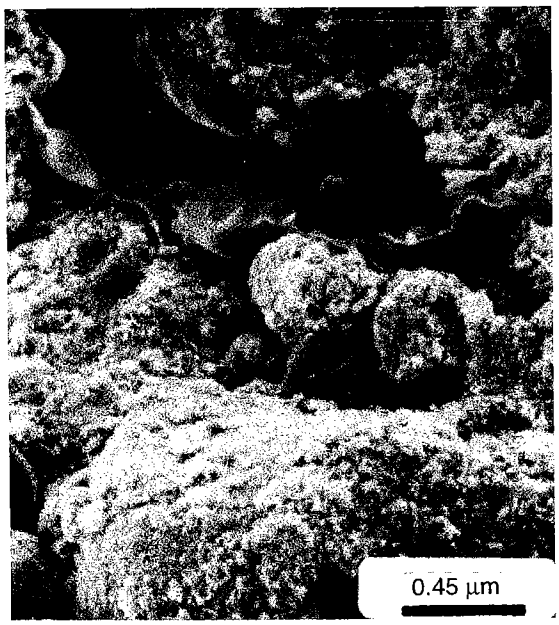

Figure 17. SEM photograph of an elongated pore space in Spiro sandstone.

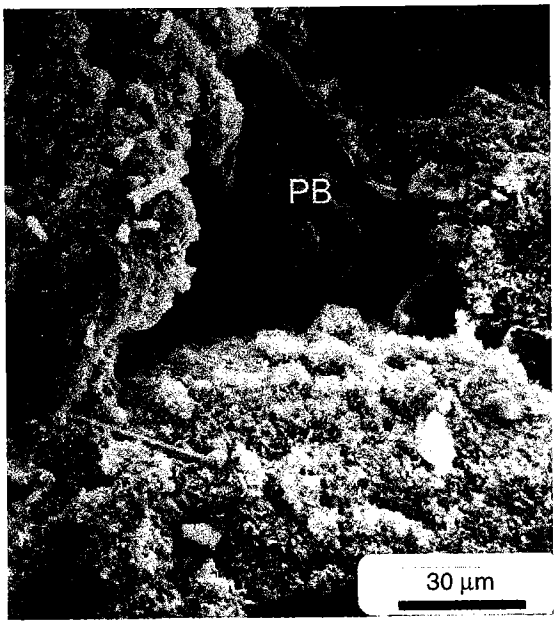

Figure 18. SEM photograph of pyrobitumen (PB) in a pore space in Spiro sandstone.

would leach siliceous components, such as chamosite and/or glauconite, along their paths. The result was partial to complete dissolution of these constituents and development of secondary porosity phase. However, in sandstones with extensive silica and/or calcite cements, Destructive Type Fluids were unable to migrate through. Moldic porosity was also observed where skeletal fragments were abundant. It is also significant to emphasize that extensive dissolution of calcite cement was not observed as suggested by Houseknecht (1987), and the contribution of the process to the porosity in the Spiro sandstone was very minor.

Following this stage, liquid hydrocarbons migrated into available voids. The oil residues can be described in thin section as pyrobitumen (Fig. 18). Another stage of quartz overgrowth followed hydrocarbon migration.

A late stage of authigenic chamosite with well-developed crystal morphology was precipitated in the available pore space. Ankerite occurs at this stage as pore filling and replacement of early carbonates. Pore-filling kaolinite was observed only in a few samples. Figure 19 shows the relationship between the various diagenetic stages and the porosity preservation and/or development in the Spiro sandstone.

CONCLUSIONS

In conclusion, berthierine and chamosite are penecontemporaneous to early-diagenetic minerals. They are considered as indicators of shallow-marine (coastal-embayment) deposition. Chamositic reservoirs exhibit a distinct diagenetic pattern. Thick clay coatings of quartz grains were the major process in preserving primary porosity in the chamosite-bearing Spiro sandstone. On the other hand, the cleaner and glauconitic sandstone showed substantial amounts of silica cementation and drastic decreases in porosity. Therefore, chamositic facies are the only hydrocarbon reservoirs in the Wilburton field area.

ACKNOWLEDGMENTS

We would like to thank Amy Close, Brad Brittain, Ryan Birkenfeld, and Melanie McPhail for their help in preparation of this manuscript.

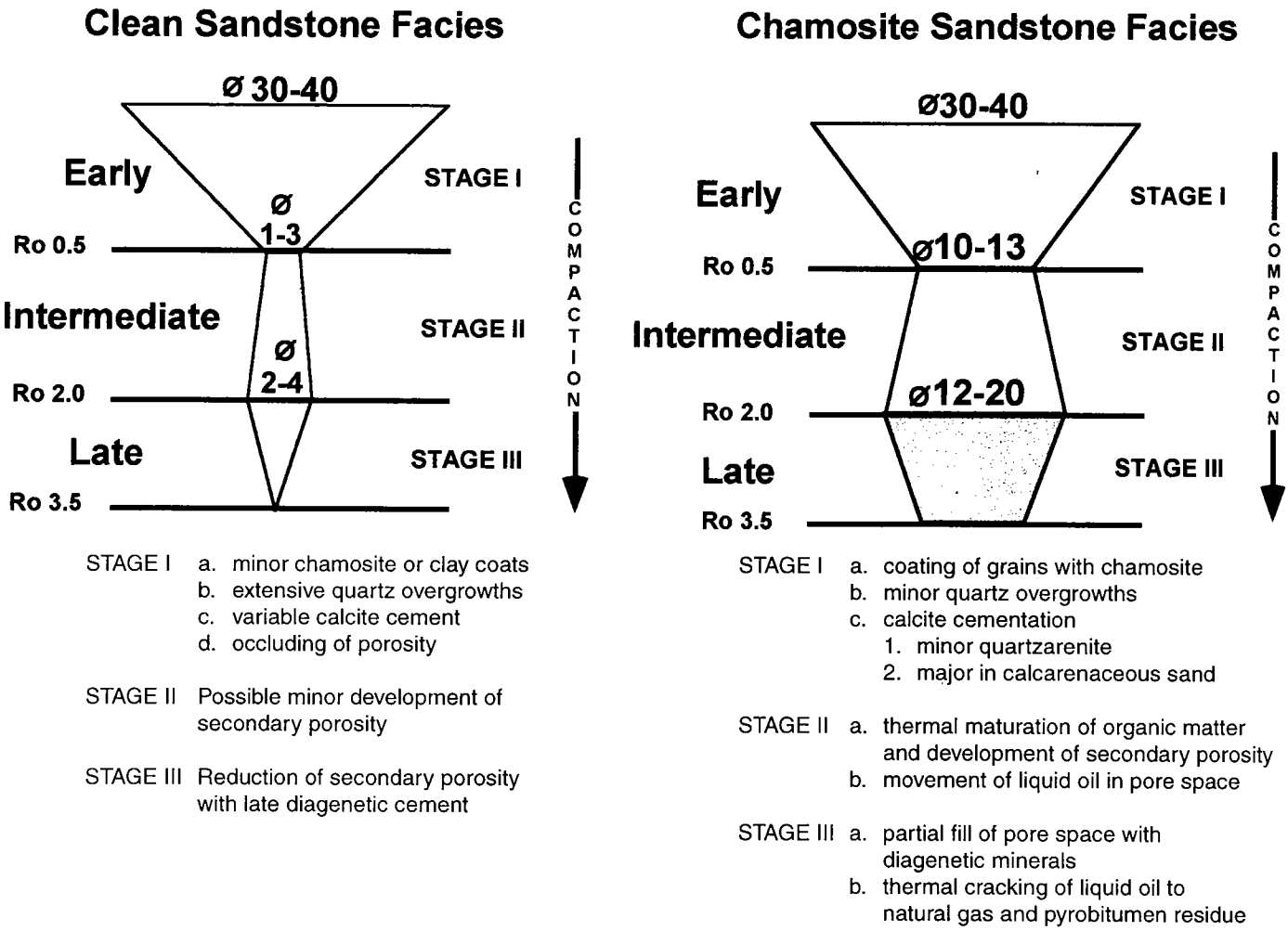

STAGE I
a. minor chamosite or clay coats
b. extensive quartz overgrowths
c. variable calcite cement
d. occluding of porosity

STAGE II
Possible minor development of secondary porosity

STAGE III
Reduction of secondary porosity with late diagenetic cement

STAGE I
a. coating of grains with chamosite
b. minor quartz overgrowths
c. calcite cementation
1. minor quartzarenite
2. major in calcarenaceous sand

STAGE II
a. thermal maturation of organic matter and development of secondary porosity
b. movement of liquid oil in pore space

STAGE III
a. partial fill of pore space with diagenetic minerals
b. thermal cracking of liquid oil to natural gas and pyrobitumen residue

Figure 19. Preservation and/or development of porosity as related to diagenetic evolution for (A) clean-sandstone facies and (B) chamosite-sandstone facies. Compare with Figure 5. R_o = vitrinite reflectance measured in oil immersion; ϕ = porosity (%).

REFERENCES CITED

Al-Shaieb, Zuhair; and Walker, P., 1987, Evolution of secondary porosity in Pennsylvanian Morrow sandstones, Anadarko basin, Oklahoma: geology of tight gas reservoirs: American Association of Petroleum Geologists Studies in Geology no. 24, p. 45–67.

Bailey, S. W., 1980, Structures of layer silicates, *in* Brindley, G. W.; and Brown, G. (eds.), Crystal structures of clay minerals and their X-ray identification: Mineralogical Society, London, p. 1–123.

Bhattacharyya, D. P., 1983, Origin of berthierine in ironstones: Clays and Clay Minerals, v. 31, p. 173–182.

Briggs, G., 1974, Carboniferous depositional environments in the Ouachita Mountains–Arkoma basin area of southeastern Oklahoma, *in* Briggs, G. (ed.), Carboniferous of the southeastern United States: Geological Society of America Special Paper 148, p. 225–239.

Brindley, G. W., 1982, Chemical composition of berthierines—a review: Clays and Clay Minerals, v. 30, p. 153–155.

Camp, W. K., 1991, Balanced cross section through Wilburton gas field, Latimer County, Oklahoma; implications for Ouachita deformation and Arbuckle (Cambro-Ordovician) exploration in Arkoma basin; Houston Geological Society Bulletin 33, no. 6.

Carothers, W. W.; and Kharaka, Y. K., 1978, Aliphatic acid anions in oil-field waters—implications for origins of natural gas: American Association of Petroleum Geologists Bulletin, v. 62, p. 2441–2453.

Curtis, C. D.; and Spears, D. A., 1968, The formations of sedimentary iron minerals: Economic Geology, v. 63, p. 257–270.

Curtis, C. D.; Hughes, C. R.; Whiteman, J. A.; and Whittle, C. K., 1985, Compositional variation within some sedimentary chlorites and some comments on their origin: Mineralogical Magazine, v. 49, p. 375–386.

Graham, S. A.; Ingersoll, R. V.; and Dickinson, W. R., 1976, Common provenance for lithic grains in Carboniferous sandstones from Ouachita Mountains and Black Warrior Basin: Journal of Sedimentary Petrology, v. 46, p. 620–632.

Heckel, P. H., 1972, Recognition of ancient shallow marine environments: Society of Economic Paleontologists and Mineralogists Special Publication 16, p. 226–286.

Houseknecht, D. W., 1987, The Atoka Formation of the Arkoma basin: tectonics, sedimentology, thermal maturity, and sandstone petrology: Tulsa Geological Society, Short Course Notes, p. 1–72.

Houseknecht, D. W.; and Kacena, J. A., 1983, Tectonic and sedimentary evolution of the Arkoma foreland basin, *in* Houseknecht, D. W., Tectonic–sedimentary evolution of the Arkoma basin: Society of Economic Paleontologists and Mineralogists, Midcontinent Section, v. 1, p. 3–33.

Iijima, A.; and Matsumoto, R., 1982, Berthierine and chamosite in coal measures of Japan: Clays and Clay Minerals, v. 30, p. 264–274.

Kimberley, M. M., 1979. Origin of oolitic iron formation: Journal of Sedimentary Petrology, v. 49, p. 111–131.

_____ 1980, The Paz de Rio oolitic inland-sea formation: Economic Geology, v. 75, p. 97–106.

Lumsden, D. N.; Pittman, E. D.; and Buchanan, R. S., 1971, Sedimentation and petrology of Spiro and Foster sands (Penn), McAlester basin, Oklahoma: American Association of Petroleum Geologists Bulletin, v. 55, p. 254–266.

Maynard, B. J., 1986, Geochemistry of oolitic iron ores, an electron microprobe study: Economic Geology, v. 81, p. 1473–1483.

Morris, R. C., 1974, Sedimentary and tectonic history of the Ouachita Mountains: Society of Economic Paleontologists and Mineralogists Special Publication 22, p. 120–142.

Odin, G. S.; and Matter, A., 1981, De glauconiarum origine: Sedimentology, v. 28, p. 611–641.

Porrenga, D. H., 1966, Glauconite and chamosite as depth indicators in the marine environment: Marine Geology, v. 5, p. 495–501.

Rohrlich, V., 1974, Microstructure and microchemistry of iron ooliths: Mineralogy Deposita, v. 9, p. 133–142.

Surdam, R. C.; Boese, S. W.; and Crossey, L. J., 1984, The chemistry of secondary porosity, *in* McDonald, D. A.; and Surdam, R. C. (eds.), Clastic diagenesis: American Association of Petroleum Geologists Memoir 37, p. 127–149.

Tucker, M. E., 1981, Sedimentary petrology: an introduction to the origin of sedimentary rocks [2nd edition]: John Wiley & Sons, New York, p. 57–58.

Van Houten, F. B.; and Purucker, M. E., 1984, Glauconitic peloids and chamositic ooids-favorable factors, constraints, and problems: Earth-Science Reviews, v. 20, p. 211–243.

Velde, B.; Raoult, J. F.; and Leikine, M., 1974, Metamorphosed berthierine pellets in mid-Cretaceous rocks from northeastern Algeria: Journal of Sedimentary Petrology, v. 44, p. 1275–1280.

Zachary, D. L.; and Sutherland, P. K., 1984, Stratigraphy and depositional framework of the Atoka Formation, Arkoma basin of Arkansas and Oklahoma, *in* Sutherland, P. K.; and Manger, W. L. (eds.), The Atoka Series (Pennsylvanian) and its boundaries—a symposium: Oklahoma Geological Survey Bulletin 136, p. 9–19.

Microbial Reservoir Characterization of a Mature Bartlesville Sandstone Reservoir, Washington County, Oklahoma

Daniel C. Hitzman, James D. Tucker, and Brooks A. Rountree
Geo-Microbial Technologies, Inc.
Ochelata, Oklahoma

ABSTRACT.—An area of approximately 720 acres of a mature Bartlesville Sandstone reservoir in Washington County, Oklahoma, was evaluated for hydrocarbon-microseepage signatures using Microbial Reservoir Characterization (MRC). This technique uses hydrocarbon-specific microorganisms found in shallow soil samples collected over producing fields to map pressure regimes in the reservoir. MRC studies anticipate reduced microbial populations above portions of the reservoir that are in direct communication with producing wells. Bypassed compartments or unswept zones can be located with elevated microbial signatures.

The study area was selected because an active infill drilling program, as well as a field rehabilitation plan were scheduled to commence soon after the survey was completed. Three hundred twenty-seven (327) soil samples were collected every 330 ft in a grid pattern. The production area with active injection wells and anticipated reservoir repressuring exhibits the highest microbial values. Areas of production with no injectors reflect expected reduced microbial values. The trends of high and low microbial values respond to suspected reservoir heterogeneities and dynamic pressure patterns.

Oil and gas fields leak light hydrocarbon gases along nearly vertical pathways. Hydrocarbon-specific microbial populations mirror this leakage. MRC surveys demonstrate reduced hydrocarbon microseepage over producing fields due to a change in drive mechanism that controls the microseepage. When a new well is brought into production, the gas drive changes from a vertically migrating buoyancy force to horizontal gas streaming to low pressure sinks created around producing wells. When this occurs, microseepage ends, and microbial populations decline rapidly. This change in drive mechanism and microbial population densities can be used to define reservoir-drainage direction, radii, and heterogeneities around existing wells. Conversely, in areas where the reservoir is being repressured, as in a waterflood, the microseepage is reestablished. Microbial counts will increase on the surface in response to increasing microseepage coming from the portion of the reservoir in direct contact with the waterflood.

INTRODUCTION

Detailed geochemical and geomicrobiological surveys and research studies document that hydrocarbon microseepage from oil and gas accumulations is common and widespread, is predominantly vertical (with obvious exceptions in some geologic settings), and is dynamic (responds quickly to changes in reservoir conditions). These characteristics create a new suite of applications for surface geochemical surveys (e.g., field development, reservoir characterization, and monitoring patterns of hydrocarbon drainage). Combined with more established uses of surface geochemistry (e.g., high-grading exploration leases, leads, and prospects), these new applications show great promise for the wider use of surface exploration methods in mature basins.

Because hydrocarbon microseepage is nearly vertical, the extent of an anomaly at the surface can approximate the productive limits of the reservoir at depth. Furthermore, the pattern of microseepage over a field can reflect reservoir heterogeneity and distinguish hydrocarbon-charged compartments from drained or uncharged compartments. Furthermore, because hydrocarbon microseepage is dynamic, seepage patterns can change rapidly in response to production-induced changes. Evidence of such changes in microseepage patterns can be identified by detailed Microbial Reservoir Characterization (MRC) technology, which responds to active microseepage.

Hitzman, D. C.; Tucker, J. D.; and Rountree, B. A., 2000, Microbial reservoir characterization of a mature Bartlesville Sandstone reservoir, Washington County, Oklahoma, *in* Johnson, K. S. (ed.), Marine clastics in the southern Midcontinent, 1997 symposium: Oklahoma Geological Survey Circular 103, p. 171–176.

INTRODUCTION TO MICROBIAL SURVEYS

The Microbial Oil Survey Technique (MOST), first developed by Phillips Petroleum Company, is based on the presence of hydrocarbon microseeps above hydrocarbon-charged reservoirs. The microseepage is detected by observing the concentrations and distributions of hydrocarbon-indicating microorganisms found in shallow soils. More specifically, when upward-migrating hydrocarbon gases from buried reservoirs enter the shallow soil environment, they are utilized by a specific group of microorganisms. There is a direct, positive relationship between the light-hydrocarbon gas concentrations in the soils and these microbial populations. Microbial anomalies have been proven to be reliable indicators of oil and gas for exploration applications (Beghtel and others, 1987; Lopez and others, 1994) as well as for field development and production (Tucker and Hitzman, 1994; Schumacher and others, 1997).

Sample patterns and sample density are selected to best define the hydrocarbon potential of the target area, subject to considerations of terrain and accessibility (Fig. 1). Both reconnaissance and more detailed surveys of acreage or prospects may be completed in this manner. The predictive value of this technology has been demonstrated by extensive field surveys in a variety of environments and targeting a wide spectrum of reservoirs. Geological and geophysical exploration and production data are greatly enhanced by the addition of microbial surveys.

MICROBIAL RESERVOIR CHARACTERIZATION EVALUATIONS

Microbial Reservoir Characterization (MRC) evaluations are an interpretative modification of the MOST methodology. MRC theory indicates that the pattern of microbial populations on the surface is directly related to pressure regimes within the reservoir.

MRC evaluations anticipate reduced microbial populations above portions of the reservoir in direct communication with the producer. This phenomenon of apparent reduced hydrocarbon microseepage over producing fields is thought to be due to a change in the drive mechanism controlling microseepage. When a well is brought into production, the drive changes from a vertically migrating buoyancy force to horizontal gas streaming to low-pressure sinks created around producing wells. When this occurs, microseepage ends and microbial populations decline rapidly. This change in drive mechanism and microbial population densities can be used to define reservoir-drainage direction and heterogeneities around existing wells in producing fields. Conversely, in areas where the reservoir is being repressured, as in a waterflood, the microseepage is reestablished. The microbial counts will increase on the surface in response to increasing microseepage coming from the portion of the reservoir in direct contact with the waterflood. Results from microbial studies surrounding producing wells that indicate the rates of light-hydrocarbon migration from the reservoir to the surface are sufficiently great to create microbial-population changes at the surface in the order of months after production has begun.

Production Only

Within producing fields, low microbial counts indicate either where the reservoir is in *direct* communication with the surrounding producers or areas never charged with hydrocarbons (clay plugs). Elevated microbial populations indicate areas within the producing reservoir not in pressure communication with surrounding producers. These areas are either isolated from the existing producers by some form of reservoir heterogeneity or indicate different hydrocarbon-charged horizons within the geologic column.

Injection and Production

Different microseepage signatures occur within producing fields where primary production has been followed by water injection. Portions of the reservoir in contact with injection fluid will once again be pressured, and hydrocarbon microseepage will be reinitiated. Therefore, elevated microbial counts in areas of fluid injection indicate which portions of the reservoir are in communication with the injectors. Low microbial counts in this injection environment indicate three scenarios: (1) the portions of the reservoir in communication with the producers within the anticipated pressure draw down away from the injector; (2) areas that are pressure depleted by production yet isolated from the nearby injector by some heterogeneity; or (3) some portion of the reservoir, such as a clay plug, that was never charged with hydrocarbons.

All of these microbial patterns are observed within the Painter Ranch MRC evaluation. It is essential to use the MRC data in conjunction with geological and geophysical information.

PAINTER RANCH GEOLOGY

The Painter Ranch production is from the Pennsylvanian Bartlesville Sandstone. Production is from a zone 20 ft thick at a depth of approximately 1,290 ft. The Bartlesville Sandstone in northeastern Oklahoma was deposited in a fluvial-dominated deltaic environment. The sequence consists of an agglomeration of prograding distributary channels, levees, crevasse splays, abandoned channels, swamps, and delta lobes intermixed with delta-plain, estuary, and marine-bay muds.

This type of depositional environment will deposit discontinuous reservoir sands and eventual reservoirs full of various heterogeneities. These will include depositional events as directional permeability trends, clay drapes, and clay plugs that will isolate compartments from production.

RESERVOIR HETEROGENEITIES

Reservoir heterogeneities are either depositional or post-depositional events that isolate, reduce, or constrict consistent fluid movement throughout the entire reservoir. Depositional features can be as large as iso-

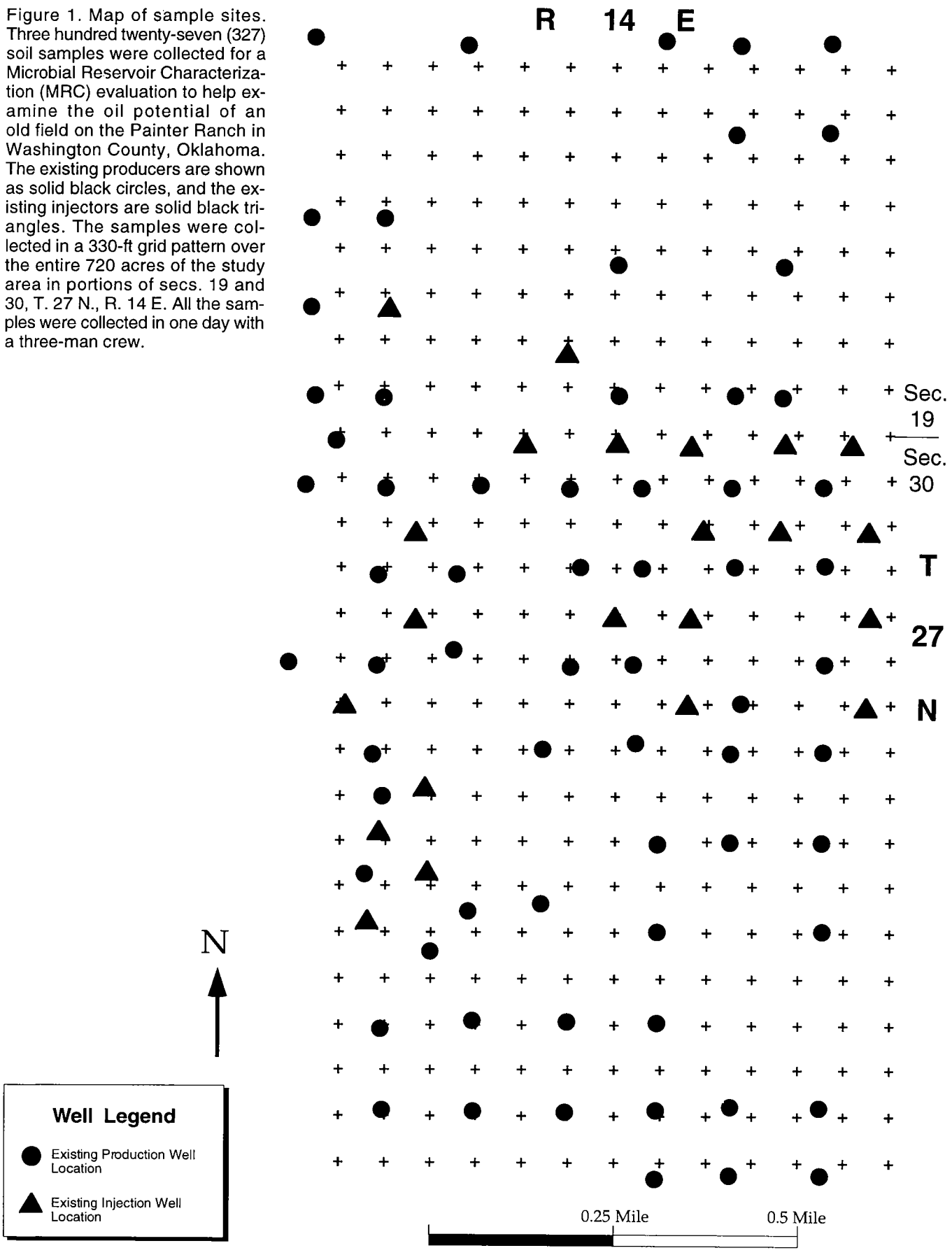

Figure 1. Map of sample sites. Three hundred twenty-seven (327) soil samples were collected for a Microbial Reservoir Characterization (MRC) evaluation to help examine the oil potential of an old field on the Painter Ranch in Washington County, Oklahoma. The existing producers are shown as solid black circles, and the existing injectors are solid black triangles. The samples were collected in a 330-ft grid pattern over the entire 720 acres of the study area in portions of secs. 19 and 30, T. 27 N., R. 14 E. All the samples were collected in one day with a three-man crew.

lated stacked channels, to grain-size differences, to clay plugs, to as subtle as clay drapes. Post-depositional events that may alter communication within the reservoir are faulting, fracture patterns, differential compaction, secondary cementation, and mineralogical alterations.

Any of these events or combinations of events can greatly affect fluid movement within producing reservoirs. Combinations of current permeability patterns, heterogeneities, and pressure differentials will control the directions and rates that fluids will move within the reservoir.

All reservoirs have some combination of the various heterogeneities, at different scales, making complete or efficient recoveries difficult to achieve. Because most reservoirs are produced as if they were uniaxial with isotropic rock types, isolated hydrocarbons are commonly bypassed and left unproduced.

MRC evaluations of producing reservoirs combined with production characteristics are very useful tools to help identify bypassed hydrocarbons. Multiple MRC studies conducted over a period of time will help identify expanding pressure regimes and any related reservoir heterogeneities. *Integrating MRC evaluations, production records, geology, and geophysics will help more completely produce the reservoir with more efficient well spacing and well patterns.*

Maps of the microbial signatures of the Painter Ranch field are shown as Figures 2 and 3. A second follow-up microbial survey—identical to the first program—has been completed recently. The results are being tabulated and compared with the first survey, along with an investigation of the engineering and production changes initiated by the new Painter Ranch injection and rehabilitation plan.

CONCLUSIONS

In areas where the reservoir has been in communication with either production or injection, the Painter Ranch MRC evaluation will help predict the following:

- Regions of the reservoir in contact with the producing wells as identified by the patterns of low microbial activity at the surface.
- The reservoir drainage radius and pattern adjacent to individual *producers* as noted by the *low* microbial activity at the surface surrounding the wells.
- Regions of the reservoir in contact with the injection wells as identified by the *high* microbial populations.
- The reservoir injection radius and pattern adjacent to individual injectors as noted by the high microbial activity at the surface surrounding each well.
- The anticipated pressure regimes within the reservoir at any location by noting the surface microbial values. Low reservoir pressure and dead oil associated are with low microbial populations and higher reservoir pressure with elevated microbial populations.
- The presence of reservoir heterogeneities and fabric by identifying organized patters and alignments of low and elevated microbial population patterns associated with production and injection.
- If significant reservoir heterogeneities are identified, infill well patterns can be adjusted to utilize the heterogeneities to maximize oil production and water injection.
- Areas of bypassed production identified by anomalously high microbial activity in areas not associated with injection, generally between existing producing wells.
- Areas of stepout potential as identified by elevated microbial activity trending away from the edges of the existing field.
- Potential hydrocarbon accumulations associated with other (shallower) formations currently not being produced. These trends are indicated by elevated microbial populations in patterns not associated with production or injection in the primary reservoir.

REFERENCES CITED

Beghtel, F. W.; Hitzman, D. O.; and Sundberg, K. R., 1987, Microbial oil survey technique (MOST) evaluation of new field wildcat wells in Kansas: Association of Petroleum Geochemical Explorationists Bulletin, v. 3, p. 1–14.

Lopez, J. P.; Hitzman, D. C.; and Tucker, J. D., 1994, Combined microbial, seismic surveys predict oil and gas occurrences in Bolivia: Oil and Gas Journal, v. 92, no. 43, p. 68–70.

Schumacher, Dietmar; Hitzman, D. C.; Tucker, James; and Rountree, Brooks, 1997, Applying high-resolution surface geochemistry to assess reservoir compartmentalization and monitor hydrocarbon drainage, *in* Kruizenga, R. J.; and Downey, M. W. (eds.), Applications of emerging technologies: unconventional methods in exploration for oil and gas, V: Southern Methodist University Press, Dallas, p. 309–322.

Tucker, James; and Hitzman, D. C., 1994, Detailed microbial surveys help improve reservoir characterization: Oil and Gas Journal, v. 92, no. 23, p. 65–68.

Figure 2. Contour map of microbial results. The microbial population patterns in this MRC survey demonstrate anticipated hydrocarbon-microseepage signatures associated with oil production and water injection. The majority of production wells are associated with reduced microbial values where little to no water injection has occurred. Conversely, the elevated microbial values are associated with the injection wells indicating which portions of the reservoir are being repressured. The patterns of high and low microbial values (i.e., the production and injection patterns) are suspected to be related to reservoir heterogeneities controlling fluid movement within the reservoir.

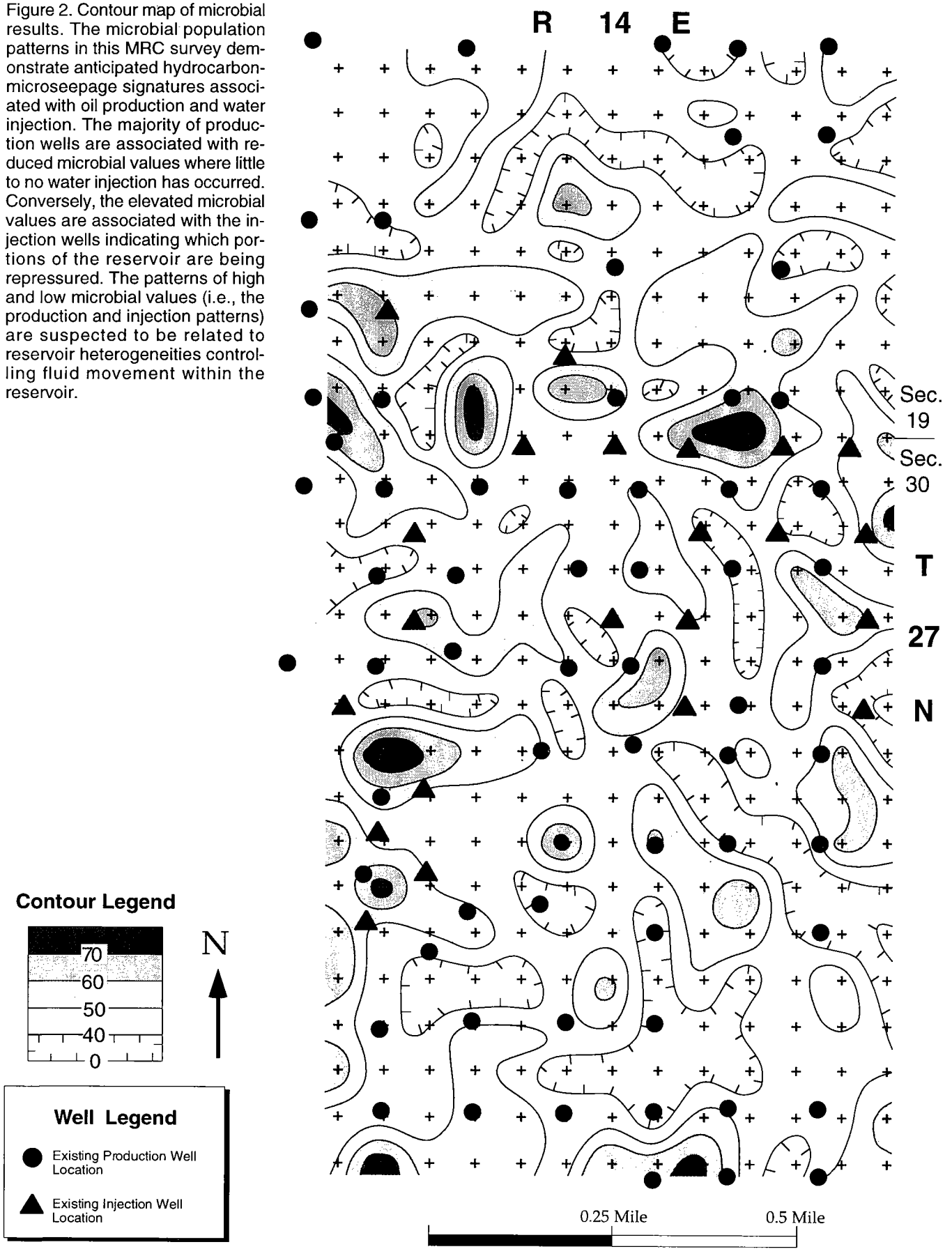

Figure 3. Contour map of smoothed microbial results. A weighted, nine-point smoothing average of the Map 2 values was utilized to examine trends in the microseepage signature rather than individual extreme values. These smoothed signatures are helpful in planning multiple-well programs and can identify larger reservoir areas in order to focus or forget development efforts.

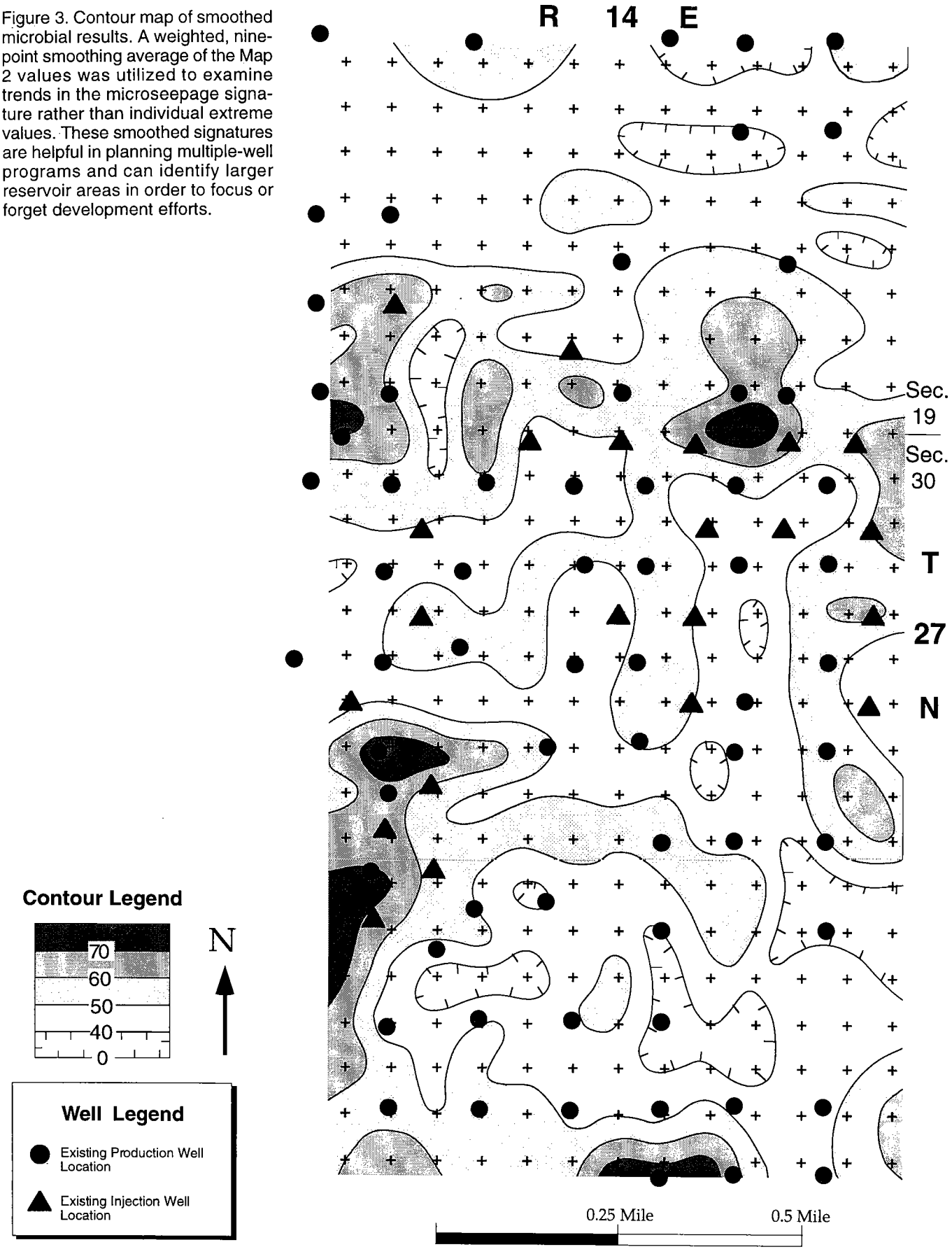

The Deep-Marine Red Fork Sandstone: A Submarine-Fan Complex

James O. Puckette
Oklahoma State University
Stillwater, Oklahoma

Charles Anderson
UnoCal Corporation
Midland, Texas

Zuhair Al-Shaieb
Oklahoma State University
Stillwater, Oklahoma

ABSTRACT.—The Red Fork Sandstone (Middle Pennsylvanian, Desmoinesian) is a prolific gas-producing reservoir in the Anadarko basin. In the greater Strong City/Butler district, production is primarily from channel-fill sandstone within suprafan lobes. Porosity is predominantly secondary and resulted from the dissolution of labile grains and matrix.

The Red Fork Sandstone was deposited primarily by a southerly flowing sediment-dispersal system. This large fluvial-deltaic complex prograded southward toward the Anadarko and Arkoma basins. In the Anadarko basin, sediments were eventually transported beyond the shelf margin and deposited as submarine fans on the basin floor. Regional mapping suggests that these fans were fed primarily by the Clinton-Weatherford channel and prograded westward. There is also evidence for northwest and southern sources. These rocks exhibit considerable lateral and vertical variability as a result of the coalescing of fan lobes and facies stacking.

The integration of core data, wireline-log characteristics, and sandstone distribution patterns allowed the reconstruction of fan facies. Elongated trends of thick sandstone are interpreted as upper and mid-fan channels. Shale-dominated intervals with thin-bedded sandstones represent lower-fan or basin-plain deposits. The stacking of fans juxtaposed upper and mid-fan facies over lower-fan and basin-plain deposits. Thick sandstone suggests multiple episodes of deposition in some areas.

Larger gas reserves are typically found in the channel facies. Suprafan lobes and channel trends can be delineated using total-sandstone–thickness maps. However, detailed correlation and mapping are necessary to identify individual reservoir compartments within these trends.

INTRODUCTION

The Red Fork Sandstone (Middle Pennsylvanian, Desmoinesian) in the western part of the Anadarko basin displays a variety of features associated with submarine-fan deposits. Successful discovery and development of Red Fork reserves are contingent on identification and delineation of fan facies. They generally occupy a low paleogeographic position beyond a well-defined shelf edge. Fan facies represent the basinal termination of the Red Fork sediment-dispersal system. This study focuses on the upper Red Fork from which most of the core data were obtained.

GEOLOGIC SETTING

The Red Fork Sandstone was deposited during the Middle Pennsylvanian (Desmoinesian) as part of a large fluvial-deltaic and submarine system. Most sediment was transported southward as a prograding fluvial-deltaic complex (Fig. 1). The Clinton-Weatherford channel was the major conduit for sediment transportation to the deeper parts of the basin (Fig. 2). These deposits contain major gas reservoirs of the Strong City/Butler district and have produced over 400 BCF of gas from submarine-fan facies.

Puckette, J. O.; Anderson, Charles; and Al-Shaieb, Zuhair, 2000, The deep-marine Red Fork Sandstone: a submarine-fan complex, *in* Johnson, K. S. (ed.), Marine clastics in the southern Midcontinent, 1997 symposium: Oklahoma Geological Survey Circular 103, p. 177–184.

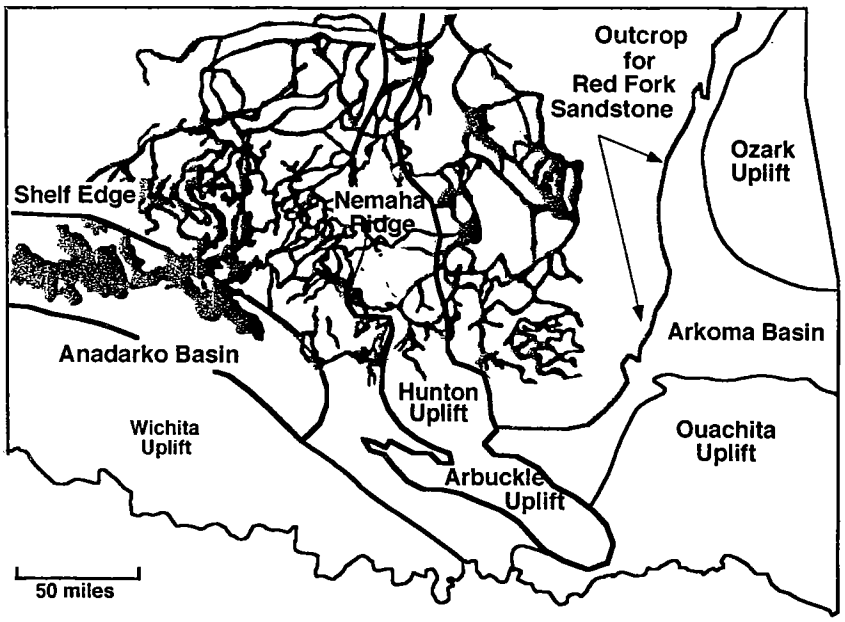

Figure 1. Geologic features of Oklahoma and distribution of the Red Fork Sandstone in Oklahoma. Red Fork sediments were dispersed by a large southerly prograding fluvial-deltaic complex (gray pattern) that eventually extended beyond the shelf edge of the Anadarko basin. From Al-Shaieb and others (1995).

PREVIOUS STUDIES

The Red Fork has been the focus of many studies in Oklahoma. Investigations pertaining to the Anadarko basin include Glass (1981), Whiting (1982), Johnson (1984), Udayashankar (1985), Schneider and Clement (1986), and Anderson (1992). Johnson (1984) and Udayashankar (1985) established electrofacies markers used to define upper and lower Red Fork intervals. Johnson (1984) recognized the lower Red Fork hinge line and described a variety of depositional environments including delta-front, submarine-channel–fill, and submarine-fan environments. Schneider and Clement (1986) defined the trend of the Clinton-Weatherford channel and its incised nature. Anderson (1992) investigated the details of the distribution of submarine-fan complexes and made interpretations of various facies utilized in this paper.

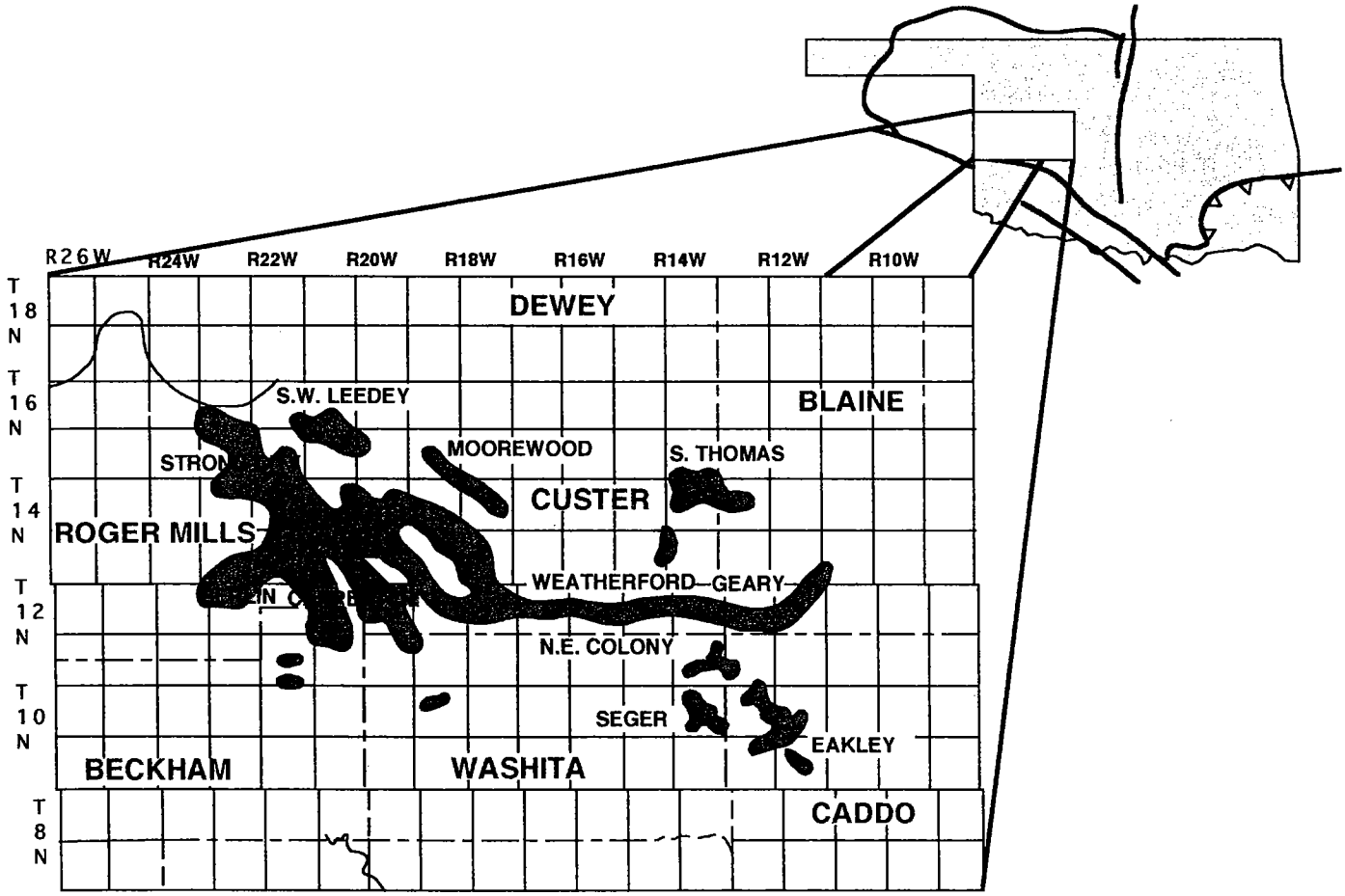

Figure 2. Gas fields of western Oklahoma producing from Red Fork Sandstone. The Weatherford-Geary fields define the position of the Clinton-Weatherford feeder channel that supplied sediment for deep-basin accumulations that became the Strong City/Butler district (Eric Anderson, personal communication, 1995).

DISTRIBUTION AND GEOMETRY OF THE UPPER RED FORK SANDSTONES

The upper Red Fork is defined as the interval between the Pink Limestone biomicrite/shale marker and the "hot" shale marker (Johnson, 1984; Anderson, 1992) (Fig. 3). This interval showed a marked increase in thickness from 150 ft in the northeast to approximately 1,000 ft to the southwest and south-central part of the area of investigation (Fig. 4). The upper Red Fork hinge zone between the shelf and slope is shown in Figure 5. This zone also represents the transition from dominantly deltaic to deeper-marine facies. Net-sandstone–isolith maps illustrate the distribution pattern of the submarine deposits. These thicknesses were determined from gamma-ray logs having reflections >30 API

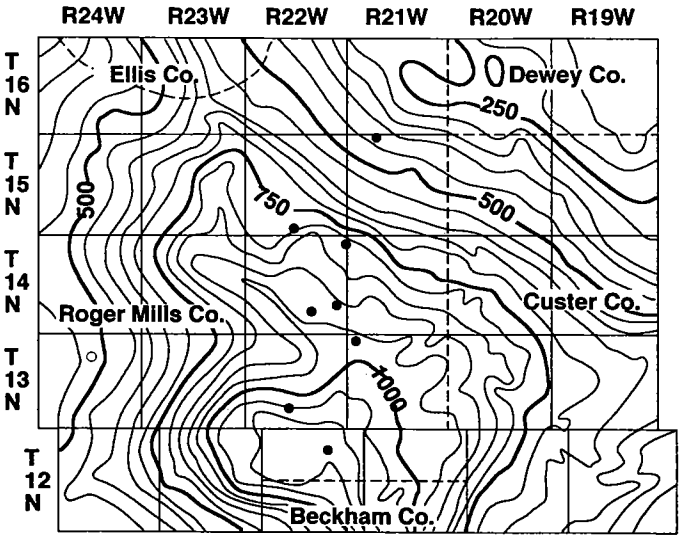

Figure 4. Isopachous map of thickness (contour interval = 50 ft) of upper Red Fork sandstone interval with locations (black dots) of wells in which the Red Fork Sandstone was cored.

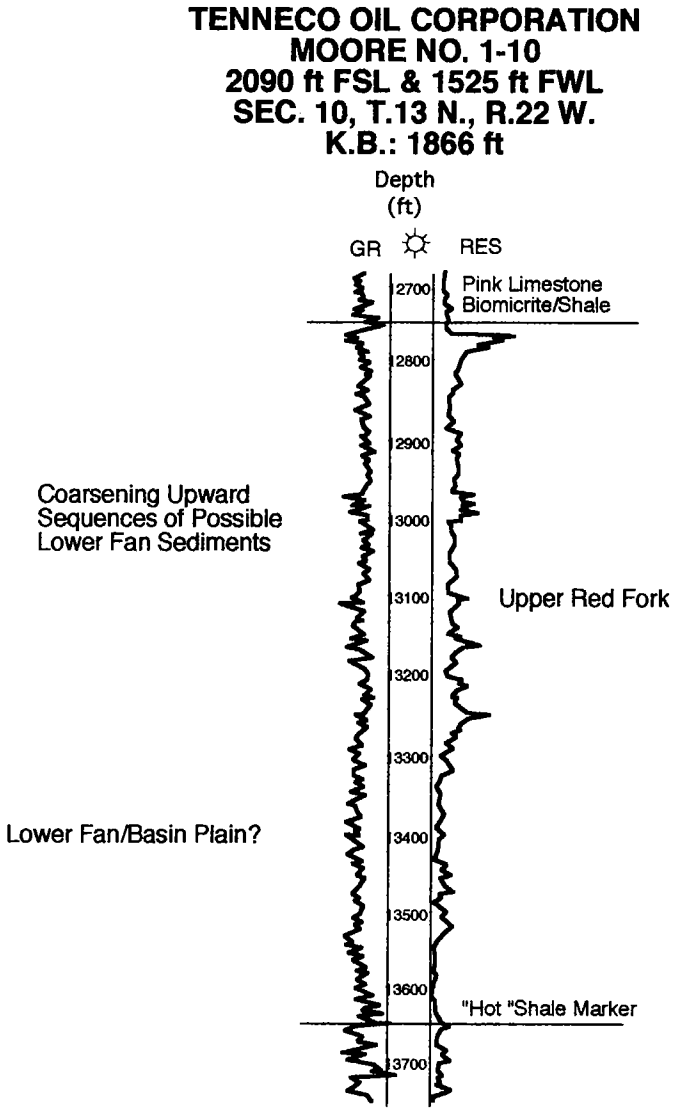

Figure 3. Wireline log from the deep Anadarko basin with markers identified that are used to define the upper Red Fork sandstone interval (after Anderson, 1992). Depth given in feet. GR = gamma-ray log; RES = resistivity log.

units from the shale base line and a corresponding increase in resistivity >10 ohm-m. Thicknesses thus determined range from <5 ft to >200 ft, and the greatest thicknesses are due to stacking of numerous sandstone units. The overall geometry of these units shows an elongated pattern to the west and northwest, indicating a major eastern source of sediments that prograded in a westerly direction (Fig. 6).

Facies Analysis

Eleven cored intervals were examined to determine sedimentary features, petrology, and diagenesis of the upper Red Fork sandstone. Sedimentary structures and depositional-facies interpretations were emphasized in this study. However, detailed description of the petrology and diagenesis is available in Anderson (1992).

A wide variety of sedimentary and biogenic structures were present in the cores. In order of decreasing abundance, they were: (1) inclined laminae, (2) ripple laminae, (3) wavy or undulating ripple laminae, (4) lenticular bedding, (5) soft-sediment deformation, (6) penecontemporaneous microfaulting, (7) slump structures, (8) parallel laminae, (9) dish and pillar structures, (10) massive bedding, (11) small-scale trough cross-bedding, (12) tabular cross-bedding, (13) climbing ripples, (14) flaser bedding, (15) interlaminated siltstone and shale, (16) burrows, (17) rounded shale clasts, (18) angular shale clasts, (19) load casts, (20) flame structures, (21) fluid-escape (pipe) structures, and (22) fossils.

Most of the cores examined contained incomplete Bouma (1962) turbidite sequences, and sedimentary features observed were very similar to those reported by Mutti and Lucchi (1972). Anderson (1992) described in detail sedimentary features and facies associated with the upper Red Fork submarine deposits in the Anadarko basin.

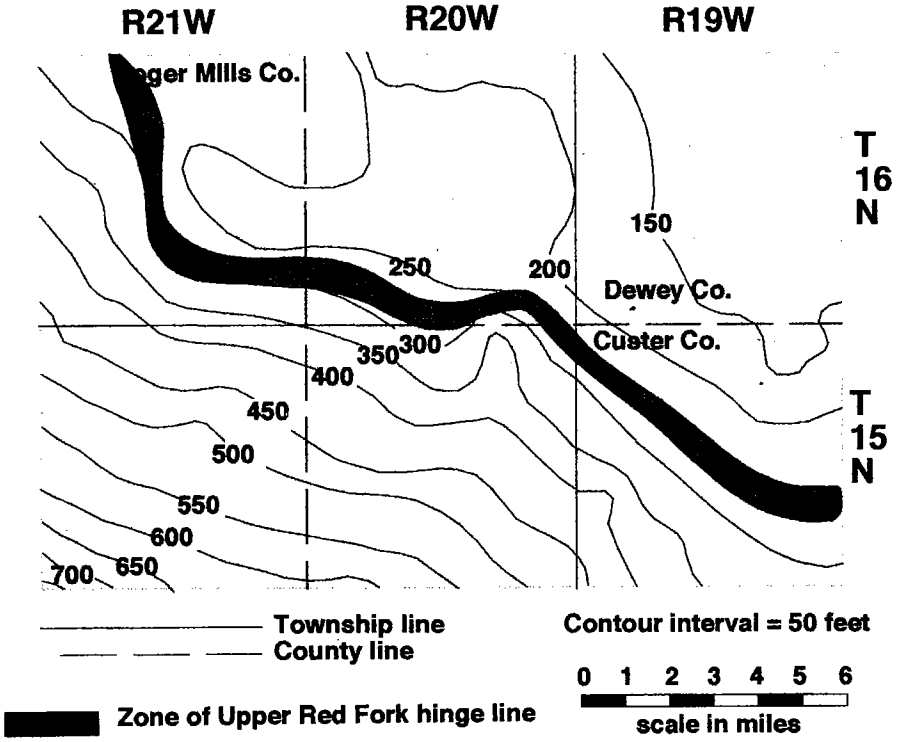

Figure 5. Map of parts of Dewey, Roger Mills, and Custer Counties, showing rapid increase in thickening (in ft) of the upper Red Fork interval that identifies the position of the shelf edge/basin hinge line.

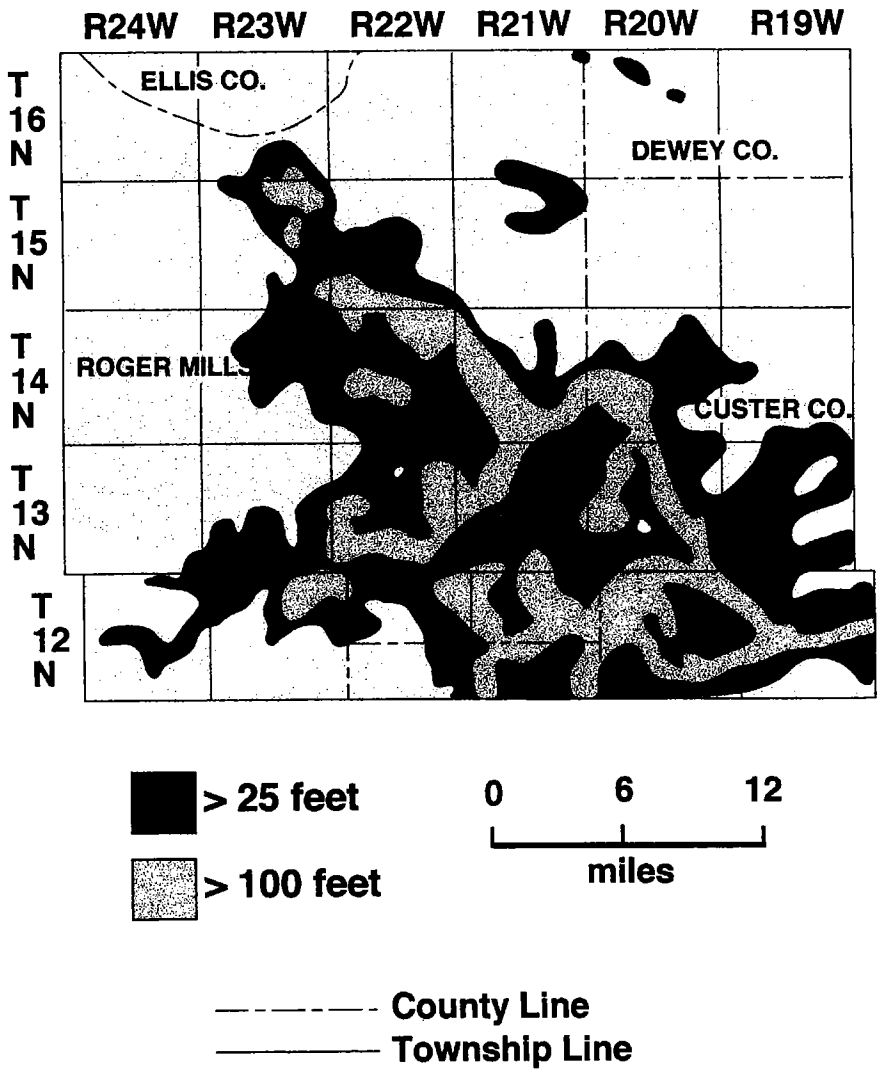

Figure 6. Map showing net thickness of upper Red Fork sandstone in portions of Ellis, Roger Mills, and Custer Counties. Sandstone trends suggest a dominant northwest-southeast trend and westward progradation of the sediment package.

Fan Morphology of the Upper Red Fork Sandstone

The facies model of Walker (1978) was used to predict facies distribution of submarine-fan complexes and to interpret fan morphology for the upper Red Fork facies (Fig. 7), and the Mutti and Lucchi (1972) facies model was used to support this interpretation. The major elements of the model consist of: (1) a feeder channel that supplies sediment; (2) a leveed-channel upper fan that transports sediment across previous depositional facies; (3) a mid-fan that consists of suprafan lobes that grade outward from non-leveed, shallow, braided channels to smooth turbidity deposits; and (4) a lower fan and basin plain with smooth relief, parallel bedding, and distal turbidites (Fig. 7).

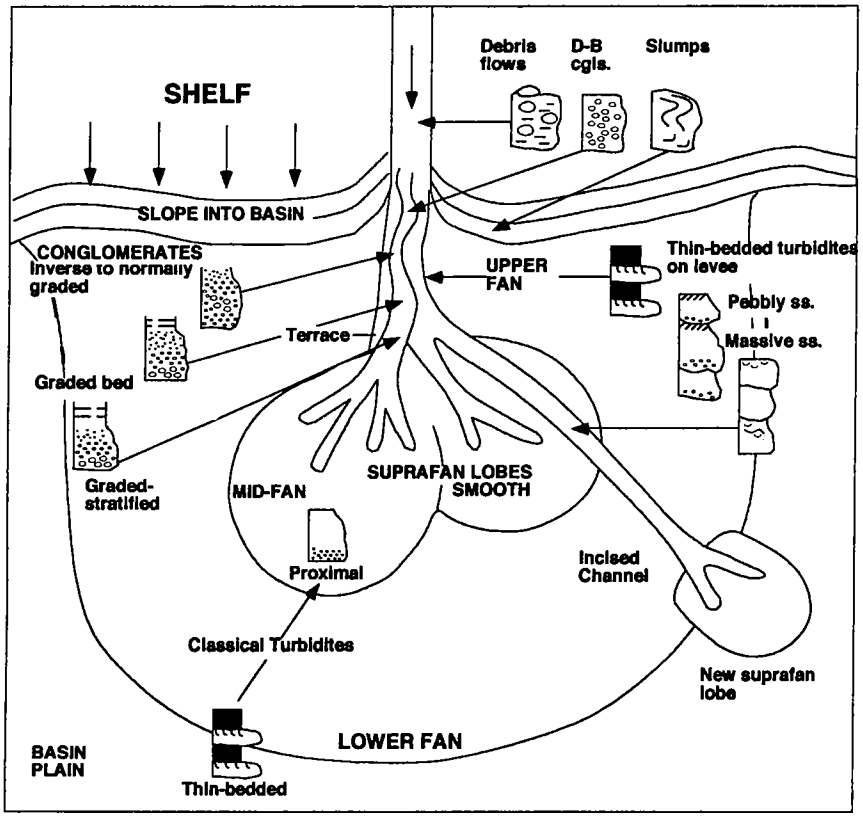

Figure 7. Submarine-fan model. From Walker (1978).

Submarine Feeder Channel Facies

Sandstone thickness of the Clinton-Weatherford trend in T. 12 N., R. 19 W. (Fig. 8) is interpreted as an upper fan feeder. The thick graded/stratified sandstone in the An-son Corp. No. 1-24 Bill well shown in Figure 9 is an example of this facies. Sandstone of this trend is dominantly very fine grained. The shale on either side of this channel may represent levee deposits.

Upper-Fan Facies

The upper-fan facies consists mainly of channel-fill sandstones. The interpretation of this facies is strictly based on log signatures because no cored material is available for examination of this interval from the study area. This facies is described as thick sandstone exceeding 20 ft in thickness that shows relatively clear gamma-ray and high-resistivity deflections of >50 ohm-m.

Mid-Fan Facies

The mid-fan facies appears to be the dominant sandstone facies found in the study area. Eight cores examined contain features that are interpreted as mid-fan deposits. Well-log signatures of this facies show serrate gamma-ray–log and resistivity-log profiles (Fig. 10). Correlation of core to wireline logs indicates the presence of interbedded, dark, silty shales that cause high gamma-ray response. The dark silty shales may represent periods of lower flow regimes with suspension settling and low-density turbidity flow as well as turbidity currents with incomplete Bouma sets. Ripple laminae are the most common sedimentary structure found in these cores and indicate a lower flow regime. Dish structures are common and represent fluidized flows. Wireline logs indicate stacking of sandstones with interbedded shales. Multiple stacked channels with interbedded shale may represent channelized turbidites of the upper mid-fan facies on suprafan lobes. Accumulation of mid-fan facies within local depocenters resulted in total sandstone thicknesses that approach several hundred feet. Local cross sections through these thick deposits illustrate lateral changes between wells (Fig. 11).

Lower-Fan Facies

Lower-fan deposits are described as parallel, thin-bedded turbidites (Mutti and Lucchi, 1972; Walker, 1978). They are recognized on wireline logs as coarsening-upward sequences with thin-bedded sandstones. This facies is present in the cored interval of Southport Exploration, No. 1-10 Merrick well (NE¼ sec. 10, T. 12 N., R. 22 W.). They consist of thin-bedded to laminar siltstones, shales, and shales with parallel bedding and soft-sediment–deformation features and microfaulting. These intervals are interpreted as having formed from low-density turbidity currents with intervals of suspension settling (Mutti and Lucchi, 1972; Walker, 1978). This results in the alternating light- and dark-colored rocks in cores.

Several wells contain apparent coarsening-upward intervals that are overlain by thick sequences of sandstone with interbedded siltstone and shale. These sandstones are interpreted as mid-fan deposits that prograded over lower-fan and basin-plain facies.

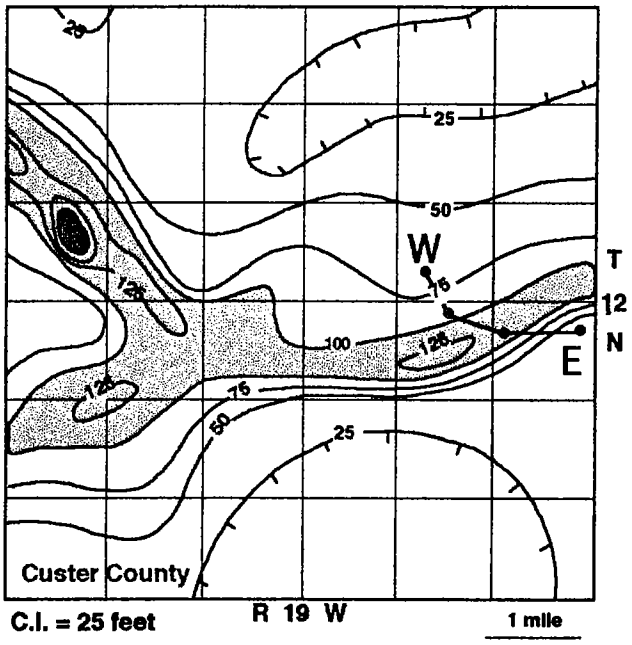

Figure 8. Net sandstone thickness (in ft) and interpreted upper-fan feeder channel in part of Custer County. Position of wells for cross section (Fig. 9) is shown by black dots.

Basin-Plain Facies

The basin-plain and lower-fan facies have similar morphologies and are difficult to separate. Plane-parallel bedding with hemipelagic sediment and minor turbidity flows represent basin-plain facies (Mutti and Lucchi, 1972; Walker, 1978). The Southport Exploration, Inc., No. 1-10 Merrick well is interpreted as an example of this facies. The cored interval consists of interbedded brown and dark-gray shales with lighter-colored siltstones and sandstones. Soft-sediment-deformation features including flowage, slump structures, and microfaulting are common. Thin beds of very fine-grained sandstone within the shale contain ripples formed by traction currents (Mutti and Lucchi, 1972).

Wireline-log signatures (Fig. 3) indicate a shale-rich lithology with high neutron porosity. The basin-plain facies is the most abundant facies in the study area. Juxtaposing basin-plain facies against other sandstone-rich facies may contribute to trapping and provide excellent source beds for hydrocarbons.

DEPOSITIONAL MODEL

The depositional model for the upper Red Fork sandstone is shown in Figure 12. This model is based on the previously described facies, fan models, and regional geology. This generalized interpretation may be used

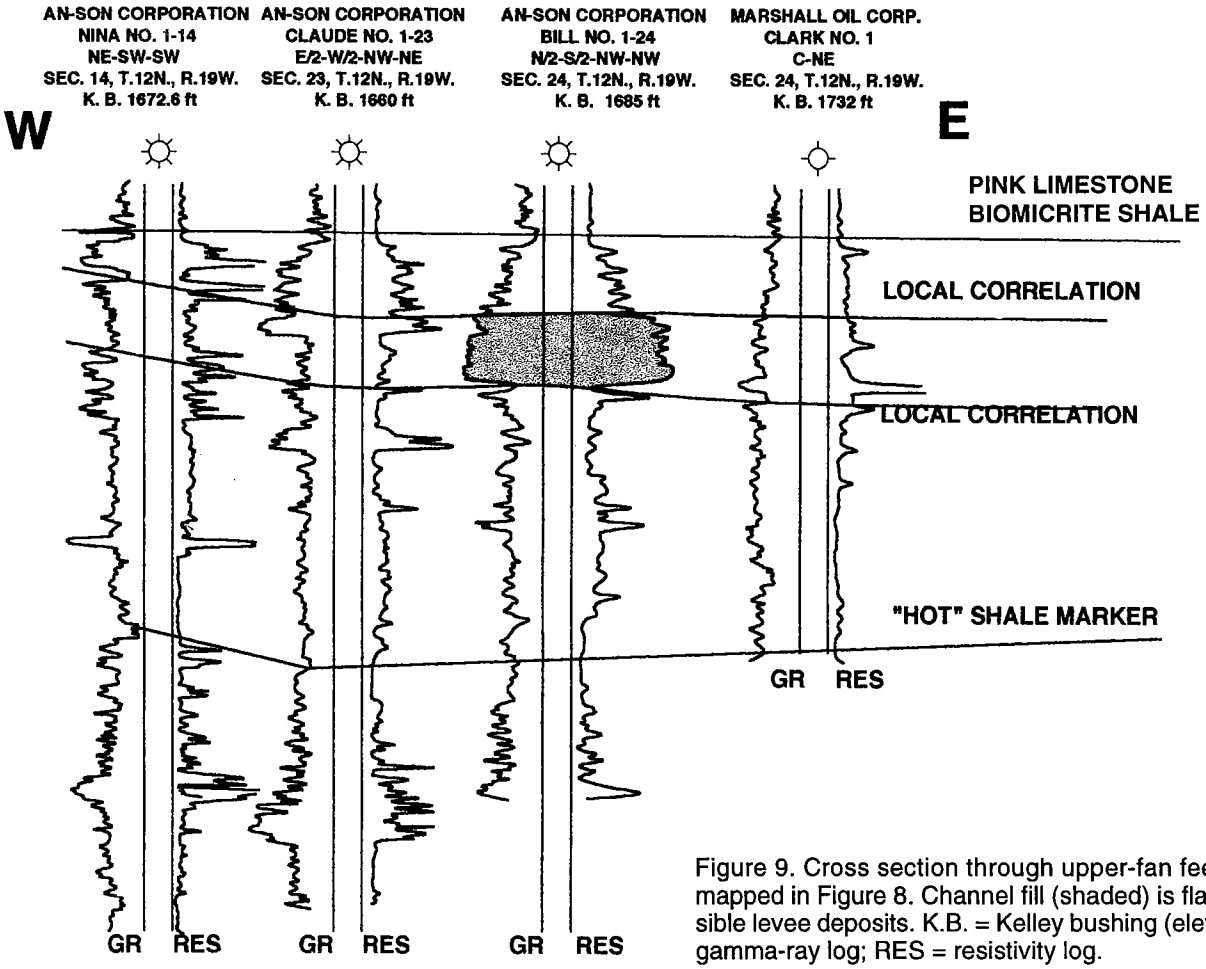

Figure 9. Cross section through upper-fan feeder channel mapped in Figure 8. Channel fill (shaded) is flanked by possible levee deposits. K.B. = Kelley bushing (elevation); GR = gamma-ray log; RES = resistivity log.

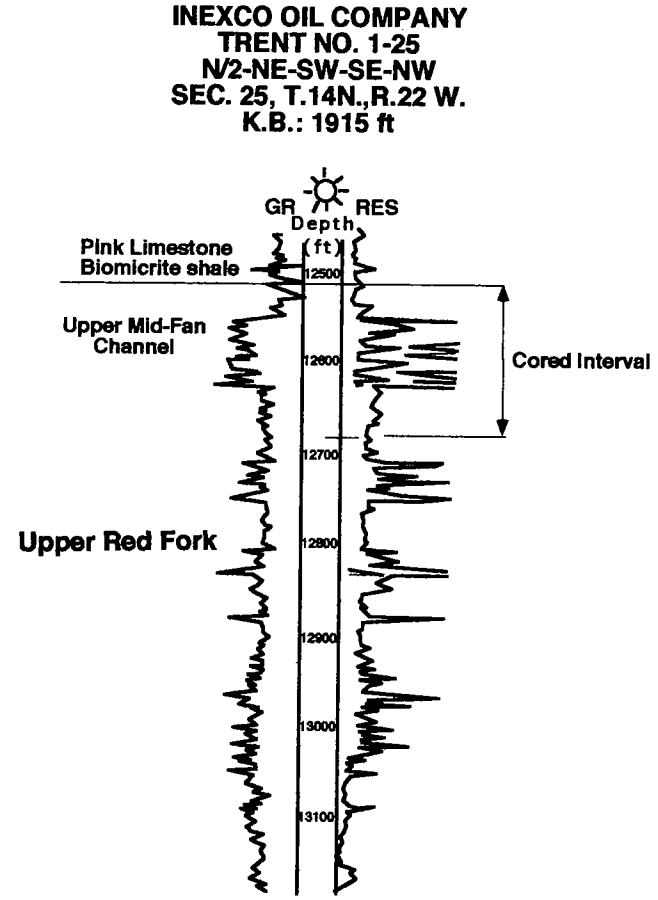

Figure 10. Upper mid-fan channel fill with serrated wireline-log signatures (from Anderson, 1992). The cored interval contains incomplete Bouma (1962) sequences, suggesting possible channelized turbidity flow. Depth in ft. GR = gamma-ray log; RES = resistivity log; K.B. = Kelley bushing (elevation).

as a guide to find thicker sandstone trends, but individual fans and sandstone packages must be examined individually to identify their facies and to predict their reservoir potential.

Upper Red Fork sediments were deposited according to the following sequence of events. (1) A submarine upper-fan feeder channel formed downslope of the Clinton-Weatherford channel located east of the study area. (2) The leveed feeder channel extended from the Clinton area westward to the basin floor. (3) The feeder-channel sediments began forming fan complexes with upper-, mid-, and lower-fan facies. (4) The channels were deflected northward as a result of aggradation that formed topographically higher areas. (5) Finally, upper-fan channels prograded across previously deposited mid- and lower-fan facies, resulting in the juxtapositioning and interfingering of different fan facies (Fig. 12).

Fan deposition may have been influenced by possible sediment sources to the north, northeast, and south. Thin-section petrography indicates that the basin-floor sandstones contain similar constituents and have a similar sediment provenance as the Red Fork to the east. Minor amounts of granophyre and microperthite indicate some contribution from a southern source from the Wichita Mountains.

POROSITY EVOLUTION

Porosity in the Red Fork is essentially all secondary and resulted from dissolution of labile grains such as metamorphic-rock fragments and feldspars. Additional porosity formed by the dissolution of matrix. Complete descriptions of the Red Fork Sandstone and its diagenetic history are found in Anderson (1992), Johnson (1984), and Udayashankar (1985).

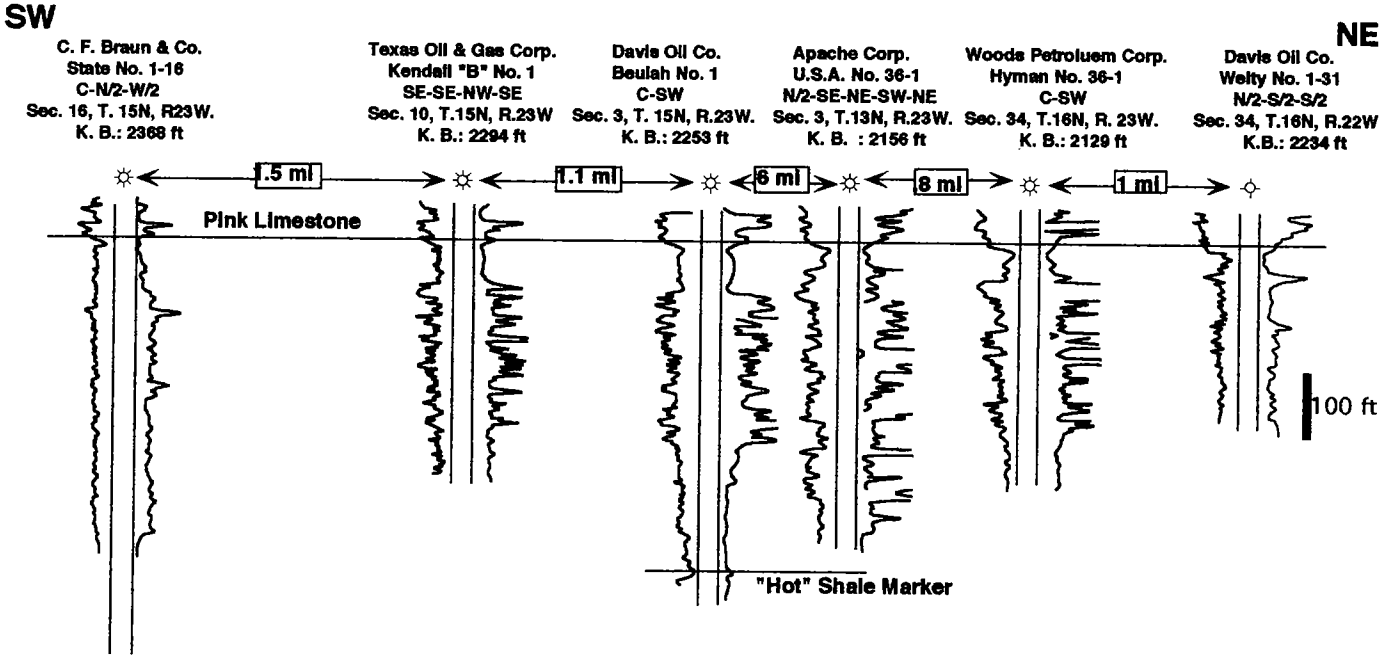

Figure 11. Local southwest-northeast cross section illustrating lateral and vertical changes in wireline-log signatures that indicate reservoir heterogeneity in the upper Red Fork sandstone. K.B. = Kelley bushing (elevation).

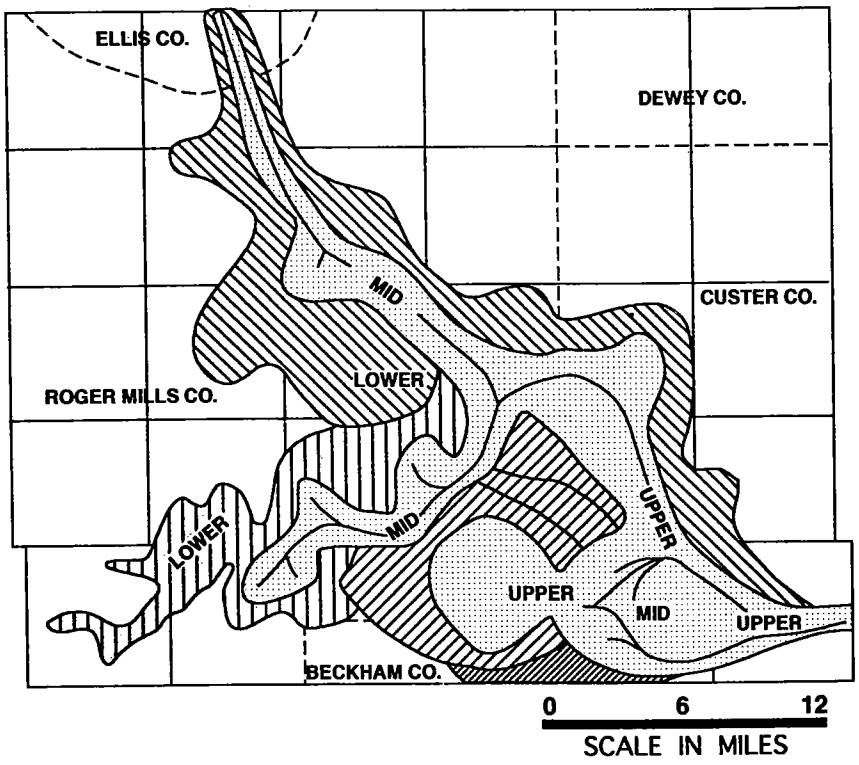

Figure 12. Extent of upper Red Fork submarine-fan progradation in the Anadarko basin. Fan morphology was based primarily on net sandstone thickness.

IMPLICATIONS

Red Fork reservoirs that produce the largest volume of gas are thick channel-fill sandstones of upper- and mid-fan facies. Prospects for fan-channel facies should be developed along thick net-sandstone trends. The multiplicity of channels that resulted from facies stacking and suprafan-lobe switching present a complex target that should be resolved with detailed mapping and/or seismic data. Lateral and vertical variability in the upper Red Fork section has resulted in extensive reservoir compartmentalization. This creates additional potential for finding untapped reserves between existing wells drilled on conventional-spacing patterns.

ACKNOWLEDGMENTS

We thank Eric Anderson for his valuable contributions to this paper. We also thank Phebe Deyhim, Brad Brittain, Ryan Birkenfeld, Amy Close, and Melanie McPhail for their help and support in preparation of the manuscript.

REFERENCES CITED

Al-Shaieb, Zuhair; Shelton, J. W.; Puckette, J. O.; and Boardman, D. B. II, 1995, Sandstone and carbonate reservoirs of the Mid-Continent: a syllabus for a short course sponsored by the Oklahoma City Geological Society, 195 p.

Anderson, C. J., Jr., 1992, Distribution of submarine fan facies of the upper Red Fork interval in the Anadarko basin, western Oklahoma: Oklahoma State University unpublished M.S. thesis, 275 p.

Bouma, A. H., 1962, Sedimentology of some flysch deposits: A graphic approach to facies interpretation: Elsevier, Amsterdam, 168 p.

Glass, J. L., 1981, Depositional environments, reservoir trends, and diagenesis of the Red Fork Sandstone in Grant and eastern Kay Counties, Oklahoma: Oklahoma State University unpublished M.S. thesis, 99 p.

Johnson, C. L., 1984, Depositional environments, reservoir trends, and diagenesis of the Red Fork sandstones in portions of Blaine, Caddo, and Custer Counties, Oklahoma: Oklahoma State University unpublished M.S. thesis, 122 p.

Mutti E.; and Lucchi F. R., 1972, Le torbiditi dell' Appennino settentrionale: Introduzione all'analisi di facies: Society Geologia Italiana Memoir, v. 11, p. 161–199.

Schneider, R. E.; and Clement, W. A., 1986, The East Clinton gas field, Custer County, Oklahoma: a seismic-stratigraphic case history: Oklahoma City Geological Society, Shale Shaker Digest XII, p. 63–67.

Udayashankar, K. V., 1985, Depositional environment, petrology and diagenesis of Red Fork Sandstone in central Dewey County, Oklahoma: Oklahoma State University unpublished M.S. thesis, 188 p.

Walker, R. G., 1978, Deep-water sandstone facies and ancient submarine fans: models for exploration for stratigraphic traps: AAPG Bulletin, v. 62, p. 932–966.

Whiting, P. H., 1982, Depositional environment of Red Fork sandstones, deep Anadarko Basin, western Oklahoma: Oklahoma City Geological Society, Shale Shaker Digest XI, p. 104–119.

Sedimentology and Geochemistry of the Hushpuckney and Upper Tackett Shales: Cyclothem Models Revisited

Anna M. Cruse[1] and Timothy W. Lyons
University of Missouri
Columbia, Missouri

ABSTRACT.—An integrated sedimentological-geochemical model has been applied to the Pennsylvanian cyclothemic Hushpuckney Shale in Iowa and the equivalent upper Tackett shale in Oklahoma to investigate the temporal dynamics of water-column redox as recorded in centimeter-scale variability. X-radiography combined with biofacies models of water-column oxygenation reveal that the gray-shale units in the deepest-water, most-offshore shale facies were deposited under an oxygenated water column, whereas the associated black shales marking maximum transgression were deposited under a water column devoid of oxygen. Thus, the gray-black boundary represents either the paleochemocline—a record of lateral migration of the water-column redox interface in phase with the transgressing and regressing sea—or rapid, basinwide onset of anoxia. Although the water column was everywhere anoxic during black-shale deposition, intersite variations in values of downcore degree of pyritization (DOP) and of iron and organic-carbon concentrations are a function of differences in local sedimentation rates.

INTRODUCTION

The oxic-anoxic boundary (chemocline) in the water column is a critical interface between two vastly different chemical environments. It is a site of enhanced chemical and biological processes, including redox cycling of transition metals (e.g., Spencer and others, 1972; German and others, 1991; Shaw and others, 1994), enhanced precipitation of authigenic apatite (Burnett and others, 1982), and increased biological activity associated with enhanced nutrient cycling (Mullins and others, 1985). Impingement of the chemocline on a basin margin with attendant redox cycling of metals has been proposed as a key factor in the development of transition-metal ore deposits, specifically Mn (Force and Cannon, 1988).

Anoxia below the chemocline arises from the interplay of two mechanisms: (1) excessive oxygen demand due to the biochemical degradation of organic matter, and (2) a deficient oxygen supply that results from inhibited vertical and lateral circulation of oxygen-rich waters. Thus, anoxic conditions occur when the demand for oxygen exceeds the supply (Demaison and Moore, 1980). Bathymetric fluctuations of the chemocline in modern settings occur through natural and anthropogenic processes on time scales of hours to decades (Murray and others, 1989; Kempe and others, 1990; Lyons and others, 1993) and can cause major biologic "kills" due to the low concentrations of dissolved O_2, high concentrations of toxic metals that are remobilized from bottom sediments, and high levels of H_2S linked to bacterial reduction of sulfate in the water column (Boesch and Rabalais, 1991; Shaw and others, 1994; Hagerman and others, 1996; Hornfelt and Nyholm, 1996; Poulson and others, 1997). Despite these potential hazards, we lack detailed models addressing the type and magnitude of the response in water-column and sediment chemistry expected if redox conditions change on time scales of 10^0 to 10^2 years. The rock record, specifically Pennsylvanian cyclothemic shales of Midcontinent North America, provides an ideal setting in which to address these issues, although the time scales of change are significantly longer than those linked to present-day anthropogenic oxygen deficiencies. The redox conditions of the epicontinental sea during deposition of these cyclic units can be constrained by sedimentological and paleontological indicators, providing an independent framework within which to examine the geochemical behavior of a wide range of redox-sensitive chemical species.

To successfully utilize these shale units as analogs for conditions of long-term dynamic anoxia, it is critical to first demonstrate that black-shale deposition occurred as a result of preferential preservation of

[1]Present address: Woods Hole Oceanographic Institution, Dept. of Marine Chemistry and Geochemistry, Woods Hole, Massachusetts

Cruse, A. M.; and Lyons, T. W., 2000, Sedimentology and geochemistry of the Hushpuckney and upper Tackett shales: cyclothem models revisited, *in* Johnson, K. S. (ed.), Marine clastics in the southern Midcontinent, 1997 symposium: Oklahoma Geological Survey Circular 103, p. 185–194.

organic matter under anoxic waters or under anoxic conditions resulting from elevated biological productivity and to characterize the geographic and temporal variation in water-column redox. We have thus undertaken a high-resolution, integrated study of the middle Upper Pennsylvanian (Missourian) Hushpuckney Shale of the Swope Cycle in Iowa and its equivalent in Oklahoma, the upper Tackett shale (P. H. Heckel, personal communication, 1997) and focused specifically on the transitions from gray- to black-shale facies. By combining sedimentological criteria and C-S-Fe systematics, new insight has been gained about redox conditions in the Pennsylvanian epicontinental sea that provides a framework within which to evaluate the accumulation of organic carbon and the behavior of redox-sensitive transition metals and rare-earth elements under conditions of dynamic redox.

GEOLOGIC SETTING

The Pennsylvanian System of the Midcontinent is characterized by fourth- to fifth-order cycles of shales and limestones known as cyclothems (Heckel, 1977, 1986). These sequences developed in response to waxing and waning of Gondwanan glaciers and ice caps most probably on Milankovich time scales (Wanless and Shepard, 1936; Heckel, 1977, 1986; Crowell, 1978), although tectonic processes may have influenced sequence development, particularly in areas proximal to the Appalachian orogenic belt (Klein, 1992; Klein and Kupperman, 1992). Earlier autocyclic models of delta shifting (Galloway and Brown, 1973; Ferm, 1975) are accommodated within the glacial-eustatic model as a mechanism for local sequence modification (Heckel, 1977, 1980).

A classic, "Kansas-type" cyclothem, which is shown schematically in Figure 1, consists of an outside shale deposited in a nearshore fluvial-deltaic environment followed upsection by a thin (0.1–1.0 m) transgressive limestone. This thin limestone is succeeded respectively by an offshore shale, a thick (2–10 m) regressive limestone, and a second outside (nearshore) shale (Heckel, 1977). The difference in thickness between the two limestone units reflects the dynamics of sea-level change—ice caps melt faster than they form (Heckel, 1986). Sequences were commonly exposed to subaerial weathering between individual transgressive-regressive cycles, as recorded by paleosols capping the uppermost outside-shale units and meteoric cements in the regressive limestones (Heckel, 1977, 1983, 1994; Goebel and others, 1989).

The offshore-shale facies (also known as the core shale) typically contains a thin (<1 m thick), laminated, black, organic-rich, phosphatic shale interbedded within overlying and underlying gray, organic-poor, bioturbated shales. The black-shale units can be correlated throughout the Midcontinent, with surface and subsurface distributions ranging between 20,000 and 100,000 km^2 (Coveney and Glascock, 1989). Sedimentation rates during black-shale deposition were generally low throughout the basin and increased toward the shoreline in western Oklahoma and Texas and in the Appalachian region due to increased detrital flux related to weathering of tectonic highlands (Heckel, 1994). Although the depositional environment of Pennsylvanian black shales has been debated (e.g., Zangerl and Richardson, 1963; Heckel, 1977, 1991; Coveney and others, 1991; Heckel and Hatch, 1992), the consensus is that Upper Pennsylvanian (Missourian and Virgilian) black shales were deposited under deep waters in relatively offshore environments (Heckel, 1977, 1991; Coveney and others, 1991; Coveney, 1992; Heckel and Hatch, 1992).

Black-shale deposition is widely believed to have occurred at maximum transgression when water depths were great enough (~100 m) to support stratification due to development of a pycnocline (Heckel, 1977; Hatch and Leventhal, 1992), with attendant anoxia leading to preferential carbon preservation. Increased productivity rather than enhanced preservation also has been proposed as a causal factor in black-shale development (e.g., Pedersen and Calvert, 1990), where water column anoxia can be viewed as an effect rather than a cause of organic enrichment. Although productivity increases may have been a significant factor, it is highly unlikely that a record of such an event would have been preserved in an environment characterized by low sedimentation rates without anoxia in the overlying waters (Heckel, 1991). The presence of water-column anoxia during deposition of the black shales is corroborated by the geochemical results presented below.

METHODS

Drill cores of the Hushpuckney Shale and the equivalent upper Tackett shale from two sites in the Midcontinent (sites IRC in Iowa and C-TW-1 in Oklahoma; Fig. 2) were sampled at centimeter-scale intervals with an emphasis on transitions between gray and black facies. The gray-black–shale boundaries were determined based on the first and last appearance of laminations in X-radiographs. The first five to eleven samples both stratigraphically above and below the determined boundary were contiguous. The next one to four samples were separated by intervals of 3–4 cm. Samples were then crushed to fine powders using an alumina ceramic ball and mill.

Concentrations of total and inorganic carbon (C_{inorg}—carbon present as $CaCO_3$) were determined by liberating the carbon via combustion at 950°C and acidification in 2N (normal) HCl, respectively. The amount of CO_2 generated was then quantified via coulometric titration, allowing organic carbon (C_{org}) concentrations to be calculated by difference. Analyses of pure $CaCO_3$ standards were reproducible to within 0.08 wt%.

Total reduced-sulfur (TRS) concentrations were measured using the chromium-reduction method described in Zhabina and Volkov (1978) and Canfield and others (1986). TRS consists of sulfur in pyrite and iron monosulfides and as elemental sulfur. Iron monosulfides and elemental sulfur are generally transient species on geologic time scales; thus, TRS can be consid-

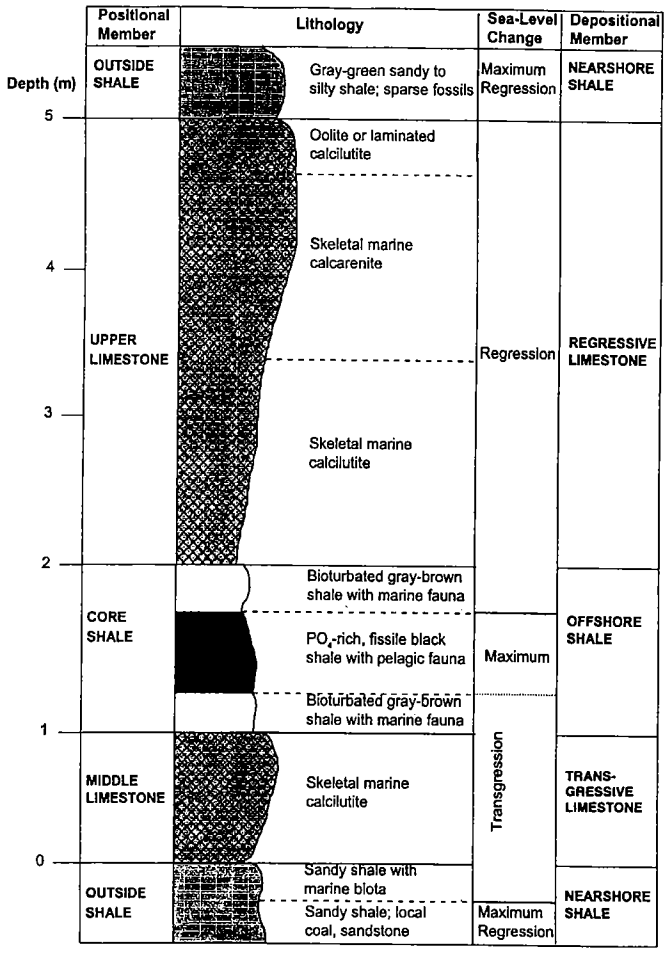

Figure 1. Generalized stratigraphic section of a "Kansas-type" cyclothem, Midcontinent North America. Modified from Heckel (1977).

ered to represent pyrite sulfur (S_{py}), given the absence of other base-metal sulfides in the samples of interest. Replicate analyses of freshly ground, pure pyrite standards yielded sulfur recoveries that were consistently greater than 96 wt%.

The extent to which the original total reactive iron reservoir has been transformed to pyrite can be assessed by calculating degree-of-pyritization (DOP) values (Berner, 1970; Raiswell and others, 1988). DOP is defined as:

$$Fe_{py}/(Fe_{py} + Fe_{HCl}),$$

where Fe_{py} is the pyrite-iron concentration calculated from measured values of S_{py}. Fe_{HCl} is the remaining, unsulfidized portion of the "reactive" iron reservoir and is defined as the fraction of iron that is extractable by boiling in 12 N HCl for 1 min (Berner, 1970; Raiswell and others, 1988). This method has been shown to cause nearly complete extraction of iron in oxide phases (including magnetite) and comparatively little extraction of silicate iron—with the possible exceptions of chlorite, nontronite, and (perhaps) biotite—as discussed by Raiswell and others (1994). This method thus overestimates the pool of iron that is readily reactive towards hydrogen sulfide, which can cause DOP calculations to be moderate, despite the persistent presence of anoxic-sulfidic (euxinic) conditions in the water column or in the sedimentary pore waters (Lyons, 1997). The extracted Fe concentrations were quantified spectrophotometrically using the ferrozine method of Stookey (1970). The standard deviation for replicate analyses was less than 9.5% of the mean, resulting in an error in calculated DOP values of only 1%. Bulk iron and titanium concentrations in each sample were measured by instrumental neutron activation analysis at the Missouri University Research Reactor.

RESULTS

X-Radiography

The Hushpuckney Shale in core IRC (Iowa) and its equivalent, the upper Tackett shale in core C-TW-1 (Oklahoma) exhibit a well-developed, microlaminated, phosphate-rich, black-shale facies that lies between nonnlaminated gray shales, with phosphate present as both discrete nodules (C-TW-1) and as bedding-parallel microlaminae (IRC) in the black shales. Bivalve fossils are present in X-radiographs of the upper and lower gray shales in core C-TW-1 and are conspicuously absent in the laminated black facies of C-TW-1 and IRC. In addition, burrows and root casts have been preserved in the upper and lower gray shales in both cores.

C-S-Fe System

Concentrations of C_{org} in the black-shale facies of both C-TW-1 and IRC are greatly enriched relative to the overlying and underlying gray shales. In C-TW-1, C_{org} ranges from 5 to 13 wt%, in contrast to 0.8 to 1.2 wt% and 1.1 to 3 wt% in the transgressive and regressive gray shales, respectively (Fig. 3). The black-shale facies in IRC is more organic-rich than C-TW-1, with concentrations ranging from 7 to 35 wt% (Fig. 3). The gray shales in IRC are very lean in organic matter, generally containing less than 0.7 wt% C_{org}. Carbonate concentrations (C_{inorg}) in C-TW-1 are highest in the lowermost gray sample and are low in the black and regressive gray shales. The black shale in IRC contains between 0.2 to 1.5 wt% C_{inorg}, with concentrations in the gray shales generally increasing with distance away from the gray-black–shale boundary. For reference, pure $CaCO_3$ is 12 wt% C_{inorg}.

The S_{py} concentrations show very different behavior in these two cores (Fig. 4), despite gross intersite similarities in C_{org} and C_{inorg} trends. In core C-TW-1, S_{py} concentrations differ by a factor of 10 in the two gray facies, averaging approximately 1 wt% in the transgressive samples and 0.1 wt% within the regressive samples. Concentrations in the regressive black shale samples are generally more enriched than in the transgressive samples. For example, in the transgressive portion of the black-shale facies, the maximum S_{py} concentration is only 4.4 wt%, in contrast to a maximum of 12.9 wt% in the regressive facies. Centimeter-scale fluctuations of 300% to 600% are imposed on this over-

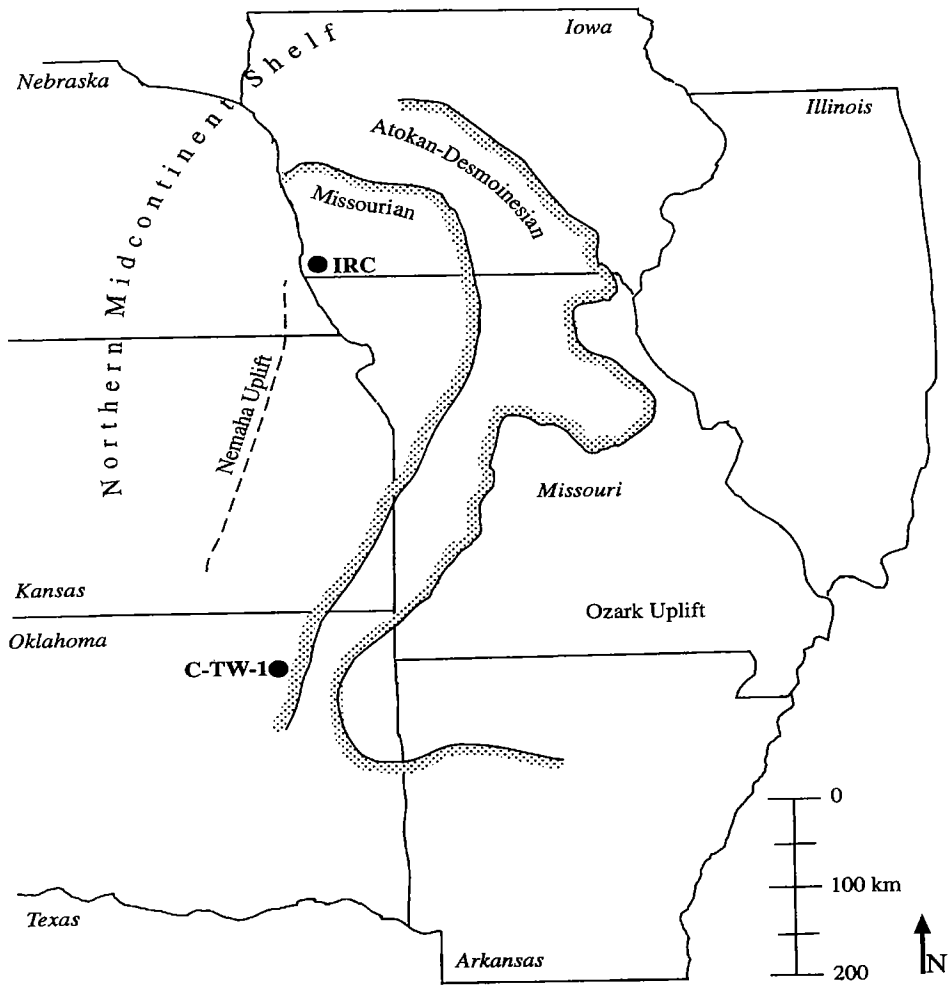

Figure 2. Location map showing generalized Pennsylvanian paleogeography, the subarial distribution of the outcrop belt (stippled area), and the two drill-core sites. Base map modified from Heckel (1977).

all trend of increasing concentrations upcore. Throughout the black facies of IRC, S_{py} concentrations are consistently near 1.5 wt%, with the highest concentration of 3.2 wt% found in the overlying regressive gray shale.

The trends for DOP versus depth in C-TW-1 and IRC are similar to those observed for S_{py} concentrations (Fig. 5). DOP values in the transgressive black shale of C-TW-1 range between 0.51 and 0.78, whereas those in the regressive organic-rich facies range between 0.68 and 0.86. There is also centimeter-scale variability in DOP values, such as the shift toward lower values between depths of 8,945 and 8,955 cm (Fig. 5). DOP values are an order of magnitude lower in the regressive gray shale than in the transgressive gray shale, as manifested in a dramatic drop in values across the regressive chemocline boundary from black to gray shale, in sharp contrast to the only slight change observed across the transgressive boundary (Fig. 5). In IRC, DOP values calculated for black-shale samples span a narrow range centered around 0.6, with higher values in the overlying and underlying gray shales (Fig. 5).

Bulk iron concentrations are a mixture of a detrital and an authigenic component. Only variations in the authigenic component, however, reflect water-column redox conditions. By normalizing the iron concentrations to the titanium concentrations, authigenic enrichments relative to the average detrital input can be discerned. In C-TW-1, ratios of Fe/Ti in the black shales subtly increase upcore, with smaller-scale decreases superimposed on this trend. The Fe/Ti ratio in the overlying and underlying gray shales are similar to crustal average values (Fig. 6). In IRC, the ratio of Fe/Ti is uniformly low, near crustal average values, throughout the black-shale facies.

DISCUSSION

Sedimentological Model for Depositional Environment

The first step in interpreting the gray-black shale boundary as a record of the paleochemocline is establishing that the redox state of the overlying water column differed during black- and gray-shale deposition. Rhoads and Morse (1971) synthesized data from modern marine environments with differing bottom-water concentrations of dissolved O_2 to develop a biofacies model of water-column redox conditions. This model allowed the recognition of three different regions of dissolved oxygen concentrations based on sedimentological structures and macrofaunal characteristics. These are: (1) anaerobic (<0.1 ml/l O_2), (2) dysaerobic (0.1–1.0 ml/l O_2), and (3) aerobic (>1.0 ml/l O_2). Subsequent work by Savrda and others (1984) and Savrda and Bottjer (1986, 1987, 1991) incorporating an ichnofossil hierarchy and new interpretations of macrofossil assemblages has resulted in a refined model that includes five distinct redox environments within the context of spatial and temporal oxygen gradients (Savrda and Bottjer, 1991). Even in the revised model, the presence of well-developed laminations indicates anoxia in the overlying water column, whereas homogenized and burrowed sediments are deposited under oxic water columns.

X-radiography of the two cores revealed that the black-shale facies is microlaminated and devoid of trace fossils or bivalves. This absence contrasts strikingly to the overlying and underlying gray shales that

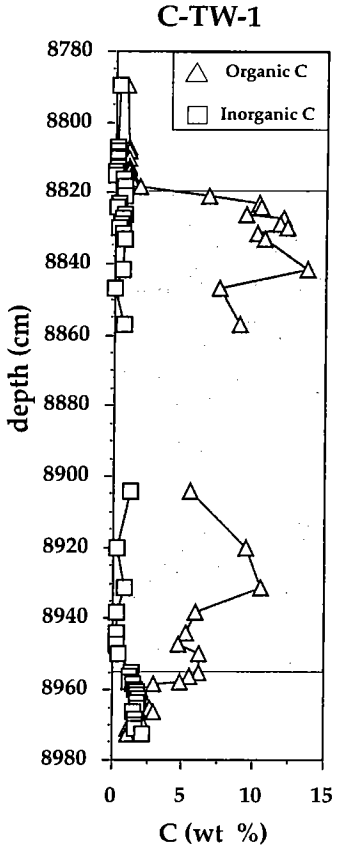

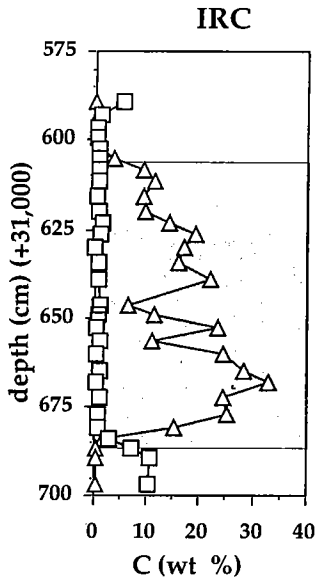

Figure 3. Organic (squares) and inorganic (triangles) carbon concentrations (wt%) versus depth (cm) for C-TW-1 and IRC. Pure carbonate represents 12 wt% C_{inorg}. Shaded area represents the interval in which laminations were observed in X-radiographs, corresponding to times of anoxia in the overlying water column. Note differing scales for each graph.

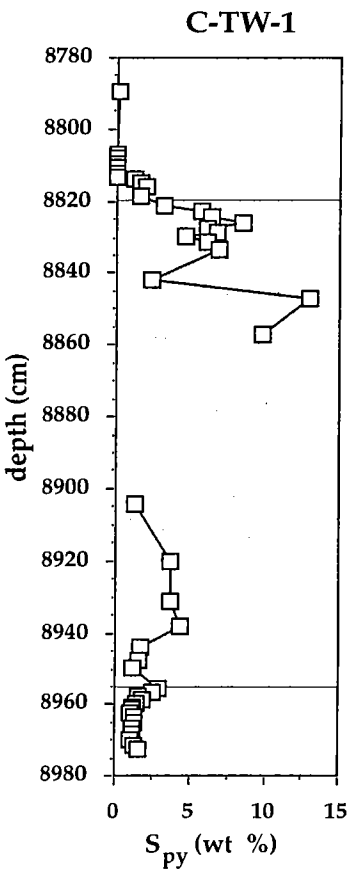

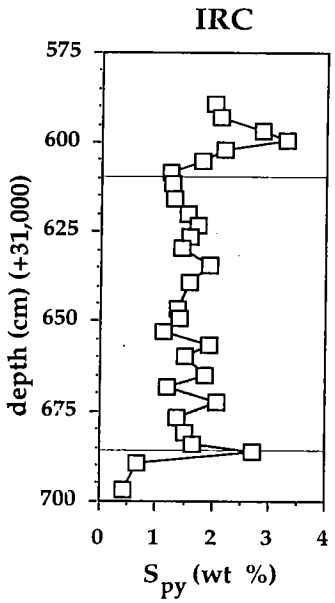

Figure 4. Pyrite sulfur concentrations (wt%) versus depth (cm) for core-holes C-TW-1 and IRC. Shaded area is the same as in Figure 3.

are homogenized due to bioturbation and contain abundant bivalves and burrows. These differences in sedimentary structures and paleontological characteristics are related to variations in the degree of water-column oxygenation. When the overlying water column is fully oxygenated, benthic fauna thrive. Through infaunal life processes, these animals bioturbate and homogenize sediments, resulting in biofabrics in the gray shales and preservation of body fossils. When bottom waters become anoxic (i.e., contain no dissolved oxygen), benthic macrofauna can no longer survive. Consequently, microlaminations are preserved, and no benthic fossils are found. The black-shale facies in C-TW-1 and IRC were deposited in an environment of water-column anoxia, and the overlying and underlying gray shales were deposited under an oxic water column. Thus, the gray-black boundary in the core shale facies represents a record of the impingement of the paleochemocline on the basin margin or sudden onset of basinwide anoxia. This sedimentological model of paleoredox conditions provides a framework within which to utilize the C-S-Fe system to provide greater temporal and spatial details of the development of water-column anoxia.

C-S-Fe Systematics

Geochemical proxies used in conjunction with oxygen-related biofacies models can provide greater detail concerning the paleoredox conditions of the water column and the evolution of anoxia. The C-S-Fe system, as it relates to sedimentary pyrite formation, has been shown to be a powerful tool in reconstructing paleoenvironments (Raiswell and Berner, 1985; Dean and Arthur, 1989; Lyons and others, 2000). The first step in the formation of sedimentary pyrite is the bacterially mediated process of sulfate reduction:

$$2\ CH_2O + SO_4^{2-} \rightarrow H_2S + 2\ HCO_3^-$$

Hydrogen sulfide generated via this reaction then combines with reactive iron minerals to form iron monosulfides and finally pyrite (FeS_2) (Berner, 1984; Hurtgen and others, 1999). The C_{org}, S, and Fe can limit the formation of bacteriogenic sedimentary pyrite in three fundamental environments: (1) freshwater, (2) normal (oxic) marine, and (3) euxinic (anoxic, sulfidic) marine (Raiswell and Berner, 1985).

Fresh-water environments are typically depleted in sulfate so that these sediments display a wide range of C_{org} concentrations with very low levels of pyrite sulfur (Lyons and Berner, 1992; see Fig. 7). The amount

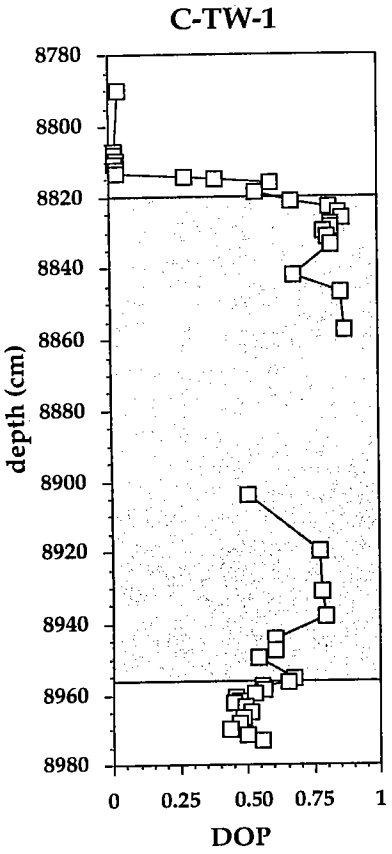

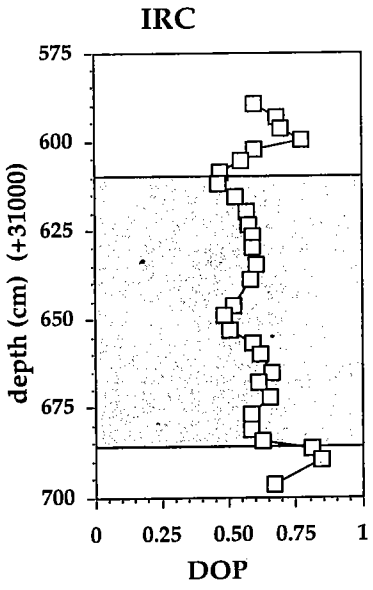

Figure 5. Calculated degree-of-pyritization (DOP) values versus depth (cm) in core-holes C-TW-1 and IRC. Shaded area is the same as in Figure 3.

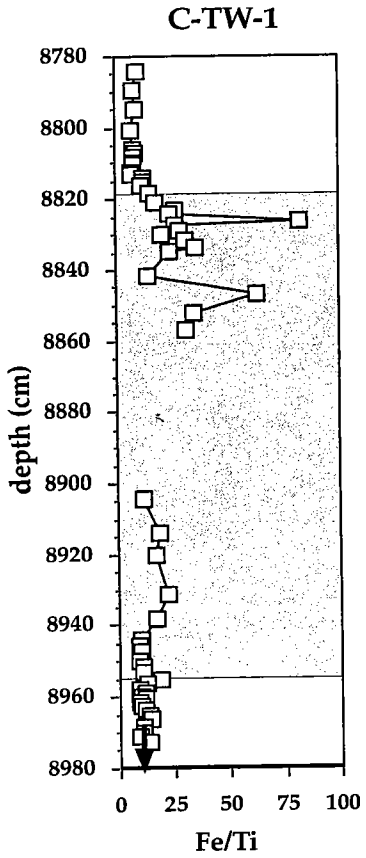

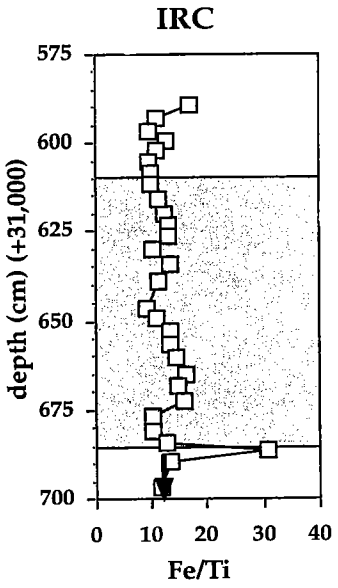

Figure 6. Iron concentrations (ppm) normalized to Ti concentrations (ppm) in core-holes C-TW-1 and IRC. Arrow indicates Fe/Ti ratio in average continental crust (Taylor and McClennan, 1985). Shaded area is the same as in Figure 3.

and reactivity of deposited organic matter is typically the limiting factor for pyrite formation in normal marine environments (Berner, 1984), which results in a strong coupling between S_{py} and C_{org} (Fig. 7).

In euxinic environments, H_2S is ubiquitous. Thus, the size of the reactive sedimentary-iron reservoir commonly becomes the limiting factor in pyrite formation (Raiswell and Berner, 1985). C-S relationships in these environments can become more complicated because of the potential for both diagenetic (sedimentary) and syngenetic (water-column) contributions to pyrite formation (Raiswell and Berner, 1985). If a large diagenetic component exists relative to the syngenetic component, the result will be a line of positive slope (a diagenetic component of increasing C_{org} and S_{py} reflecting C_{org} limitations during burial) that has a nonzero intercept (syngenetic component) (Fig. 7). However, the line of positive slope can also represent an environment where most of the pyrite formed in the water-column with Fe deposition that was strongly coupled to C_{org} (Raiswell and Berner, 1985). A line of zero-slope (fixed S_{py} and increasing C_{org}) characterizes euxinic environments where pyrite formation is strongly Fe-limited and where C_{org} and Fe deposition are decoupled (Lyons and Berner, 1992) (Fig. 7).

Degree-of-pyritization (DOP) values can be utilized both to indicate water-column redox conditions as well as to distinguish between Fe limitation and C_{org} limitation in producing the euxinic line of positive slope (Raiswell and Berner, 1985; Raiswell and others, 1988; Lyons and Berner, 1992). Raiswell and others (1988) showed that decreasing water-column oxygen concentrations is strongly correlated with increasing values of DOP. The DOP values can be utilized to distinguish between three types of bottom-water conditions: (1) aerobic, with DOP <0.46; (2) restricted, with DOP between 0.46 and 0.80; (3) inhospitable, with DOP generally >0.76 (Raiswell and others, 1988). However, some caution is required in the interpretation of DOP values. In euxinic environments where the sedimentation rate is high and the detrital iron reservoir is highly unreactive, DOP values can be rather low despite the ubiquity of H_2S in the water column (Canfield and others, 1996; Lyons, 1997; Raiswell and Canfield, 1998).

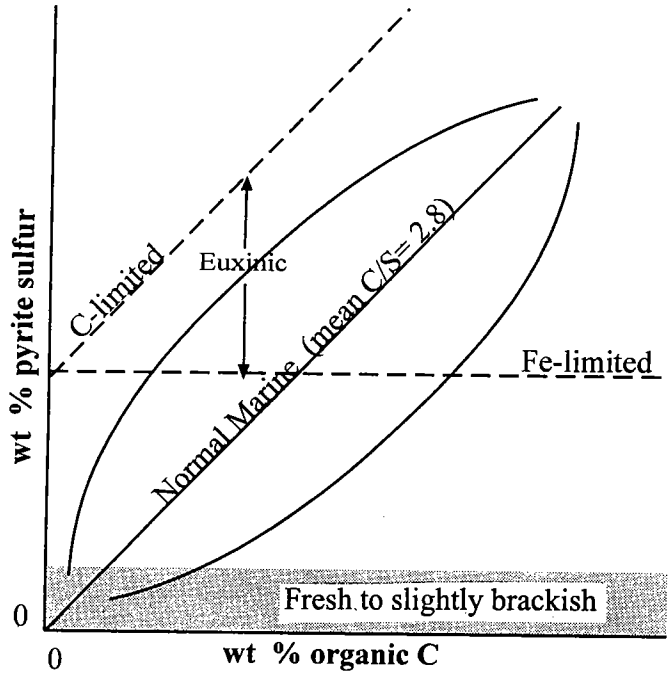

Figure 7. Schematic diagram showing variations in C-S relationships in fresh-water, normal-, and euxinic-marine environments. Redrawn from Lyons and Berner (1992).

Although the black-shale facies in both cores contain elevated concentrations of C_{org}, the very different trends in S_{py} concentrations and DOP values may indicate geographic variation in water-column redox conditions or inputs of detritally delivered Fe. The overall range of calculated DOP values in core C-TW-1 (0.51–0.78, Fig. 5) indicates that the water column was largely euxinic (anoxic-sulfidic) as the black facies was deposited. There is a subtle increase in DOP values upcore within the black shale (Fig. 5), which is also manifested in an increase in the Fe/Ti ratio (Fig. 6). These increases likely reflect an overall decrease in sedimentation rate upcore. Superimposed on this overall trend are shifts toward lower DOP values, S_{py} concentrations and Fe/Ti (e.g., between 8,945 and 8,955 cm depth) (Figs. 4–6). These shorter-term events may have resulted from a temporary weakening of the stratification of the water column that allowed increased vertical mixing (Hatch and Leventhal, 1992). Alternatively, these decreases could also represent short-term increases in sedimentation rate, with a subsequent dilution of the authigenic Fe and S_{py} concentrations. That is, Fe scavenged from the water column with S would be decoupled from the local detrital flux. Preliminary $\delta^{34}S$ measurements of authigenic sulfide are uniformly low (approximately –40‰ relative to the Canyon Diablo troilite (CDT) standard) throughout the black-shale facies in C-TW-1, indicative of bacterial reduction of sulfate to sulfide within the open-reservoir conditions of the water column (Lyons, 1997). This scenario is most consistent with a decrease in sedimentation rate upcore. If the bottom waters were periodically ventilated to produce the lower S_{py} concentrations and DOP values, this would result in higher $\delta^{34}S$ values as the locus of sulfate reduction shifted to the pore waters. In pore waters, the sulfate pool can become limited, driving the $\delta^{34}S$ of sulfate and sulfide toward higher values.

Concentrations of S_{py} and DOP values in C-TW-1 drop dramatically across the regressive chemocline (from black to gray shale), in sharp contrast to the slight change observed across the transgressive boundary (Figs. 4 and 5). As anoxic waters inundated the sediments and sulfate reduction initiated, H_2S likely diffused downward into the underlying transgressive gray-shale facies, sulfidizing reactive iron that was still present (Pruysers and others, 1993; Passier and others, 1996) and producing relatively high S_{py} concentrations and DOP values. The order of magnitude lower S_{py} concentrations and calculated DOP values in the regressive gray shale likely reflect penetration of oxygenated meteoric waters into this unit during subaerial exposure at maximum sea-level lowstand, as well as clastic dilution due to an increased sedimentation rate. The absence of a diffusion overprint and lower sulfide availability relative to the black shales is due to C_{org} limitation. The penetrating waters also produced the paleocaliche and vadose-zone cements observed in the overlying Bethany Falls Limestone (P. H. Heckel, personal communication, 1997). As the oxygen burndown occurred, S_{py} would have been oxidized to sulfate and remobilized from the shale, resulting in dramatically lower concentrations and DOP values. Similar events have been reported from the overlying Stark Shale by Hatch and Leventhal (1997).

In C-TW-1, black-shale samples from both the transgressive (GT) and regressive (GR) gray shales as well as the transgressive black-shale samples (BT) tend to cluster around the Holocene normal-marine line, although some black-shale samples do lie both above and below the line (Fig. 8). This supports the interpretation of the gray shales being deposited under normal-marine (i.e., oxygenated) conditions. The black-shale results are likely skewed by the effects of Fe limitation. The regressive black-shale samples (BR) deposited under euxinic conditions with inferred low sediment inputs, however, define a line of negative slope rather than conforming to one of the predicted relationships (Figs. 7 and 8). Again, this discrepancy results from the decrease in the sedimentation rate of clastic components upcore. The samples with the highest concentrations of S_{py} represent a time of highly sediment-starved depositional conditions, with syngenetically formed pyrite from the water column forming a dominant portion of the buried sulfur and iron fluxes. In this case, C-S relationships still reflect paleoceanographic conditions because the source for the preserved carbon and sulfur was the overlying water column.

Concentrations of S_{py} and calculated DOP values for black-shale samples from IRC both span a narrow range. DOP values range from 0.47 to 0.66, commonly indicative of dysoxic to anoxic rather than euxinic conditions (Fig. 5). On a plot of C_{org} versus S_{py}, the black-shale samples (BR, BT) define a straight line that is below the Holocene normal-marine trend, a relationship

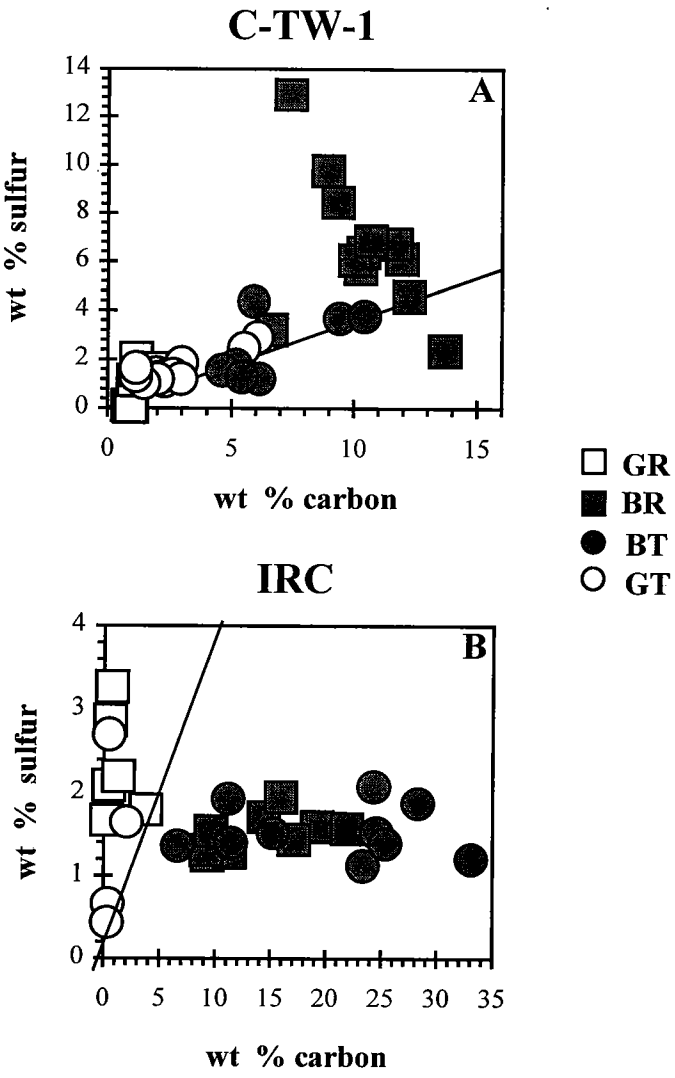

Figure 8. S_{py} (wt%) versus C_{org} (wt%) for core-holes *A.* C-TW-1 and *B.* IRC. Note differing scales on each graph. Solid line represents the mean C/S weight ratio of 2.8 for normal-marine Holocene sediments.

that is indicative of Fe-limited pyrite formation under an euxinic water column (Fig. 8). Thus, the relatively low DOP values are a manifestation of the lability of the detrital-iron reservoir rather than paleoredox conditions. As is hypothesized for C-TW-1, the water column at IRC appears to have remained euxinic throughout black-shale deposition. Iron-limited pyrite formation can characterize basin-margin environments where the influx of weathered detrital iron swamps the amount of iron scavenged in a sulfidic water column independent of clastic inputs (Canfield and others, 1996; Hurtgen and others, 1999). Paleogeographic reconstructions (Heckel, 1980) place IRC in a location toward the center of the basin, removed from the marginal environment where euxinic, iron-limited pyrite formation would be expected. However, this most likely reflects the nature of the rock record, so that such reconstructions tend to simplify coastlines rather than portraying the complexities observed in modern environments, indicating the potential role of geochemical proxies to enhance models developed using traditional sedimentological techniques alone.

Calculated DOP values for the overlying regressive gray-shale samples from IRC are higher than in the black-shale facies, despite low carbonate concentrations (Figs. 3 and 5). S_{py} concentrations are extremely high in comparison to the concentration of C_{org}, as can be seen on the C-S plot (Fig. 8). Low-temperature diagenetic processes are unlikely to produce this relationship, suggesting that the relatively high S_{py} concentrations decoupled from C_{org} concentrations and high DOP values resulted from the epigenetic addition of some pyrite from circulating basinal brines. The C-S-Fe relationships in the black shale do not appear to have been affected by this process, suggesting that the brines may have flowed preferentially through the gray shale due perhaps to a lower permeability associated with the bioturbated sediment fabric.

In summary, the C-S-Fe relationships for C-TW-1 and IRC appear to indicate black-shale deposition under euxinic conditions throughout the Pennsylvanian epicontinental sea. DOP and S_{py} trends versus depth in core C-TW-1 appear to reflect euxinic water-column conditions with smaller scale variations in sediment input (detrital-iron inputs). Black-shale deposition in IRC appears also to have occurred exclusively within an euxinic water column, but, with S_{py}, DOP, and Fe/Ti relationships controlled by the consistently high inferred inputs of clastic sediment. Additionally, there appears to have been slight postdepositional augmentation of the sedimentary pyrite reservoir in the regressive gray shales in IRC. However, this process did not affect the underlying black shales, suggesting preferential fluid flow linked to biofabric-controlled heterogeneities in permeability.

CONCLUSIONS

A combined sedimentological-geochemical approach has been applied to Pennsylvanian cyclothemic shales in Oklahoma and Iowa in order to demonstrate that black-shale formation was caused by enhanced preservation of organic carbon, and likely enhanced productivity, under an anoxic-sulfidic water column. Anoxia was maintained underneath a pycnocline that migrated in phase with the transgressions and regressions of the epicontinental sea. The addition of geochemical proxies to sedimentological models of depositional environment allows the discernment of additional temporal and geographic detail concerning the development and maintenance of water-column anoxia on 1,000- to 10,000-yr time scales. The depositional model developed here for the Hushpuckney/upper Tackett shales provides a framework within which the behavior of redox-sensitive chemical species can now be investigated to answer questions concerning the consequences of long-term anoxia in the natural environment and short-term redox changes linked to anthropogenic environmental change.

REFERENCES CITED

Berner, R. A., 1970, Sedimentary pyrite formation: American Journal of Science, v. 267, p. 19–42.

_____ 1984, Sedimentary pyrite formation: An update: Geochimica et Cosmochimica Acta, v. 48, p. 605–615.

Boesch, D. F.; and Rabalais, N. N., 1991, Effects of hypoxia on continental shelf benthos: comparisons between the New York Bight and the northern Gulf of Mexico, *in* Tyson, R. V.; and Pearson, T. H. (eds.). Modern and ancient continental shelf anoxia: Geological Society of America Special Publication 58, p. 27–34.

Burnett, W. C; Beers, M. J.; and Roe, K. K., 1982, Growth rates of phosphate nodules from the continental margin off Peru: Science, v. 215, p. 1616–1618.

Canfield, D. E.; Lyons, T. W.; and Raiswell, R., 1996, A model for iron deposition to euxinic Black Sea sediments: American Journal of Science, v. 296, p. 818–834.

Canfield, D. E.; Raiswell, R.; Westrich, J. T.; Reaves, C. M.; and Berner, R. A., 1986, The use of chromium reduction in the analysis of reduced inorganic sulfur in sediments and shales: Chemical Geology, v. 54, p. 149–155.

Coveney, R. M., Jr., 1992, Evidence for expulsion of hydrothermal fluids and hydrocarbons in the Midcontinent during the Pennsylvanian, *in* Johnson, K. S.; and Cardott, B. C. (eds.), Source rocks in the southern Midcontinent, 1990 symposium: Oklahoma Geological Survey Circular 93, p. 133–144.

Coveney, R. M., Jr.; and Glascock, M. D., 1989, A review of the origins of metal-rich Pennsylvanian black shales, central U.S.A., with an inferred role for basinal brines: Applied Geochemistry, v. 4, p. 347–367.

Coveney, R. M., Jr.; Watney, W. L.; and Maples, C. G., 1991, Contrasting depositional models for Pennsylvanian black shales discerned from molybdenum abundances: Geology, v. 19, p. 147–150.

Crowell, J. C., 1978, Gondwanan glaciation, cyclothems, continental positioning, and climate change: American Journal of Science, v. 278, p. 1345–1372.

Dean, W. E.; and Arthur, M. A., 1989, Iron-sulfur-carbon relationships in organic-carbon-rich sequences I: Cretaceous Western Interior Seaway: American Journal of Science, v. 289, p. 708–746.

Demaison, G. J.; and Moore, G. T., 1980, Anoxic environments and oil source bed genesis: American Association of Petroleum Geologists Bulletin, v. 64, p. 1179–1209.

Ferm, J. C., 1975., Pennsylvanian cyclothems of the Appalachian plateau, a retrospective view, *in* McKee, E. D.; and Crosby, E. J. (eds.), Paleotectonic investigations of the Pennsylvanian System in the United States: Part II.—Interpretive summary and special features of the Pennsylvanian System: U.S. Geological Survey Professional Paper 853, p. 57–64.

Force, E. R.; and Cannon, W. F., 1988, Depositional model for shallow-marine manganese deposits around black shale basins: Economic Geology, v. 83, p. 93–117.

Galloway, W. E.; and Brown, L. F., Jr., 1973, Depositional systems and shelf-slope relations on cratonic basin margin, uppermost Pennsylvanian of north-central Texas: American Association of Petroleum Geologists Bulletin, v. 57, p. 1185–1218.

German, C. R.; Holliday, B. P.; and Elderfield, H., 1991, Redox cycling of rare earth elements in the suboxic zone of the Black Sea: Geochimca et Cosmochimca Acta, v. 55, p. 3553–3558.

Goebel, K. A.; Bettis, E. A., III; and Heckel, P. H., 1989, Upper Pennsylvanain paleosol in Stranger Shale and underlying Iatan Limestone, southwestern Iowa: Journal of Sedimentary Petrology, v. 59, p. 224–232.

Hagerman, L.; Josefson, A. B.; and Jensen, J. N., 1996, Benthic macrofauna and demersal fish, *in* Jorgensen, B. B.; and Richardson, K. (eds.), Eutrophication in coastal marine systems: American Geophysical Union Coastal and Estuarine Studies, v. 52, , p. 155–178.

Hatch, J. R.; and Leventhal, J. S., 1992, Relationship between inferred redox potential of the depositional environment and geochemistry of the Upper Pennsylvanian (Missourian) Stark Shale Member of the Dennis Limestone, Wabaunsee County, Kansas, U.S.A.: Chemical Geology, v. 99, p. 65–82.

Hatch, J. R.; and Leventhal, J. S., 1997, Early diagenetic partial oxidation of organic matter and sulfides in the Middle Pennsylvanian (Desmoinesian) Excello Shale Member of the Fort Scott Limestone and equivalents, northern Midcontinent region, USA: Chemical Geology, v. 134, p. 215–235.

Heckel, P. H., 1977, Origin of phosphatic black shale facies in Pennsylvanian cyclothems of mid-continent North America: American Association of Petroleum Geologists Bulletin, v. 61, p. 1045–1068.

_____ 1980, Paleogeography of eustatic model for deposition of Midcontinent Upper Pennsylvanian cyclothems, *in* Fouch, T. D.; and Magathan, E. R. (eds.), Paleozoic paleogeography of west-central United States: Society of Economic Paleontologists and Mineralogists, Rocky Mountain Section, Paleogeography Symposium 1, p. 197–215.

_____ 1983, Diagenetic model for carbonate rocks in Midcontinent Pennsylvanian eustatic cyclothems: Journal of Sedimentary Petrology, v. 53, p. 733–759.

_____ 1986, Sea-level curve for Pennsylvanian eustatic marine transgressive-regressive depositional cycles along Midcontinent outcrop belt, North America: Geology, v. 14, 330–334.

_____ 1991, Thin widespread Pennsylvanian black shales of Midcontinent North America: a record of cyclic succession of widespread pycnoclines in a fluctuating epeiric sea, *in* Tyson, R. V.; and Pearson, T. H. (eds.), Modern and ancient continental shelf anoxia: Geological Society of America Special Publication 58, p. 259–273.

_____ 1994, Evaluation of evidence for glacio-eustatic control over marine Pennsylvanian cyclothems in North America and consideration of possible tectonic effects, *in* Dennison, J. M.; and Ettensohn, F. R. (eds.), Tectonic and eustatic controls on sedimentary cycles: Society of Economic Paleontologists and Mineralogists, Concepts in Sedimentology and Paleontology, v. 4, p. 65–87.

Heckel, P. H.; and Hatch, J. R., 1992, Contrasting depositional models for Pennsylvanian black shale discerned from molybdenum abundances; comment: Geology, v. 20, p. 88–89.

Hornfelt, B.; and Nyholm, N. E. I., 1996, Breeding performance of Tengmalm's owl in a heavy metal pollution gradient: Journal of Applied Ecology, v. 33, p. 377–386.

Hurtgen, M. T.; Lyons, T. W.; Ingall, E. D.; and Cruse, A. M., 1999, Anomalous enrichments of iron monosulfide in euxinic marine sediments and the role of H_2S in iron

sulfide transformations: Examples from Effingham Inlet, Orca basin, and the Black Sea: American Journal of Science, v. 299, p. 556–588.

Kempe, S.; Liebezett, G.; Direcks, A.-R.; and Asper, V., 1990, Water balance in the Black Sea: Nature, v. 346, p. 419.

Klein, G. deV., 1992, Climatic and tectonic sea-level gauge for Midcontinent Pennsylvanian cyclothems: Geology, v. 20, p. 363–366.

Klein, G. deV.; and Kupperman, J. B., 1992, Pennsylvanian cyclothems: methods of distinguishing tectonically induced changes in sea level from climatically induced changes: Geological Society of America Bulletin, v. 104, p. 166–175.

Lyons, T. W. 1997, Sulfur isotope trends and pathways of iron sulfide formation in upper Holocene sediments of the anoxic Black Sea: Geochimica et Cosmochimica, v. 61, p. 3367–3382.

Lyons, T. W.; and Berner, R. A., 1992, Carbon-sulfur-iron systematics of the uppermost deep-water sediments of the Black Sea: Chemical Geology, v. 99, p. 1–27.

Lyons, T. W.; Berner, R. A.; and Anderson, R. F., 1993, Evidence for large pre-industrial perturbations of the Black Sea chemocline: Nature, v. 365, p. 538–540.

Lyons, T. W.; Luepke, J. J.; Schreiber, M. E.; and Zieg, G. A., 2000, Sulfur geochemical constraints on Mesoproterozoic restricted marine deposition: Lower Belt Supergroup, northwestern United States: Geochimica et Cosmochimica Acta, v. 64, p. 427–437.

Mullins, H. T.; Thompson, J. B.; McDougall, K.; and Vercoutere, T., 1985, Oxygen-minimum zone edge effects: Evidence from the central California coastal upwelling system: Geology, v. 13, p. 491–494.

Murray, J. W.; Jannasch, H. W.; Honjo, S.; Anderson, R. F.; Reeburgh, W. S.; Top, Z.; Friedrich, L. A.; Codispoti, L. A.; and Izdar, E., 1989, Unexpected changes in the oxic/anoxic interface in the Black Sea: Nature, v. 338, p. 411–413.

Passier, H. F.; Middleburg, J. J.; Van Os, B. J. H.; and De Lange, G. J., 1996, Diagenetic pyritization under eastern Mediterranean sapropels caused by downward sulphide diffusion: Geochimica et Cosmochimica Acta, v. 60, p. 751–763.

Pedersen, T. F.; and Calvert, S. E., 1990, Anoxia vs. productivity: what controls the formation of organic-carbon-rich sediments and sedimentary rocks?: American Association of Petroleum Geologists Bulletin, v. 74, p. 454–466.

Poulson, S. R.; Colberg, P. J. S.; Drever, J. I., 1997, Toxicity of heavy metals (Ni, Zn) to *Desulfovibrio desufuricans*: Geomicrobiology Journal, v. 14, p. 41–49.

Pruysers, P. A.; De Lange, G. J.; Middelburg, J.; and Hydes, D. J., 1993, The diagenetic formation of metal-rich layers in sapropel-containing sediments in the eastern Mediterranean: Geochimica et Cosmochimica Acta, v. 57, p. 527–536.

Raiswell, R.; and Berner, R. A., 1985, Pyrite formation in euxinic and semi-euxinic sediments: American Journal of Science, v. 285, p. 710–724.

Raiswell, R.; and Canfield, D., 1998, Sources of iron for pyrite formation in marine sediments: American Journal of Science, v. 298, p. 219–245.

Raiswell, R.; Buckley, F.; Berner, R. A.; and Anderson, T. F., 1988, Degree of pyritization of iron as a paleoenvironmental indicator of bottom-water oxygenation: Journal of Sedimentary Petrology, v. 58, p. 812–819.

Raiswell, R.; Canfield, D. E.; and Berner, R. A., 1994, A comparison of iron extraction methods for the determination of degree of pyritization and the recognition of iron-limited pyrite formation: Chemical Geology, v. 111, p. 101–110.

Rhoads, D. C.; and Morse, J. W., 1971, Evolutionary and ecologic significance of oxygen-deficient marine basins: Lethia, v. 4, p. 413–428.

Savrda, C. E.; and Bottjer, D. J., 1986, Trace-fossil model for reconstruction of paleo-oxygenation in bottom waters: Geology, v. 14, p. 3–6.

_____ 1987, The exaerobic zone, a new oxygen-deficient marine biofacies: Nature, v. 327, p. 54–56.

_____ 1991, Oxygen-related biofacies in marine strata: an overview and update, *in* Tyson, R. V.; and Pearson, T. H. (eds.), Modern and ancient continental shelf anoxia: Geological Society of America Special Publication 58, p. 201–219.

Savrda, C. E.; Bottjer, D. J.; and Gorsline, D. S., 1984, Development of a comprehensive oxygen-deficient marine biofacies model: Evidence from Santa Monica, San Pedro, and Santa Barbara basins, California continental borderland: American Association of Petroleum Geologists Bulletin, v. 68, p. 1179–1192.

Shaw, T. J.; Sholkovitz, E. R.; and Klinkhammer, G., 1994, Redox dynamics in the Chesapeake Bay: the effect on sediment/water redox exchange: Geochimica et Cosmochimica Acta, v. 58, p. 2985–2995.

Spencer, D. W.; Brewer, P. G.; and Sachs, P. L., 1972, Aspects of the distribution and trace metal composition of suspended matter in the Black Sea: Geochimica et Cosmochimica Acta, v. 36, p. 71–86.

Stookey, L. L., 1970, Ferrozine—a new spectrophotometric reagent for iron: Analytical Chemistry, v. 42, p. 779–781.

Taylor, S. R.; and McClennan, S. M., 1985, The continental crust: Its composition and evolution: Blackwell Scientific, Oxford, 312 p.

Wanless, H. R.; and Shepard, F. P., 1936, Sea level and climatic changes related to late Paleozoic cycles: Geological Society of America Bulletin, v. 47, p. 1177–1206.

Zangerl, R.; and Richardson, E. S., 1963, The paleoecological history of two Pennsylvanian black shales: Chicago Natural History Museum, Fieldiana: Geology Memoir, v. 4, 352 p.

Zhabina, N. N.; and Volkov, I. I., 1978, A method of determination of various sulfur compounds in sea sediments and rocks, *in* Krumbein, W. E. (ed.), Environmental biogeochemistry: methods, metals and assessment, v. 3: Ann Arbor Science Publishers, Ann Arbor, Michigan, p. 734–745.

Depositional Environments of Marine Sandstones in the Midcontinent

Richard D. Fritz and Larry D. Gerken
Masera Corporation
Tulsa, Oklahoma

ABSTRACT.—Marine sandstones were deposited in a variety of structural and stratigraphic settings in the Midcontinent. Deposition was controlled and can be characterized by three structural stages: (1) rifting stage, (2) subsiding stage, and (3) deformational stage. Stratigraphically, these structural stages can be roughly defined by Sloss sequences as follows: (1) pre-Sauk (to perhaps earliest Sauk), (2) Sauk to Tippecanoe, and (3) Kaskaskia to Absaroka.

Relatively little deposition occurred during the rifting stage, which was dominated in the Midcontinent by igneous and metamorphic rock and metasediment. At the end of this stage, the transgressive marine Reagan Sandstone was deposited, which marked the beginning of subsidence in the Anadarko and Arkoma basins.

The subsiding stage of the Midcontinent began with deposition of the Cambrian–Ordovician Arbuckle Group, which is mostly carbonate but also contains several widespread marine-clastic deposits such as the Gunter sandstone. Arbuckle deposition was immediately followed by the deposition of the thick clastic sequence of the Ordovician Simpson Group. This group can be subdivided in ascending order into the Joins, Oil Creek, McLish, Tulip Creek, and Bromide Formations. The sandstones that make up much of these formations were deposited in a mixed-carbonate–clastic environment. Simpson sands were most likely derived from the north and northeast by marine, coastal, fluvial, and eolian processes across a vast plain sometimes referred to as the "Great American Carbonate Bank."

Another thick carbonate sequence followed Simpson deposition and was composed of limestones, dolomites, and thin shales of the Viola to Hunton Groups. The thin, marine to estuarine Misener sandstones were deposited from and along the Simpson outcrop on the post-Hunton unconformity.

The first major clastic wedges to be deposited during the deformational stage of the Midcontinent are represented by the Carboniferous Stanley–Jackfork section, which was deposited in the Ouachita trough, and by the Springer Group, which was deposited in the southern Oklahoma aulacogen and current Anadarko basin. In the Ouachita uplift, a thick turbidite complex represents the Carboniferous Stanley–Jackfork Groups with sediment derived from the east, north, and south. It is followed by the Morrowan Johns Valley clastic wedge, which is characterized by chaotic slump features. To the north, the Union Valley contains thin marine-sandstone deposits.

Westward on the Anadarko shelf, the Springer Group consists of fluvial-deltaic sediments, most of which were truncated. The basinal remnant is dominated by nearshore-marine bars and sheet sandstones encased in thick marine shales. In the Anadarko basin, the Springer Group is overlain by the Pennsylvanian Morrow Group, which is one of the most significant and widespread clastic wedges in the Midcontinent. In the Anadarko basin, the Morrow can be divided into upper and lower sequences. Deltaic-coastal sediments to the north and west and nearshore-marine deposits along the Anadarko shelf edge and basin can characterize sandstone deposition in the lower section. The upper Morrow is characterized by cherts derived from the uplift of carbonates along the Amarillo-Wichita uplift and then deposited in fan-delta complexes.

Although Atokan sediments are relatively thin in the Anadarko basin, in the Arkoma basin/Ouachita uplift, the Atoka is represented by a thick clastic wedge, which was derived primarily from the advancing Ouachita orogenic belt. The basal Atokan is represented by the rather widespread Spiro Sandstone, which is predominantly a marine sequence deposited on a wide shelf. The Spiro was most likely sourced from the north and east by deltas advancing along the Reelfoot rift. Most of the overlying Atoka section consists of an extremely thick, foreland-basin sequence of deltaic to marine sandstones and shales.

The remainder of the Pennsylvanian (Desmoinesian to Virgilian) was dominated by clastic cyclic sequences, especially in Oklahoma. The Red Fork was the most extensive of these sequences and was deposited over much of the Midcontinent. The Red Fork can be divided into upper, middle, and lower units, most of which are fluvial-deltaic deposits; however, in the slope and basinal areas, the Red Fork sandstones are represented by a complex of deltaic deposits, nearsh ore-marine bars, estuarine deposits, and shallow submarine fans. The upper Red Fork sandstone may represent a thick, low-stand delta instead of a submarine-fan complex.

Multiple Upper Pennsylvanian to Permian deltaic to marine sequences overlie the Desmoinesian units. One

Fritz, R. D.; and Gerken, L. D., 2000, Depositional environments of marine sandstones in the Midcontinent, *in* Johnson, K. S. (ed.), Marine clastics in the southern Midcontinent, 1997 symposium: Oklahoma Geological Survey Circular 103, p. 195–196.

of the most notable of these marine sequences is the Cottage Grove section, which contains large offshore-bar deposits.

Marine deposits are also found in the Cretaceous in southern Oklahoma.

Most of the marine sandstones described above have economic importance as fair to excellent oil and gas reservoirs. It is important to understand their reservoir characteristics and geometry for future exploration and exploitation evaluation.

Sequence Stratigraphy of the Jackfork Sandstone in the Ouachita Mountains—Applications for Petroleum Exploration

Richard D. Fritz
Masera Corporation
Tulsa, Oklahoma

Michael Kuykendall
Solid Rock Resources, Inc.
Tulsa, Oklahoma

ABSTRACT.—Recent drilling for Jackfork reservoirs in southeastern Oklahoma has renewed interest in the structural and stratigraphic framework of the Ouachita uplift. Structurally, the uplift can be divided into two areas by the Ti Valley fault: (1) a frontal, imbricated zone north of the fault and (2) the central thrust belt south of the fault. Morrowan age strata can also be divided by the Ti Valley fault, with dominantly platform sediments to the north and basin deposits to the south.

The Jackfork Group consists of a thick sequence of alternating sandstones and shales. This sequence represents an elongate submarine-fan complex that extends from Alabama to Oklahoma. The sandstones are composed of slumps, debris flows, and turbidites, which were primarily derived from nonvolcanic landmass east of the present-day Black Warrior basin. Secondarily, some of these sediments were derived from the north from Simpson outcrops and from a large drainage basin to the northeast, which terminated with advancing deltas through the Reelfoot rift area. Some sediment may also be derived from the south from the emergent, advancing Ouachita thrust belt.

Multiple fan models have been used to explain Jackfork deposition. A combination of the Walker and Vail models appears to be most applicable to Jackfork deposition. Recent study of Jackfork sequence stratigraphy indicates that the submarine fans may be subdivided into intervals that represent pulses during third-order, sea-level changes.

The central Ouachita thrust belt is a largely unexplored zone of over four million acres in Oklahoma and Arkansas. Sohio initiated an exploration program from 1980 to 1988, during which they drilled a large "channel" identified from seismic in a syncline. Although there were multiple gas shows, the well was not economic. In the early 1990s, H&H Star be-gan drilling for the Spiro sandstone along the Ti Valley faults and found several wells with productive Jackfork. This resulted in a marginally economic gas play exploited by Amoco, Chesapeake, Ward, and others along a large very elongate anticline. More recently, Vastar, Texaco, and Chevron have drilled along the Windingstair fault to evaluate Jackfork potential.

This new round of Jackfork exploration has focused thus far partly on porous and permeable, massive-appearing, "channel-like" sandstones. Outcrop comparisons to the subsurface show that these reservoirs are compositionally quartzarenites and sublitharenites. These sandstones are poorly to moderately sorted, moderately compacted, subrounded to subangular, very fine to medium-grained, with distinctive thin quartz-granule lag layers. The more porous outcrop sandstones were originally more feldspathic and lithic; however, surficial dissolution of these more unstable detrital constituents creates secondary porosity that masks the original sandstone composition as well as the true reservoir pore geometry.

Fritz, R. D.; and Kuykendall, Michael, 2000, Sequence stratigraphy of the Jackfork Sandstone in the Ouachita Mountains—applications for petroleum exploration, *in* Johnson, K. S. (ed.), Marine clastics in the southern Midcontinent, 1997 symposium: Oklahoma Geological Survey Circular 103, p. 197.

Trends in Production, Reservoir Characteristics, and Stratigraphic and Depositional Boundaries of the Clastic Facies of the Springer Group, Anadarko Basin, Oklahoma

Walter J. Hendrickson, Paul W. Smith, Craig M. Williams, and Ronald J. Woods
Petroleum Information/Dwights LLC
Oklahoma City, Oklahoma

ABSTRACT.—As part of a regional study, the logs from every producing well in a large portion of the Anadarko basin and shelf of Oklahoma were reviewed to verify the actual producing reservoir. Both detail and regional cross sections were constructed and used to determine stratigraphic relationships and to develop a system of stratigraphic nomenclature that could be used across the area with accuracy, detail, and consistency. Correlations were made from the Heebner Shale (Cisco Group, Upper Pennsylvanian) to the deepest zones penetrated. Allocation of the production within the study area was made based on these correlations and the associated stratigraphic nomenclature.

The Springer Group in the study area consists of the Boatwright, Britt, and Cunningham sandstones, in ascending order. Whereas the Cunningham was found always to be a sandstone, extensive correlations indicated that the Boatwright and Britt, which are predominantly sandstones in the southeastern portion of the study area, develop an equivalent carbonate facies to the northwest. The cross sections demonstrate this lateral facies change as well as permitting identification of the various subdivisions of the Springer. Facies and production maps are presented for the individual subdivisions of the Springer Group. A comparative analysis of the three Springer formations was made for productive depth, thickness, porosity, water saturations, and hydrocarbon recovery.

Approximately 2.1 trillion cubic feet of gas has been produced from 702 completions in the Boatwright, Britt, and Cunningham sandstones as therein defined.

Hendrickson, W. J.; Smith, P. W.; Williams, C. M.; and Woods, R. J., 2000, Trends in production, reservoir characteristics, and stratigraphic and depositional boundaries of the clastic facies of the Springer Group, Anadarko basin, Oklahoma, *in* Johnson, K. S. (ed.), Marine clastics in the southern Midcontinent, 1997 symposium: Oklahoma Geological Survey Circular 103, p. 198.

Depositional Environments of the Upper Permian Childress Sandstone and Gypsum, Eastern Flank Permian Basin, Texas

James O. Jones[1]
The University of Texas at San Antonio
San Antonio, Texas

ABSTRACT.—The Childress Dolomite on the eastern flank of the Permian basin has long been mapped as extending from northern Childress County, Texas, to south of Sweetwater in Nolan County, Texas. Near the Childress and Cottle County line, however, the Childress Dolomite thins and disappears to the south in northern Cottle County. In that area, and at about the same interval as the Childress Dolomite, a resistant unit is present that is composed of gypsum and gypsum-cemented sandstone. On geologic maps of the area, it is referred to as the Childress Dolomite. The gypsiferous unit is herein referred to as the Childress Sandstone and Gypsum.

Depositional strike in this area is approximately N. 10° E. with a dip of less than a degree to the west. This gypsiferous unit extends south for at least 200 km from southern Childress County into Nolan County. It is exposed as the cap of east-facing cliffs and scarp slopes on westward dipping cuestas of the region. It can generally be viewed to the west of U.S. Highway 83 from northern King County to southern Stonewall County. It forms the resistive surfaces of buttes and mesas that are updip from the cuestas.

The sandstone is a well preserved, very fine to fine-grained quartzarenite that typically does not contain primary sedimentary structures. It has been cemented with gypsum that was probably derived by dissolution from the overlying alabaster gypsum bed.

A few exposures contain excellent sedimentary structures. Large cross-stratification of >1 m in thickness and 10 m in horizontal extent, as well as smaller cross-bedding are present. Symmetrical ripple marks with wave heights of 2 cm and lengths of 4 cm, as well as linguoid ripple marks up to 20 cm wide and up to 10 cm high are preserved. Flow direction of linguoid ripple marks trends north of west. Larger cross-stratifications are part of megaripples or dunes developed on large, siliciclastic tidal flats of the eastern flank of the basin. Linguoid ripples are ebb-tide structures in multiple packets with parallel laminae produced by the flood tides.

Most cross-bedding is preserved because larger fragments of well-rounded quartz grains, oolites, and carbonate fragments are in relief on weathered surfaces. Sandstone with gypsum cement removed by dissolution is friable and generally structureless. Larger fragments of carbonate pebbles and very coarse quartz grains are commonly present at the toe of lee slopes of larger cross-beds. Dune lee slopes trend northeast indicating tide flow from west to east.

Tidal sedimentary structures the size of the large dunes that are present on this tidal shelf are the result of strong tidal flow and were probably generated in water depths in the mesotidal to macrotidal range.

[1]Deceased

Jones, J. O., 2000, Depositional environments of the upper Permian Childress Sandstone and Gypsum, eastern flank Permian basin, Texas, *in* Johnson, K. S. (ed.), Marine clastics in the southern Midcontinent, 1997 symposium: Oklahoma Geological Survey Circular 103, p. 199.

Evidence for a Spiro-Equivalent Lowstand Fan in the Ouachita Overthrust Belt, Southeastern Oklahoma—A New Exploratory Target

Mark R. Longden and Daniel J. Patterson
Vastar Resources
Houston, Texas

Steven Scott Demecs
Scott Services International Inc.
Plano, Texas

ABSTRACT.—The Atoka Formation of the Ouachita thrust belt has historically been interpreted as a muddy flysch deposit derived from the eroding Appalachians and deposited as a large, westward-directed axial fan. Sublithic-sandstone composition and low textural maturity indicate a recycled orogenic source terrain consistent with this interpretation. However, examination of more than 90 outcrops within the Ti Valley thrust plate in western Arkansas and eastern Oklahoma reveals an anomalous quartzarenite-sandstone facies, which locally forms the basal sandstone of the Atoka Formation. At least four distinct sites of deposition are recognized. Petrographic studies indicate a cratonic provenance for these sandstones. High textural maturity and shallow-marine fossil debris indicate derivation from a high-energy, shallow-marine–shelf environment. Stratigraphic position (basal Atoka), provenance, sandstone composition and texture, and fossil assemblage are identical to the shelfal Spiro sandstone of the adjacent Arkoma basin, and a genetic relationship is thus inferred.

Stratigraphically, the quartzarenite sandstone rests in sharp contact with the underlying Johns Valley Formation, an olistostrome-bearing unit that is widely interpreted as having been deposited in a mud-rich, slope to base-of-slope environment. Immediately overlying the quartzarenite facies and occasionally interbedded with it are thin turbidite sandstones typical of the deep-water Atoka Formation. These relationships constrain the unit to a deep-water environment, dominated by gravity-driven depositional processes.

Three depositional facies are recognized in outcrop. The first facies occurs as lenticular or channel-form sandstone bodies 1–3 mi wide and up to 265 ft thick. Sedimentary structures observed include massive, structureless beds up to 50 ft thick, as well as parallel laminae, convolute bedding, water-escape structures and sparse flute casts. The second depositional facies occurs laterally and distally(?) to the channel facies and consists of beds 3 in. to 20 ft thick, which are commonly structureless. Less common are beds having massive bases and parallel to ripple-laminated tops resembling partial Bouma sequences. Sparse inverse grading and "floating clasts" occur locally. This facies may represent nonchannelized overbank or levy deposits. The third depositional facies consists of a progradational parasequence-set with an aggregate thickness of greater than 640 ft. Beds within this facies range from 2 in. to 9 ft thick and are generally massive or parallel laminated. Deformed parallel laminae and/or cross-stratification are common at bed tops. Normal grading and partial Bouma sequences, as well as flute casts, occur locally. This facies is interpreted as representing prograding fan lobes.

The thick channel sands are confined to the northernmost thrust plates of the Ti Valley system. Thinner-bedded facies occur basinward. A palinspastically restored isopach map indicates north-south depositional trends and is consistent with a cratonic source and sparse south-directed flute casts. We interpret these deposits as small (50–200 mi^2?) sand-rich fans derived from the craton during the sea-level lowstand during Spiro time.

The lowstand fan-channels have lateral continuity measured in miles, comparable reservoir quality to Spiro producers, and greater potential reservoir thickness than typical Spiro producers in the Arkoma basin. They, thus, represent a viable exploratory target in the frontal Ouachita Mountains of southeastern Oklahoma and western Arkansas.

Longden, M. R.; Patterson, D. J.; and Demecs, S. S., 2000, Evidence for a Spiro-equivalent lowstand fan in the Ouachita overthrust belt, southeastern Oklahoma—a new exploratory target, *in* Johnson, K. S. (ed.), Marine clastics in the southern Midcontinent, 1997 symposium: Oklahoma Geological Survey Circular 103, p. 200.

Palinspastic Restoration of the Choctaw, Pine Mountain, and Ti Valley Thrust Plates—Constraints on Spiro Paleogeography and Sequence Analysis

Mark R. Longden and Daniel J. Patterson
Vastar Resources
Houston, Texas

Steven Scott Demecs
Scott Services International, Inc.
Plano, Texas

ABSTRACT.—Integration of recent well-control, surface, and seismic data has allowed construction of a balanced cross-section through the Arkoma basin and frontal Ouachita Mountains, which constrains the restored position of the Choctaw, Pine Mountain, and Ti Valley thrusts with greater certainty than previous studies. Central to the interpretation is the recognition of preserved hanging-wall and footwall cutoffs at the basal Atoka (Spiro) level both between the Ti Valley and Pine Mountain plates and between the Pine Mountain and Choctaw plates. The Choctaw hanging-wall cutoff is not locally preserved due to erosion, and, thus, the restoration represents a minimum value. However, mapping by the Oklahoma Geological Survey indicates erosion may be minimal.

The Ti Valley thrust has approximately 5 mi of shortening with respect to the underlying Pine Mountain plate, whereas the Pine Mountain thrust has less than 2 mi of shortening with respect to the Choctaw plate. The Choctaw thrust displays the greatest shortening with at least 7.5 mi of displacement with respect to the underlying duplex. The subthrust duplex has 6 mi of shortening at the Spiro level. Summation of both fold and thrust shortening between and within the thrust plates—at the Spiro level—yields a restored position for the Ti Valley thrust approximately 23 mi south of its present location. The Pine Mountain thrust and Choctaw thrusts restore 19 mi and 14 mi, respectively, south of their present position. This is considerably less than many previously published estimates and provides constraints on the reconstruction of Spiro paleogeography. It also indicates that the transition to the "Ouachita facies" of the Pennsylvanian section occurred well north of the Broken Bow uplift, near the current-day location of the Octavia thrust fault.

Spiro strata in the southern Arkoma basin consist of shallow-marine, siliciclastic and carbonate rocks that have been interpreted as representing portions of the lowstand and transgressive systems tracts. The Spiro sandstone exposed on the Choctaw thrust consists predominately of shoreline and shelf sediments of the lowstand and transgressive systems tracts deposited near the shelf/slope break, with possible slope-canyon turbidites in the southern part of the thrust plate. The Spiro interval of the Pine Mountain plate consists largely of shale, muddy spiculite, and thin, very fine grained, turbidite sandstones deposited on the slope. Sparse, thick-bedded Spiro sandstone accumulations are present in wells and outcrop and represent ponded sediment in slope-canyon or gully systems. The Spiro of the Ti Valley thrust plate is interpreted as a base-of-slope, lowstand fan and reaches a gross thickness of >640 ft, with amalgamated channel sands up to 265 ft thick.

The restoration and facies interpretations presented here constitute an internally consistent facies model and place deposits of the Ti Valley thrust plate in relatively close proximity to the Spiro shelf edge. The distance from the shelf edge to the base of slope defines a slope width of about 5–10 mi, a range consistent with modern, tectonically active margins.

Longden, M. R.; Patterson, D. J.; and Demecs, S. S., 2000, Palinspastic restoration of the Choctaw, Pine Mountain, and Ti Valley thrust plates—constraints on Spiro paleogeography and sequence analysis, *in* Johnson, K. S. (ed.), Marine clastics in the southern Midcontinent, 1997 symposium: Oklahoma Geological Survey Circular 103, p. 201.

Geology of the Brentwood Shallow Gas Field, Washington County, Arkansas

Walter L. Manger
University of Arkansas
Fayetteville, Arkansas

Phillip R. Shelby
Shelby Geological Consulting
Ozark, Arkansas

ABSTRACT.—The Brentwood shallow gas field occupies an area of approximately 24 mi^2 occupying portions of T. 14 N., R. 29 W. and R. 30 W., near the community of Brentwood, Washington County, Arkansas. The discovery well was the No. 1 Archie Goad, drilled by Arkansas Western Gas Company in March 1959; however, that well was never produced. In 1977, the Arkansas Western Gas Company No. 1 Harmon was reentered by Bistate Energy, and production began in April 1978. The field has been delimited by 30 productive wells and at least 23 nonproductive wells. All wells are shallower than 1,000 ft, and most are less than 800 ft. Peak production approached 150 thousand cubic feet (Mcf) of gas per day, and through December 1994, the Brentwood field had cumulative production of 1.83 billion cubic feet, principally dry methane. There is no commercial production at the present time.

The Brentwood field produces from the Wedington Sandstone Member, Fayetteville Shale (Upper Mississippian, Chesterian). This unit is a well-known constructional delta, but most of the production in the field is from marine sheet sands basinward of the distributary system. Black shales entombed the delta system and adjacent shelf sandstones to provide the seal for the reservoir. Logs record an average thickness of 20 ft for the Wedington in the Brentwood field, with a distinctive signature expressing a shaly top and base for the interval. Reported porosity ranged from 12% to 20%, but there were few log suites and no cores upon which to characterize the productive interval. Drillers reported a cementation cap—identified by slow drilling—that trapped gas immediately below the top of the Wedington in most productive wells. Open-hole completions below a wireline packer were typical of the field, and there was no stimulation of the reservoir.

A series of northeast-southwest–trending normal faults that are downthrown on their southeastern sides occur at approximately 2–25-mi spacing across the southern Ozark region. These faults intersect the east-west boundary faults of the northern Arkoma basin and extend nearly to the Arkansas-Missouri border. In northwestern Arkansas, this system is represented by the Fayetteville and Drakes Creek faults. Smaller, east-west–trending normal faults, downthrown to the south, connect these major faults. The Brentwood field is bisected by the Brentwood fault with displacement of 90–150 ft. The bulk of production occurs in anticlinal closures of approximately 300 ft on the upthrown (north) side of that fault. Production is also recorded from the downthrown (south) side of the Brentwood fault.

Production from the Brentwood field is dry methane that we believe was produced from sources in the Arkoma basin and then migrated along the major northeast-trending faults into the shallow gas province of northwestern Arkansas. Since the first discovery in 1953, and with the peak of production in the 1980s, 14 fields, including Brentwood, constituting more than 170 wells, have produced 10.17 billion cubic feet of gas from this province.

Manger, W. L.; and Shelby, P. R., 2000, Geology of the Brentwood shallow gas field, Washington County, Arkansas, *in* Johnson, K. S. (ed.), Marine clastics in the southern Midcontinent, 1997 symposium: Oklahoma Geological Survey Circular 103, p. 202.

Reservoir Development and Production from the Clifty-Sylamore Interval (Devonian), Shallow Gas Province, Northwestern Arkansas

Walter L. Manger
University of Arkansas
Fayetteville, Arkansas

Phillip R. Shelby
Shelby Geological Consulting
Ozark, Arkansas

ABSTRACT.—The shallow gas province of northwestern Arkansas is confined essentially to Washington and Madison Counties (generally bounded by T. 13 N. to T. 16 N. and R. 26 W. to R. 33 W.). The first commercial well was the Threkeld No. 1, completed by Arkansas Western Gas Company in June 1953. At its most active stage in the late 1980s, the province consisted of 14 small fields and more than 170 wells. Cumulative production through December 1994 has exceeded 10.17 billion cubic feet. Producing wells are typically less than 1,000 ft, and many are less than 600 ft. Production has been recorded from the St. Peter (Middle Ordovician), Clifty (Middle Devonian), Sylamore (Upper Devonian), Boone Formation (Lower Mississippian), and Wedington Sandstone (Upper Mississippian), but most wells produce from a single horizon. Most fields are located in proximity to either the Fayetteville or Drakes Creek faults, major northeast-southwest–trending normal faults, and associated with local anticlinal closures. All wells produce dry methane, with trace amounts of other gases, condensate, and water. Initial shut-in pressures range from 90 to 140 psi, and pressure declines of 20–30% are typical of the first year. Field rules allow 40- or 80-acre well spacing, depending on the field.

The Devonian succession of the southern Ozarks in northern Arkansas consists of the Penters Chert, Clifty Formation, and Chattanooga Shale, which are regarded as representing the Lower, Middle, and Upper portions of the system, respectively. Each of the units is bounded by a regional, erosional unconformity (type 1 sequence boundary), and each lacks persistency; the complete sequence is generally not developed in any one well or surface section. The bulk of the production in the shallow gas province is encountered immediately below the Chattanooga Shale (Upper Devonian) in orthoquartzitic sandstones sealed by black shale. These sandstones represent transgressive marine deposits reworking erosional products derived from the underlying units. They are typically referred to the Sylamore Member. The Sylamore is thin and phosphatic and has the highest persistency of any of the Devonian units except the Chattanooga. In contrast, the Clifty is sporadic, and favorable porosity and permeability are associated with high areas on the pre-Devonian erosional surface. Low areas may develop green, nonproductive shale below the Chattanooga. Unfortunately, the lack of cores has limited understanding of the reservoir interval.

Gas appears to have migrated from the Arkoma basin into the shallow gas province along the major northeast-trending normal faults. There is no production between the shallow gas province and the boundary faults of the northern Arkoma basin, a distance of approximately 20 mi. Migrating gas would have had the opportunity to invade any reservoir-quality lithologies in a suitable structural setting in that region, which represents a potential, but unproven, focus for future exploration.

Manger, W. L.; and Shelby, P. R., 2000, Reservoir development and production from the Clifty-Sylamore interval (Devonian), shallow gas province, northwestern Arkansas, *in* Johnson, K. S. (ed.), Marine clastics in the southern Midcontinent, 1997 symposium: Oklahoma Geological Survey Circular 103, p. 203.

Interpreting Formation MicroScanner Log Images of Gulf of Mexico Pliocene Deep-Water Clastics by Comparison with Pennsylvanian Jackfork Group Deep-Water Clastics, West-Central Arkansas

Roger M. Slatt[1]
Colorado School of Mines
Golden, Colorado

Robert J. Davis
Schlumberger Indonesia
Jakarta, Indonesia

Charles G. Stone
Arkansas Geological Commission
Little Rock, Arkansas

Douglas W. Jordan
Arco Venezuela, Inc.
Caracas, Venezuela

ABSTRACT.—A comprehensive picture has emerged recently of the variety of deep-water, clastic depositional elements present in the Jackfork Group of west-central Arkansas. The details of our investigations have been reported on industry field trips and discussed in several recent publications and presentations. We now add another applied dimension to this picture by comparing small- to large-scale sedimentary features observed in the outcrops with what we interpret as identical features observed on Formation MicroScanner (FMS) logs from Pliocene Gulf of Mexico deep-water clastics.

Small-scale features displayed on the FMS logs include slumps, erosional surfaces, thin sand-shale interbeds, mud-lined depressions/scours, isolated sandstone clasts in shaly debris-flow beds, remnant bedding in various stages of disruption because of flowage, and load structures. These features are similar in size and character to those observed in outcrop. On a larger scale, thin- and thick-bedded intervals and major, probably regionally correlative surfaces are recognized.

Based upon the outcrop criteria, recognition of these features on FMS (and FMI) images from the Jackfork, Gulf of Mexico, or other deep-water clastics can lead to improved interpretation of depositional processes, facies and their three-dimensional geometry, relative reservoir quality, and lateral and vertical continuity of beds. This understanding can prove valuable in resolving reservoir management, development drilling, and exploration issues.

[1]Current address: University of Oklahoma, Norman, Oklahoma.

Slatt, R. M.; Davis, R. J.; Stone, C. G.; and Jordan, D. W., 2000, Interpreting Formation MicroScanner log images of Gulf of Mexico Pliocene deep-water clastics by comparison with Pennsylvanian Jackfork Group deep-water clastics, west-central Arkansas, *in* Johnson, K. S. (ed.), Marine clastics in the southern Midcontinent, 1997 symposium: Oklahoma Geological Survey Circular 103, p. 204.

Outcrop Analogs of Turbidite Petroleum Reservoirs for Assessing Volumetric, Development Drilling, and Simulation Scenarios

Roger M. Slatt[1]
Colorado School of Mines
Golden, Colorado

Paul Weimer
University of Colorado
Boulder, Colorado

Hisham A. Al-Siyabi and Eugene T. Williams
Colorado School of Mines
Golden, Colorado

ABSTRACT.—The Pennsylvanian upper Jackfork Formation has been mapped in detail in superbly exposed quarries, dam exposures, and other outcrops in the DeGray Lake–Hollywood area, central Arkansas, to develop three-dimensional analog models of turbidite reservoirs. If it is imagined that the floor of quarry or dam exposures are fluid/water contacts and their upper ground surfaces are unconformities, then it is possible to map "fluid" contacts, and, when standing on these contacts, to imagine yourself within a turbidite reservoir. On this basis, "volumetrics" can be calculated and "development drilling" and "simulation" scenarios can be assessed for the different observed geologic conditions. Two examples are presented.

Hollywood Quarry sits near the crest of a faulted anticline. A lower interval of shallowly dipping, thick, amalgamated, lenticular sandstones is separated from an upper interval of thin, laterally continuous, interlayered sandstones and shales by a thick, laterally continuous shale. Numerous faults dissect the quarry and compartmentalize strata over short distances. "Volumetrics" have been calculated at about 300,000 stock tank barrels of oil originally in place for this "reservoir" using psuedo values for porosity, water saturation, and bulk volume of oil. For "reservoir simulation," a two-layer geologic model is adequate. Several "development drilling" scenarios are possible owing to complex fault and stratigraphic compartmentalization.

At DeGray Lake Spillway, a 1,000-ft-thick, steeply dipping, outcrop succession of thin- and thick-bedded sandstone intervals separated by thick shales has been correlated with numerous shallow core borings from the DeGray Lake Dam area, about 1 mi away. "Volumetrics" for this "reservoir" have been calculated at about 2 MMSTBOOIP using psuedo values for porosity, water saturation, and bulk volume of oil. A number of vertical, deviated, and horizontal "development drilling" scenarios can be applied to this analog of a steeply dipping, unconformity-capped turbidite reservoir.

[1]Current address: University of Oklahoma, Norman, Oklahoma.

Slatt, R. M.; Weimer, Paul; Al-Siyabi, H. A.; and Williams, E. T.., 2000, Outcrop analogs of turbidite petroleum reservoirs for assessing volumetric, development drilling, and simulation scenarios, *in* Johnson, K. S. (ed.), Marine clastics in the southern Midcontinent, 1997 symposium: Oklahoma Geological Survey Circular 103, p. 205.

Comparative Sedimentology of the Dutcher and Cromwell (Pennsylvanian) Sandstones of the Northeastern Oklahoma Platform

Dorothy L. Swindler and J. Glenn Cole
Independent Geologists
Tulsa, Oklahoma

ABSTRACT.—The Dutcher and Cromwell sandstones are poorly understood, although they have produced much oil and gas in eastern Oklahoma. The term Dutcher is used for sandstones of the Atoka Formation in the subsurface of the northeastern Oklahoma platform (north and northwest of the Arkoma basin and as far west as the Seminole-Cushing uplift). Northward from the Arkoma basin, the Atoka Formation rests on progressively older Morrowan and then Mississippian rocks. The Morrow Group thins northward and westward depositionally and by erosional truncation. Where the Wapanucka limestone is absent, it is difficult to know with certainty whether the shale that separates the Dutcher from the Union Valley is Morrowan, Atokan, or both. Based on log character alone, it is difficult, and in places not possible, to distinguish between Dutcher sandstone (Atokan) and sandy Morrowan beds.

The Cromwell sandstone is the main oil-producing sandstone in the Cromwell field (northeastern Seminole County). The Cromwell sandstone in a core from the Cromwell field consists of interbedded sandstone, fossiliferous sandstone, and sandy grainstone. Almost half of the core contains roughly equal amounts of quartz-sand and carbonate grains. Eastward, the ratio of sandstone to limestone decreases, and the interval becomes dominantly limestone. We consider the Cromwell sandstone to be a sandstone facies of the Union Valley Formation.

The Dutcher interval is interpreted to have been deposited in a storm-dominated, muddy-shelf environment. The best porosity and permeability was found in sandstones that contained a small amount of detrital clay in the form of mud–rip-up clasts, chamosite, or rock fragments. The detrital clay was apparently the source of authigenic clay that inhibited pervasive silica cementation. Sandstones with no clay tended to be cemented with quartz overgrowths. Of the Dutcher cores studied, the best reservoir quality was in a sandstone consisting of stacked storm deposits, reworked in part by waves. Authigenic clay was replaced by carbonate that was later dissolved. Disseminated traces of authigenic sphalerite and one concentration (8% by point count) suggest that the location of this well on the Depew uplift adjacent to the Keokuk fault zone contributed to the exceptional reservoir quality.

The Cromwell sandstone was deposited on an open-marine shelf at the transition between siliciclastic-dominated and carbonate-dominated environments. Sandstone, fossiliferous sandstone, and sandy grainstone are interbedded, and transitions between lithologies are, for the most part, gradational. Vertical gradations in lithology are also expected to be found laterally. The best porosity was in sandstone and fossiliferous sandstone in which bryozoan fragments are the dominant carbonate-grain type. Porosity in the sandy grainstone formed mostly by dissolution of bryozoans. Porosity in the fine-grained sandstone without bryozoans is occluded by quartz overgrowths.

Swindler, D. L.; and Cole, J. G., 2000, Comparative sedimentology of the Dutcher and Cromwell (Pennsylvanian) sandstones of the northeastern Oklahoma platform, *in* Johnson, K. S. (ed.), Marine clastics in the southern Midcontinent, 1997 symposium: Oklahoma Geological Survey Circular 103, p. 206.

Effects of Depth on Gas Well Recovery in Marine Sandstones in the Anadarko Basin

Thomas J. Woods
Ziff Energy Group
Houston, Texas

Paul W. Smith
Dwights Energydata
Oklahoma City, Oklahoma

ABSTRACT.—A decade ago, industry perceptions were that expenses, risks, and deeper sediment quality would only support expanding industry activity into deeper sediments if gas prices grew very rapidly, approaching $4–$5 per thousand cubic feet (Mcf). Since the mid-1980s, however, gas prices have averaged less than $1.75 per Mcf and have not remained above $2.00 per Mcf for much more than a year. Nevertheless, industry activity has begun to move into deeper sediments at an accelerating rate in the 1990s.

Currently, the average depth of an onshore gas well is approaching 6,500 ft, its greatest value ever. Despite declining drilling activity, the number of gas wells deeper than 15,000 ft is also approaching a record level. The changes that have occurred reflect a combination of new technology that has reduced the expenses and risks associated with deeper drilling as well as the basic "quality" of deeper sediments, none of which were expected a decade ago.

In the marine sandstones of the Anadarko basin, results above 15,000 ft, where more than 90% of industry activity has occurred to date, suggest that the prospects of finding significant recoveries is quite limited, particularly below 10,000 ft. However, a more detailed review of industry results suggests the opposite scenario, particularly below 14,000 ft. Thus, the probability of finding large targets in the Anadarko basin grows with depth. It should be noted that similar observations are seen in Arkoma basin sandstones as well.

This paper will review the trends in gas recovery for Anadarko basin sandstones with depth by formation and age. Physical reservoir volumes will be discussed, along with the effects of overpressuring on the observations. Recent changes in the expenses and risks associated with drilling activity in Oklahoma will also be discussed. Overall, the results of our analysis suggest significant prospects for new gas reserves should exist in the deeper sediments of the Anadarko basin, and the expenses and risks associated with bringing those reserves into production are quite low.

Woods, T. J.; and Smith, P. W., 2000, Effects of depth on gas well recovery in marine sandstones in the Anadarko basin, *in* Johnson, K. S. (ed.), Marine clastics in the southern Midcontinent, 1997 symposium: Oklahoma Geological Survey Circular 103, p. 207.

Clastics as Seismic Markers—Images and Imaginings from the Mountain Front, Southwest Oklahoma: 1979–1996

Roger A. Young, David Thomas, and Zhi-Ming Liu
University of Oklahoma
Norman, Oklahoma

ABSTRACT.—The COCORP seismic-reflection lines in southwest Oklahoma were acquired in 1979 and have formed a historical reference for subsequent reflection studies of the deep Anadarko basin and the adjacent Wichita Mountains frontal zone. The standard for discussion of crustal structure in this area has remained the interpretation of these lines by J. A. Brewer and others (1983, COCORP profiling across the southern Oklahoma aulacogen: overthrusting of the Wichita Mountains and compression within the Anadarko basin: Geology, v. 11, p. 109–114). Oil-industry seismic lines in the late 1980s improved the resolution of shallow and mid-crustal images enormously, so that, armed with these images, one can discern the much lower-resolution appearance of the same features on the earlier sections.

This paper examines the seismic expression of some of the most prominent seismic markers in the clastics of the lower Pennsylvanian. Coincident COCORP and Seismic Exchange, Inc., lines show a remarkable contrast in the character of the same seismic reflections. Improvements in acquisition design and processing are responsible, in part, for the great improvement in imaging, but the flexibility and dynamic range afforded by workstation visualization can be at least as important. Lessons learned from comparison of the old and the new encourage optimistic imaginings for future 3-D acquisition and prestack processing of data from the same areas.

Young, R. E.; Thomas, D.; and Liu, Z-M, 2000, Clastics as seismic markers—images and imaginings from the mountain front, southwest Oklahoma: 1979–1996, *in* Johnson, K. S. (ed.), Marine clastics in the southern Midcontinent, 1997 symposium: Oklahoma Geological Survey Circular 103, p. 208.

LMU: An Expandable, Alpha-Numeric, Trichotomous, Informal, Rock-Stratigraphic–Classification System Based on Marker-Defined, Stratigraphic Reference Surfaces

R. E. Young
Consulting Geologist
Edmond, Oklahoma

Abstract.—A marker-defined, stratigraphic reference surface is any recognizable, laterally traceable, soil- or rock-stratigraphic boundary, which was also a former surface of deposition, or transportation, or erosion; or an *in situ* remnant of a former surface of deposition, or transportation, or erosion.

These reference surfaces may be (1) *primary*—bedding planes in core or outcrop; (2) *secondary*— interpreted "marker-beds" on mechanical logs; or (3) *abstract*—onlapped, offlapped, eroded, or faulted-out "mental images" of reference surfaces.

This informal, trichotomous classification of strata, based on reference surfaces, begins with a division into three categories as follows: L for Lower, M for Middle, and U for Upper. To preserve in the informal name the unique vertical position of each stratal unit as well as the original intent of the stratigrapher, two steps are required as follows: (1) the number 1 is added to the right of L, M, or U each time a stratal unit is trichotomously classified; and (2) the informal, alpha-numeric name of each stratal unit includes all of the letters and numbers in the previous name.

For example, after three trichotomous classification steps the individual stratal unit spoken of as "the third upper, of the second lower, of the first middle, of the Cunningham Formation" would be annotated from larger to smaller as follows: CmF, M-1, L-2, U-3. This same stratal unit would be diagrammed as shown in Figure 1.

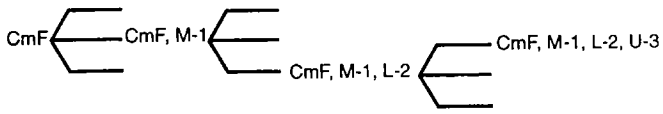

Figure 1. Example of trichotomous classification steps.

Young, R. E., 2000, LMU: an expandable, alpha-numeric, trichotomous, informal, rock-stratigraphic–classification system based on marker-defined, stratigraphic reference surfaces, *in* Johnson, K. S. (ed.), Marine clastics in the southern Midcontinent, 1997 symposium: Oklahoma Geological Survey Circular 103, p. 209.

Origin and Distribution of Porosity in a Carbonate-Cemented Reservoir, Hale Formation (Morrowan), Arkoma Basin, Arkansas

Doy Zachry
University of Arkansas
Fayetteville, Arkansas

ABSTRACT.—The distribution of porous and permeable strata in reservoirs of the Hale Formation is controlled by the proximity of those units to carbonate mud-mound complexes.

Morrowan units including the upper part of the Hale Formation crop out in the Boston Mountains of northwest Arkansas. Southward, the units are displaced by normal fault systems into the subsurface of the Arkoma basin where they contain significant reservoirs of natural gas. Productive intervals occur less than 15 mi from the outcrop belt.

The Hale Formation in the outcrop belt is divided into a lower Cane Hill Member and an upper Prairie Grove Member. The Prairie Grove is mainly composed of calcareous quartzarenite. The carbonate content ranges from 0% to 45% and occurs as skeletal grains and as calcite cement. Terrigenous grains are well sorted, and large-scale cross-stratification is common. A secondary component in the Prairie Grove Member is limestone consisting of skeletal grains and carbonate mud. Intervals of limestone are normally characterized by small bioherms that range from 2 to 15 ft in thickness but form laterally continuous complexes bounded above and below by quartzarenite units.

Adjacent to the bioherms, the sandstones contain abundant skeletal grains, and porosity is occluded by calcite cement. Partially dissolved skeletal grains are abundant and may have contributed to the cement and loss of porosity. Distally positioned quartzarenite units contain little calcite and only small quantities of quartz cement. Porosity ranges to 22% determined petrographically, and reservoir quality is high.

The Prairie Grove Member accumulated on a high-energy shelf prior to the formation of the Arkoma basin. Competent tidal currents generated large bed forms and prominent cross-stratification. Carbonate mud, stabilized by bryozoans, calcareous algae, and other organisms, formed low mounds that coalesced laterally into banks. Skeletal grains were derived and moved laterally away from the banks by tidal currents, extending the distribution of carbonate material over an area substantially greater than the mounds themselves. Porosity in these intervals was occluded by the partial dissolution of skeletal grains and precipitation of calcite cement. More distally positioned sand bodies lack skeletal grains, and porosity was preserved.

Zachry, D., 2000, Origin and distribution of porosity in a carbonate-cemented reservoir, Hale Formation (Morrowan), Arkoma basin, Arkansas, *in* Johnson, K. S. (ed.), Marine clastics in the southern Midcontinent, 1997 symposium: Oklahoma Geological Survey Circular 103, p. 210.